Copyright Warning & Restrictions

The copyright law of the United States (Title 17, United States Code) governs the making of photocopies or other reproductions of copyrighted material.

Under certain conditions specified in the law, libraries and archives are authorized to furnish a photocopy or other reproduction. One of these specified conditions is that the photocopy or reproduction is not to be "used for any purpose other than private study, scholarship, or research." If a, user makes a request for, or later uses, a photocopy or reproduction for purposes in excess of "fair use" that user may be liable for copyright infringement,

This institution reserves the right to refuse to accept a copying order if, in its judgment, fulfillment of the order would involve violation of copyright law.

Please Note: The author retains the copyright while the New Jersey Institute of Technology reserves the right to distribute this thesis or dissertation

Printing note: If you do not wish to print this page, then select "Pages from: first page # to: last page #" on the print dialog screen

ABSTRACT

COMPUTATIONAL THERMOCHEMISTRY OF HYDROCARBONS, OXYGENATES, CYCLIC ALKANES, AND FURANS

by
Jason Michael Hudzik

Fundamental thermochemical properties including enthalpies ($\Delta H^{\circ}_{f\,298}$), entropies ($S^{\circ}(T)$), heat capacities ($C_p(T)$), and bond dissociation energies (BDEs) for several common and complex hydrocarbon fuel species are determined using computational chemical methods. $\Delta H^{\circ}_{f\,298}$ values are calculated using work reactions with the B3LYP (6-31G(d,p) and 6-311G(2d,2p) basis sets), CBS-QB3, and G3MP2B3 calculation methods. Structures, moments of inertia, vibrational frequencies, and internal rotor potentials are calculated for contributions to entropies and heat capacities. Kinetic rate parameters are calculated for hydrogen abstraction and chemical activation reactions.

Recommended $\Delta H^{\circ}_{f\,298}$ and carbon-hydrogen (C–H) BDEs for several normal and branched alkanes and ketones including corresponding radicals from loss of hydrogen atoms show strong comparisons to available literature values. Ketone C–H BDEs in the α position decrease by 6-9 kcal mol^{-1} with increasing substitution compared to normal alkane C–H BDEs. Group additivity (GA) and hydrogen-bond increment (HBI) values for these ketones are determined.

Thermodynamic parameters for *exo*-tricyclo[5.2.1.$0^{2,6}$]decane (TCD), principle component of the hydrocarbon fuel JP-10, and its radicals, diradicals, and carbenes are determined. $\Delta H^{\circ}_{f\,298}$ for TCD is found to be -19.5 kcal mol^{-1} and used to calculate C–H and C–C BDEs for TCD radical, diradical, and carbene formations. Hydrogen

abstraction reactions by a pool of radical species are analyzed using the modified Arrhenius equation for calculation of temperature-dependent rate constants.

High-energy substituted furans created from sustainable biomass sources are of interest in biofuel production due to their high-energy density, and physical properties which are comparable to modern fuel blends. Methoxyfurans show strong furan ring C–H BDEs of 120 kcal mol^{-1} with a decrease to 98 kcal mol^{-1} for the methoxy-methyl C–H bonds. 2-methylfuran hydroperoxide and alcohol species have over 40 kcal mol^{-1} ranges for the O–O BDEs and alcohol O–H BDEs. Oxidation of 2-methylfuran radical, at the furan carbon across from the methyl group, has a 50.6 kcal mol^{-1} well depth. Reaction pathways including abstractions, group transfers, dissociations, and radical peroxy oxygen additions are considered. Temperature- and pressure-dependent rate constants are calculated using quantum Rice-Ramsperger-Kassel analysis and master equation for falloff and stabilization.

COMPUTATIONAL THERMOCHEMISTRY OF HYDROCARBONS, OXYGENATES, CYCLIC ALKANES, AND FURANS

by
Jason Michael Hudzik

A Dissertation
Submitted to the Faculty of
New Jersey Institute of Technology
in Partial Fulfillment of the Requirements for the Degree of
Doctor of Philosophy in Chemistry

Department of Chemistry and Environmental Science

May 2013

APPROVAL PAGE

COMPUTATIONAL THERMOCHEMISTRY OF HYDROCARBONS, OXYGENATES, CYCLIC ALKANES, AND FURANS

Jason Michael Hudzik

Dr. Joseph W. Bozzelli, Dissertation Advisor — Date
Distinguished Professor of Chemistry and Environmental Science, NJIT

Dr. Carol A. Venanzi, Committee Member — Date
Distinguished Professor of Chemistry and Environmental Science, NJIT

Dr. Tamara Gund, Committee Member — Date
Professor of Chemistry and Environmental Science, NJIT

Dr. Haidong Huang, Committee Member — Date
Assistant Professor of Chemistry and Environmental Science, NJIT

Dr. Li Zhu, Committee Member — Date
Research Scientist, Celgene Corporation, Summit, NJ

BIOGRAPHICAL SKETCH

Author: Jason Michael Hudzik

Degree: Doctor of Philosophy

Date: May 2013

Undergraduate and Graduate Education:

- Doctor of Philosophy in Chemistry,
  New Jersey Institute of Technology, Newark, NJ, 2013
- Associate in Science in Business Administration,
  County College of Morris, Randolph, NJ, 2012
- Master of Science in Chemistry,
  New Jersey Institute of Technology, Newark, NJ, 2009
- Bachelor of Science in Chemistry,
  New Jersey Institute of Technology, Newark, NJ, 2007
- Associate in Science in Biology,
  County College of Morris, Randolph, NJ, 2005

Major: Chemistry

Presentations and Publications:

Jason M. Hudzik and Joseph W. Bozzelli, "Thermochemistry and bond dissociation energies of ketones," The Journal of Physical Chemistry A, 2012, 116, 5707-5722.

Jason M. Hudzik, Rubik Asatryan, and Joseph W. Bozzelli, "Thermochemical properties of *exo*-tricyclo[5.2.1.$0^{2,6}$]decane (JP-10 Jet Fuel) and derived tricyclodecyl radicals," The Journal of Physical Chemistry A, 2010, 114, 9545-9553.

Jason M. Hudzik and Joseph W. Bozzelli, "Structure and thermochemical properties of 2-methoxyfuran, 3-methoxyfuran, and their carbon-centered radicals using computational chemistry," The Journal of Physical Chemistry A, 2010, 114, 7984-7995.

Dedicated to

my loving parents, Judith and Michael

my wonderful sister, Jennifer

my wife and best friend, Erin

my beautiful daughters, Alexa and Brianna.

I am truly a lucky man.

ACKNOWLEDGMENT

I would like to extend my sincerest gratitude to my advisor, Dr. Joseph W. Bozzelli, for the opportunity to study under his guidance as a graduate student at NJIT. His encouragement, patience, and caring has served as motivation which will forever inspire me. I am forever grateful for this experience I have been given.

Other members of the Bozzelli Research Group including Dr. Rubik Asatryan, Dr. Alvaro Castillo, Suarwee Snitsiriwat, and Itsaso Auzmendi Murua are also acknowledged for their helpful discussions and friendship. You have all lead through example and made me want to work to the best of my abilities. Thank you so much for this.

I am also very grateful to Dr. Carol Venanzi, Dr. Tamara Gund, Dr. Haidong Huang, and Dr. Li Zhu for serving on my dissertation committee and contributing their helpful comments.

Funding provided through the STTR program by the US Navy (contract number 68335-09-C-0376) is gratefully acknowledged.

The last few years would not have been possible without the constant love and support from all of my family, friends, and coworkers. This enabled me to be able to pursue my dreams and aspirations. I will never be able to say thank you enough to everyone.

TABLE OF CONTENTS

TABLE OF CONTENTS
(Continued)

Chapter **Page**

TABLE OF CONTENTS
(Continued)

Chapter **Page**

TABLE OF CONTENTS
(Continued)

Chapter **Page**

TABLE OF CONTENTS
(Continued)

Chapter **Page**

TABLE OF CONTENTS
(Continued)

Chapter **Page**

TABLE OF CONTENTS
(Continued)

LIST OF TABLES

LIST OF TABLES
(Continued)

LIST OF TABLES
(Continued)

LIST OF TABLES
(Continued)

LIST OF TABLES
(Continued)

LIST OF TABLES
(Continued)

LIST OF TABLES
(Continued)

LIST OF TABLES
(Continued)

LIST OF FIGURES

LIST OF FIGURES
(Continued)

LIST OF FIGURES
(Continued)

LIST OF FIGURES
(Continued)

LIST OF FIGURES
(Continued)

CHAPTER 1

INTRODUCTION

Fuel and energy sources are a major component of the global community, which will certainly continue into the future, so their continual monitoring and analysis is essential. The demand for energy will need to keep pace ensuring worldwide growth and expansion. There are several research evaluations that have shown, with continued growth of the world population, that within a few decades, the current petroleum industry and supply chain will not be able to meet the projected demands.[1,2] There is significant current research focused on the development of alternative fuel supplies, including biofuels which, considering bioproduction, have minimum influx of CO_2 into the environment,[3,4] to satisfy the projected shortfall of fuel supplies.

A key to moving forward in meeting these needs and developing new fuel types is to understand the combustion and combustion effluent chemistry of current fuels. Understanding fuel combustion is necessary in improving engine and combustion efficiency while simultaneously reducing emissions. A crucial component for successful analysis is in understanding the reaction mechanisms and kinetic pathways for all stable, radical, intermediate, and transition state species under realistic combustion conditions.

Linear and branched hydrocarbon alkanes are the most fundamental structures in organic and hydrocarbon chemistry and are components in a majority of transportation fuels. Accurate analysis and modeling is not easy when typical fuels can be comprised of individual components up to complex mixtures of hundreds, in some cases even thousands, of species. Atmospheric and combustion reactions can create hundreds more

intermediate species which further increases the difficulty. Modeling requires thermochemical properties for all of these species to understand their role within the reaction system and for calculating rate constant expressions.

Surrogate fuels represent the physical and chemical properties of a desired fuel by incorporating only a limited number of representative species from chemical classes such as alkanes, cycloalkanes, alkenes, and aromatics. Progress in modeling surrogate fuels, including the chemical kinetic models of species such as *n*-heptane,[5-14] has allowed for creation of reaction mechanisms under combustion system conditions. *n*-Heptane is also a primary reference fuel for the octane and cetane scales and is used as an auto ignition diesel surrogate due to similarities in cetane rating. Although *n*-heptane and its carbon-centered radicals are involved in several chemical systems, their thermochemical properties are not readily available.

Ketones are another major class of organic compounds which play important roles in atmospheric chemistry and as intermediates in combustion processes. They are also used as fuel tracers for monitoring fuel properties[15-17] and as fuel additives in reducing soot emissions.[18,19] Detailed chemical kinetic models for hydrocarbon combustion exist, but there are far less studies focusing on ketones.

Experimental studies have looked at the influence that acetone and acetyl radical have on the chemistry of ozone production in the earth's atmosphere. Hydrogen abstractions by hydroxyl radicals and photolysis are important atmospheric loss processed for ketones which is partially controlled by carbon-hydrogen bond dissociation energies (C–H BDEs).[20-22] Comprehensive studies on C–H BDEs of ketones, especially

for the carbons adjacent to the carbonyl group which affect both unimolecular dissociation and abstraction kinetics, are not available.

Fuels including the high-energy density military propellant fuel JP-10 can also contain more complex hydrocarbons such as *exo*-tricyclo[5.2.1.$0^{2,6}$]decane (TCD). TCD is the principal component of JP-10 and an excellent candidate for use as a missile fuel with its three cyclic rings and multiple strained carbon sites allowing for efficient energy storage and high thermal stability. The size and intricacy of the compound makes analysis of the unimolecular decomposition difficult, as seen in the wide range of initial products for pyrolysis, combustion, and cracking of TCD by several research groups.[23-33]

No experimental or calculated BDEs for TCD are available which are of interest due to the high strain in the molecule. Cyclic and linear hydrocarbon carbon-carbon (C–C) bonds are approximately 10 kcal mol^{-1} weaker than C–H bonds. Diradical and carbene formation from C–C bond dissociation in ring systems allow release of strain energy resulting in lower energy species which can quickly undergo further reactions. C–C bond cleavage is also important in initiation during combustion and pyrolysis. There is a higher entropy gain in cleavage of these bonds, compared to C–H bonds, resulting in faster cleavage at high temperatures. C–H bond energies aid in abstraction reaction analysis from a pool of several radical species for calculation of rate constants. Abstraction locations aid in determining which sites are more prone for initial reaction pathways. Calculation of these properties would allow for TCD to serve as a model for larger complex hydrocarbons.

Global concerns for the development of new fuels hinges on the availability of the fuel sources and their scalability. Economic and environmental concerns also need to be

addressed before large scale production can be implemented. Biofuels are of high value as future fuels due to their sustainability and regeneration reusing CO_2 from the atmosphere.[34-36]

Biofuel sources, such as lignocellulosic biomass, are broken down into valuable smaller carbon- and oxygen-containing compounds. Biomass conversion processes attempt to utilize all of the available carbon while minimizing chemical energy loss ensuring the integrity and usefulness of the fuels.[37] Understanding the thermochemistry and reaction kinetics controlling biomass breakdown are necessary for the modeling and design of the processing, product selectivity, energy efficiency, and carbon recycling.[38]

One of the versatile compounds created during biomass processing is 5-hydroxymethylfurfural which can be converted into organic acids, aldehydes, alcohols, amines, ethers, and substituted furans.[39-43] Experimental information is lacking for the thermochemistry of high-energy furan-based compounds, including methyl and methoxyfurans, which are shown to have possible biofuel application.[1,37,44] Simmie and Curran[45] determined that furan and methylfuran ring C–H BDEs are in excess of 120 kcal mol^{-1} with lower energies in the methyl substituents. Aromaticity and the oxygen atom's location within the cyclic structure creates these extremely strong C–H bonds. A large chemical activation energy could then be created for the initial adduct formed from the association of these furan radicals with O_2. Thermochemical properties for methyl, methoxy, hydroperoxide and alcohol substituted furans will allow for analysis of key intermediates formed in furan oxidation reactions.

The objective of this dissertation is to apply well-known density functional theory and composite computational methods to calculate thermochemical properties and

kinetics of hydrocarbons, oxygenates, cyclic alkanes, and furans which are not readily available. Calculating accurate and reliable thermochemical properties, including enthalpies of formation ($\Delta H^{\circ}_{f\ 298}$), entropies ($S(T)$), heat capacities ($C_p(T)$), and bond dissociation energies (BDEs), will aid in the creation of chemical kinetic models while serving as representative species for larger related compounds. Calculated values are compared to experimental data, where available, or to high level calculations to gauge their accuracy and thus justifying their use. Groups are developed for use in the group additivity (GA) and hydrogen-bond increment (HBI) methods allowing for the rapid estimation of thermochemical properties. Chemical activation reactions of 2-methylfuran radical and O_2 including important product formation and reaction pathways including abstractions, group transfers, dissociations, and radical peroxy oxygen additions are explored. Temperature- and pressure-dependent rate constants are calculated using quantum Rice-Ramsperger-Kassel analysis and master equation for falloff and stabilization.

CHAPTER 2

COMPUTATIONAL METHODS

2.1 Background

Electronic structure theory, based on the laws of motion for microscopic particles from quantum mechanics, is used to determine the energy of a species using different approximations to solve the Schrödinger equation. This energy, along with several other calculated properties from statistical mechanics, allows for the determination of key fundamental thermochemical properties which are vital due to their influence on reaction mechanisms and in creating detailed chemical kinetic models.

The Schrödinger equation can be represented as,

$$\mathrm{H}\Psi = \mathrm{E}\Psi \tag{2.1}$$

where H is the Hamiltonian operator composed of kinetic and potential energy terms, Ψ, is the wave function, a set of solutions of the Hamiltonian, describing the positions of the electrons and nuclei, and E is the energy of the system, an eigenvalue of the eigenfunction Ψ. The wave function describes the state of the system which is a function of the particles' coordinates (x) and time (t), giving the relationship $\Psi=\Psi(x,t)$ for a one-particle, one-dimension system. This is used to define an equation which describes the system and how the wave function changes with time,

$$-\frac{\hbar}{i}\frac{\partial\Psi(x,t)}{\partial t} = -\frac{\hbar^2}{2m}\frac{\partial^2\Psi(x,t)}{\partial x^2} + V(x,t)\Psi(x,t) \tag{2.2}$$

where ħ is Planck's constant divided by 2π, i is $\sqrt{-1}$, m is the mass of the particle, and $V(x,t)$ is the potential energy of the system. Specific positions of the coordinates cannot be determined with certainty, but the probability density,

$$\left|\Psi(x,t)\right|^2$$

can be used to find the probability,

$$\left|\Psi(x,t)\right|^2 dx$$

of locating the particle within a specific region between x and $x + dx$ at a certain time.

A simplifying approximation can be made using a stationary state where a time-independent potential energy exists. Solutions of equation 2.2 can be found which satisfy,

$$\Psi(x,t) = f(t)\psi(x) \tag{2.3}$$

where $f(t)$ is a function of time and ψ is a function of just position. The system can then exist in a number of fixed energy stationary states where the wave function satisfies,

$$\Psi(x,t) = e^{\frac{-iEt}{\hbar}}\psi(x) \tag{2.4}$$

For the one-particle, one-dimensional case, the time-independent Schrödinger equation can then be written as,

$$-\frac{\hbar^2}{2m}\frac{d^2\psi(x)}{dx^2} + V(x)\psi(x) = E\psi(x) \tag{2.5}$$

where the left-hand side of the equation can be rearranged into an operator expression, denoted by brackets, which transforms a function into another function as,

$$\left[-\frac{\hbar^2}{2m}\frac{d^2}{dx^2} + V(x) \right] \psi(x) = E\psi(x) \tag{2.6}$$

This equation implies that an allowed energy value can be determined from an energy operator operating on the wave function. The Hamiltonian operator, $\hat{H}$, is the energy operator representing the total energy from the potential, $\hat{V}$, and kinetic, $\hat{T}$, energy operators as,

$$\hat{H} = \hat{T} + \hat{V} = -\frac{\hbar^2}{2m}\frac{d^2}{dx^2} + V(x) \tag{2.7}$$

The Hamiltonian can also be written to include *n* particles where each particle *i* has mass m_i and coordinates (x_i,y_i,z_i),

$$\hat{H} = -\sum_{i=1}^{n} \frac{\hbar^2}{2m_i}\nabla_i^2 + V(x_1,...,z_n) \tag{2.8}$$

where ∇^2 is the Laplacian operator defined as,

$$\nabla_i^2 = \frac{\partial^2}{\partial x_i^2} + \frac{\partial^2}{\partial y_i^2} + \frac{\partial^2}{\partial z_i^2} \tag{2.9}$$

The time-independent Schrödinger equation in equation 2.6 can then be written as,

$$\left[-\sum_{i=1}^{n}\frac{\hbar^2}{2m_i}\nabla_i^2+V(x_1,...,z_n)\right]\psi=E\psi \tag{2.10}$$

where the time-independent wave function incorporates each of the coordinates from the *n* particles as,

$$\psi=\psi(x_1,y_1,z_1,...x_n,y_n,z_n) \tag{2.11}$$

The Born-Oppenheimer approximation can also be applied allowing for the separation of the nuclear and electronic motions. The mass of an electron is so tiny compared to the nuclei that electrons appear to be moving through a system of fixed position nuclei. Electrons will assume an optimal distribution representing the lowest energy, ground state, based on the arrangement of the nuclei. This approximation creates two independent problems and reducing the complexity of the solution to the Schrödinger equation. The Hamiltonian operator in equation 2.8 involving interactions of numerous electrons and nuclei can then be represented as,

$$\hat{H}=T_N+T_E+V_{NE}+V_{EE}+V_{NN} \tag{2.12}$$

which includes, the kinetic energy operators of the nuclei (T_N) and electrons (T_E) and the potential energy operators of the repulsions between the nuclei (V_{NN}), attractions between the electrons and nuclei (V_{NE}), and the repulsions from the electrons (V_{EE}).

Solving the Schrödinger equation at this point is still a formidable task. For *n* electrons, there are 3*n* degrees of freedom and *n* spin coordinates resulting in having to calculate many electronic wave functions while simultaneously considering the repulsions from the other electrons. Different methods, or levels of theory, will utilize further approximations affecting both the accuracy and computational cost, including time and computer resources. These further approximations depend on the calculation method and can be broadly categorized as semi-empirical, *ab initio*, and density functional theory.

The first two calculation types are based on molecular orbital theory where the lower energy orbitals are occupied with electrons before the higher energy orbitals. Semi-empirical methods are the most basic quantum mechanical methods and require minimal computational resources. Approximate solutions to the Schrödinger equation are calculated using a simpler Hamiltonian with parameters fit to experimental data. Higher level calculations are currently available, but semi-empirical methods are still practical for the analysis of very large species.

The second type, *ab initio*, are more resource demanding and use mathematical representations of orbitals from linear combinations of basis functions, called a basis set, which constrain electrons into specific orbitals. These approximated orbitals are centered on the nucleus of an atom and range in size. Larger basis sets allow for a more accurate representation of the orbitals by decreasing the restrictions on the electrons, but this comes with a computational cost. These calculations do not incorporate empirical parameters and vary in the degrees of treating instantaneous electron-electron interaction, known as the electron correlation energy. Hartree-Fock (HF) is the simplest *ab initio*

method which calculates a wave function based on an average repulsion between the electrons instead of the instantaneous interaction. This limitation in HF decreases its accuracy, but serves as a starting point for other methods. Higher level methods such as configuration interaction, perturbation theory, and coupled cluster theory, referred to as post-HF, improve on the HF wave function but have higher computational costs to accompany the increase in accuracy.

The final calculation method, density functional theory (DFT), does not calculate molecular wave functions. Basis sets are used to determine the electron probability density and then a functional calculates the electronic energy including electron correlation. Hohenberg and Kohn put forth two mathematical theorems which serve as the basis for DFT. The first theorem proved that the ground state electronic energy, E_0, from the Schrödinger equation is a unique functional of the ground state electron probability density, $\rho_0(x, y, z)$, which relies only on three variables. The Hohenberg-Kohn variational theorem then shows that the minimal energy functional corresponds to the true ground state electron density.

The Kohn-Sham (KS) method serves as a blueprint to solve the Hohenberg-Kohn theorem by finding ρ_0 and then E_0 from a set of the KS equations which, in theory, can determine the exact solution. Approximations are still required because the functional describing the exchange and correlation treatment of the electron interaction and repulsion energies is unknown.

2.2 Density Functional Theory Methods

The steady development of more efficient and accurate functionals has allowed DFT calculations for chemical properties in a variety of fields. Analysis of larger molecules is

possible with DFT due to its lower calculation time and computational costs while providing equivalent accuracy compared to other calculation methods. DFT is the primary tool for the analysis of species in this dissertation while use of *ab initio* calculations is primarily restricted to their use in composite methods.

One of the most widely used DFT methods is B3LYP which combines the three-parameter Becke exchange functional, B3[46], with Lee-Yang-Parr correlation functional, LYP.[47] B3LYP is one of the most frequently used and reliable DFT methods available.[48] Curtiss et al.[49] reported that it has the smallest average absolute deviation, 3.11 kcal mol^{-1}, of the seven DFT methods studied using the G2 test set of molecules. For the analysis of certain species, other DFT methods including BB1K,[50] MPWB1K,[51] BMK,[52] *w*B97X-D,[53,54] and M06-2X[55,56] are used.

Molecular orbitals are represented using linear combinations of basis functions, which are commonly the resource efficient Gaussian Type Orbtials (GTO). Pople basis sets, including the split-valence double zeta basis set 6-31G(d,p), are selected for analysis of the species. This basis set is of moderate size and provides a good combination between accuracy and computational resources. Six primitives for each core atomic orbital basis functions and used with two basis functions for the valence shells, where one is composed of three primitives and the other only one primitive. Five d-type and three p-type polarization functions are added to the non-hydrogen and hydrogen species, respectively, adding additional orbital space for the electron. A larger split-valence triple-zeta 6-311G(2d,2p) basis set is also utilized and serves as a comparison to 6-31G(d,p). This basis set includes an additional basis function for the valence shells and an

additional two sets of d-type and p-type polarization functions to the non-hydrogen and hydrogen species, respectively.

2.3 Composite Methods

A tradeoff between accuracy and computational resources always exists. To attain the most accurate calculations, high level methods using large basis sets are necessary, but often the size of the molecular system makes applications of such methods difficult if not impossible.

The development of composite, or compound, methods has allowed for high level calculations to be performed on large chemical systems while producing values within standard chemical accuracy of 1 kcal mol^{-1}. Composite methods use predetermined procedures of combining results from multiple levels of theory to mimic much higher, and more expensive, calculations while running in significantly less time. These methods are continually modified for improved accuracy and efficiency to help offset the high computational cost and resource demands of these methods.

The composite method G3MP2B3[57,58] is a modified version of G3MP2[59] with geometries and zero-point vibrational energies (ZPVE), scaled by 0.96, from a B3LYP/6-31G(d) calculation. This method has an improved average absolute deviation of 1.25 kcal $mol^{-1}$from the G2/97 test set as compared to G3MP2[57] where the geometries are from MP2(FU)/6-31G(d) with the scaled ZPVE from HF/6-31G(d). Single point energies are calculated using frozen core approximations (FC) in QCISD(T,FC)/6-31G(d) followed by a MP2(FC)/G3MP2large calculation. The G3MP2large basis set is a modified version of the 6-311+G(3df,2p) with diffuse function on hydrogens and 2df polarization functions on the second row atoms, Li-Ne. Spin-orbit corrections are

included for atomic species from a combination of experimental and theoretical values. Higher level corrections which compensate for remaining deficiencies are incorporated in the energy calculation.

Another commonly utilized composite method is the complete basis set method CBS-QB3[60,61] from Petersson and coworkers where energies from several calculations are extrapolated to the complete basis set limit. A mean absolute deviation of 1.10 kcal mol^{-1} from the G2/97 test set for CBS-QB3 has been calculated[61] which is similar to G3MP2B3. Geometries and frequencies are determined from the B3LYP/6-311G(2d,d,p) level with ZPVE, scaled by 0.99 and single point energy calculations at the CCSD(T)/6-31+G(d'), MP4SDQ/CBSB4, and MP2/CBSB3 levels. The complete basis set is extrapolated with corrections for spin contamination to calculate the final energy.

2.4 Calculated Thermochemical Properties

Calculation of thermochemical properties for each species is outlined in the following sections.

2.4.1 Initial Species Parameters

Species are initially optimized using the B3LYP/6-31G(d,p) method[46,47] as implemented in the Gaussian 03[62] and Gaussian 09[63] program suites. In certain situations where B3LYP is not able to converge on an appropriate geometry, other calculation types such as the semi-empirical PM3[64,65] or the *ab initio* MP2[66-70] methods are used. Vibrational frequencies are examined to verify stable, all positive frequencies, and transition state, one negative frequency, species.

Potential energy curves for single bond internal rotations are calculated at 10° intervals while the rest of the species is allowed to relax. The curves verify the converged optimized species is in the lowest energy conformation. If a lower energy conformation is found, this geometry is optimized and potential energy curves are calculated again. The potential energy barriers from these curves are also utilized to determine entropy and heat capacity contributions from internal rotations.

2.4.2 Enthalpy

DFT methods are popular in this type of analysis due to their lower computation costs, but their accuracy is not as high compared to the results of composite methods.[71-74] Errors, which may seem insignificant in small molecule systems, compound as the size of the molecule increases. To improve the accuracy in the enthalpy calculations, it is common to implement different work reactions which conserves mass balance, hybridization, and bond type for the reactants and products. Work reactions allow for significant systematic method error cancellation due to similar chemical environments on both sides of the reaction. This allows lower level and less computationally demanding methods, such as DFT, to be used without sacrificing accuracy.[73]

Isodesmic work reactions are used to calculate $\Delta H^{\circ}_{f\ 298}$ for all species which incorporate molecules with similar bonding and atomic arrangement on both sides of the reaction. Total enthalpies, including zero-point vibrational and thermal corrections, for the optimized products and reactants are calculated at different levels of theory. The enthalpy change for each reaction, $\Delta H^{\circ}_{rxn\ 298}$, is then calculated using Hess's Law in equation 2.13. Combining $\Delta H^{\circ}_{rxn\ 298}$ with literature enthalpies of formation values,

Lit $\Delta H^{\circ}_{f\,298}$, of the known products and reactants results in a $\Delta H^{\circ}_{f\,298}$ for the target species in equation 2.14. An example calculation is provided in Appendix A.

$$\Delta H^{o}_{rxn\ 298} = \sum(\text{Total Enthalpy of Products}) - \sum(\text{Total Enthalpy of Reactants}) \tag{2.13}$$

$$\Delta H^{o}_{rxn\ 298} = \sum(\text{Lit } \Delta H^{o}_{f\,298}\ \text{Products}) - \sum(\text{Lit } \Delta H^{o}_{f\,298}\ \text{Reactants} + \Delta H^{o}_{f\,298}\ \text{Target Species}) \tag{2.14}$$

Comparison of the DFT values to experimental data or higher level composite methods, which provide more accurate thermochemical properties,[58,73,75] allows for comparison and gauging the accuracy of the work reaction method using DFT calculations.

Enthalpy calculations for species where either convergence was unsuccessful or an unacceptable geometry was determined, are calculated using single point energies. In these cases, an acceptable optimized geometry is used and the energy is calculated using another method without optimization. Single point energies are common when geometry optimization using a high level or resource demanding method is not feasible. For example, single point energies are used for diradicals and carbenes of TCD, a large ten carbon polycyclic hydrocarbon, where optimization with high level calculation methods is difficult. The coupled cluster method with single, double, and perturbative triple excitation calculations, CCSD(T),[76-82] one of the highest level calculations available, is used for single point energies based on optimized B3LYP/6-31G(d,p) geometries.

2.4.3 Bond Dissociation Energy

Bond dissociation energies (BDE) are important to determine initial reaction pathways and kinetics. The stability of the radical determines the relative energy needed to cleave a carbon-hydrogen or a carbon-carbon bond in beta scission reactions in hydrocarbons, for example. Lower bond energies are more susceptible to hydrogen abstraction by radical species.

BDEs for the species in this study include carbon-hydrogen (C–H), oxygen-hydrogen (O–H), carbon-carbon (C–C), and oxygen-oxygen (O–O) bonds. For the homo and heteroatomic bonds, C–H, O–H, and O–O, a bond cleavage reaction with the calculated $\Delta H^{\circ}_{f\,298}$ values is utilized. For example, the bond cleavage reaction used to calculate C–H or O–H BDEs is the difference in the calculated $\Delta H^{\circ}_{f\,298}$ for the parent compound (R–H) and the corresponding radical (R•) plus hydrogen atom (H•),

$$\text{R–H} \quad \rightarrow \quad \text{R•} + \text{H•}$$

A sample calculation is provided in Appendix A. In the case of the O–O BDE calculation, the bond is in a hydroperoxide group, so a hydroxyl radical is formed and a similar bond cleavage reaction is used,

$$\text{RO–OH} \quad \rightarrow \quad \text{RO•} + \text{OH•}$$

Established literature values of 52.10 kcal mol^{-1} for a hydrogen atom[83] and 8.89 kcal mol^{-1} for a hydroxyl radical[84] are used in these calculations.

The calculated C–C BDEs are in polycyclic hydrocarbons corresponds to ring opening and does not generate two separate species. For these calculations, the difference between the $\Delta H^{\circ}_{f\,298}$ values for the parent and radical is used to determine the C–C BDE.

2.4.4 Entropy and Heat Capacity

Entropy (*S(T)*) and heat capacity ($C_p(T)$) calculations utilize the simple rigid-rotor harmonic-oscillator (HO) to describe the 3*n*-6 vibrations for non-linear species. It is well-known that there are accuracy issues in determining the lower frequency torsions corresponding to internal rotations using this approximation. Replacing these frequencies with methods to treat the internal rotations as hindered rotors increases the accuracy for *S(T)* and $C_p(T)$.

The initial research of Pitzer and Gwinn[85-87] addressed contributions from symmetrical and unsymmetrical rotating groups on a rigid frame. Later, work by Kilpatrick and Pitzer[88] was expanded to include balanced and unbalanced linked rotating groups. These studies still serve as a basis for current research and development for new methods for treating internal rotations.

Determining which low range frequency corresponds to a given bond rotation can often times be challenging and is characteristic of large molecules containing multiple rotating species. Coupling can also occur between various rotations or other types of motion which increases the difficulty in properly accounting for rotational contributions. A number of studies utilizing different techniques for handling coupled and uncoupled internal rotors contributions have been reported.[89-96] Although more advanced methods addressing coupled internal rotators are available, basic treatment of internal rotations as uncoupled rotations provides improved accuracy over the HO approximation alone.[90,93,97]

The HO approximation from translations, vibrations, and external rotation contributions to entropy and heat capacity are determined using the Statistical Mechanics for Heat Capacity and Entropy (SMCPS) program.[98] The program uses the geometry, frequencies, and moments of inertia from the optimized methods calculation for the structure along with the mass, electronic degeneracy, symmetry, and number of optical isomers for the species. ZPVEs are scaled as recommended by Scott and Radom.[99] Vibrations corresponding to torsion frequencies are removed and treated using a hindered rotor model. Internal rotation contributions are then added to the SMCPS values.

The equations for entropy and heat capacity used in SMCPS come from standard statistical mechanics allowing for macroscopic thermochemical properties to be calculated based on molecular energies from electronic structure calculations. These equations are summed from the individual contributions where entropy is calculated as,

$$S(T) = S_{Trans} + S_{Rot} + S_{Vib} + S_{Elec} + S_{OI} + S_{Sym} \tag{2.15}$$

$$S_{Trans} = 37.0 + \frac{3}{2}R\ln\left(\frac{m}{40}\right) + \frac{3}{2}R\ln\left(\frac{T}{298}\right)$$

$$S_{Rot} = 11.5 + \frac{R}{2}\ln\left(\frac{I_m{}^3}{\sigma_e}\right) + \frac{3}{2}R\ln\left(\frac{T}{298}\right) \text{ (non-linear molecules)}$$

$$= 6.9 + R\ln\left(\frac{I}{\sigma_e}\right) + R\ln\left(\frac{T}{298}\right) \text{ (linear molecules)}$$

$$= 4.6 + R\ln\left(\frac{I_r{}^{1/2}}{\sigma_i}\right) + \frac{R}{2}\ln\left(\frac{T}{298}\right) \text{ (one-dimensional, free rotor)}$$

$$S_{Vib} = R\sum_{K=1}^{3N-6}\left(\frac{h\nu_k / k_B T}{\left(e^{h\nu_k/k_B T} - 1\right)} - \ln\left(1 - e^{-h\nu_k/k_B T}\right)\right)$$

$$S_{Elec} = R\ln(sm)$$

$$S_{OI} = R\ln(n)$$

$$S_{Sym} = -R\ln(\sigma_e)$$

and heat capacity is calculated as,

$$C_p(T) = C_{Trans} + C_{Rot} + C_{Vib} + C_{Elec} + R \tag{2.16}$$

$$C_{Trans} = \frac{3}{2}R$$

$$C_{Rot} = \frac{3}{2}R \text{ (non-linear molecules)}$$

$$= R \text{ (linear molecules)}$$

$$= \frac{1}{2}R \text{ (one-dimensional, free rotor)}$$

$$C_{Vib} = R\sum_{k=1}^{3N-6}\left(\frac{h\nu_k / k_BT\ ^2 e^{h\nu_k/k_BT}}{e^{h\nu_k/k_BT}\ \text{-}1\ ^2}\right)$$

$$C_{Elec} = R\ln(sm)$$

Notation in equations 2.15 and 2.16 includes: molecular weight in amu (m), temperature in Kelvin (T), ideal gas constant (R), number of optical isomers (n), Planck's constant (h), vibrational frequency for the kth normal mode (ν_k), Boltzmann's constant (k_B), external symmetry number of the molecule (σ_e), symmetry of the internal rotation (σ_i), moment of inertia for a linear molecule about its center of mass (I), product of the three principle moments of inertia about its center of gravity (I_m^3), reduced moment of inertia for the internal rotation (I_r), and spin multiplicity (sm).

Internal rotation contributions are calculated using the Pitzer and Gwinn[85-87] approximation method as calculated in the VIBIR[100] code. This method is best suited for rotations where the potential energy as a function of the angle, $V(\phi)$, can be expressed as

$$V(\phi) = \sum_m \frac{1}{2}V_m\ \ 1 - \cos\sigma_m\phi_m \tag{2.17}$$

where V_m is the height of the potential barriers and σ_m is the foldness of the potential energy graphs for each bond rotation. Reduced moments of inertia are calculated based on the optimized geometries using the mass and radius of rotation for the rotational groups. There are no adjustments for coupling of internal rotor motion with vibration and VIBIR assumes that the rotational groups are symmetrical, which is accurate for primary and terminal methyl group rotation, for example. Other types of rotational barriers are also estimated using averages of the calculated barrier heights.

A second method for calculation of internal rotation contribution is the ROTATOR code.[101] This code uses the potential energy curves with expansion of the hindrance potential at discrete torsion angles in the truncated Fourier series,

$$V(\phi) = a_0 + \sum a_i \cos(i\phi) + \sum b_i \sin(i\phi), \quad \text{where } i = 1-7 \tag{2.18}$$

where a_o, a_i, and b_i provide the minima and maxima of the torsion potentials with allowance for a shift of the theoretical extreme angular positions. ROTATOR calculates the Hamiltonian matrix in the basis of wave functions of free internal rotor with subsequent calculation of energy levels by direct diagonalization. Direct summation over the energy levels allows for calculation of the partition function where the entropy and heat capacity contributions are found using standard statistical thermodynamics. By fitting to the actual potential energy graph of a rotational bond, ROTATOR can accurately describe both symmetrical and unsymmetrical group rotations.

2.4.5 Group Additivity

The group additivity (GA) method, as developed by Benson,[102] is a practical method for rapid estimation of thermochemical properties, particularly for larger compounds. The success of this empirical method is based on the accurate knowledge of the contributions of representative groups, obtained from smaller molecules, and their established linear consistency in thermochemical property contribution. Corrections for rotors, symmetry, electron degeneracy, optical isomers, and other interactions are also taken into account. The hydrogen-bond increment (HBI) method for group additivity[100] allows calculation of the thermochemical properties of radicals with only one additional group to that of the parent species. Thermodynamic properties including $\Delta H^{\circ}_{f\ 298}$, S°_{298}, and $C_p(T)$ can be approximated as the sum of the individual groups and used as a comparison for calculated values.[102-104] The GA and HBI methods are implemented using the Thermodynamic Property Estimation for Radicals and Molecules (THERM) code.[105,106]

Versatility of the GA and HBI methods allows for application to a wide range of compounds where thermochemical properties can be estimated for use in development of engineering and chemical kinetic modeling. Groups are constantly being developed for unique classes of compounds which are gaining attention. Possible biofuel compounds, for example, can be easily approximated and applied in models as the search for alternative fuel sources advance.

2.4.6 Kinetic Analysis

Canonical transition state theory (CTST), where a transition state maximum energy barrier connecting the reactants and products exists, is used to calculate high-pressure rate constants, k(T), in the 300-2000 K temperature range. Using the previously

calculated enthalpies, entropies, and heat capacities for the reactants and the transition state species, high-pressure rate constants are calculated,

$$k(T) = \frac{k_B T}{h} \exp\left(\frac{\Delta S^{\ddagger}}{R}\right) \exp\left(\frac{-\Delta H^{\ddagger}}{RT}\right) \left(\frac{RT}{P^0}\right)^{\Delta n^{\ddagger}} \tag{2.19}$$

where k_B is Boltzmann's constant, h is Planck's constant, T is temperature, P^0 is standard pressure, R is the ideal gas constant, and $\Delta S^{\ddagger}$, $\Delta H^{\ddagger}$, and $\Delta n^{\ddagger}$ are the changes in entropy, enthalpy, and the number of molecules between the reactant and transition state, respectively.

These high-pressure rate constants are fit using a nonlinear least-squares method to the modified form of the Arrhenius equation,

$$k(T) = AT^n \exp\left(\frac{-E_a}{RT}\right) \tag{2.20}$$

to determine the elementary rate parameters, A, n, and E_a. The program Thermkin is used in calculating both the high-pressure rate constants and the elementary rate parameters.

Variational transition state theory (VTST) is used in barrier-less, no transition state, situations common for radical and O_2 association. A scan of the bond length for the radical + O_2 adduct is completed by incrementing the length until a limit in the maximum energy is reached. High-pressure rate constants for each bond length position are then calculated, equation 2.19, for the 300-2000 K temperature range. The minimum rate constants at each temperature are fit to the modified Arrhenius equation, equation 2.20, to determine the elementary rate parameters.

Chemical activation bimolecular reactions involve the formation of an energized adduct containing a large excess of energy from the bond formation. The adduct can undergo unimolecular reactions, including isomerization, dissociation, including back to the original reactants, and deactivation through collisional stabilization. These reactions compete with both temperature- and pressure-dependence, but the energy dependence of the rate constant, *k*(E), must also be considered to correctly account for product distributions. Full descriptions of the models utilized for chemical activation and unimolecular dissociation is given by Sheng et al.[107]

Quantum Rice-Ramsperger-Kassel (QRRK) analysis is used for *k*(E) calculation based on statistical assumptions for the number of ways in which energy can be distributed among the vibrational degrees of freedom in a molecule. The proportion of energy located in a critical oscillator leading to a reaction allows for calculation of the rate constants. Although more accurate models exist, such as Rice-Ramsperger-Kassel-Marcus (RRKM), higher demands for specific details about the transition state species are necessary. With uncertainty and questionable accuracy of geometrical structure and modes of vibration in some of these transition state structures, QRRK provides acceptable analysis with fewer input parameters.

Bimolecular chemical activation reactions in this analysis can be schematically represented in Figure 2.1 where A_e^* is the entrance isomer activated complex formed from the initial reactants R and R' and A_e is the entrance isomer collisionally stabilized adduct. A_e^* can go to a products, back to reactants, or subsequent isomerizations, A_i^*, which can further dissociate to products, be collisionally stabilized to A_i, or reisomerize.

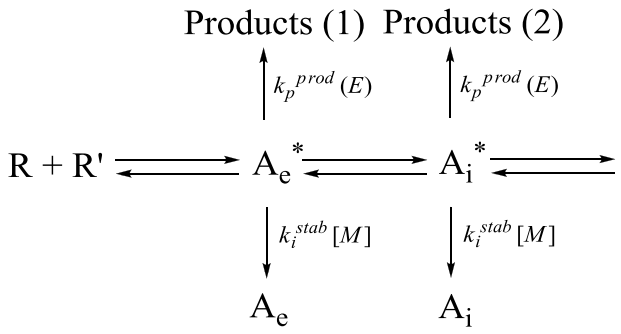

Figure 2.1 Schematic representation of chemical activation reactions.

Rate constants for chemical activations can be defined as a function of temperature, pressure, and collision parameters as,

$$\frac{d[A_i]}{dt} = [R][R']k_i^{stab}(T,P) \tag{2.21}$$

$$\frac{d[\text{Products}]}{dt} = [R][R']k_p^{prod}(T,P) \tag{2.22}$$

Overall rate constants to a given product channel can be determined from parameters in the master equation model by summing the dissociation differential rate constant, $d_{p,i}^q$, from isomer i to product p at energy q times the population vectors, n_i^q, which are functions of temperature, pressure, and collider molecule properties,

$$k_p^{prod}(T,P) = \sum_q d_{p,i}^q n_i^q \tag{2.23}$$

Rate constants for formation of a stabilized adduct are calculated from the product of the population, n_i^r, frequency of collisions between the adduct and the bath gas, ω, using the standard Lennard-Jones model, and the probability matrix representing the fraction of deactivating collisions resulting in a change from energy level *r* to *q* (where $q_{\min}^i$ is the lowest activated energy level) of isomer *i*, P_i^{qr},

$$k_i^{stab}(T,P) = \omega \sum_r \left(1 - \sum_{q>q_{\min}^i} P_i^{qr} \right) n_i^r \tag{2.24}$$

Although substantial information is generated from the rate constants from chemical activation analysis, additional dissociation analysis is necessary to completely build chemical kinetic models. Dissociation reactions are schematically represented as,

$$A_e \xrightarrow{k_p^{prod}} \text{Products (1)}$$

$$\xrightarrow{k_p^{prod}} \text{Products (2)}$$

where isomers are treated as irreversible product channels, immediately stabilized, with no distinction made for the activated and stabilized adducts. With this simplification, product channels, including isomers, are defined as,

$$\frac{d[\text{Products}]}{dt} = [A_i] k_p^{prod}(T,P) \tag{2.25}$$

Rate constants can be determined from parameters in the master equation model by summing, over all energy levels *q*, the product of the differential rate constant, $d_{p,i}^{q}$, and the normalized population distribution function, g_i^q,

$$k_p^{prod} = \frac{\sum_q d_{p,i}^{q} g_i^q}{\sum_q g_i^q} \tag{2.26}$$

These calculations for the temperature- and pressure-dependent rate constants are implemented in the CHEMASTER code[107] which uses a multifrequency QRRK analysis for *k*(E) with master equation for falloff and stabilization. The steady-state assumption is applied to the energized adduct(s) where both forward and reverse reaction paths are calculated while formation of adjacent products is not reversible. Chemical activation analysis includes all products, but dissociation analysis only considers immediate reactions from the well species. Further reaction needs to be considered separately.

CHEMASTER input includes temperature and pressure ranges of interest, mass of the species, the previously calculated elementary rate parameters from the high pressure rate constants, Lennard-Jones transport parameters of collisional diameter and well depth for the collider molecule, the third body bath gas, and reactants, and a reduced set of three representative vibrations and their degeneracies. These vibrations are from the full set of 3*n*-6 vibrations and reproduce heat capacity including one external rotation which can be used for estimation of the molecular density of states.[108] The average energy removed, on a per collision basis from the adduct, and the energy grid integration interval with corresponding maximum energy level for the adduct are also included in the input.

CHAPTER 3

THERMOCHEMISTRY AND BOND DISSOCIATION ENERGIES OF C_7H_{16} ISOMERS

3.1 Overview

Hydrocarbon alkanes are one of the most fundamental structures in chemistry and are at the center of a wide range of chemical systems inclusive of energy production. The presence of methane and small hydrocarbons in natural gas is the force behind major efforts on their geochemical formation and on methods to synthesize larger molecules and for advancing natural gas exploration and development.[109,110]

Linear and branched hydrocarbons are components in the vast majority of transportation fuels. The analysis of fuel combustion is crucial for improving engine and combustion efficiency while reducing emission. This requires understanding the reaction mechanisms and kinetic pathways of existing fuels under various reaction conditions of realistic combustion systems.

This is not easily accomplished because jet fuel, diesel fuel, and gasoline contain complex mixtures of hundreds, in some cases even thousands, of species which quickly raises the difficulty of accurate modeling the oxidation reaction systems. To combat this, surrogate fuels are utilized to represent the physical and chemical properties of the desired fuel by incorporating only a handful of species from representative chemical classes such as alkanes, cycloalkanes, alkenes, and aromatics. Over the years, there has been significant progress in the development, experimentation, and modeling of diesel surrogate fuels.[111] This is due in part to the progress that has been made in the chemical

kinetic models of the representative species used in surrogate fuels, with a particular interest in *n*-heptane[5-14] because it is cetane rated at 100.

Stability, thermochemical properties, and chemical kinetics of alkane parent and radical species are important to understanding their overall reaction paths and mechanisms in combustion processes and atmospheric chemistry. These properties strongly influence their roles in these systems where having accurate and reliable values would offer improvement in understanding and developing reaction paths and detailed chemical kinetic models.

Modeling work for rate constant expressions are dependent upon knowing thermochemical properties such as enthalpies, entropies, and heat capacities for all of the reacting species. The group additivity (GA) method, as developed by Benson,[102] allows for the rapid estimation of thermochemical properties based on the accurate knowledge of the contributions of representative groups from smaller molecules and their established linear consistency in thermochemical property contribution. This method is commonly implemented to estimate properties for species that are not well known.[5,9,112-114]

Although C_7 alkanes and their radicals are involved in a variety of different chemical systems, basic gas phase thermochemical properties are not readily available or experimental and theoretical values have discrepancies. There have been some studies on liquid and solid phases for linear and branched heptanes.[115,116]

By employing high level computational methods, a set of thermochemical properties for these species can be calculated which otherwise might be difficult to determine. There has been previous success using theoretical calculation methods in

determining key thermochemical properties for varying length linear and branched alkanes.[117-119]

This manuscript provides a set of thermochemical properties including enthalpies ($\Delta H^{\circ}_{f\,298}$), entropies ($S^{\circ}(T)$), and heat capacities ($C_p(T)$) along with primary, secondary, and tertiary C–H BDEs for three C_7H_{16} isomers, shown in Figure 3.1, and their corresponding carbon-centered radicals. Calculated $\Delta H^{\circ}_{f\,298}$ for parent species show good agreement compared to available literature values. Bond energies for radical formation are also determined from the parent and are compared to conventional normal primary, secondary, and tertiary bond energies from alkane hydrocarbons. Entropies and heat capacities for *n*-heptane, 2-methylhexane, and 2,3-dimethylpentane are calculated using different methods to account for internal rotation contributions and compared to available literature data. Entropies and heat capacities for their carbon-centered radicals are calculated using the methods that most accurately reproduce experimental data on the stable alkanes.

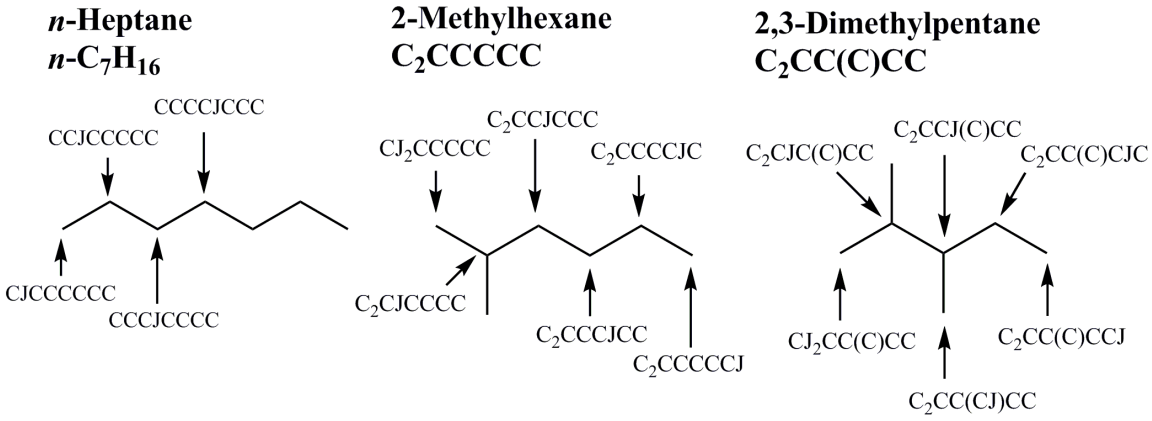

Figure 3.1 Nomenclature for C_7H_{16} parent and radical species.

3.2 Nomenclature

Abbreviations are utilized in this chapter as illustrated below:

- – represents a bond between two atoms,
- J represents a radical site on the preceding carbon atom,
- (C) represents a methyl substituent on the preceding carbon atom.

3.3 Computational Methods

Optimized geometries for all of the species are initially calculated at the B3LYP/6-31G(d,p) density function theory (DFT) method.[46,47] Potential energy curves, presented in Appendix B, for the internal rotation barriers are used to identify and to verify that the optimized structures are the lowest energy conformation.

Isodesmic work reactions are implemented for calculation of the enthalpies of formation ($\Delta H^{\circ}_{f\,298}$) using the B3LYP method with the 6-31G(d,p) and 6-311G(d,p) basis sets. Comparisons to the higher level composite methods G3MP2B3[57,58] and CBS-QB3[60,61] verify the accuracy and the use of the DFT method for these alkanes. Carbon-hydrogen bond dissociation energies (C–H BDE) are determined from the calculated $\Delta H^{\circ}_{f\,298}$ energies and the well-established literature value of 52.10 kcal mol^{-1} for a hydrogen atom.[83] All calculations are performed using the Gaussian 03 program suite.[62]

Several methods are used for the calculation of entropies and heat capacities for *n*-heptane, 2-methylhexane, 2,3-dimethylpentane beginning with the rigid-rotor harmonic-oscillator (HO) approximation as calculated by the Statistical Mechanics for Heat Capacity and Entropy (SMCPS[98]) program. Due to the error which exists with

applying the HO approximation to low frequency vibrational modes of internal rotations, these frequencies are removed and replaced with contributions from single bond hindered rotor analysis using the VIBIR[100] and ROTATOR[101] codes. These results are compared to available literature values and then the optimal method(s) are used to calculate entropy and heat capacity data for their carbon-centered radicals. The group additivity (GA) method, as developed by Benson,[102] serves as a comparison for the calculated parent $\Delta H^{\circ}_{f\,298}$, $S^{\circ}(T)$, and $C_p(T)$ values.

3.4 Results and Discussion

Isodesmic work reactions incorporate reference species that have well-established $\Delta H^{\circ}_{f\,298}$ values listed in Table 3.1. Each of the parent C_7H_{16} compounds are analyzed with four to five work reactions where the parent compound is reacted with a straight chain alkane yielding smaller linear and branched alkanes. The work reactions with the calculated $\Delta H^{\circ}_{f\ \ 298}$ for each species using the B3LYP/6-31G(d,p), B3LYP/6-311G(2d,2p), CBS-QB3, and G3MP2B3 methods are presented for the parent species in Table 3.2. The work reactions for the alkane radicals have the radical species reacted with a small hydrocarbon yielding the parent species plus a hydrocarbon radical. The work reactions and the calculated $\Delta H^{\circ}_{f\,298}$ for each radical species using the DFT and composite methods are presented in Table 3.3.

Properties for all species including optimized structure parameters, symmetry values, moments of inertia, vibrational frequencies, internal rotor potentials, entropies, and heat capacities are presented in Appendix B.

Table 3.1 Standard Enthalpies of Formation for Reference Species

Species	$\Delta H^{\circ}_{f\,298}$ (kcal mol^{-1})	Reference
H	52.10	83
CH_3CH_3	-20.0 ± 0.1	120
$CH_3CH_2CH_3$	-25.0 ± 0.1	120
$CH_3CH_2CH_2CH_3$	-30.0 ± 0.1	120
$(CH_3)_3CH$	-32.1 ± 0.1	120
n-C_5H_{12}	-35.1 ± 0.2	120
CC_2CC	-36.7 ± 0.2	120
n-C_6H_{14}	-39.9 ± 0.2	120
CC_2C_2C	-42.6 ± 0.2	120
CH_3CJH_2	29.0 ± 0.4	121
CH_3CJHCH_3	21.5 ± 0.4	121
$(CH_3)_3CJ$	12.3 ± 0.4	121
$CH_3CJHCH_2CH_3$	16.1 ± 0.5	121

Table 3.2 Isodesmic Work Reactions and Calculated $\Delta H^{\circ}_{f\,298}$ for C_7H_{16} Parent Species

Isodesmic Reactions							$\Delta H^{\circ}_{f\,298}$ (kcal mol^{-1})			
							B3LYP		CBS-QB3	G3MP2B3
							6-31G(d,p)	6-311G(2d,2p)		
n-C_7H_{16} System										
n-C_7H_{16}	+	CH_3CH_3	→	$CH_3CH_2CH_3$	+	n-C_6H_{14}	-44.77	-44.71	-44.97	-44.95
n-C_7H_{16}	+	CH_3CH_3	→	$CH_3CH_2CH_2CH_3$	+	n-C_5H_{12}	-44.95	-44.90	-45.22	-45.17
n-C_7H_{16}	+	$CH_3CH_2CH_3$	→	n-C_5H_{12}	+	n-C_5H_{12}	-45.14	-45.15	-45.23	-45.21
n-C_7H_{16}	+	$CH_3CH_2CH_3$	→	$CH_3CH_2CH_2CH_3$	+	n-C_6H_{14}	-44.81	-44.83	-44.88	-44.86
n-C_7H_{16}	+	$CH_3CH_2CH_2CH_3$	→	n-C_5H_{12}	+	n-C_6H_{14}	-44.96	-44.97	-44.99	-44.98
						Average	**-44.93**	**-44.91**	**-45.06**	**-45.03**
						Method Average	**-44.9**		**-45.0**	
C_2CCCCC System										
C_2CCCCC	+	CH_3CH_3	→	$(CH_3)_3CH$	+	n-C_5H_{12}	-46.09	-45.98	-46.88	-46.87
C_2CCCCC	+	$CH_3CH_2CH_3$	→	$(CH_3)_3CH$	+	n-C_6H_{14}	-45.95	-45.91	-46.53	-46.56
C_2CCCCC	+	CH_3CH_3	→	CC_2CC	+	$CH_3CH_2CH_2CH_3$	-46.50	-46.44	-46.88	-46.84
C_2CCCCC	+	$CH_3CH_2CH_3$	→	CC_2CC	+	n-C_5H_{12}	-46.69	-46.69	-46.89	-46.88
C_2CCCCC	+	$CH_3CH_2CH_2CH_3$	→	CC_2CC	+	n-C_6H_{14}	-46.51	-46.51	-46.65	-46.65
						Average	**-46.35**	**-46.31**	**-46.77**	**-46.76**
						Method Average	**-46.3**		**-46.8**	
$C_2CC(C)CC$ System										
$C_2CC(C)CC$	+	CH_3CH_3	→	CC_2C_2C	+	$CH_3CH_2CH_3$	-46.36	-46.23	-47.06	-47.05
$C_2CC(C)CC$	+	$CH_3CH_2CH_3$	→	CC_2C_2C	+	$CH_3CH_2CH_2CH_3$	-46.40	-46.34	-46.96	-46.96
$C_2CC(C)CC$	+	$CH_3CH_2CH_2CH_3$	→	CC_2C_2C	+	n-C_5H_{12}	-46.55	-46.48	-47.07	-47.08
$C_2CC(C)CC$	+	n-C_5H_{12}	→	CC_2C_2C	+	n-C_6H_{14}	-46.22	-46.16	-46.72	-46.73
						Average	**-46.38**	**-46.30**	**-46.95**	**-46.96**
						Method Average	**-46.3**		**-47.0**	

Table 3.3 Isodesmic Work Reactions, Calculated $\Delta H^{\circ}_{f\,298}$, and Bond Dissociation Energies for C_7H_{16} Radical Species

Isodesmic Reactions	$\Delta H^{\circ}_{f\,298}$ (kcal mol^{-1}) B3LYP 6-31G(d,p)	B3LYP 6-311G(2d,2p)	CBS-QB3	G3MP2B3
CJCCCCCC System				
CJCCCCCC + CH_3CH_3 → *n*-C_7H_{16} + CH_3CJH_2	4.15	4.09	4.19	4.23
CJCCCCCC + $CH_3CH_2CH_3$ → *n*-C_7H_{16} + CH_3CJHCH_3	5.55	5.39	4.44	4.05
CJCCCCCC + $(CH_3)_3CH$ → *n*-C_7H_{16} + $(CH_3)_3CJ$	6.54	6.22	4.07	3.32
CJCCCCCC + $CH_3CH_2CH_2CH_3$ → *n*-C_7H_{16} + $CH_3CJHCH_2CH_3$	4.92	4.86	3.82	3.40
Average	**5.29**	**5.14**	**4.13**	**3.75**
Method Average	**5.2**		**3.9**	
Bond Dissociation Energy	**102.4**	**102.3**	**101.3**	**100.9**
CCJCCCCC System				
CCJCCCCC + CH_3CH_3 → *n*-C_7H_{16} + CH_3CJH_2	0.18	0.21	1.36	1.82
CCJCCCCC + $CH_3CH_2CH_3$ → *n*-C_7H_{16} + CH_3CJHCH_3	1.58	1.51	1.62	1.64
CCJCCCCC + $(CH_3)_3CH$ → *n*-C_7H_{16} + $(CH_3)_3CJ$	2.56	2.34	1.24	0.90
CCJCCCCC + $CH_3CH_2CH_2CH_3$ → *n*-C_7H_{16} + $CH_3CJHCH_2CH_3$	0.95	0.98	0.99	0.99
Average	**1.32**	**1.26**	**1.30**	**1.34**
Method Average	**1.3**		**1.3**	
Bond Dissociation Energy	**98.5**	**98.4**	**98.5**	**98.5**
CCCJCCCC System				
CCCJCCCC + CH_3CH_3 → *n*-C_7H_{16} + CH_3CJH_2	0.39	0.33	1.57	2.07
CCCJCCCC + $CH_3CH_2CH_3$ → *n*-C_7H_{16} + CH_3CJHCH_3	1.80	1.63	1.82	1.89
CCCJCCCC + $(CH_3)_3CH$ → *n*-C_7H_{16} + $(CH_3)_3CJ$	2.78	2.46	1.45	1.15
CCCJCCCC + $CH_3CH_2CH_2CH_3$ → *n*-C_7H_{16} + $CH_3CJHCH_2CH_3$	1.17	1.10	1.20	1.24
Average	**1.53**	**1.38**	**1.51**	**1.59**
Method Average	**1.5**		**1.5**	
Bond Dissociation Energy	**98.7**	**98.5**	**98.7**	**98.7**

Table 3.3 Isodesmic Work Reactions, Calculated $\Delta H^{\circ}_{f\,298}$, and Bond Dissociation Energies for C_7H_{16} Radical Species (Continued A)

Isodesmic Reactions							$\Delta H^{\circ}_{f\,298}$ (kcal mol^{-1}) B3LYP 6-31G(d,p)	B3LYP 6-311G(2d,2p)	CBS-QB3	G3MP2B3
CCCCJCCC System										
CCCCJCCC	+	CH_3CH_3	→	*n*-C_7H_{16}	+	CH_3CJH_2	0.33	0.29	1.57	2.06
CCCCJCCC	+	$CH_3CH_2CH_3$	→	*n*-C_7H_{16}	+	CH_3CJHCH_3	1.73	1.59	1.82	1.88
CCCCJCCC	+	$(CH_3)_3CH$	→	*n*-C_7H_{16}	+	$(CH_3)_3CJ$	2.72	2.42	1.45	1.15
CCCCJCCC	+	$CH_3CH_2CH_2CH_3$	→	*n*-C_7H_{16}	+	$CH_3CJHCH_2CH_3$	1.10	1.06	1.20	1.23
						Average	**1.47**	**1.34**	**1.51**	**1.58**
						Method Average	**1.4**		**1.5**	
						Bond Dissociation Energy	**98.6**	**98.5**	**98.7**	**98.7**
CJ_2CCCCC System										
CJ_2CCCCC	+	CH_3CH_3	→	C_2CCCCC	+	CH_3CJH_2	2.36	2.32	2.72	2.90
CJ_2CCCCC	+	$CH_3CH_2CH_3$	→	C_2CCCCC	+	CH_3CJHCH_3	3.76	3.62	2.97	2.72
CJ_2CCCCC	+	$(CH_3)_3CH$	→	C_2CCCCC	+	$(CH_3)_3CJ$	4.75	4.45	2.60	1.98
CJ_2CCCCC	+	$CH_3CH_2CH_2CH_3$	→	C_2CCCCC	+	$CH_3CJHCH_2CH_3$	3.13	3.09	2.35	2.07
						Average	**3.50**	**3.37**	**2.66**	**2.42**
						Method Average	**3.4**		**2.5**	
						Bond Dissociation Energy	**102.4**	**102.2**	**101.5**	**101.3**
$C_2CJCCCC$ System										
$C_2CJCCCC$	+	CH_3CH_3	→	C_2CCCCC	+	CH_3CJH_2	-4.91	-4.62	-2.40	-1.52
$C_2CJCCCC$	+	$CH_3CH_2CH_3$	→	C_2CCCCC	+	CH_3CJHCH_3	-3.50	-3.32	-2.14	-1.70
$C_2CJCCCC$	+	$(CH_3)_3CH$	→	C_2CCCCC	+	$(CH_3)_3CJ$	-2.52	-2.49	-2.52	-2.44
$C_2CJCCCC$	+	$CH_3CH_2CH_2CH_3$	→	C_2CCCCC	+	$CH_3CJHCH_2CH_3$	-4.13	-3.85	-2.77	-2.35
						Average	**-3.76**	**-3.57**	**-2.46**	**-2.00**
						Method Average	**-3.7**		**-2.2**	
						Bond Dissociation Energy	**95.1**	**95.3**	**96.4**	**96.9**

Table 3.3 Isodesmic Work Reactions, Calculated $\Delta H^{\circ}_{f\,298}$, and Bond Dissociation Energies for C_7H_{16} Radical Species (Continued B)

Isodesmic Reactions							$\Delta H^{\circ}_{f\,298}$ (kcal mol^{-1}) B3LYP 6-31G(d,p)	B3LYP 6-311G(2d,2p)	CBS-QB3	G3MP2B3
$C_2CCJCCC$ System										
$C_2CCJCCC$	+	CH_3CH_3	→	C_2CCCCC	+	CH_3CJH_2	-1.45	-1.48	-0.01	0.55
$C_2CCJCCC$	+	$CH_3CH_2CH_3$	→	C_2CCCCC	+	CH_3CJHCH_3	-0.05	-0.18	0.25	0.38
$C_2CCJCCC$	+	$(CH_3)_3CH$	→	C_2CCCCC	+	$(CH_3)_3CJ$	0.94	0.65	-0.13	-0.36
$C_2CCJCCC$	+	$CH_3CH_2CH_2CH_3$	→	C_2CCCCC	+	$CH_3CJHCH_2CH_3$	-0.68	-0.70	-0.37	-0.27
						Average	**-0.31**	**-0.43**	**-0.06**	**0.08**
						Method Average	**-0.4**		**0.0**	
						Bond Dissociation Energy	**98.6**	**98.4**	**98.8**	**98.9**
$C_2CCCJCC$ System										
$C_2CCCJCC$	+	CH_3CH_3	→	C_2CCCCC	+	CH_3CJH_2	-2.04	-2.01	-0.57	-0.06
$C_2CCCJCC$	+	$CH_3CH_2CH_3$	→	C_2CCCCC	+	CH_3CJHCH_3	-0.63	-0.71	-0.32	-0.24
$C_2CCCJCC$	+	$(CH_3)_3CH$	→	C_2CCCCC	+	$(CH_3)_3CJ$	0.35	0.11	-0.69	-0.97
$C_2CCCJCC$	+	$CH_3CH_2CH_2CH_3$	→	C_2CCCCC	+	$CH_3CJHCH_2CH_3$	-1.26	-1.24	-0.94	-0.89
						Average	**-0.89**	**-0.96**	**-0.63**	**-0.54**
						Method Average	**-0.9**		**-0.6**	
						Bond Dissociation Energy	**98.0**	**97.9**	**98.2**	**98.3**
$C_2CCCCJC$ System										
$C_2CCCCJC$	+	CH_3CH_3	→	C_2CCCCC	+	CH_3CJH_2	-1.54	-1.50	-0.32	0.15
$C_2CCCCJC$	+	$CH_3CH_2CH_3$	→	C_2CCCCC	+	CH_3CJHCH_3	-0.13	-0.20	-0.07	-0.03
$C_2CCCCJC$	+	$(CH_3)_3CH$	→	C_2CCCCC	+	$(CH_3)_3CJ$	0.85	0.62	-0.44	-0.77
$C_2CCCCJC$	+	$CH_3CH_2CH_2CH_3$	→	C_2CCCCC	+	$CH_3CJHCH_2CH_3$	-0.76	-0.73	-0.69	-0.68
						Average	**-0.39**	**-0.45**	**-0.38**	**-0.33**
						Method Average	**-0.4**		**-0.4**	
						Bond Dissociation Energy	**98.5**	**98.4**	**98.5**	**98.5**

Table 3.3 Isodesmic Work Reactions, Calculated $\Delta H^{\circ}_{f\,298}$, and Bond Dissociation Energies for C_7H_{16} Radical Species (Continued C)

Isodesmic Reactions							$\Delta H^{\circ}_{f\,298}$ (kcal mol^{-1}) B3LYP 6-31G(d,p)	B3LYP 6-311G(2d,2p)	CBS-QB3	G3MP2B3
$C_2CCCCCJ$ System										
$C_2CCCCCJ$	+	CH_3CH_3	→	C_2CCCCC	+	CH_3CJH_2	2.44	2.38	2.50	2.56
$C_2CCCCCJ$	+	$CH_3CH_2CH_3$	→	C_2CCCCC	+	CH_3CJHCH_3	3.85	3.68	2.76	2.38
$C_2CCCCCJ$	+	$(CH_3)_3CH$	→	C_2CCCCC	+	$(CH_3)_3CJ$	4.83	4.50	2.38	1.64
$C_2CCCCCJ$	+	$CH_3CH_2CH_2CH_3$	→	C_2CCCCC	+	$CH_3CJHCH_2CH_3$	3.22	3.15	2.13	1.73
						Average	**3.59**	**3.43**	**2.44**	**2.08**
						Method Average	**3.5**		**2.3**	
						Bond Dissociation Energy	**102.5**	**102.3**	**101.3**	**100.9**
$CJ_2CC(C)CC$ System										
$CJ_2CC(C)CC$	+	CH_3CH_3	→	$C_2CC(C)CC$	+	CH_3CJH_2	1.53	1.51	1.83	1.95
$CJ_2CC(C)CC$	+	$CH_3CH_2CH_3$	→	$C_2CC(C)CC$	+	CH_3CJHCH_3	2.94	2.81	2.09	1.77
$CJ_2CC(C)CC$	+	$(CH_3)_3CH$	→	$C_2CC(C)CC$	+	$(CH_3)_3CJ$	3.92	3.64	1.71	1.04
$CJ_2CC(C)CC$	+	$CH_3CH_2CH_2CH_3$	→	$C_2CC(C)CC$	+	$CH_3CJHCH_2CH_3$	2.31	2.29	1.46	1.12
						Average	**2.68**	**2.56**	**1.77**	**1.47**
						Method Average	**2.6**		**1.6**	
						Bond Dissociation Energy	**101.7**	**101.6**	**100.8**	**100.5**
$C_2CJC(C)CC$ System										
$C_2CJC(C)CC$	+	CH_3CH_3	→	$C_2CC(C)CC$	+	CH_3CJH_2	-6.43	-6.20	-3.79	-2.84
$C_2CJC(C)CC$	+	$CH_3CH_2CH_3$	→	$C_2CC(C)CC$	+	CH_3CJHCH_3	-5.02	-4.90	-3.53	-3.02
$C_2CJC(C)CC$	+	$(CH_3)_3CH$	→	$C_2CC(C)CC$	+	$(CH_3)_3CJ$	-4.04	-4.07	-3.91	-3.75
$C_2CJC(C)CC$	+	$CH_3CH_2CH_2CH_3$	→	$C_2CC(C)CC$	+	$CH_3CJHCH_2CH_3$	-5.65	-5.42	-4.15	-3.67
						Average	**-5.28**	**-5.15**	**-3.85**	**-3.32**
						Method Average	**-5.2**		**-3.6**	
						Bond Dissociation Energy	**93.8**	**93.9**	**95.2**	**95.7**

Table 3.3 Isodesmic Work Reactions, Calculated $\Delta H^{\circ}_{f\,298}$, and Bond Dissociation Energies for C_7H_{16} Radical Species (Continued D)

Isodesmic Reactions							$\Delta H^{\circ}_{f\,298}$ (kcal mol^{-1}) B3LYP 6-31G(d,p)	B3LYP 6-311G(2d,2p)	CBS-QB3	G3MP2B3
$C_2CCJ(C)CC$ System										
$C_2CCJ(C)CC$	+	CH_3CH_3	→	$C_2CC(C)CC$	+	CH_3CJH_2	-5.62	-5.37	-2.85	-1.87
$C_2CCJ(C)CC$	+	$CH_3CH_2CH_3$	→	$C_2CC(C)CC$	+	CH_3CJHCH_3	-4.21	-4.07	-2.60	-2.05
$C_2CCJ(C)CC$	+	$(CH_3)_3CH$	→	$C_2CC(C)CC$	+	$(CH_3)_3CJ$	-3.23	-3.24	-2.97	-2.78
$C_2CCJ(C)CC$	+	$CH_3CH_2CH_2CH_3$	→	$C_2CC(C)CC$	+	$CH_3CJHCH_2CH_3$	-4.85	-4.60	-3.22	-2.70
						Average	**-4.48**	**-4.32**	**-2.91**	**-2.35**
						Method Average	**-4.4**		**-2.6**	
						Bond Dissociation Energy	**94.6**	**94.7**	**96.1**	**96.7**
$C_2CC(CJ)CC$ System										
$C_2CC(CJ)CC$	+	CH_3CH_3	→	$C_2CC(C)CC$	+	CH_3CJH_2	0.99	1.01	1.53	1.72
$C_2CC(CJ)CC$	+	$CH_3CH_2CH_3$	→	$C_2CC(C)CC$	+	CH_3CJHCH_3	2.40	2.31	1.78	1.54
$C_2CC(CJ)CC$	+	$(CH_3)_3CH$	→	$C_2CC(C)CC$	+	$(CH_3)_3CJ$	3.38	3.14	1.41	0.81
$C_2CC(CJ)CC$	+	$CH_3CH_2CH_2CH_3$	→	$C_2CC(C)CC$	+	$CH_3CJHCH_2CH_3$	1.77	1.78	1.16	0.89
						Average	**2.13**	**2.06**	**1.47**	**1.24**
						Method Average	**2.1**		**1.4**	
						Bond Dissociation Energy	**101.2**	**101.1**	**100.5**	**100.3**
$C_2CC(C)CJC$ System										
$C_2CC(C)CJC$	+	CH_3CH_3	→	$C_2CC(C)CC$	+	CH_3CJH_2	-3.08	-2.93	-1.44	-0.84
$C_2CC(C)CJC$	+	$CH_3CH_2CH_3$	→	$C_2CC(C)CC$	+	CH_3CJHCH_3	-1.68	-1.63	-1.18	-1.02
$C_2CC(C)CJC$	+	$(CH_3)_3CH$	→	$C_2CC(C)CC$	+	$(CH_3)_3CJ$	-0.69	-0.81	-1.55	-1.76
$C_2CC(C)CJC$	+	$CH_3CH_2CH_2CH_3$	→	$C_2CC(C)CC$	+	$CH_3CJHCH_2CH_3$	-2.31	-2.16	-1.80	-1.67
						Average	**-1.94**	**-1.88**	**-1.49**	**-1.32**
						Method Average	**-1.9**		**-1.4**	
						Bond Dissociation Energy	**97.1**	**97.2**	**97.6**	**97.7**

Table 3.3 Isodesmic Work Reactions, Calculated $\Delta H^{\circ}_{f\,298}$, and Bond Dissociation Energies for C_7H_{16} Radical Species (Continued E)

Isodesmic Reactions							$\Delta H^{\circ}_{f\,298}$ (kcal mol^{-1})			
							B3LYP		CBS-QB3	G3MP2B3
							6-31G(d,p)	6-311G(2d,2p)		
$C_2CC(C)CCJ$ System										
$C_2CC(C)CCJ$	+	CH_3CH_3	→	$C_2CC(C)CC$	+	CH_3CJH_2	1.34	1.33	1.56	1.67
$C_2CC(C)CCJ$	+	$CH_3CH_2CH_3$	→	$C_2CC(C)CC$	+	CH_3CJHCH_3	2.75	2.64	1.82	1.49
$C_2CC(C)CCJ$	+	$(CH_3)_3CH$	→	$C_2CC(C)CC$	+	$(CH_3)_3CJ$	3.73	3.46	1.44	0.76
$C_2CC(C)CCJ$	+	$CH_3CH_2CH_2CH_3$	→	$C_2CC(C)CC$	+	$CH_3CJHCH_2CH_3$	2.12	2.11	1.20	0.85
						Average	**2.48**	**2.38**	**1.50**	**1.19**
						Method Average	**2.4**		**1.3**	
						Bond Dissociation Energy	**101.5**	**101.4**	**100.6**	**100.2**

3.4.1 Heat of Formation $\Delta H^{\circ}_{f\,298}$

Tables 3.2 and 3.3 list the work reactions with a summary of the average $\Delta H^{\circ}_{f\,298}$ values from the DFT and the composite methods, CBS-QB3 and G3MP2B3, in Table 3.4. Overall from these values there is very good agreement for the $\Delta H^{\circ}_{f\,298}$ values between the DFT and composite which results from the use of the error cancelling work reactions. Error for the $\Delta H^{\circ}_{f\,298}$ values is reported as the standard deviation from the work reactions. These values coincide with the root-mean-square (rms) deviation of 0.73 kcal mol^{-1}, 95% confidence limit of 1.56 kcal mol^{-1}, between experimental and CBS-QB3 ΔH°_{rxn} values for fifteen straight and branched alkane reactions reported by Snitsiriwat and Bozzelli.[122]

Table 3.4 Summary of $\Delta H^{\circ}_{f\,298}$ and C–H Bond Dissociation Energies for C_7H_{16} Isomers[a]

Species	DFT		Composite	
	$\Delta H^{\circ}_{f\,298}$	C–H BDE	$\Delta H^{\circ}_{f\,298}$	C–H BDE
n-C_7H_{16}	-44.9 ± 0.1	-	-45.0 ± 0.1	-
CJCCCCCC	5.2 ± 0.9	102.4	3.9 ± 0.4	101.1
CCJCCCCC	1.3 ± 0.9	98.4	1.3 ± 0.3	98.5
CCCJCCCC	1.5 ± 0.9	98.6	1.5 ± 0.3	98.7
CCCCJCCC	1.4 ± 0.9	98.6	1.5 ± 0.3	98.7
C_2CCCCC	-46.3 ± 0.3	-	-46.8 ± 0.1	-
CJ_2CCCCC	3.4 ± 0.9	102.3	2.5 ± 0.4	101.4
C_2CJCCCC	-3.7 ± 0.9	95.2	-2.2 ± 0.4	96.6
C_2CCJCCC	-0.4 ± 0.9	98.5	0.0 ± 0.4	98.9
C_2CCCJCC	-0.9 ± 0.9	97.9	-0.6 ± 0.3	98.3
C_2CCCCJC	-0.4 ± 0.9	98.4	-0.4 ± 0.3	98.5
C_2CCCCCJ	3.5 ± 0.9	102.4	2.3 ± 0.4	101.1
C_2CC(C)CC	-46.3 ± 0.1	-	-47.0 ± 0.1	-
CJ_2CC(C)CC	2.6 ± 0.9	101.7	1.6 ± 0.4	100.7
C_2CJC(C)CC	-5.2 ± 0.9	93.8	-3.6 ± 0.4	95.5
C_2CCJ(C)CC	-4.4 ± 0.9	94.7	-2.6 ± 0.5	96.4
C_2CC(CJ)CC	2.1 ± 0.9	101.2	1.4 ± 0.4	100.4
C_2CC(C)CJC	-1.9 ± 0.9	97.1	-1.4 ± 0.4	97.6
C_2CC(C)CCJ	2.4 ± 0.9	101.5	1.3 ± 0.4	100.4

[a] Units kcal mol^{-1}.

The parent species show that the lower computational level DFT methods provide acceptable analysis compared to the higher level composite methods with an average absolute difference of 0.4 kcal mol^{-1}. It should be noted that the differences between the methods increase with the amount of branching and should be considered when applying these DFT methods.

There is a higher average absolute difference of 0.8 kcal mol^{-1} between the two levels of theory for the radical species. This shows that the DFT methods provide acceptable analysis for these alkane radicals with, in similar fashion to the parent species, the differences increase as the branching increases.

Recommended $\Delta H^{\circ}_{f\,298}$ values, from the average of the CBS-QB3 and G3MP2B3 methods, are presented in Table 3.4. The calculated $\Delta H^{\circ}_{f\,298}$ for the parent species are compared to other available literature values in Table 3.5.

Calculated values of -45.0 kcal mol^{-1} and -46.8 kcal mol^{-1} for *n*-C_7H_{16} and C_2CCCCC respectively, are within small ranges of the available literature values. This good consistency determines that the work reactions and calculation methods are appropriate for analyzing these types of hydrocarbons. Calculated value of -47.0 kcal mol^{-1} for $C_2CC(C)CC$ falls in the middle of the range of the literature values, but is within accepted chemical accuracy, as defined as 1 kcal mol^{-1}.

Comparison to the group additivity (GA) method shows excellent agreement for *n*-heptane, but there is an increasing derivation as the chain branching increases. It is important to note that the GA values also increase in derivation, more than the calculated values, from the reported literature values seen in the 2-3 kcal mol^{-1} underestimation for $C_2CC(C)CC$.

Table 3.5 Comparison of Calculated $\Delta H^{\circ}_{f\,298}$ Values for C_7H_{16} Isomers to Available Literature Values

Species	This Study $\Delta H^{\circ}_{f\,298}$	Literature Values $\Delta H^{\circ}_{f\,298}$	Reference
n-C_7H_{16}	-45.0 ± 0.1	-44.8 ± 0.3	120
		-44.89 ± 0.19	123
		-44.9	124
		-44.88	116
		-44.74	118
		-44.84	125
		-45.05	*a*
C_2CCCCC	-46.8 ± 0.1	-46.5 ± 0.2	120
		-46.60 ± 0.30	123
		-46.59	116
		-46.43	118
		-46.48	125
		-47.29	*a*
$C_2CC(C)CC$	-47.0 ± 0.1	-47.5 ± 0.3	120
		-47.62 ± 0.30	123
		-46.39	125
		-49.53	*a*

[a] Determined using group additivity.

3.4.2 Carbon-Hydrogen Bond Dissociation Energies (C–H BDEs)

C–H BDEs are computed from the work reactions listed in Table 3.3 where the calculated $\Delta H^{\circ}_{f\,298}$ of the parent and radical molecules are combined with the well-established literature value of 52.10 kcal mol^{-1} for the hydrogen atom.[83] A summary from the DFT and higher level calculations are listed in Table 3.4 where there is good consistency between the two levels of calculations for these BDEs. Recommended values, from the CBS-QB3 and G3MP2B3 average, show good agreement to standard reference C–H BDEs of 101.1, 98.5, and 96.5 kcal mol^{-1} for primary, secondary, and tertiary alkanes, respectively. These values are confirmed by multiple studies where primary C–H BDEs for ethane, *n*-propane, and *n*-butane in the 100-101 kcal mol^{-1} range and secondary C–H

BDEs of approximately 98 kcal mol^{-1} for *n*-propane and *n*-butane.[121,126,127] Tertiary C–H BDE from *t*-butyl reported values range 95.7-97.2 kcal mol^{-1}.[121,126,128]

Calculated primary C–H BDEs for these alkanes fall in a tight 1 kcal mol^{-1} range of 100.4-101.4 kcal mol^{-1} with nearly identical strength to the standard 101.1 kcal mol^{-1} value. Secondary and tertiary calculated C–H BDEs give a slightly larger range of 97.6-98.9 and 95.5-96.6 kcal mol^{-1}, respectively, but still are consistent with the standard values.

Work by Snitsiriwat and Bozzelli on isooctane[122] depicts a trend of decreasing C–H BDEs for tertiary and adjacent secondary locations for species of increasing size with numerous branching groups. Combining their secondary and tertiary values for isooctane of 97.3 and 94.2 kcal mol^{-1} with these calculated values yield average C–H BDEs of 98.3 and 95.7 kcal mol^{-1} for secondary and tertiary branched alkanes respectively. These are an approximate decrease of 0.2 and 0.8 kcal mol^{-1} from normal alkane C–H BDEs.

3.4.3 Internal Rotors

Potential energy curves for internal rotation of single bonds for the parent and radical species are determined using the B3LYP/6-31G(d,p) level of theory. Relaxed scans at 10° intervals are used to determine the lowest energy geometries. If a lower energy conformation is found, previous scan were re-run to insure the lowest energy conformation. These potential energy curves are presented in Appendix B and are used to calculate entropy and heat capacity contributions from internal rotations.

3.4.4 Entropies (*S(T)*) and Heat Capacities ($C_p(T)$)

The methods to calculate entropies and heat capacities are broken up into four groupings where abbreviations for the methods are denoted in italics:

1. *SMCPS*: applies only the rigid-rotor harmonic-oscillator (HO) approximation without correction (subtraction) of R ln(σ) for the three-fold symmetry of the primary methyl groups using the torsion frequencies.
2. *SMCPS/Methyl*: applies the HO approximation with corrections from VIBIR for only methyl group rotations.
3. *SMCPS/VIBIR*: applies the HO approximation for vibrations with all torsion frequencies removed from SMCPS and replaced with contributions for internal rotors from use of VIBIR.
4. *SMCPS/ROTATOR***:** applies the HO approximation for vibrations with all torsion frequencies removed from SMCPS and replaced with contributions for internal rotors from use of ROTATOR.

Comparison between the calculated entropies and heat capacities to available reference literature values for the three molecule parent systems are presented Tables 3.6 and 3.7. These comparisons provide a gauge on the calculation methods. To determine the overall performance of the different methods, relative difference in the entropies and heat capacities between 298-1500 K, based on literature values from Scott,[125] are calculated and presented in Figures 3.2 and 3.3.

Table 3.6 Comparison of Calculated Entropies for C_7H_{16} Parent Species to Available Literature Values[a,b]

Species	*S(T)* (cal mol^{-1} K^{-1})							Method
	298 K	400 K	500 K	600 K	800 K	1000 K	1500 K	
n-C_7H_{16}	95.43	107.58	119.24	130.57	151.90	171.31	212.40	SMCPS (1)
	90.46	102.14	113.40	124.36	144.96	163.73	203.47	SMCPS/Methyl (18)
	101.58	112.39	123.07	133.56	153.39	171.42	209.33	SMCPS/VIBIR (18)
	104.14	117.49	129.66	141.13	162.23	181.11	220.57	SMCPS/ROTATOR (18)
	102.27	115.46	127.77	139.47	161.01	180.29		Ref. 129
	102.29	115.41	127.72	139.5	161.2	180.5	220.5	Ref. 125
	102.78	116.09	128.46	140.18	161.73	180.99	221.20	Ref. 130
C_2CCCCC	94.95	107.28	119.07	130.48	151.89	171.35	212.48	SMCPS (1)
	90.10	101.73	112.94	123.81	144.19	162.69	201.82	SMCPS/Methyl (27)
	100.14	111.16	121.93	132.46	152.26	170.22	208.03	SMCPS/VIBIR (27)
	102.72	116.18	128.51	140.12	161.40	180.37	219.94	SMCPS/ROTATOR (27)
	100.38	113.57	125.88	137.58	159.12	178.40		Ref. 129
	100.48	113.63	126.03	137.9	159.7	179.3	220.0	Ref. 125
	101.33	114.71	127.13	138.89	160.48	179.75	219.96	Ref. 130
$C_2CC(C)CC$	94.72	107.21	119.10	130.58	152.06	171.54	212.67	SMCPS (1)
	91.55	103.14	114.21	124.91	144.89	163.02	201.42	SMCPS/Methyl (81)
	98.61	109.77	120.54	131.01	150.63	168.46	206.10	SMCPS/VIBIR (81)
	98.95	112.15	124.37	135.93	157.14	176.11	215.72	SMCPS/ROTATOR (81)
	98.96	112.15	124.46	136.16	157.70	176.98		Ref. 129
	99.08	112.09	124.5	136.3	158.3	177.9	219.3	Ref. 125

[a] Subtracted 0.026 cal mol^{-1} K^{-1} from values in Ref. 130 to convert from a standard pressure of 1 bar to 1 atm.
[b] Symmetry values are given in parenthesis for our methods.

Table 3.7 Comparison of Calculated Heat Capacities for C_7H_{16} Parent Species to Available Literature Values[a]

Species	*Cp(T)* (cal mol^{-1} K^{-1})							Method
	298 K	400 K	500 K	600 K	800 K	1000 K	1500 K	
n-C_7H_{16}	36.12	47.25	57.71	66.90	81.58	92.54	109.55	SMCPS (1)
	36.48	47.59	57.80	66.67	80.83	91.44	108.00	SMCPS/Methyl (18)
	37.36	48.77	59.21	68.13	81.85	91.72	106.68	SMCPS/VIBIR (18)
	41.08	50.32	59.19	67.06	79.86	89.54	104.56	SMCPS/ROTATOR (18)
	39.67	50.42	60.07	68.33	81.43	91.20		Ref. 129
	39.48	50.35	60.25	68.7	81.8	91.2	106	Ref. 125
		50.74	60.25	68.41	81.40	91.18	106.52	Ref. 130
C_2CCCCC	36.73	47.84	58.21	67.29	81.82	92.69	109.60	SMCPS (1)
	37.28	48.43	58.44	67.07	80.81	91.13	107.34	SMCPS/Methyl (27)
	38.09	49.38	59.52	68.16	81.61	91.43	106.47	SMCPS/VIBIR (27)
	41.11	50.97	59.94	67.77	80.37	89.89	104.75	SMCPS/ROTATOR (27)
	39.67	50.42	60.07	68.33	81.43	91.20		Ref. 129
	39.32	50.66	60.66	69.2	82.6	92.4	108	Ref. 125
		50.98	60.46	68.59	81.49	91.20	106.48	Ref. 130
$C_2CC(C)CC$	37.29	48.36	58.62	67.60	81.97	92.75	109.58	SMCPS (1)
	38.30	49.03	58.63	66.93	80.27	90.39	106.40	SMCPS/Methyl (81)
	38.84	49.59	59.28	67.66	80.98	90.88	106.16	SMCPS/VIBIR (81)
	39.98	50.33	59.55	67.51	80.25	89.89	105.03	SMCPS/ROTATOR (81)
	39.67	50.42	60.07	68.33	81.43	91.20		Ref. 129
	38.44	50.44	60.64	69.3	83.1	93.5	110	Ref. 125

[a] Symmetry values are given in parenthesis for our methods.

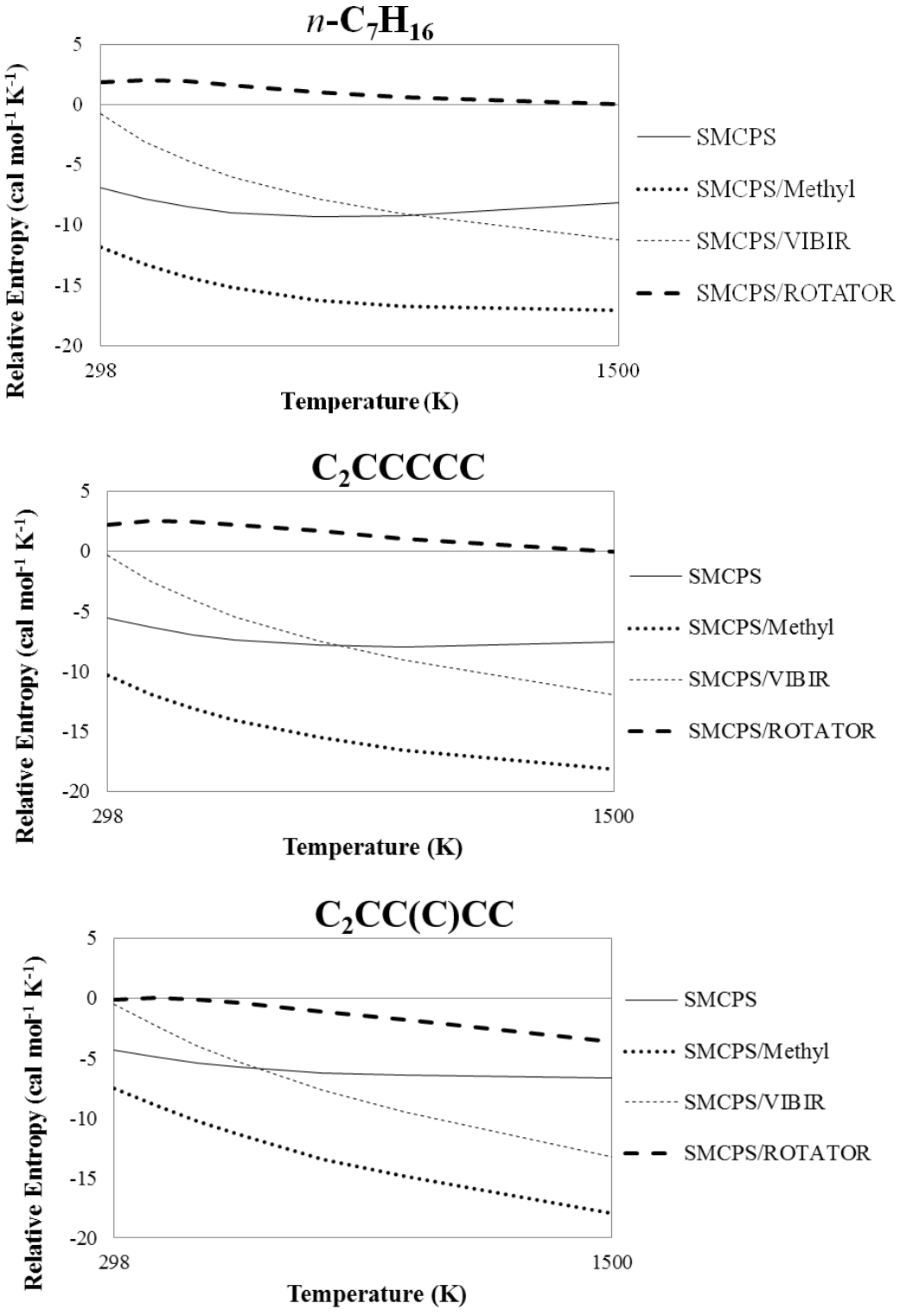

Figure 3.2 Comparison of calculated entropies to literature values.

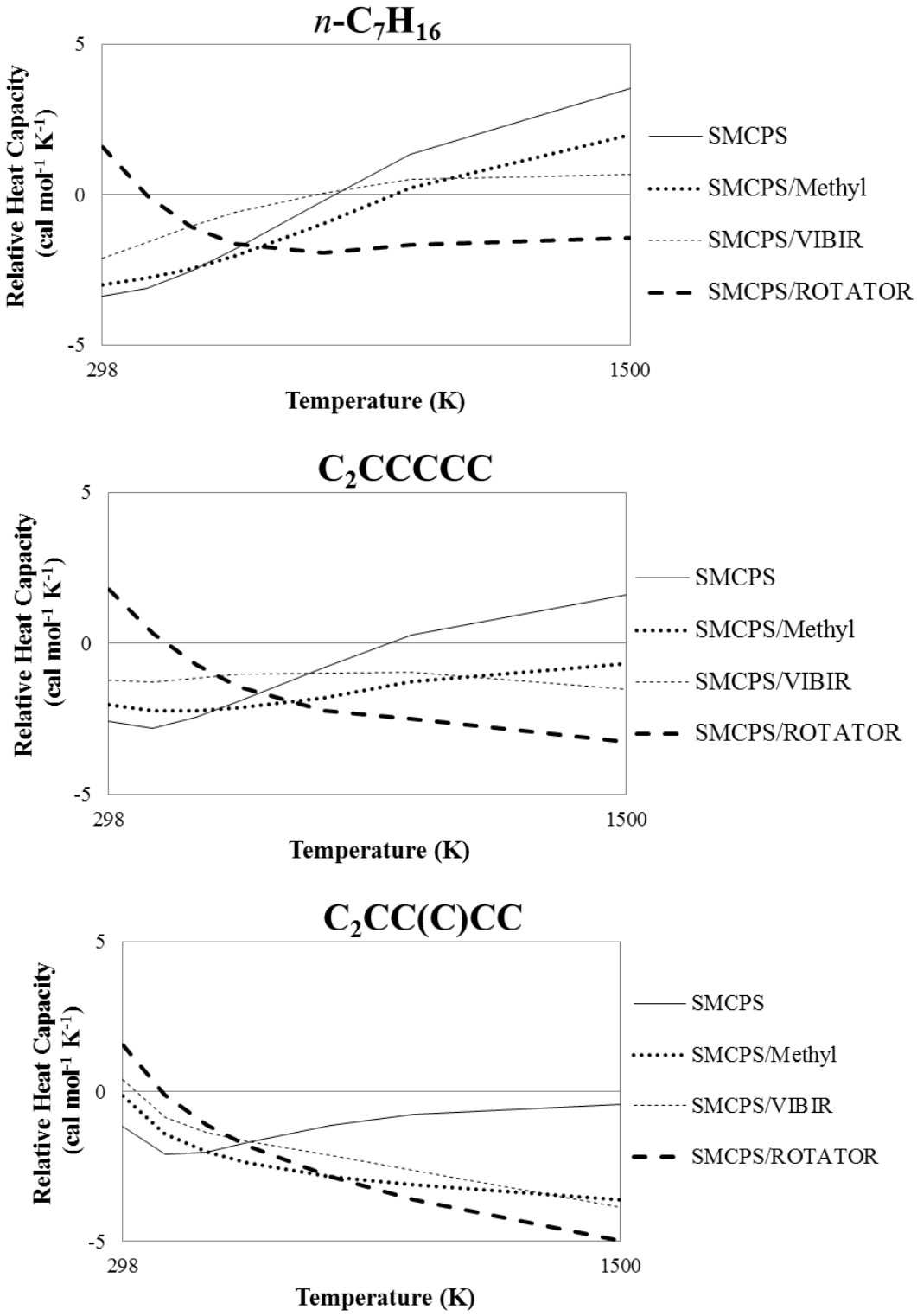

Figure 3.3 Comparison of calculated heat capacities to literature values.

The data in Table 3.6 for the parent molecules by the HO approximation method, as implemented in the SMCPS code, are shown to consistently underpredict entropies by 4 to 9 cal mol^{-1} K^{-1} in this 298-1500 K temperature range. It is seen that as the branching of these isomers increases, the HO approximation provides a slight increase in accuracy.

The second calculation method provides corrections using the Pitzer and Gwinn method, as implemented in the VIBIR code, for symmetrical terminal methyl rotations. Contributions from the torsion frequencies associated with the methyl rotations are replaced with VIBIR values and incorporated with the remaining vibration contributions at each temperature.

These SMCPS/Methyl values, in Figure 3.2, are observed to significantly underestimate the entropies by 7 to 12 cal mol^{-1} K^{-1} at 298 K and 17 to 18 cal mol^{-1} K^{-1} at 1500 K. In this case, the HO approximation from SMCPS is a better estimate than only considering corrections for methyl rotations.

Entropy contributions using all internal rotors are calculated using both VIBIR and ROTATOR. Determining the corresponding rotation-vibration torsions are problematic due to the coupling of several internal rotors. To overcome this, numerous different pair combinations are removed and it is observed that there is an insignificant change in the results. To maintain consistency, the first six vibration frequencies are removed for each species.

At 298 K, the SMCPS/VIBIR values provide accuracy within 1 cal mol^{-1} K^{-1} to the reference values for all of the parent species; SMCPS/ROTATOR provides a slightly closer value for $C_2CC(C)CC$. As the temperature increases, the SMCPS/VIBIR values quickly begin to underestimate the Scott values by 11-13 cal mol^{-1} K^{-1} at 1500 K. In

contrast, SMCPS/ROTATOR provides much closer agreement throughout the temperature range. In general, modeling the rotational energy barriers provides for a better approximation to entropy.

The HO approximation with corrections for internal rotations by the ROTATOR code provides the best comparison to available entropy reference values. It is important to note that SMCPS/VIBIR provides very good agreement with literature entropy values at 298 K.

Heat capacity values show much better consistency between the methods than the entropies with maximum deviation of approximately 5 cal mol^{-1} K^{-1} from the Scott[125] values in Figure 3.3. For *n*-C_7H_{16} and C_2CCCCC, the SMCPS/Methyl and SMCPS/VIBIR values show a lower deviation from the Scott values compared to SMCPS/ROTATOR while all three methods deviate further for $C_2CC(C)CC$. In Table 3.7, it is seen that the Scott[125] values range between 1-2 cal mol^{-1} K^{-1} higher than the Stull[129] values for C_2CCCCC and $C_2CC(C)CC$. Use of the Stull values reduces the deviation for the calculated heat capacities methods resulting in acceptable values when accounting for internal rotations.

Due to the importance in accounting for internal rotation in the parent entropy values, entropies and heat capacities are calculated using both SMCPS/ROTATOR and SMCPS/VIBIR, for the radical species in Tables 3.8 and 3.9. The SMCPS/VIBIR entropy values under predict compared to SMCPS/ROTATOR with an increase in deviation as temperature increases. In several instances, specifically for the $C_2CC(C)CC$ radicals, SMCPS/VIBIR provides acceptable approximation to the SMCPS/ROTATOR values at 298 K as it did for the parent species. However, the deviation between the methods

quickly increases to over 9 cal mol^{-1} K^{-1} at 1500 K. For heat capacities, this trend does not exist and the methods are consistent in this temperature range with a maximum deviation of approximately 3 cal mol^{-1} K^{-1}.

Experimental literature values do not exist for these radical species, and entropies and heat capacities from the SMCPS/ROTATOR method are recommended based on the consistency in the entropy and heat capacity values for the parent species. Calculated SMCPS/ROTATOR entropies and heat capacities for the extended 50-5000 K range are presented in Appendix B, although it is difficult to comment on the accuracy of these values.

Table 3.8 Comparison of Calculated Entropies for C_7H_{16} Radical Species[a]

Species	*S(T)* (cal mol^{-1} K^{-1})							Method
	298 K	400 K	500 K	600 K	800 K	1000 K	1500 K	
CJCCCCCC (3)	106.41	117.09	127.56	137.78	156.96	174.30	210.56	SMCPS/VIBIR
	110.52	123.61	135.53	146.73	167.19	185.40	223.26	SMCPS/ROTATOR
CCJCCCCC (9)	106.14	116.68	126.95	136.97	155.82	172.92	208.88	SMCPS/VIBIR
	110.37	122.98	134.57	145.53	165.71	183.77	221.45	SMCPS/ROTATOR
CCCJCCCC (9)	106.55	117.35	127.71	137.75	156.53	173.54	209.33	SMCPS/VIBIR
	110.68	123.20	134.77	145.73	165.90	183.95	221.63	SMCPS/ROTATOR
CCCCJCCC (9)	106.57	117.39	127.76	137.81	156.58	173.58	209.34	SMCPS/VIBIR
	110.89	123.30	134.83	145.78	165.95	184.01	221.69	SMCPS/ROTATOR
CJ_2CCCCC (9)	105.12	116.02	126.60	136.86	156.03	173.31	209.45	SMCPS/VIBIR
	106.23	119.60	131.72	143.06	163.69	181.97	219.90	SMCPS/ROTATOR
$C_2CJCCCC$ (54)	103.43	113.75	123.76	133.55	152.04	168.88	204.51	SMCPS/VIBIR
	106.60	118.81	130.12	140.88	160.78	178.68	216.19	SMCPS/ROTATOR
$C_2CCJCCC$ (27)	103.94	114.91	125.37	135.44	154.20	171.13	206.77	SMCPS/VIBIR
	106.71	119.40	131.11	142.17	162.46	180.56	218.28	SMCPS/ROTATOR
$C_2CCCJCC$ (27)	102.28	113.40	124.04	134.28	153.30	170.42	206.31	SMCPS/VIBIR
	105.35	118.23	130.09	141.28	161.74	179.96	217.84	SMCPS/ROTATOR
$C_2CCCCJC$ (27)	103.36	114.13	124.51	134.58	153.41	170.46	206.31	SMCPS/VIBIR
	106.40	119.09	130.77	141.81	162.09	180.21	217.97	SMCPS/ROTATOR
$C_2CCCCCJ$ (9)	103.60	114.48	125.04	135.28	154.44	171.71	207.88	SMCPS/VIBIR
	106.21	119.37	131.42	142.73	163.36	181.67	219.65	SMCPS/ROTATOR
$CJ_2CC(C)CC$ (27)	102.45	113.64	124.28	134.53	153.59	170.79	206.91	SMCPS/VIBIR
	101.47	114.80	126.99	138.42	159.19	177.59	215.73	SMCPS/ROTATOR
$C_2CJC(C)CC$ (81)	102.41	113.00	123.25	133.19	151.82	168.72	204.36	SMCPS/VIBIR
	102.95	115.46	127.01	137.94	158.07	176.10	213.82	SMCPS/ROTATOR

[a] Symmetry values are given in parenthesis.

Table 3.8 Comparison of Calculated Entropies for C_7H_{16} Radical Species[a] (Continued)

Species	*S(T)* (cal mol^{-1} K^{-1})							Method
	298 K	400 K	500 K	600 K	800 K	1000 K	1500 K	
$C_2CCJ(C)CC$ (81)	102.01	112.63	122.80	132.62	151.00	167.67	202.97	SMCPS/VIBIR
	103.90	116.05	127.38	138.18	158.14	176.06	213.61	SMCPS/ROTATOR
$C_2CC(CJ)CC$ (27)	101.47	112.59	123.24	133.50	152.62	169.86	206.01	SMCPS/VIBIR
	101.32	114.70	126.91	138.35	159.13	177.53	215.66	SMCPS/ROTATOR
$C_2CC(C)CJC$ (81)	100.32	111.32	121.90	132.10	151.07	168.18	204.10	SMCPS/VIBIR
	100.25	113.35	125.37	136.67	157.25	175.54	213.55	SMCPS/ROTATOR
$C_2CC(C)CCJ$ (27)	101.71	112.87	123.53	133.78	152.84	170.03	206.08	SMCPS/VIBIR
	101.77	115.18	127.36	138.74	159.40	177.72	215.73	SMCPS/ROTATOR

[a] Symmetry values are given in parenthesis.

Table 3.9 Comparison of Calculated Heat Capacities for C_7H_{16} Radical Species[a]

Species	*Cp(T)* (cal mol^{-1} K^{-1})							Method
	298 K	400 K	500 K	600 K	800 K	1000 K	1500 K	
CJCCCCCC (3)	37.31	48.07	57.97	66.34	79.10	88.23	102.10	SMCPS/VIBIR
	40.45	49.36	57.85	65.29	77.21	86.17	100.04	SMCPS/ROTATOR
CCJCCCCC (9)	37.13	47.35	56.94	65.18	77.97	87.27	101.53	SMCPS/VIBIR
	38.73	47.78	56.48	64.12	76.39	85.59	99.76	SMCPS/ROTATOR
CCCJCCCC (9)	38.16	48.00	57.20	65.12	77.59	86.82	101.17	SMCPS/VIBIR
	38.32	47.63	56.42	64.09	76.37	85.58	99.77	SMCPS/ROTATOR
CCCCJCCC (9)	38.23	48.08	57.26	65.14	77.55	86.76	101.10	SMCPS/VIBIR
	37.77	47.38	56.32	64.06	76.39	85.59	99.75	SMCPS/ROTATOR
CJ_2CCCCC (9)	38.13	48.72	58.34	66.45	78.90	87.93	101.82	SMCPS/VIBIR
	41.25	50.34	58.71	65.97	77.63	86.43	100.20	SMCPS/ROTATOR
$C_2CJCCCC$ (54)	36.51	46.36	55.73	63.89	76.75	86.25	100.91	SMCPS/VIBIR
	37.39	46.47	55.27	63.04	75.57	84.98	99.52	SMCPS/ROTATOR
$C_2CCJCCC$ (27)	38.78	48.57	57.52	65.20	77.35	86.46	100.83	SMCPS/VIBIR
	38.78	48.28	57.04	64.60	76.67	85.73	99.84	SMCPS/ROTATOR
$C_2CCCJCC$ (27)	39.08	49.24	58.40	66.14	78.24	87.22	101.30	SMCPS/VIBIR
	39.31	48.97	57.74	65.26	77.22	86.19	100.17	SMCPS/ROTATOR
$C_2CCCCJC$ (27)	37.96	48.03	57.33	65.29	77.79	87.01	101.29	SMCPS/VIBIR
	38.84	48.17	56.91	64.52	76.69	85.82	99.97	SMCPS/ROTATOR
$C_2CCCCCJ$ (9)	38.03	48.65	58.25	66.37	78.87	87.96	101.90	SMCPS/VIBIR
	40.29	49.86	58.50	65.92	77.70	86.55	100.34	SMCPS/ROTATOR
$CJ_2CC(C)CC$ (27)	39.43	49.33	58.38	66.17	78.54	87.71	101.84	SMCPS/VIBIR
	40.88	50.49	59.11	66.47	78.14	86.94	100.78	SMCPS/ROTATOR
$C_2CJC(C)CC$ (81)	37.39	47.42	56.66	64.60	77.10	86.38	100.88	SMCPS/VIBIR
	38.31	47.56	56.29	63.93	76.24	85.52	100.02	SMCPS/ROTATOR

[a] Symmetry values are given in parenthesis.

Table 3.9 Comparison of Calculated Heat Capacities for C_7H_{16} Radical Species[a] (Continued)

Species	*Cp(T)* (cal mol^{-1} K^{-1})							Method
	298 K	400 K	500 K	600 K	800 K	1000 K	1500 K	
$C_2CCJ(C)CC$ (81)	37.69	47.29	56.15	63.81	76.11	85.43	100.21	SMCPS/VIBIR
	36.85	46.51	55.48	63.26	75.70	85.06	99.69	SMCPS/ROTATOR
$C_2CC(CJ)CC$ (27)	39.06	49.25	58.47	66.34	78.71	87.83	101.89	SMCPS/VIBIR
	41.03	50.61	59.20	66.52	78.15	86.92	100.75	SMCPS/ROTATOR
$C_2CC(C)CJC$ (81)	38.67	48.94	58.11	65.91	78.15	87.24	101.42	SMCPS/VIBIR
	40.11	49.71	58.36	65.77	77.58	86.49	100.55	SMCPS/ROTATOR
$C_2CC(C)CCJ$ (27)	39.27	49.33	58.43	66.23	78.49	87.58	101.66	SMCPS/VIBIR
	41.32	50.55	58.92	66.15	77.76	86.57	100.51	SMCPS/ROTATOR

[a] Symmetry values are given in parenthesis.

Table 3.10 Comparison of Calculated Entropy and Heat Capacities for C_7H_{16} Parent Species to Other Available Literature Values[a]

Species	S°_{298}[b]	$C_p(T)$[b]							Method
		300 K	400 K	500 K	600 K	800 K	1000 K	1500 K	
n-C_7H_{16} (18)	102.18	39.88	50.43	60.05	68.33	81.39	91.24	106.16	GA
	104.14	41.25	50.32	59.19	67.06	79.86	89.54	104.56	SMCPS/ROTATOR
	102.27	39.86	50.42	60.07	68.33	81.43	91.20		Ref. 129
	102.29	39.67	50.35	60.25	68.7	81.8	91.2	106	Ref. 125
	102.78[c]	40.42	50.74	60.25	68.41	81.40	91.18	106.52	Ref. 130
C_2CCCCC (27)	100.87	39.61	50.37	60.12	68.47	81.58	91.38	106.52	GA
	102.72	41.30	50.97	59.94	67.77	80.37	89.89	104.75	SMCPS/ROTATOR
	100.38	39.86	50.42	60.07	68.33	81.43	91.20		Ref. 129
	100.48	39.52	50.66	60.66	69.2	82.6	92.4	108	Ref. 125
	101.33[c]	40.28	50.98	60.46	68.59	81.49	91.20	106.48	Ref. 130
$C_2CC(C)CC$ (81)	99.56	39.34	50.31	60.19	68.61	81.77	91.52	106.88	GA
	98.95	40.19	50.33	59.55	67.51	80.25	89.89	105.03	SMCPS/ROTATOR
	98.96	39.86	50.42	60.07	68.33	81.43	91.20		Ref. 129
	99.08	38.68	50.44	60.64	69.3	83.1	93.5	110	Ref. 125

[a] Symmetry values are given in parenthesis.
[b] Units of cal mol^{-1} K^{-1}.
[c] Subtracted 0.026 cal mol^{-1} K^{-1} from referenced value to convert from a standard pressure of 1 bar to 1 atm.

3.5 Conclusions

Thermochemical properties are calculated for enthalpies ($\Delta H^{\circ}_{f\,298}$), entropies ($S^{\circ}(T)$), heat capacities ($C_p(T)$), and carbon-hydrogen bond dissociation energies (C–H BDEs) for *n*-heptane, 2-methylhexane, 2,3-dimethylpentane, and their carbon-centered radicals. Internal rotor potentials are determined using B3LYP/6-31G(d,p) to verify the lowest energy structure and for calculating contributions to entropies and heat capacities. $\Delta H^{\circ}_{f\,298}$ values are calculated using isodesmic work reactions with density functional theory and higher level composite computational methods. Comparisons of the enthalpies for the parent species with referenced literature data are within chemical accuracy of 1 kcal mol^{-1}. Calculated C–H bond dissociation energies for the radicals are within acceptable limits compared to standard *n*-alkane primary, secondary, and tertiary bonds. Entropies and heat capacities are calculated between 50-5000 K. There is good agreement for the calculation methods to the referenced available literature values when corrections for all internal rotations are accounted for using the SMCPS/ROTATOR method over the 298-1500 K temperature range.

CHAPTER 4

THERMOCHEMISTRY AND BOND DISSOCIATION ENERGIES OF KETONES

4.1 Overview

The role of ketones in the chemistry of the earth's atmosphere has been studied experimentally using field measurements and has been incorporated into modeling studies.[131-135] Sources of atmospheric acetone, for example, include emissions from dead plant matter, burning of biomass, oxidation of hydrocarbons, and anthropogenic emissions.[20,136-139] Acetone and the acetonyl radical, formed by hydroxyl radical abstraction,[140] have been shown to play an important role in atmospheric chemistry by influencing ozone production through withdrawing nitrogen oxides in the form of peroxyacetyl nitrates (PAN) and generating HO_x free radicals.[132-136,141-143] Important atmospheric loss processes for ketones involve hydrogen abstractions by hydroxyl radicals, a process that is partially controlled by carbon-hydrogen bond dissociation energies (C–H BDEs), and by photolysis.[20-22]

Besides their importance in the atmosphere, ketones are a major class of organic compounds. They make up a significant portion of organic cleaning solvents, paint thinners, nail polish removers, and as solvents in chemical processes. Ketones have also been used as fuel tracers for monitoring fuel properties such as concentration, temperature, density, pressure, velocity, and distribution using laser-induced fluorescence[15-17] and as fuel additives in reducing soot emissions.[18,19]

Detailed chemical kinetic models have been developed and are readily available for hydrocarbon combustion[6] with some, but far fewer, studies for ketones. Some

chemical kinetic models have been developed involving smaller ketones such as for the oxidation of acetone[144-146] and several reactions involving acetonyl radicals.[147-149] Chemical kinetic models for 2-butanone and 3-pentanone oxidation have recently been reported[150,151] where properties for radicals formed from hydrogen abstraction had to be estimated using group additivity and comparisons to acetone. The value used for the secondary carbon-hydrogen bonds was several kcal mol^{-1} higher than the actual value, and this could affect both unimolecular dissociation and abstraction kinetics in the model. Sebbar et al.[152] in kinetic analysis of butanone oxidation have recently reported weak carbon-hydrogen bond dissociation energies in 2-butanone for the carbons adjacent to the carbonyl group to support this. Rate constants for abstraction reactions in modeling atmospheric and combustion chemistry are commonly estimated using well-studied smaller compounds having similar bond dissociation energies.

There have been previous microwave spectroscopy studies on the molecular geometry of several smaller ketones.[153-156] However, there are no comprehensive studies on bond energies of ketones and radicals corresponding to loss of H atom as a class of compounds with the exception of acetone, which has reported C–H bond energies of 92-101 kcal mol^{-1}.[157-166] The more recent theoretical and experimental studies however seem to converge on a value of 96 ± 1 kcal mol^{-1}.[157,159,160,164] Although ketones have many applications and involvement in different chemical systems, basic thermochemical properties for several representative compounds are not available. Accurate and reliable enthalpies of formation and bond dissociation energies for these species are necessary for improvement in understanding ketonyl radicals, transition states, reaction paths, and in developing detailed chemical kinetic models.[45,167,168]

The objective of this chapter is to provide a set of thermochemical properties including enthalpies ($\Delta H^{\circ}_{f\ 298}$), entropies ($S(T)$), and heat capacities ($C_p(T)$) along with primary, secondary, and tertiary C–H BDEs adjacent to the carbonyl group for five small ketone species, presented in Figure 4.1. Calculated $\Delta H^{\circ}_{f\ 298}$ for 2-butanone, 3-pentanone, 2-pentanone, 3-methyl-2-butanone, and 2-methyl-3-pentanone show good agreement compared to available literature values. $\Delta H^{\circ}_{f\ 298}$ values are calculated for all of the radicals corresponding to the loss of hydrogen atom (J represents the radical site on a preceding carbon atom). Bond energies are determined from the parent and radical species and compared to the available literature values and conventional normal primary, secondary, and tertiary bond energies from alkane hydrocarbons.

4.2 Nomenclature

Abbreviations are utilized in this chapter as illustrated below:

- – represents a bond between two atoms,
- C(=O) represents a carbonyl group,
- (C) represents a methyl substituent on the preceding carbon atom,
- J represents a radical site on the preceding carbon atom,
- TVR denotes translation, vibration, and external rotation,
- IR denotes internal rotation.

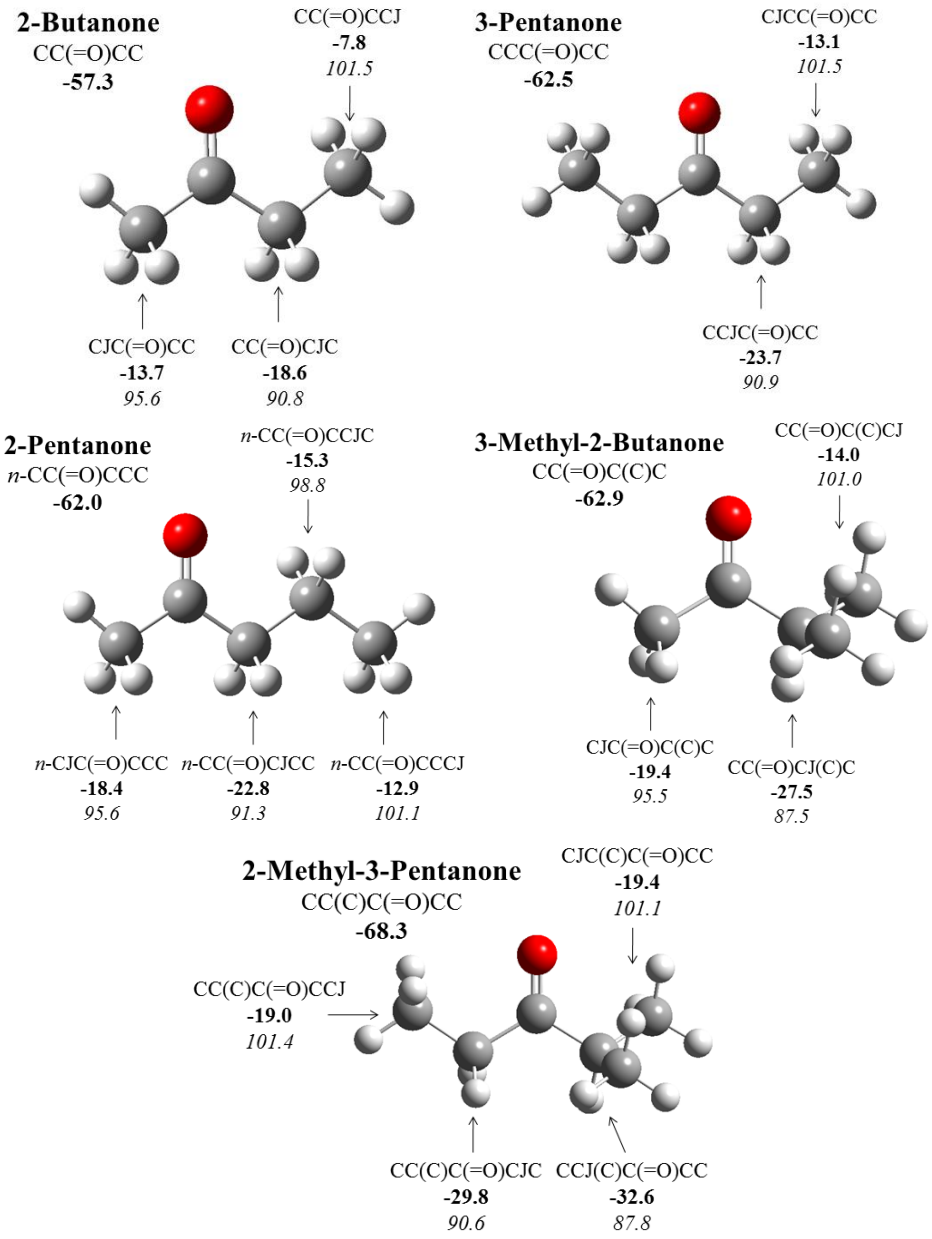

Figure 4.1 Nomenclature, recommended $\Delta H^{\circ}_{f\ 298}$ (bold, kcal mol^{-1}), and carbon-hydrogen bond dissociation energies (italic, kcal mol^{-1}) for ketones.

4.3 Computational Methods

Optimized geometries for the parent and radicals are initially calculated at the B3LYP/ 6-31G(d,p) level of theory.[46,47] Potential energy curves for the single bond internal

rotation barriers are used to verify the lowest energy conformation and for calculation of entropies and heat capacities. These potential energy graphs are available in Appendix C.

Isodesmic work reactions are implemented for calculation of the enthalpies of formation ($\Delta H^{\circ}_{f\,298}$) using the B3LYP method with the 6-31G(d,p) and 6-311G(d,p) basis sets. Higher level composite methods, G3MP2B3[57,58] and CBS-QB3,[60,61] are used as a comparison for the DFT methods. Carbon-hydrogen bond dissociation energies (C–H BDE) are determined from the calculated $\Delta H^{\circ}_{f\,298}$ energies and the well-established literature value of 52.10 kcal mol^{-1} for a hydrogen atom.[83] All calculations are performed using the Gaussian 03 program suite.[62]

Contributions to entropies and heat capacities from translations, vibrations, and external rotations, represented as TVR, are calculated using the Statistical Mechanics for Heat Capacity and Entropy (SMCPS) program[98] using B3LYP/6-31G(d,p) calculations. Contributions from internal rotations, represented as IR, are incorporated using the Pitzer and Gwinn[85-87] approximation method in the VIBIR[100] code. Total entropies and heat capacity values are determined by summing the TVR and IR contributions in the 100-5000 K temperature range.

The group additivity (GA) method, as developed by Benson,[102] serves as a comparison for the calculated $\Delta H^{\circ}_{f\,298}$, S°_{298}, and $C_p(T)$ values. Hydrogen-bond increment (HBI) values for the primary, secondary, and tertiary positions adjacent to the carbonyl group in these ketones are derived.

4.4 Results and Discussion

Isodesmic work reactions are used to calculate the $\Delta H^{\circ}_{f\,298}$ for each target species at the B3LYP/6-31G(d,p), B3LYP/6-311G(2d,2p), CBS-QB3, and G3MP2B3 levels of theory.

All of the species in the work reactions, except for the target compound, have standard well-established $\Delta H^{\circ}_{f\,298}$ values; [83,120,121,168] these are listed in Table 4.1. In some cases, the work reactions incorporate a ketone compound that is analyzed in this study. The reference $\Delta H^{\circ}_{f\,298}$ values in these cases are from literature values[169-172] shown in Table 4.1. The work reactions are presented in Table 4.2.

Table 4.1 Standard Enthalpies of Formation for Reference Species

Species	$\Delta H^{\circ}_{f\,298}$ (kcal mol^{-1})	Reference
H	52.10	83
CH_4[a]	-17.8 ± 0.1	120
CH_3CH_3	-20.0 ± 0.1	120
$CH_3CH_2CH_3$	-25.0 ± 0.1	120
$CH_3CH_2CH_2CH_3$	-30.0 ± 0.1	120
$(CH_3)_3CH$	-32.1 ± 0.1	120
CC(=O)	-39.72 ± 0.16	168
CC(=O)C	-51.9 ± 0.2	120
CC(=O)CC	-57.02 ± 0.20	169
CCC(=O)CC	-62.25 ± 0.39	*b*
CC(=O)C(C)C	-62.76 ± 0.21	172
CJH_3[a]	35.1 ± 0.2	173
CH_3CJH_2	29.0 ± 0.4	121
CH_3CJHCH_3	21.5 ± 0.4	121
$(CH_3)_3CJ$	12.3 ± 0.4	121
$CH_3CJHCH_2CH_3$	16.1 ± 0.5	121
CC(=O)CJ[a]	-8.3 ± 0.5	157

[a] Used in reference reactions in Scheme 4.2.
[b] Reported on NIST WebBook as the reanalyzed value of Ref. 170 by Ref. 171.

Table 4.2 Isodesmic Work Reactions and Calculated $\Delta H^{\circ}_{f\,298}$ for Ketone Parent Species

Isodesmic Reactions							$\Delta H^{\circ}_{f\,298}$ (kcal mol^{-1})				Average Reference Species Uncertainty
							B3LYP		CBS-QB3	G3MP2B3	
							6-31G(d,p)	6-311G(2d,2p)			
CC(=O)CC System											
CC(=O)CC	+	CH_3CH_3	→	CC(=O)C	+	$CH_3CH_2CH_3$	-57.42	-57.31	-57.36	-57.24	0.13
CC(=O)CC	+	CH_3CH_3	→	CC(=O)	+	$CH_3CH_2CH_2CH_3$	-57.86	-57.92	-57.21	-56.85	0.12
CC(=O)CC	+	$CH_3CH_2CH_3$	→	CC(=O)C	+	$CH_3CH_2CH_2CH_3$	-57.49	-57.46	-57.29	-57.19	0.13
CC(=O)CC	+	CC(=O)	→	CC(=O)C	+	CC(=O)C	-57.05	-56.85	-57.45	-57.57	0.19
						Average	**-57.45**	**-57.39**	**-57.33**	**-57.21**	**0.14**
						Method Std Dev		**0.36**		**0.21**	
CCC(=O)CC System											
CCC(=O)CC	+	CH_3CH_3	→	CC(=O)C	+	$CH_3CH_2CH_2CH_3$	-62.88	-62.75	-62.71	-62.53	0.13
CCC(=O)CC	+	CH_3CH_3	→	CC(=O)CC	+	$CH_3CH_2CH_3$	-62.41	-62.31	-62.44	-62.37	0.13
CCC(=O)CC	+	$CH_3CH_2CH_3$	→	CC(=O)CC	+	$CH_3CH_2CH_2CH_3$	-62.49	-62.46	-62.37	-62.31	0.13
CCC(=O)CC	+	CC(=O)	→	CC(=O)CC	+	CC(=O)C	-62.05	-61.85	-62.53	-62.70	0.19
						Average	**-62.46**	**-62.34**	**-62.51**	**-62.48**	**0.15**
						Method Std Dev		**0.34**		**0.15**	
***n*-CC(=O)CCC System**											
n-CC(=O)CCC	+	CH_3CH_3	→	CC(=O)CC	+	$CH_3CH_2CH_3$	-61.87	-61.74	-61.94	-61.93	0.13
n-CC(=O)CCC	+	CH_3CH_3	→	CC(=O)C	+	$CH_3CH_2CH_2CH_3$	-62.34	-62.18	-62.21	-62.10	0.13
n-CC(=O)CCC	+	$CH_3CH_2CH_3$	→	CC(=O)CC	+	$CH_3CH_2CH_2CH_3$	-61.94	-61.89	-61.87	-61.88	0.13
n-CC(=O)CCC	+	CC(=O)	→	CC(=O)C	+	CC(=O)CC	-61.50	-61.29	-62.02	-62.26	0.19
n-CC(=O)CCC	+	CC(=O)C	→	CC(=O)CC	+	CC(=O)CC	-61.47	-61.45	-61.60	-61.71	0.20
						Average	**-61.82**	**-61.71**	**-61.93**	**-61.98**	**0.16**
						Method Std Dev		**0.34**		**0.21**	
CC(=O)C(C)C System											
CC(=O)C(C)C	+	CH_3CH_3	→	CC(=O)C	+	$CH_3CH_2CH_2CH_3$	-61.73	-61.64	-63.14	-63.01	0.13
CC(=O)C(C)C	+	CH_3CH_3	→	CC(=O)CC	+	$CH_3CH_2CH_3$	-61.26	-61.21	-62.87	-62.84	0.13
CC(=O)C(C)C	+	$CH_3CH_2CH_3$	→	CC(=O)CC	+	$CH_3CH_2CH_2CH_3$	-61.34	-61.35	-62.80	-62.79	0.13
CC(=O)C(C)C	+	CC(=O)	→	CC(=O)CC	+	CC(=O)C	-60.89	-60.75	-62.95	-63.17	0.19
CC(=O)C(C)C	+	CC(=O)C	→	CC(=O)CC	+	CC(=O)CC	-60.87	-60.91	-62.53	-62.62	0.20
						Average	**-61.22**	**-61.17**	**-62.86**	**-62.89**	**0.16**
						Method Std Dev		**0.34**		**0.21**	

Table 4.2 Isodesmic Work Reactions and Calculated $\Delta H^{\circ}_{f\,298}$ for Ketone Parent Species (Continued)

Isodesmic Reactions	$\Delta H^{\circ}_{f\,298}$ (kcal mol^{-1}) B3LYP 6-31G(d,p)	B3LYP 6-311G(2d,2p)	CBS-QB3	G3MP2B3	Average Reference Species Uncertainty
CC(C)C(=O)CC System					
CC(C)C(=O)CC + CH_3CH_3 → CC(=O)CC + $CH_3CH_2CH_2CH_3$	-66.88	-66.79	-68.39	-68.29	0.13
CC(C)C(=O)CC + CH_3CH_3 → CC(=O)C(C)C + $CH_3CH_2CH_3$	-68.31	-68.20	-68.35	-68.27	0.14
CC(C)C(=O)CC + CH_3CH_3 → CCC(=O)CC + $CH_3CH_2CH_3$	-66.65	-66.58	-68.27	-68.23	0.20
CC(C)C(=O)CC + CC(=O) → CC(=O)CC + CC(=O)CC	-66.05	-65.89	-68.21	-68.46	0.19
Average	**-66.97**	**-66.87**	**-68.31**	**-68.31**	**0.17**
Method Std Dev	**0.89**		**0.09**		

Each of the ketone parent compounds are analyzed with four to five isodesmic work reactions where the parent compound is reacted with ethane, propane, acetaldehyde, or acetone and yields a small three- or four-carbon *n*-alkane and, in most cases, acetone or 2-butanone. Slightly larger species are generated for the 2-methyl-3-pentanone work reactions.

The radical work reactions are slightly different where the compound is reacted with a small hydrocarbon and yields the parent ketone plus a hydrocarbon radical as seen in Scheme 4.1. The radical work reactions are presented in Table 4.3.

Scheme 4.1 Radical Isodesmic Work Reactions

Radical	+	CH_3CH_3	→	Parent	+	CH_3CJH_2
Radical	+	$CH_3CH_2CH_3$	→	Parent	+	CH_3CJHCH_3
Radical	+	$(CH_3)_3CH$	→	Parent	+	$(CH_3)_3CJ$
Radical	+	$CH_3CH_2CH_2CH_3$	→	Parent	+	$CH_3CJHCH_2CH_3$

The optimized structure parameters, symmetry values, moments of inertia, vibrational frequencies, internal rotor potentials, entropies, and heat capacities for each species from the B3LYP/6-31G(d,p) level of theory are presented in Appendix C.

Table 4.3 Isodesmic Work Reactions, Calculated $\Delta H^{\circ}_{f\,298}$, and Bond Dissociation Energies for Ketone Radical Species

Isodesmic Reactions							$\Delta H^{\circ}_{f\,298}$ (kcal mol^{-1}) B3LYP 6-31G(d,p)	$\Delta H^{\circ}_{f\,298}$ (kcal mol^{-1}) B3LYP 6-311G(2d,2p)	$\Delta H^{\circ}_{f\,298}$ (kcal mol^{-1}) CBS-QB3	$\Delta H^{\circ}_{f\,298}$ (kcal mol^{-1}) G3MP2B3	Average Reference Species Uncertainty
CJC(=O)CC System											
CJC(=O)CC	+	CH_3CH_3	→	CC(=O)CC	+	CH_3CJH_2	-14.61	-13.96	-13.65	-13.24	0.23
CJC(=O)CC	+	$CH_3CH_2CH_3$	→	CC(=O)CC	+	CH_3CJHCH_3	-13.21	-12.67	-13.40	-13.42	0.23
CJC(=O)CC	+	$(CH_3)_3CH$	→	CC(=O)CC	+	$(CH_3)_3CJ$	-12.28	-11.89	-13.83	-14.21	0.23
CJC(=O)CC	+	$CH_3CH_2CH_2CH_3$	→	CC(=O)CC	+	$CH_3CJHCH_2CH_3$	-13.82	-13.18	-14.01	-14.05	0.27
						Average	**-13.48**	**-12.92**	**-13.72**	**-13.73**	**0.24**
						Method Std Dev		**0.91**		**0.35**	
						Bond Dissociation Energy	**95.89**	**96.45**	**95.65**	**95.64**	
CC(=O)CJC System											
CC(=O)CJC	+	CH_3CH_3	→	CC(=O)CC	+	CH_3CJH_2	-20.88	-20.28	-18.59	-17.98	0.23
CC(=O)CJC	+	$CH_3CH_2CH_3$	→	CC(=O)CC	+	CH_3CJHCH_3	-19.49	-18.99	-18.35	-18.17	0.23
CC(=O)CJC	+	$(CH_3)_3CH$	→	CC(=O)CC	+	$(CH_3)_3CJ$	-18.55	-18.21	-18.77	-18.95	0.23
CC(=O)CJC	+	$CH_3CH_2CH_2CH_3$	→	CC(=O)CC	+	$CH_3CJHCH_2CH_3$	-20.10	-19.50	-18.95	-18.80	0.27
						Average	**-19.75**	**-19.24**	**-18.67**	**-18.47**	**0.24**
						Method Std Dev		**0.90**		**0.37**	
						Bond Dissociation Energy	**89.62**	**90.13**	**90.70**	**90.90**	
CC(=O)CCJ System											
CC(=O)CCJ	+	CH_3CH_3	→	CC(=O)CC	+	CH_3CJH_2	-7.97	-7.91	-7.54	-7.56	0.23
CC(=O)CCJ	+	$CH_3CH_2CH_3$	→	CC(=O)CC	+	CH_3CJHCH_3	-6.58	-6.62	-7.29	-7.75	0.23
CC(=O)CCJ	+	$(CH_3)_3CH$	→	CC(=O)CC	+	$(CH_3)_3CJ$	-5.64	-5.84	-7.72	-8.53	0.23
CC(=O)CCJ	+	$CH_3CH_2CH_2CH_3$	→	CC(=O)CC	+	$CH_3CJHCH_2CH_3$	-7.19	-7.13	-7.90	-8.38	0.27
						Average	**-6.85**	**-6.87**	**-7.61**	**-8.06**	**0.24**
						Method Std Dev		**0.86**		**0.43**	
						Bond Dissociation Energy	**102.52**	**102.50**	**101.76**	**101.31**	
CJCC(=O)CC System											
CJCC(=O)CC	+	CH_3CH_3	→	CCC(=O)CC	+	CH_3CJH_2	-13.21	-13.14	-12.81	-12.79	0.23
CJCC(=O)CC	+	$CH_3CH_2CH_3$	→	CCC(=O)CC	+	CH_3CJHCH_3	-11.82	-11.84	-12.56	-12.98	0.23
CJCC(=O)CC	+	$(CH_3)_3CH$	→	CCC(=O)CC	+	$(CH_3)_3CJ$	-10.88	-11.07	-12.99	-13.77	0.23
CJCC(=O)CC	+	$CH_3CH_2CH_2CH_3$	→	CCC(=O)CC	+	$CH_3CJHCH_2CH_3$	-12.43	-12.35	-13.16	-13.61	0.27
						Average	**-12.08**	**-12.10**	**-12.88**	**-13.29**	**0.24**
						Method Std Dev		**0.86**		**0.41**	
						Bond Dissociation Energy	**102.51**	**102.50**	**101.71**	**101.31**	

Table 4.3 Isodesmic Work Reactions, Calculated $\Delta H^{\circ}_{f\,298}$, and Bond Dissociation Energies for Ketone Radical Species (Continued A)

Isodesmic Reactions							$\Delta H^{\circ}_{f\,298}$ (kcal mol^{-1}) B3LYP 6-31G(d,p)	$\Delta H^{\circ}_{f\,298}$ (kcal mol^{-1}) B3LYP 6-311G(2d,2p)	$\Delta H^{\circ}_{f\,298}$ (kcal mol^{-1}) CBS-QB3	$\Delta H^{\circ}_{f\,298}$ (kcal mol^{-1}) G3MP2B3	Average Reference Species Uncertainty
CCJC(=O)CC System											
CCJC(=O)CC	+	CH_3CH_3	→	CCC(=O)CC	+	CH_3CJH_2	-26.12	-25.49	-23.76	-23.10	0.23
CCJC(=O)CC	+	$CH_3CH_2CH_3$	→	CCC(=O)CC	+	CH_3CJHCH_3	-24.73	-24.20	-23.51	-23.29	0.23
CCJC(=O)CC	+	$(CH_3)_3CH$	→	CCC(=O)CC	+	$(CH_3)_3CJ$	-23.80	-23.42	-23.93	-24.07	0.23
CCJC(=O)CC	+	$CH_3CH_2CH_2CH_3$	→	CCC(=O)CC	+	$CH_3CJHCH_2CH_3$	-25.34	-24.71	-24.11	-23.91	0.27
						Average	**-25.00**	**-24.46**	**-23.83**	**-23.59**	**0.24**
						Method Std Dev		**0.91**		**0.37**	
						Bond Dissociation Energy	**89.60**	**90.14**	**90.77**	**91.00**	
***n*-CJC(=O)CCC System**											
n-CJC(=O)CCC	+	CH_3CH_3	→	*n*-CC(=O)CCC	+	CH_3CJH_2	-19.31	-18.66	-18.35	-17.92	0.23
n-CJC(=O)CCC	+	$CH_3CH_2CH_3$	→	*n*-CC(=O)CCC	+	CH_3CJHCH_3	-17.91	-17.37	-18.10	-18.11	0.23
n-CJC(=O)CCC	+	$(CH_3)_3CH$	→	*n*-CC(=O)CCC	+	$(CH_3)_3CJ$	-16.98	-16.59	-18.53	-18.90	0.23
n-CJC(=O)CCC	+	$CH_3CH_2CH_2CH_3$	→	*n*-CC(=O)CCC	+	$CH_3CJHCH_2CH_3$	-18.52	-17.88	-18.70	-18.74	0.27
						Average	**-18.18**	**-17.63**	**-18.42**	**-18.42**	**0.24**
						Method Std Dev		**0.91**		**0.35**	
						Bond Dissociation Energy	**95.87**	**96.42**	**95.63**	**95.63**	
***n*-CC(=O)CJCC System**											
n-CC(=O)CJCC	+	CH_3CH_3	→	*n*-CC(=O)CCC	+	CH_3CJH_2	-25.05	-24.52	-22.86	-22.15	0.23
n-CC(=O)CJCC	+	$CH_3CH_2CH_3$	→	*n*-CC(=O)CCC	+	CH_3CJHCH_3	-23.65	-23.23	-22.62	-22.34	0.23
n-CC(=O)CJCC	+	$(CH_3)_3CH$	→	*n*-CC(=O)CCC	+	$(CH_3)_3CJ$	-22.72	-22.46	-23.04	-23.12	0.23
n-CC(=O)CJCC	+	$CH_3CH_2CH_2CH_3$	→	*n*-CC(=O)CCC	+	$CH_3CJHCH_2CH_3$	-24.26	-23.74	-23.22	-22.97	0.27
						Average	**-23.92**	**-23.49**	**-22.93**	**-22.65**	**0.24**
						Method Std Dev		**0.89**		**0.39**	
						Bond Dissociation Energy	**90.13**	**90.56**	**91.12**	**91.41**	
***n*-CC(=O)CCJC System**											
n-CC(=O)CCJC	+	CH_3CH_3	→	*n*-CC(=O)CCC	+	CH_3CJH_2	-16.78	-16.61	-15.18	-14.76	0.23
n-CC(=O)CCJC	+	$CH_3CH_2CH_3$	→	*n*-CC(=O)CCC	+	CH_3CJHCH_3	-15.38	-15.32	-14.94	-14.95	0.23
n-CC(=O)CCJC	+	$(CH_3)_3CH$	→	*n*-CC(=O)CCC	+	$(CH_3)_3CJ$	-14.45	-14.54	-15.36	-15.73	0.23
n-CC(=O)CCJC	+	$CH_3CH_2CH_2CH_3$	→	*n*-CC(=O)CCC	+	$CH_3CJHCH_2CH_3$	-15.99	-15.83	-15.54	-15.58	0.27
						Average	**-15.65**	**-15.57**	**-15.25**	**-15.26**	**0.24**
						Method Std Dev		**0.86**		**0.35**	
						Bond Dissociation Energy	**98.40**	**98.48**	**98.80**	**98.80**	

Table 4.3 Isodesmic Work Reactions, Calculated $\Delta H^{\circ}_{f\,298}$, and Bond Dissociation Energies for Ketone Radical Species (Continued B)

Isodesmic Reactions							$\Delta H^{\circ}_{f\,298}$ (kcal mol^{-1}) B3LYP 6-31G(d,p)	$\Delta H^{\circ}_{f\,298}$ (kcal mol^{-1}) B3LYP 6-311G(2d,2p)	$\Delta H^{\circ}_{f\,298}$ (kcal mol^{-1}) CBS-QB3	$\Delta H^{\circ}_{f\,298}$ (kcal mol^{-1}) G3MP2B3	Average Reference Species Uncertainty
***n*-CC(=O)CCCJ System**											
n-CC(=O)CCCJ	+	CH_3CH_3	→	*n*-CC(=O)CCC	+	CH_3CJH_2	-12.78	-12.82	-12.66	-12.59	0.23
n-CC(=O)CCCJ	+	$CH_3CH_2CH_3$	→	*n*-CC(=O)CCC	+	CH_3CJHCH_3	-11.38	-11.52	-12.41	-12.78	0.23
n-CC(=O)CCCJ	+	$(CH_3)_3CH$	→	*n*-CC(=O)CCC	+	$(CH_3)_3CJ$	-10.45	-10.75	-12.84	-13.57	0.23
n-CC(=O)CCCJ	+	$CH_3CH_2CH_2CH_3$	→	*n*-CC(=O)CCC	+	$CH_3CJHCH_2CH_3$	-11.99	-12.03	-13.01	-13.41	0.27
						Average	**-11.65**	**-11.78**	**-12.73**	**-13.09**	**0.24**
						Method Std Dev		**0.86**		**0.40**	
						Bond Dissociation Energy	**102.40**	**102.27**	**101.32**	**100.96**	
CJC(=O)C(C)C System											
CJC(=O)C(C)C	+	CH_3CH_3	→	CC(=O)C(C)C	+	CH_3CJH_2	-20.69	-20.08	-19.49	-18.85	0.23
CJC(=O)C(C)C	+	$CH_3CH_2CH_3$	→	CC(=O)C(C)C	+	CH_3CJHCH_3	-19.29	-18.79	-19.24	-19.04	0.23
CJC(=O)C(C)C	+	$(CH_3)_3CH$	→	CC(=O)C(C)C	+	$(CH_3)_3CJ$	-18.36	-18.01	-19.66	-19.82	0.23
CJC(=O)C(C)C	+	$CH_3CH_2CH_2CH_3$	→	CC(=O)C(C)C	+	$CH_3CJHCH_2CH_3$	-19.90	-19.30	-19.84	-19.67	0.27
						Average	**-19.56**	**-19.04**	**-19.56**	**-19.34**	**0.24**
						Method Std Dev		**0.90**		**0.37**	
						Bond Dissociation Energy	**95.41**	**95.93**	**95.41**	**95.63**	
CC(=O)CJ(C)C System											
CC(=O)CJ(C)C	+	CH_3CH_3	→	CC(=O)C(C)C	+	CH_3CJH_2	-31.21	-30.35	-27.69	-26.75	0.23
CC(=O)CJ(C)C	+	$CH_3CH_2CH_3$	→	CC(=O)C(C)C	+	CH_3CJHCH_3	-29.82	-29.06	-27.44	-26.94	0.23
CC(=O)CJ(C)C	+	$(CH_3)_3CH$	→	CC(=O)C(C)C	+	$(CH_3)_3CJ$	-28.88	-28.28	-27.87	-27.72	0.23
CC(=O)CJ(C)C	+	$CH_3CH_2CH_2CH_3$	→	CC(=O)C(C)C	+	$CH_3CJHCH_2CH_3$	-30.43	-29.57	-28.04	-27.57	0.27
						Average	**-30.08**	**-29.31**	**-27.76**	**-27.25**	**0.24**
						Method Std Dev		**0.95**		**0.45**	
						Bond Dissociation Energy	**84.89**	**85.66**	**87.21**	**87.73**	
CC(=O)C(C)CJ System											
CC(=O)C(C)CJ	+	CH_3CH_3	→	CC(=O)C(C)C	+	CH_3CJH_2	-14.47	-14.43	-13.76	-13.58	0.23
CC(=O)C(C)CJ	+	$CH_3CH_2CH_3$	→	CC(=O)C(C)C	+	CH_3CJHCH_3	-13.08	-13.14	-13.51	-13.77	0.23
CC(=O)C(C)CJ	+	$(CH_3)_3CH$	→	CC(=O)C(C)C	+	$(CH_3)_3CJ$	-12.14	-12.36	-13.94	-14.56	0.23
CC(=O)C(C)CJ	+	$CH_3CH_2CH_2CH_3$	→	CC(=O)C(C)C	+	$CH_3CJHCH_2CH_3$	-13.69	-13.65	-14.11	-14.40	0.27
						Average	**-13.35**	**-13.39**	**-13.83**	**-14.08**	**0.24**
						Method Std Dev		**0.86**		**0.38**	
						Bond Dissociation Energy	**101.63**	**101.58**	**101.14**	**100.89**	

Table 4.3 Isodesmic Work Reactions, Calculated $\Delta H^{\circ}_{f\,298}$, and Bond Dissociation Energies for Ketone Radical Species (Continued C)

Isodesmic Reactions							$\Delta H^{\circ}_{f\,298}$ (kcal mol^{-1}) B3LYP 6-31G(d,p)	$\Delta H^{\circ}_{f\,298}$ (kcal mol^{-1}) B3LYP 6-311G(2d,2p)	$\Delta H^{\circ}_{f\,298}$ (kcal mol^{-1}) CBS-QB3	$\Delta H^{\circ}_{f\,298}$ (kcal mol^{-1}) G3MP2B3	Average Reference Species Uncertainty
CJC(C)C(=O)CC System											
CJC(C)C(=O)CC	+	CH_3CH_3	→	CC(C)C(=O)CC	+	CH_3CJH_2	-19.82	-19.78	-19.16	-18.98	0.20
CJC(C)C(=O)CC	+	$CH_3CH_2CH_3$	→	CC(C)C(=O)CC	+	CH_3CJHCH_3	-18.42	-18.49	-18.92	-19.16	0.20
CJC(C)C(=O)CC	+	$(CH_3)_3CH$	→	CC(C)C(=O)CC	+	$(CH_3)_3CJ$	-17.49	-17.71	-19.34	-19.95	0.20
CJC(C)C(=O)CC	+	$CH_3CH_2CH_2CH_3$	→	CC(C)C(=O)CC	+	$CH_3CJHCH_2CH_3$	-19.04	-19.00	-19.52	-19.79	0.23
						Average	**-18.69**	**-18.75**	**-19.24**	**-19.47**	**0.21**
						Method Std Dev		**0.86**		**0.37**	
						Bond Dissociation Energy	**101.72**	**101.66**	**101.17**	**100.94**	
CCJ(C)C(=O)CC System											
CCJ(C)C(=O)CC	+	CH_3CH_3	→	CC(C)C(=O)CC	+	CH_3CJH_2	-36.26	-35.38	-32.81	-31.83	0.20
CCJ(C)C(=O)CC	+	$CH_3CH_2CH_3$	→	CC(C)C(=O)CC	+	CH_3CJHCH_3	-34.86	-34.08	-32.56	-32.01	0.20
CCJ(C)C(=O)CC	+	$(CH_3)_3CH$	→	CC(C)C(=O)CC	+	$(CH_3)_3CJ$	-33.93	-33.31	-32.99	-32.80	0.20
CCJ(C)C(=O)CC	+	$CH_3CH_2CH_2CH_3$	→	CC(C)C(=O)CC	+	$CH_3CJHCH_2CH_3$	-35.47	-34.59	-33.16	-32.64	0.23
						Average	**-35.13**	**-34.34**	**-32.88**	**-32.32**	**0.21**
						Method Std Dev		**0.96**		**0.46**	
						Bond Dissociation Energy	**85.28**	**86.07**	**87.53**	**88.09**	
CC(C)C(=O)CJC System											
CC(C)C(=O)CJC	+	CH_3CH_3	→	CC(C)C(=O)CC	+	CH_3CJH_2	-32.43	-31.86	-29.92	-29.04	0.20
CC(C)C(=O)CJC	+	$CH_3CH_2CH_3$	→	CC(C)C(=O)CC	+	CH_3CJHCH_3	-31.03	-30.56	-29.67	-29.23	0.20
CC(C)C(=O)CJC	+	$(CH_3)_3CH$	→	CC(C)C(=O)CC	+	$(CH_3)_3CJ$	-30.10	-29.79	-30.10	-30.01	0.20
CC(C)C(=O)CJC	+	$CH_3CH_2CH_2CH_3$	→	CC(C)C(=O)CC	+	$CH_3CJHCH_2CH_3$	-31.64	-31.07	-30.27	-29.86	0.23
						Average	**-31.30**	**-30.82**	**-29.99**	**-29.54**	**0.21**
						Method Std Dev		**0.90**		**0.43**	
						Bond Dissociation Energy	**89.11**	**89.59**	**90.42**	**90.87**	
CC(C)C(=O)CCJ System											
CC(C)C(=O)CCJ	+	CH_3CH_3	→	CC(C)C(=O)CC	+	CH_3CJH_2	-19.10	-19.03	-18.69	-18.67	0.20
CC(C)C(=O)CCJ	+	$CH_3CH_2CH_3$	→	CC(C)C(=O)CC	+	CH_3CJHCH_3	-17.70	-17.74	-18.44	-18.85	0.20
CC(C)C(=O)CCJ	+	$(CH_3)_3CH$	→	CC(C)C(=O)CC	+	$(CH_3)_3CJ$	-16.77	-16.96	-18.87	-19.64	0.20
CC(C)C(=O)CCJ	+	$CH_3CH_2CH_2CH_3$	→	CC(C)C(=O)CC	+	$CH_3CJHCH_2CH_3$	-18.32	-18.25	-19.04	-19.48	0.23
						Average	**-17.97**	**-18.00**	**-18.76**	**-19.16**	**0.21**
						Method Std Dev		**0.86**		**0.41**	
						Bond Dissociation Energy	**102.44**	**102.41**	**101.65**	**101.25**	

4.4.1 Heat of Formation $\Delta H^{\circ}_{f\,298}$

A summary of the $\Delta H^{\circ}_{f\,298}$ averages from the DFT and composite methods for parent and radical ketones from the work reactions in Tables 4.2 and 4.3 is summarized in Table 4.4 and Figure 4.1. Evaluation of the error for these standard enthalpies is provided in several ways. Tables 4.2 and 4.3 list the average reference species uncertainty along with the standard deviation from the calculated $\Delta H^{\circ}_{f\,298}$ values from the DFT and the combined CBS-QB3 and G3MP2B3 work reactions. In addition, standard deviations for five reference reactions, Scheme 4.2, involving standard species with known enthalpies, given in Table 4.1, are determined from the difference of the literature versus calculated $\Delta H^{\circ}_{reaction}$ values. The resulting standard deviations from the reference reactions show an average of 1.2 and 0.4 kcal mol^{-1} for the DFT and composite methods, respectively. These standard deviations coincide with the average standard deviations, on a per work reaction basis, determined in Tables 4.2 and 4.3. Values from Scheme 4.2 are recommended for evaluation of accuracy and note that the uncertainty in the reference species also needs to be considered.

On the basis of the correlations in these different techniques, error values are provided in Table 4.4 using the standard deviation from the individual calculated $\Delta H^{\circ}_{f\,298}$ values.

Table 4.4 Summary of Average $\Delta H^{\circ}_{f\,298}$ and Bond Dissociation Energies[a]

Species	DFT		CBS-QB3/G3MP2B3	
	$\Delta H^{\circ}_{f\,298}$	C–H BDE	$\Delta H^{\circ}_{f\,298}$	C–H BDE
CC(=O)CC	-57.4 ± 0.4	-	-57.3 ± 0.2	-
CJC(=O)CC	-13.2 ± 0.9	96.2	-13.7 ± 0.4	95.6
CC(=O)CJC	-19.5 ± 0.9	89.9	-18.6 ± 0.4	90.8
CC(=O)CCJ	-6.9 ± 0.9	102.5	-7.8 ± 0.4	101.5
CCC(=O)CC	-62.4 ± 0.3	-	-62.5 ± 0.2	-
CJCC(=O)CC	-12.1 ± 0.9	102.5	-13.1 ± 0.4	101.5
CCJC(=O)CC	-24.7 ± 0.9	89.9	-23.7 ± 0.4	90.9
n-CC(=O)CCC	-61.8 ± 0.3	-	-62.0 ± 0.2	-
n-CJC(=O)CCC	-17.9 ± 0.9	96.1	-18.4 ± 0.4	95.6
n-CC(=O)CJCC	-23.7 ± 0.9	90.3	-22.8 ± 0.4	91.3
n-CC(=O)CCJC	-15.6 ± 0.9	98.4	-15.3 ± 0.4	98.8
n-CC(=O)CCCJ	-11.7 ± 0.9	102.3	-12.9 ± 0.4	101.1
CC(=O)C(C)C	-61.2 ± 0.3	-	-62.9 ± 0.2	-
CJC(=O)C(C)C	-19.3 ± 0.9	95.7	-19.4 ± 0.4	95.5
CC(=O)CJ(C)C	-29.7 ± 1.0	85.3	-27.5 ± 0.4	87.5
CC(=O)C(C)CJ	-13.4 ± 0.9	101.6	-14.0 ± 0.4	101.0
CC(C)C(=O)CC	-66.9 ± 0.9	-	-68.3 ± 0.1	-
CJC(C)C(=O)CC	-18.7 ± 0.9	101.7	-19.4 ± 0.4	101.1
CCJ(C)C(=O)CC	-34.7 ± 1.0	85.7	-32.6 ± 0.5	87.8
CC(C)C(=O)CJC	-31.1 ± 0.9	89.3	-29.8 ± 0.4	90.6
CC(C)C(=O)CCJ	-18.0 ± 0.9	102.4	-19.0 ± 0.4	101.4

[a] Units kcal mol^{-1}. Error is standard deviation from work reaction tables; see also Scheme 4.2 for error analysis on reference reactions and Table 4.1 for reference species uncertainties.

Scheme 4.2 Reference Reactions for Comparison of Literature and Calculated $\Delta H^{\circ}_{reaction}$ Values

Reference Reactions							Literature Values	$\Delta H^{\circ}_{reaction}$ (kcal mol^{-1}) B3LYP 6-31G(d,p)	B3LYP 6-311G(2d,2p)	CBS-QB3	G3MP2B3
CC(=O)CJ	+	CH_4	→	CC(=O)C	+	CJH_3	9.30	11.15	10.43	9.18	8.31
CC(=O)CJ	+	CH_3CH_3	→	CC(=O)C	+	CH_3CJH_2	5.40	6.38	5.71	5.47	5.04
CC(=O)CJ	+	$CH_3CH_2CH_3$	→	CC(=O)C	+	CH_3CJHCH_3	2.90	2.47	1.91	2.71	2.71
CC(=O)CJ	+	$(CH_3)_3CH$	→	CC(=O)C	+	$(CH_3)_3CJ$	0.80	-0.61	-1.02	0.99	1.35
CC(=O)CJ	+	$CH_3CH_2CH_2CH_3$	→	CC(=O)C	+	$CH_3CJHCH_2CH_3$	2.50	2.71	2.03	2.94	2.96
						Method Std Dev		**1.20**		**0.44**	

These data demonstrate good agreement for the $\Delta H^{\circ}_{f\,298}$ values between the DFT and the higher level methods, which results from the use of work reactions. The parent ketones show an average difference of 0.7 kcal mol^{-1}. The maximum difference is 0.2 kcal mol^{-1} for the smaller ketones (2-butanone, 3-pentanone, and 2-pentanone) which shows that DFT provides an acceptable analysis compared to the higher level calculation methods. For the two larger ketones, the average difference increases to 1.7 and 1.4 kcal mol^{-1}, which supports the known problems of additive errors in DFT methods;[73,174] this should be considered in applying these time and computational resource effective DFT methods.

The radical compounds have an average enthalpy difference of 1.0 kcal mol^{-1}. If CC(=O)CJ(C)C and CCJ(C)C(=O)CC are removed, which have differences over 2 kcal mol^{-1} from consideration, the average difference is reduced to 0.8 kcal mol^{-1}. Calculated $\Delta H^{\circ}_{f\,298}$ values are recommended from the average of the CBS-QB3 and G3MP2B3 levels of theory for all of the parent and radical ketone species, which are summarized in Figure 4.1 and Table 4.4.

Table 4.5 shows a comparison of the recommended $\Delta H^{\circ}_{f\,298}$ values to literature values. Literature values for all of the parent ketones are shown, but only values for 2-butanone and 3-pentanone radicals are found in the literature for comparison.

Table 4.5 Comparison of $\Delta H^{\circ}_{f\,298}$ and Carbon-Hydrogen Bond Dissociation Energy for Ketones and Radicals to Literature Values

Species	$\Delta H^{\circ}_{f\,298}$ (kcal mol^{-1})		Ref.	C–H BDE (kcal mol^{-1})		Ref.
	This Study	Literature		This Study	Literature	
CC(=O)CC	-57.3	-57.02 ± 0.20	169			
		-57.05 ± 0.23	*a*			
		-56.90	175			
		-57.0 ± 0.2	120			
		-56.88[b]	151			
CJC(=O)CC	-13.7	-14.60[b]	151	95.6	96.5	160
		-13.3	157		95.48[b]	151
					95.8	157
					95.55	152
CC(=O)CJC	-18.6	-17.08[b]	151	90.8	92.3	176
		-18.6	157		93.2	160
					93.8	177
					91.3	178
					90.3	157
					90.50[b]	151
					90.29	152
CC(=O)CCJ	-7.8	-7.88[b]	151	101.5	101.09[b]	151
		-7.2	157		102.1	157
					100.65	152
CCC(=O)CC	-62.5	-61.65 ± 0.20	172			
		-62.25 ± 0.39	*a*			
		-62.20[b]	150			
CJCC(=O)CC	-13.1	-13.20[b]	150	101.5	101.8	157
		-11.8	157			
CCJC(=O)CC	-23.7	-18.25[b]	150	90.9	93.4	160
		-22.7	157		94.8	177
					88.4	166
					90.8	157
					88	158
n-CC(=O)CCC	-62.0	-61.91 ± 0.26	172			
		-61.9 ± 0.2	120			
CC(=O)C(C)C	-62.9	-62.76 ± 0.21	172			
CC(C)C(=O)CC	-68.3	-68.4 ± 0.2	179			
		-68.4 ± 0.2	120			

[a] Reported on NIST WebBook as the reanalyzed value of Ref. 170 by Ref. 171.
[b] Values calculated using group additivity.

2-Butanone is the smallest ketone analyzed, and the calculated value of -57.3 kcal mol^{-1} has a maximum derivation of 0.4 kcal mol^{-1} of the reported literature values. Literature values are reported for 2-butanone radicals for comparison along with values determined using group additivity (GA) and hydrogen-bond increment (HBI) methods.[100,102] When comparing calculated values to the literature values for the three radical sites on 2-butanone, there is very good agreement with a maximum difference of only 0.6 kcal mol^{-1}. However, the current group additivity for the two radical sites adjacent to the carbonyl range in difference between 0.9-1.5 kcal mol^{-1}.

The calculated value of -62.5 kcal mol^{-1} for 3-pentanone also shows agreement below 0.9 kcal mol^{-1} to the reported literature value. The primary methyl radical CJCC(=O)CC, where the methyl is not adjacent to the carbonyl group, is also within 1.3 kcal mol^{-1} of the reported GA and literature values. There is, however, an approximately 7 kcal mol^{-1} wide range in the reported bond energies for the secondary radical CCJC(=O)CC which creates a 5 kcal mol^{-1} difference in the calculated $\Delta H^{\circ}_{f\ 298}$ value compared to the GA hydrogen-bond increment value, while only a 1 kcal mol^{-1} difference from one recent literature value. The data suggests the previous estimates of secondary bond dissociation energies adjacent to the carbonyl group in ketones are high and that kinetic estimates to C–H bond scission and abstraction are underestimated. New group additivity data for the ketone radicals are provided below.

Calculated $\Delta H^{\circ}_{f\ 298}$ values for the other three ketone parent species are below 0.2 kcal mol^{-1}, which is well within chemical accuracy of 1 kcal mol^{-1}. Due to the close agreement between the CBS-QB3 and G3MP2B3 $\Delta H^{\circ}_{f\ 298}$ values, the average $\Delta H^{\circ}_{f\ 298}$ values from these methods are recommended.

4.4.2 Carbon-Hydrogen Bond Dissociation Energies (C–H BDEs)

C–H BDEs are computed from the work reactions listed in Table 4.3. The calculated $\Delta H^{\circ}_{f\ 298}$ of the parent and radical molecules are combined with the well-established literature value of 52.10 kcal mol^{-1} for the hydrogen atom.[83]

Primary C–H BDEs for ethane, *n*-propane, and *n*-butane have been previously shown by multiple studies to be in the 100.5-101 kcal mol^{-1} range.[121,126,127] These studies also all report similarly lower values for secondary C–H BDEs of approximately 98.5 kcal mol^{-1} for *n*-propane and *n*-butane. The standard tertiary C–H BDE of 96.5 kcal mol^{-1} is averaged from *t*-butyl reported values which range 95.7-97.2 kcal mol^{-1}.[121,126,128] Calculated C–H BDEs for the ketones in this study from the DFT and higher level calculations are listed in Table 4.4 with the recommended values from the average of the CBS-QB3 and G3MP2B3 methods in Figure 4.1.

Analysis of the BDE for these ketones can be broken down into five bond types or classes:

1. primary,
2. primary adjacent to the carbonyl,
3. secondary,
4. secondary adjacent to the carbonyl,
5. tertiary adjacent to the carbonyl.

Table 4.6 summarizes these different bond classes for each parent compound where there is consistency for each bond type. Recent theoretical and experimental studies for the C–H BDEs in acetone are also included for comparison.

Table 4.6 Summary of Carbon-Hydrogen Bond Dissociation Energies[a,b] for Non-Cyclic Ketone Radical Species

Species	Carbon-Hydrogen Bond Dissociation Classes				
	Primary	**Primary Adjacent to Carbonyl**	**Secondary**	**Secondary Adjacent to Carbonyl**	**Tertiary Adjacent to Carbonyl**
CC(=O)C		96 ± 1[c]			
CC(=O)CC	101.5	95.6		90.8	
CCC(=O)CC	101.5			90.9	
n-CC(=O)CCC	101.1	95.6	98.8	91.3	
CC(=O)C(C)C	101.0	95.5			87.5
CC(C)C(=O)CC	101.1, 101.4			90.6	87.8

[a] Recommended values from CBS-QB3/G3MP2B3 average.
[b] Units kcal mol^{-1}.
[c] Average of available literature values from Ref. 157,159,160, and 164.

Primary C–H positions have at least one carbon atom between the primary carbon and the carbonyl group. BDEs for these ketones provide a tight range from 101.0-101.5 kcal mol^{-1} from primary methyl groups in six different locations with various other effects from each parent. This provides a good distribution where these six C–H BDEs are near identical strength to those in *n*-alkanes of 101.1 kcal mol^{-1}.

Bond energies decrease by about 6 kcal mol^{-1} for the three species that have primary groups directly adjacent to the carbonyl group. The determined values are 95.5-95.6 kcal mol^{-1} and compare with the C–H BDE of acetone. This lower bond energy results from resonance with the carbonyl group.

The secondary bond energies on carbons adjacent to the carbonyl are another 4-5 kcal mol^{-1} lower at 90.6-91.3 kcal mol^{-1}. Overall, this is an 8 kcal mol^{-1} bond energy reduction from an alkane secondary carbon. There is only one secondary carbon that is at one or more carbons removed from the carbonyl group, *n*-CC(=O)CCJC, which has a normal secondary bond energy of 98.8 kcal mol^{-1}.

Tertiary bond energies adjacent to the carbonyl are also strongly influenced with lower bond energies of 87.5 and 87.8 kcal mol^{-1}, 9 kcal mol^{-1} lower than the 96.5 kcal mol^{-1} commonly observed for an alkyl tertiary bond.

Comparison of the calculated BDEs to literature values is limited to 2-butanone and 3-pentanone and presented in Table 4.5. The bond energies for CJC(=O)CC and CC(=O)CCJ are within approximately 0.2 kcal mol^{-1} to the averages of the GA and literature values while there is a difference of approximately 0.9 kcal mol^{-1} for CC(=O)CJC. There is an 88-94.8 kcal mol^{-1} range of values for CCJC(=O)CC from 3-pentanone in the literature; the calculated value of 90.9 kcal mol^{-1} falls within. The calculated value for the primary methyl on CJCC(=O)CC is within 0.3 kcal mol^{-1} of the literature value.

Figure 4.1 and Table 4.4 have the recommended bond energies from the average of the CBS-QB3 and G3MP2B3 levels of theory.

4.4.3 Internal Rotors

Potential energy curves for internal rotations within the parent and radical species are calculated using the B3LYP/6-31G(d,p) level of theory. Relaxed scans at 10° intervals are used to determine the lowest energy geometries. If a lower energy conformation is found, previous scans are re-run to insure the lowest energy conformation is located. These potential energy curves are also used to determine entropy and heat capacity internal rotational contributions.

All of the parent ketone terminal methyl (not adjacent to the carbonyl) groups, exhibit three-fold symmetry with energy barriers between 2-3 kcal mol^{-1}. The three-fold barriers are 0.5 kcal mol^{-1} for methyl rotations adjacent to the carbonyl group. Upon

radical formation at the methyl site, there is a decrease to two-fold symmetry and a decrease in the barrier energy ranging from below 0.1 to 3.0 kcal mol^{-1} except for the groups adjacent to the carbonyl. Radical sites adjacent to the carbonyl group, regardless of primary, secondary, or tertiary location, have energy barriers over 10 kcal mol^{-1} upon radical formation resulting from the resonance with the carbonyl group.

A comparison of the calculated barrier heights to those of Nickerson et al.[180] and Sinke et al.[175] is illustrated in Figure 4.2. Overall, there is reasonable agreement for the ethyl and methyl rotations adjacent to the carbonyl. There are slightly larger deviations between the values with the terminal methyl group barrier. There is a 1 kcal mol^{-1} range in the values for the terminal methyl group on 2-butanone. The B3LYP calculations show 1.98 kcal mol^{-1}, while Nickerson and Sinke determined 2.4 and 2.95 kcal mol^{-1}, respectively, which are typical barrier heights for terminal methyl rotation.[181-184] While relaxed scans are needed to determine the lowest energy configuration, they do not necessarily represent the accurate internal rotation barrier.

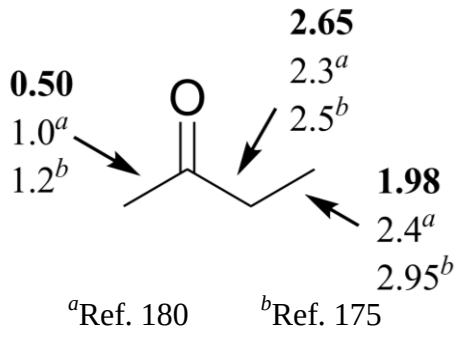

Figure 4.2 Comparison of calculated rotational barriers to literature values for 2-butanone.

4.4.4 Entropies (*S(T)*) and Heat Capacities ($C_p(T)$)

Contributions from each compound's translations, vibration frequencies, and external rotations, represented as TVR, are calculated using the rigid-rotor harmonic-oscillator approximation SMCPS[98] code with the zero-point vibration energies (ZPVE) scaled by 0.9806 for B3LYP/6-31G(d,p) as recommended by Scott and Radom.[99] The optical isomers' contribution to entropy for the radicals CC(=O)C(C)CJ and CJC(C)C(=O)CC code resulting from the chiral center created at the tertiary carbon center upon methyl radical formation are included in the SMCPS calculation.

The contributions from internal rotations, represented by IR, are determined using the calculated potential energy rotational barriers, moments of inertia for each group in the rotor, and barrier foldness. Internal rotor torsion frequencies, including terminal methyl groups, are identified using visual inspection in GaussView and removed from vibration contribution. In cases where identification of a frequency is uncertain due to coupling to other motions, the lower frequency is selected. These are replaced with entropy and heat capacity contributions from the Pitzer and Gwinn method for hindered rotor analysis. Use of the Pitzer and Gwinn methods is described in detail in Ref. 100.

Table 4.7 illustrates results from several different models for inclusion of internal rotor versus torsion frequency contributions; it also provides comparison with experimental data for the species where it is available. Entropy and heat capacities for acetone CC(=O)C are also calculated to show the agreement to other available values. Values from the group additivity (GA) method are also included which coincide well with the experimental data providing some support for considering the GA data as reference in the comparisons.

Table 4.7 Comparison of Entropy and Heat Capacities for Ketone Parent Species to Other Available Methods

Species	S°_{298}[a]	$C_p(T)$[a]							Method	Rotors
		300 K	400 K	500 K	600 K	800 K	1000 K	1500 K		
CC(=O)C	70.09	17.97	22.00	25.89	29.34	34.93	39.15	45.26	GA	
σ = 18	70.49	17.97	22.00	25.89	29.34	34.93	39.15		Ref 185	
	71.72								Gaussian	0[b]
	70.67	17.51	21.47	25.26	28.61	34.02	38.12	44.56	SMCPS + VIBIR	2[d]
CC(=O)CC	80.88	23.47	28.95	34.14	38.69	46.00	51.49	59.46	GA	
σ = 9	80.81	24.68	29.81	34.76	39.09	46.08	51.33		Ref 185	
	81.11	24.78	29.87	34.72	39.02	46.00	51.26	59.41	Ref 169	
	80.60								Gaussian	0[b]
	80.55	23.74	29.51	34.89	39.58	47.07	52.66	61.36	SMCPS	0[b]
	77.68	22.99	28.48	33.63	38.15	45.43	50.90	59.49	SMCPS + VIBIR	2[c]
	81.58	23.47	28.75	33.68	38.00	45.00	50.30	58.68	SMCPS + VIBIR	3[d]
CCC(=O)CC	89.29	30.37	37.40	43.29	48.34	57.13	63.55	73.40	GA	
σ = 18	86.37								Gaussian	0[b]
	86.30	28.60	35.93	42.79	48.75	58.23	65.28	76.21	SMCPS	0[b]
	81.69	28.72	35.63	42.09	47.76	56.88	63.72	74.43	SMCPS + VIBIR	2[c]
	89.58	29.63	36.10	42.10	47.37	55.95	62.47	72.79	SMCPS + VIBIR	4[d]

[a] Units cal mol^{-1} K^{-1}.
[b] No rotors. Use of torsion frequencies for rotor contributions without reduction (correction) in entropy for equivalent hydrogen atoms in CH_3 groups.
[c] Only methyl rotors.
[d] All internal rotors.

Table 4.7 Comparison of Entropy and Heat Capacities for Ketone Parent Species to Other Available Methods (Continued)

Species	S°_{298} [a]	$C_p(T)$ [a]							Method	Rotors
		300 K	400 K	500 K	600 K	800 K	1000 K	1500 K		
n-CC(=O)CCC	90.48	29.67	36.65	42.84	48.19	57.10	63.69	73.53	GA	
σ = 9	89.91	29.06	36.42	42.80	48.62	57.13	63.61		Ref 185	
	88.37								Gaussian	0[b]
	88.31	28.60	35.95	42.81	48.78	58.26	65.31	76.24	SMCPS	0[b]
	84.14	27.95	35.23	41.94	47.73	56.94	63.80	74.49	SMCPS + VIBIR	2[c]
	90.41	28.67	35.84	42.32	47.83	56.51	62.98	73.12	SMCPS + VIBIR	4[d]
CC(=O)C(C)C	87.99	28.32	35.75	42.63	48.32	57.41	64.11	74.13	GA	
σ = 27	85.53								Gaussian	0[b]
	85.46	29.10	36.37	43.13	49.01	58.37	65.35	76.21	SMCPS	0[b]
	83.52	28.82	35.83	42.23	47.74	56.56	63.20	73.64	SMCPS + VIBIR	3[c]
	88.70	29.06	35.71	41.86	47.22	55.85	62.40	72.74	SMCPS + VIBIR	4[d]
CC(C)C(=O)CC	97.59	34.52	43.45	51.33	57.82	68.51	76.31	88.20	GA	
σ = 27	93.02								Gaussian	0[b]
	92.95	33.95	42.79	51.02	58.17	69.53	77.97	91.07	SMCPS	0[b]
	88.42	34.49	42.93	50.62	57.29	67.96	75.98	88.57	SMCPS + VIBIR	3[c]
	96.40	35.00	43.09	50.59	57.14	67.64	75.46	87.58	SMCPS + VIBIR	5[d]

[a] Units cal mol^{-1} K^{-1}.
[b] No rotors. Use of torsion frequencies for rotor contributions without reduction (correction) in entropy for equivalent hydrogen atoms in CH_3 groups.
[c] Only methyl rotors.
[d] All internal rotors.

For this limited set of ketones, contributions to entropy and heat capacity from all of the internal rotors in each of the parent ketones need to be included in order to match the literature data from Stull.[185] In Table 4.7, entropy is significantly underestimated when only the low barrier methyl rotors are considered, in one case by more than 5 cal mol^{-1} K^{-1}, relative to the Stull data. There is much better agreement to Stull for acetone, 2-butanone, and 2-pentanone when all of the rotors are considered with maximum absolute differences of 0.8 cal mol^{-1} K^{-1} for S°_{298} and 1.2 cal mol^{-1} K^{-1} for $C_p(T)$ between 300 and 1000 K. Similar agreement for 2-butanone to data from Chao[169] is also observed.

Ketone sp^3 carbon bonds have lower barriers than those in alkane hydrocarbons, and these internal rotors should have important contributions, but there are also internal rotors in the larger ketones that have barriers higher than 6 kcal mol^{-1}. There are a number of studies on methods and the importance for calculating contributions from internal rotations to obtain more accurate entropies and heat capacity estimates.[89-96] Further analysis using several of these methods are a goal of future work.

It is known that a torsion frequency estimate of the contributions to heat capacity contribute a full R (ideal gas constant) to $C_p(T)$ at high temperatures, while a free rotor contributes only R/2. The computer code THERM,[105,106] which is often used to extrapolate $C_p(T)$ data to higher temperatures and generate NASA polynomials, allows one to incorporate the number of internal rotors in the target $C_p(T)_{(infinity)}$ value. This allows some adjustment for anharmonic effects by under-representing the number of rotors, one can add R/2 to $C_p(T)_{(infinity)}$, where each rotor omitted would be counted by

THERM as frequency contribution. Our recommendation is to underestimate the number of rotors contribution to $C_p(T)_{(infinity)}$ by one-half.

Entropies and heat capacities in the 100-5000 K temperature range for the ketone parents and radicals from B3LYP/6-31G(d,p) calculations are presented in Appendix C. For the radical ketone species, all of the single bond rotations are included except for the radical sites directly adjacent to the carbonyl group. The energy barriers for these primary, secondary, and tertiary locations are all in excess of 10 kcal mol^{-1} where contributions are treated as torsion frequencies. These barriers result from resonance between the radical site and the adjacent, electronegative carbonyl group. The resonance also accounts for the low bond dissociation energies. Potential barriers for rotors, where $S(T)$ and $C_p(T)$ values are determined from torsion frequencies, are denoted in the potential energy diagrams in Appendix C with asterisks.

4.4.5 Group Additivity (GA)

The group additivity (GA) method, as developed by Benson,[102] is a rapid estimation method for $\Delta H^{\circ}_{f\ 298}$, S°_{298}, and $C_p(T)$ of stable species. The hydrogen-bond increment method (HBI) for group additivity of radical species, as developed by this research group,[100] is implemented for the ketone radical species. The HBI method allows calculation of the thermochemical properties of radicals with only one additional group to that of the parent species. Group additivity for the thermochemical properties of ketones will be useful in the development of their chemical kinetic modeling.

The known groups that are used in the GA method calculation are listed in Table 4.8. As previously described, the bond dissociation energies for primary, secondary, and tertiary C–H bonds located adjacent to the carbonyl site have energies approximately

6-9 kcal mol^{-1} lower than those found for alkanes. This difference is a major concern. Therefore, recommended ketone bond groups are presented; KETOP (CJC(=O)), KETOS (CCJC(=O)), and KETOT (C2CJC(=O)) correspond to the ketone primary, secondary, and tertiary locations respectively. These groups result in the thermochemical properties of the radical compounds when the entropy and heat capacities are added to the parent species. The bond group enthalpy corresponds to the average C–H BDE for the specific adjacent ketone classes in Table 4.6, while the entropy and heat capacities are averaged from the difference in the radical and parent compounds.

Table 4.8 Literature and Recommended Hydrogen-Bond Increment Group Values for Ketones

Group	$\Delta H^{\circ}_{f\,298}$ [a]	S°_{298} [b]	$C_p(T)$ [b]						
			300 K	400 K	500 K	600 K	800 K	1000 K	1500 K
Known Groups									
C/CO/H3	-10.08	30.41	6.19	7.84	9.40	10.79	13.02	14.77	17.58
CO/C2	-31.40	15.01	5.59	6.32	7.09	7.76	8.89	9.61	10.10
C/C2/H2	-4.93	9.42	5.50	6.95	8.25	9.35	11.07	12.34	14.20
C/C/H3	-10.20	30.41	6.19	7.84	9.40	10.79	13.02	14.77	17.58
C/C/CO/H2	-5.20	9.60	6.20	7.70	8.70	9.50	11.10	12.20	14.07
C/C2/CO/H	-1.7	-11.70	4.16	5.91	7.34	8.19	9.46	10.19	11.29
Recommended Hydrogen-Bond Increment Groups									
KETOP	95.6	-2.37	-0.01	-0.43	-1.02	-1.58	-2.74	-3.58	-4.34
KETOS	90.9	-3.13	-1.68	-2.27	-2.61	-2.85	-3.64	-4.14	-4.54
KETOT	87.7	-4.59	-1.74	-2.74	-3.39	-3.61	-4.18	-4.55	-4.89

[a] Units kcal mol^{-1}.

[b] Units cal mol^{-1} K^{-1}.

4.5 Conclusions

Enthalpies of formation for five ketones and sixteen radicals with their corresponding carbon-hydrogen bond dissociation energies (C–H BDEs) are analyzed using density functional theory and higher level composite computational methods, many for the first time. Isodesmic work reactions are used to improve accuracy by cancelling error associated with the levels of theory. Comparisons with literature data shows the calculated enthalpies of formation for the ketone parent molecules are within 1 kcal mol^{-1} chemical accuracy. C–H BDEs for the ketones are determined and shown to be 6-9 kcal mol^{-1} lower than a corresponding alkane BDE for the respective primary, secondary, and tertiary C–H bonds when adjacent to the electronegative and radical stabilizing carbonyl group. C–H bond energies on a carbon that is not adjacent to a carbonyl group are similar to the standard *n*-alkanes for primary and secondary bonds. Results from the enthalpies of formation and bond dissociation energies from the DFT calculation methods are in acceptable agreement with composite method values utilizing work reactions that effectively cancel errors. For entropy and heat capacities, inclusion of internal rotors is required to have agreement with accepted literature compendiums on thermochemical properties of organic molecules for the parent ketones.

CHAPTER 5

THERMOCHEMICAL PROPERTIES OF *EXO*-TRICYCLO[5.2.1.0^{2,6}]DECANE (JP-10 JET FUEL) AND DERIVED TRICYCLODECYL RADICALS

5.1 Overview

exo-Tricyclo[5.2.1.0^{2,6}]decane (TCD), also called *exo*-tetrahydrodicyclopentadiene, is the principal component of the high-energy density hydrocarbon fuel JP-10 synthetically produced from the hydrogenation of dicyclopentadiene.[30] The compound's strained cyclic geometry allows for efficient energy storage and high thermal stability leading to its use as a missile fuel.[23,24,29,186] TCD is also a component in lubricating and cutting oils, paint solvents, waxes, and semiconductor washing agents.[187,188]

Although this is a single-component fuel, the compound's size and intricacy, viz., three rings with several strained carbon sites, results in complexity in trying to understand its reactions. The need to properly account for all the important and multifaceted product channels in combustion, thermal decomposition, atmospheric chemistry, and pyrolysis models results in significant complexity. Several researchers have used molecular dynamics, multi-element flux analysis, and experimental conditions including high-temperature thermal decomposition and cracking of JP-10 at various temperatures and pressures using spectroscopic, gas chromatography, and mass spectrometric analysis procedures to try and identify the important, initial products.[23-29] Somewhat controversial observations in different studies have resulted in a wide range of varied initial products along with some conflicting data, for pyrolysis, combustion, and cracking of TCD by several research groups.[23-33]

Knowledge of accurate thermochemistry of TCD is an important initial data set to understanding its combustion chemistry and reaction kinetics. Screening of the literature reveals one experimental study reporting the enthalpy of combustion and formation for the gas phase,[189] one study for liquid phase,[190] one high level computational study,[191] and estimated bond energies interpreted as based as secondary and tertiary bond energies in simple non-strained hydrocarbons.[26] The experimentally determined gas phase $\Delta H^{\circ}_{f\,298}$ of TCD is -14.38 ± 0.90 kcal mol^{-1} as reported by Boyd et al.[189] in 1971, which Chickos et al.[192] indicates is the endo isomer. This value is used in the kinetic mechanisms used to model JP-10 pyrolysis by Herbinet et al.[26] Chenowidth et al.[23] used the Boyd strain energy data in their force field dynamics modeling of pyrolysis.

Smith and Good[190] report a liquid phase enthalpy of -29.35 ± 0.35 kcal mol^{-1} for the exo isomer at 298.15 K. Chickos et al.[192] has determined vaporization enthalpies of 12.0 and 11.7 kcal mol^{-1} at 298.15 K for *endo*- and *exo*-TCD by correlation gas chromatography. They also report gas phase enthalpies of formation of -17.6 ± 0.6 kcal mol^{-1} for the exo and -14.8 ± 0.8 kcal mol^{-1} for the endo isomer.

Zehe and Jaffe[191] have recently determined gas phase formation enthalpies, $\Delta H^{\circ}_{f\,298}$, of -18.5 and -15.4 kcal mol^{-1} for the *exo*- and *endo*-TCD isomers from the averages generated using an isodesmic bond separation reaction G3(MP2), G3(MP2)//B3LYP, and CBS-QB3. These values with the heat of vaporization values from Chickos et al.[192] yield liquid phase enthalpies of formation of -30.2 kcal mol^{-1} for the exo and -27.4 kcal mol^{-1} for the endo isomers.

Currently there are no experimental or calculated bond dissociation energies (BDE) for TCD. The work of Herbinet et al.[26] is interpreted as possible use of generic

primary, secondary, and tertiary bond energies (approximately 101.1, 98.5, 96.5 kcal mol^{-1}, respectively). The bond energies are particularly interesting because of the high strain in the molecule. It is, for example, known that the bond energy on cyclopropane[126,193] of 106 kcal mol^{-1} is 8.5 kcal mol^{-1} higher than that of a normal secondary C–H bond energy (98.5 kcal mol^{-1}) due to the strain of the three-carbon ring. Analysis of these properties will enable a better understanding of reaction paths and detailed chemical kinetic mechanisms.

In this chapter, enthalpies of formation for the TCD parent molecule and the tricyclodecyl radicals corresponding to endo and exo positions at each carbon site are calculated. Bond energies determined for the TCD radicals are shown to follow trends known for molecules having carbons with similar ring strain and only a few sites follow conventional normal secondary and tertiary bond energies from smaller hydrocarbons. Entropy and heat capacity values, as a function of temperature, are also determined for each species. NASA polynomials of the thermodynamic data from TCD and tricyclodecyl radicals are calculated.

5.2 Nomenclature

Abbreviations are utilized in this chapter as illustrated below:

- – represents a bond between two atoms,
- Y represents a cyclic ring structure,
- YY represents a bicyclic ring structure,
- J represents a radical site on the preceding carbon atom,
- en (endo) represents the hydrogen position pointing toward the peak ch_2 group on the bridging carbon,

- ex (exo) represents the hydrogen position pointing away from the peak ch_2 group on the bridging carbon,
- C_i denotes carbon *i* according to numbering in Figure 5.1,
- TCD and JP-10 denotes *exo*-tricyclo[$5.2.1.0^{2,6}$]decane.

5.3 Isomers of TCD

TCD exists in either exo or endo form depending on the respective hydrogen atom/cyclopentane ring positions relative to the single CH_2 bridge carbon of the cyclohexane moiety in the molecule. In addition, there are chair and boat conformations for these two isomers. This results from the CH_2 group at C_4 position flop in this non-bridged cyclopentane ring, see Figure 5.1 for numbering scheme. Figures 5.2 and 5.3 illustrate the exo and endo isomers along with their respective chair and boat conformations. The energy of the transition state structure (*exo*-TCD TS) for the interconversion between chair and boat conformers in the *exo*-TCD isomer is also calculated. *exo*-TCD TS is the first order transition state with one relatively low negative (imaginary) frequency at -163 cm^{-1}. Appendix D includes the optimized geometry parameters, moments of inertia, and vibrational frequencies calculated at the B3LYP/6-31G(d,p) level, for these isomers. The B3LYP/6-31G(d,p), CBS-QB3, and G3MP2B3 levels of theory are further used for the thermochemical enthalpy analysis of these isomers also included in Appendix D.

The main compound of interest in this analysis, *exo*-TCD chair, is referred to as TCD from this point.

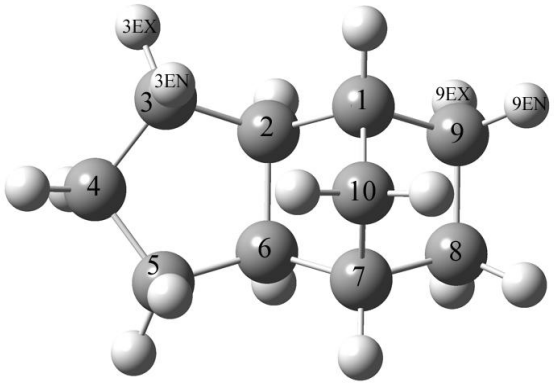

Figure 5.1 Numbering scheme for carbon and hydrogen sites of TCD.

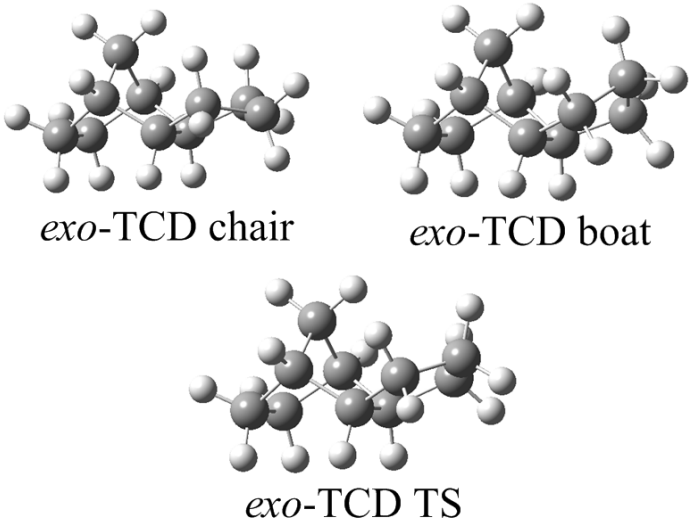

Figure 5.2 Conformations of *exo*-TCD.

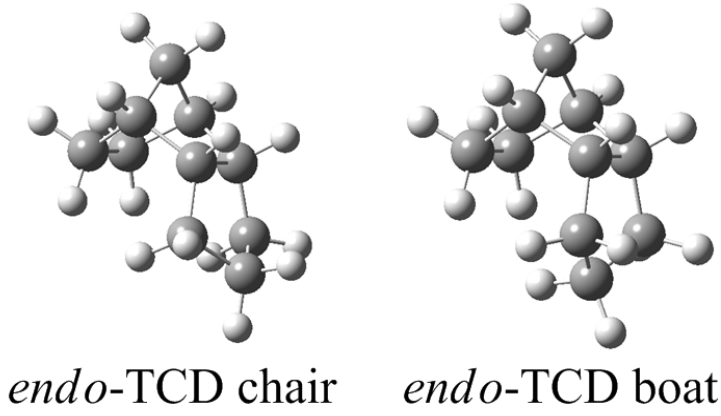

Figure 5.3 Conformations of *endo*-TCD.

5.4 Computational Methods

Structural parameters for this set of compounds are optimized at the density functional theory (DFT) B3LYP/6-31G(d,p) level of theory.[46,47] Bond dissociation energies and heats of formation are determined from isodesmic reactions using the B3LYP, BB1K,[50] MPWB1K,[51] and BMK[52] methods in conjunction with the moderate 6-31G(d,p) basis set. The larger 6-311G(2d,2p) basis set, which includes additional polarization functions on carbon and hydrogen atoms, is also employed with the B3LYP functional. The composite methods, G3MP2B3[57,58] and CBS-QB3,[60,61] are also utilized and serve as a comparison. All calculations are performed using the Gaussian 03 program suite.[62]

The Statistical Mechanics for Heat Capacity and Entropy (SMCPS) program[98] is utilized to calculate the entropy and heat capacities for TCD and corresponding tricyclodecyl radicals using the B3LYP/6-31G(d,p) level of theory. Entropy and heat capacity values are determined for the 1-5000 K temperature range and are presented in Appendix D.

5.5 Results and Discussion

A series of isodesmic work reactions, containing similar bond environments on both sides of the equations, are utilized to reduce systematic errors from each level of theory in calculating the enthalpies of formation for target compounds. The enthalpy for the TCD parent species is calculated from five work reactions. Three of the work reactions have near identical bond environments with similar strained bridged molecules on each side. The last two reactions use smaller molecules, where the reactions do not incorporate bridged hydrocarbons in the products, which are more common in the published literature

for enthalpy determination studies.[194,195] The well-established heat of formation literature values for the reference species are listed in Table 5.1.

Table 5.1 Standard Enthalpies of Formation for Reference Species

Species	$\Delta H^{\circ}_{f\,298}$ (kcal mol^{-1})	Reference
H	52.10 ± 0.001	83
CH_4	-17.78 ± 0.1	120
CH_3CH_3	-20.03 ± 0.07	120
$CH_3CH_2CH_3$	-25.02 ± 0.12	120
$(CH_3)_3CH$	-32.07 ± 0.14	120
$CH_3CH_2CH_2CH_3$	-30.04 ± 0.14	120
YC_3H_6	12.74 ± 0.12	120
YC_4H_8	6.62 ± 0.26	120
YC_5H_{10}	-18.26 ± 0.17	120
YC_6H_{12}	-29.47 ± 0.19	120
YYC_7H_{12}	-13.1 ± 1.1	120
YYC_8H_{14}	-23.66 ± 0.26	120
CH_3CJH_2	29.0 ± 0.4	121
CH_3CJHCH_3	21.5 ± 0.4	121
$(CH_3)_3CJ$	12.3 ± 0.4	121
$CH_3CJHCH_2CH_3$	16.1 ± 0.5	121
$YYCJ_7H_{11}$	33.9[a]	*b*

[a] Error not reported.
[b] See Appendix D for the enthalpy calculations.

$\Delta H^{\circ}_{f\,298}$ values are calculated using the B3LYP, BB1K, MPWB1K, and BMK methods with the 6-31G(d,p) basis set. The larger basis set, 6-311G(2d,2p), is also utilized with the B3LYP functional. These results are compared with the results from the G3MP2B3 and CBS-QB3 levels of theory. Calculated $\Delta H^{\circ}_{f\,298}$ and ΔH°_{rxn} for the TCD parent work reactions are listed in Tables 5.2 and 5.3. Figure 5.4 illustrates the abbreviations for the cyclic compound nomenclature in the work reactions.

Work reactions for the analysis of target radical enthalpy values include given radical and the parent on both sides along with the smaller, representative hydrocarbon

molecules and their corresponding radicals with accurately known enthalpies. Here the TCD radical (TCD-R*i* with *i* indicating the given carbon center) plus a hydrocarbon (HC) molecule is set equal to a HC radical plus the TCD parent. Thus, the absolute value of the radical enthalpy is calculated separately. Figure 5.1 illustrates the numbering for carbon atoms in TCD, where C_1 represents the highly strained bridge carbons to the three rings. The reactions for radicals are illustrated in Scheme 5.1 and the work reactions are presented in Table 5.4.

Optimized geometry parameters, moments of inertia, and vibrational frequencies at the B3LYP/6-31G(d,p) level for TCD and tricyclodecyl radicals are presented in Appendix D.

5.5.1 Heat of Formation $\Delta H^{\circ}_{f\,298}$

Tables 5.2 and 5.4 show that there is a good correlation for the $\Delta H^{\circ}_{f\,298}$ values between the DFT methods and the higher level calculations for TCD and its radicals, when using the work reactions that contain a balance of ring strain on each side. The radicals formed do not reveal differences in energy for the exo and endo positions for any of the calculation methods, which indicates that the radical formed from loss of either the endo or exo hydrogen atom site is identical in structure.

Table 5.2 Isodesmic Reactions and Calculated Enthalpies of Formations for TCD[a]

Isodesmic Reactions	$\Delta H^{\circ}_{f\,298}$ (kcal mol^{-1})					
	B3LYP		BB1K	MPWB1K	BMK	CBS-QB3	G3MP2B3
	6-31G(d,p)	6-311G(2d,2p)	6-31G(d,p)	6-31G(d,p)	6-31G(d,p)		
TCD System							
TCD + YC_4H_8 → YYC_7H_{12} + YYC_7H_{12}	-19.34	-19.28	-20.09	-19.97	-20.81	-17.50	-17.58
TCD + YC_5H_{10} → YYC_7H_{12} + YYC_8H_{14}	-19.01	-19.39	-20.06	-19.85	-20.56	-18.56	-18.59
TCD + YC_6H_{12} → YYC_8H_{14} + YYC_8H_{14}	-19.95	-20.12	-22.10	-21.90	-21.99	-20.19	-20.26
TCD + 3 CH_3CH_3 → 3 YC_4H_8 + $CH_3CH_2CH_2CH_3$						-20.23	-20.00
TCD + 4 CH_3CH_3 → 2 $CH_3CH_2CH_2CH_3$ + YC_4H_8 + 2 YC_3H_6						-20.96	-20.73
Average	**-19.43**	**-19.59**	**-20.75**	**-20.57**	**-21.12**	**-19.49**	**-19.43**
Atomization	**-5.22**					**-14.92**	**-18.35**
Osmont et al. Corrected Atomization	**-15.0**						

[a] Zehe and Jaffe[191] value from work reaction analysis -18.5 kcal mol^{-1}.

Table 5.3 Reaction Enthalpies for Isodesmic Reactions Used in TCD Analysis

Isodesmic Reactions	ΔH°_{rxn} B3LYP 6-31G(d,p)	B3LYP 6-311G(2d,2p)	BB1K 6-31G(d,p)	MPWB1K 6-31G(d,p)	BMK 6-31G(d,p)	CBS-QB3	G3MP2B3
TCD System							
TCD + YC_4H_8 → YYC_7H_{12} + YYC_7H_{12}	-13.48	-13.54	-12.73	-12.85	-12.01	-15.32	-15.24
TCD + YC_5H_{10} → YYC_7H_{12} + YYC_8H_{14}	0.51	0.89	1.56	1.35	2.06	0.06	0.09
TCD + YC_6H_{12} → YYC_8H_{14} + YYC_8H_{14}	2.10	2.27	4.25	4.05	4.14	2.34	2.41
TCD + 3 CH_3CH_3 → 3 YC_4H_8 + $CH_3CH_2CH_2CH_3$						70.14	69.91
TCD + 4 CH_3CH_3 → 2 $CH_3CH_2CH_2CH_3$ + YC_4H_8 + 2 YC_3H_6						73.10	72.87

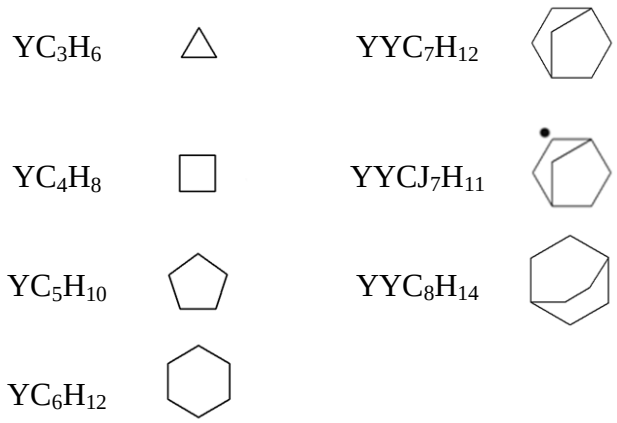

Figure 5.4 Nomenclature of cyclic species as used in work reactions.

Scheme 5.1 Radical Isodesmic Work Reactions

TCD-R*i*	+	CH_3CH_3	→	TCD	+	CH_3CJH_2
TCD-R*i*	+	$CH_3CH_2CH_3$	→	TCD	+	CH_3CJHCH_3
TCD-R*i*	+	$(CH_3)_3CH$	→	TCD	+	$(CH_3)_3CJ$
TCD-R*i*	+	$CH_3CH_2CH_2CH_3$	→	TCD	+	$CH_3CJHCH_2CH_3$
TCD-R*i*	+	YYC_7H_{12}	→	TCD	+	$YYCJ_7H_{11}$

Table 5.4 Isodesmic Reactions, Enthalpies of Formations, and Bond Dissociation Energies for Tricyclodecyl Radicals

Isodesmic Reactions							$\Delta H^{\circ}_{f\,298}$ (kcal mol^{-1})						
							B3LYP		BB1K	MPWB1K	BMK	CBS-QB3	G3MP2B3
							6-31G(d,p)	6-311G(2d,2p)	6-31G(d,p)	6-31G(d,p)	6-31G(d,p)		
TCD-R1 System													
TCD-R1	+	CH_3CH_3	→	TCD	+	CH_3CJH_2	34.47	34.84	32.82	32.93	34.31	35.49	36.05
TCD-R1	+	$CH_3CH_2CH_3$	→	TCD	+	CH_3CJHCH_3	35.86	36.13	35.10	35.17	34.89	35.73	35.86
TCD-R1	+	$(CH_3)_3CH$	→	TCD	+	$(CH_3)_3CJ$	36.80	36.91	36.63	36.60	35.51	35.31	35.08
TCD-R1	+	$CH_3CH_2CH_2CH_3$	→	TCD	+	$CH_3CJHCH_2CH_3$	35.25	35.62	34.44	34.46	34.62	35.13	35.23
TCD-R1	+	YYC_7H_{12}	→	TCD	+	$YYCJ_7H_{11}$	36.09	36.22	35.80	35.84	35.55	36.33	36.30
						Average	**35.70**	**35.94**	**34.96**	**35.00**	**34.98**	**35.60**	**35.71**
						Bond Dissociation Energy	**107.26**	**107.50**	**106.52**	**106.56**	**106.54**	**107.16**	**107.27**
TCD-R2 System													
TCD-R2	+	CH_3CH_3	→	TCD	+	CH_3CJH_2	26.14	26.52	24.76	24.93	27.17	28.16	29.07
TCD-R2	+	$CH_3CH_2CH_3$	→	TCD	+	CH_3CJHCH_3	27.53	27.81	27.04	27.17	27.75	28.41	28.88
TCD-R2	+	$(CH_3)_3CH$	→	TCD	+	$(CH_3)_3CJ$	28.47	28.59	28.57	28.61	28.37	27.98	28.10
TCD-R2	+	$CH_3CH_2CH_2CH_3$	→	TCD	+	$CH_3CJHCH_2CH_3$	26.92	27.30	26.38	26.47	27.48	27.80	28.25
TCD-R2	+	YYC_7H_{12}	→	TCD	+	$YYCJ_7H_{11}$	27.76	27.91	27.74	27.84	28.41	29.00	29.31
						Average	**27.37**	**27.63**	**26.90**	**27.00**	**27.84**	**28.27**	**28.72**
						Bond Dissociation Energy	**98.93**	**99.19**	**98.46**	**98.56**	**99.40**	**99.83**	**100.28**
TCD-R3EX System													
TCD-R3EX	+	CH_3CH_3	→	TCD	+	CH_3CJH_2	24.62	24.75	23.77	23.87	25.88	26.27	26.84
TCD-R3EX	+	$CH_3CH_2CH_3$	→	TCD	+	CH_3CJHCH_3	26.02	26.04	26.05	26.11	26.46	26.52	26.65
TCD-R3EX	+	$(CH_3)_3CH$	→	TCD	+	$(CH_3)_3CJ$	26.95	26.82	27.58	27.54	27.08	26.09	25.87
TCD-R3EX	+	$CH_3CH_2CH_2CH_3$	→	TCD	+	$CH_3CJHCH_2CH_3$	25.40	25.53	25.39	25.40	26.19	25.92	26.02
TCD-R3EX	+	YYC_7H_{12}	→	TCD	+	$YYCJ_7H_{11}$	26.25	26.13	26.75	26.78	27.12	27.11	27.09
						Average	**25.85**	**25.85**	**25.91**	**25.94**	**26.55**	**26.38**	**26.49**
						Bond Dissociation Energy	**97.41**	**97.41**	**97.47**	**97.50**	**98.11**	**97.94**	**98.05**
TCD-R3EN System													
TCD-R3EN	+	CH_3CH_3	→	TCD	+	CH_3CJH_2	24.62	24.75	23.77	23.87	25.88	26.27	26.84
TCD-R3EN	+	$CH_3CH_2CH_3$	→	TCD	+	CH_3CJHCH_3	26.02	26.04	26.06	26.11	26.46	26.52	26.65
TCD-R3EN	+	$(CH_3)_3CH$	→	TCD	+	$(CH_3)_3CJ$	26.95	26.82	27.58	27.54	27.08	26.09	25.87
TCD-R3EN	+	$CH_3CH_2CH_2CH_3$	→	TCD	+	$CH_3CJHCH_2CH_3$	25.40	25.53	25.39	25.40	26.19	25.91	26.02
TCD-R3EN	+	YYC_7H_{12}	→	TCD	+	$YYCJ_7H_{11}$	26.25	26.13	26.75	26.78	27.12	27.11	27.09
						Average	**25.85**	**25.85**	**25.91**	**25.94**	**26.55**	**26.38**	**26.49**
						Bond Dissociation Energy	**97.41**	**97.41**	**97.47**	**97.50**	**98.11**	**97.94**	**98.05**

Table 5.4 Isodesmic Reactions, Enthalpies of Formations, and Bond Dissociation Energies for Tricyclodecyl Radicals (Continued)

Isodesmic Reactions							$\Delta H^{\circ}_{f\,298}$ (kcal mol^{-1})						
							B3LYP		BB1K	MPWB1K	BMK	CBS-QB3	G3MP2B3
							6-31G(d,p)	6-311G(2d,2p)	6-31G(d,p)	6-31G(d,p)	6-31G(d,p)		
TCD-R4EX System													
TCD-R4EX	+	CH_3CH_3	→	TCD	+	CH_3CJH_2	25.17	25.27	24.38	24.40	26.47	26.83	27.35
TCD-R4EX	+	$CH_3CH_2CH_3$	→	TCD	+	CH_3CJHCH_3	26.56	26.56	26.66	26.64	27.05	27.08	27.16
TCD-R4EX	+	$(CH_3)_3CH$	→	TCD	+	$(CH_3)_3CJ$	27.50	27.34	28.18	28.08	27.67	26.66	26.37
TCD-R4EX	+	$CH_3CH_2CH_2CH_3$	→	TCD	+	$CH_3CJHCH_2CH_3$	25.95	26.05	25.99	25.94	26.77	26.48	26.53
TCD-R4EX	+	YYC_7H_{12}	→	TCD	+	$YYCJ_7H_{11}$	26.79	26.66	27.35	27.31	27.71	27.67	27.59
						Average	**26.39**	**26.38**	**26.51**	**26.47**	**27.13**	**26.95**	**27.00**
						Bond Dissociation Energy	**97.95**	**97.94**	**98.07**	**98.03**	**98.69**	**98.51**	**98.56**
TCD-R4EN System													
TCD-R4EN	+	CH_3CH_3	→	TCD	+	CH_3CJH_2	25.17	25.27	24.38	24.40	26.47	26.83	27.35
TCD-R4EN	+	$CH_3CH_2CH_3$	→	TCD	+	CH_3CJHCH_3	26.56	26.56	26.66	26.64	27.04	27.08	27.16
TCD-R4EN	+	$(CH_3)_3CH$	→	TCD	+	$(CH_3)_3CJ$	27.50	27.34	28.18	28.08	27.66	26.66	26.37
TCD-R4EN	+	$CH_3CH_2CH_2CH_3$	→	TCD	+	$CH_3CJHCH_2CH_3$	25.95	26.06	25.99	25.94	26.77	26.48	26.53
TCD-R4EN	+	YYC_7H_{12}	→	TCD	+	$YYCJ_7H_{11}$	26.79	26.66	27.35	27.31	27.71	27.67	27.59
						Average	**26.39**	**26.38**	**26.51**	**26.47**	**27.13**	**26.95**	**27.00**
						Bond Dissociation Energy	**97.95**	**97.94**	**98.07**	**98.03**	**98.69**	**98.51**	**98.56**
TCD-R9EX System													
TCD-R9EX	+	CH_3CH_3	→	TCD	+	CH_3CJH_2	26.12	26.37	24.86	24.94	26.56	26.96	27.55
TCD-R9EX	+	$CH_3CH_2CH_3$	→	TCD	+	CH_3CJHCH_3	27.52	27.66	27.14	27.18	27.14	27.21	27.36
TCD-R9EX	+	$(CH_3)_3CH$	→	TCD	+	$(CH_3)_3CJ$	28.45	28.44	28.67	28.62	27.76	26.79	26.58
TCD-R9EX	+	$CH_3CH_2CH_2CH_3$	→	TCD	+	$CH_3CJHCH_2CH_3$	26.91	27.16	26.48	26.48	26.87	26.61	26.73
TCD-R9EX	+	YYC_7H_{12}	→	TCD	+	$YYCJ_7H_{11}$	27.75	27.76	27.84	27.86	27.80	27.80	27.79
						Average	**27.35**	**27.48**	**27.00**	**27.01**	**27.23**	**27.07**	**27.20**
						Bond Dissociation Energy	**98.91**	**99.04**	**98.56**	**98.57**	**98.79**	**98.63**	**98.76**
TCD-R9EN System													
TCD-R9EN	+	CH_3CH_3	→	TCD	+	CH_3CJH_2	26.12	26.37	24.86	24.94	26.57	26.96	27.55
TCD-R9EN	+	$CH_3CH_2CH_3$	→	TCD	+	CH_3CJHCH_3	27.52	27.66	27.15	27.18	27.14	27.21	27.36
TCD-R9EN	+	$(CH_3)_3CH$	→	TCD	+	$(CH_3)_3CJ$	28.45	28.44	28.67	28.62	27.76	26.79	26.58
TCD-R9EN	+	$CH_3CH_2CH_2CH_3$	→	TCD	+	$CH_3CJHCH_2CH_3$	26.91	27.16	26.48	26.48	26.87	26.61	26.73
TCD-R9EN	+	YYC_7H_{12}	→	TCD	+	$YYCJ_7H_{11}$	27.75	27.76	27.84	27.86	27.81	27.80	27.79
						Average	**27.35**	**27.48**	**27.00**	**27.01**	**27.23**	**27.07**	**27.20**
						Bond Dissociation Energy	**98.91**	**99.04**	**98.56**	**98.57**	**98.79**	**98.63**	**98.76**

Table 5.4 Isodesmic Reactions, Enthalpies of Formations, and Bond Dissociation Energies for Tricyclodecyl Radicals (Continued)

Isodesmic Reactions							$\Delta H^{\circ}_{f\,298}$ (kcal mol^{-1})						
							B3LYP		BB1K	MPWB1K	BMK	CBS-QB3	G3MP2B3
							6-31G(d,p)	6-311G(2d,2p)	6-31G(d,p)	6-31G(d,p)	6-31G(d,p)		
TCD-R10EX System													
TCD-R10EX	+	CH_3CH_3	→	TCD	+	CH_3CJH_2	31.09	31.23	30.45	30.61	31.78	32.40	32.92
TCD-R10EX	+	$CH_3CH_2CH_3$	→	TCD	+	CH_3CJHCH_3	32.49	32.52	32.73	32.85	32.36	32.65	32.73
TCD-R10EX	+	$(CH_3)_3CH$	→	TCD	+	$(CH_3)_3CJ$	33.42	33.29	34.26	34.28	32.98	32.23	31.95
TCD-R10EX	+	$CH_3CH_2CH_2CH_3$	→	TCD	+	$CH_3CJHCH_2CH_3$	31.88	32.01	32.07	32.14	32.08	32.05	32.10
TCD-R10EX	+	YYC_7H_{12}	→	TCD	+	$YYCJ_7H_{11}$	32.72	32.61	33.43	33.52	33.02	33.24	33.16
						Average	**32.32**	**32.33**	**32.59**	**32.68**	**32.44**	**32.51**	**32.57**
						Bond Dissociation Energy	**103.88**	**103.89**	**104.15**	**104.24**	**104.00**	**104.07**	**104.13**
TCD-R10EN System													
TCD-R10EN	+	CH_3CH_3	→	TCD	+	CH_3CJH_2	31.09	31.23	30.45	30.61	31.78	32.40	32.92
TCD-R10EN	+	$CH_3CH_2CH_3$	→	TCD	+	CH_3CJHCH_3	32.49	32.52	32.73	32.85	32.35	32.65	32.73
TCD-R10EN	+	$(CH_3)_3CH$	→	TCD	+	$(CH_3)_3CJ$	33.42	33.30	34.26	34.28	32.97	32.22	31.95
TCD-R10EN	+	$CH_3CH_2CH_2CH_3$	→	TCD	+	$CH_3CJHCH_2CH_3$	31.88	32.01	32.07	32.14	32.08	32.04	32.10
TCD-R10EN	+	YYC_7H_{12}	→	TCD	+	$YYCJ_7H_{11}$	32.72	32.61	33.43	33.52	33.02	33.24	33.16
						Average	**32.32**	**32.33**	**32.59**	**32.68**	**32.44**	**32.51**	**32.57**
						Bond Dissociation Energy	**103.88**	**103.89**	**104.15**	**104.24**	**104.00**	**104.07**	**104.13**

For the DFT methods, there is a maximum difference of 0.26 kcal mol^{-1} for the B3LYP method when comparing the average results using the 6-31G(d,p) and 6-311G(2d,2p) basis sets for the parent and radicals. For the BB1K, MPWB1K, and BMK methods, there is a larger difference of 0.94 kcal mol^{-1} between the averages of these methods using the same 6-31G(d,p) basis set. The difference between the average energy values for all five DFT methods is consistent within 1 kcal mol^{-1} with the exception of the parent compound which is slightly higher at 1.7 kcal mol^{-1} due to an overestimation by the BMK method.

The CBS-QB3 and G3MP2B3 higher level calculations are significantly more consistent with a maximum difference of 0.5 kcal mol^{-1} where a majority of the calculations are approximately 0.1 kcal mol^{-1}. The close agreement between these two high level composite methods suggests accuracy in addition to the obvious precision.

Table 5.5 lists the average values for the combined five DFT methods and the CBS-QB3 and G3MP2B3 methods. Overall the DFT level of theory provides an acceptable analysis result, as compared to higher level calculations with a maximum difference of 1.2 kcal mol^{-1}, when the work reaction includes balance of ring strain.

Table 5.5 Recommended $\Delta H^{\circ}_{f\,298}$ and Bond Dissociation Energies for TCD and Radicals[a]

Species	DFT		CBS-QB3/G3MP2B3	
	$\Delta H^{\circ}_{f\,298}$	C–H BDE	$\Delta H^{\circ}_{f\,298}$	C–H BDE
TCD	-20.3 ± 1.0		-19.5 ± 1.3	
TCD-R1	35.3 ± 1.1	106.9	35.7 ± 0.5	107.2
TCD-R2	27.3 ± 1.0	98.9	28.5 ± 0.5	100.1
TCD-R3	26.0 ± 1.0	97.6	26.4 ± 0.5	98.0
TCD-R4	26.6 ± 1.0	98.1	27.0 ± 0.5	98.5
TCD-R9	27.2 ± 1.0	98.8	27.1 ± 0.5	98.7
TCD-R10	32.5 ± 1.0	104.0	32.5 ± 0.5	104.1

[a] Units kcal mol^{-1}.

Enthalpies of formation of -19.5, 35.7, 28.5, 26.4, 27.0, 27.1, and 32.5 kcal mol^{-1} for TCD, TCD-R1, TCD-R2, TCD-R3, TCD-R4, TCD-R9, and TCD-R10, respectively, are recommended from the averages of the CBS-QB3 and G3MP2B3 methods where standard deviations from the work reactions are included as error in Table 5.5.

5.5.2 Heat of Formation $\Delta H^{\circ}_{f\,298}$ Calculated by Atomization Reaction Methods

An atomization reaction method is also utilized to determine the enthalpy of formation for TCD at the B3LYP/6-31G(d,p), CBS-QB3, and G3MP2B3 levels of theory. Calculation details have been described previously.[196,197] In this method, ΔH_f (o+tc), a hypothetical atomization reaction is employed in a similar fashion to the above isodesmic work reactions. The target molecule, TCD, is balanced with its constituent atoms, C and H, in the gas phase with revised temperature correction values. For TCD, the reaction is:

$$\text{TCD} \rightarrow 10\,\text{C} + 16\,\text{H}$$

Table 5.2 has the values for the atomization reaction where the B3LYP/6-31G(d,p) value of -5.22 kcal mol^{-1} is apparently not acceptable and the -14.92 kcal mol^{-1} value from CBS-QB3 is a significant 4.6 kcal mol^{-1} overestimate from the recommended -19.5 kcal mol^{-1} value from the isodesmic work reaction analysis from composite calculations. On the other hand, the G3MP2B3 value of -18.35 kcal mol^{-1} is only higher by 1.1 kcal mol^{-1}. Hence, the G3MP2B3 atomization method appears to be a reliable alternative method with good accuracy for hydrocarbon systems.

Osmont et al. empirically corrected the atomization method for polycyclic hydrocarbons[198] from a B3LYP/6-31G(d,p) calculation and is presented in Table 5.2. A calculated value of -15.0 kcal mol^{-1} is calculated, 4.5 kcal mol^{-1} higher than the -19.5 kcal mol^{-1} recommended value. While the authors show good agreement of their method with non-cyclic hydrocarbons and oxy-hydrocarbons, they do show the method performs less well for complex polycyclic hydrocarbons.[199-202]

5.5.3 Heat of Formation $\Delta H^{\circ}_{f\,298}$ Calculated by Isomerization Reaction Methods

The calculated heat of formation for the lower energy chair form of the *exo*-TCD, -19.5 kcal mol^{-1}, is combined with the isomerization work reaction below in Scheme 5.2 to determine the standard enthalpies of formation for the boat and TS forms of *exo*-TCD and the chair and boat forms of *endo*-TCD:

Scheme 5.2 Isomerization Work Reactions

exo-TCD boat $\rightarrow$ *exo*-TCD chair
exo-TCD TS $\rightarrow$ *exo*-TCD chair
endo-TCD chair $\rightarrow$ *exo*-TCD chair
*end*o-TCD boat $\rightarrow$ *exo*-TCD chair

This reaction allows for a maximum degree of error cancellation because of the similar strain in the endo and exo isomer structures and systematic errors on specific atom groups will cancel. Table 5.6 has a summary of the values calculated for the work reactions. Data for each of the work reactions are available in Appendix D.

Table 5.6 TCD Isomers $\Delta H^{\circ}_{f\,298}$ from Unimolecular Isomerization and Bimolecular Isodesmic Work Reactions

Species	Isomerization Reaction ($\Delta H^{\circ}_{f\,298}$, kcal mol^{-1})			Isodesmic Reaction ($\Delta H^{\circ}_{f\,298}$, kcal mol^{-1})		
	B3LYP 6-31G(d,p)	CBS-QB3	G3MP2B3	B3LYP 6-31G(d,p)	CBS-QB3	G3MP2B3
exo-TCD chair				-19.4	-19.5	-19.4
exo-TCD boat	-17.5	-17.4	-17.4	-17.5	-17.5	-17.4
exo-TCD TS	-16.0	-15.4	-15.4	-16.0	-15.5	-15.4
endo-TCD chair	-15.6	-15.3	-15.3	-15.5	-15.4	-15.3
endo-TCD boat	-15.8	-16.4	-16.5	-15.7	-16.4	-16.5

Structures of the different exo and endo isomers are illustrated in Figures 5.2 and 5.3, respectively. The *exo*-TCD structure is more stable than the *endo*-TCD isomer by about 2.6 kcal mol^{-1}. The *exo*-TCD chair is shown to be approximately 2 kcal mol^{-1} more stable than the *exo*-TCD boat conformation. For the *exo*-TCD TS, conversion of the chair form to the boat form, the transition state energy is calculated to be higher than the *exo*-TCD chair by a 4 kcal mol^{-1} barrier. The energies of the *endo*-TCD boat and chair conformations show a smaller energy difference, approximately 1 kcal mol^{-1}, with the boat conformation lower in energy. Overall, there is good correlation between the data generated from the isomerization and isodesmic work reactions. Recommended values for these isomers, given in Table 5.7, are -19.5, -17.4, -15.4, -15.3, and -16.5 kcal mol^{-1} for the *exo*-TCD chair, *exo*-TCD boat, *exo*-TCD TS, *endo*-TCD chair, and *endo*-TCD

boat, respectively. Errors are again assigned using the standard deviations from the isodesmic work reaction values.

Table 5.7 Recommended $\Delta H^{\circ}_{f\,298}$ for TCD Isomers

Species	$\Delta H^{\circ}_{f\,298}$ (kcal mol^{-1})
exo-TCD chair	-19.5 ± 1.3
exo-TCD boat	-17.4 ± 1.3
exo-TCD TS	-15.4 ± 1.3
endo-TCD chair	-15.3 ± 1.3
endo-TCD boat	-16.5 ± 1.3

Recommended values of -19.5 and -16.5 kcal mol^{-1} for exo and endo are within 1 kcal mol^{-1} to the Zehe and Jaffe[191] values of -18.5 and -15.4 kcal mol^{-1} for the exo and endo isomers. The *endo*-TCD values of -15.3 and -16.5 kcal mol^{-1} for the chair and boat conformations are similar to the -14.38 kcal mol^{-1} reported by Boyd.[189] Using the recommended calculated values with the heat of vaporization values from Chickos,[192] gives liquid phase enthalpies of -31.2 and -28.5 kcal mol^{-1} for *exo*- and *endo*-TCD. These values are within 2 kcal mol^{-1} of the reported liquid phase enthalpies of Zehe and Jaffe[191] and Smith and Good.[190]

5.5.4 Entropies ($S(T)$) and Heat Capacities ($C_p(T)$)

Entropy and heat capacities for TCD and tricyclodecyl radicals, presented for the temperature range of 1-5000 K in Appendix D, calculated at the B3LYP/6-31G(d,p) level of theory using the Statistical Mechanics for Heat Capacity and Entropy (SMCPS) program.[98] Zero-point vibration energies (ZPVE) are scaled by 0.9806 for B3LYP/6-31G(d,p) as recommended by Scott and Radom.[99] NASA Polynomials for use

in kinetic and thermochemical calculations for modeling are also presented in Appendix D.

5.5.5 Carbon-Hydrogen Bond Dissociation Energies (C–H BDEs)

Bond dissociation energies corresponding to the loss of a hydrogen atom are computed from the work reactions listed in Table 5.4 using the $\Delta H^{\circ}_{f\,298}$ of the parent molecule and carbon site radicals with the standard enthalpy of the hydrogen atom. Determining these bond energies facilitates understanding the initial reaction pathways and kinetics the compound will undergo with lower bond energies being more susceptible to hydrogen abstraction. Standard bond dissociation energies for primary, secondary, and tertiary alkanes of 101.1, 98.5, and 96.5 kcal mol^{-1} along with energies for secondary one- and two-carbon bridges and bridgeheads for norbornane[203] of 104.9, 98.7, and 107.3 kcal mol^{-1} are used for values of the standard reference species.

TCD has two tertiary bridgehead radical sites related to the C_1 and C_2 atoms in the numbering scheme of Figure 5.1. TCD-R1 and TCD-R2 have bond energies of 107.2 and 100.1 kcal mol^{-1}, which are significantly different from the common 96.5 kcal mol^{-1} for a tertiary alkane C–H bond. TCD-R1 is similar to the 107.3 kcal mol^{-1} for the bridgehead position of norbornane and 106 kcal mol^{-1} found both in cyclopropane[126,193] and bicyclo[1.1.1]pentane[128] resulting from the ring strain present. This strain also accounts for the relative difference in energy for the two tertiary sites, TCD-R1 and TCD-R2, where the more highly strained TCD-R1 has about a 7 kcal mol^{-1} higher bond energy than the less strained TCD-R2. The increasing strain and energy is caused by an unfavorable non-planar geometry created upon radical formation.

TCD-R3, TCD-R4, and TCD-R9 are all secondary carbons with energies of 98.0, 98.5, and 98.7 kcal mol^{-1}; these values are slightly lower than the 98.5 kcal mol^{-1} for secondary alkanes C–H bonds. These TCD radical values are consistent with the 98.7 kcal mol^{-1} for the secondary two-carbon bridge bond energy for norbornane,[203] 97-98 kcal mol^{-1} for the secondary two- and three-carbon bridges of bicyclo[3.1.1]heptane, tricyclo[$3.1.1.0^{1,5}$]heptane, tricyclo[$2.2.1.0^{1,4}$]heptane, and bicyclo[2.2.2]octane,[128] and 96-97 kcal mol^{-1} for cyclopentane.[126,204-206]

TCD-R10 is a strained, single bridging, carbon with strain that is probably similar to TCD-R1 and TCD-R2, although now in a secondary structure. The resulting bond energy for TCD-R10 of 104.1 kcal mol^{-1} is indicative of this strain and is similar to 104.9 kcal mol^{-1} found for the secondary one-carbon bridged bond energy in norbornane[203] and 103-105 kcal mol^{-1} for the single bridging positions in bicyclo[2.1.1]hexane and bicyclo[3.1.1]heptane.[128] This can be compared to the 100 kcal mol^{-1} bond energy observed in cyclohexane, where there is little strain.[126,204-206]

The carbon sites for the exo and endo hydrogen atoms, see Figure 5.1, are shown to have identical bond energies, Table 5.4, and therefore are not separately discussed.

5.6 Conclusions

Standard enthalpies of formation for the parent TCD molecule and the different tricyclodecyl radicals corresponding to loss of hydrogen atoms from the carbons sites are evaluated using five density functional methods and the G3MP2B3 and CBS-QB3 composite computational methods. A series of five isodesmic work reactions, that include reference molecules of similar ring strain, is used to effect a cancelation of calculation errors. The enthalpy of formation for TCD of -19.5 kcal mol^{-1} is found to be several kcal

mol^{-1} lower than the commonly used literature values. Carbon-hydrogen bond energies for the TCD carbon sites (TCD-R*i*) are determined as follows: TCD-R1, 107.2; TCD-R2, 100.1; TCD-R3, 98.0; TCD-R4, 98.5; TCD-R9, 98.7; TCD-R10, 104.1 kcal mol^{-1}. Results from use of five different DFT methods are in very good agreement with composite method values for work reactions that contain similar bridged hydrocarbons on both sides and for the radicals. NASA polynomials for the thermodynamic data for TCD and tricyclodecyl radicals are also determined.

CHAPTER 6

BOND ENERGIES AND THERMOCHEMICAL PROPERTIES OF RING OPENED DIRADICALS AND CARBENES OF *EXO*-TRICYCLO[5.2.1.0^{2,6}]DECANE

6.1 Overview

Carbon-carbon (C–C) bonds in cyclic and linear hydrocarbons are typically weaker than corresponding carbon-hydrogen (C–H) bonds by about 10 kcal mol^{-1}, and with a higher entropy gain in cleavage of these bonds, they will cleave faster under high temperature, unimolecular dissociation conditions than the C–H bonds. This cleavage reaction creates two radical species, chain branching, and while reverse reaction is also rapid and highly competitive with further reaction, the forward reactions are important to initiation of combustion and pyrolysis.

Thermodynamic data for *exo*-tricyclo[5.2.1.0^{2,6}]decane (TCD) diradicals, including their carbon-carbon bond dissociation energies (C–C BDEs) is valuable to understanding reaction pathways of the complex hydrocarbons in fuels and in petroleum and other cracking reactors.[207,208] Accurate thermochemical data can provide a basis for understanding the initiation and reaction kinetics. Initial ring opening reactions in strained ring systems allow release of strain energy and result in lower energy species. Ring opening of smaller cyclic hydrocarbons can also undergo an intramolecular hydrogen transfer leading to highly exothermic double bond formation.

The role of diradical species created from breaking C–C bonds in ring opening processes for cyclic and polycyclic compounds have been previously studied.[26,208-216] Williams and coworkers[30] suggested a mechanism where breaking the central C–C bond

shared by two five-member rings or a C–H bond of a CH_2 group would likely be the initiation step in the unimolecular decomposition of TCD. The significant study by Herbinet et al.[26] presented some thermochemistry and a comprehensive detailed kinetic model including diradical species created from initial unimolecular cleavage of the C–C bonds in TCD. They compared their model with experimental results for the thermal decomposition of TCD. Xing et al.[29] similarly developed a probable diradical mechanism for the thermal cracking of TCD under elevated pressures.

Nakra et al.[27] studied pyrolysis of TCD in a flow reactor where they observed decomposition around 1000 K and complete decomposition at approximately 1350 K. They also determined important products by mass spectrometry analysis indicating that cyclopentadiene was a major initial product, but is transient at these conditions and begins to decompose at approximately 1350 K. The computational studies, molecular dynamics simulations at several thousand degrees K, of Goddard's research group reported C–C bond cleavage forming either ethylene with a C_8 hydrocarbon or two C_5 hydrocarbons from initial thermal decomposition.[23]

As the roles of carbenes as reactive intermediates in combustion reactions increases, the need for accurate thermochemical properties will become more important. Research involving carbenes has increased as theoretical computations are aligned with experimental results. Computational studies for carbenes include heats of formation for small species such as ethylidene[217] and hydroxyl-substituted carbenes[218] to larger saturated and unsaturated diaminocarbenes[219] and phenylcarbene.[220] Carbene stabilities have been studied computationally for trifluoromethyl and ammonium cationic ligand substitutions,[221] mono- and di-aryl substituents,[222] and monoheteroatom substitution for

acyclic and cyclic carbenes.[223] Electronic structure effects from ortho-, meta-, and para-substitutions for phenylcarbene[224] have also been investigated.

In this chapter, each of the seven C*m*–C*n* bond energies are studied (*m* and *n* denote carbons according to numbering in Figure 6.1). Each of the C–C bonds in TCD is cleaved and the radical sites capped with a hydrogen atom, for completion of valence, resulting in seven stable parent compounds (TCD-H2 *m*-*n*). For the radical (TCD-H2 *m*J-*n* and *m*-*n*J), diradical (TCD-H2 *m*J-*n*J), and carbene (TCD-H2 *m*JJ-*n* and *m*-*n*JJ) species, J represents a radical site from the loss of a hydrogen atom on the preceding carbon atom. Standard enthalpies of formation of each parent, radical, diradical, and carbene species are determined. The C–H BDEs corresponding to loss of H at the capped sites are determined for the radicals while the C–C BDEs are calculated as the difference between the enthalpy of TCD and the diradical and carbene species. Entropies (*S(T)*) and heat capacities ($C_p(T)$) are also determined for each species.

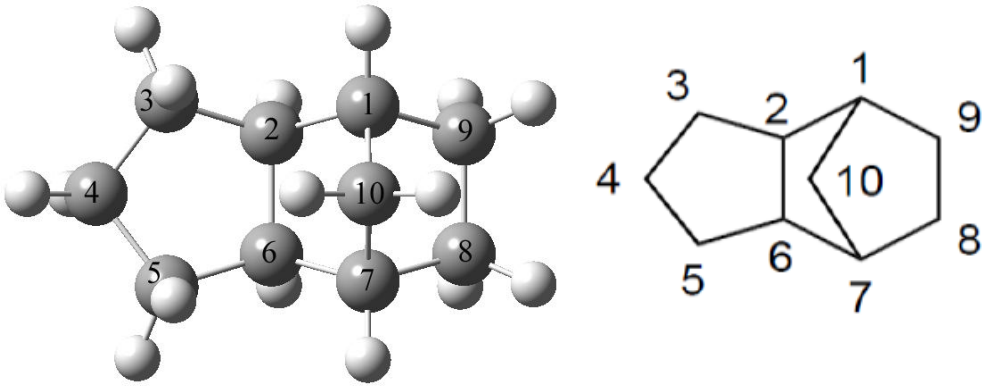

Figure 6.1 Numbering scheme for carbon and hydrogen sites of TCD.

6.2 Nomenclature

Abbreviations are utilized in this chapter as illustrated below:

- = represents a double bond between two atoms,
- Y represents a cyclic ring structure,
- YY represents a bicyclic ring structure,
- J or · represents a radical site on the preceding carbon atom,
- JJ or **:** represents a carbene site on the preceding carbon atom,
- (s) or (t) represents a singlet or triplet state species,
- *m* and *n* denotes carbons according to numbering in Figure 6.1,
- TCD and JP-10 denotes *exo*-tricyclo[5.2.1.$0^{2,6}$]decane.

Figure 6.2 has an example of the nomenclature used for the parent, radical, diradical, and carbene species based on the numbering in Figure 6.1. The structures in this figure are kept close to the parent structure for ease of identification and do not reflect their optimized geometries.

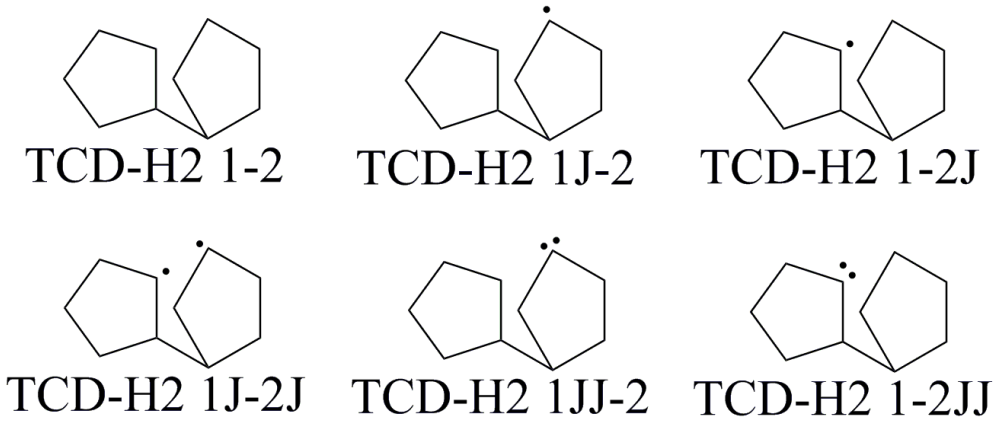

Figure 6.2 Example nomenclature for TCD-H2 1-2 parent, radical, diradical, and carbene species.

6.3 Computational Methods

Initial structural parameters including geometries, vibrational frequencies, moments of inertia, and internal rotor potentials are analyzed using the density functional theory (DFT) B3LYP[46,47] method with the 6-31G(d,p) basis set.

Enthalpy of formation ($\Delta H^{\circ}_{f\ 298}$) values are calculated using isodesmic work reactions having similar bonding environments for the products and reactants using the Gaussian 03[62] and Gaussian 09[63] program suites. The parent work reactions incorporate similar bridged structures on both sides of the reaction for minimization of error which is important for accuracy in enthalpy calculations.[225] DFT values calculated using B3LYP with the 6-31G(d,p) and the larger 6-311G(2d,2p) basis set are compared to values from the *w*B97X-D[53,54] and M06-2X[55,56] DFT methods using the 6-31G(d,p) basis set. Higher level composite methods G3MP2B3[57,58] and CBS-QB3[60,61] are used to gauge the accuracy of the DFT methods.

For the diradicals and carbenes, single point energies are calculated using the coupled cluster method with single, double, and perturbative triple excitation calculations, CCSD(T)[76-82], based on the optimized B3LYP/6-31G(d,p) geometries. Atomic spin densities for the carbon radical sites confirmed singlet, opposite spins, and triplet states, same spin, for the diradical species.

The spin-projection method, developed by Yamaguchi and coworkers,[226] is applied to the energies for the singlet diradicals and carbenes from the DFT methods. This correction aims to remove the spin contamination error from the triplet state in the open shell singlet calculations. Ess and Cook[227] showed that DFT methods give inadequate singlet-triplet (S-T) energies without spin correction. They also showed that

only corrected M06-2X and *w*B97X-D values give reasonable accuracy for S-T gap energies for open shell singlet diradicals. Calculated CBS-QB3 singlet diradical values are also corrected, as recommended by Sirjean et al.,[228] to remove error created in this method from strong spin contamination. The correction term was optimized against S-T gaps for hydrocarbon diradicals from CASSCF calculations and was shown to produce acceptable formation enthalpies for twenty two hydrocarbon and heteroatomic diradicals.

Optimization of the singlet TCD 2J-6J species is not possible with the any of the methods used in this study. A stable singlet structure is obtained using semi-empirical methods, but optimization at higher levels yielded ring closure back to TCD. To provide an approximate and acceptable geometry for the singlet, single point energies are calculated from the optimized triplet geometry. The methods all provide one negative frequency corresponding to a ring inversion. The inverse of the frequency is used to calculate its zero-point vibrational energy (ZPVE) contribution, then scaled by 0.9806 for B3LYP, as recommended by Scott and Radom,[99] and 0.967 for M06-2X and 0.975 for *w*B97X-D, as recommended by Truhlar and coworkers.[229] The calculated enthalpy values include this ZPVE contribution as well as the spin correction. A similar procedure is followed for the composite methods with adjusting for the negative frequency ZPVE correction.

The Statistical Mechanics for Heat Capacity and Entropy (SMCPS) program[98] is utilized to calculate the entropy and heat capacities for all of the compounds using the B3LYP/6-31G(d,p) level of theory. Internal rotors also are incorporated using the Pitzer and Gwinn[85-87] approximation method where the potential energy barriers to rotation are calculated at the B3LYP/6-31G(d,p) level. Internal rotor torsions below 4.5 kcal mol^{-1} are

removed and replaced with entropy and heat capacity contributions as hindered rotors. Total entropy and heat capacity values are determined by summing these contributions.

6.4 Results and Discussion

The primary objectives in this chapter are to determine the BDEs for the seven different C–C bonds in TCD and to calculate the thermochemical properties of the singlet diradicals. Diradicals and carbenes can be formed from the cleavage of the TCD C–C bonds, as illustrated in Figure 6.3. These species have different relative stabilities which affect their C–C BDEs and thus the ring opening kinetics. The thermochemical properties determine initial decomposition kinetics and reaction pathways.

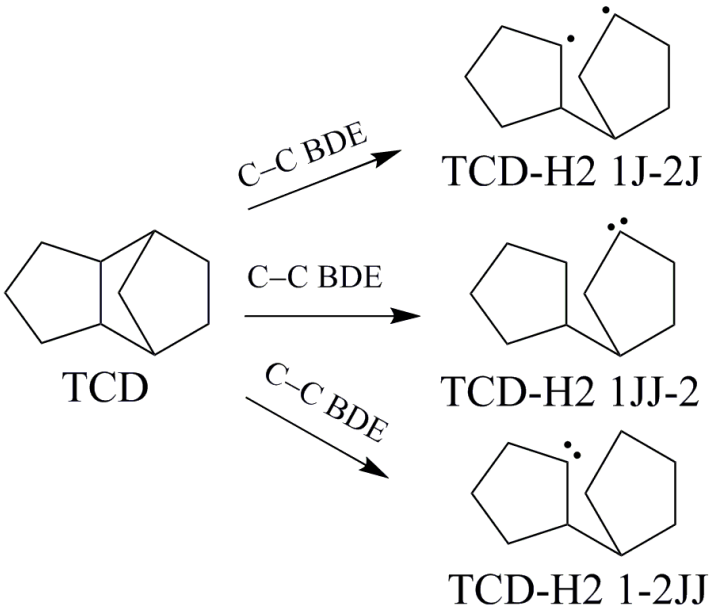

Figure 6.3 Overall calculated carbon-carbon bond dissociation energies (C–C BDE) for ring opening of TCD to diradicals and carbenes.

With the main focus on the TCD diradicals, Figure 6.4 has the stepwise calculations for the intermediate radical species and bond dissociation energies calculated in this study.

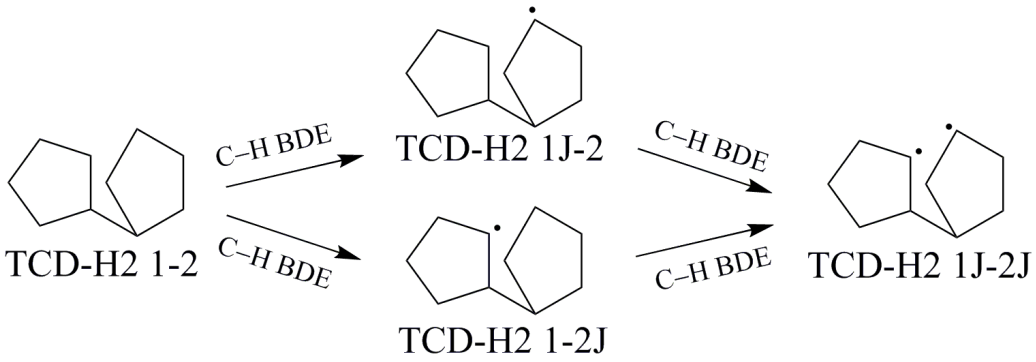

Figure 6.4 Stepwise calculation of radicals and bond dissociation energies from hydrogen atom removal from TCD-H2 parent species.

The TCD-H2 *m*-*n* nomenclature, as shown in Figures 6.2 and 6.4, corresponds to a starting TCD structure that has had the *m*-*n* bond cleaved, and a H atom added to each carbon radical. The C*m*–C*n* bonds correspond to the TCD numbering in Figure 6.1. These structures with the *m*-*n* opened bond and capped carbon radical sites are then optimized.

A mono radical (doublet) species, denoted TCD-H2 *m*J-*n* or TCD-H2 *m*-*n*J, are determined from the optimized TCD-H2 *m*-*n*. The standard enthalpy and bond energy are calculated for the TCD-H2 *m*J-*n* and TCD-H2 *m*-*n*J species. Then from the mono radicals, the hydrogen on the second carbon of the bond cleavage is removed and optimized to create the diradical, for both the singlet and triplet states. This diradical is denoted TCD-H2 *m*J-*n*J.

A separate calculation beginning with the mono radicals removed a second hydrogen atom from the first radical site to create the carbene, for both the singlet and triplet states, denoted TCD-H2 *m*JJ-*n* and TCD-H2 *m*-*n*JJ.

6.4.1 Heat of Formation $\Delta H^{\circ}_{f\,298}$

Calculation and validation of the enthalpies of formation ($\Delta H^{\circ}_{f\,298}$) for the parent compounds is completed with two sets of isodesmic work reactions to reduce systematic errors from the calculation methods. The first set of work reactions, Scheme 6.1, is used to calculate $\Delta H^{\circ}_{f\,298}$ values using four reactions. The first three contain reference species with similar strain in bridged cyclic bonding environments on both sides of the equations. The fourth reaction uses smaller molecules, which are not bridged, but their enthalpies are known to higher accuracy, which allows some comparison of calculation errors where ring strain is not cancelled. The reactions are similar to ones which provided good precision previously for TCD.[225] The standard enthalpies of formation for the reference species are listed in Table 6.1.

Scheme 6.1 Work Reactions for Calculating $\Delta H^{\circ}_{f\,298}$ of Parent TCD-H2 m-n

TCD-H2 *m*-*n*	+	YC_4H_8	→	YYC_7H_{12}	+	YC_7H_{14}
TCD-H2 *m*-*n*	+	YC_5H_{10}	→	YYC_7H_{12}	+	YC_8H_{16}
TCD-H2 *m*-*n*	+	YC_6H_{12}	→	YYC_8H_{14}	+	YC_8H_{16}
TCD-H2 *m*-*n*	+	3 CH_3CH_3	→	2 YC_4H_8	+	2 $CH_3CH_2CH_2CH_3$

Table 6.1 Standard Enthalpies of Formation for Reference Species

Species	$\Delta H^{\circ}_{f\,298}$ (kcal mol^{-1})	Reference
H	52.10	83
CH_4	-17.8 ± 0.1	120
CH_3CH_3	-20.0 ± 0.1	120
$CH_3CH_2CH_3$	-25.0 ± 0.1	120
$(CH_3)_3CH$	-32.1 ± 0.1	120
$CH_3CH_2CH_2CH_3$	-30.0 ± 0.1	120
$CH_3CH_2CH_2CH_2CH_3$	-35.1 ± 0.2	120
$CH_2=CH_2$	12.5 ± 0.1	120
$CH_2=CHCH_3$	4.8 ± 0.2	120
$CH_3CH=CHCH_3$	-2.7 ± 0.2	120
CH_3CH_2OH	-56.2 ± 0.1	120
YC_4H_8	6.6 ± 0.3	120
YC_5H_{10}	-18.3 ± 0.2	120
YC_6H_{12}	-29.5 ± 0.2	120
YC_7H_{14}	-37.0 ± 0.2	120
YYC_7H_{12}	-13.1 ± 1.1	120
YC_8H_{16}	-44.1 ± 0.4	120
YYC_8H_{14}	-23.7 ± 0.3	120
TCD	-19.5 ± 1.3	225
CH_3CJH_2	29.0 ± 0.4	121
CH_3CJHCH_3	21.5 ± 0.4	121
$(CH_3)_3CJ$	12.3 ± 0.4	121
$CH_3CJHCH_2CH_3$	16.1 ± 0.5	121
$:CH_2$ (s)	102.31 ± 0.20	230
$:CH_2$ (t)	93.31 ± 0.20	230
$CH_3C:OH$ (s)	11.2 ± 1	218
$CH_3C:OH$ (t)	42.3[a]	218
$YYCJ_7H_{11}$	33.9[a]	*b*

[a] Error not reported.
[b] See Appendix D for enthalpy calculation.

A second set of work reactions for the parent compounds, illustrated in Scheme 6.2, incorporate ring opened species and the parent TCD compound. These are not included in the $\Delta H^{\circ}_{f\,298}$ calculation, but serve to validate the Scheme 6.1 work reactions and mimic the TCD to TCD-H2 *m-n* ring opening system. The first two reactions in this set have similar strain in bridged bicyclic compounds, which open to their single cyclic

counterparts. The third and fourth reactions involve cyclic ring opening to normal straight chain alkanes. The nomenclature of the cyclic species used in these work reactions is illustrated in Figure 6.5, while the eight work reactions for the parent compounds are presented in Appendix E.

Scheme 6.2 Work Reactions using TCD Species for Validation of $\Delta H^{\circ}_{f\,298}$ for Parent TCD-H2 *m-n*

TCD-H2 *m-n*	+	YYC_7H_{12}	→	YC_7H_{14}	+	TCD
TCD-H2 *m-n*	+	YYC_8H_{14}	→	YC_8H_{16}	+	TCD
TCD-H2 *m-n*	+	YC_5H_{10}	→	$CH_3CH_2CH_2CH_2CH_3$	+	TCD
TCD-H2 *m-n*	+	YC_4H_8	→	$CH_3CH_2CH_2CH_3$	+	TCD

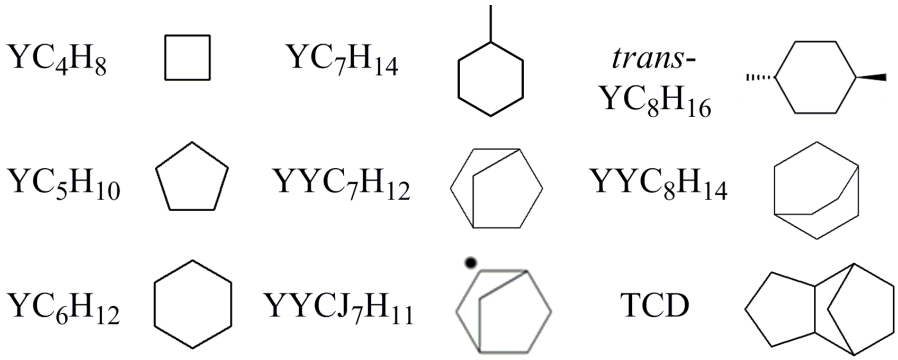

Figure 6.5 Nomenclature of cyclic species as used in work reactions.

Work reactions used to calculate $\Delta H^{\circ}_{f\,298}$ for the TCD-H2 *m*J-*n* and *m*-*n*J radicals are listed in Scheme 6.3. These work reactions use smaller radical and parent compounds as reference species where their heats of formation are accurately known; they also use a near TCD structure on both sides for strain cancelation.

Scheme 6.3 Work Reactions for Calculating $\Delta H^{\circ}_{f\,298}$ of Single Radicals (Doublets)

TCD-H2 *m*-*n* Radical	+	CH_3CH_3	→	TCD-H2 *m*-*n*	+	CH_3CJH_2
TCD-H2 *m*-*n* Radical	+	$CH_3CH_2CH_3$	→	TCD-H2 *m*-*n*	+	CH_3CJHCH_3
TCD-H2 *m*-*n* Radical	+	$(CH_3)_3CH$	→	TCD-H2 *m*-*n*	+	$(CH_3)_3CJ$
TCD-H2 *m*-*n* Radical	+	$CH_3CH_2CH_2CH_3$	→	TCD-H2 *m*-*n*	+	$CH_3CJHCH_2CH_3$
TCD-H2 *m*-*n* Radical	+	YYC_7H_{12}	→	TCD-H2 *m*-*n*	+	$YYCJ_7H_{11}$

The work reactions for the singlet and triplet diradicals are listed in Scheme 6.4; they involve one reference species radical and one TCD-H2 *m*-*n* radical. Since there are two TCD-H2 *m*-*n* single radical sites, one for *m* and one for *n* of each C*m*–C*n* location, diradical $\Delta H^{\circ}_{f\,298}$ values are averaged from all ten work reactions.

Scheme 6.4 Work Reactions for Calculating $\Delta H^{\circ}_{f\,298}$ of Diradicals

TCD-H2 *m*J-*n*J	+	CH_3CH_3	→	TCD-H2 *m*-*n* Radical	+	CH_3CJH_2
TCD-H2 *m*J-*n*J	+	$CH_3CH_2CH_3$	→	TCD-H2 *m*-*n* Radical	+	CH_3CJHCH_3
TCD-H2 *m*J-*n*J	+	$(CH_3)_3CH$	→	TCD-H2 *m*-*n* Radical	+	$(CH_3)_3CJ$
TCD-H2 *m*J-*n*J	+	$CH_3CH_2CH_2CH_3$	→	TCD-H2 *m*-*n* Radical	+	$CH_3CJHCH_2CH_3$
TCD-H2 *m*J-*n*J	+	YYC_7H_{12}	→	TCD-H2 *m*-*n* Radical	+	$YYCJ_7H_{11}$

Work reactions for calculation of the $\Delta H^{\circ}_{f\,298}$ for the TCD-H2 carbenes are listed in Scheme 6.5. Two work reactions have smaller carbene (singlet and triplet) species while the three others incorporate small *n*-alkane hydrocarbons and their olefins.

Scheme 6.5 Work Reactions for Calculating $\Delta H^{\circ}_{f\,298}$ of Carbenes

TCD-H2 *m-n* Carbenes	+	CH_4	→	TCD-H2 *m-n*	+	$:CH_2$
TCD-H2 *m-n* Carbenes	+	CH_3CH_2OH	→	TCD-H2 *m-n*	+	$CH_3C:OH$
TCD-H2 *m-n* Carbenes	+	CH_3CH_3	→	TCD-H2 *m-n*	+	$CH_2=CH_2$
TCD-H2 *m-n* Carbenes	+	$CH_3CH_2CH_3$	→	TCD-H2 *m-n*	+	$CH_2=CHCH_3$
TCD-H2 *m-n* Carbenes	+	$CH_3CH_2CH_2CH_3$	→	TCD-H2 *m-n*	+	$CH_3CH=CHCH_3$

Optimized structures, moments of inertia, and vibration frequencies at the B3LYP/6-31G(d,p) level for all of the TCD-H2 *m-n* parent, radical, diradical (triplet), and carbene (triplet) species are included in Appendix E.

6.4.1.1 Parent $\Delta H^{\circ}_{f\,298}$: TCD-H2 m-nJ. The work reactions for calculation of the $\Delta H^{\circ}_{f\,298}$ for the parent TCD-H2 *m-n* parent species are presented in Appendix E. Work reactions from Scheme 6.1 used to calculate $\Delta H^{\circ}_{f\,298}$ show excellent agreement to those from Scheme 6.2 and validate these findings for the TCD-H2 *m-n* parent species. There is good consistency between the two sets of work reactions and the different levels of theory which serves as a check on the calculated $\Delta H^{\circ}_{f\,298}$ values. The validation of these values from a second set of reactions is important as these parent species serve in the subsequent radical, diradical, and carbene work reactions.

Calculated $\Delta H^{\circ}_{f\,298}$ values are summarized in Table 6.2. The values from the B3LYP methods using the 6-31G(d,p) and 6-311G(2d,2p) basis sets are averaged along with the two composite methods CBS-QB3 and G3MP2B3. Averages from the composite methods are recommended and are used in the subsequent reactions.

Table 6.2 Summary of $\Delta H^{\circ}_{f\,298}$ and C–H Bond Dissociation Energies for TCD-H2 *m-n* Parent and Radical Species[a]

Species	B3LYP[b]			Composite[c]		
	$\Delta H^{\circ}_{f\,298}$	C–H BDE	C–H BDE[d]	$\Delta H^{\circ}_{f\,298}$	C–H BDE	C–H BDE[d]
TCD-H2 1-2	-33.9 ± 0.6			-30.5 ± 0.9		
TCD-H2 1J-2	13.5 ± 0.8	96.1	96.4	13.4 ± 0.5	96.0	96.8
TCD-H2 1-2J	13.9 ± 0.8	96.4	96.0	13.9 ± 0.5	96.4	96.3
TCD-H2 2-3	-31.4 ± 0.5			-30.8 ± 0.9		
TCD-H2 2J-3	15.9 ± 0.8	98.8	102.5	15.9 ± 0.5	98.8	101.6
TCD-H2 2-3J	19.5 ± 0.8	102.4	98.9	18.3 ± 0.5	101.2	99.2
TCD-H2 3-4	-29.1 ± 0.4			-30.4 ± 0.9		
TCD-H2 3J-4	18.8 ± 0.8	101.3	100.5	18.2 ± 0.5	100.7	100.8
TCD-H2 3-4J	19.2 ± 0.8	101.7	100.0	18.3 ± 0.5	100.8	100.7
TCD-H2 2-6	-25.1 ± 0.4			-24.1 ± 0.9		
TCD-H2 2J-6	17.2 ± 0.8	93.3	90.2	17.1 ± 0.5	93.2	94.4
TCD-H2 2-6J	17.2 ± 0.8	93.3	90.2	17.1 ± 0.5	93.2	94.4
TCD-H2 1-10	-32.2 ± 0.4			-31.5 ± 0.9		
TCD-H2 1J-10	11.6 ± 0.8	95.1	101.0	12.0 ± 0.5	95.6	100.0
TCD-H2 1-10J	17.2 ± 0.8	100.7	95.4	16.5 ± 0.5	100.1	95.5
TCD-H2 1-9	-35.7 ± 0.5			-34.2 ± 0.9		
TCD-H2 1J-9	10.9 ± 0.8	97.2	101.0	11.5 ± 0.5	97.8	100.8
TCD-H2 1-9J	15.5 ± 0.8	101.7	96.4	14.5 ± 0.5	100.7	97.8
TCD-H2 9-8	-38.2 ± 0.5			-36.3 ± 0.9		
TCD-H2 9J-8	13.8 ± 0.8	102.2	100.1	12.8 ± 0.5	101.2	100.8
TCD-H2 9-8J	13.8 ± 0.8	102.2	100.1	12.8 ± 0.5	101.2	100.8

[a] Units kcal mol^{-1} with error provided from standard deviation of work reaction values.
[b] Average from 6-31G(d,p) and 6-311G(2d,2p) basis sets.
[c] Average from CBS-QB3 and G3MP2B3 methods.
[d] C–H BDE for the loss of the second hydrogen from the radical species generating diradical singlet species.

6.4.1.2 Radical $\Delta H^{\circ}_{f\,298}$: TCD-H2 mJ-n and TCD-H2 m-nJ. Calculated $\Delta H^{\circ}_{f\ \ 298}$ and corresponding C–H BDEs values for the radicals created from the loss of a single hydrogen atom from the TCD parent species are given in Appendix E from the five work reactions in Scheme 6.3. As expected, the heats of formation for the radicals at the 2-6 and 9-8 positions are nearly identical. In similar fashion for the parent species, there is excellent precision in the $\Delta H^{\circ}_{f\ 298}$ values. Averages from the B3LYP and composite methods are summarized in Table 6.2. The average composite method values are recommended and further used as the standard reference $\Delta H^{\circ}_{f\ 298}$ values in the diradical work reactions.

6.4.1.3 Diradical $\Delta H^{\circ}_{f\,298}$: TCD-H2 mJ-nJ. Table 6.3 lists the two sets of work reactions used to determine the heat of formation for the singlet and triplet diradicals using the calculated $\Delta H^{\circ}_{f\ 298}$ from respective TCD-H2 *m*J-*n* and *m*-*n*J radicals. The M06-2X and *w*B97X-D functionals are also included in the diradical analysis to show the applicability of other DFT methods for these highly strained cyclic species. Use of work reactions with the spin-correction methods of Yamaguchi et al.[226] and Sirjean et al.[228] show that satisfactory results are obtained from the less time and computationally demanding DFT methods compared to higher level results. The single point energies from the CCSD(T) calculations, based on optimized B3LYP/6-31G(d,p) geometries, are also in line with the these methods. A summary of the singlet and triplet $\Delta H^{\circ}_{f\,298}$ values is presented in Table 6.4.

Table 6.3 Isodesmic Reactions, Calculated $\Delta H^{\circ}_{f\,298}$, and Bond Dissociation Energies for TCD-H2 *m*J-*n*J Diradicals

Isodesmic Reactions						$\Delta H^{\circ}_{f\,298}$ (kcal mol^{-1})												
						B3LYP/ 6-31G(d,p)	**B3LYP/ 6-311G(2d,2p)**	**M06-2X/ 6-31G(d,p)**	***w*B97X-D/ 6-31G(d,p)**	**CCSD(T)**	**CBS-QB3**	**G3MP2B3**	**B3LYP/ 6-31G(d,p)**	**B3LYP/ 6-311G(2d,2p)**	**M06-2X/ 6-31G(d,p)**	***w*B97X-D/ 6-31G(d,p)**	**CCSD(T)**	**CBS-QB3**	**G3MP2B3**
TCD-H2 1J-2J System						**Singlets**							**Triplets**						
TCD-H2 1J-2J	+	CH_3CH_3	→	TCD-H2 1J-2	+	CH_3CJH_2	56.38	56.65	57.34	57.21	58.38	58.33	58.07	56.38	56.65	57.33	57.21	58.38	57.60	58.09
TCD-H2 1J-2J	+	$CH_3CH_2CH_3$	→	TCD-H2 1J-2	+	CH_3CJHCH_3	57.78	57.95	58.13	58.12	58.40	58.59	57.89	57.77	57.95	58.12	58.13	58.39	57.86	57.91
TCD-H2 1J-2J	+	$(CH_3)_3CH$	→	TCD-H2 1J-2	+	$(CH_3)_3CJ$	58.76	58.78	58.03	58.49	57.88	58.21	57.16	58.76	58.78	58.02	58.49	57.87	57.48	57.18
TCD-H2 1J-2J	+	$CH_3CH_2CH_2CH_3$	→	TCD-H2 1J-2	+	$CH_3CJHCH_2CH_3$	57.15	57.42	57.10	57.31	57.60	57.96	57.24	57.14	57.43	57.09	57.32	57.60	57.23	57.26
TCD-H2 1J-2J	+	YYC_7H_{12}	→	TCD-H2 1J-2	+	$YYCJ_7H_{11}$	58.03	58.06	58.25	58.13	58.55	59.20	58.34	58.02	58.07	58.24	58.14	58.55	58.47	58.36
						Average	**57.6**	**57.8**	**57.8**	**57.9**	**58.2**	**58.5**	**57.7**	**57.6**	**57.8**	**57.8**	**57.9**	**58.2**	**57.7**	**57.8**
						C–H Bond Energy	**96.3**	**96.5**	**96.5**	**96.6**	**96.9**	**97.2**	**96.4**	**96.3**	**96.5**	**96.5**	**96.6**	**96.9**	**96.4**	**96.5**
TCD-H2 1J-2J	+	CH_3CH_3	→	TCD-H2 1-2J	+	CH_3CJH_2	56.48	56.79	57.29	56.96	58.04	58.36	58.04	56.47	56.79	57.28	56.96	58.04	57.63	58.06
TCD-H2 1J-2J	+	$CH_3CH_2CH_3$	→	TCD-H2 1-2J	+	CH_3CJHCH_3	57.88	58.09	58.08	57.87	58.05	58.61	57.86	57.87	58.09	58.08	57.88	58.05	57.89	57.88
TCD-H2 1J-2J	+	$(CH_3)_3CH$	→	TCD-H2 1-2J	+	$(CH_3)_3CJ$	58.86	58.92	57.99	58.24	57.54	58.24	57.13	58.85	58.92	57.98	58.24	57.53	57.51	57.15
TCD-H2 1J-2J	+	$CH_3CH_2CH_2CH_3$	→	TCD-H2 1-2J	+	$CH_3CJHCH_2CH_3$	57.25	57.56	57.05	57.06	57.26	57.99	57.21	57.24	57.57	57.04	57.07	57.25	57.26	57.23
TCD-H2 1J-2J	+	YYC_7H_{12}	→	TCD-H2 1-2J	+	$YYCJ_7H_{11}$	58.13	58.20	58.20	57.88	58.21	59.23	58.32	58.12	58.21	58.19	57.89	58.20	58.50	58.34
						Average	**57.7**	**57.9**	**57.7**	**57.6**	**57.8**	**58.5**	**57.7**	**57.7**	**57.9**	**57.7**	**57.6**	**57.8**	**57.8**	**57.7**
						C–H Bond Energy	**95.9**	**96.1**	**95.9**	**95.8**	**96.0**	**96.7**	**95.9**	**95.9**	**96.1**	**95.9**	**95.8**	**96.0**	**96.0**	**96.0**
						TCD C_1–C_2 *Bond Energy*	**77.1**	**77.3**	**77.2**	**77.2**	**77.5**	**77.9**	**77.2**	**77.1**	**77.3**	**77.2**	**77.2**	**77.4**	**77.2**	**77.2**
TCD-H2 2J-3J System						**Singlets**							**Triplets**						
TCD-H2 2J-3J	+	CH_3CH_3	→	TCD-H2 2J-3	+	CH_3CJH_2	65.09	65.03	65.20	64.90	65.42	65.81	65.24	65.10	65.02	65.21	65.36	65.49	65.15	65.20
TCD-H2 2J-3J	+	$CH_3CH_2CH_3$	→	TCD-H2 2J-3	+	CH_3CJHCH_3	66.49	66.33	65.99	65.82	65.44	66.07	65.06	66.50	66.32	66.00	66.28	65.51	65.40	65.02
TCD-H2 2J-3J	+	$(CH_3)_3CH$	→	TCD-H2 2J-3	+	$(CH_3)_3CJ$	67.48	67.16	65.90	66.18	64.92	65.70	64.33	67.48	67.15	65.90	66.64	64.99	65.03	64.29
TCD-H2 2J-3J	+	$CH_3CH_2CH_2CH_3$	→	TCD-H2 2J-3	+	$CH_3CJHCH_2CH_3$	65.86	65.80	64.96	65.01	64.64	65.45	64.41	65.87	65.79	64.97	65.47	64.71	64.78	64.37
TCD-H2 2J-3J	+	YYC_7H_{12}	→	TCD-H2 2J-3	+	$YYCJ_7H_{11}$	66.74	66.44	66.11	65.83	65.59	66.68	65.52	66.75	66.43	66.12	66.29	65.66	66.02	65.48
						Average	**66.3**	**66.2**	**65.6**	**65.5**	**65.2**	**65.9**	**64.9**	**66.3**	**66.1**	**65.6**	**66.0**	**65.3**	**65.3**	**64.9**
						C–H Bond Energy	**102.5**	**102.4**	**101.8**	**101.8**	**101.4**	**102.2**	**101.1**	**102.5**	**102.4**	**101.9**	**102.2**	**101.5**	**101.5**	**101.1**
TCD-H2 2J-3J	+	CH_3CH_3	→	TCD-H2 2-3J	+	CH_3CJH_2	63.83	64.05	64.72	64.57	65.67	65.52	65.53	63.83	64.04	64.73	65.03	65.74	64.86	65.49
TCD-H2 2J-3J	+	$CH_3CH_2CH_3$	→	TCD-H2 2-3J	+	CH_3CJHCH_3	65.23	65.35	65.51	65.48	65.68	65.78	65.36	65.23	65.34	65.52	65.94	65.75	65.11	65.32
TCD-H2 2J-3J	+	$(CH_3)_3CH$	→	TCD-H2 2-3J	+	$(CH_3)_3CJ$	66.21	66.18	65.42	65.84	65.16	65.41	64.62	66.21	66.17	65.42	66.30	65.23	64.74	64.58
TCD-H2 2J-3J	+	$CH_3CH_2CH_2CH_3$	→	TCD-H2 2-3J	+	$CH_3CJHCH_2CH_3$	64.60	64.82	64.48	64.67	64.89	65.16	64.71	64.60	64.81	64.49	65.13	64.96	64.49	64.67
TCD-H2 2J-3J	+	YYC_7H_{12}	→	TCD-H2 2-3J	+	$YYCJ_7H_{11}$	65.48	65.46	65.63	65.49	65.84	66.39	65.81	65.48	65.45	65.63	65.95	65.91	65.73	65.77
						Average	**65.1**	**65.2**	**65.2**	**65.2**	**65.4**	**65.7**	**65.2**	**65.1**	**65.2**	**65.2**	**65.7**	**65.5**	**65.0**	**65.2**
						C–H Bond Energy	**98.9**	**99.0**	**98.9**	**99.0**	**99.2**	**99.4**	**99.0**	**98.9**	**98.9**	**98.9**	**99.5**	**99.3**	**98.8**	**99.0**
						TCD C_2–C_3 *Bond Energy*	**85.2**	**85.1**	**84.9**	**84.8**	**84.8**	**85.3**	**84.5**	**85.2**	**85.1**	**84.9**	**85.3**	**84.9**	**84.6**	**84.5**

Table 6.3 Isodesmic Reactions, Calculated $\Delta H^{\circ}_{f\,298}$, and Bond Dissociation Energies for TCD-H2 *m*J-*n*J Diradicals (Continued A)

Isodesmic Reactions							$\Delta H^{\circ}_{f\,298}$ (kcal mol^{-1})												
							B3LYP/ 6-31G(d,p)	B3LYP/ 6-311G(2d,2p)	M06-2X/ 6-31G(d,p)	*w*B97X-D/ 6-31G(d,p)	CCSD(T)	CBS-QB3	G3MP2B3	B3LYP/ 6-31G(d,p)	B3LYP/ 6-311G(2d,2p)	M06-2X/ 6-31G(d,p)	*w*B97X-D/ 6-31G(d,p)	CCSD(T)	CBS-QB3	G3MP2B3
TCD-H2 3J-4J System							**Singlets**							**Triplets**						
TCD-H2 3J-4J	+	CH_3CH_3	→	TCD-H2 3J-4	+	CH_3CJH_2	65.49	65.32	66.25	66.48	67.03	67.15	66.76	66.75	66.72	66.60	66.82	67.05	66.94	67.02
TCD-H2 3J-4J	+	$CH_3CH_2CH_3$	→	TCD-H2 3J-4	+	CH_3CJHCH_3	66.89	66.62	67.05	67.40	67.04	67.41	66.59	68.14	68.02	67.39	67.74	67.06	67.20	66.85
TCD-H2 3J-4J	+	$(CH_3)_3CH$	→	TCD-H2 3J-4	+	$(CH_3)_3CJ$	67.88	67.45	66.95	67.76	66.52	67.03	65.85	69.13	68.84	67.30	68.10	66.54	66.83	66.11
TCD-H2 3J-4J	+	$CH_3CH_2CH_2CH_3$	→	TCD-H2 3J-4	+	$CH_3CJHCH_2CH_3$	66.26	66.09	66.02	66.59	66.25	66.78	65.94	67.51	67.49	66.36	66.93	66.27	66.58	66.20
TCD-H2 3J-4J	+	YYC_7H_{12}	→	TCD-H2 3J-4	+	$YYCJ_7H_{11}$	67.14	66.74	67.16	67.40	67.20	68.02	67.04	68.40	68.13	67.51	67.74	67.22	67.81	67.30
						Average	**66.7**	**66.4**	**66.7**	**67.1**	**66.8**	**67.3**	**66.4**	**68.0**	**67.8**	**67.0**	**67.5**	**66.8**	**67.1**	**66.7**
						C–H Bond Energy	**100.7**	**100.4**	**100.6**	**101.1**	**100.7**	**101.2**	**100.4**	**101.9**	**101.8**	**101.0**	**101.4**	**100.8**	**101.0**	**100.6**
TCD-H2 3J-4J	+	CH_3CH_3	→	TCD-H2 3-4J	+	CH_3CJH_2	65.12	64.95	66.12	66.66	67.04	67.09	66.83	66.37	66.35	66.47	67.00	67.06	66.88	67.09
TCD-H2 3J-4J	+	$CH_3CH_2CH_3$	→	TCD-H2 3-4J	+	CH_3CJHCH_3	66.52	66.25	66.91	67.57	67.06	67.34	66.65	67.77	67.65	67.26	67.91	67.08	67.14	66.91
TCD-H2 3J-4J	+	$(CH_3)_3CH$	→	TCD-H2 3-4J	+	$(CH_3)_3CJ$	67.50	67.08	66.82	67.93	66.54	66.97	65.91	68.75	68.48	67.16	68.27	66.56	66.76	66.18
TCD-H2 3J-4J	+	$CH_3CH_2CH_2CH_3$	→	TCD-H2 3-4J	+	$CH_3CJHCH_2CH_3$	65.89	65.73	65.88	66.76	66.26	66.72	66.00	67.14	67.12	66.23	67.10	66.28	66.52	66.26
TCD-H2 3J-4J	+	YYC_7H_{12}	→	TCD-H2 3-4J	+	$YYCJ_7H_{11}$	66.77	66.37	67.03	67.58	67.21	67.96	67.10	68.02	67.76	67.38	67.92	67.23	67.75	67.36
						Average	**66.4**	**66.1**	**66.6**	**67.3**	**66.8**	**67.2**	**66.5**	**67.6**	**67.5**	**66.9**	**67.6**	**66.8**	**67.0**	**66.8**
						C–H Bond Energy	**100.2**	**99.9**	**100.4**	**101.1**	**100.6**	**101.0**	**100.3**	**101.4**	**101.3**	**100.7**	**101.5**	**100.7**	**100.8**	**100.6**
						TCD-H2 *C_3–C_4 Bond Energy*	**86.0**	**85.7**	**86.1**	**86.7**	**86.3**	**86.7**	**85.9**	**87.3**	**87.1**	**86.4**	**87.0**	**86.3**	**86.5**	**86.2**
TCD-H2 2J-6J System							**Singlets**							**Triplets**						
TCD-H2 2J-6J	+	CH_3CH_3	→	TCD-H2 2J-6	+	CH_3CJH_2	53.76	54.19	56.06	54.91	59.37	59.49	59.36	59.75	59.90	60.74	61.09	61.93	61.64	62.23
TCD-H2 2J-6J	+	$CH_3CH_2CH_3$	→	TCD-H2 2J-6	+	CH_3CJHCH_3	55.16	55.50	56.85	55.82	59.39	59.74	59.18	61.15	61.21	61.53	62.00	61.94	61.90	62.05
TCD-H2 2J-6J	+	$(CH_3)_3CH$	→	TCD-H2 2J-6	+	$(CH_3)_3CJ$	56.14	56.32	56.75	56.18	58.87	59.37	58.44	62.13	62.03	61.43	62.37	61.42	61.52	61.31
TCD-H2 2J-6J	+	$CH_3CH_2CH_2CH_3$	→	TCD-H2 2J-6	+	$CH_3CJHCH_2CH_3$	54.52	54.97	55.82	55.01	58.59	59.12	58.53	60.52	60.68	60.50	61.19	61.14	61.27	61.40
TCD-H2 2J-6J	+	YYC_7H_{12}	→	TCD-H2 2J-6	+	$YYCJ_7H_{11}$	55.41	55.61	56.96	55.83	59.54	60.36	59.63	61.40	61.32	61.64	62.01	62.09	62.51	62.50
						Average	**55.0**	**55.3**	**56.5**	**55.6**	**59.2**	**59.6**	**59.0**	**61.0**	**61.0**	**61.2**	**61.7**	**61.7**	**61.8**	**61.9**
						C–H Bond Energy	**90.0**	**90.4**	**91.5**	**90.6**	**94.2**	**94.7**	**94.1**	**96.0**	**96.1**	**96.2**	**96.8**	**96.7**	**96.8**	**96.9**
TCD-H2 2J-6J	+	CH_3CH_3	→	TCD-H2 2-6J	+	CH_3CJH_2	53.76	54.20	56.06	54.91	59.38	59.48	59.36	59.75	59.91	60.74	61.09	61.93	61.64	62.23
TCD-H2 2J-6J	+	$CH_3CH_2CH_3$	→	TCD-H2 2-6J	+	CH_3CJHCH_3	55.16	55.50	56.85	55.82	59.39	59.74	59.18	61.15	61.21	61.53	62.01	61.94	61.90	62.05
TCD-H2 2J-6J	+	$(CH_3)_3CH$	→	TCD-H2 2-6J	+	$(CH_3)_3CJ$	56.14	56.32	56.75	56.19	58.87	59.37	58.45	62.13	62.03	61.43	62.37	61.42	61.52	61.31
TCD-H2 2J-6J	+	$CH_3CH_2CH_2CH_3$	→	TCD-H2 2-6J	+	$CH_3CJHCH_2CH_3$	54.53	54.97	55.82	55.01	58.59	59.12	58.53	60.52	60.68	60.50	61.20	61.14	61.27	61.40
TCD-H2 2J-6J	+	YYC_7H_{12}	→	TCD-H2 2-6J	+	$YYCJ_7H_{11}$	55.41	55.61	56.97	55.83	59.54	60.35	59.64	61.40	61.32	61.65	62.01	62.10	62.51	62.50
						Average	**55.0**	**55.3**	**56.5**	**55.6**	**59.2**	**59.6**	**59.0**	**61.0**	**61.0**	**61.2**	**61.7**	**61.7**	**61.8**	**61.9**
						C–H Bond Energy	**90.0**	**90.4**	**91.5**	**90.6**	**94.2**	**94.6**	**94.1**	**96.0**	**96.1**	**96.2**	**96.8**	**96.7**	**96.8**	**96.9**
						TCD *C_2–C_6 Bond Energy*	**74.5**	**74.8**	**75.9**	**75.0**	**78.6**	**79.1**	**78.5**	**80.4**	**80.5**	**80.6**	**81.2**	**81.2**	**81.2**	**81.4**

Table 6.3 Isodesmic Reactions, Calculated $\Delta H^{\circ}_{f\,298}$, and Bond Dissociation Energies for TCD-H2 *m*J-*n*J Diradicals (Continued B)

Isodesmic Reactions						$\Delta H^{\circ}_{f\,298}$ (kcal mol^{-1})													
						B3LYP/ 6-31G(d,p)	B3LYP/ 6-311G(2d,2p)	M06-2X/ 6-31G(d,p)	*w*B97X-D/ 6-31G(d,p)	CCSD(T)	CBS-QB3	G3MP2B3	B3LYP/ 6-31G(d,p)	B3LYP/ 6-311G(2d,2p)	M06-2X/ 6-31G(d,p)	*w*B97X-D/ 6-31G(d,p)	CCSD(T)	CBS-QB3	G3MP2B3
TCD-H2 1J-10J System						**Singlets**							**Triplets**						
TCD-H2 1J-10J	+	CH_3CH_3	→	TCD-H2 1J-10	+	CH_3CJH_2	59.71	59.68	58.99	59.59	60.26	60.28	59.74	59.85	59.84	59.17	59.73	60.38	59.75	59.97
TCD-H2 1J-10J	+	$CH_3CH_2CH_3$	→	TCD-H2 1J-10	+	CH_3CJHCH_3	61.11	60.98	59.78	60.51	60.27	60.53	59.56	61.25	61.14	59.96	60.64	60.39	60.01	59.80
TCD-H2 1J-10J	+	$(CH_3)_3CH$	→	TCD-H2 1J-10	+	$(CH_3)_3CJ$	62.10	61.81	59.69	60.87	59.75	60.16	58.83	62.23	61.97	59.86	61.01	59.87	59.63	59.06
TCD-H2 1J-10J	+	$CH_3CH_2CH_2CH_3$	→	TCD-H2 1J-10	+	$CH_3CJHCH_2CH_3$	60.48	60.46	58.75	59.70	59.47	59.91	58.91	60.61	60.61	58.93	59.83	59.59	59.38	59.15
TCD-H2 1J-10J	+	YYC_7H_{12}	→	TCD-H2 1J-10	+	$YYCJ_7H_{11}$	61.36	61.10	59.90	60.52	60.43	61.15	60.01	61.50	61.26	60.08	60.65	60.54	60.62	60.25
						Average	**61.0**	**60.8**	**59.4**	**60.2**	**60.0**	**60.4**	**59.4**	**61.1**	**61.0**	**59.6**	**60.4**	**60.2**	**59.9**	**59.6**
						C–H Bond Energy	**101.1**	**100.9**	**99.5**	**100.3**	**100.1**	**100.5**	**99.5**	**101.2**	**101.1**	**99.7**	**100.5**	**100.3**	**100.0**	**99.7**
TCD-H2 1J-10J	+	CH_3CH_3	→	TCD-H2 1-10J	+	CH_3CJH_2	58.54	58.67	58.73	58.66	60.44	60.07	59.94	58.68	58.83	58.91	58.80	60.56	59.55	60.18
TCD-H2 1J-10J	+	$CH_3CH_2CH_3$	→	TCD-H2 1-10J	+	CH_3CJHCH_3	59.94	59.97	59.52	59.58	60.45	60.33	59.76	60.07	60.13	59.70	59.71	60.57	59.80	60.00
TCD-H2 1J-10J	+	$(CH_3)_3CH$	→	TCD-H2 1-10J	+	$(CH_3)_3CJ$	60.93	60.80	59.43	59.94	59.94	59.96	59.03	61.06	60.96	59.60	60.08	60.05	59.43	59.26
TCD-H2 1J-10J	+	$CH_3CH_2CH_2CH_3$	→	TCD-H2 1-10J	+	$CH_3CJHCH_2CH_3$	59.31	59.44	58.49	58.77	59.66	59.71	59.11	59.44	59.60	58.67	58.90	59.78	59.18	59.35
TCD-H2 1J-10J	+	YYC_7H_{12}	→	TCD-H2 1-10J	+	$YYCJ_7H_{11}$	60.19	60.08	59.64	59.59	60.61	60.94	60.22	60.33	60.24	59.82	59.72	60.73	60.42	60.45
						Average	**59.8**	**59.8**	**59.2**	**59.3**	**60.2**	**60.2**	**59.6**	**59.9**	**60.0**	**59.3**	**59.4**	**60.3**	**59.7**	**59.8**
						C–H Bond Energy	**95.4**	**95.4**	**94.7**	**94.9**	**95.8**	**95.8**	**95.2**	**95.5**	**95.5**	**94.9**	**95.0**	**95.9**	**95.3**	**95.4**
						TCD C_1–C_{10} *Bond Energy*	**79.8**	**79.8**	**78.8**	**79.2**	**79.6**	**79.8**	**79.0**	**80.0**	**79.9**	**78.9**	**79.4**	**79.7**	**79.2**	**79.2**
TCD-H2 1J-9J System						**Singlets**							**Triplets**						
TCD-H2 1J-9J	+	CH_3CH_3	→	TCD-H2 1J-9	+	CH_3CJH_2	59.23	59.19	59.00	59.44	60.21	60.59	60.06	60.12	60.10	60.06	60.34	60.49	60.37	60.44
TCD-H2 1J-9J	+	$CH_3CH_2CH_3$	→	TCD-H2 1J-9	+	CH_3CJHCH_3	60.63	60.49	59.79	60.36	60.22	60.84	59.88	61.52	61.40	60.85	61.26	60.50	60.63	60.26
TCD-H2 1J-9J	+	$(CH_3)_3CH$	→	TCD-H2 1J-9	+	$(CH_3)_3CJ$	61.61	61.32	59.69	60.72	59.71	60.47	59.14	62.50	62.23	60.75	61.62	59.98	60.25	59.52
TCD-H2 1J-9J	+	$CH_3CH_2CH_2CH_3$	→	TCD-H2 1J-9	+	$CH_3CJHCH_2CH_3$	60.00	59.96	58.76	59.55	59.43	60.22	59.23	60.89	60.87	59.82	60.45	59.70	60.01	59.61
TCD-H2 1J-9J	+	YYC_7H_{12}	→	TCD-H2 1J-9	+	$YYCJ_7H_{11}$	60.88	60.60	59.91	60.36	60.38	61.46	60.33	61.77	61.52	60.96	61.27	60.65	61.24	60.71
						Average	**60.5**	**60.3**	**59.4**	**60.1**	**60.0**	**60.7**	**59.7**	**61.4**	**61.2**	**60.5**	**61.0**	**60.3**	**60.5**	**60.1**
						C–H Bond Energy	**101.1**	**100.9**	**100.0**	**100.7**	**100.6**	**101.3**	**100.3**	**102.0**	**101.8**	**101.1**	**101.6**	**100.9**	**101.1**	**100.7**
TCD-H2 1J-9J	+	CH_3CH_3	→	TCD-H2 1-9J	+	CH_3CJH_2	57.60	57.64	58.67	58.67	60.33	60.32	60.32	58.49	58.56	59.73	59.57	60.60	60.11	60.70
TCD-H2 1J-9J	+	$CH_3CH_2CH_3$	→	TCD-H2 1-9J	+	CH_3CJHCH_3	59.00	58.95	59.47	59.58	60.34	60.58	60.14	59.89	59.86	60.52	60.48	60.61	60.37	60.52
TCD-H2 1J-9J	+	$(CH_3)_3CH$	→	TCD-H2 1-9J	+	$(CH_3)_3CJ$	59.98	59.77	59.37	59.95	59.82	60.21	59.41	60.87	60.68	60.43	60.85	60.10	59.99	59.79
TCD-H2 1J-9J	+	$CH_3CH_2CH_2CH_3$	→	TCD-H2 1-9J	+	$CH_3CJHCH_2CH_3$	58.37	58.42	58.44	58.77	59.54	59.96	59.49	59.26	59.33	59.49	59.67	59.82	59.74	59.87
TCD-H2 1J-9J	+	YYC_7H_{12}	→	TCD-H2 1-9J	+	$YYCJ_7H_{11}$	59.25	59.06	59.58	59.59	60.49	61.19	60.59	60.14	59.97	60.64	60.49	60.77	60.98	60.98
						Average	**58.8**	**58.8**	**59.1**	**59.3**	**60.1**	**60.5**	**60.0**	**59.7**	**59.7**	**60.2**	**60.2**	**60.4**	**60.2**	**60.4**
						C–H Bond Energy	**96.5**	**96.4**	**96.7**	**96.9**	**97.7**	**98.1**	**97.6**	**97.4**	**97.3**	**97.8**	**97.8**	**98.0**	**97.9**	**98.0**
						TCD C_1–C_9 *Bond Energy*	**79.1**	**79.0**	**78.7**	**79.2**	**79.5**	**80.0**	**79.3**	**80.0**	**79.9**	**79.8**	**80.1**	**79.8**	**79.8**	**79.7**

Table 6.3 Isodesmic Reactions, Calculated $\Delta H^{\circ}_{f\,298}$, and Bond Dissociation Energies for TCD-H2 *m*J-*n*J Diradicals (Continued C)

Isodesmic Reactions						$\Delta H^{\circ}_{f\,298}$ (kcal mol^{-1})													
						B3LYP/ 6-31G(d,p)	**B3LYP/ 6-311G(2d,2p)**	**M06-2X/ 6-31G(d,p)**	***w*B97X-D/ 6-31G(d,p)**	**CCSD(T)**	**CBS-QB3**	**G3MP2B3**	**B3LYP/ 6-31G(d,p)**	**B3LYP/ 6-311G(2d,2p)**	**M06-2X/ 6-31G(d,p)**	***w*B97X-D/ 6-31G(d,p)**	**CCSD(T)**	**CBS-QB3**	**G3MP2B3**
TCD-H2 9J-8J System						**Singlets**							**Triplets**						
TCD-H2 9J-8J	+	CH_3CH_3	→	TCD-H2 9J-8	+	CH_3CJH_2	59.67	59.43	61.04	60.88	62.35	61.75	61.41	61.99	61.91	62.32	62.68	62.75	62.10	62.34
TCD-H2 9J-8J	+	$CH_3CH_2CH_3$	→	TCD-H2 9J-8	+	CH_3CJHCH_3	61.07	60.73	61.83	61.79	62.36	62.01	61.23	63.39	63.21	63.11	63.60	62.76	62.36	62.16
TCD-H2 9J-8J	+	$(CH_3)_3CH$	→	TCD-H2 9J-8	+	$(CH_3)_3CJ$	62.05	61.56	61.73	62.15	61.85	61.63	60.50	64.37	64.04	63.02	63.96	62.25	61.98	61.43
TCD-H2 9J-8J	+	$CH_3CH_2CH_2CH_3$	→	TCD-H2 9J-8	+	$CH_3CJHCH_2CH_3$	60.44	60.20	60.80	60.98	61.57	61.39	60.58	62.75	62.69	62.08	62.79	61.97	61.74	61.51
TCD-H2 9J-8J	+	YYC_7H_{12}	→	TCD-H2 9J-8	+	$YYCJ_7H_{11}$	61.32	60.85	61.94	61.80	62.52	62.62	61.68	63.64	63.33	63.23	63.61	62.92	62.97	62.61
						Average	**60.9**	**60.6**	**61.5**	**61.5**	**62.1**	**61.9**	**61.1**	**63.2**	**63.0**	**62.8**	**63.3**	**62.5**	**62.2**	**62.0**
						C–H Bond Energy	**100.2**	**99.9**	**100.8**	**100.9**	**101.5**	**101.2**	**100.4**	**102.6**	**102.4**	**102.1**	**102.7**	**101.9**	**101.6**	**101.3**
TCD-H2 9J-8J	+	CH_3CH_3	→	TCD-H2 9-8J	+	CH_3CJH_2	59.67	59.43	61.04	60.88	62.35	61.75	61.41	61.99	61.91	62.32	62.68	62.75	62.10	62.34
TCD-H2 9J-8J	+	$CH_3CH_2CH_3$	→	TCD-H2 9-8J	+	CH_3CJHCH_3	61.07	60.73	61.83	61.79	62.36	62.01	61.23	63.39	63.21	63.11	63.60	62.76	62.36	62.16
TCD-H2 9J-8J	+	$(CH_3)_3CH$	→	TCD-H2 9-8J	+	$(CH_3)_3CJ$	62.05	61.56	61.73	62.15	61.85	61.63	60.50	64.37	64.04	63.02	63.96	62.25	61.98	61.43
TCD-H2 9J-8J	+	$CH_3CH_2CH_2CH_3$	→	TCD-H2 9-8J	+	$CH_3CJHCH_2CH_3$	60.44	60.20	60.80	60.98	61.57	61.39	60.58	62.75	62.69	62.08	62.79	61.97	61.74	61.51
TCD-H2 9J-8J	+	YYC_7H_{12}	→	TCD-H2 9-8J	+	$YYCJ_7H_{11}$	61.32	60.85	61.94	61.80	62.52	62.62	61.68	63.64	63.33	63.23	63.61	62.92	62.97	62.61
						Average	**60.9**	**60.6**	**61.5**	**61.5**	**62.1**	**61.9**	**61.1**	**63.2**	**63.0**	**62.8**	**63.3**	**62.5**	**62.2**	**62.0**
						C–H Bond Energy	**100.2**	**99.9**	**100.8**	**100.9**	**101.5**	**101.2**	**100.4**	**102.6**	**102.4**	**102.1**	**102.7**	**101.9**	**101.6**	**101.3**
						TCD C_9–C_8 *Bond Energy*	**80.4**	**80.0**	**80.9**	**81.0**	**81.6**	**81.3**	**80.5**	**82.7**	**82.5**	**82.2**	**82.8**	**82.0**	**81.7**	**81.5**

Table 6.4 Summary of Calculated $\Delta H^{\circ}_{f\,298}$ for TCD-H2 *m*J-*n*J Diradicals with Comparison to Literature Values[a]

Species	B3LYP[b]		M06-2X		*w*B97X-D		CCSD(T)		CBS-QB3		G3MP2B3		Literature[c]
	Singlet	Triplet	Singlet	Triplet	Singlet	Triplet	Singlet	Triplet	Singlet	Triplet	Singlet	Triplet	
TCD-H2 1J-2J	57.8 ± 0.8	57.8 ± 0.8	57.7 ± 0.5	57.7 ± 0.5	57.7 ± 0.5	57.7 ± 0.5	58.0 ± 0.4	58.0 ± 0.4	58.5 ± 0.4	57.7 ± 0.4	57.7 ± 0.5	57.7 ± 0.5	57.41
TCD-H2 2J-3J	65.7 ± 1.0	65.7 ± 1.0	65.4 ± 0.5	65.4 ± 0.5	65.4 ± 0.6	65.8 ± 0.6	65.3 ± 0.4	65.4 ± 0.4	65.8 ± 0.5	65.1 ± 0.5	65.1 ± 0.5	65.0 ± 0.5	67.80
TCD-H2 3J-4J	66.4 ± 0.8	67.7 ± 0.8	66.6 ± 0.5	67.0 ± 0.5	67.2 ± 0.5	67.6 ± 0.5	66.8 ± 0.4	66.8 ± 0.4	67.2 ± 0.4	67.0 ± 0.4	66.5 ± 0.5	66.7 ± 0.5	68.14
TCD-H2 2J-6J	55.2 ± 0.8	61.0 ± 0.8	56.5 ± 0.5	61.2 ± 0.5	55.6 ± 0.5	61.7 ± 0.5	59.2 ± 0.4	61.7 ± 0.4	59.6 ± 0.4	61.8 ± 0.4	59.0 ± 0.5	61.9 ± 0.5	72.21
TCD-H2 1J-10J	60.3 ± 1.0	60.5 ± 1.0	59.3 ± 0.5	59.5 ± 0.5	59.8 ± 0.7	59.9 ± 0.7	60.1 ± 0.4	60.2 ± 0.4	60.3 ± 0.5	59.8 ± 0.5	59.5 ± 0.5	59.7 ± 0.5	61.79
TCD-H2 1J-9J	59.6 ± 1.1	60.5 ± 1.1	59.3 ± 0.5	60.3 ± 0.5	59.7 ± 0.7	60.6 ± 0.7	60.0 ± 0.4	60.3 ± 0.4	60.6 ± 0.5	60.4 ± 0.5	59.9 ± 0.5	60.2 ± 0.5	67.49
TCD-H2 9J-8J	60.7 ± 0.8	63.1 ± 0.8	61.5 ± 0.5	62.8 ± 0.5	61.5 ± 0.5	63.3 ± 0.5	62.1 ± 0.4	62.5 ± 0.4	61.9 ± 0.4	62.2 ± 0.4	61.1 ± 0.5	62.0 ± 0.5	67.39

[a] Units kcal mol^{-1} with error provided from standard deviation of work reaction values.

[b] Average from 6-31G(d,p) and 6-311G(2d,2p) basis sets.

[c] Ref. 26.

Differences in the singlet and triplet energies for the diradicals, fall primarily below 1 kcal mol^{-1}. The DFT methods predict larger differences for TCD-H2 9J-8J with a maximum of 2.4 kcal mol^{-1} from the B3LYP calculations. All of the methods show much larger differences for TCD-H2 2J-6J where singlet and triplet energies range from 5-6 kcal mol^{-1} from the DFT methods to 2-3 kcal mol^{-1} for the higher level methods. For all of the methods, except CBS-QB3, it is shown that the singlet is preferred to the triplet state for all species. There is one exception from G3MP2B3 for TCD-H2 2J-3J where the triplet is favored by only 0.1 kcal mol^{-1}. For the CBS-QB3 calculations, it is seen that the triplet is lower in energy except for TCD-H2 2J-6J and 9J-8J where there are 2.2 and 0.3 kcal mol^{-1} differences respectively. This could be from the spin-correction method applied to these values. Based on the results from the DFT, CCSD(T), and G3MP2B3 methods, the singlet state is interpreted to be preferred for these TCD diradicals.

6.4.1.4 Comparison of $\Delta H^{\circ}_{f\,298}$ TCD-H2 *m*J-*n*J to Literature. Herbinet et al.[26] also estimated thermochemical properties for these TCD diradicals. They used a combination of the THERGAS software,[231] which is based on group additivity,[102] and estimated corrections assuming no interaction between the two radical sites. A comparison between the Herbinet values and this study is presented in Table 6.4.

The calculated singlet diradical values, regardless of the method, show that the TCD-H2 1J-2J, 2J-6J, 1J-10J, and 1J-9J positions are the lowest energy structures and fall within an approximate 4 kcal mol^{-1} range. These sites reflect the ring strain relief upon bond breakage into a more relaxed geometry and are consistent with the TCD-H2 1J-2J and 1J-10J values determined by Herbinet while the 1J-9J position is over 7 kcal mol^{-1} higher in energy suggesting less relief of ring strain. They also determined that the 2J-6J

position has the highest $\Delta H^{\circ}_{f\,298}$ for these diradicals while this study shows it to be one of the lowest for both the singlet and triplet states. Li et al.[30] suggested that cleavage of the 2-6 bond could be the first ring opening position and Davidson et al.[24] noted that this location might also be most susceptible to bond reformation.

The TCD-H2 2J-3J, 3J-4J, and 9J-8J diradicals all have reported enthalpies within less than 1 kcal mol^{-1} to each other in the Herbinet study. These calculations show good correlation to these values for the 2-3 and 3-4 positions, but the 9-8 position is approximately 6 kcal mol^{-1} lower in energy.

6.4.1.5 Carbene $\Delta H^{\circ}_{f\,298}$: TCD-H2 *m*JJ-*n* and TCD-H2 *m*-*n*JJ. Initial $\Delta H^{\circ}_{f\,298}$ values for TCD carbene species are calculated for comparison to the diradicals. Optimization of the triplet state carbenes are straightforward, similar to the triplet diradicals, while careful singlet optimization is necessary. Singlet carbenes with terminal alkane locations (2-3JJ, 3-4JJ, 1-9JJ, and 9JJ-8) quickly converge to more stable bicyclic olefins via a hydrogen transfer from an adjacent carbon. Keeping this in mind, $\Delta H^{\circ}_{f\,298}$ values for all singlet and triplet species using work reactions are calculated and summarized in Table 6.5. Since the same enthalpy values are seen for the radicals and diradicals for 2-6 and 9-8, only one carbene species is analyzed for each location.

Table 6.5 Isodesmic Reactions, Calculated $\Delta H^{\circ}_{f\,298}$, and Bond Dissociation Energies for TCD-H2 *m-n* Carbenes

Isodesmic Reactions						$\Delta H^{\circ}_{f\,298}$ (kcal mol^{-1})													
						B3LYP/ 6-31G(d,p)	B3LYP/ 6-311G(2d,2p)	M06-2X/ 6-31G(d,p)	*w*B97X-D/ 6-31G(d,p)	CCSD(T)	CBS-QB3	G3MP2B3	B3LYP/ 6-31G(d,p)	B3LYP/ 6-311G(2d,2p)	M06-2X/ 6-31G(d,p)	*w*B97X-D/ 6-31G(d,p)	CCSD(T)	CBS-QB3	G3MP2B3
TCD-H2 1JJ-2 System						**Singlets**											**Triplets**		
TCD-H2 1JJ-2	+	CH_4	→	TCD-H2 1-2	+	$:CH_2$	60.17	60.49	58.53	60.30	70.14	67.98	68.77	67.22	67.68	70.31	68.95	73.29	70.28	71.97
TCD-H2 1JJ-2	+	CH_3CH_2OH	→	TCD-H2 1-2	+	$CH_3C{:}OH$	61.17	61.58	63.24	63.09	63.57	60.63	64.47	73.53	73.61	72.19	73.98	72.95	71.74	71.98
TCD-H2 1JJ-2	+	CH_3CH_3	→	TCD-H2 1-2	+	$CH_2{=}CH_2$	58.33	58.64	60.90	59.56	61.21	60.60	64.43	65.28	67.02	65.65	65.07	65.72	71.18	71.40
TCD-H2 1JJ-2	+	$CH_3CH_2CH_3$	→	TCD-H2 1-2	+	$CH_2{=}CHCH_3$	59.51	59.64	61.70	60.07	61.10	60.60	64.31	66.47	68.03	66.45	65.58	65.61	71.17	71.27
TCD-H2 1JJ-2	+	$CH_3CH_2CH_2CH_3$	→	TCD-H2 1-2	+	$CH_3CH{=}CHCH_3$	60.50	60.39	61.79	60.40	61.27	60.43	63.94	67.46	68.77	66.54	65.91	65.78	71.00	70.90
						Average	**59.9**	**60.1**	**61.2**	**60.7**	**63.5**	**62.0**	**65.2**	**68.0**	**69.0**	**68.2**	**67.9**	**68.7**	**71.1**	**71.5**
						TCD C_1–C_2 *Bond Energy*	**79.4**	**79.6**	**80.7**	**80.1**	**82.9**	**81.5**	**84.6**	**87.5**	**88.5**	**87.7**	**87.4**	**88.1**	**90.5**	**91.0**
TCD-H2 1-2JJ System						**Singlets**											**Triplets**		
TCD-H2 1-2JJ	+	CH_4	→	TCD-H2 1-2	+	$:CH_2$	60.26	60.61	58.59	61.04	69.16	69.46	68.61	67.21	67.58	70.55	69.77	73.85	70.70	72.46
TCD-H2 1-2JJ	+	CH_3CH_2OH	→	TCD-H2 1-2	+	$CH_3C{:}OH$	61.26	61.71	63.30	63.84	62.60	62.11	64.30	73.52	73.50	72.43	74.80	73.51	72.16	72.47
TCD-H2 1-2JJ	+	CH_3CH_3	→	TCD-H2 1-2	+	$CH_2{=}CH_2$	58.42	58.76	60.96	60.30	60.23	62.08	64.27	65.27	66.91	65.89	65.89	66.28	71.60	71.89
TCD-H2 1-2JJ	+	$CH_3CH_2CH_3$	→	TCD-H2 1-2	+	$CH_2{=}CHCH_3$	59.60	59.77	61.77	60.81	60.12	62.07	64.14	66.46	67.92	66.69	66.40	66.17	71.59	71.76
TCD-H2 1-2JJ	+	$CH_3CH_2CH_2CH_3$	→	TCD-H2 1-2	+	$CH_3CH{=}CHCH_3$	60.59	60.51	61.85	61.15	60.30	61.90	63.77	67.45	68.67	66.78	66.74	66.35	71.42	71.39
						Average	**60.0**	**60.3**	**61.3**	**61.4**	**62.5**	**63.5**	**65.0**	**68.0**	**68.9**	**68.5**	**68.7**	**69.2**	**71.5**	**72.0**
						TCD C_1–C_2 *Bond Energy*	**79.5**	**79.7**	**80.8**	**80.9**	**81.9**	**83.0**	**84.5**	**87.4**	**88.4**	**87.9**	**88.2**	**88.7**	**91.0**	**91.5**

Table 6.5 Isodesmic Reactions, Calculated $\Delta H^{\circ}_{f\,298}$, and Bond Dissociation Energies for TCD-H2 *m-n* Carbenes (Continued A)

Isodesmic Reactions							$\Delta H^{\circ}_{f\,298}$ (kcal mol^{-1})													
							B3LYP/ 6-31G(d,p)	**B3LYP/ 6-311G(2d,2p)**	**M06-2X/ 6-31G(d,p)**	***w*B97X-D/ 6-31G(d,p)**	**CCSD(T)**	**CBS-QB3**	**G3MP2B3**	**B3LYP/ 6-31G(d,p)**	**B3LYP/ 6-311G(2d,2p)**	**M06-2X/ 6-31G(d,p)**	***w*B97X-D/ 6-31G(d,p)**	**CCSD(T)**	**CBS-QB3**	**G3MP2B3**
TCD-H2 2JJ-3 System														**Singlets**						**Triplets**
TCD-H2 2JJ-3	+	CH_4	→	TCD-H2 2-3	+	$:CH_2$	62.68	62.47	59.95	63.28	70.87	70.05	67.29	69.44	69.82	72.91	72.39	76.01	74.94	74.76
TCD-H2 2JJ-3	+	CH_3CH_2OH	→	TCD-H2 2-3	+	$CH_3C{:}OH$	63.68	63.57	64.65	66.08	64.31	62.70	62.99	75.76	75.75	74.79	77.42	75.66	74.40	74.78
TCD-H2 2JJ-3	+	CH_3CH_3	→	TCD-H2 2-3	+	$CH_2{=}CH_2$	60.83	60.62	62.31	62.54	61.94	62.67	62.95	67.51	69.16	68.25	68.51	68.44	73.84	74.19
TCD-H2 2JJ-3	+	$CH_3CH_2CH_3$	→	TCD-H2 2-3	+	$CH_2{=}CHCH_3$	62.02	61.63	63.12	63.05	61.83	62.66	62.82	68.70	70.17	69.05	69.03	68.33	73.83	74.07
TCD-H2 2JJ-3	+	$CH_3CH_2CH_2CH_3$	→	TCD-H2 2-3	+	$CH_3CH{=}CHCH_3$	63.01	62.37	63.20	63.38	62.01	62.50	62.45	69.69	70.91	69.13	69.36	68.50	73.66	73.70
						Average	**62.4**	**62.1**	**62.6**	**63.7**	**64.2**	**64.1**	**63.7**	**70.2**	**71.2**	**70.8**	**71.3**	**71.4**	**73.7**	**74.3**
						TCD C_2–C_3 *Bond Energy*	**81.9**	**81.6**	**82.1**	**83.1**	**83.7**	**83.6**	**83.2**	**89.7**	**90.6**	**90.3**	**90.8**	**90.8**	**93.2**	**93.8**
TCD-H2 2-3JJ System														**Singlets**						**Triplets**
TCD-H2 2-3JJ	+	CH_4	→	TCD-H2 2-3	+	$:CH_2$	75.46	75.57	74.45	75.76	84.24	82.87	84.06	71.83	71.82	73.76	73.15	75.74	73.92	74.88
TCD-H2 2-3JJ	+	CH_3CH_2OH	→	TCD-H2 2-3	+	$CH_3C{:}OH$	76.46	76.67	79.16	78.56	77.67	75.52	79.76	78.15	77.75	75.64	78.18	75.40	75.38	74.89
TCD-H2 2-3JJ	+	CH_3CH_3	→	TCD-H2 2-3	+	$CH_2{=}CH_2$	73.61	73.72	76.82	75.02	75.31	75.49	79.72	69.90	71.16	69.09	69.28	68.17	74.82	74.30
TCD-H2 2-3JJ	+	$CH_3CH_2CH_3$	→	TCD-H2 2-3	+	$CH_2{=}CHCH_3$	74.80	74.73	77.62	75.53	75.20	75.48	79.60	71.09	72.16	69.90	69.79	68.06	74.81	74.18
TCD-H2 2-3JJ	+	$CH_3CH_2CH_2CH_3$	→	TCD-H2 2-3	+	$CH_3CH{=}CHCH_3$	75.79	75.47	77.71	75.87	75.37	75.31	79.23	72.08	72.91	69.98	70.12	68.23	74.64	73.81
						Average	**75.2**	**75.2**	**77.2**	**76.1**	**77.6**	**76.9**	**80.5**	**72.6**	**73.2**	**71.7**	**72.1**	**71.1**	**74.7**	**74.4**
						TCD C_2–C_3 *Bond Energy*	**94.7**	**94.7**	**96.6**	**95.6**	**97.0**	**96.4**	**99.9**	**92.1**	**92.6**	**91.1**	**91.6**	**90.6**	**94.2**	**93.9**

Table 6.5 Isodesmic Reactions, Calculated $\Delta H^{\circ}_{f\,298}$, and Bond Dissociation Energies for TCD-H2 *m-n* Carbenes (Continued B)

Isodesmic Reactions							$\Delta H^{\circ}_{f\,298}$ (kcal mol^{-1})													
							B3LYP/ 6-31G(d,p)	**B3LYP/ 6-311G(2d,2p)**	**M06-2X/ 6-31G(d,p)**	***w*B97X-D/ 6-31G(d,p)**	**CCSD(T)**	**CBS-QB3**	**G3MP2B3**	**B3LYP/ 6-31G(d,p)**	**B3LYP/ 6-311G(2d,2p)**	**M06-2X/ 6-31G(d,p)**	***w*B97X-D/ 6-31G(d,p)**	**CCSD(T)**	**CBS-QB3**	**G3MP2B3**
TCD-H2 3JJ-4 System														**Singlets**						**Triplets**
TCD-H2 3JJ-4	+	CH_4	→	TCD-H2 3-4	+	$:CH_2$	72.82	72.91	74.28	73.96	82.39	81.46	82.79	69.87	69.85	71.67	72.16	74.58	72.85	74.06
TCD-H2 3JJ-4	+	CH_3CH_2OH	→	TCD-H2 3-4	+	$CH_3C{:}OH$	73.82	74.00	78.99	76.76	75.83	74.10	78.49	76.19	75.78	73.55	77.19	74.24	74.31	74.08
TCD-H2 3JJ-4	+	CH_3CH_3	→	TCD-H2 3-4	+	$CH_2{=}CH_2$	70.98	71.06	76.64	73.22	73.46	74.08	78.45	67.94	69.19	67.00	68.28	67.01	73.75	73.49
TCD-H2 3JJ-4	+	$CH_3CH_2CH_3$	→	TCD-H2 3-4	+	$CH_2{=}CHCH_3$	72.16	72.06	77.45	73.73	73.36	74.07	78.33	69.12	70.20	67.81	68.79	66.90	73.74	73.37
TCD-H2 3JJ-4	+	$CH_3CH_2CH_2CH_3$	→	TCD-H2 3-4	+	$CH_3CH{=}CHCH_3$	73.15	72.81	77.53	74.06	73.53	73.90	77.96	70.12	70.94	67.89	69.13	67.08	73.57	73.00
						Average	**72.6**	**72.6**	**77.0**	**74.3**	**75.7**	**75.5**	**79.2**	**70.6**	**71.2**	**69.6**	**71.1**	**70.0**	**73.6**	**73.6**
						TCD C_3–C_4 *Bond Energy*	**92.0**	**92.0**	**96.4**	**93.8**	**95.2**	**95.0**	**98.7**	**90.1**	**90.7**	**89.0**	**90.6**	**89.4**	**93.1**	**93.1**
TCD-H2 3-4JJ System														**Singlets**						**Triplets**
TCD-H2 3-4JJ	+	CH_4	→	TCD-H2 3-4	+	$:CH_2$	74.81	74.79	74.34	75.17	83.80	82.41	83.71	71.54	71.54	73.29	72.78	75.60	73.87	74.89
TCD-H2 3-4JJ	+	CH_3CH_2OH	→	TCD-H2 3-4	+	$CH_3C{:}OH$	75.81	75.89	79.05	77.97	77.24	75.06	79.40	77.85	77.47	75.17	77.81	75.26	75.32	74.90
TCD-H2 3-4JJ	+	CH_3CH_3	→	TCD-H2 3-4	+	$CH_2{=}CH_2$	72.97	72.94	76.71	74.43	74.87	75.03	79.36	69.61	70.88	68.62	68.91	68.03	74.76	74.32
TCD-H2 3-4JJ	+	$CH_3CH_2CH_3$	→	TCD-H2 3-4	+	$CH_2{=}CHCH_3$	74.15	73.95	77.51	74.94	74.76	75.03	79.24	70.79	71.89	69.43	69.42	67.92	74.75	74.19
TCD-H2 3-4JJ	+	$CH_3CH_2CH_2CH_3$	→	TCD-H2 3-4	+	$CH_3CH{=}CHCH_3$	75.15	74.70	77.60	75.28	74.94	74.86	78.87	71.78	72.63	69.51	69.75	68.09	74.59	73.82
						Average	**74.6**	**74.5**	**77.0**	**75.6**	**77.1**	**76.5**	**80.1**	**72.3**	**72.9**	**71.2**	**71.7**	**71.0**	**74.7**	**74.4**
						TCD C_3–C_4 *Bond Energy*	**94.0**	**93.9**	**96.5**	**95.0**	**96.6**	**95.9**	**99.6**	**91.8**	**92.3**	**90.7**	**91.2**	**90.4**	**94.1**	**93.9**

Table 6.5 Isodesmic Reactions, Calculated $\Delta H^{\circ}_{f\,298}$, and Bond Dissociation Energies for TCD-H2 *m-n* Carbenes (Continued C)

Isodesmic Reactions							$\Delta H^{\circ}_{f\,298}$ (kcal mol^{-1})												
							B3LYP/ 6-31G(d,p)	B3LYP/ 6-311G(2d,2p)	M06-2X/ 6-31G(d,p)	*w*B97X-D/ 6-31G(d,p)	CCSD(T)	CBS-QB3	G3MP2B3	B3LYP/ 6-31G(d,p)	B3LYP/ 6-311G(2d,2p)	M06-2X/ 6-31G(d,p)	*w*B97X-D/ 6-31G(d,p)	CCSD(T)	CBS-QB3	G3MP2B3
TCD-H2 2JJ-6 System												**Singlets**						**Triplets**	
TCD-H2 2JJ-6	+	CH_4	→	TCD-H2 2-6	+	$:CH_2$	65.58	65.76	64.03	66.65	76.33	73.63	75.27	65.85	66.15	69.12	68.53	72.42	69.72	71.71
TCD-H2 2JJ-6	+	CH_3CH_2OH	→	TCD-H2 2-6	+	$CH_3C{:}OH$	66.59	66.86	68.73	69.45	69.76	66.27	70.97	72.17	72.08	71.00	73.56	72.08	71.18	71.72
TCD-H2 2JJ-6	+	CH_3CH_3	→	TCD-H2 2-6	+	$CH_2{=}CH_2$	63.74	63.91	66.39	65.91	67.40	66.25	70.93	63.92	65.49	64.45	64.65	64.85	70.62	71.14
TCD-H2 2JJ-6	+	$CH_3CH_2CH_3$	→	TCD-H2 2-6	+	$CH_2{=}CHCH_3$	64.93	64.92	67.20	66.42	67.29	66.24	70.80	65.11	66.49	65.26	65.16	64.74	70.61	71.01
TCD-H2 2JJ-6	+	$CH_3CH_2CH_2CH_3$	→	TCD-H2 2-6	+	$CH_3CH{=}CHCH_3$	65.92	65.66	67.28	66.75	67.46	66.07	70.43	66.10	67.24	65.34	65.50	64.92	70.44	70.64
						Average	**65.4**	**65.4**	**66.7**	**67.0**	**69.6**	**67.7**	**71.7**	**66.6**	**67.5**	**67.0**	**67.5**	**67.8**	**70.5**	**71.2**
						TCD C_2–C_6 *Bond Energy*	**84.8**	**84.9**	**86.2**	**86.5**	**89.1**	**87.2**	**91.1**	**86.1**	**86.9**	**86.5**	**86.9**	**87.3**	**90.0**	**90.7**
TCD-H2 1JJ-10 System												**Singlets**						**Triplets**	
TCD-H2 1JJ-10	+	CH_4	→	TCD-H2 1-10	+	$:CH_2$	58.23	58.04	57.65	59.58	69.74	67.07	68.77	61.30	61.57	65.22	63.77	68.34	65.04	67.01
TCD-H2 1JJ-10	+	CH_3CH_2OH	→	TCD-H2 1-10	+	$CH_3C{:}OH$	59.23	59.14	62.36	62.38	63.18	59.72	64.47	67.61	67.50	67.10	68.79	68.00	66.49	67.03
TCD-H2 1JJ-10	+	CH_3CH_3	→	TCD-H2 1-10	+	$CH_2{=}CH_2$	56.39	56.19	60.01	58.84	60.81	59.69	64.43	59.36	60.91	60.56	59.89	60.77	65.93	66.44
TCD-H2 1JJ-10	+	$CH_3CH_2CH_3$	→	TCD-H2 1-10	+	$CH_2{=}CHCH_3$	57.58	57.19	60.82	59.35	60.70	59.68	64.31	60.55	61.91	61.36	60.40	60.66	65.93	66.32
TCD-H2 1JJ-10	+	$CH_3CH_2CH_2CH_3$	→	TCD-H2 1-10	+	$CH_3CH{=}CHCH_3$	58.57	57.94	60.90	59.68	60.88	59.52	63.94	61.54	62.66	61.45	60.73	60.83	65.76	65.95
						Average	**58.0**	**57.7**	**60.3**	**60.0**	**63.1**	**61.1**	**65.2**	**62.1**	**62.9**	**63.1**	**62.7**	**63.7**	**65.8**	**66.5**
						TCD C_1–C_{10} *Bond Energy*	**77.5**	**77.2**	**79.8**	**79.4**	**82.5**	**80.6**	**84.6**	**81.5**	**82.4**	**82.6**	**82.2**	**83.2**	**85.3**	**86.0**

Table 6.5 Isodesmic Reactions, Calculated $\Delta H^{\circ}_{f\,298}$, and Bond Dissociation Energies for TCD-H2 *m-n* Carbenes (Continued D)

Isodesmic Reactions						$\Delta H^{\circ}_{f\,298}$ (kcal mol^{-1})													
						B3LYP/ 6-31G(d,p)	B3LYP/ 6-311G(2d,2p)	M06-2X/ 6-31G(d,p)	*w*B97X-D/ 6-31G(d,p)	CCSD(T)	CBS-QB3	G3MP2B3	B3LYP/ 6-31G(d,p)	B3LYP/ 6-311G(2d,2p)	M06-2X/ 6-31G(d,p)	*w*B97X-D/ 6-31G(d,p)	CCSD(T)	CBS-QB3	G3MP2B3
TCD-H2 1-10JJ System						**Singlets**										**Triplets**			
TCD-H2 1-10JJ	+	CH_4	→	TCD-H2 1-10	+	$:CH_2$	68.61	68.86	67.36	70.11	78.77	77.35	78.92	68.36	68.40	69.60	70.55	72.95	71.47	72.70
TCD-H2 1-10JJ	+	CH_3CH_2OH	→	TCD-H2 1-10	+	$CH_3C{:}OH$	69.61	69.96	72.07	72.91	72.21	69.99	74.62	74.67	74.33	71.48	75.58	72.61	72.92	72.72
TCD-H2 1-10JJ	+	CH_3CH_3	→	TCD-H2 1-10	+	$CH_2{=}CH_2$	66.77	67.01	69.72	69.37	69.84	69.97	74.58	66.42	67.74	64.93	66.68	65.38	72.36	72.13
TCD-H2 1-10JJ	+	$CH_3CH_2CH_3$	→	TCD-H2 1-10	+	$CH_2{=}CHCH_3$	67.95	68.02	70.53	69.88	69.73	69.96	74.46	67.61	68.74	65.74	67.19	65.27	72.36	72.01
TCD-H2 1-10JJ	+	$CH_3CH_2CH_2CH_3$	→	TCD-H2 1-10	+	$CH_3CH{=}CHCH_3$	68.95	68.77	70.61	70.22	69.91	69.79	74.09	68.60	69.49	65.82	67.52	65.44	72.19	71.64
						Average	**68.4**	**68.5**	**70.1**	**70.5**	**72.1**	**71.4**	**75.3**	**69.1**	**69.7**	**67.5**	**69.5**	**68.3**	**72.3**	**72.2**
						TCD C_1–C_{10} *Bond Energy*	**87.8**	**88.0**	**89.5**	**90.0**	**91.6**	**90.9**	**94.8**	**88.6**	**89.2**	**87.0**	**89.0**	**87.8**	**91.7**	**91.7**
TCD-H2 1JJ-9 System						**Singlets**										**Triplets**			
TCD-H2 1JJ-9	+	CH_4	→	TCD-H2 1-9	+	$:CH_2$	58.26	58.18	58.02	59.41	69.48	67.44	68.59	64.10	64.24	67.79	66.76	70.75	67.88	69.74
TCD-H2 1JJ-9	+	CH_3CH_2OH	→	TCD-H2 1-9	+	$CH_3C{:}OH$	59.26	59.28	62.73	62.21	62.92	60.08	64.29	70.42	70.17	69.67	71.79	70.41	69.34	69.76
TCD-H2 1JJ-9	+	CH_3CH_3	→	TCD-H2 1-9	+	$CH_2{=}CH_2$	56.42	56.33	60.39	58.67	60.55	60.06	64.25	62.17	63.58	63.12	62.88	63.18	68.78	69.17
TCD-H2 1JJ-9	+	$CH_3CH_2CH_3$	→	TCD-H2 1-9	+	$CH_2{=}CHCH_3$	57.60	57.34	61.19	59.18	60.44	60.05	64.12	63.35	64.59	63.93	63.40	63.07	68.77	69.05
TCD-H2 1JJ-9	+	$CH_3CH_2CH_2CH_3$	→	TCD-H2 1-9	+	$CH_3CH{=}CHCH_3$	58.59	58.09	61.28	59.52	60.62	59.88	63.75	64.35	65.33	64.01	63.73	63.25	68.60	68.68
						Average	**58.0**	**57.8**	**60.7**	**59.8**	**62.8**	**61.5**	**65.0**	**64.9**	**65.6**	**65.7**	**65.7**	**66.1**	**68.7**	**69.3**
						TCD C_1–C_9 *Bond Energy*	**77.5**	**77.3**	**80.2**	**79.3**	**82.3**	**81.0**	**84.5**	**84.3**	**85.0**	**85.2**	**85.2**	**85.6**	**88.1**	**88.7**

Table 6.5 Isodesmic Reactions, Calculated $\Delta H^{\circ}_{f\,298}$, and Bond Dissociation Energies for TCD-H2 *m-n* Carbenes (Continued E)

Isodesmic Reactions							$\Delta H^{\circ}_{f\,298}$ (kcal mol^{-1})												
							B3LYP/ 6-31G(d,p)	**B3LYP/ 6-311G(2d,2p)**	**M06-2X/ 6-31G(d,p)**	***w*B97X-D/ 6-31G(d,p)**	**CCSD(T)**	**CBS-QB3**	**G3MP2B3**	**B3LYP/ 6-31G(d,p)**	**B3LYP/ 6-311G(2d,2p)**	**M06-2X/ 6-31G(d,p)**	***w*B97X-D/ 6-31G(d,p)**	**CCSD(T)**	**CBS-QB3**	**G3MP2B3**
TCD-H2 1-9JJ System														**Singlets**						
TCD-H2 1-9JJ	+	CH_4	→	TCD-H2 1-9	+	$:CH_2$	71.44	71.48	70.38	71.63	80.07	78.84	80.07	67.60	67.61	69.29	68.97	71.65	69.93	70.95
TCD-H2 1-9JJ	+	CH_3CH_2OH	→	TCD-H2 1-9	+	$CH_3C{:}OH$	72.44	72.58	75.09	74.43	73.51	71.48	75.76	73.91	73.54	71.17	74.00	71.31	71.39	70.96
TCD-H2 1-9JJ	+	CH_3CH_3	→	TCD-H2 1-9	+	$CH_2{=}CH_2$	69.60	69.63	72.75	70.89	71.14	71.46	75.73	65.66	66.95	64.62	65.10	64.08	70.83	70.37
TCD-H2 1-9JJ	+	$CH_3CH_2CH_3$	→	TCD-H2 1-9	+	$CH_2{=}CHCH_3$	70.78	70.64	73.55	71.40	71.03	71.45	75.60	66.85	67.96	65.43	65.61	63.97	70.82	70.25
TCD-H2 1-9JJ	+	$CH_3CH_2CH_2CH_3$	→	TCD-H2 1-9	+	$CH_3CH{=}CHCH_3$	71.77	71.38	73.64	71.74	71.21	71.28	75.23	67.84	68.70	65.51	65.94	64.15	70.65	69.88
						Average	**71.2**	**71.1**	**73.1**	**72.0**	**73.4**	**72.9**	**76.5**	**68.4**	**69.0**	**67.2**	**67.9**	**67.0**	**70.7**	**70.5**
						TCD C_1–C_9 *Bond Energy*	**90.7**	**90.6**	**92.5**	**91.5**	**92.9**	**92.4**	**95.9**	**87.8**	**88.4**	**86.7**	**87.4**	**86.5**	**90.2**	**89.9**
TCD-H2 9JJ-8 System														**Singlets**						
TCD-H2 9JJ-8	+	CH_4	→	TCD-H2 9-8	+	$:CH_2$	69.90	69.74	70.41	70.50	79.13	76.83	78.28	66.07	66.01	68.37	67.87	70.64	68.27	69.48
TCD-H2 9JJ-8	+	CH_3CH_2OH	→	TCD-H2 9-8	+	$CH_3C{:}OH$	70.90	70.83	75.12	73.29	72.57	69.47	73.97	72.38	71.94	70.25	72.90	70.29	69.73	69.50
TCD-H2 9JJ-8	+	CH_3CH_3	→	TCD-H2 9-8	+	$CH_2{=}CH_2$	68.06	67.89	72.77	69.75	70.20	69.45	73.93	64.14	65.35	63.70	63.99	63.06	69.17	68.91
TCD-H2 9JJ-8	+	$CH_3CH_2CH_3$	→	TCD-H2 9-8	+	$CH_2{=}CHCH_3$	69.24	68.89	73.58	70.27	70.09	69.44	73.81	65.32	66.36	64.51	64.50	62.96	69.16	68.78
TCD-H2 9JJ-8	+	$CH_3CH_2CH_2CH_3$	→	TCD-H2 9-8	+	$CH_3CH{=}CHCH_3$	70.23	69.64	73.66	70.60	70.27	69.27	73.44	66.31	67.10	64.59	64.83	63.13	68.99	68.41
						Average	**69.7**	**69.4**	**73.1**	**70.9**	**72.4**	**70.9**	**74.7**	**66.8**	**67.4**	**66.3**	**66.8**	**66.0**	**69.1**	**69.0**
						TCD C_9–C_8 *Bond Energy*	**89.1**	**88.9**	**92.6**	**90.3**	**91.9**	**90.4**	**94.1**	**86.3**	**86.8**	**85.7**	**86.3**	**85.5**	**88.5**	**88.5**

All of the DFT methods have been corrected using the same spin-projection method used for the diradicals. A summary of the calculated $\Delta H^{\circ}_{f\,298}$ values is presented in Table 6.6 where, in general, there are similar values for the DFT methods while the values from CCSD(T), CBS-QB3, and G3MP2B3 are higher. Error for these values is determined as the standard deviation from the work reactions for each level of theory. In the subsequent analysis, the entire range of values is considered from all of the calculation methods.

The singlet-triplet gaps for these carbenes have a much larger range as compared to the diradicals from under 1 to over 10 kcal mol^{-1}. This is expected due to the proximity of the two electrons on the single carbon. Except for two cases, TCD-H2 2JJ-6 and 1-10JJ, all of the methods show agreement in preference for either the singlet or triplet state. The singlets are more stable for secondary cyclic positions while the triplets show favorable stability for the terminal methyl locations.

These calculations show that some of the carbenes are similar in energy to the diradicals. TCD-H2 1JJ-2, 1-2JJ, 2JJ-3, 1JJ-10, and 1JJ-9 singlet species all have energies between approximately 58-65 kcal mol^{-1}. All of the methods show 1JJ-9, 1JJ-10, and 1-2JJ are the lowest energy species. Energies for the most stable state of the other carbenes all begin close to the maximum diradical energy around 65 kcal mol^{-1} and continue up to about 75 kcal mol^{-1}. The higher energy states for these carbenes show energies with an even higher maximum of about 80 kcal mol^{-1}.

Table 6.6 Summary of Calculated $\Delta H^{\circ}_{f\,298}$[a] for TCD-H2 *m-n* Carbenes

Species	B3LYP[b]		M06-2X		*w*B97X-D		CCSD(T)		CBS-QB3		G3MP2B3	
	Singlet	**Triplet**	**Singlet**	**Triplet**	**Singlet**	**Triplet**	**Singlet**	**Triplet**	**Singlet**	**Triplet**	**Singlet**	**Triplet**
TCD-H2 1JJ-2	60.0	68.5	61.2	68.2	60.7	67.9	63.5	68.7	62.0	71.1	65.2	71.5
TCD-H2 1-2JJ	60.2	68.4	61.3	68.5	61.4	68.7	62.5	69.2	63.5	71.5	65.0	72.0
TCD-H2 2JJ-3	62.3	70.7	62.6	70.8	63.7	71.3	64.2	71.4	64.1	73.7	63.7	74.3
TCD-H2 2-3JJ	75.2	72.9	77.2	71.7	76.1	72.1	77.6	71.1	76.9	74.7	80.5	74.4
TCD-H2 3JJ-4	72.6	70.9	77.0	69.6	74.3	71.1	75.7	70.0	75.5	73.6	79.2	73.6
TCD-H2 3-4JJ	74.5	72.6	77.0	71.2	75.6	71.7	77.1	71.0	76.5	74.7	80.1	74.4
TCD-H2 2JJ-6	65.4	67.1	66.7	67.0	67.0	67.5	69.6	67.8	67.7	70.5	71.7	71.2
TCD-H2 1JJ-10	57.8	62.5	60.3	63.1	60.0	62.7	63.1	63.7	61.1	65.8	65.2	66.5
TCD-H2 1-10JJ	68.5	69.4	70.1	67.5	70.5	69.5	72.1	68.3	71.4	72.3	75.3	72.2
TCD-H2 1JJ-9	57.9	65.2	60.7	65.7	59.8	65.7	62.8	66.1	61.5	68.7	65.0	69.3
TCD-H2 1-9JJ	71.2	68.7	73.1	67.2	72.0	67.9	73.4	67.0	72.9	70.7	76.5	70.5
TCD-H2 9JJ-8	69.5	67.1	73.1	66.3	70.9	66.8	72.4	66.0	70.9	69.1	74.7	69.0
σ[c]	1.0	2.8	1.7	2.9	1.4	3.7	3.9	4.1	3.3	0.5	2.0	0.5

[a] Units kcal mol^{-1}.

[b] Average from 6-31G(d,p) and 6-311G(2d,2p) basis sets.

[c] Error provided from standard deviation of work reaction values.

6.4.2 Carbon-Hydrogen Bond Dissociation Energies (C–H BDEs)

6.4.2.1 C–H BDE: Parent to Radical . C–H BDEs are computed from the calculated parent and radical enthalpies listed in Table 6.2 with the standard enthalpy of the hydrogen atom in Table 6.1 according to the reaction:

TCD-H2 *m*-*n* Parent → TCD-H2 *m*-*n* Radical + H

When comparing the DFT and composite calculation, similar ranges exist for the BDE as was previously seen with the heat of formation values. C–H BDEs in Table 6.2 show the DFT methods provide acceptable values compared to the higher levels. Average values from the composite methods are recommended and referenced in the subsequent analysis.

The secondary cyclic carbon radicals TCD-H2 1J-2, 1-2J, 2J-3, 1J-9, and 1J-10 have bond energies ranging from 95.6-98.8 kcal mol^{-1}. These are consistent with the standard BDEs for secondary alkanes of 98.5 kcal mol^{-1} and the 97-99 kcal mol^{-1} range of the secondary cyclic carbon radicals of TCD[225] (TCD-R3, TCD-R4, TCD-R9), norbornane,[203] bicyclo[3.1.1]heptane,[128] and bicyclo[2.2.2]octane.[128]

The TCD-H2 2-6 radicals have lower bond energies of 93.2 kcal mol^{-1} seemingly due to better radical stability with a larger ring of eight or more carbons. This is consistent with bond energies seen of 96-97 kcal mol^{-1} for cyclopentane, 99-100 kcal mol^{-1} for cyclohexane and 95.7 kcal mol^{-1} for cyclooctane.[126,128,204-206]

Radical formation on primary sites of an alkane branch for the TCD-H2 3-4, 9-8, 2-3J, 1-10J, and 1-9J have bond energies ranging from 100.1-101.2 kcal mol^{-1}, with only a 1.1 kcal mol^{-1} difference from these methyl, ethyl, or *n*-propyl groups. There is excellent agreement to a standard 101.1 kcal mol^{-1} primary alkane and the 100-101 kcal

mol^{-1} primary C–H BDE range reported for ethane, *n*-propane, and *n*-butane.[121,126,127] A search of the literature for substituted cycloalkane BDEs provided only values for the primary C–H BDE for the methyl group in methylcyclopropane ranging from 97-99 kcal mol^{-1}.[126,206] These values from primary alkanes and alkane substituted cyclics are consistent with these calculations.

6.4.2.2 Second C–H BDE: Radical to Diradical. Table 6.2 also summarizes the energy required to remove the second hydrogen from each TCD-H2 radical to generate the diradical singlet species using the reaction:

TCD-H2 *m*-*n* Radical → TCD-H2 *m*J-*n*J Diradical + H

These second C–H BDEs are calculated based on the singlet diradical composite method average. As was the case for the hydrogen removal, the average from the B3LYP and the composite methods are in good agreement. Overall, these species are not affected by the existence of the first radical site. The maximum difference for these second C–H BDEs as compared to the first is only 1.2 kcal mol^{-1} which allows for the same conclusions for these BDEs as seen in the first energies.

6.4.3 Carbon-Carbon Bond Dissociation Energies (C–C BDEs)

6.4.3.1 C–C BDE: Diradicals. The C–C BDE are computed as the difference in energy of the $\Delta H^{\circ}_{f\,298}$ for TCD,[225] -19.5 kcal mol^{-1}, and $\Delta H^{\circ}_{f\,298}$ for the diradical species. For reference, the C–C standard BDE for methyl groups in the C_2-C_6 *n*-alkanes are 88-90 kcal mol^{-1} while ethyl and propyl group C–C BDEs in the C_4-C_8 and C_6-C_8 for *n*-alkanes are slightly lower in the 86-88 kcal mol^{-1} range.[126] C–C BDE for several *n*-aldehydes

have been shown to be 82-85 kcal mol^{-1} with larger energies of 88-90 kcal mol^{-1} for bond dissociations more than three carbon atoms away from the carbonyl group.[168]

C–C BDEs for cyclopentane and cyclohexane are estimated using calculated $\Delta H^{\circ}_{f\,298}$ values by Sirjean et al.[208] for the parent and corresponding diradicals. Values of 81 and 88 kcal mol^{-1} for C–C BDE cyclopentane and cyclohexane are calculated with each cyclic compound opening to a diradical with a normal alkane conformation. Sirjean et al.[208] report rate parameters for unimolecular cyclopentane and cyclohexane ring opening to singlet diradicals with activation energies of approximately 85 (log A (s^{-1}) of 18.11 and n -0.466) and 93 (log A (s^{-1}) of 21.32 and n -0.972) kcal mol^{-1} respectively at temperatures between 600-2000 K.

A summary of the C–C BDEs, in Table 6.7, representing the TCD ring opening to singlet and triplet diradicals range from 77-87 kcal mol^{-1} with good correlations between the DFT and the higher level calculations. For all of the diradicals, there are minimal differences between the singlet and triplet energies except for TCD-H2 2J-6J. This species has a large difference in the calculated $\Delta H^{\circ}_{f\,298}$ which translates into large differences for the C–C BDEs. Singlet C–C BDEs values from the average of the CBS-QB3 and G3MP2B3 values from Table 6.7, which provide good representative C–C BDEs for all of our methods, are considered in the subsequent analysis.

Table 6.7 Summary of Calculated C–C Bond Dissociation Energies[a] for TCD-H2 *m*J-*n*J Diradicals

Species	B3LYP[b]		M06-2X		*w*B97X-D		CCSD(T)		CBS-QB3		G3MP2B3	
	Singlet	**Triplet**	**Singlet**	**Triplet**	**Singlet**	**Triplet**	**Singlet**	**Triplet**	**Singlet**	**Triplet**	**Singlet**	**Triplet**
TCD-H2 1J-2J	77.2	77.2	77.2	77.2	77.2	77.2	77.5	77.4	77.9	77.2	77.2	77.2
TCD-H2 2J-3J	85.1	85.1	84.9	84.9	84.8	85.3	84.8	84.9	85.3	84.6	84.5	84.5
TCD-H2 3J-4J	85.9	87.2	86.1	86.4	86.7	87.0	86.3	86.3	86.7	86.5	85.9	86.2
TCD-H2 2J-6J	74.6	80.5	75.9	80.6	75.0	81.2	78.6	81.2	79.1	81.2	78.5	81.4
TCD-H2 1J-10J	79.8	79.9	78.8	78.9	79.2	79.4	79.6	79.7	79.8	79.2	79.0	79.2
TCD-H2 1J-9J	79.1	80.0	78.7	79.8	79.2	80.1	79.5	79.8	80.0	79.8	79.3	79.7
TCD-H2 9J-8J	80.2	82.6	80.9	82.2	81.0	82.8	81.6	82.0	81.3	81.7	80.5	81.5

[a] Units kcal mol^{-1}.

[b] Average from 6-31G(d,p) and 6-311G(2d,2p) basis sets.

Calculations show that five of the seven C–C BDEs fall within a tight 3.3 kcal mol^{-1} range. The 1-2 position is determined to be the most favorable site for initial ring opening reactions which connects the two cyclopentane rings through the C_1 and C_2 bridgehead carbons. Formation of this singlet diradical is the weakest relative C–C BDE of 77.6 kcal mol^{-1} for TCD.

The next four bond energies have differences of about 2 kcal mol^{-1} with the 2-6 only slightly stronger than the 1-2 bond at 78.8 kcal mol^{-1}. The next highest energies, 1-10 and 1-9, have only a 0.3 kcal mol^{-1} difference, 79.4 and 79.7 kcal mol^{-1} respectively, and involve breaking bonds to the same C_1 bridgehead carbon. The final energy in this grouping is only approximately 1 kcal mol^{-1} higher at 80.9 kcal mol^{-1} for the 9-8 position. These four C–C BDEs are only slightly lower than the 81 kcal mol^{-1} estimated for cyclopentane.

The two strongest BDEs are 84.9 and 86.3 kcal mol^{-1} for TCD-H2 2J-3J and 3J-4J. These correspond to opening a five carbon ring and do not show as great a relief from ring strain as the other locations on TCD.

6.4.3.2 C–C BDE: Carbenes. For comparison, the C–C BDE for generating the singlet and triplet carbenes are determined and given in Table 6.8. The methods give consistent values with slightly lower values for the DFT methods and higher values for the composite methods. Subsequent analysis of the carbene products was planned; but our calculations show that carbene formation is not as important as diradical formation.

Table 6.8 Summary of Calculated C–C Bond Dissociation Energies[a] for TCD-H2 *m-n* Carbenes

Species	B3LYP[b]		M06-2X		*w*B97X-D		CCSD(T)		CBS-QB3		G3MP2B3	
	Singlet	**Triplet**	**Singlet**	**Triplet**	**Singlet**	**Triplet**	**Singlet**	**Triplet**	**Singlet**	**Triplet**	**Singlet**	**Triplet**
TCD-H2 1JJ-2	79.5	88.0	80.7	87.7	80.1	87.4	82.9	88.1	81.5	90.5	84.6	91.0
TCD-H2 1-2JJ	79.6	87.9	80.8	87.9	80.9	88.2	81.9	88.7	83.0	91.0	84.5	91.5
TCD-H2 2JJ-3	81.7	90.2	82.1	90.3	83.1	90.8	83.7	90.8	83.6	93.2	83.2	93.8
TCD-H2 2-3JJ	94.7	92.3	96.6	91.1	95.6	91.6	97.0	90.6	96.4	94.2	99.9	93.9
TCD-H2 3JJ-4	92.0	90.4	96.4	89.0	93.8	90.6	95.2	89.4	95.0	93.1	98.7	93.1
TCD-H2 3-4JJ	94.0	92.1	96.5	90.7	95.0	91.2	96.6	90.4	95.9	94.1	99.6	93.9
TCD-H2 2JJ-6	84.8	86.5	86.2	86.5	86.5	86.9	89.1	87.3	87.2	90.0	91.1	90.7
TCD-H2 1JJ-10	77.3	82.0	79.8	82.6	79.4	82.2	82.5	83.2	80.6	85.3	84.6	86.0
TCD-H2 1-10JJ	87.9	88.9	89.5	87.0	90.0	89.0	91.6	87.8	90.9	91.7	94.8	91.7
TCD-H2 1JJ-9	77.4	84.7	80.2	85.2	79.3	85.2	82.3	85.6	81.0	88.1	84.5	88.7
TCD-H2 1-9JJ	90.6	88.1	92.5	86.7	91.5	87.4	92.9	86.5	92.4	90.2	95.9	89.9
TCD-H2 9JJ-8	89.0	86.6	92.6	85.7	90.3	86.3	91.9	85.5	90.4	88.5	94.1	88.5

[a] Units kcal mol^{-1}.

[b] Average from 6-31G(d,p) and 6-311G(2d,2p) basis sets.

Several of the DFT methods predict C–C BDEs in a similar range seen for the diradical BDEs and extending to over 90 kcal mol^{-1}. The composite methods have a higher starting range for the carbene C–C BDEs and extend to almost 100 kcal mol^{-1}.

6.4.4 Internal Rotors

Internal rotor analysis is needed for determination of the lowest energy geometries and for internal rotor contributions to entropy and heat capacity. Potential curves at 298 K for internal rotors in the parent, radical, diradical, and carbene species are determined using relaxed scans at the B3LYP/6-31G(d,p) level of theory at 10° intervals. If a lower energy conformer is found, previous scans are re-run to insure the lowest energy conformation. Figure 6.6 illustrates the bond numbering for compounds that have more than one internal rotor. Note that these structures do not reflect their optimized geometries. Plots of internal rotation potentials at 298 K are available in Appendix E.

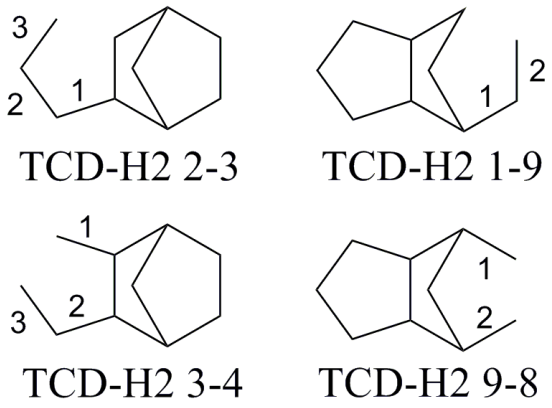

Figure 6.6 Internal rotor notation for species with multiple rotational bonds.

6.4.4.1 Methyl Rotation. Internal rotational potential barriers in the parent TCD-H2 *m*-*n* compounds exhibit three-fold barrier heights between 2.4-3.4 kcal mol^{-1} which are near the typical rotor potential for methyl groups in hydrocarbons[181-184] at approximately 3 kcal mol^{-1}. Locations which are more crowded, for example rotor 1 in TCD-H2 3-4, have larger barriers while less hindered rotors, rotor 3 in TCD-H2 3-4 and in the TCD-H2 1-10 rotor, have lower barriers.

When the methyl group is the radical site, there are two-fold barriers with reduced heights of 0.2-1.0 kcal mol^{-1} while the diradicals are 0.4-0.8 kcal mol^{-1}. The carbenes exhibit similarities to the parents, radicals, and diradicals with methyl rotation barrier heights between 0.5-3.4 kcal mol^{-1}.

6.4.4.2 Methyl and Ethyl Group Rotation. Barriers that involve methyl and ethyl group rotors for TCD-H2 2-3 and 1-9 have a 5.6-6.3 kcal mol^{-1} range. These compare with similar values in *n*-alkanes groups; for example the central C–C rotor barrier in *n*-butane has been reported as between 5.0-5.5 kcal mol^{-1}.[232-234] The barrier increases to 10.8 kcal mol^{-1} for ethyl rotation, rotor 2, in TCD-H2 3-4 due to the closeness of the two methyl groups.

In radical, diradical, and carbene formation, a similar decrease in barrier height energy occurres in the methyl radicals, but these barriers are still in excess of 4.3 kcal mol^{-1}. There is a 2.2 kcal mol^{-1} maximum barrier energy difference between the parent, radical, diradical, and carbene compounds for TCD-H2 2-3 and TCD-H2 1-9 while the TCD-H2 3-4 compounds show a larger 3.2 kcal mol^{-1} maximum difference.

6.4.4.3 Cyclopentane Rotation. TCD-H2 1-2 is unique in that it has rotation about a bond joining two cyclopentane rings. This barrier energy is similar to that for the methyl and ethyl substituent group rotors. The parent compound has a non-symmetrical maximum barrier of 7.1 kcal mol^{-1} which decreases slightly to 6.1-7.0 kcal mol^{-1} upon radical, diradical, and carbene formation. Similar energy barriers are seen for the central O–O rotor in dimethyl tetraoxide[235] and the central C–O rotor in methyl ethyl ether.[236]

6.4.5 Entropies (*S(T)*) and Heat Capacities ($C_p(T)$)

Entropies and heat capacities for the TCD-H2 *m*J-*n*J diradical singlet state species at the B3LYP/6-31G(d,p) level of theory for the 50-5000 K temperature range (JANNAF format) are presented in Table 6.9. The entropy values determined from the diradical triplet species are reduced down by R ln(3) to account for the multiplicity difference. Total entropies and heat capacities for the other species are presented in Appendix E.

Table 6.9 Calculated Total Entropies[a] and Heat Capacities[a] for TCD-H2 *m*J-*n*J Singlet Diradical Species

Temperature	TCD-H2 1J-2J		TCD-H2 2J-3J		TCD-H2 3J-4J		TCD-H2 2J-6J		TCD-H2 1J-10J		TCD-H2 1J-9J		TCD-H2 9J-8J	
(K)	**Cp**	**S**	**Cp**	**S**	**Cp**	**S**	**Cp**	**S**	**Cp**	**S**	**Cp**	**S**	**Cp**	**S**
50	12.35	60.93	12.92	61.36	12.82	63.38	10.53	56.98	11.41	59.69	12.81	60.85	13.41	62.09
100	18.25	71.35	17.86	71.37	18.43	73.23	15.57	65.72	16.94	68.92	18.32	71.10	18.30	72.03
150	23.38	79.72	22.75	79.10	23.55	80.85	21.30	73.10	22.22	76.37	23.26	79.04	23.44	79.58
200	28.76	87.15	28.24	86.08	29.10	87.78	27.36	80.03	27.95	83.22	28.71	86.16	29.14	86.50
250	35.07	94.21	34.75	92.83	35.54	94.49	34.10	86.83	34.50	89.91	35.09	92.99	35.58	93.23
298	41.88	100.93	41.70	99.32	42.37	100.94	41.11	93.39	41.39	96.36	41.90	99.54	42.32	99.68
400	56.79	115.32	56.72	113.39	57.07	114.87	56.17	107.58	56.23	110.31	56.70	113.64	56.81	113.56
500	69.86	129.40	69.71	127.23	69.77	128.53	69.30	121.53	69.15	124.03	69.59	127.46	69.42	127.16
600	80.75	143.10	80.45	140.71	80.26	141.82	80.23	135.13	79.91	137.41	80.31	140.91	79.91	140.38
700	89.76	156.23	89.29	153.62	88.92	154.54	89.28	148.18	88.82	150.24	89.17	153.81	88.59	153.04
800	97.29	168.70	96.67	165.89	96.16	166.61	96.85	160.59	96.28	162.45	96.59	166.06	95.88	165.08
1000	109.12	191.72	108.27	188.52	107.58	188.89	108.75	183.52	108.02	185.01	108.26	188.68	107.37	187.30
1500	126.93	239.72	125.87	235.72	124.98	235.36	126.69	231.39	125.79	232.15	125.91	235.89	124.88	233.71
2000	135.87	277.57	134.79	272.98	133.83	272.06	135.71	269.19	134.76	269.39	134.83	273.16	133.78	270.39
2500	140.76	308.45	139.69	303.40	138.72	302.04	140.65	300.04	139.68	299.81	139.73	303.59	138.68	300.36
3000	143.66	334.38	142.61	328.95	141.63	327.24	143.58	325.96	142.60	325.36	142.64	329.15	141.60	325.55
3500	145.51	356.67	144.46	350.93	143.48	348.91	145.45	348.23	144.46	347.34	144.49	351.13	143.46	347.22
4000	146.75	376.19	145.71	370.17	144.72	367.89	146.70	367.74	145.71	366.58	145.73	370.37	144.71	366.20
4500	147.61	393.52	146.59	387.27	145.60	384.75	147.58	385.07	146.59	383.67	146.60	387.47	145.59	383.06
5000	148.24	409.11	147.22	402.64	146.23	399.91	148.21	400.65	147.22	399.05	147.24	402.85	146.23	398.22
Zero Point Energy[b]	143.197		143.034		142.180		144.605		143.726		142.868		142.406	

[a] Units of cal mol^{-1} K^{-1}.

[b] Units of kcal mol^{-1}.

6.5 Conclusions

Carbon-carbon bonds dissociation energies in *exo*-tricyclo[5.2.1.$0^{2,6}$]decane (TCD) corresponding to diradical and carbene formation are determined. $\Delta H^{\circ}_{f\ 298}$ values are calculated for the parent (TCD-H2 *m*-*n*), radicals (TCD-H2 *m*J-*n* and *m*-*n*J), diradicals (TCD-H2 *m*J-*n*J), and carbenes (TCD-H2 *m*JJ-*n* and *m*-*n*JJ) which are used to determine C–H BDEs in going from parent to radical to diradical species. The density functional theory B3LYP method and the CBS-QB3 and G3MP2B3 composite computational methods are used in conjunction with a series of work reactions to increase accuracy. The use of work reactions with similar bridged hydrocarbons show that results from DFT methods can result in accurate data. Entropies (*S(T)*) and heat capacities ($C_p(T)$) are also determined for all species. C–C BDEs range from 77.6-86.3 kcal mol^{-1} for TCD diradical singlet state species. Analysis of the TCD carbene C–C BDEs show a wider range from about 77-100 kcal mol^{-1} due to the variation in the singlet and triplet $\Delta H^{\circ}_{f\ 298}$ values for the individual methods.

CHAPTER 7

HYDROGEN ABSTRACTION FROM *EXO*-TRICYCLO[5.2.1.0^{2,6}]DECANE (TCD) BY HYDROGEN AND OXYGEN ATOMS AND METHYL, HYDROXYL, AND HYDROPEROXYL RADICALS

7.1 Overview

Chemical kinetic modeling for gas phase oxidation of hydrocarbon fuels is an important analysis and optimization tool in order to optimize and control the combustion process in propulsion and energy release applications. Optimization and control via computer modeling versus more expensive experiment has become a commonly implemented tool in our arsenal of method improvement. The ability to accurately model combustion systems in the 300-2000 K temperature range becomes paramount. In combustion of hydrocarbons, one to the most important initiation processes is abstraction of hydrogen atoms from the parent hydrocarbon by radical pool species such as hydrogen and oxygen atoms, OH, HO_2, CH_3 radicals, and molecular oxygen. In this chapter, previously calculated thermochemical properties, $\Delta H^{\circ}_{f\ 298}$, $S^{\circ}(T)$, and $C_p(T)$, for TCD are incorporated to estimate the rate constants for forward and reverse abstraction reactions. Six different abstraction sites using the hydrogen and oxygen atoms and methyl, hydroxyl, and hydroperoxyl radical species. Thermodynamic properties are calculated for all of the transition states in this study in order to estimate the the abstraction rate constants. Kinetic mechanisms for TCD rests upon having reliable thermochemical properties for parent, radicals, and diradicals. The previous studies on gas phase formation enthalpies for TCD and its radicals, with corresponding carbon-hydrogen bond dissociation energies (C–H BDE),[225] assists in determining which sites are more prone to

hydrogen abstraction in initial reaction pathways. Radical stability affects the C–H BDE where an increasing radical stability will decrease the corresponding BDE.

Rate constants are expressed over the above temperature range in the three parameter modified Arrhenius form in equation 2.20. It has been previously shown[225] that the C–H bond dissociation energies for the endo (en) or exo (ex) position hydrogen atoms in TCD are identical, see Figure 7.1. The endo position for C_3, C_4, and C_9 abstraction is selected for analysis. For C_{10} abstraction, the hydrogen from the less bulky cyclohexane side (opposite to the cyclopentane moiety) of the single CH_2 bridge has been selected for calculation of the transition state structures.

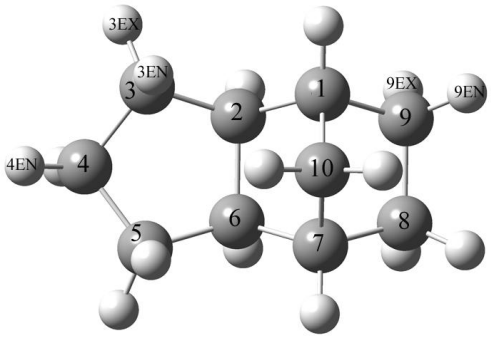

Figure 7.1 Numbering scheme for carbon and hydrogen sites of TCD.

7.2 Nomenclature

Abbreviations are utilized in this chapter as illustrated below:

- TS-TCD R*i*-*X* represents a hydrogen abstraction TCD transition state species, where *X* is the abstraction species (H, CH_3, O, OH, or OOH) and *i* is the carbon center corresponding to Figure 7.1,
- J represents a radical site on the preceding carbon atom,
- TCD and JP-10 denotes *exo*-tricyclo[5.2.1.$0^{2,6}$]decane.

7.3 Computational Methods

Density functional theory (DFT) is initially utilized to determine structural parameters for the TS-TCD abstraction species using the Gaussian 03 program suite.[62] Optimized structures for the TS-TCD R*i*-H, -CH_3, -O, and -OOH species are determined using B3LYP[46,47] with the 6-31G(d,p) basis set. For the TS-TCD R*i*-OH species, saddle point geometries were not possible with B3LYP. The MP2[66-70] method with the 6-31G(d,p) basis set was found to converge on acceptable structures with the transition states having a characteristic single imaginary frequency corresponding to the mode of vibration connecting the reactant and product. Potential energy diagrams for the hindered internal rotor for methyl, hydroxyl, and hydroperoxyl abstractions are calculated to verify the structure is the lowest energy.

Isodesmic work reactions having similar bridged structures, and subsequently similar ring strain environments, for the products and reactants are employed to determine $\Delta H^{\circ}_{f\,298}$ values for the TS-TCD species using B3LYP and the G3MP2B3[57,58] and CBS-QB3[60,61] composite methods.

Entropies, $S^{\circ}(T)$, and heat capacities, $C_p(T)$, from translations, vibrations, and external rotations for the TS-TCD abstraction species are determined using the calculated strctures and frequencies using the Statistical Mechanics for Heat Capacity and Entropy (SMCPS) program.[98] Internal rotation created from the methyl, hydroxyl, and hydroperoxyl abstraction groups are analyzed for their contributions to the entropies and heat capacities using the Pitzer and Gwinn[85-87] approximation method. These contributions are added to those from the SMCPS analysis to determine total entropies and heat capacities.

The Arrhenius pre-exponential factors (A, *n*, and E_a) are fit in a three parameter modified Arrhenius equation to describe the temperature dependenct of the rate constants, k(T), over the 300-2000 K temperature range. Rate constants and A factors are reported with units of $cm^3\ mol^{-1}\ s^{-1}$ and Ea with kcal mol^{-1}.

7.4 Results and Discussion

7.4.1 Transition State Structures

The nomenclature and optimized geometries for the TS-TCD abstraction species are illustrated in Figures 7.2-7.6. Important bond distances and angles are listed to allow for direct comparison. In these figures, the angle of attack for all of the abstraction species is within approximately 15° of being linear. Analyzing each transition state structures for each atom or radical pool species (R•), showed that the R•--H and TCD(C—H) bond distances of the abstracted hydrogen are all within 0.1 Å for each R• and corresponding TCD carbon

Appendix F has the optimized geometry parameters, moments of inertia, and vibrational frequencies for the transition state species.

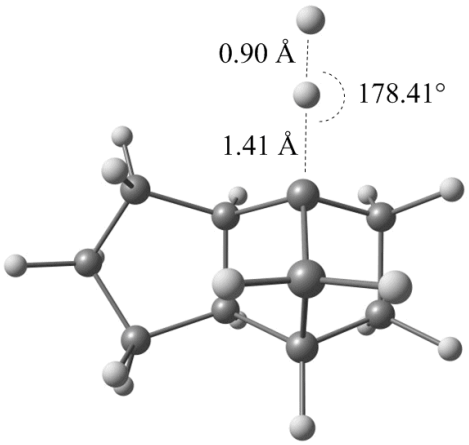

TS-TCD R1-H

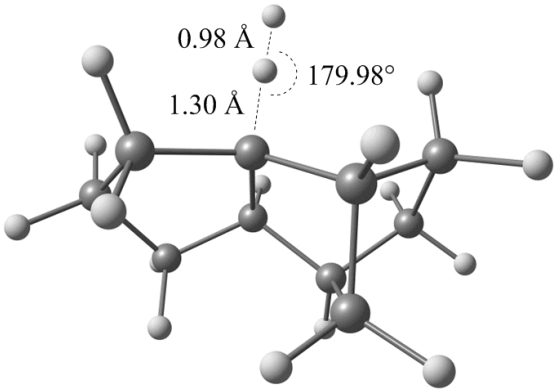

TS-TCD R2-H

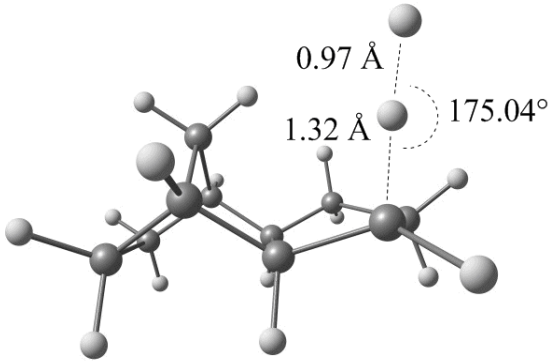

TS-TCD R3-H

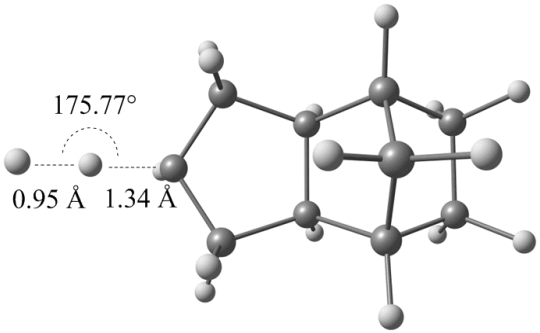

TS-TCD R4-H

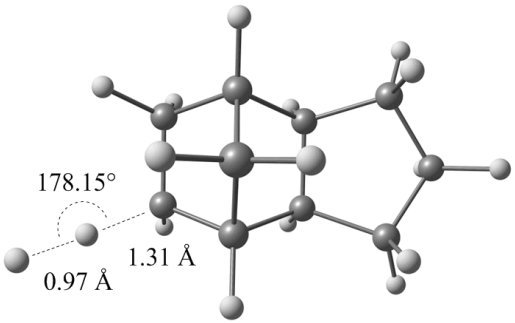

TS-TCD R9-H

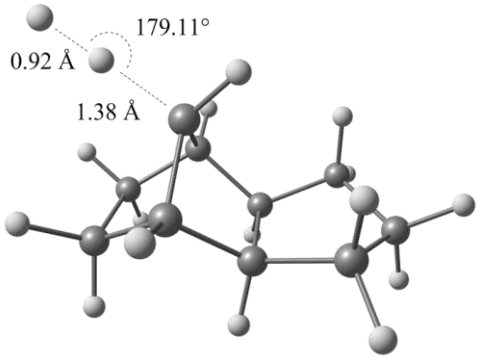

TS-TCD R10-H

Figure 7.2 TS-TCD R*i*-H bond lengths and angles from B3LYP/6-31G(d,p).

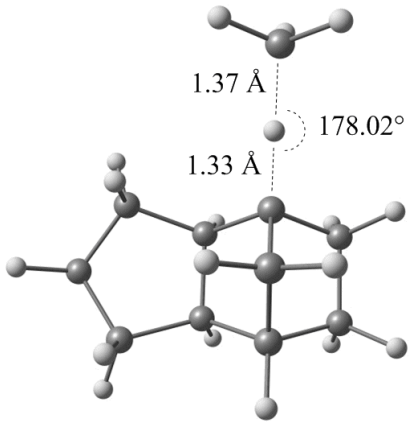

TS-TCD R1-CH_3

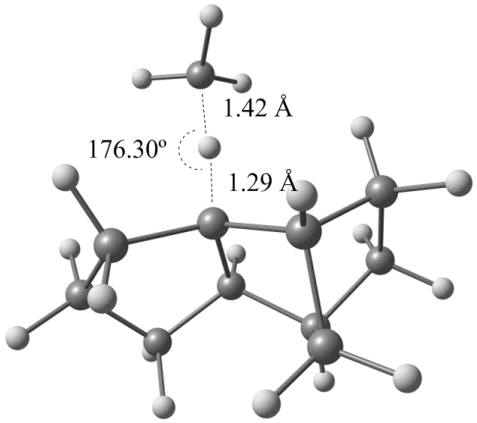

TS-TCD R2-CH_3

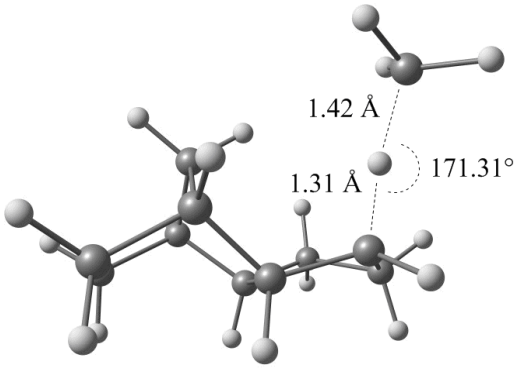

TS-TCD R3-CH_3

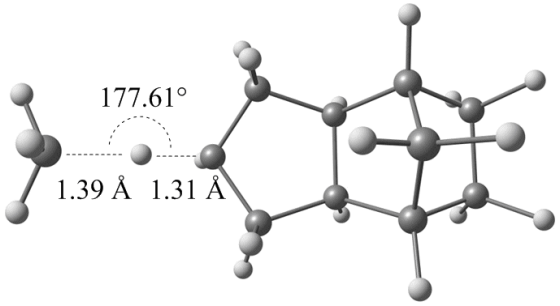

TS-TCD R4-CH_3

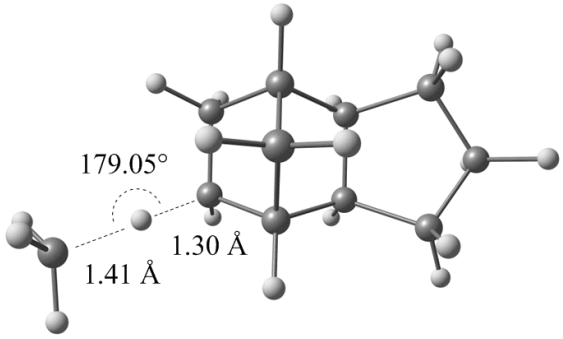

TS-TCD R9-CH_3

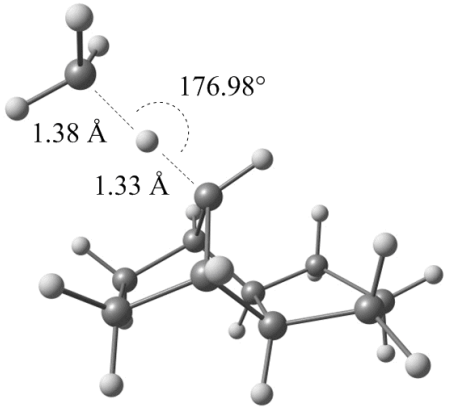

TS-TCD R10-CH_3

Figure 7.3 TS-TCD R*i*-CH_3 bond lengths and angles from B3LYP/6-31G(d,p).

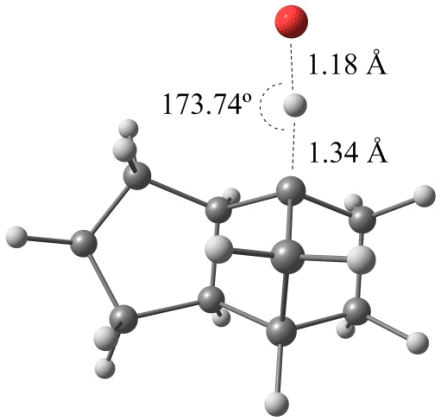

TS-TCD R1-O

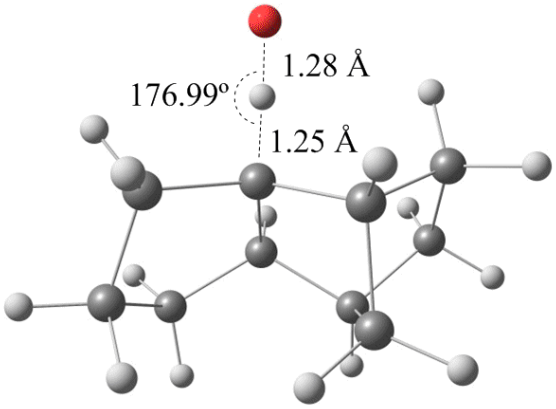

TS-TCD R2-O

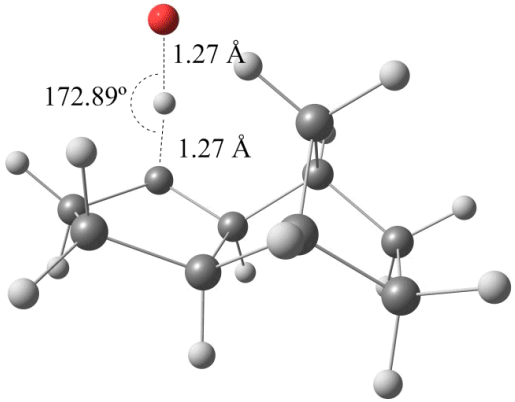

TS-TCD R3-O

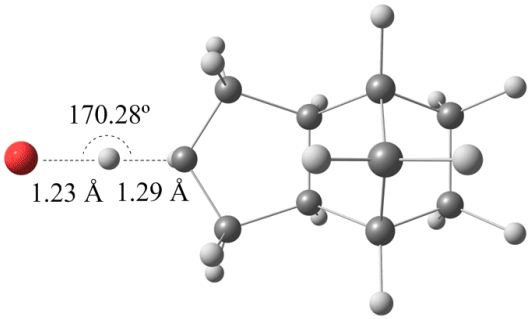

TS-TCD R4-O

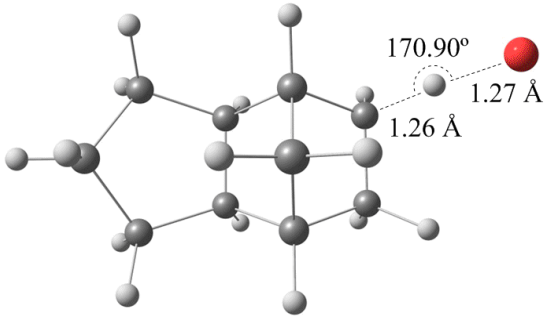

TS-TCD R9-O

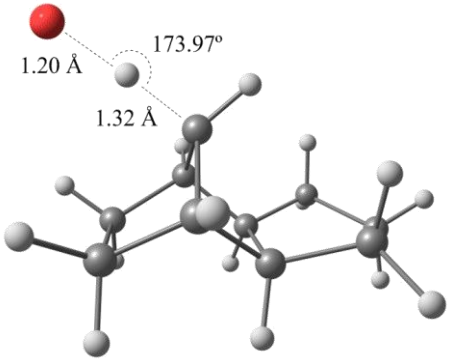

TS-TCD R10-O

Figure 7.4 TS-TCD R*i*-O bond lengths and angles from B3LYP/6-31G(d,p).

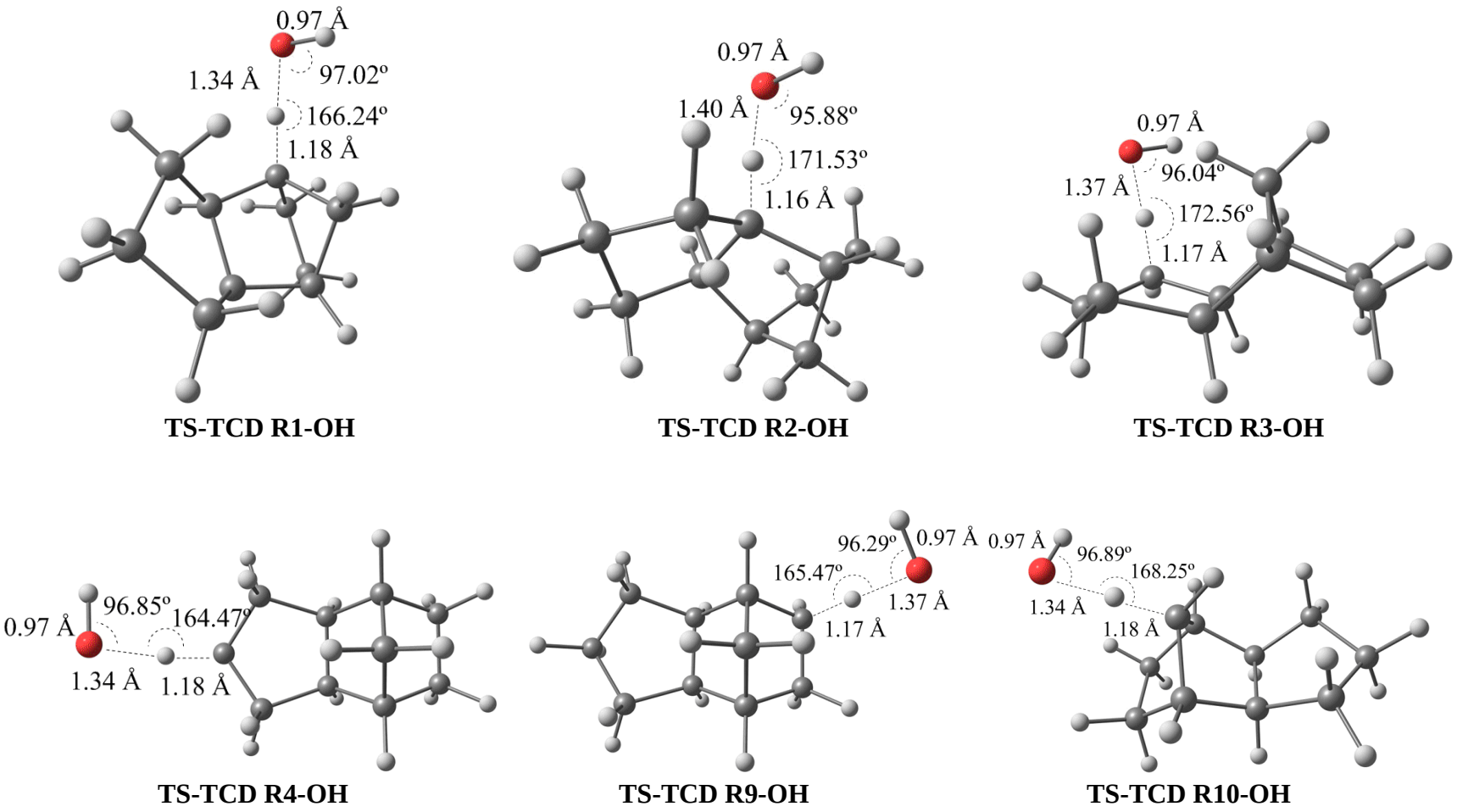

Figure 7.5 TS-TCD R*i*-OH bond lengths and angles from MP2/6-31G(d,p).

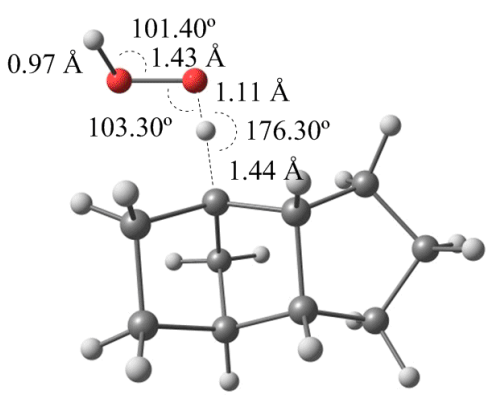

TS-TCD R1-OOH

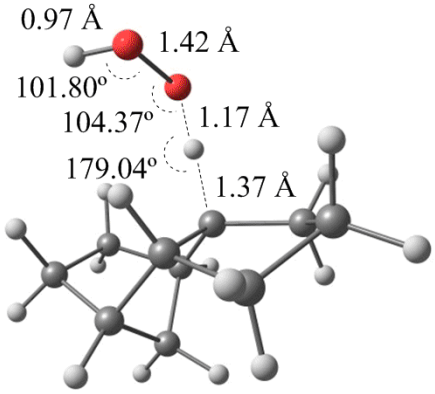

TS-TCD R2-OOH

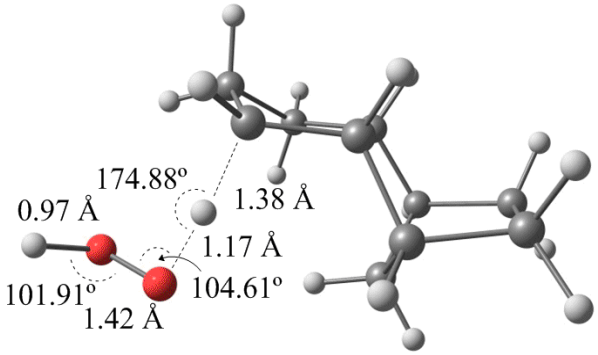

TS-TCD R3-OOH

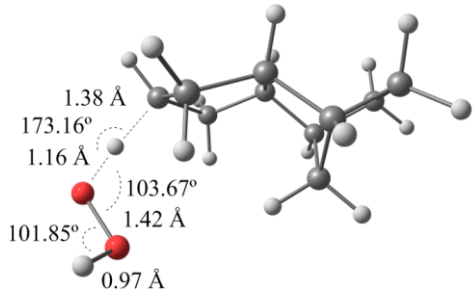

TS-TCD R4-OOH

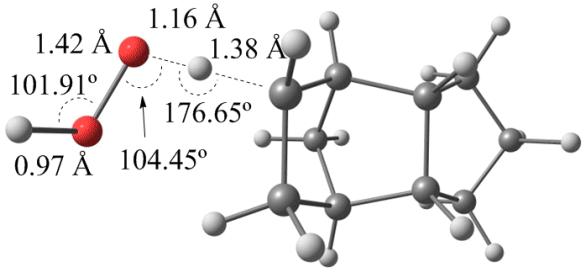

TS-TCD R9-OOH

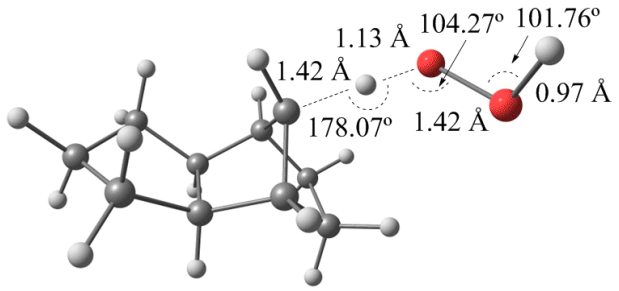

TS-TCD R10-OOH

Figure 7.6 TS-TCD R*i*-OOH bond lengths and angles from B3LYP/6-31G(d,p).

7.4.2 Heat of Formation $\Delta H^{\circ}_{f\,298}$

Isodemsic work reactions are utilized by each calculation methods to cancel error and determine accurate heat of formations for the TS-TCD abstraction species. These isodesmic work reactions incorporate the TCD transition state structure as a reactant and the TCD parent compound as a product which provides similar ring strain environments. Normal straight chain alkanes, alcohols, and alkyl hydroperoxides with their corresponding radicals are incorporated as the other species in the reactions. These species have well-known gas phase heats of formations listed in Table 7.1.

Table 7.2 has a summary of the calculated $\Delta H^{\circ}_{f\,298}$ for TS-TCD abstraction species from the averages of the B3LYP and the CBS-QB3 and G3MP2B3 methods. The individual work reactions for these species are presented in Appendix F. Due to the difficulties in determining suitable transition state geometries for the TS-TCD R*i*-OH species, single point energies using the DFT and composite methods are calculated based on the optimized MP2/6-31G(d,p) transition state geometries. In these tables, there is a good correlation for the CBS-QB3 and G3MP2B3 methods. Comparison of the averages of the DFT and the composite methods shows that there is a much larger absolute difference ranging from 4-8 kcal mol^{-1} between the calculation methods. The DFT method consistently under predicts the TS-TCD abstraction energies. Average $\Delta H^{\circ}_{f\,298}$ values from the CBS-QB3 and G3MP2B3 methods are recommended in Table 7.2.

Reaction energetics at the CBS-QB3 and G3MP2B3 levels, between the calculated transition state structure and the reactant radical and TCD parent, are used to determine the reaction barrier. In a second analysis, reactions shown in Scheme 7.1 use the reaction energies from the corresponding transition state structure and the product

TCD radical and product of the radical pool species with hydrogen atom: (H_2, CH_4, OH, HOOH, and H_2O) are also used in calculation of the barriers.

Table 7.1 Standard Enthalpies of Formation for Reference Species

Species	$\Delta H^{\circ}_{f\,298}$ (kcal mol^{-1})	Reference
H	52.10	83
H_2	0	
O	59.56 ± 0.02	237
OH	8.9 ± 0.1	167
H_2O	-57.80	83
HOOH	-32.53	83
HOOJ	2.94 ± 0.06	238
CH_4	-17.8 ± 0.1	120
CJH_3	34.82	83
CH_3CH_3	-20.0 ± 0.1	120
CH_3CJH_2	29.0 ± 0.4	121
$CH_3CH_2CH_3$	-25.0 ± 0.1	120
$CH_3CH_2CJH_2$	23.9 ± 0.5	173
$CH_3CH_2CH_2CH_3$	-30.0 ± 0.1	120
$CH_3CH_2CH_2CJH_2$	19.3 ± 0.5	239
CH_3OH	-48.2 ± 0.1	120
CH_3OJ	4.1 ± 1	173
CH_3CH_2OH	-56.2 ± 0.1	120
CH_3CH_2OJ	-3.6 ± 0.8	240
$CH_3CH_2CH_2OH$	-61.0 ± 0.1	120
$CH_3CH_2CH_2OJ$	-8.6 ± 0.3	*a*
$CH_3CH_2CH_2CH_2OH$	-65.7 ± 0.1	120
$CH_3CH_2CH_2CH_2OJ$	-13.4 ± 0.3	*a*
CH_3OOH	-31.0 ± 0.2	241
CH_3CH_2OOH	-39.1 ± 0.2	241
$CH_3CH_2CH_2OOH$	-43.8 ± 0.3	241
$CH_3CH_2CH_2CH_2OOH$	-48.4 ± 0.2	241
TCD	-19.5 ± 1.3	225
TCD-R1	35.7 ± 0.5	225
TCD-R2	28.5 ± 0.5	225
TCD-R3	26.4 ± 0.5	225
TCD-R4	27.0 ± 0.5	225
TCD-R9	27.1 ± 0.5	225
TCD-R10	32.5 ± 0.5	225

[a] See Appendix F for enthalpy calculation.

Table 7.2 Summary of Calculated $\Delta H^{\circ}_{f\,298}$ for TS-TCD Species

Species	$\Delta H^{\circ}_{f\,298}$ (kcal mol^{-1})				Barrier Height[c]
	DFT[a]	CBS-QB3	G3MP2B3	Composite[b]	
TS-TCD R1-H	36.9	42.6	42.5	42.5	9.9
TS-TCD R2-H	32.6	37.9	37.9	37.9	5.3
TS-TCD R3-H	34.0	39.6	39.4	39.5	6.9
TS-TCD R4-H	34.9	41.1	40.9	41.0	8.4
TS-TCD R9-H	33.5	39.2	39.0	39.1	6.5
TS-TCD R10-H	36.4	42.2	41.9	42.0	9.4
TS-TCD R1-CH_3	23.1	28.4	28.7	28.5	13.2
TS-TCD R2-CH_3	20.5	25.0	25.2	25.1	9.8
TS-TCD R3-CH_3	21.8	27.0	27.0	27.0	11.7
TS-TCD R4-CH_3	21.8	28.1	28.2	28.2	12.9
TS-TCD R9-CH_3	20.7	26.5	26.6	26.6	11.3
TS-TCD R10-CH_3	23.1	28.7	28.7	28.7	13.4
TS-TCD R1-O	39.9	43.9	43.1	43.5	3.4
TS-TCD R2-O	37.9	43.2	42.2	42.7	2.6
TS-TCD R3-O	37.4	42.2	40.9	41.5	1.4
TS-TCD R4-O	39.5	44.6	43.2	43.9	3.8
TS-TCD R9-O	39.3	44.7	43.4	44.1	4.0
TS-TCD R10-O	40.0	44.5	43.3	43.9	3.8
TS-TCD R1-OH	-17.4	-10.1	-11.2	-10.7	-0.1
TS-TCD R2-OH	-20.0	-12.0	-12.1	-12.1	-1.5
TS-TCD R3-OH	-19.1	-10.9	-11.8	-11.3	-0.7
TS-TCD R4-OH	-17.4	-9.5	-10.8	-10.2	0.4
TS-TCD R9-OH	-18.8	-10.7	-11.5	-11.1	-0.5
TS-TCD R10-OH	-17.2	-9.7	-10.4	-10.0	0.6
TS-TCD R1-OOH	-6.0	0.3	0.3	0.3	16.9
TS-TCD R2-OOH	-11.3	-4.7	-4.2	-4.4	12.2
TS-TCD R3-OOH	-9.9	-2.2	-2.3	-2.2	14.4
TS-TCD R4-OOH	-8.3	-0.5	-0.6	-0.6	16.0
TS-TCD R9-OOH	-10.3	-3.0	-3.0	-3.0	13.6
TS-TCD R10-OOH	-6.2	0.7	0.2	0.5	17.1

[a] Average from B3LYP/6-31G(d,p) and B3LYP/6-311G(2d,2p).

[b] Average from CBS-QB3 and G3MP2B3.

[c] From reactions in Scheme 7.1, units kcal mol^{-1}.

Scheme 7.1 Forward TS-TCD Abstraction Reactions

TCD	+	H	→	TS-TCD R*i*-H	→	TCD-R*i*	+	H_2
TCD	+	CJH_3	→	TS-TCD R*i*-CH_3	→	TCD-R*i*	+	CH_4
TCD	+	O	→	TS-TCD R*i*-O	→	TCD-R*i*	+	OH
TCD	+	OH	→	TS-TCD R*i*-OH	→	TCD-R*i*	+	H_2O
TCD	+	HOOJ	→	TS-TCD R*i*-OOH	→	TCD-R*i*	+	HOOH

7.4.3 Internal Rotors

Internal rotor analysis is conducted for the TS-TCD R*i*-CH_3, R*i*-OH, and R*i*-OOH compounds. Potential energy diagrams using relaxed scans at 10° rotation intervals are determined using B3LYP/6-31G(d,p) for -CH_3 and -OOH and MP2/6-31G(d,p) for -OH abstractions. These scans are used to determine the lowest energy conformations. If lower energy conformations are found, the scans are re-run to ensure the lowest energy conformation. The potential energy diagrams for the hindered rotors are provided in Appendix F.

The methyl abstraction species have a maximum rotational barrier of approximately 0.25 kcal mol^{-1} for TS-TCD R2-CH_3 and R3-CH_3. The remaing four compounds have lower energy barriers, below 0.09 kcal mol^{-1}.

The hydroxyl abstraction species, rotation from the hydroxyl group (R-OH) shows maximum rotational barrier heights of approximately 0.90 kcal mol^{-1} except for TS-TCD R2-OH and R3-OH again. These species are slightly higher at 1.2 and 1.7 kcal mol^{-1}, respectively.

The hydroperoxyl abstraction species, the first internal rotor (R-OOH) has barriers all below 1.4 kcal mol^{-1}, except for TS-TCD R3-OOH which is higher at

2.8 kcal mol^{-1}. The second rotation for the hydroxyl group (R-OH) has higher maximum barriers between 8.8-10.9 kcal mol^{-1}.

7.4.4 Entropy ($S^{\circ}(T)$) and Heat Capacities ($C_p(T)$)

Entropies and heat capacities are calculated using the Statistical Mechanics for Heat Capacity and Entropy (SMCPS) program.[98] Contributions from geometry, frequencies, moments of inertia, and internal rotors are included with zero-point vibration energies (ZPVE) scaled by 0.9806 for B3LYP/6-31G(d,p) and by 0.9608 for MP2/6-31G(d,p) as recommended by Scott and Radom.[99]

For the methyl, hydroxyl, and hydroperoxyl radical abstraction transition states, the frequency corresponding to internal rotations with barriers below 4.5 kcal mol^{-1} are removed and treated more accurately as a hindered rotor. These energy barriers, along with their reduced moments of inertia, are used in the Pitzer and Gwinn[85-87] approximation method for their contributions to entropies and heat capacities. These contributions are added to the values from the SMCPS analysis to determine the total entropies and heat capacities in the temperature range of 50-5000 K. These are presented in Appendix F with **c**ommonly reported values, S°_{298} and $C_p(T)$ from 300-1500 K, in Table 7.3.

7.4.5 Potential Energy Diagrams

Potential energy diagrams for the hydrogen abstractions are determined from $\Delta H^{\circ}_{f\ 298}$ from each species following the forward, and corresponding reverse, reactions in Scheme 7.1. The energy barriers are calculated as the difference in the $\Delta H^{\circ}_{f\ 298}$ for the standard values in Table 7.1 including the TCD radicals previously determined[225] and the

calculated values for the TS-TCD abstraction species from Table 7.2. The potential energy diagrams are presented in Figures 7.7-7.11 where the values are the relative resulting energies in units of kcal mol^{-1}.

Table 7.3 Calculated Entropy and Heat Capacities for TS-TCD Abstraction Species[a]

Species	S°_{298}[b]	$C_p(T)$[b]						
		300 K	400 K	500 K	600 K	800 K	1000 K	1500 K
TS-TCD R1-H	90.48	39.98	56.13	70.44	82.26	99.94	112.33	130.63
TS-TCD R2-H	89.85	39.70	55.99	70.44	82.35	100.09	112.49	130.75
TS-TCD R3-H	89.60	39.42	55.84	70.39	82.34	100.12	112.52	130.77
TS-TCD R4-H	90.38	39.61	55.93	70.41	82.33	100.08	112.47	130.73
TS-TCD R9-H	89.85	39.54	55.92	70.44	82.38	100.14	112.53	130.77
TS-TCD R10-H	90.24	39.76	56.05	70.48	82.36	100.07	112.45	130.71
TS-TCD R1-CH_3	102.29	45.34	62.51	77.79	90.49	109.68	123.35	143.91
TS-TCD R2-CH_3	101.36	45.28	62.49	77.80	90.51	109.71	123.37	143.93
TS-TCD R3-CH_3	100.85	44.92	62.28	77.70	90.47	109.72	123.39	143.94
TS-TCD R4-CH_3	102.34	44.97	62.31	77.72	90.48	109.72	123.39	143.93
TS-TCD R9-CH_3	101.83	44.96	62.32	77.73	90.50	109.73	123.40	143.95
TS-TCD R10-CH_3	101.82	45.05	62.34	77.73	90.47	109.70	123.37	143.92
TS-TCD R1-O	96.24	42.05	58.17	72.34	83.94	101.18	113.24	131.10
TS-TCD R2-O	95.72	41.63	57.80	72.03	83.69	101.02	113.12	131.03
TS-TCD R3-O	93.95	41.27	57.57	71.89	83.61	101.00	113.13	131.05
TS-TCD R4-O	96.19	41.44	57.62	71.87	83.56	100.94	113.07	131.02
TS-TCD R9-O	96.00	41.38	57.67	71.99	83.70	101.06	113.17	131.07
TS-TCD R10-O	95.24	41.76	57.99	72.25	83.91	101.20	113.27	131.12
TS-TCD R1-OH	98.63	41.43	57.30	71.63	83.55	101.44	114.09	133.20
TS-TCD R2-OH	96.72	41.30	57.15	71.49	83.44	101.37	114.05	133.18
TS-TCD R3-OH	95.72	41.85	57.68	71.96	83.83	101.65	114.24	133.28
TS-TCD R4-OH	98.04	41.05	57.00	71.43	83.42	101.39	114.07	133.20
TS-TCD R9-OH	97.47	41.15	57.03	71.43	83.41	101.39	114.07	133.21
TS-TCD R10-OH	97.23	41.38	57.24	71.60	83.55	101.47	114.12	133.22
TS-TCD R1-OOH	110.31	46.61	63.43	78.24	90.42	108.55	121.27	140.22
TS-TCD R2-OOH	108.23	46.94	63.61	78.38	90.53	108.65	121.36	140.28
TS-TCD R3-OOH	107.25	47.09	63.90	78.69	90.82	108.89	121.54	140.38
TS-TCD R4-OOH	109.54	46.87	63.70	78.53	90.70	108.80	121.48	140.34
TS-TCD R9-OOH	108.28	46.76	63.62	78.48	90.66	108.78	121.47	140.34
TS-TCD R10-OOH	109.48	46.48	63.39	78.29	90.50	108.65	121.36	140.27

[a] Values based on B3LYP/6-31G(d,p) calculations except those for TS-TCD R*i*-OH species which are from MP2/6-31G(d,p) level of theory.
[b] Units cal mol^{-1} K^{-1}.

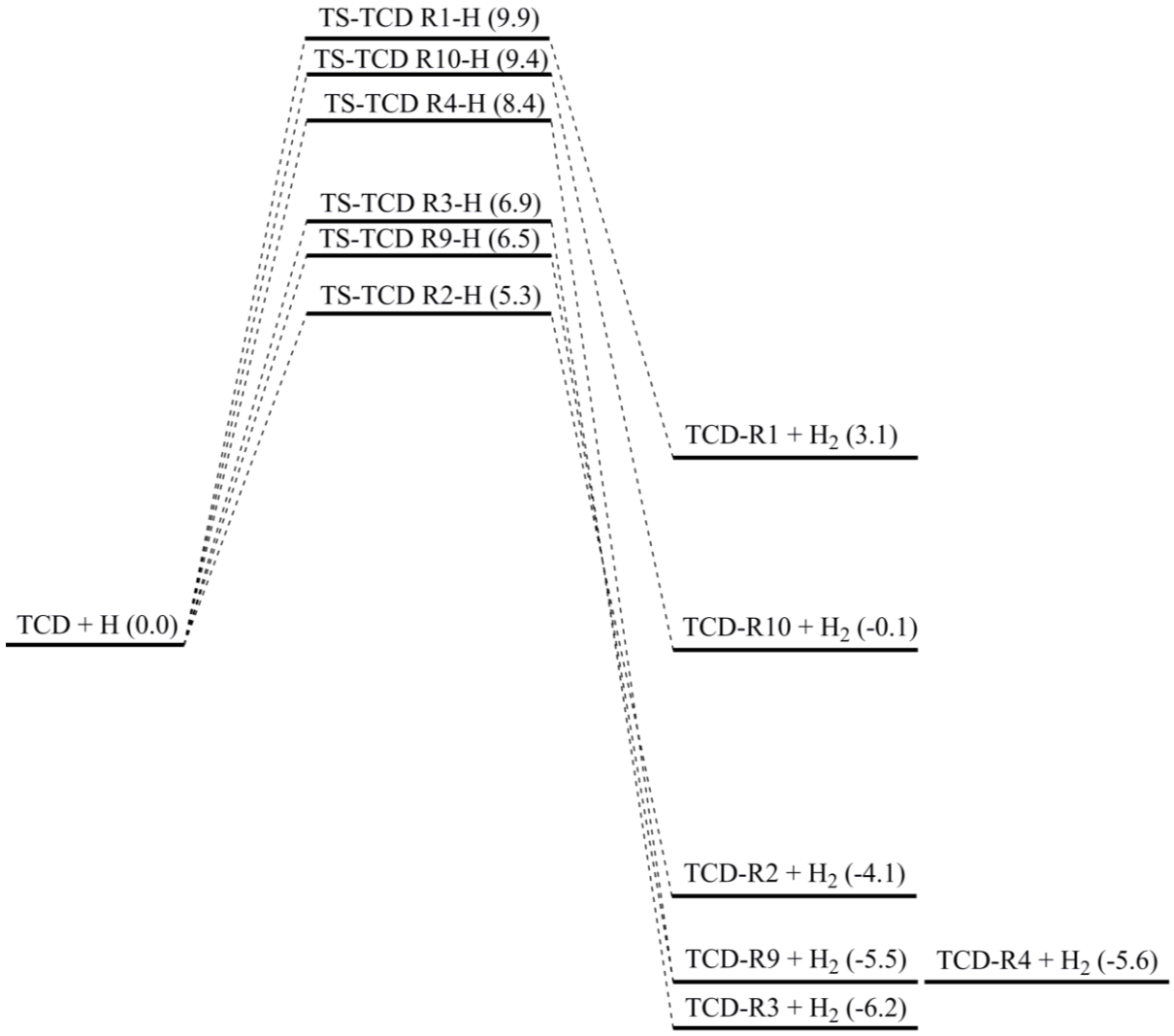

Figure 7.7 Potential energy barrier diagram for H atom abstraction reactions.

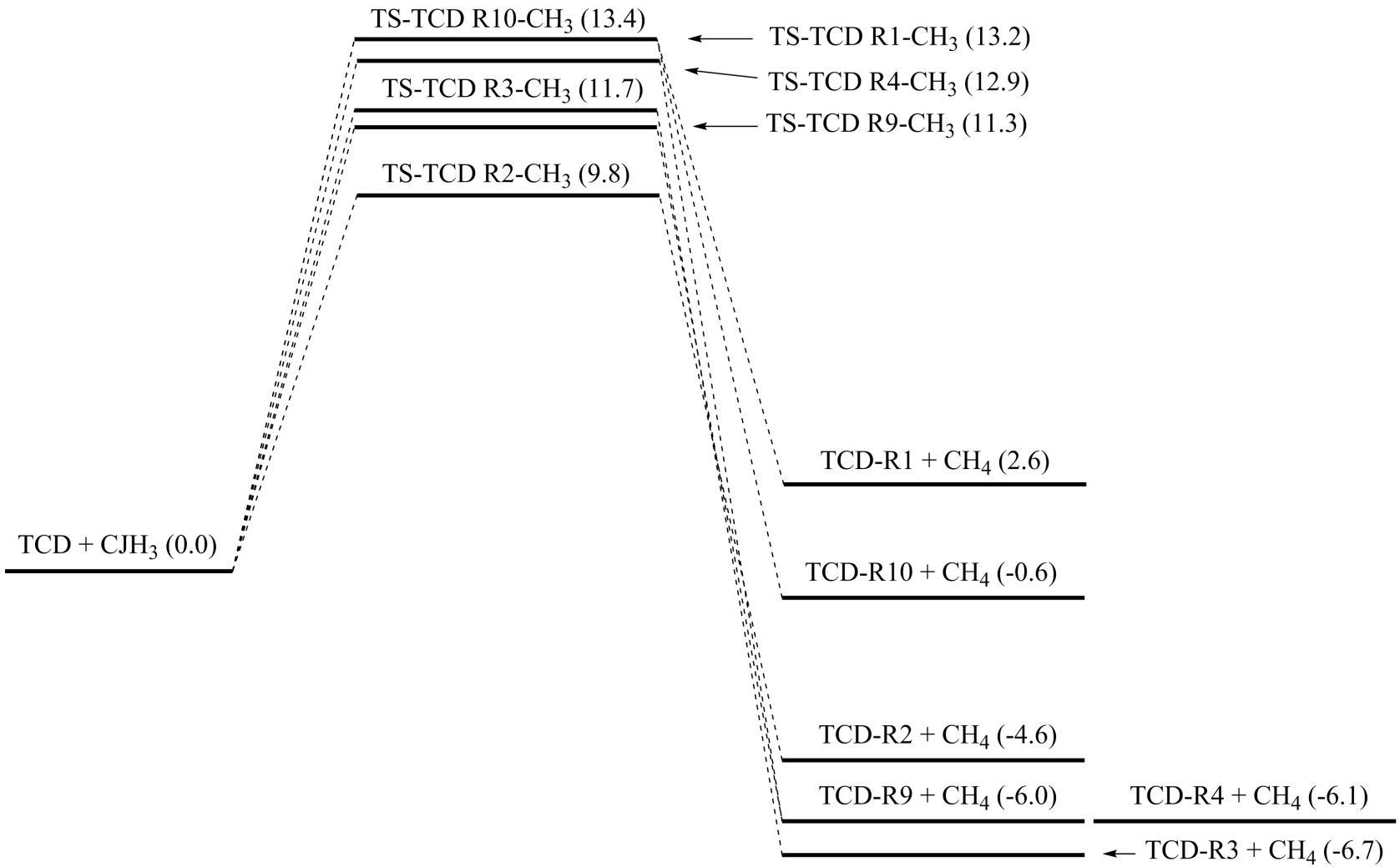

Figure 7.8 Potential energy barrier diagram for CH_3 radical abstraction reactions.

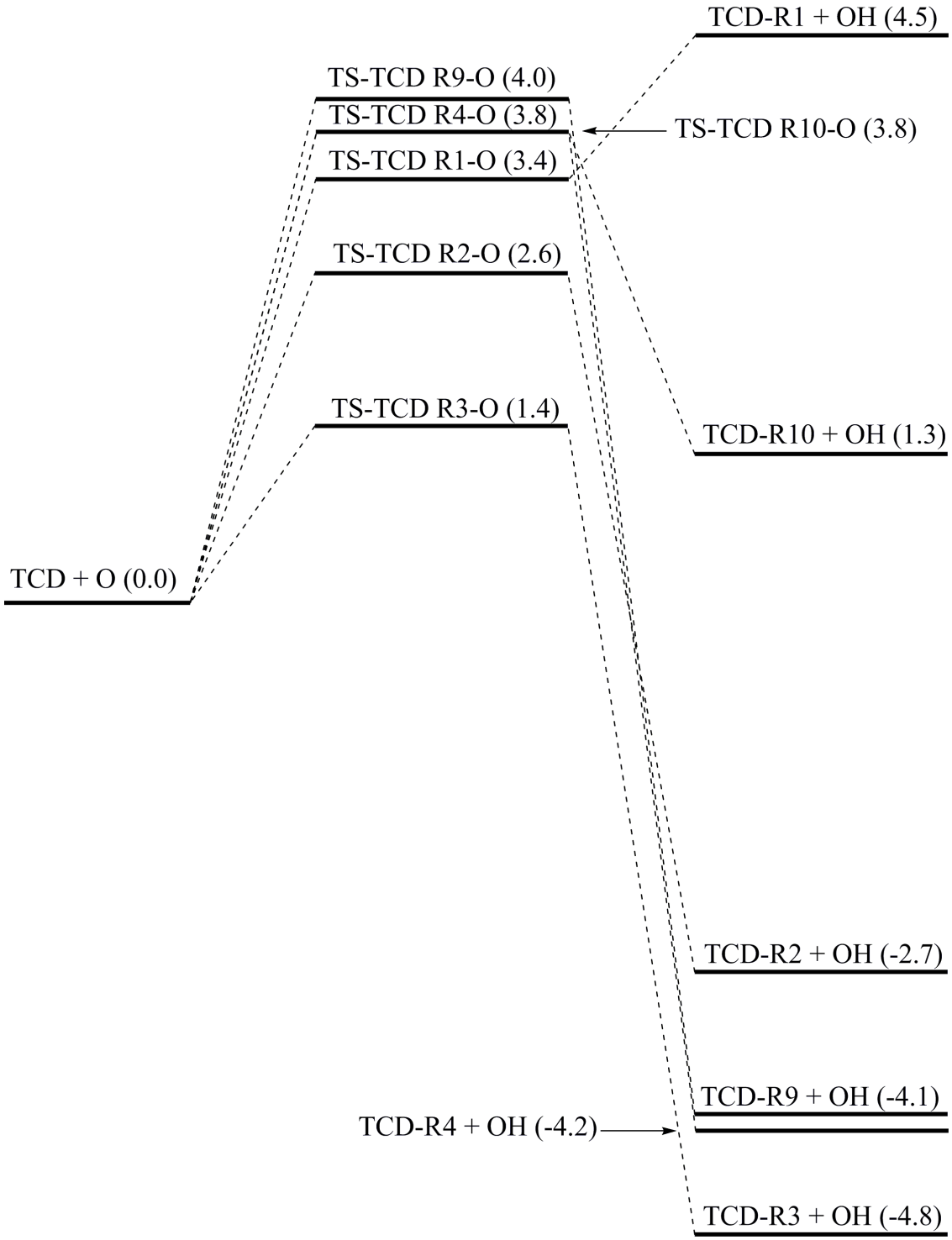

Figure 7.9 Potential energy barrier diagram for O atom abstraction reactions.

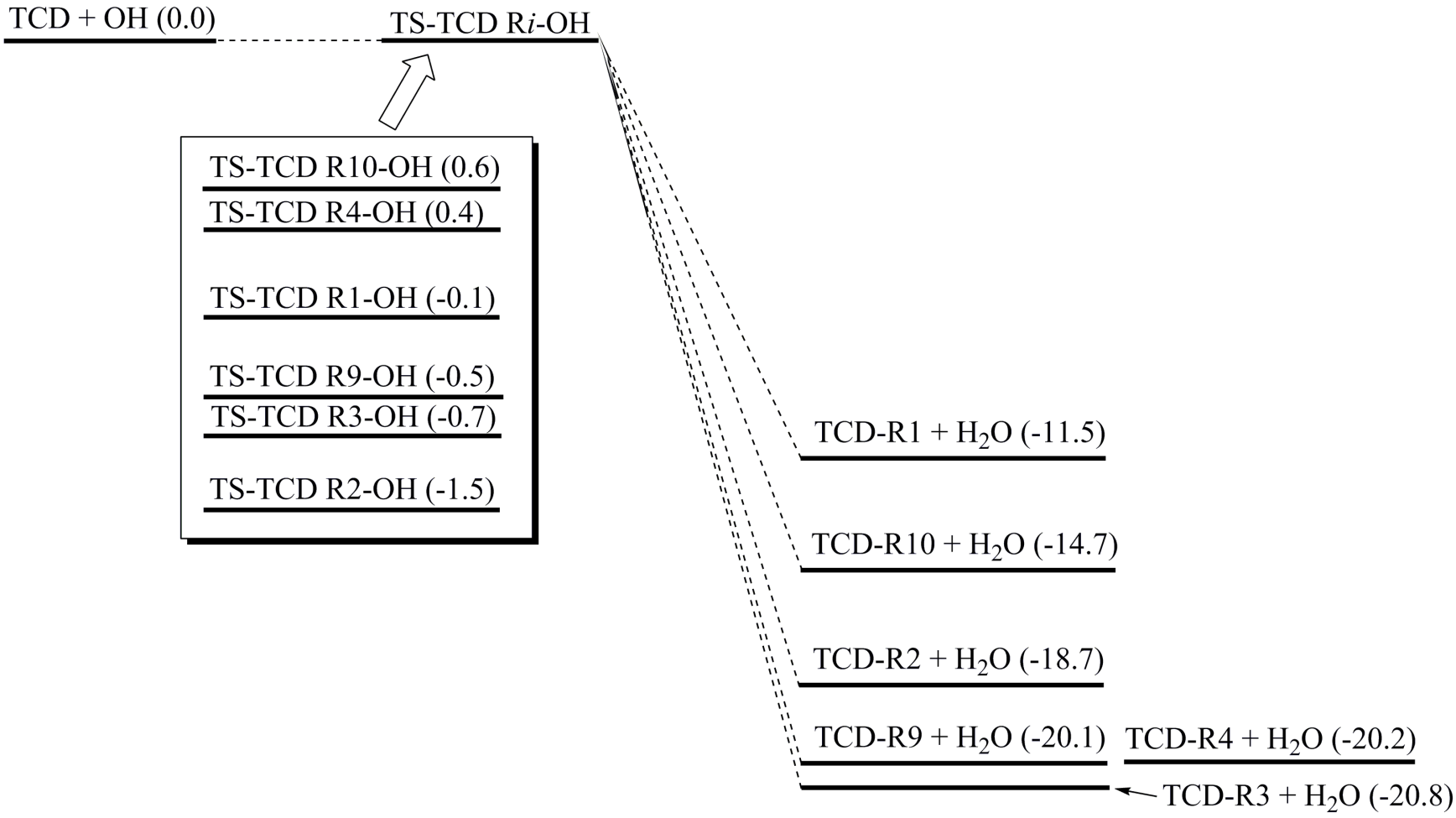

Figure 7.10 Potential energy barrier diagram for OH radical abstraction reactions.

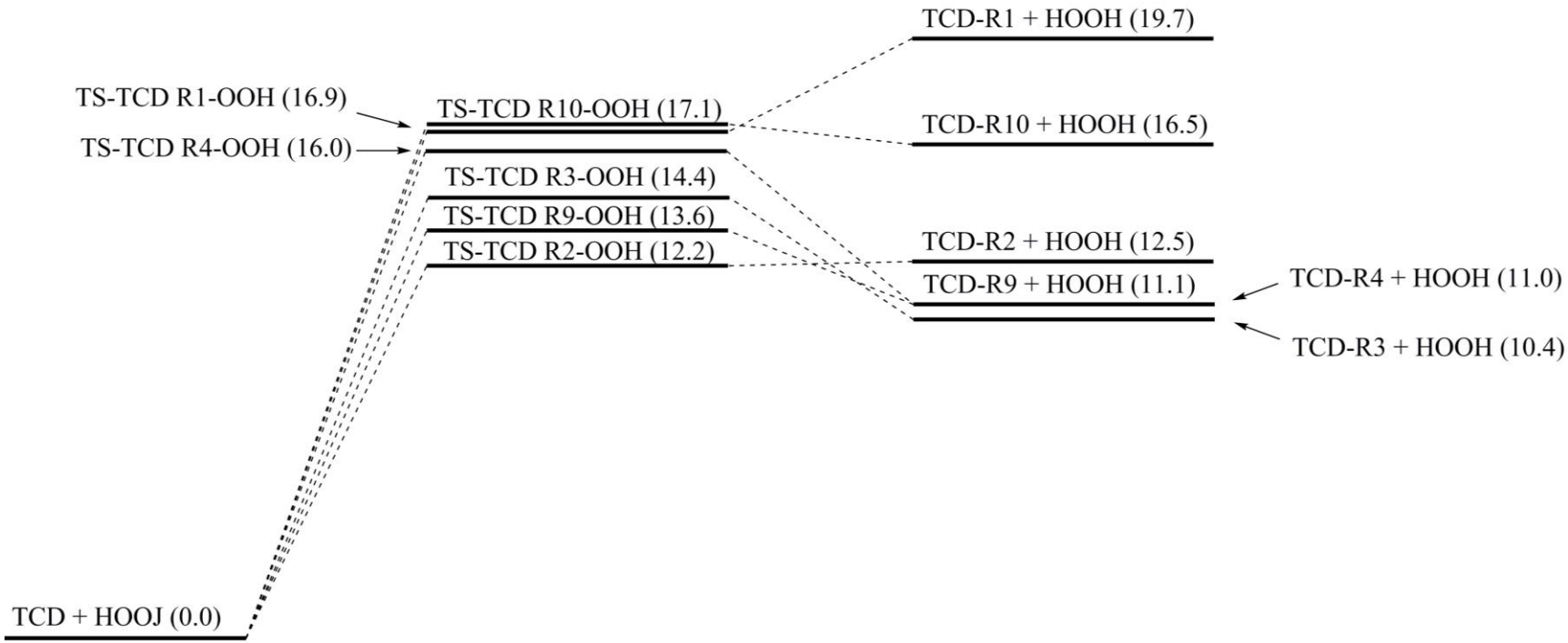

Figure 7.11 Potential energy barrier diagram for OOH radical abstraction reactions.

Abstraction by the hydrogen and oxygen atoms and the methyl radical species are exothermic with exceptions from the C_1 positions and from the C_{10} position for the oxygen atom. The most exothermic reactions occur for the hydroxyl abstraction with a range of -11 to -21 kcal mol^{-1}. The heat of formation for the TS-TCD R*i*-OH species fall within a very tight range seen in Figure 7.10 in the 0.6 to -1.5 kcal mol^{-1} range of the relative energies. Consequently, the stability created in the product formation creates reverse barriers in excess of 11 kcal mol^{-1}. In contrast, all of the abstractions by the hydroperoxyl radical are endothermic by 10 to 20 kcal mol^{-1}.

For the products that are created from the abstractions in Figures 7.7-7.11, their relative stabilities are consistent with the hydrogen bond dissociation energies (BDEs) previously calculated. For each series of abstractions, the C_1 position yields the highest energy product followed by C_{10}, C_2, C_9, C_4, and C_3 respectively. This also shows the relationship to BDEs and how it allows for the prediction of the most susceptible hydrogen abstraction location for initial reaction pathways. The high BDE at the tertiary bridgehead C_1 caused by the unfavorable strain, and corresponding non-planar radical geometry, is why the abstractions from C_1 have the highest product energy. The C_3 secondary position location allows for a more stable radical formation, in comparison, and correspondingly lowest product energy.

7.4.6 Kinetics and Rate Constant Expression

The elementary rate parameters A, *n*, and E_a, summarized in Table 7.4, are fitted to the calculated rate constants between 300-2000 K. Rate constants are calculated per one site location and assumed to scale with the number of hydrogens on the respective TCD carbon (identical hydrogens).

Figures 7.7 to 7.11 show that the calculated rate constant barriers are correlated to enthalpy of reaction for each radical pool species. Table 7.5 presents the CBS-QB3 calculated ΔH°_{rxn} for the forward abstraction reactions in Scheme 7.1 and the corresponding calculated transition state barrier energies. Figure 7.12 shows the overall comparison of the calculated ΔH°_{rxn} versus barrier energy for each of the abstraction species. As shown in the potential energy diagrams, hydroxyl group abstractions are the most exothermic and the hydroperoxyl abstractions the most endothermic. The remaining abstractions are centralized between -5 and 5 kcal mol^{-1} for ΔH°_{rxn}. Figures 7.13- 7.17 show the ΔH°_{rxn} versus barrier energy for each of the individual radical species depicting the linear relationship.

Plots of the log k vs. 1000/T are given in Figures 7.18-7.22 for the forward and reverse reactions. In these figures, both the forward and reverse reaction rates correspond with the barrier heights determined in Figures 7.7-7.11. Higher barriers that need to be overcome translate into a slower reactivity while lower barriers allow for faster reactivity. At lower temperatures, there is a broader range of rates as compared to the convergence seen as the temperature increases. For this temperature range, the rate constants increase up to 2000 K.

Table 7.4 Elementary Rate Parameters for Forward (f) and Reverse (r) Abstraction Reactions.

Species	A^a (f)	n (f)	$E_a{}^b$ (f)	A^a (r)	n (r)	$E_a{}^b$ (r)
TS-TCD R1-H	$6.489x10^7$	1.828	9.91	$8.153x10^5$	2.021	6.51
TS-TCD R2-H	$3.332x10^7$	1.873	5.22	$3.848x10^5$	1.985	9.01
TS-TCD R3-H	$2.884x10^7$	1.870	6.84	$8.110x10^5$	1.819	12.75
TS-TCD R4-H	$4.621x10^7$	1.862	8.35	$6.232x10^5$	1.783	13.74
TS-TCD R9-H	$3.016x10^7$	1.884	6.41	$1.526x10^6$	1.817	11.62
TS-TCD R10-H	$4.223x10^7$	1.869	9.37	$1.103x10^6$	1.857	9.15
TS-TCD R1-CH_3	$4.909x10^3$	2.689	12.61	$6.451x10^2$	3.033	9.93
TS-TCD R2-CH_3	$2.877x10^3$	2.698	9.19	$3.476x10^2$	2.960	13.70
TS-TCD R3-CH_3	$2.371x10^3$	2.682	11.05	$6.973x10^2$	2.781	17.68
TS-TCD R4-CH_3	$4.955x10^3$	2.685	12.23	$6.989x10^2$	2.756	18.35
TS-TCD R9-CH_3	$3.663x10^3$	2.691	10.63	$1.938x10^3$	2.774	16.57
TS-TCD R10-CH_3	$3.967x10^3$	2.681	12.75	$1.084x10^3$	2.819	13.25
TS-TCD R1-O	$1.004x10^5$	2.422	3.19	$5.401x10^2$	2.625	-1.67
TS-TCD R2-O	$1.408x10^5$	2.327	2.41	$6.958x10^2$	2.447	4.75
TS-TCD R3-O	$6.592x10^4$	2.300	1.25	$7.934x10^2$	2.258	5.71
TS-TCD R4-O	$2.384x10^5$	2.280	3.64	$1.376x10^3$	2.210	7.58
TS-TCD R9-O	$1.510x10^5$	2.332	3.78	$3.269x10^3$	2.273	7.54
TS-TCD R10-O	$6.207x10^4$	2.413	3.60	$6.940x10^2$	2.410	1.93
TS-TCD R1-OH	$9.299x10^6$	1.488	0.10	$3.695x10^5$	1.731	11.39
TS-TCD R2-OH	$4.506x10^6$	1.450	-1.27	$1.646x10^5$	1.612	17.21
TS-TCD R3-OH	$1.068x10^6$	1.598	-0.61	$9.501x10^4$	1.597	19.99
TS-TCD R4-OH	$8.942x10^6$	1.442	0.60	$3.814x10^5$	1.413	20.70
TS-TCD R9-OH	$6.733x10^6$	1.443	-0.33	$1.077x10^6$	1.425	19.58
TS-TCD R10-OH	$4.426x10^6$	1.492	0.72	$3.657x10^5$	1.530	15.19
TS-TCD R1-OOH	$1.073x10^2$	3.268	16.03	$6.203x10^2$	2.794	-3.47
TS-TCD R2-OOH	$2.692x10^1$	3.322	11.36	$1.431x10^2$	2.767	-0.96
TS-TCD R3-OOH	$7.732x10^0$	3.436	13.46	$1.001x10^2$	2.718	3.27
TS-TCD R4-OOH	$3.354x10^1$	3.385	15.15	$2.081x10^2$	2.639	4.45
TS-TCD R9-OOH	$1.929x10^1$	3.371	12.74	$4.491x10^2$	2.636	1.84
TS-TCD R10-OOH	$5.512x10^1$	3.301	16.20	$6.626x10^2$	2.622	-0.12

[a] Units of $cm^3\ mol^{-1}\ s^{-1}$.

[b] Units of $kcal\ mol^{-1}$.

Table 7.5 Calculated ΔH°_{rxn} and Barrier Energies for TCD Forward Abstraction Reactions

Forward Abstraction Reactions		ΔH°_{rxn} [a,b]	Barrier Energy [a]
TS-TCD R*i*-H System			
TCD + H → TCD-R*i* + H_2			
	TCD-R1	2.3	9.9
	TCD-R2	-5.1	5.3
	TCD-R3	-7.0	6.9
	TCD-R4	-6.4	8.4
	TCD-R9	-6.3	6.5
	TCD-R10	-0.8	9.4
TS-TCD R*i*-CH_3 System			
TCD + CJH_3 → TCD-R*i* + CH_4			
	TCD-R1	2.2	13.2
	TCD-R2	-5.1	9.8
	TCD-R3	-7.0	11.7
	TCD-R4	-6.4	12.8
	TCD-R9	-6.3	11.3
	TCD-R10	-0.9	13.4
TS-TCD R*i*-O System			
TCD + O → TCD-R*i* + OH			
	TCD-R1	4.9	3.4
	TCD-R2	-2.4	2.6
	TCD-R3	-4.3	1.4
	TCD-R4	-3.8	3.8
	TCD-R9	-3.6	4.0
	TCD-R10	1.8	3.8
TS-TCD R*i*-OH System			
TCD + OH → TCD-R*i* + H_2O			
	TCD-R1	-11.5	-0.1
	TCD-R2	-18.9	-1.5
	TCD-R3	-20.7	-0.7
	TCD-R4	-20.2	0.4
	TCD-R9	-20.1	-0.5
	TCD-R10	-14.6	0.6
TS-TCD R*i*-OOH System			
TCD + HOOJ → TCD-R*i* + HOOH			
	TCD-R1	19.9	16.8
	TCD-R2	12.5	12.2
	TCD-R3	10.6	14.3
	TCD-R4	11.2	16.0
	TCD-R9	11.3	13.6
	TCD-R10	16.8	17.0

[a] Units of kcal mol^{-1}.
[b] From CBS-QB3 calculation.

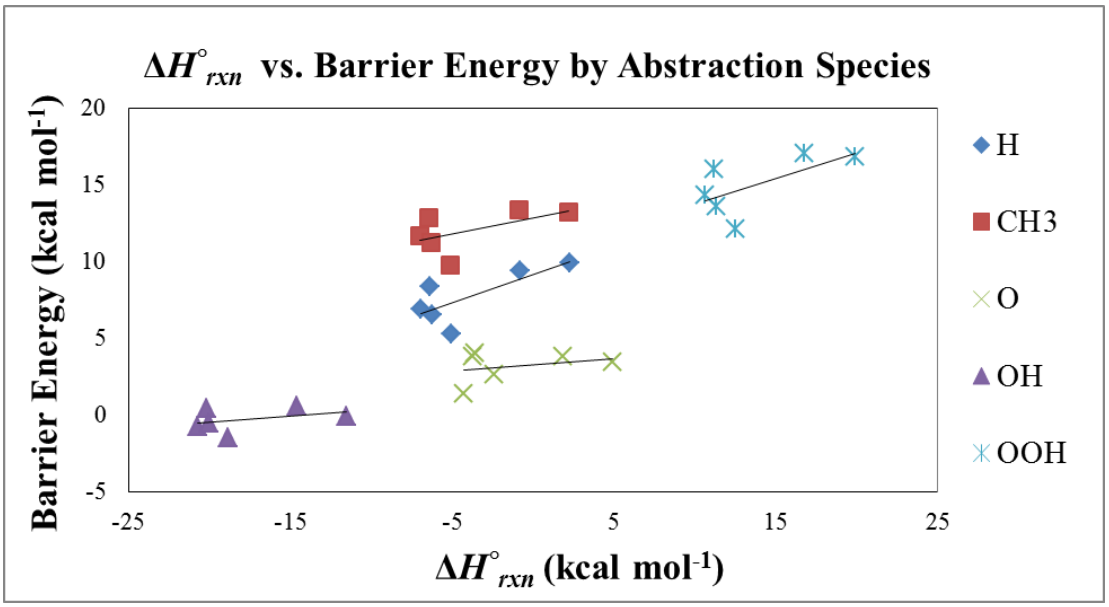

Figure 7.12 Overall comparison of calculated ΔH°_{rxn} vs. barrier energy for abstraction by H, CH_3, O, OH, and OOH from TCD.

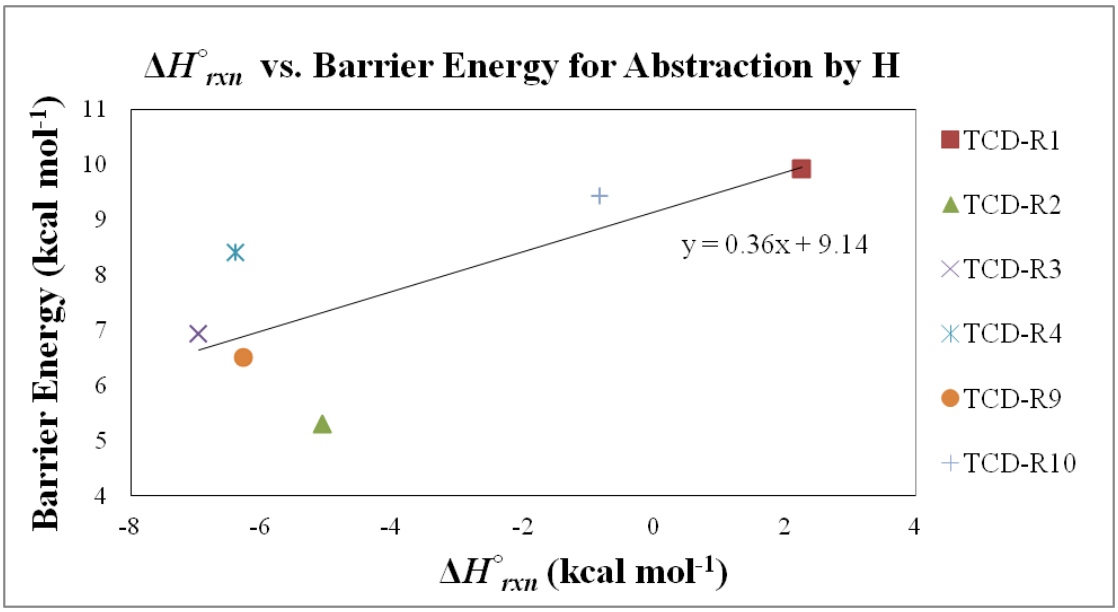

Figure 7.13 Calculated ΔH°_{rxn} vs. barrier energy for abstraction by H from TCD.

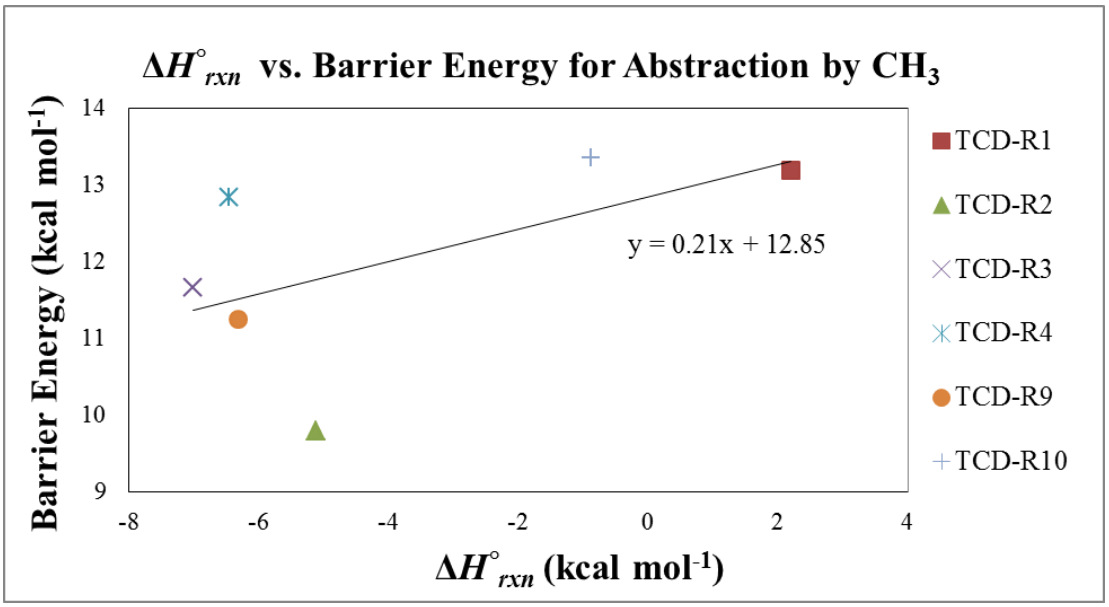

Figure 7.14 Calculated ΔH°_{rxn} vs. barrier energy for abstraction by CH_3 from TCD.

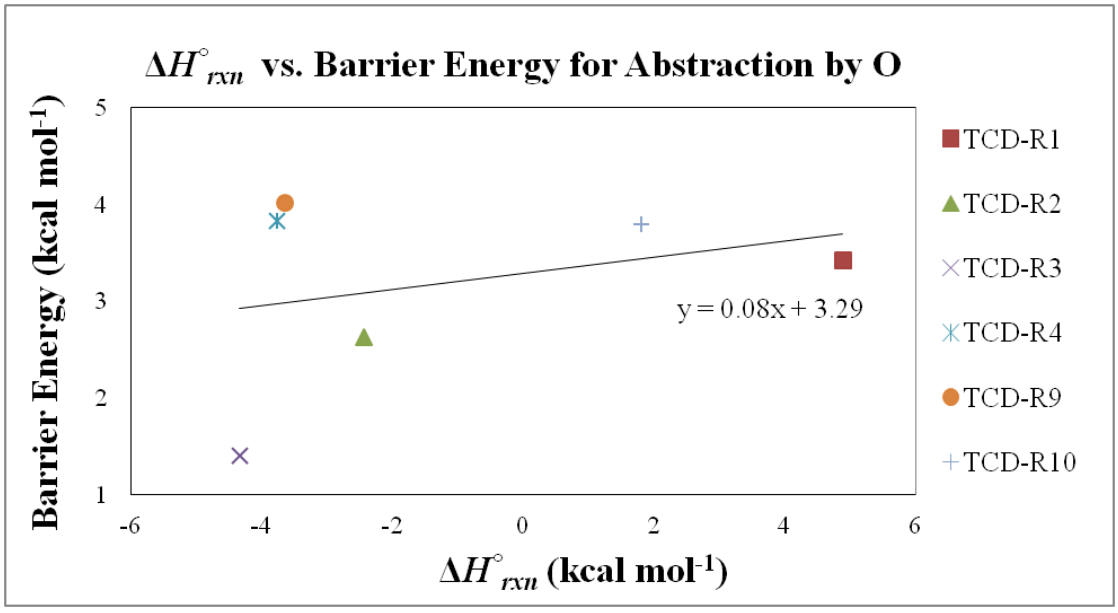

Figure 7.15 Calculated ΔH°_{rxn} vs. barrier energy for abstraction by O from TCD.

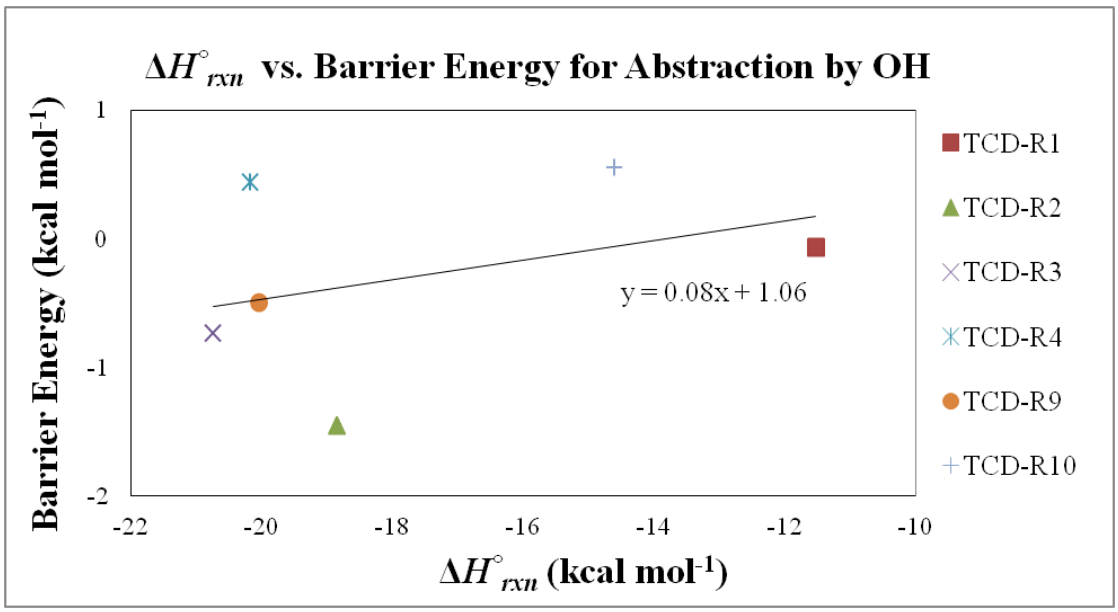

Figure 7.16 Calculated ΔH°_{rxn} vs. barrier energy for abstraction by OH from TCD.

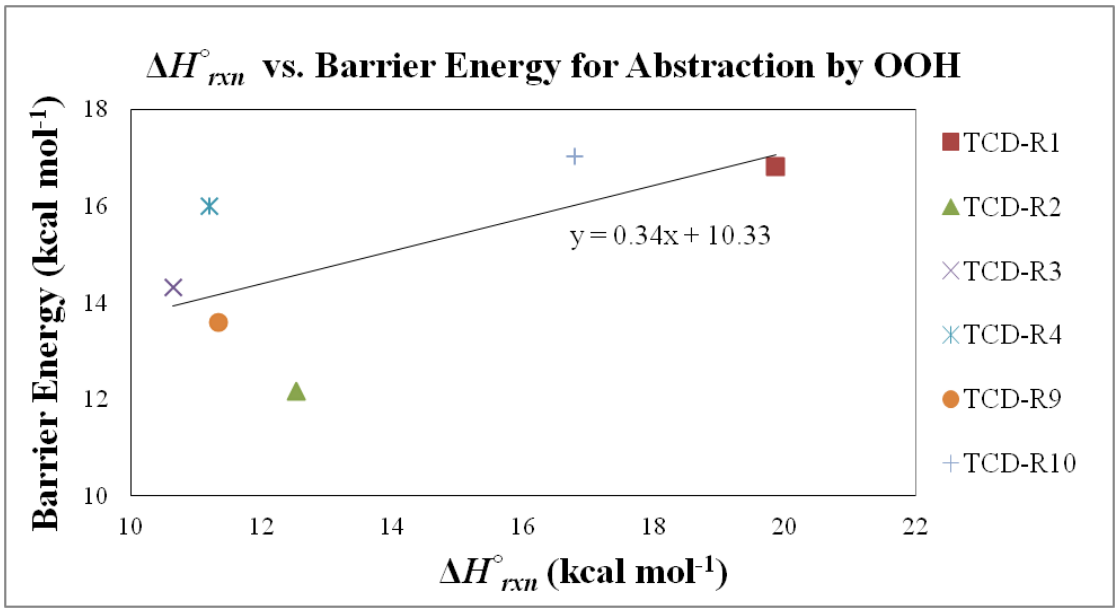

Figure 7.17 Calculated ΔH°_{rxn} vs. barrier energy for abstraction by OOH from TCD.

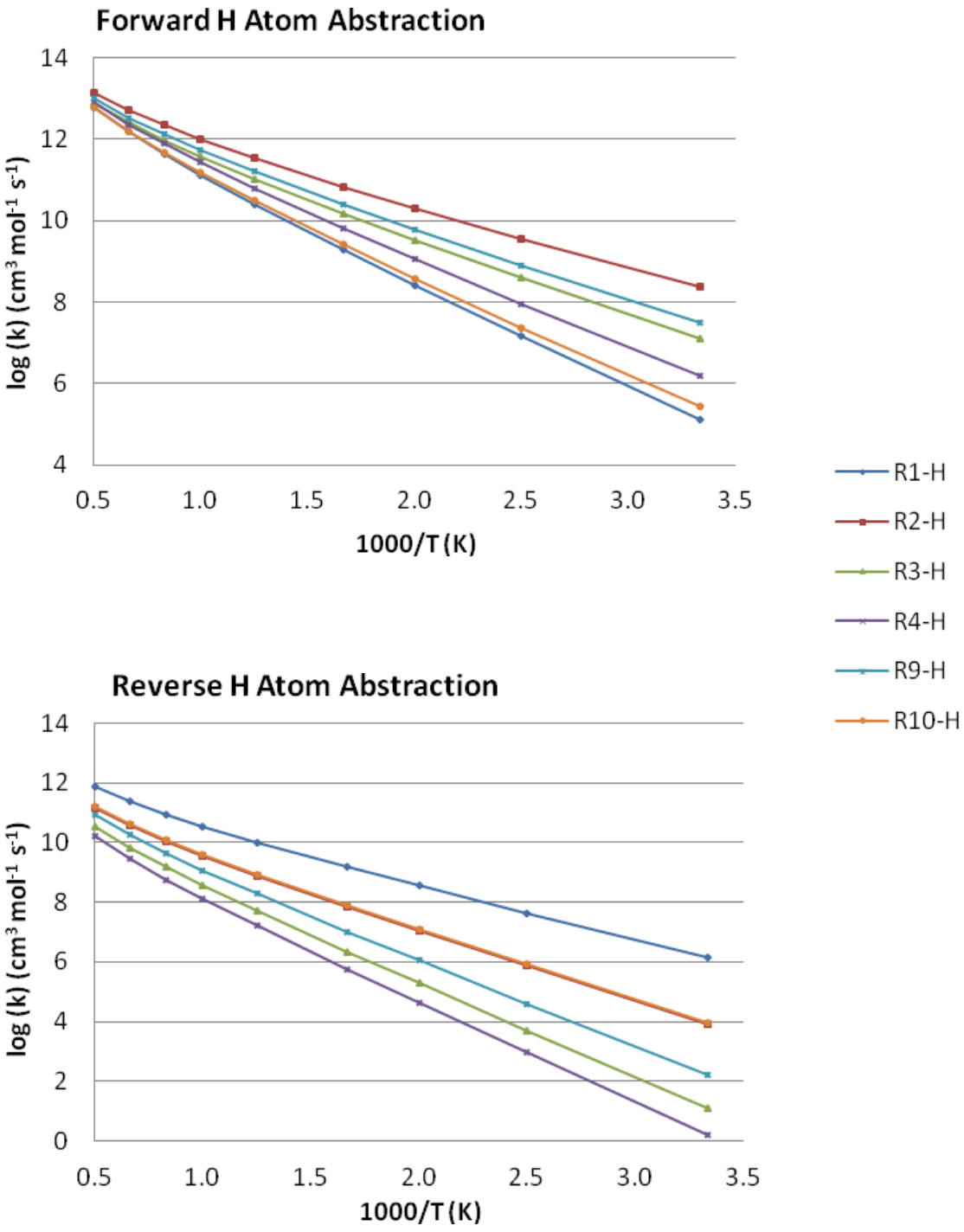

Figure 7.18 Rate constants for H atom abstractions from TCD.

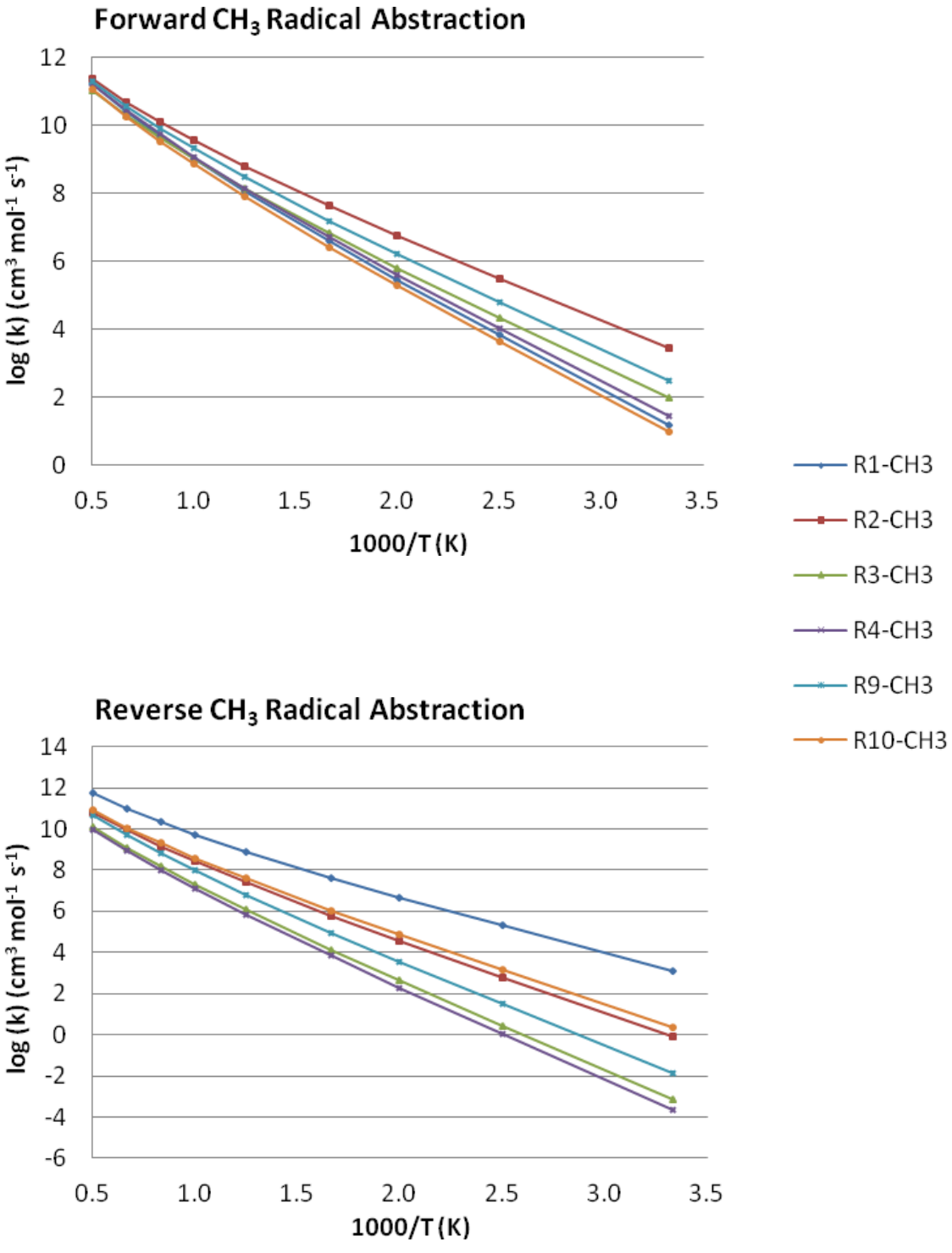

Figure 7.19 Rate constants for CH_3 radical abstractions from TCD.

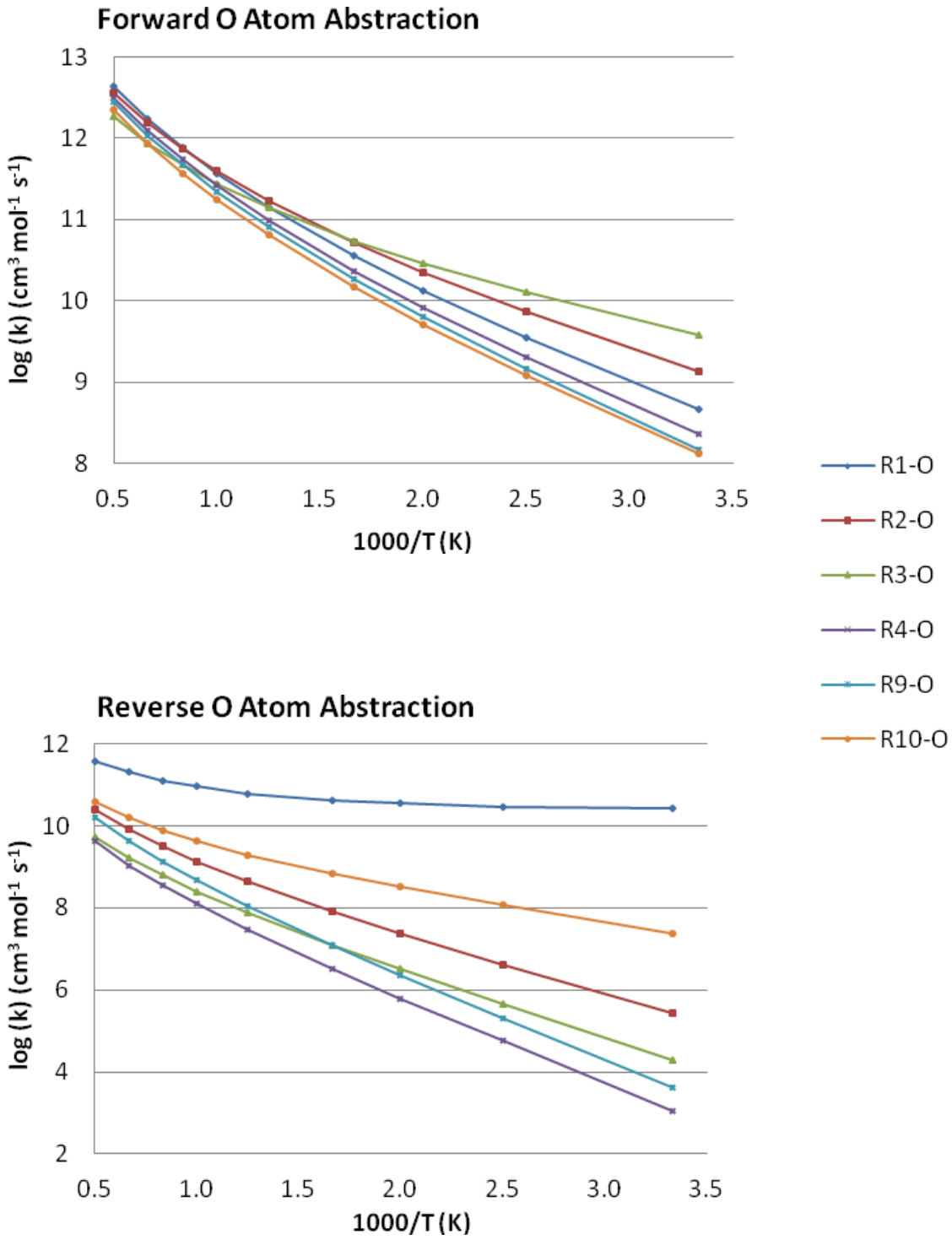

Figure 7.20 Rate constants for O atom abstractions from TCD.

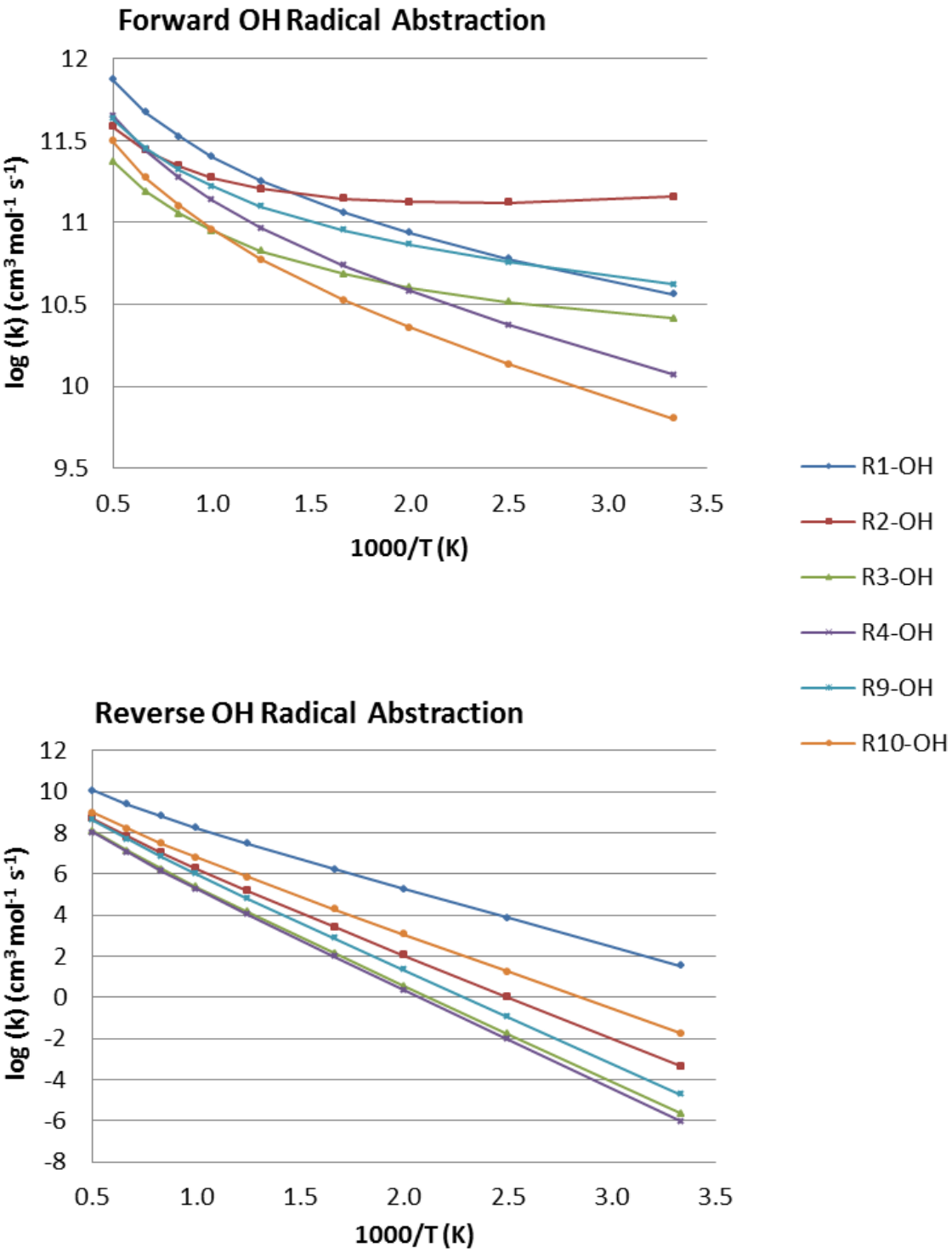

Figure 7.21 Rate constants for OH radical abstractions from TCD.

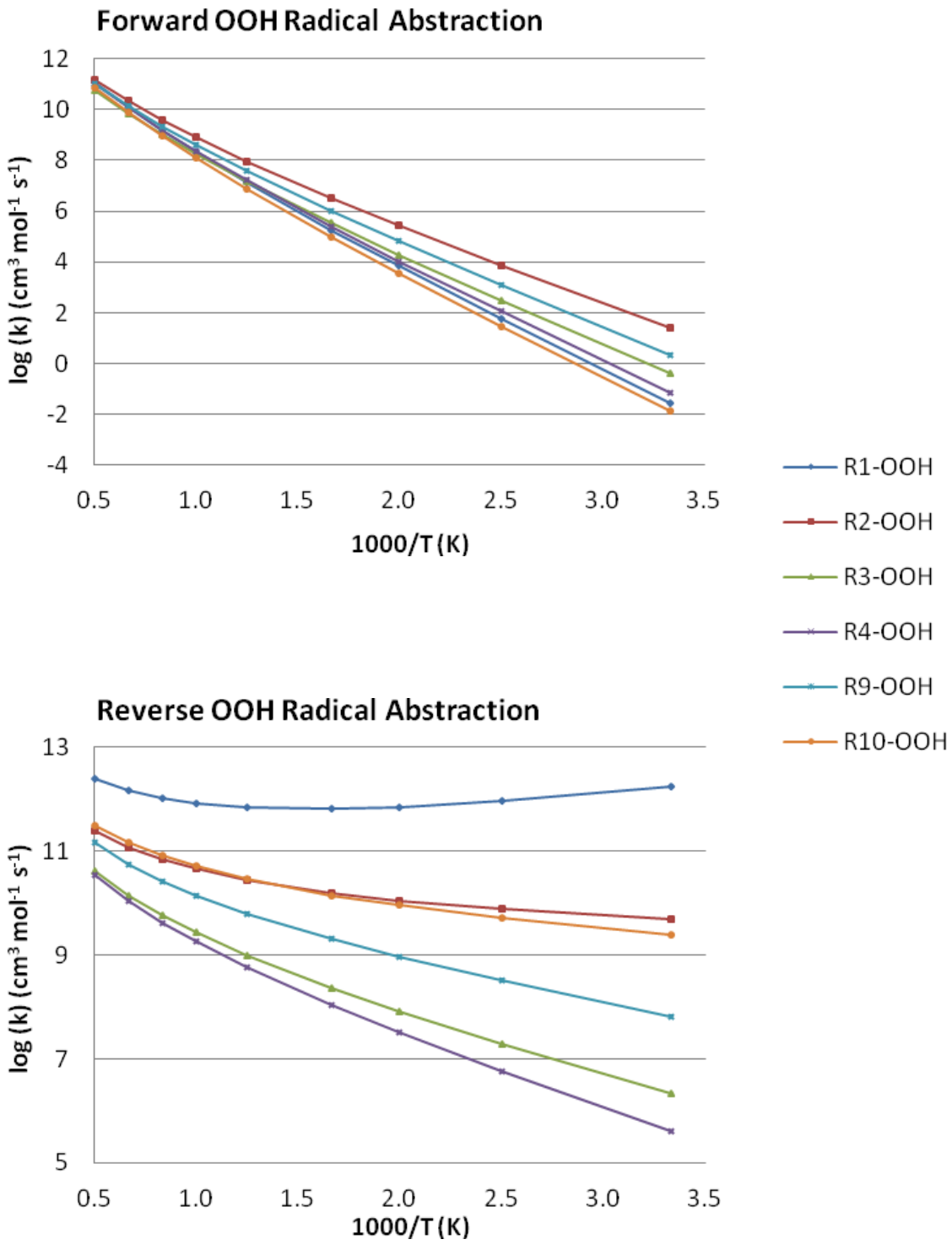

Figure 7.22 Rate constants for OOH radical abstractions from TCD.

7.5 Conclusions

Abstraction of hydrogen atoms form the different sites of e*xo*-tricyclo[5.2.1.$0^{2,6}$]decane (TCD) by hydrogen and oxygen atoms and methyl, hydroxyl, and hydroperoxyl radicals are analyzed in the 300-2000 K temperature range. Enthalpies ($\Delta H^{\circ}_{f\ 298}$), entropies ($S^{\circ}(T)$), and heat capacities ($C_p(T)$) are calculated for the TCD transition state species (TS-TCD). Standard $\Delta H^{\circ}_{f\,298}$ values are recommended from the average of the G3MP2B3 and CBS-QB3 calculation methods due to the constant under prediction in the energy from the density functional theory B3LYP method. Elementary rate parameters, A, *n*, and E_a, are fit in the three parameter modified Arrhenius equation to calculate temperature dependent rate constants, k(T), over the 300-2000 K temperature range. The calculated rate constants are directly proportional to the nature of the abstraction site and shows the relationship that bond dissociation energies have to corresponding product energies.

CHAPTER 8

STRUCTURE AND THERMOCHEMICAL PROPERTIES OF 2-METHOXYFURAN, 3-METHOXYFURAN, AND THEIR CARBON-CENTERED RADICALS

8.1 Overview

Biofuels, with their regeneration reusing CO_2 from the atmosphere, are considered important future fuels and of high value for sustainability.[34-36] Biofuels start with materials such as lignocellulosic biomass, which is high in carbohydrates; these are then converted into smaller carbon- and oxygen-containing compounds in various types of processing. This is currently used to produce bioethanol[242] and is being analyzed as a possible source for other biofuel compounds.[243,244] A major obstacle during the breakdown of biomass into fuels or other products is the loss of chemical energy. Minimizing this loss enhances the integrity and usefulness of the created compounds as fuels.[37] One goal of an optimized conversion process is to utilize all of the carbon available in the biomass for energy efficiency.

A wide range of research using various types of conversion processes such as pyrolysis, supercritical fluid extractions, gasification, and liquefaction in hopes to improve the chemical yields from biomass.[245,246] Understanding the thermochemistry and reaction kinetics in the hydrolysis, dehydration, oxidation, and hydrogenation of biomass will be valuable to modeling and design of the processing, product selectivity, energy efficiency, and carbon recycling.[38] Other considerations such as type and available amount of biomass, economical limitations, and environmental concerns are also important factors controlling process selection.[247]

One of the more versatile compounds created from biofuel production is 5-hydroxymethylfurfural (HMF); it has been isolated through several feed-stocks including glucose, fructose, cellulose,[42,248,249] and lignocelluloses.[1,250] Although HMF cannot itself be used as a fuel,[249] it can be converted into a number of promising products, such as organic acids, aldehydes, alcohols, amines, and ethers.[39-41] Substituted furan molecules are a group of compounds that can also be created from HMF.[42,43] Methyl and methoxyfurans are two types of high-energy furans that have been shown to have possible biofuel application.[1,37,44]

Methoxyfurans are the simplest furan ethers, and their synthesis has been studied by several research groups.[251-253] Methoxyfurans have been utilized in the synthesis of a variety of compounds and reactions such as 1,2,3-trisubstituted cyclopropanes,[254] (±)-avenaciolide and (±)-isoavenaciolide,[255] maleic anhydride,[256,257] and *N*-methylmaleimide[256] cycloadducts, and Friedel-Crafts catalyzed reactions with nitroalkenes[258] and with selenoaldehydes to generate methyl penta-2,4-dienoates.[259] 2-Methoxyfuran has also successfully been employed to study the reaction enthalpy and kinetic parameters in the synthesis of oxanorbornadiene.[260]

The structure of 2-methoxyfuran has been studied with the MP2/6-311++G**, B3LYP/6-311++G**, and B3LYP/cc-pVTZ calculation methods by Beukes et al.[261] where its lowest energy structure was determined to be when the methyl is in the syn configuration with respect to the double bonded carbons in the furan ring. This study confirms this.

There is little experimental information on the thermochemistry of furan ethers and radicals corresponding to loss of hydrogen atoms. Furan and methyl-substituted

furans have been analyzed by Simmie and Curran[45] where bond dissociation energies and formation enthalpies were determined. This group of compounds poses extremely strong carbon-hydrogen (C–H) bonds due to the aromaticity and the oxygen atom's location in their cyclic structure. Bond dissociation energies in excess of 120 kcal mol^{-1} were observed for C–H bonds on the furan ring with lower energies for the bonds of substituent groups.

In this chapter, thermochemical properties are determined for 2-methoxyfuran, 3-methoxyfuran, and their carbon-centered radicals for their possible biofuel applications. Standard heat of formations ($\Delta H^{\circ}_{f\ 298}$), entropies ($S(T)$), heat capacities ($C_p(T)$), bond dissociation energies, and internal rotation potentials are calculated. Data from this study is used to develop groups for use in the group additivity (GA) method. Valuable thermochemical data is provided to hopefully assist in creating chemical kinetic models for these and similar compounds.

8.2 Nomenclature

Abbreviations are utilized in this chapter as illustrated below:

- – represents a bond between two atoms,
- = represents a double bond between two atoms,
- Y represents a cyclic ring structure,
- [OCH_3] represents a OCH_3 substituent on the preceding carbon atom,
- • represents a radical site on the preceding carbon atom.

8.3 Computational Methods

Structures, vibration frequencies, zero-point vibrational energies (ZPVE), and internal rotor potentials are initially analyzed with the hybrid density functional theory (DFT) B3LYP[46,47] method with the 6-31G(d,p) basis set.

Isodesmic work reactions are used to calculate enthalpies of formation ($\Delta H^{\circ}_{f\,298}$) for the target methoxyfuran compounds using B3LYP with the 6-31G(d,p) and 6-311G(2d,2p) basis sets. These values are compared to composite methods G3,[58] G3MP2B3,[57,58] and CBS-QB3[60,61] which serves as a way to evaluate the accuracy of the DFT methods for these furan-based compounds. All calculations are performed using the Gaussian 03 program suite.[62] The natural bond orbital (NBO) analysis is also performed as implemented in the Gaussian 03 code (NBO Version 3.1).[262]

Entropies and heat capacities for the compounds are calculated at the B3LYP/6-31G(d,p) level of theory using the Statistical Mechanics for Heat Capacity and Entropy, SMCPS,[98] program. The Pitzer and Gwinn[85-87] approximation method for entropy and heat capacity contributions from internal rotations use internal rotor potential energy barriers calculated at the B3LYP/6-31G(d,p) level. Total entropies and heat capacities for each compound are determined by summing these contributions.

8.4 Results and Discussion

8.4.1 Configuration and Geometry

Figure 8.1 illustrates the numbering convention for the methoxyfurans and radicals in this study. Optimized geometries for the compounds from the B3LYP/6-31G(d,p) level of theory with corresponding nomenclature are presented in Figure 8.2. Optimized geometry parameters, vibrational frequencies, and moments of inertia for all structures along with a

comparison showing excellent agreement of the high level calculation methods to the previously determined bond lengths and angles for 2-methoxyfuran by Beukes et al.[261] are available in Appendix G.

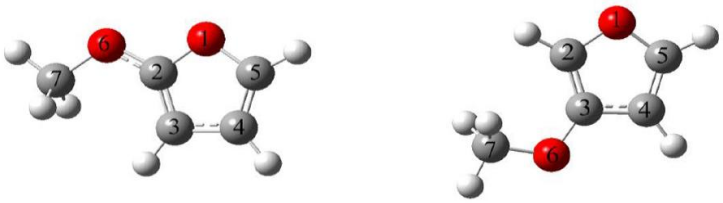

Figure 8.1 Numbering convention for 2-methoxyfuran, 3-methoxyfuran, and radicals.

2-Methoxyfuran and each of the radicals have two low-energy conformations for the methyl group in the methoxy substituent, shown in Figure 8.3. Syn signifies the methyl group is adjacent to the double bonded carbons in the furan ring and anti has it rotated toward the oxygen of the furan ring. Figure 8.2 shows that Y(OC[OCH_3]CCC), Y(OC[OCH_3]CC$^{\bullet}$C), and Y(OC[OCH_3]C$^{\bullet}$CC) attain their lowest energies in the syn conformation with small energy increases of 0.6, 0.6, and 1.4 kcal mol^{-1} for their anti conformations.

The other 2-methoxyfuran radicals, Y(OC[OCH_3]CCC$^{\bullet}$) and Y(OC[OC$^{\bullet}H_2$]CCC), have their lowest energy in the anti configuration with only a slight 0.3 kcal mol^{-1} energy increase to the syn conformation. Hydrogen bonding occurs in the anti configuration to stabilize the radicals seen in the methyl hydrogen to furan oxygen bond distances of 2.6 Å and 2.4 Å for Y(OC[OCH_3]CCC$^{\bullet}$) and Y(OC[OC$^{\bullet}H_2$]CCC).

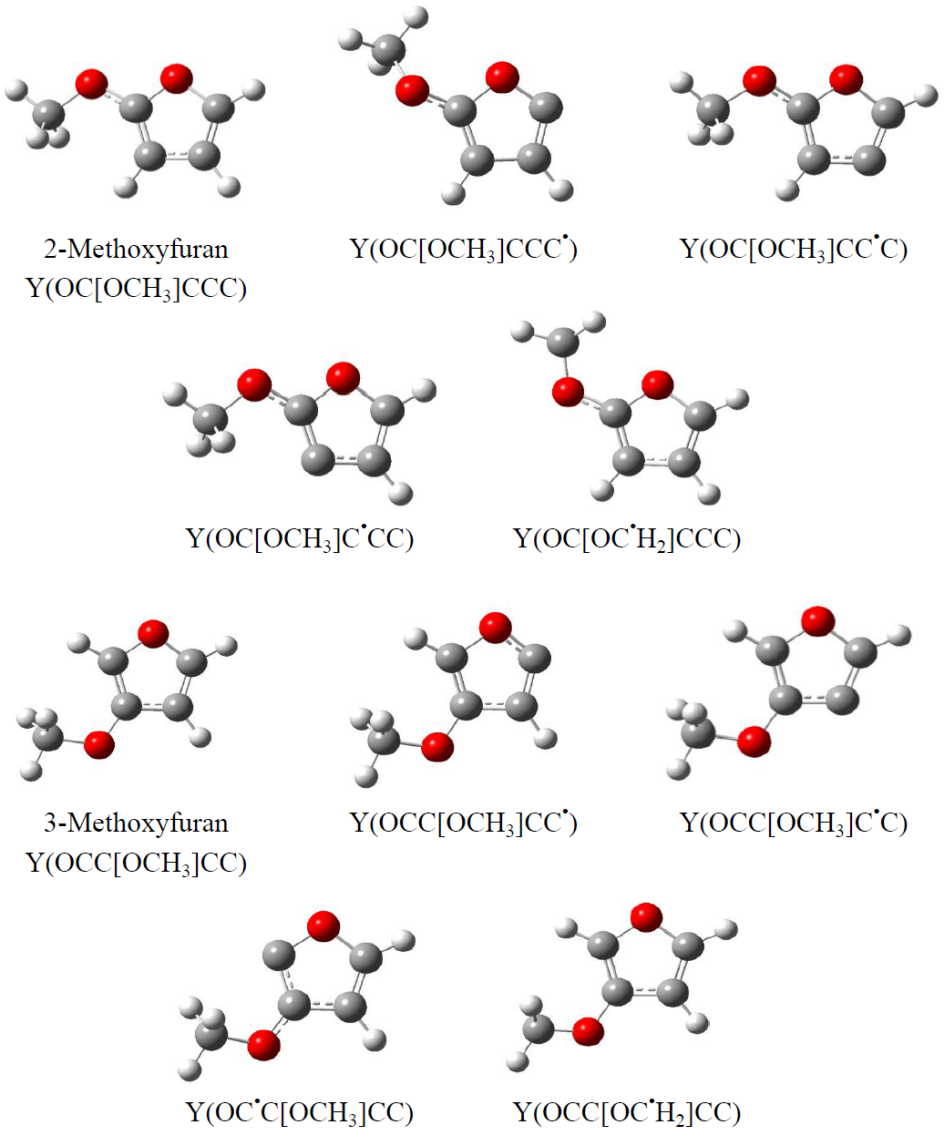

Figure 8.2 Nomenclature and illustration of the lowest energy conformation for each species from the B3LYP/6-31G(d,p) level of theory.

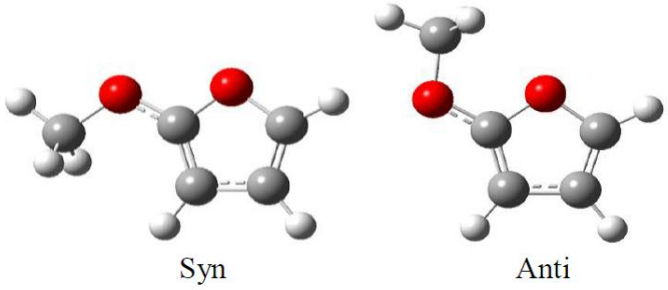

Figure 8.3 Syn and anti conformations for 2-methoxyfuran.

3-Methoxyfuran and its radicals, in contrast, consistently show preference to the conformation where the methyl group is rotated away from the base of the furan ring as shown in Figure 8.2.

Each compound in this analysis, except Y(OC[OCH_3]CCC$^{\bullet}$), has its lowest energy, regardless if syn or anti, when the methyl carbon is in the same plane as the furan ring creating a planar geometry. Each of the analysis methods for Y(OC[OCH_3]CCC$^{\bullet}$) shows the methyl group is approximately half way between parallel and perpendicular to the furan ring at a 50° angle. The G3 method deviates slightly here with a 60° angle in the optimized geometry.

Data on the geometries and the NBO charges are presented in Table 8.1, for 2-methoxyfuran and Y(OC[OCH_3]CCC$^{\bullet}$) which assist in explaining the stable out of plane conformation. The shortening of the C_2–O_6, 1.342 Å to 1.336 Å, and O_1–C_5, 1.379 Å to 1.346 Å, bonds with the elongation of the O_1–C_2, 1.351 Å to 1.388 Å, suggests a partial double bond formation is occurring for C_2–O_6. This is further supported by the shortened C_2–C_3 bond, relaxation of the C_2–C_3–C_4 angle, increased charge on C_3, decreased charges for C_2 and O_6, and the increase of the bond angle, closer to that of a sp^2 bond, to 115.8° for C_7–O_6–C_2. Finally, the O_6–C_2–O_1 bond angle increase to 117.7° would position the C_7 methyl group slightly further from O_1. The methoxy group in the Y(OC[OCH_3]CCC$^{\bullet}$) radical would rotate to this out of plane methyl configuration to be able to hydrogen bond to the oxygen for increasing stability.

Table 8.1 Comparison of Charges, Bond Lengths, and Bond Angles for 2-Methoxyfuran and Y(OC[OCH_3]CCC$^{\bullet}$)[a]

	NBO Charge	
	Y(OC[OCH_3]CCC)	Y(OC[OCH_3]CCC$^{\bullet}$)
O_1	-0.464	-0.523
C_2	0.628	0.591
C_3	-0.440	-0.366
C_4	-0.319	-0.442
C_5	0.060	0.416
O_6	-0.520	-0.527
C_7	-0.324	-0.326

	Bond Length (Å)	
	Y(OC[OCH_3]CCC)	Y(OC[OCH_3]CCC$^{\bullet}$)
O_1–C_2	1.351	1.388
C_2–C_3	1.367	1.361
C_3–C_4	1.440	1.448
C_4–C_5	1.356	1.356
O_1–C_5	1.379	1.346
C_2–O_6	1.342	1.336
O_6–C_7	1.424	1.438

	Bond Angle (°)	
	Y(OC[OCH_3]CCC)	Y(OC[OCH_3]CCC$^{\bullet}$)
O_1–C_2–C_3	111.6	110.2
C_2–C_3–C_4	105.0	106.6
C_3–C_4–C_5	106.9	104.5
C_4–C_5–O_1	110.1	113.2
C_7–O_6–C_2	114.6	115.8
O_6–C_2–O_1	113.4	117.7
C_2–O_1–C_5	106.4	105.4

[a] B3LYP/6-31G(d,p) level of theory.

8.4.2 Heat of Formation $\Delta H^{\circ}_{f\,298}$

Enthalpies of formation ($\Delta H^{\circ}_{f\,298}$) are determined for the target furan compounds in this study using isodesmic reactions. $\Delta H^{\circ}_{f\ 298}$ values for the reference species and uncertainties are summarized in Table 8.2.

Table 8.2 Standard Enthalpies of Formation for Reference Species

Species	$\Delta H^{\circ}_{f\,298}$ (kcal mol^{-1})	Reference
H	52.10 ± 0.001	83
CH_4	-17.89 ± 0.08	123
CH_3CH_3	-20.04 ± 0.07	263
$CH_3CH_2CH_3$	-24.82 ± 0.14	123
$CH_2=CH_2$	12.54 ± 0.07	83
$CH_2=CHCH_3$	4.88 ± 0.08	264
CH_3OCH_3	-43.99 ± 0.12	265
$CH_3CH_2CH_2OCH_3$	-56.89 ± 0.20	266
$CH_2=CHCH_2OCH_3$	-25.68[a]	267
Y(OCCCC)	-8.29[a]	268
$Y(C_6H_6)$	19.81 ± 0.13	171
$Y(C_6H_5[OCH_3])$	-17.27 ± 0.93	83
$C^{\bullet}H_3$	34.82 ± 0.2	83
$CH_3C^{\bullet}H_2$	28.40 ± 0.5	173
$CH_3CH_2C^{\bullet}H_2$	23.90 ± 0.5	83
$CH_2=C^{\bullet}H$	70.90 ± 0.3	269
$CH_2=CHC^{\bullet}H_2$	39.13 ± 0.13	100
$Y(C^{\bullet}_6H_5)$	81.4 ± 0.16	83

[a] Error not reported.

The enthalpies of formation for 2- and 3-methoxyfuran for each work reaction is shown in Tables 8.3 and 8.4 for the five levels of theory. There is good consistency with the B3LYP method for the $\Delta H^{\circ}_{f\,298}$ values between the 6-31G(d,p) and 6-311G(2d,2p) basis sets, with all differences less than 0.65 kcal mol^{-1} for the methoxyfurans and their radicals. The higher level composite calculations from the CBS-QB3 and G3MP2B3 methods also have consistent values within 0.04 and 0.10 kcal mol^{-1} for 2- and 3-methoxyfuran but do show deviations ranging from 0.02 to 1.02 kcal mol^{-1} for the radical species. Values for the radicals from the G3 level of theory are presented but are excluded from the recommended averages, due to their average deviation of 1.8 kcal mol^{-1} higher than the CBS-QB3 and G3MP2B3 values. This is consistent with the

discussion in the radicals section of the article by Simmie and Curran[45] and references therein. Differences in the ZPVE and geometry optimization methods in G3 versus the CBS-QB3 and G3MP2B3 calculation methods could also be a reason for the consistently higher G3 energy values.

Enthalpy of formation values for 2- and 3-methoxyfuran parent and radical species are recommended from the averages from the CBS-QB3 and G3MP2B3 methods presented in Table 8.5.

The DFT method is shown to provide acceptable enthalpy values by comparison to the higher level calculations. There is only a 0.5 to 0.8 kcal mol^{-1} difference for 2- and 3-methoxyfuran from the DFT method work reactions relative to the higher calculation levels. The enthalpy analysis for the radicals shows a larger deviation ranging from 0.01 to 1.23 kcal mol^{-1}. This suggests that the B3LYP density functional calculations with work reactions provide reasonable estimates for these molecules and radicals.

Table 8.3 Isodesmic Reactions, Calculated Enthalpies of Formation, and Bond Energies for 2-Methoxyfuran and Radicals

Isodesmic Reactions							$\Delta H^{\circ}_{f\,298}$ (kcal mol^{-1})				
							B3LYP		CBS-QB3	G3MP2B3	G3
							6-31G(d,p)	6-311G(2d,2p)			
Y(OC[OCH$_3$]CCC) System											
Y(OC[OCH$_3$]CCC)	+	CH_4	→	Y(OCCCC)	+	CH_3OCH_3	-45.05	-44.80	-44.86	-44.79	-45.61
Y(OC[OCH$_3$]CCC)	+	$CH_3CH_2CH_3$	→	Y(OCCCC)	+	$CH_3CH_2CH_2OCH_3$	-45.89	-45.37	-44.75	-44.78	-45.41
Y(OC[OCH$_3$]CCC)	+	CH_2=$CHCH_3$	→	Y(OCCCC)	+	CH_2=$CHCH_2OCH_3$	-46.16	-45.92	-45.13	-45.14	-45.70
Y(OC[OCH$_3$]CCC)	+	Y(C_6H_6)	→	Y(OCCCC)	+	Y(C_6H_5[OCH_3])	-45.15	-45.23	-45.35	-45.21	-45.24
						Average	**-45.56**	**-45.33**	**-45.02**	**-44.98**	**-45.49**
						Osmont et al. Corrected Atomization	**-46.0**				
Y(OC[OCH$_3$]CCC$^{\bullet}$) System											
Y(OC[OCH$_3$]CCC$^{\bullet}$)	+	CH_4	→	Y(OC[OCH$_3$]CCC)	+	$C^{\bullet}H_3$	21.70	22.20	23.55	25.37	25.82
Y(OC[OCH$_3$]CCC$^{\bullet}$)	+	CH_3CH_3	→	Y(OC[OCH$_3$]CCC)	+	$CH_3C^{\bullet}H_2$	22.19	22.65	22.99	24.38	24.63
Y(OC[OCH$_3$]CCC$^{\bullet}$)	+	$CH_3CH_2CH_3$	→	Y(OC[OCH$_3$]CCC)	+	$CH_3CH_2C^{\bullet}H_2$	22.19	22.71	22.99	24.33	24.59
Y(OC[OCH$_3$]CCC$^{\bullet}$)	+	CH_2=CH_2	→	Y(OC[OCH$_3$]CCC)	+	CH_2=$C^{\bullet}H$	22.98	23.20	23.99	24.89	25.42
Y(OC[OCH$_3$]CCC$^{\bullet}$)	+	CH_2=$CHCH_3$	→	Y(OC[OCH$_3$]CCC)	+	CH_2=$CHC^{\bullet}H_2$	23.09	23.21	23.26	23.14	24.70
Y(OC[OCH$_3$]CCC$^{\bullet}$)	+	Y(C_6H_6)	→	Y(OC[OCH$_3$]CCC)	+	Y($C^{\bullet}_6H_5$)	24.47	24.30	22.37	23.14	26.84
						Average	**22.77**	**23.04**	**23.19**	**24.21**	**25.33**
						Osmont et al. Corrected Atomization	**22.8**				
						C–H Bond Energy	**119.87**	**120.15**	**120.29**	**121.31**	**122.43**

Table 8.3 Isodesmic Reactions, Calculated Enthalpies of Formation, and Bond Energies for 2-Methoxyfuran and Radicals (Continued)

Isodesmic Reactions							$\Delta H^{\circ}_{f\,298}$ (kcal mol^{-1})				
							B3LYP		CBS-QB3	G3MP2B3	G3
							6-31G(d,p)	6-311G(2d,2p)			
Y(OC[OCH$_3$]CC$^{\bullet}$C) System											
Y(OC[OCH$_3$]CC$^{\bullet}$C)	+	CH$_4$	→	Y(OC[OCH$_3$]CCC)	+	C$^{\bullet}$H$_3$	20.77	21.59	22.23	23.54	23.78
Y(OC[OCH$_3$]CC$^{\bullet}$C)	+	CH$_3$CH$_3$	→	Y(OC[OCH$_3$]CCC)	+	CH$_3$C$^{\bullet}$H$_2$	21.26	22.05	21.67	22.54	22.59
Y(OC[OCH$_3$]CC$^{\bullet}$C)	+	CH$_3$CH$_2$CH$_3$	→	Y(OC[OCH$_3$]CCC)	+	CH$_3$CH$_2$C$^{\bullet}$H$_2$	21.26	22.11	21.66	22.50	22.55
Y(OC[OCH$_3$]CC$^{\bullet}$C)	+	CH$_2$=CH$_2$	→	Y(OC[OCH$_3$]CCC)	+	CH$_2$=C$^{\bullet}$H	22.05	22.60	22.67	23.05	23.38
Y(OC[OCH$_3$]CC$^{\bullet}$C)	+	CH$_2$=CHCH$_3$	→	Y(OC[OCH$_3$]CCC)	+	CH$_2$=CHC$^{\bullet}$H$_2$	22.16	22.60	21.93	21.31	22.65
Y(OC[OCH$_3$]CC$^{\bullet}$C)	+	Y(C$_6$H$_6$)	→	Y(OC[OCH$_3$]CCC)	+	Y(C$^{\bullet}$$_6H_5$)	23.54	23.70	21.05	21.30	24.79
						Average	**21.84**	**22.44**	**21.87**	**22.37**	**23.29**
						Osmont et al. Corrected Atomization	**21.9**				
						C–H Bond Energy	**118.94**	**119.54**	**118.97**	**119.47**	**120.39**
Y(OC[OCH$_3$]C$^{\bullet}$CC) System											
Y(OC[OCH$_3$]C$^{\bullet}$CC)	+	CH$_4$	→	Y(OC[OCH$_3$]CCC)	+	C$^{\bullet}$H$_3$	22.01	22.75	23.50	24.73	25.50
Y(OC[OCH$_3$]C$^{\bullet}$CC)	+	CH$_3$CH$_3$	→	Y(OC[OCH$_3$]CCC)	+	CH$_3$C$^{\bullet}$H$_2$	22.51	23.20	22.94	23.73	24.31
Y(OC[OCH$_3$]C$^{\bullet}$CC)	+	CH$_3$CH$_2$CH$_3$	→	Y(OC[OCH$_3$]CCC)	+	CH$_3$CH$_2$C$^{\bullet}$H$_2$	22.51	23.27	22.93	23.68	24.27
Y(OC[OCH$_3$]C$^{\bullet}$CC)	+	CH$_2$=CH$_2$	→	Y(OC[OCH$_3$]CCC)	+	CH$_2$=C$^{\bullet}$H	23.30	23.75	23.94	24.24	25.10
Y(OC[OCH$_3$]C$^{\bullet}$CC)	+	CH$_2$=CHCH$_3$	→	Y(OC[OCH$_3$]CCC)	+	CH$_2$=CHC$^{\bullet}$H$_2$	23.41	23.76	23.20	22.49	24.37
Y(OC[OCH$_3$]C$^{\bullet}$CC)	+	Y(C$_6$H$_6$)	→	Y(OC[OCH$_3$]CCC)	+	Y(C$^{\bullet}$$_6H_5$)	24.78	24.86	22.32	22.49	26.51
						Average	**23.09**	**23.60**	**23.14**	**23.56**	**25.01**
						Osmont et al. Corrected Atomization	**23.1**				
						C–H Bond Energy	**120.19**	**120.70**	**120.24**	**120.66**	**122.11**

Table 8.3 Isodesmic Reactions, Calculated Enthalpies of Formation, and Bond Energies for 2-Methoxyfuran and Radicals (Continued)

Isodesmic Reactions							$\Delta H^{\circ}_{f\,298}$ (kcal mol^{-1})				
							B3LYP		CBS-QB3	G3MP2B3	G3
							6-31G(d,p)	6-311G(2d,2p)			
Y(OC[OC$^{\bullet}$H$_2$]CCC) System											
Y(OC[OC$^{\bullet}$H$_2$]CCC)	+	CH_4	→	Y(OC[OCH_3]CCC)	+	$C^{\bullet}H_3$	-0.57	-0.48	2.04	2.82	3.59
Y(OC[OC$^{\bullet}$H$_2$]CCC)	+	CH_3CH_3	→	Y(OC[OCH_3]CCC)	+	$CH_3C^{\bullet}H_2$	-0.07	-0.03	1.48	1.82	2.40
Y(OC[OC$^{\bullet}$H$_2$]CCC)	+	$CH_3CH_2CH_3$	→	Y(OC[OCH_3]CCC)	+	$CH_3CH_2C^{\bullet}H_2$	-0.07	0.04	1.48	1.78	2.36
Y(OC[OC$^{\bullet}$H$_2$]CCC)	+	$CH_2=CH_2$	→	Y(OC[OCH_3]CCC)	+	$CH_2=C^{\bullet}H$	0.72	0.52	2.48	2.34	3.19
Y(OC[OC$^{\bullet}$H$_2$]CCC)	+	$CH_2=CHCH_3$	→	Y(OC[OCH_3]CCC)	+	$CH_2=CHC^{\bullet}H_2$	0.83	0.53	1.75	0.59	2.47
Y(OC[OC$^{\bullet}$H$_2$]CCC)	+	Y(C_6H_6)	→	Y(OC[OCH_3]CCC)	+	Y($C^{\bullet}_6H_5$)	2.21	1.63	0.86	0.59	4.61
						Average	**0.51**	**0.37**	**1.68**	**1.66**	**3.10**
						Osmont et al. Corrected Atomization	**0.5**				
						C—H Bond Energy	**97.61**	**97.47**	**98.78**	**98.76**	**100.20**

Table 8.4 Isodesmic Reactions, Calculated Enthalpies of Formation, and Bond Energies for 3-Methoxyfuran and Radicals

Isodesmic Reactions							$\Delta H^{\circ}_{f\,298}$ (kcal mol^{-1})				
							B3LYP		CBS-QB3	G3MP2B3	G3
							6-31G(d,p)	6-311G(2d,2p)			
Y(OCC[OCH$_3$]CC) System											
Y(OCC[OCH$_3$]CC)	+	CH$_4$	→	Y(OCCCC)	+	CH$_3$OCH$_3$	-41.56	-41.16	-40.95	-40.82	-41.61
Y(OCC[OCH$_3$]CC)	+	CH$_3$CH$_2$CH$_3$	→	Y(OCCCC)	+	CH$_3$CH$_2$CH$_2$OCH$_3$	-42.40	-41.74	-40.84	-40.81	-41.41
Y(OCC[OCH$_3$]CC)	+	CH$_2$=CHCH$_3$	→	Y(OCCCC)	+	CH$_2$=CHCH$_2$OCH$_3$	-42.67	-42.28	-41.22	-41.17	-41.70
Y(OCC[OCH$_3$]CC)	+	Y(C$_6$H$_6$)	→	Y(OCCCC)	+	Y(C$_6$H$_5$[OCH$_3$])	-41.66	-41.60	-41.44	-41.24	-41.25
						Average	**-42.07**	**-41.70**	**-41.11**	**-41.01**	**-41.49**
						Osmont et al. Corrected Atomization	**-42.5**				
Y(OCC[OCH$_3$]CC$^{\bullet}$) System											
Y(OCC[OCH$_3$]CC$^{\bullet}$)	+	CH$_4$	→	Y(OCC[OCH$_3$]CC)	+	C$^{\bullet}$H$_3$	24.71	25.58	25.95	27.35	28.05
Y(OCC[OCH$_3$]CC$^{\bullet}$)	+	CH$_3$CH$_3$	→	Y(OCC[OCH$_3$]CC)	+	CH$_3$C$^{\bullet}$H$_2$	25.20	26.04	25.39	26.35	26.86
Y(OCC[OCH$_3$]CC$^{\bullet}$)	+	CH$_3$CH$_2$CH$_3$	→	Y(OCC[OCH$_3$]CC)	+	CH$_3$CH$_2$C$^{\bullet}$H$_2$	25.20	26.10	25.39	26.31	26.82
Y(OCC[OCH$_3$]CC$^{\bullet}$)	+	CH$_2$=CH$_2$	→	Y(OCC[OCH$_3$]CC)	+	CH$_2$=C$^{\bullet}$H	25.99	26.59	26.39	26.87	27.65
Y(OCC[OCH$_3$]CC$^{\bullet}$)	+	CH$_2$=CHCH$_3$	→	Y(OCC[OCH$_3$]CC)	+	CH$_2$=CHC$^{\bullet}$H$_2$	26.10	26.59	25.66	25.12	26.93
Y(OCC[OCH$_3$]CC$^{\bullet}$)	+	Y(C$_6$H$_6$)	→	Y(OCC[OCH$_3$]CC)	+	Y(C$^{\bullet}$$_6H_5$)	27.48	27.69	24.78	25.12	29.07
						Average	**25.78**	**26.43**	**25.59**	**26.19**	**27.56**
						Osmont et al. Corrected Atomization	**25.4**				
						C–H Bond Energy	**118.94**	**119.59**	**118.75**	**119.35**	**120.72**

Table 8.4 Isodesmic Reactions, Calculated Enthalpies of Formation, and Bond Energies for 3-Methoxyfuran and Radicals (Continued)

Isodesmic Reactions							$\Delta H^{\circ}_{f\,298}$ (kcal mol^{-1})				
							B3LYP		CBS-QB3	G3MP2B3	G3
							6-31G(d,p)	6-311G(2d,2p)			
Y(OCC[OCH$_3$]C$^{\bullet}$C) System											
Y(OCC[OCH$_3$]C$^{\bullet}$C)	+	CH_4	→	Y(OCC[OCH$_3$]CC)	+	C$^{\bullet}$H$_3$	26.42	27.18	27.89	29.25	29.86
Y(OCC[OCH$_3$]C$^{\bullet}$C)	+	CH_3CH_3	→	Y(OCC[OCH$_3$]CC)	+	$CH_3C^{\bullet}H_2$	26.91	27.64	27.33	28.25	28.67
Y(OCC[OCH$_3$]C$^{\bullet}$C)	+	$CH_3CH_2CH_3$	→	Y(OCC[OCH$_3$]CC)	+	$CH_3CH_2C^{\bullet}H_2$	26.91	27.70	27.33	28.20	28.63
Y(OCC[OCH$_3$]C$^{\bullet}$C)	+	$CH_2=CH_2$	→	Y(OCC[OCH$_3$]CC)	+	$CH_2=C^{\bullet}H$	27.70	28.19	28.33	28.76	29.46
Y(OCC[OCH$_3$]C$^{\bullet}$C)	+	$CH_2=CHCH_3$	→	Y(OCC[OCH$_3$]CC)	+	$CH_2=CHC^{\bullet}H_2$	27.81	28.19	27.60	27.02	28.74
Y(OCC[OCH$_3$]C$^{\bullet}$C)	+	Y(C_6H_6)	→	Y(OCC[OCH$_3$]CC)	+	Y($C^{\bullet}_6H_5$)	29.19	29.29	26.72	27.01	30.88
						Average	**27.49**	**28.03**	**27.54**	**28.08**	**29.37**
						Osmont et al. Corrected Atomization	**27.1**				
						C–H Bond Energy	**120.65**	**121.19**	**120.70**	**121.24**	**122.53**
Y(OC$^{\bullet}$C[OCH$_3$]CC) System											
Y(OC$^{\bullet}$C[OCH$_3$]CC)	+	CH_4	→	Y(OCC[OCH$_3$]CC)	+	C$^{\bullet}$H$_3$	25.10	25.63	27.91	28.31	31.15
Y(OC$^{\bullet}$C[OCH$_3$]CC)	+	CH_3CH_3	→	Y(OCC[OCH$_3$]CC)	+	$CH_3C^{\bullet}H_2$	25.59	26.09	27.35	27.31	29.96
Y(OC$^{\bullet}$C[OCH$_3$]CC)	+	$CH_3CH_2CH_3$	→	Y(OCC[OCH$_3$]CC)	+	$CH_3CH_2C^{\bullet}H_2$	25.59	26.15	27.34	27.26	29.92
Y(OC$^{\bullet}$C[OCH$_3$]CC)	+	$CH_2=CH_2$	→	Y(OCC[OCH$_3$]CC)	+	$CH_2=C^{\bullet}H$	26.38	26.64	28.35	27.82	30.75
Y(OC$^{\bullet}$C[OCH$_3$]CC)	+	$CH_2=CHCH_3$	→	Y(OCC[OCH$_3$]CC)	+	$CH_2=CHC^{\bullet}H_2$	26.49	26.65	27.61	26.07	30.03
Y(OC$^{\bullet}$C[OCH$_3$]CC)	+	Y(C_6H_6)	→	Y(OCC[OCH$_3$]CC)	+	Y($C^{\bullet}_6H_5$)	27.87	27.74	26.73	26.07	32.17
						Average	**26.17**	**26.48**	**27.55**	**27.14**	**30.66**
						Osmont et al. Corrected Atomization	**25.7**				
						C–H Bond Energy	**119.33**	**119.64**	**120.71**	**120.30**	**123.82**

Table 8.4 Isodesmic Reactions, Calculated Enthalpies of Formation, and Bond Energies for 3-Methoxyfuran and Radicals (Continued)

Isodesmic Reactions							$\Delta H^{\circ}_{f\,298}$ (kcal mol^{-1})				
							B3LYP		CBS-QB3	G3MP2B3	G3
							6-31G(d,p)	6-311G(2d,2p)			
Y(OCC[OC$^{\bullet}$H$_2$]CC) System											
Y(OCC[OC$^{\bullet}$H$_2$]CC)	+	CH_4	→	Y(OCC[OCH$_3$]CC)	+	C$^{\bullet}$H$_3$	3.06	3.21	5.26	5.39	6.35
Y(OCC[OC$^{\bullet}$H$_2$]CC)	+	CH_3CH_3	→	Y(OCC[OCH$_3$]CC)	+	$CH_3C^{\bullet}H_2$	3.56	3.67	4.70	4.39	5.16
Y(OCC[OC$^{\bullet}$H$_2$]CC)	+	$CH_3CH_2CH_3$	→	Y(OCC[OCH$_3$]CC)	+	$CH_3CH_2C^{\bullet}H_2$	3.55	3.73	4.70	4.35	5.12
Y(OCC[OC$^{\bullet}$H$_2$]CC)	+	CH_2=CH_2	→	Y(OCC[OCH$_3$]CC)	+	CH_2=C$^{\bullet}$H	4.34	4.22	5.70	4.91	5.95
Y(OCC[OC$^{\bullet}$H$_2$]CC)	+	CH_2=$CHCH_3$	→	Y(OCC[OCH$_3$]CC)	+	CH_2=$CHC^{\bullet}H_2$	4.46	4.22	4.97	3.16	5.23
Y(OCC[OC$^{\bullet}$H$_2$]CC)	+	Y(C_6H_6)	→	Y(OCC[OCH$_3$]CC)	+	Y(C$^{\bullet}$$_6H_5$)	5.32	5.45	4.09	3.16	7.37
						Average	**4.05**	**4.08**	**4.91**	**4.23**	**5.86**
						Osmont et al. Corrected Atomization	**3.7**				
						C—H Bond Energy	**97.22**	**97.23**	**98.07**	**97.39**	**99.02**

Table 8.5 Recommended $\Delta H^{\circ}_{f\,298}$[a] and C–H Bond Dissociation Energies[a] (BDE) for 2-Methoxyfuran, 3-Methoxyfuran, and Radicals

Species	DFT		CBS-QB3/ G3MP2B3	
	$\Delta H^{\circ}_{f\,298}$	C–H BDE	$\Delta H^{\circ}_{f\,298}$	C–H BDE
Y(OC[OCH_3]CCC)	-45.45		-45.00	
Y(OC[OCH_3]CCC$^{\bullet}$)	22.91	120.01	23.70	120.80
Y(OC[OCH_3]CC$^{\bullet}$C)	22.14	119.24	22.12	119.22
Y(OC[OCH_3]C$^{\bullet}$CC)	23.34	120.44	23.35	120.45
Y(OC[OC$^{\bullet}H_2$]CCC)	0.44	97.54	1.67	98.77
Y(OCC[OCH_3]CC)	-41.88		-41.06	
Y(OCC[OCH_3]CC$^{\bullet}$)	26.11	119.27	25.89	119.05
Y(OCC[OCH_3]C$^{\bullet}$C)	27.76	120.92	27.81	120.97
Y(OC$^{\bullet}$C[OCH_3]CC)	26.33	119.49	27.34	120.51
Y(OCC[OC$^{\bullet}H_2$]CC)	4.07	97.23	4.57	97.73

[a] Units of kcal mol^{-1}.

8.4.3 Enthalpies of Formation Calculated by Atomization Reaction Method

Atomization reactions are also used to determine the enthalpy of formation for a compound by considering the compound's decomposition to its balanced number of constituent atoms, C, H, and O. Osmont et al.[199-202] developed an empirically corrected atomization method for gas phase heterocyclic oxygenated compounds using the B3LYP/6-31G(d,p) calculation and is presented in Tables 8.3 and 8.4. This method, while partially calibrated on furan-like molecules, has been shown to produce good agreement to experimental standard enthalpies of formation for the related compounds furan, tetrahydrofuran, and 2,5-dimethylfuran.[199]

Comparison of values from the Osmont method show good agreement to the calculated DFT values in this study. For the parent compounds, the work reaction values of -45.6 kcal mol^{-1} for 2-methoxyfuran and -42.1 kcal mol^{-1} for 3-methoxyfuran are 0.4 kcal mol^{-1} lower than the Osmont method values of -46.0 and -42.5 kcal mol^{-1}, respectively. This method also shows good comparison to the recommended higher

calculation level average values with deviations of 1.0 kcal mol^{-1} for 2-methoxyfuran and 1.4 kcal mol^{-1} for 3-methoxyfuran.

Radical analysis from this method by incorporation of a carbon atom radical correction[200,201] is also presented in Tables 8.3 and 8.4. The eight methoxyfuran radicals show acceptable results similar to the parent compounds. There is a 0.2 kcal mol^{-1} average difference for the work reactions to the Osmont method and only a 0.9 kcal mol^{-1} difference to the recommended values. This consistency validates the use and choices of our work reactions employed overall in this analysis for the B3LYP/6-31G(d,p) level of theory.

8.4.4 Carbon-Hydrogen Bond Dissociation Energies (C–H BDEs)

Differences in bond dissociation energies for a compound are important to determine the reaction pathways and kinetics for abstraction and dissociation reactions. The bond dissociation energies from the radicals are listed in Tables 8.3 and 8.4 along with a summary of the averages in Table 8.5.

The methoxyfurans have four different C–H bond types. Bond energies are determined by using the reaction Parent → Radical + H, where the calculated $\Delta H^{\circ}_{f\ 298}$ values for both the parent and radicals are combined with the established $\Delta H^{\circ}_{f\ 298}$ literature value[83] of 52.1 kcal mol^{-1} for the hydrogen atom.

For the radicals formed from hydrogen loss on the furan ring, Y(OC[OCH_3]CCC$^{\bullet}$), Y(OC[OCH_3]CC$^{\bullet}$C), Y(OC[OCH_3]C$^{\bullet}$CC), Y(OCC[OCH_3]CC$^{\bullet}$), Y(OCC[OCH_3]C$^{\bullet}$C), and Y(OC$^{\bullet}$C[OCH_3]CC), the bond energy averages from the CBS-QB3 and G3MP2B3 calculations of 120.8, 119.2, 120.5, 119.1, 121.0, and 120.5 kcal mol^{-1} are recommended. These energies create a 1.9 kcal mol^{-1} range for the

different ring positions on these methoxy-substituted furans and are among the highest currently known for hydrocarbon aromatics. These furan ring bond energies are consistent with other multiposition heterocyclic compounds. For example, furan[45,270] has bond energies of 118-121 kcal mol^{-1} depending on the C–H bond position, pyrrole[270-272] with 118-120 kcal mol^{-1}, and thiophene[270] with 114-117 kcal mol^{-1}. Unsaturated cyclic hydrocarbons such as benzene[45,126,270,273] have lower bond energies of 110-113 kcal mol^{-1}. Saturated cyclic hydrocarbons have even lower bond dissociation energies of approximately 95 kcal mol^{-1} for cyclopentane[126,193,204-206] and 100 kcal mol^{-1} for cyclohexane.[126,204-206]

The radicals on the methyl group for 2- and 3-methoxyfuran have recommended bond energies of 98.8 and 97.7 kcal mol^{-1}. This is 20 kcal mol^{-1} lower in energy than the furan ring C–H bonds; but is 10 kcal mol^{-1} higher than the benzylic C–H bond on the methyl groups of toluene, xylenes, and other multi-methyl-substituted benzenes. These lower bond energies are due to the increase in stability from the resonance of the electron with the adjacent oxygen atom and somewhat through to the furan ring. Benzyl radical formation in toluene[121,126] and the methyl radical formation in 2-methylfuran[45,126] also have similarly low C–H bond energies, from resonance stabilized radicals, of 86-90 kcal mol^{-1}. Primary C–H bond energies in dimethyl ether[126,274] and secondary bond energies in ethyl methyl ether[126] also have similar bond energies of 96 and 93 kcal mol^{-1}, which are low compared to the equivalent bond energies, 98.5-101 kcal mol^{-1}, of the primary and secondary bonds in the hydrocarbons ethane, *n*-propane, and *n*-butane.[121,126,127,206]

8.4.5 Internal Rotors

Potential energy curves for the internal rotation barriers across the methoxy and the methyl rotors in 2- and 3-methoxyfuran are calculated using B3LYP/6-31G(d,p). The lowest energy conformation is first determined, and potential energy profiles are then created using a relaxed scan at 10° intervals. Graphs of the potential energies of the two hindered rotors versus the dihedral angle for the compounds are available in Appendix G.

The methyl rotors, Y([O–CH_3]), in the 2- and 3-methoxyfuran parent molecules and on the radicals of the furan ring all have three-fold symmetric barriers near 3 kcal mol^{-1} with two exceptions, Y(OC[OCH_3]CCC$^{\bullet}$) and Y(OC$^{\bullet}$C[OCH_3]CC), which have barriers of only 1.5 and 2 kcal mol^{-1}. Overall, the methyl rotor potentials are similar to the 3 kcal mol^{-1} typically found for methyl groups in hydrocarbons.[181-184]

The methoxy rotors, Y([–OCH_3]), in the 2- and 3-methoxyfuran parent molecules and on the radicals of the furan ring all have a single minimum point with a broad potential (~300^{o}) of 1.5-2.8 kcal mol^{-1}. This barrier has a central minimum that decreases from several tenths to 1.5 kcal mol^{-1} from the maximum with one exception. The Y(OC[OCH_3]CCC$^{\bullet}$) barrier is three-fold and is non-symmetrical. Methyl vinyl ether was calculated to have a similar, between 2-4 kcal mol^{-1}, rotation barrier by da Silva, Kim, and Bozzelli.[275]

Methylene and methoxy rotors in Y(OC[OC$^{\bullet}H_2$]CCC) and Y(OCC[OC$^{\bullet}H_2$]CC) have similar two-fold symmetric barriers of 2.3 kcal mol^{-1} at approximately equivalent dihedral angles. The Y([O–C$^{\bullet}H_2$]) rotors both show an expected decrease from three-fold to two-fold symmetry with higher barriers of near 6.0 kcal mol^{-1} resulting from partial

π-bonding between the methyl radical and the oxygen of the ether. These energies are similar to the 5 kcal mol^{-1} barriers found for methyl vinyl ether radicals.[275]

8.4.6 Entropies (*S(T)*) and Heat Capacities ($C_p(T)$)

Contributions to entropy, S°_{298}, and heat capacities, $C_p(T)$, for 300-1500 K from translations, vibration frequencies, and external rotations, represented as TVR in Table 8.6, are calculated using the rigid-rotor harmonic-oscillator approximation implemented in the SMCPS[98] code. Here the two torsion frequencies have been omitted and contributions from the Y([–OCH_3]) and Y([O–CH_3]) internal bond rotations, represented as IR, using the barrier energies from the potential energy graphs are calculated. Summing the TVR and IR contributions give the total entropy and heat capacities at the temperatures. Data similar to JANNAF format tables over the larger temperature range of 100-5000 K for both the entropies and heat capacities are listed in Appendix G.

Table 8.6 Calculated Entropy (S°_{298}) and Heat Capacities ($C_p(T)$) for 2-Methoxyfuran, 3-Methoxyfuran, and Radicals

Species		S°_{298}[a]	$C_p(T)$[a]								
			300 K	400 K	500 K	600 K	700 K	800 K	900 K	1000 K	1500 K
Y(OC[OCH_3]CCC)	TVR	70.72	20.85	27.78	33.83	38.81	42.88	46.23	49.04	51.42	59.11
σ (symmetry) = 3	IR 1 (–OCH_3)	6.58	2.11	1.99	1.77	1.60	1.47	1.38	1.32	1.26	1.12
	IR 2 (O–CH_3)	4.47	2.13	2.10	1.94	1.78	1.65	1.54	1.46	1.38	1.18
	Total	81.76	25.08	31.87	37.54	42.19	46.00	49.15	51.82	54.05	61.41
Y(OC[OCH_3]CCC$^{\bullet}$)	TVR	74.75	20.70	26.96	32.40	36.85	40.47	43.44	45.91	47.99	54.67
σ (symmetry) = 1	IR 1 (–OCH_3)	6.96	1.79	1.65	1.46	1.35	1.26	1.20	1.17	1.13	1.06
	IR 2 (O–CH_3)	5.26	1.57	1.46	1.33	1.24	1.18	1.14	1.11	1.09	1.04
	Total	86.97	24.06	30.07	35.19	39.44	42.91	45.78	48.19	50.21	56.76
Y(OC[OCH_3]CC$^{\bullet}$C)	TVR	74.25	20.48	26.70	32.14	36.61	40.25	43.24	45.74	47.84	54.59
σ (symmetry) = 1	IR 1 (–OCH_3)	6.62	2.09	1.96	1.74	1.57	1.45	1.36	1.30	1.24	1.11
	IR 2 (O–CH_3)	4.51	2.12	2.08	1.92	1.75	1.62	1.51	1.44	1.36	1.17
	Total	85.37	24.68	30.74	35.79	39.93	43.32	46.12	48.48	50.45	56.87
Y(OC[OCH_3]C$^{\bullet}$CC)	TVR	74.67	20.48	26.65	32.08	36.55	40.20	43.21	45.72	47.83	54.59
σ (symmetry) = 1	IR 1 (–OCH_3)	6.62	2.09	1.96	1.74	1.57	1.45	1.36	1.30	1.24	1.11
	IR 2 (O–CH_3)	4.84	1.95	1.85	1.66	1.51	1.40	1.33	1.27	1.22	1.10
	Total	86.12	24.52	30.46	35.47	39.63	43.05	45.90	48.29	50.28	56.80
Y(OC[OC$^{\bullet}H_2$]CCC)[b]	TVR	74.46	21.58	28.13	33.56	37.87	41.31	44.11	46.44	48.40	54.77
σ (symmetry) = 1	IR 1 (–OC$^{\bullet}H_2$)	6.47	2.16	2.05	1.83	1.66	1.52	1.42	1.36	1.29	1.13
	IR 2 (O–C$^{\bullet}H_2$)	3.13	1.99	2.09	2.21	2.27	2.27	2.23	2.16	2.09	1.70
	Total	84.05	25.73	32.27	37.60	41.80	45.10	47.76	49.95	51.77	57.61

[a] Units of cal mol^{-1} K^{-1}.
[b] 152.3° H–C_7–O_6–H dihedral angle from B3LYP/6-31G(d,p) level of theory.
[c] 148.2° H–C_7–O_6–H dihedral angle from B3LYP/6-31G(d,p) level of theory.

Table 8.6 Calculated Entropy (S°_{298}) and Heat Capacities ($C_p(T)$) for 2-Methoxyfuran, 3-Methoxyfuran, and Radicals (Continued)

Species		S°_{298}[a]	$C_p(T)$[a]								
			300 K	400 K	500 K	600 K	700 K	800 K	900 K	1000 K	1500 K
Y(OCC[OCH_3]CC)	TVR	70.78	20.91	27.82	33.85	38.82	42.89	46.24	49.05	51.42	59.11
σ (symmetry) = 3	IR 1 (–OCH_3)	6.09	2.32	2.32	2.28	2.13	1.96	1.81	1.68	1.49	1.24
	IR 2 (O–CH_3)	4.29	2.12	2.18	2.18	2.07	1.93	1.79	1.67	1.48	1.25
	Total	81.16	25.35	32.32	38.31	43.02	46.77	49.83	52.39	54.39	61.60
Y(OCC[OCH_3]CC$^{\bullet}$)	TVR	74.48	20.67	26.88	32.28	36.73	40.36	43.34	45.83	47.92	54.63
σ (symmetry) = 1	IR 1 (–OCH_3)	6.24	2.32	2.29	2.21	2.02	1.84	1.69	1.57	1.40	1.19
	IR 2 (O–CH_3)	4.32	2.14	2.18	2.16	2.05	1.90	1.76	1.64	1.46	1.23
	Total	85.04	25.13	31.34	36.66	40.80	44.10	46.79	49.04	50.78	57.06
Y(OCC[OCH_3]C$^{\bullet}$C)	TVR	74.22	20.38	26.58	32.02	36.50	40.16	43.18	45.69	47.81	54.58
σ (symmetry) = 1	IR 1 (–OCH_3)	6.20	2.33	2.30	2.23	2.05	1.87	1.72	1.60	1.42	1.20
	IR 2 (O–CH_3)	4.31	2.13	2.18	2.17	2.05	1.91	1.76	1.65	1.47	1.24
	Total	84.73	24.84	31.06	36.41	40.61	43.94	46.66	48.93	50.69	57.02
Y(OC$^{\bullet}$C[OCH_3]CC)	TVR	74.80	20.94	27.23	32.67	37.10	40.69	43.64	46.09	48.15	54.76
σ (symmetry) = 1	IR 1 (–OCH_3)	6.09	2.32	2.32	2.28	2.13	1.96	1.80	1.68	1.48	1.24
	IR 2 (O–CH_3)	4.90	2.02	1.91	1.80	1.61	1.47	1.37	1.30	1.20	1.09
	Total	85.79	25.28	31.47	36.75	40.84	44.12	46.81	49.07	50.83	57.09
Y(OCC[OC$^{\bullet}H_2$]CC)[c]	TVR	74.03	21.17	27.78	33.27	37.64	41.13	43.97	46.33	48.32	54.75
σ (symmetry) = 1	IR 1 (–OC$^{\bullet}H_2$)	6.39	2.29	2.21	2.10	1.89	1.71	1.57	1.46	1.32	1.15
	IR 2 (O–C$^{\bullet}H_2$)	3.22	1.94	2.05	2.14	2.24	2.27	2.25	2.18	2.00	1.62
	Total	83.65	25.40	32.04	37.51	41.77	45.12	47.79	49.97	51.64	57.51

[a] Units of cal mol^{-1} K^{-1}.
[b] 152.3° H–C_7–O_6–H dihedral angle from B3LYP/6-31G(d,p) level of theory.
[c] 148.2° H–C_7–O_6–H dihedral angle from B3LYP/6-31G(d,p) level of theory.

8.4.7 Group Additivity Method

The group additivity method, as developed by Benson,[102] is a practical method for rapid estimation of thermochemical properties, particularly for larger compounds. The method relies on the knowledge of the contributions of representative groups in the molecule(s), usually obtained from smaller molecules, and their established linear consistency in thermochemical property contribution. A significant number of molecular properties such as molar volume, molar refraction, refractive index, and magnetic susceptibility along with thermodynamic properties such as entropy, molar heat capacity, and heat of formation can be accurately approximated as the sum of the individual groups.[102-104] Group additivity for the thermochemical properties of biofuel molecules and intermediates will be needed for use in engineering models, with the increasing importance of biofuels in our energy supply.

The 120 kcal mol^{-1} C–H bond energies determined in this study, and in previous studies on furan ring carbons, are approximately 7 to 9 kcal mol^{-1} stronger than those on benzenes[45,126,270,273] and 9 to 13 kcal mol^{-1} stronger than those on primary and secondary vinyl groups.[275,276] The furan-based molecules are unique and should have special groups for the ring oxygen and carbons similar to group names for benzene. Currently, the method of group additivity for furans involves using carbon double bond groups; one O/Cd2, two Cd/H/O, two Cd/Cd/H, and one furan ring group to correct for the inadequate components of the carbon double bond groups. Carbon double bond notation becomes untenable when there is a group on a furan ring carbon that can interact uniquely with the furan ring. The methoxy or ether group on the furan ring carbon is one example of this with clear resonance into the ring. Here one would implement a Cd/O_2 group for

2-methoxyfuran, but this group in furan is very different from a Cd/O_2 group in a dialcohol, diether, or alcohol plus an ether, that would be bonded to a carbon double bond. One Cd/O_2 group cannot represent these very different systems.

Due to growing importance in furan research, specific groups should be calculated to aid in thermochemical properties. For example, OF/CF2, CF/OF/H, and CF/H groups could be developed where a separate ring correction group would not be needed. This will be a focus of future work. In this study, two groups for the bonding of the methoxy group to a furan carbon; CF/OF/O (replaces Cd/O_2) for 2-methoxyfuran and CF/O for 3-methoxyfuran are calculated. The previously known[102,277] and the developed groups from this study are summarized in Table 8.7; future studies will likely supplement these.

Separate bond dissociation groups are listed in Table 8.7, which result in thermochemical properties of the radicals when the entropy and heat capacity properties are added to the corresponding methoxyfuran parent molecules. The bond group enthalpy value is different however; it corresponds to the C–H bond energy at the indicated site.[100] The enthalpy of the radical is determined by a C–H bond dissociation reaction, knowing the enthalpy of the parent, the H atom, and the bond energy. Upon inspection of these bond groups, there is only a 2 kcal mol^{-1} range in the bond energies from this study as well as in the study of Simmie and Curran.[45] The average bond energy over the species in both studies is 120.2 kcal mol^{-1}. Separately, entropy and heat capacity data for the parent furan and its two radical sites are determined and it is observed that the values in these bond groups from the two methoxyfurans and in the two sites of furan are also similar. The average bond energy for CFJ from this study and that of Simmie, 120.2 kcal mol^{-1}, is used.

Table 8.7 Calculated and Literature Group Additivity and Bond Dissociation Energies for Methoxyfurans

Group	$\Delta H^{\circ}_{f\,298}$ (kcal mol^{-1})	S°_{298} (cal mol^{-1} K^{-1})	$C_p(T)$ (cal mol^{-1} K^{-1})						
			300 K	400 K	500 K	600 K	800 K	1000 K	1500 K
Known Groups									
O/CD2	-32.80	10.00	3.40	3.70	3.70	3.80	4.40	4.60	4.80
CD/H/O[a]	8.60	6.20	4.75	6.46	7.64	8.35	9.10	9.56	10.46
CD/CD/H[a]	6.74	6.38	4.46	5.79	6.75	7.42	8.35	9.11	10.09
O/C/CD	-29.70	5.44	4.04	4.73	4.99	5.04	4.97	4.81	4.49
C/H3/O[b]	-10.00	30.41	6.19	7.84	9.40	10.79	13.03	14.77	17.58
CY/FURAN	-6.84	30.09	-6.08	-6.98	-6.71	-6.00	-4.85	-4.03	-2.95
Groups Developed in this Study									
CF/O	14.34	-11.38	3.84	4.32	4.90	5.27	5.73	6.01	6.67
CF/OF/O[c]	12.26	-10.96	3.86	4.54	5.02	5.37	5.80	6.12	6.85
2CF5JOC	120.80	5.207	-1.019	-1.802	-2.350	-2.752	-3.370	-3.835	-4.647
2CF4JOC	119.22	3.611	-0.401	-1.132	-1.754	-2.262	-3.033	-3.602	-4.540
2CF3JOC	120.45	4.365	-0.558	-1.406	-2.071	-2.559	-3.253	-3.766	-4.613
2CFOCJ	98.77	2.295	0.651	0.402	0.057	-0.394	-1.389	-2.275	-3.804
3CF5JOC	119.05	3.883	-0.220	-0.980	-1.652	-2.220	-3.039	-3.605	-4.543
3CF4JOC	120.97	3.570	-0.515	-1.263	-1.896	-2.414	-3.167	-3.696	-4.583
3CF2JOC	120.51	4.627	-0.071	-0.854	-1.560	-2.180	-3.016	-3.555	-4.506
3CFOCJ	97.73	2.487	0.046	-0.282	-0.800	-1.250	-2.041	-2.755	-4.090
Recommended Bond Dissociation Groups									
CFJ	120.2[d]	2.46	-0.72	-1.51	-2.15	-2.65	-3.42	-3.99	-4.85
CFJ/O/C	120.2[d]	4.21	-0.46	-1.24	-1.88	-2.40	-3.15	-3.68	-4.57
CF/O/CJ	98.3	2.39	0.35	0.06	-0.37	-0.82	-1.72	-2.51	-3.95

[a] Ref. 277.
[b] Ref. 102.
[c] CF and OF represent carbon furan and oxygen furan.
[d] Average from Ref. 45 and this study.

Use of the CFJ, CFJ/O/C, and CF/O/CJ bond groups, where J represents radical site, are recommended where the values are average values of the sites in the lower section of Table 8.7. These groups are intrinsic and contributions from symmetry, electron degeneracy, optical isomers, gauche, and other interactions, as clearly illustrated by Benson,[102] must also be considered.

8.5 Conclusions

Density functional theory and higher level composite calculation methods are used to determine thermochemical properties for 2-methoxyfuran, 3-methoxyfuran, and radicals corresponding to loss of hydrogen atoms. There is a close agreement between the density functional theory B3LYP and the composite CBS-QB3 and G3MP2B3 calculations for both the parent and the radical compounds when work reactions are used. The recommended $\Delta H^{\circ}_{f\ 298}$ for Y(OC[OCH_3]CCC) and Y(OCC[OCH_3]CC) are -45.0 and -41.1 kcal mol^{-1}. Bond energies for the C–H bonds on the furan ring are approximately 120 kcal mol^{-1} and decrease to 98 kcal mol^{-1} for the methoxy-methyl C–H bonds. The furan ring bond energies are similar to those reported for furan and hydrocarbon-substituted furans. The lower energy methyl C–H bonds are a more favored abstraction site. Thermodynamic properties for group additivity are determined for CF/O, CF/OF/O, furan ring carbon-hydrogen bonds, and methyl radicals of the methoxy groups.

CHAPTER 9

THERMOCHEMISTRY OF 2-METHYLFURAN HYDROPEROXIDE AND ALCOHOL SPECIES

9.1 Overview

The strong incentive to develop biofuels as renewable fuels in order to limit carbon dioxides emissions and help control global warming, certain groups of compounds are emerging as potential next generation fuels. The versatile intermediate compounds, such as high-energy substituted furans, created in the production processes of these fuels are sometimes just as important. The review by Lewkowski[39] summarizes the importance of one such compound, 5-hydroxymethylfurfural (HMF), and its use in deriving a vast array of compounds including organic acids, aldehydes, amines, and ethers. Other substituted furans, such as 2,5-dimethylfuran (25DMF), can also be produced from HMF and are shown to have possible biofuel applications.[1,42]

2-Methylfuran (2MF) has been the basis for a lot work with involvement in several chemical systems. It has been used in testing cycloaurated gold (III) complex catalytic activities[278] and in producing second-generation biofuels suitable for high-quality diesel fuels.[279] 2MF synthesis has been explored through a coupling process involving the simultaneous furfural hydrogenation and cyclohexanol dehydrogenation[280] and through conversion of pentoses.[281] The products formed from 2MF hydrogenation,[282,283] and hydrogen-abstraction and pyrolysis[284] along with reactions with hydroxyl radicals[285-288] and chlorine atoms[289,290] have also been studied. Substituted furan-based compounds are being developed where the thermochemistry and decomposition kinetics of 25DMF[291] has been analyzed by Simmie and Metcalfe.

Furan-based species have been shown to have unique thermochemical properties. In initial work on 2- and 3-methoxyfuran,[292] reported carbon-hydrogen bond dissociation energies (C–H BDE) on the furan ring are very high, some 7 kcal mol^{-1} stronger than even those on benzene. Similar findings are observed for the methoxy-methyl bonds, approximately 7.5 kcal mol^{-1} stronger than the benzylic C–H bonds of toluene and xylenes. Thermochemical properties for the hydroperoxide and alcohol species are necessary for the development of oxidation reactions for 2MF radicals. Since literature values are not available, high level calculations are utilized to provide accurate and reliable values.

In this chapter, enthalpies ($\Delta H^{\circ}_{f\,298}$), entropies ($S^{\circ}_{298}$), and heat capacities ($C_p(T)$) including radicals corresponding to the loss of hydrogen atom are calculated. Oxygen-hydrogen and oxygen-oxygen bond dissociation energies (O–H and O–O BDE) are determined from the parent and radical species and allow for the prediction of initial reaction pathways for these compounds. Bond energies for these substituted 2MF species are determined to be very low, specifically for the O–O bonds in the hydroperoxides.

9.2 Nomenclature

Abbreviations are utilized as illustrated below:

- – represents a bond between two atoms,
- Y represents a cyclic ring structure,
- [CH_3] represents a methyl substituent on the preceding carbon atom,
- J represents a radical site on the preceding carbon atom.

9.3 Computational Methods

Optimized geometries for the parent and radicals are initially determined using the density functional theory (DFT) B3LYP[46,47] method. Potential energy curves for internal rotation verified that the structure is the lowest energy conformation. Enthalpies of formation are calculated using isodesmic work reactions to achieve greater accuracy using the B3LYP with both the 6-31G(d,p) and 6-311G(2d,2p) basis sets. Higher level composite methods G3MP2B3[57,58] and CBS-QB3[60,61] are also utilized to validate the use of the lower level DFT methods. All calculations are performed using the Gaussian 03 program suite.[62] O–H and O–O BDE are derived using a bond cleavage reaction with the calculated $\Delta H^{\circ}_{f\ 298}$ energies. Established literature values of 52.10 kcal mol^{-1} for a hydrogen atom[83] and 8.89 kcal mol^{-1} for a hydroxyl radical[84] are used.

Contributions to entropy and heat capacities from translations, vibrations, and external rotations are calculated using the rigid-rotor harmonic-oscillator approximation with the Statistical Mechanics for Heat Capacity and Entropy (SMCPS) program.[98] The ROTATOR program is used to determine contributions from internal rotational potential energy curves from the B3LYP/6-31G(d,p) level to entropy and heat capacities.[101] Summing the SMCPS and ROTATOR contributions gives the total entropy and heat capacity values for these species.

9.4 Results and Discussion

9.4.1 Heat of Formation $\Delta H^{\circ}_{f\ 298}$

Isodesmic work reactions are used to calculate the $\Delta H^{\circ}_{f\ 298}$ for each target species. The species in the work reactions, except for the target compounds and $CH_3CH_2CH_2OJ$, have standard well-established $\Delta H^{\circ}_{f\ 298}$ values that are listed in Table 9.1. Calculation of the

$\Delta H^{\circ}_{f\,298}$ for $CH_3CH_2CH_2OJ$ comes from a series of five isodesmic work reactions and is presented in Appendix F. The work reactions for the substituted methylfurans are presented in Table 9.2.

Table 9.1 Standard Enthalpies of Formation for Reference Species

Species	$\Delta H^{\circ}_{f\,298}$ (kcal mol^{-1})	Reference
H	52.10	83
OH	8.89 ± 0.09	84
CH_4	-17.8 ± 0.1	120
CH_3CH_3	-20.0 ± 0.1	120
$CH_3CH_2CH_3$	-25.0 ± 0.1	120
CH_3OH	-48.2 ± 0.1	120
CH_3CH_2OH	-56.2 ± 0.1	120
$CH_3CH_2CH_2OH$	-61.0 ± 0.1	120
CH_3OOH	-31.0 ± 0.2	241
CH_3CH_2OOH	-39.1 ± 0.2	241
$CH_3CH_2CH_2OOH$	-43.8 ± 0.3	241
Y(OC[CH_3]CCC)	-19.3 ± 0.1	45
CH_3OJ	4.1 ± 1	173
CH_3CH_2OJ	-3.6 ± 0.8	240
$CH_3CH_2CH_2OJ$	-8.6 ± 0.3	*a*
CH_3OOJ	2.9 ± 0.2	241
CH_3CH_2OOJ	-5.6 ± 0.2	241
$CH_3CH_2CH_2OOJ$	-10.5 ± 0.3	241

[a] See Appendix F for enthalpy calculation.

Table 9.2 Isodesmic Work Reactions, Calculated $\Delta H^{\circ}_{f\,298}$, and Bond Dissociation Energies for 2-Methylfuran Hydroperoxide and Alcohol Species

Isodesmic Reactions							$\Delta H^{\circ}_{f\,298}$ (kcal mol^{-1})			
							B3LYP		CBS-QB3	G3MP2B3
							6-31G(d,p)	6-311G(2d,2p)		
Y(OC[CH_3]CCC[OOH]) System										
Y(OC[CH_3]CCC[OOH])	+	CH_4	→	Y(OC[CH_3]CCC)	+	CH_3OOH	-42.82	-42.14	-40.83	-40.45
Y(OC[CH_3]CCC[OOH])	+	CH_3CH_3	→	Y(OC[CH_3]CCC)	+	CH_3CH_2OOH	-43.52	-42.74	-41.06	-40.73
Y(OC[CH_3]CCC[OOH])	+	$CH_3CH_2CH_3$	→	Y(OC[CH_3]CCC)	+	$CH_3CH_2CH_2OOH$	-43.24	-42.49	-40.66	-40.37
						Average	**-43.2**	**-42.5**	**-40.9**	**-40.5**
						Method Average	**-42.8 ± 0.5**		**-40.7 ± 0.3**	
Y(OC[CH_3]CCC[OOJ]) System										
Y(OC[CH_3]CCC[OOJ])	+	CH_3OOH	→	Y(OC[CH_3]CCC[OOH])	+	CH_3OOJ	-2.72	-2.72	-1.91	-1.44
Y(OC[CH_3]CCC[OOJ])	+	CH_3CH_2OOH	→	Y(OC[CH_3]CCC[OOH])	+	CH_3CH_2OOJ	-2.57	-2.66	-1.67	-1.29
Y(OC[CH_3]CCC[OOJ])	+	$CH_3CH_2CH_2OOH$	→	Y(OC[CH_3]CCC[OOH])	+	$CH_3CH_2CH_2OOJ$	-2.75	-2.79	-1.80	-1.42
						Average	**-2.7**	**-2.7**	**-1.8**	**-1.4**
						Method Average	**-2.7 ± 0.1**		**-1.6 ± 0.2**	
						O–H Bond Dissociation Energy	**90.1**		**91.2**	
Y(OC[CH_3]CCC[OH]) System										
Y(OC[CH_3]CCC[OH])	+	CH_4	→	Y(OC[CH_3]CCC)	+	CH_3OH	-62.58	-62.07	-60.72	-60.32
Y(OC[CH_3]CCC[OH])	+	CH_3CH_3	→	Y(OC[CH_3]CCC)	+	CH_3CH_2OH	-62.89	-62.27	-60.86	-60.45
Y(OC[CH_3]CCC[OH])	+	$CH_3CH_2CH_3$	→	Y(OC[CH_3]CCC)	+	$CH_3CH_2CH_2OH$	-62.54	-61.84	-60.68	-60.31
						Average	**-62.7**	**-62.1**	**-60.8**	**-60.4**
						Method Average	**-62.4 ± 0.4**		**-60.6 ± 0.2**	

Table 9.2 Isodesmic Work Reactions, Calculated $\Delta H^{\circ}_{f\,298}$, and Bond Dissociation Energies for 2-Methylfuran Hydroperoxide and Alcohol Species (Continued A)

Isodesmic Reactions							$\Delta H^{\circ}_{f\,298}$ (kcal mol^{-1})			
							B3LYP		CBS-QB3	G3MP2B3
							6-31G(d,p)	6-311G(2d,2p)		
Y(OC[CH_3]CCC[OJ]) System										
Y(OC[CH_3]CCC[OJ])	+	CH_3OH	→	Y(OC[CH_3]CCC[OH])	+	CH_3OJ	-46.95	-47.48	-49.12	-47.75
Y(OC[CH_3]CCC[OJ])	+	CH_3CH_2OH	→	Y(OC[CH_3]CCC[OH])	+	CH_3CH_2OJ	-46.44	-46.36	-48.13	-47.54
Y(OC[CH_3]CCC[OJ])	+	$CH_3CH_2CH_2OH$	→	Y(OC[CH_3]CCC[OH])	+	$CH_3CH_2CH_2OJ$	-46.58	-47.15	-48.86	-47.58
						Average	**-46.7**	**-47.0**	**-48.7**	**-47.6**
						Method Average	**-46.8 ± 0.4**		**-48.2 ± 0.7**	
						O–H Bond Dissociation Energy	**65.8**		**64.5**	
						O–O Bond Dissociation Energy	**2.7**		**1.4**	
Y(OC[CH_3]CC[OOH]C) System										
Y(OC[CH_3]CC[OOH]C)	+	CH_4	→	Y(OC[CH_3]CCC)	+	CH_3OOH	-37.09	-36.56	-35.95	-35.65
Y(OC[CH_3]CC[OOH]C)	+	CH_3CH_3	→	Y(OC[CH_3]CCC)	+	CH_3CH_2OOH	-37.80	-37.15	-36.18	-35.92
Y(OC[CH_3]CC[OOH]C)	+	$CH_3CH_2CH_3$	→	Y(OC[CH_3]CCC)	+	$CH_3CH_2CH_2OOH$	-37.51	-36.90	-35.78	-35.56
						Average	**-37.5**	**-36.9**	**-36.0**	**-35.7**
						Method Average	**-37.2 ± 0.4**		**-35.8 ± 0.2**	
Y(OC[CH_3]CC[OOJ]C) System										
Y(OC[CH_3]CC[OOJ]C)	+	CH_3OOH	→	Y(OC[CH_3]CC[OOH]C)	+	CH_3OOJ	-2.19	-2.12	-1.25	-0.73
Y(OC[CH_3]CC[OOJ]C)	+	CH_3CH_2OOH	→	Y(OC[CH_3]CC[OOH]C)	+	CH_3CH_2OOJ	-2.05	-2.06	-1.01	-0.58
Y(OC[CH_3]CC[OOJ]C)	+	$CH_3CH_2CH_2OOH$	→	Y(OC[CH_3]CC[OOH]C)	+	$CH_3CH_2CH_2OOJ$	-2.22	-2.19	-1.14	-0.71
						Average	**-2.2**	**-2.1**	**-1.1**	**-0.7**
						Method Average	**-2.1 ± 0.1**		**-0.9 ± 0.3**	
						O–H Bond Dissociation Energy	**85.8**		**87.0**	

Table 9.2 Isodesmic Work Reactions, Calculated $\Delta H^{\circ}_{f\,298}$, and Bond Dissociation Energies for 2-Methylfuran Hydroperoxide and Alcohol Species (Continued B)

Isodesmic Reactions							$\Delta H^{\circ}_{f\,298}$ (kcal mol^{-1})			
							B3LYP		CBS-QB3	G3MP2B3
							6-31G(d,p)	6-311G(2d,2p)		
Y(OC[CH_3]CC[OH]C) System										
Y(OC[CH_3]CC[OH]C)	+	CH_4	→	Y(OC[CH_3]CCC)	+	CH_3OH	-58.22	-57.66	-56.14	-55.80
Y(OC[CH_3]CC[OH]C)	+	CH_3CH_3	→	Y(OC[CH_3]CCC)	+	CH_3CH_2OH	-58.53	-57.87	-56.28	-55.92
Y(OC[CH_3]CC[OH]C)	+	$CH_3CH_2CH_3$	→	Y(OC[CH_3]CCC)	+	$CH_3CH_2CH_2OH$	-58.18	-57.44	-56.10	-55.78
						Average	**-58.3**	**-57.7**	**-56.2**	**-55.8**
						Method Average	**-58.0 ± 0.4**		**-56.0 ± 0.2**	
Y(OC[CH_3]CC[OJ]C) System										
Y(OC[CH_3]CC[OJ]C)	+	CH_3OH	→	Y(OC[CH_3]CC[OH]C)	+	CH_3OJ	-27.89	-28.09	-30.15	-29.83
Y(OC[CH_3]CC[OJ]C)	+	CH_3CH_2OH	→	Y(OC[CH_3]CC[OH]C)	+	CH_3CH_2OJ	-27.37	-26.97	-29.15	-29.62
Y(OC[CH_3]CC[OJ]C)	+	$CH_3CH_2CH_2OH$	→	Y(OC[CH_3]CC[OH]C)	+	$CH_3CH_2CH_2OJ$	-27.52	-27.76	-29.89	-29.66
						Average	**-27.6**	**-27.6**	**-29.7**	**-29.7**
						Method Average	**-27.6 ± 0.4**		**-29.7 ± 0.3**	
						O–H Bond Dissociation Energy	**80.5**		**78.4**	
						O–O Bond Dissociation Energy	**17.1**		**15.0**	
Y(OC[CH_3]C[OOH]CC) System										
Y(OC[CH_3]C[OOH]CC)	+	CH_4	→	Y(OC[CH_3]CCC)	+	CH_3OOH	-37.92	-37.42	-36.81	-36.37
Y(OC[CH_3]C[OOH]CC)	+	CH_3CH_3	→	Y(OC[CH_3]CCC)	+	CH_3CH_2OOH	-38.62	-38.02	-37.04	-36.64
Y(OC[CH_3]C[OOH]CC)	+	$CH_3CH_2CH_3$	→	Y(OC[CH_3]CCC)	+	$CH_3CH_2CH_2OOH$	-38.34	-37.76	-36.64	-36.28
						Average	**-38.3**	**-37.7**	**-36.8**	**-36.4**
						Method Average	**-38.0 ± 0.4**		**-36.6 ± 0.3**	

Table 9.2 Isodesmic Work Reactions, Calculated $\Delta H^{\circ}_{f\,298}$, and Bond Dissociation Energies for 2-Methylfuran Hydroperoxide and Alcohol Species (Continued C)

Isodesmic Reactions							$\Delta H^{\circ}_{f\,298}$ (kcal mol^{-1})			
							B3LYP		CBS-QB3	G3MP2B3
							6-31G(d,p)	6-311G(2d,2p)		
Y(OC[CH$_3$]C[OOJ]CC) System										
Y(OC[CH$_3$]C[OOJ]CC)	+	CH$_3$OOH	→	Y(OC[CH$_3$]C[OOH]CC)	+	CH$_3$OOJ	-2.58	-2.48	-1.62	-1.20
Y(OC[CH$_3$]C[OOJ]CC)	+	CH$_3$CH$_2$OOH	→	Y(OC[CH$_3$]C[OOH]CC)	+	CH$_3$CH$_2$OOJ	-2.43	-2.41	-1.39	-1.05
Y(OC[CH$_3$]C[OOJ]CC)	+	CH$_3$CH$_2$CH$_2$OOH	→	Y(OC[CH$_3$]C[OOH]CC)	+	CH$_3$CH$_2$CH$_2$OOJ	-2.61	-2.54	-1.51	-1.18
						Average	**-2.5**	**-2.5**	**-1.5**	**-1.1**
						Method Average	**-2.5 ± 0.1**		**-1.3 ± 0.2**	
						O–H Bond Dissociation Energy	**86.2**		**87.4**	
Y(OC[CH$_3$]C[OH]CC) System										
Y(OC[CH$_3$]C[OH]CC)	+	CH$_4$	→	Y(OC[CH$_3$]CCC)	+	CH$_3$OH	-57.74	-57.82	-56.62	-55.65
Y(OC[CH$_3$]C[OH]CC)	+	CH$_3$CH$_3$	→	Y(OC[CH$_3$]CCC)	+	CH$_3$CH$_2$OH	-58.05	-58.03	-56.77	-55.78
Y(OC[CH$_3$]C[OH]CC)	+	CH$_3$CH$_2$CH$_3$	→	Y(OC[CH$_3$]CCC)	+	CH$_3$CH$_2$CH$_2$OH	-57.70	-57.60	-56.58	-55.63
						Average	**-57.8**	**-57.8**	**-56.7**	**-55.7**
						Method Average	**-57.8 ± 0.2**		**-56.2 ± 0.5**	
Y(OC[CH$_3$]C[OJ]CC) System										
Y(OC[CH$_3$]C[OJ]CC)	+	CH$_3$OH	→	Y(OC[CH$_3$]C[OH]CC)	+	CH$_3$OJ	-30.17	-29.89	-31.33	-31.47
Y(OC[CH$_3$]C[OJ]CC)	+	CH$_3$CH$_2$OH	→	Y(OC[CH$_3$]C[OH]CC)	+	CH$_3$CH$_2$OJ	-29.66	-28.76	-30.34	-31.26
Y(OC[CH$_3$]C[OJ]CC)	+	CH$_3$CH$_2$CH$_2$OH	→	Y(OC[CH$_3$]C[OH]CC)	+	CH$_3$CH$_2$CH$_2$OJ	-29.80	-29.55	-31.07	-31.30
						Average	**-29.9**	**-29.4**	**-30.9**	**-31.3**
						Method Average	**-29.6 ± 0.5**		**-31.1 ± 0.4**	
						O–H Bond Dissociation Energy	**78.6**		**77.1**	
						O–O Bond Dissociation Energy	**15.9**		**14.4**	

Table 9.2 Isodesmic Work Reactions, Calculated $\Delta H^{\circ}_{f\,298}$, and Bond Dissociation Energies for 2-Methylfuran Hydroperoxide and Alcohol Species (Continued D)

Isodesmic Reactions							$\Delta H^{\circ}_{f\,298}$ (kcal mol^{-1})			
							B3LYP		CBS-QB3	G3MP2B3
							6-31G(d,p)	6-311G(2d,2p)		
Y(OC[CH_2OOH]CCC) System										
Y(OC[CH_2OOH]CCC)	+	CH_4	→	Y(OC[CH_3]CCC)	+	CH_3OOH	-36.08	-36.11	-36.67	-36.51
Y(OC[CH_2OOH]CCC)	+	CH_3CH_3	→	Y(OC[CH_3]CCC)	+	CH_3CH_2OOH	-36.78	-36.70	-36.90	-36.79
Y(OC[CH_2OOH]CCC)	+	$CH_3CH_2CH_3$	→	Y(OC[CH_3]CCC)	+	$CH_3CH_2CH_2OOH$	-36.50	-36.45	-36.50	-36.43
						Average	**-36.5**	**-36.4**	**-36.7**	**-36.6**
						Method Average	**-36.4 ± 0.3**		**-36.6 ± 0.2**	
Y(OC[CH_2OOJ]CCC) System										
Y(OC[CH_2OOJ]CCC)	+	CH_3OOH	→	Y(OC[CH_2OOH]CCC)	+	CH_3OOJ	-1.94	-1.83	-1.60	-1.44
Y(OC[CH_2OOJ]CCC)	+	CH_3CH_2OOH	→	Y(OC[CH_2OOH]CCC)	+	CH_3CH_2OOJ	-1.79	-1.76	-1.37	-1.29
Y(OC[CH_2OOJ]CCC)	+	$CH_3CH_2CH_2OOH$	→	Y(OC[CH_2OOH]CCC)	+	$CH_3CH_2CH_2OOJ$	-1.97	-1.90	-1.49	-1.42
						Average	**-1.9**	**-1.8**	**-1.5**	**-1.4**
						Method Average	**-1.9 ± 0.1**		**-1.4 ± 0.1**	
						O–H Bond Dissociation Energy	**86.9**		**87.3**	
Y(OC[CH_2OH]CCC) System										
Y(OC[CH_2OH]CCC)	+	CH_4	→	Y(OC[CH_3]CCC)	+	CH_3OH	-53.65	-53.51	-53.72	-53.64
Y(OC[CH_2OH]CCC)	+	CH_3CH_3	→	Y(OC[CH_3]CCC)	+	CH_3CH_2OH	-53.97	-53.72	-53.87	-53.76
Y(OC[CH_2OH]CCC)	+	$CH_3CH_2CH_3$	→	Y(OC[CH_3]CCC)	+	$CH_3CH_2CH_2OH$	-53.61	-53.29	-53.68	-53.62
						Average	**-53.7**	**-53.5**	**-53.8**	**-53.7**
						Method Average	**-53.6 ± 0.2**		**-53.7 ± 0.1**	

Table 9.2 Isodesmic Work Reactions, Calculated $\Delta H^{\circ}_{f\,298}$, and Bond Dissociation Energies for 2-Methylfuran Hydroperoxide and Alcohol Species (Continued E)

Isodesmic Reactions							$\Delta H^{\circ}_{f\,298}$ (kcal mol^{-1})			
							B3LYP		CBS-QB3	G3MP2B3
							6-31G(d,p)	6-311G(2d,2p)		
Y(OC[CH_2OJ]CCC) System										
Y(OC[CH_2OJ]CCC)	+	CH_3OH	→	Y(OC[CH_2OH]CCC)	+	CH_3OJ	-0.73	-0.97	0.13	0.42
Y(OC[CH_2OJ]CCC)	+	CH_3CH_2OH	→	Y(OC[CH_2OH]CCC)	+	CH_3CH_2OJ	-0.21	0.15	1.13	0.63
Y(OC[CH_2OJ]CCC)	+	$CH_3CH_2CH_2OH$	→	Y(OC[CH_2OH]CCC)	+	$CH_3CH_2CH_2OJ$	-0.36	-0.64	0.39	0.59
						Average	**-0.4**	**-0.5**	**0.6**	**0.5**
						Method Average	**-0.5 ± 0.4**		**0.5 ± 0.3**	
						O–H Bond Dissociation Energy	**105.4**		**106.4**	
						O–O Bond Dissociation Energy	**45.1**		**46.1**	

There is a good correlation for the lower level DFT methods compared to the higher level composite method calculations. Uncertainty in the values is given as the standard deviation in the work reactions. $\Delta H^{\circ}_{f\ 298}$ values from the average of the CBS-QB3 and G3MP2B3 levels of theory for all of the parent and radical species are recommended and presented in Figure 9.1.

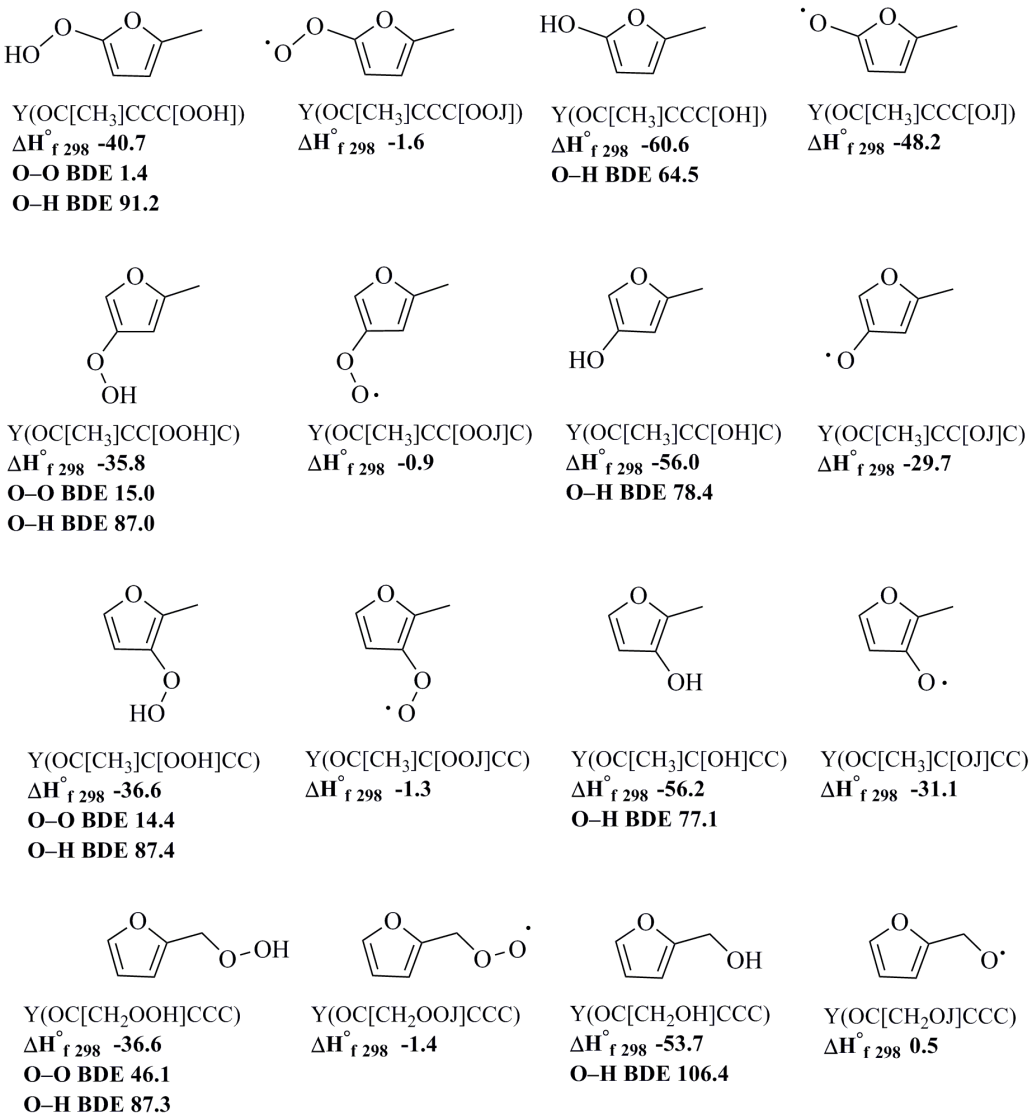

Figure 9.1 Nomenclature, recommended $\Delta H^{\circ}_{f\ 298}$, oxygen-hydrogen, and oxygen-oxygen bond dissociation energies (O–H and O–O BDEs) for 2-methylfuran hydroperoxide and alcohol species.

9.4.2 Oxygen-Hydrogen and Oxygen-Oxygen Bond Dissociation Energies (O–H and O–O BDEs)

O–H BDEs for the hydroperoxide species fall in a tight range of 87.0-87.4 kcal mol^{-1} when attached to the furan ring in the 3 and 4 positions and to the methyl substituent. These are similar to the energies of 84-88 kcal mol^{-1} seen in primary, secondary, and tertiary alkyls, and vinylic, allyl, and phenyl hydroperoxides.[121,126,241,267,293] A slightly higher energy, 91.2 kcal mol^{-1}, occurs when the hydroperoxide group is attached to the 5 position of the furan ring is similar to the 91-94 kcal mol^{-1} for ethynyl and substituted phenyl hydroperoxides.[126,267]

Common hydroperoxide O–O BDEs are very weak and have energies from 43-47 kcal mol^{-1} for primary, secondary, and tertiary alkyl hydroperoxides.[126,241,267,294] The calculated value of 46.1 kcal mol^{-1} for Y(OC[CH_2OJ]CCC) is right in line with this and is slightly higher than the 36-40 kcal mol^{-1} seen for the O–O BDEs in alkyl peroxides.[126,295] Much lower energies are calculated for the 3 and 4 positions substitutions, 14-15 kcal mol^{-1}, and for the 5 position, 1.4 kcal mol^{-1}. These low energies are due to both the weak O–O bonds and the formation of the strong resonance within the furan moiety creating an easily stabilized radical.

O–H BDEs for the 2-methylfuran alcohol species follow a similar trend to the O–O BDEs. The alcohol group on the methyl substituent has a bond energy of 106.4 kcal mol^{-1} which is similar to the 103-106 kcal mol^{-1} energies for primary, secondary, and tertiary alcohols and 105-106 kcal mol^{-1} for benzyl alcohol and cyclohexanol.[121,126,193,295] The energies for the 3 and 4 position are lower ranging between 77-78 kcal mol^{-1} with the 5 position almost 40 kcal mol^{-1} lower in energy at 64.5 kcal mol^{-1} than the alkyl alcohol

bond energies and the 89-90 kcal mol^{-1} for phenol.[121,296] Again, a much more favorable environment for the radical formation from the bond dissociation is created generating lower bond dissociation energies.

9.4.3 Bond Lengths

Figure 9.2 has the optimized 2-methylfuran hydroperoxide and alcohol species from the B3LYP/6-31G(d,p) level of theory with the carbon-carbon, carbon-oxygen, and oxygen-hydrogen bond lengths in Å.

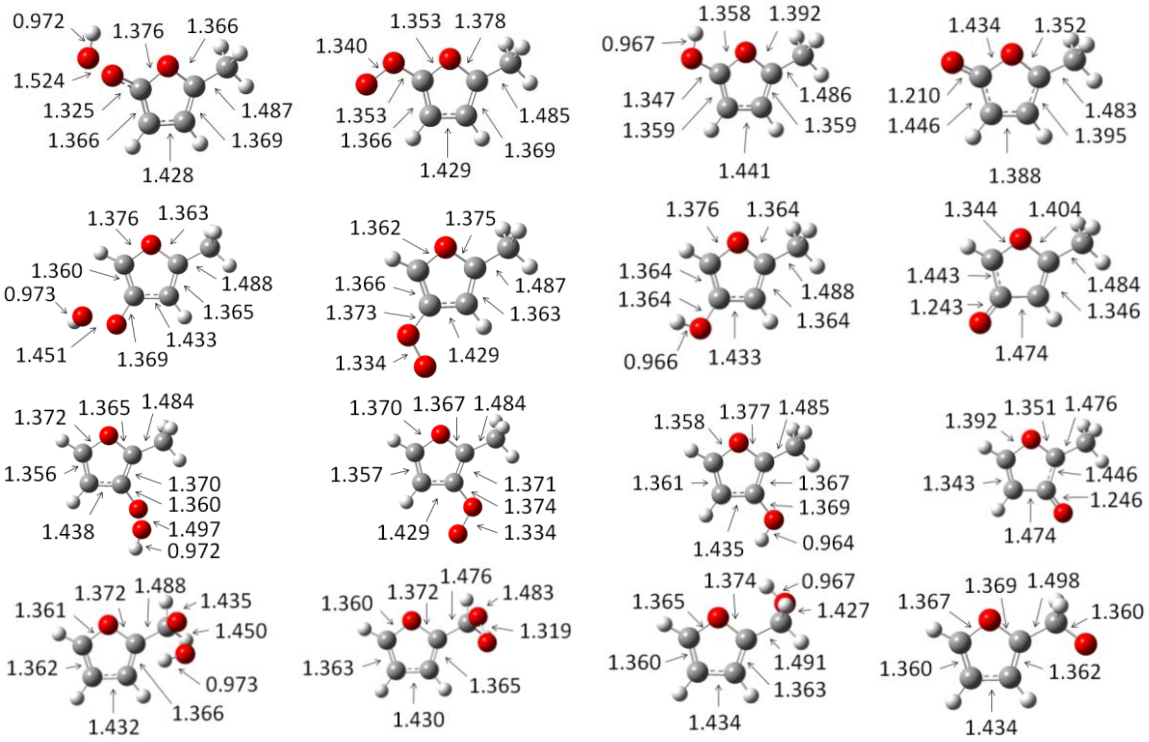

Figure 9.2 Bond lengths (Å) for 2-methylfuran hydroperoxide and alcohol species from B3LYP/6-31G(d,p) level of theory.

In general, the C_f –CH_3, where f denotes an atom within the furan ring, bond lengths are consistently between 1.48 and 1.50 Å. There is relatively no change for the furan moiety bond lengths for the methyl substituted position in going from the parent to the radical. This is not the case for the other three substitution locations where, upon radical formation for both the hydroperoxides and alcohols, one of the C_f–O_f–C_f bonds elongates while the other compresses. This change is more pronounced with the alcohols with one less oxygen atom by which the electron can be stabilized via full or partial double bond formation.

Upon radical formation, the O–O bonds in the peroxides and the C–O bonds in the alcohols shorten due to the resonance stabilization. Specifically for Y(OC[CH_3]CCC[OJ]), there is an elongation to 1.434 Å and a shortening to 1.352 Å for the C_f–O_f –C_f bond, respectively. This would be a target location for ring opening.

9.4.4 Entropy (S°_{298}) and Heat Capacities ($C_p(T)$)

S°_{298} and $C_p(T)$ for these species are determined by summing the contributions from the translations, vibrations, and external rotations to those from internal rotation. These total entropy and heat capacity values are presented in Table 9.3.

Table 9.3 Calculated Entropy (S°_{298}) and Heat Capacities ($C_p(T)$) for 2-Methylfuran Hydroperoxide and Alcohol Species

Species	S°_{298} [a]	$C_p(T)$ [a]						
		300 K	400 K	500 K	600 K	800 K	1000 K	1500 K
Y(OC[CH_3]CCC[OOH])	91.57	30.88	37.73	43.62	48.37	55.25	59.95	66.82
Y(OC[CH_3]CCC[OOJ])	86.36	28.50	35.17	40.84	45.39	51.96	56.42	62.89
Y(OC[CH_3]CCC[OH])	81.75	26.59	32.67	38.02	42.47	49.20	53.98	61.25
Y(OC[CH_3]CCC[OJ])	78.38	24.03	30.34	35.72	40.10	46.58	51.09	57.71
Y(OC[CH_3]CC[OOH]C)	93.85	29.22	35.97	41.84	46.66	53.79	58.76	66.16
Y(OC[CH_3]CC[OOJ]C)	86.81	28.07	34.84	40.59	45.20	51.85	56.35	62.86
Y(OC[CH_3]CC[OH]C)	81.38	25.81	32.21	37.73	42.28	49.10	53.92	61.21
Y(OC[CH_3]CC[OJ]C)	78.36	24.38	30.61	35.94	40.28	46.71	51.17	57.75
Y(OC[CH_3]C[OOH]CC)	93.64	30.11	36.86	42.63	47.32	54.25	59.08	66.28
Y(OC[CH_3]C[OOJ]CC)	86.79	28.67	35.18	40.73	45.21	51.75	56.24	62.77
Y(OC[CH_3]C[OH]CC)	82.59	25.56	31.89	37.44	42.04	48.93	53.81	61.16
Y(OC[CH_3]C[OJ]CC)	78.62	23.96	30.23	35.63	40.04	46.56	51.08	57.72
Y(OC[CH_2OOH]CCC)	92.19	31.84	38.62	44.21	48.68	55.26	59.82	66.53
Y(OC[CH_2OOJ]CCC)	90.42	27.05	34.05	39.95	44.66	51.42	55.98	62.48
Y(OC[CH_2OH]CCC)	82.96	25.03	31.87	37.69	42.38	49.27	54.07	61.29
Y(OC[CH_2OJ]CCC)	81.60	24.38	30.71	36.20	40.64	47.13	51.57	58.02

[a] Units cal mol^{-1} K^{-1}.

9.5 Conclusions

Enthalpies of formation for the four hydroperoxide and four alcohol species of 2-methyfuran and their radicals are determined using density functional theory and higher level composite computational methods. Isodesmic work reactions are employed to improve accuracy by cancelling error and show good consistency between the levels of theory. Corresponding oxygen-hydrogen and oxygen-oxygen bond dissociation energies are determined and compared to other similar species. Due to the stability and high resonance stabilization, including aromatization, of the furans, the radical compounds in some cases have bond energies that are much lower than would be expected. There is good consistency between the O–H BDEs for the 2-methylfuran hydroperoxides, but a wide 45 kcal mol^{-1} range for the O–O BDEs and a similar 42 kcal mol^{-1} range for the O–H BDEs in the alcohol species. S°_{298} and $C_p(T)$ values are also determined for the parent and radicals species. Results from this study will serve as useful data for this important family of compounds.

CHAPTER 10

CHEMICAL ACTIVATION REACTIONS OF 2-METHYLFURAN WITH $^3O_2$

10.1 Overview

The search for replacement of current day fossil fuels has been an ongoing process now for over a decade. Compounds created during the conversion process of starting material, such as biomass, are just as important as the fuels themselves. Lignocellulosic biomass is an abundant renewable feedstock, composed of cellulose, hemicelluloses, and lignin, which serves as an excellent source for a variety of compounds. One such group of compounds getting much of the attention are high-energy substituted furans for their possible biofuel applications.[42]

5-Hydroxymethylfurfural (HMF) is a furan of great interest as it can be converted from fructose[41,43,249] and cellulose biomass[1,297-299] with the latter capable of being a large scale sustainable source. HMF can be transformed into numerous organic acids, aldehydes, alcohols, amines, and ethers[39-41] making it versatile and able to replace chemicals for industrial processes derived from petroleum sources. HMF along with furan, furfural, furfuryl alcohol, 2- and 3-methylfuran (2MF and 3MF), 2,5-dimethylfuran (25DMF), and nine other furan-based compounds have been shown as products created from pyrolysis of ^{13}C isotopically labeled D-glucose.[300]

Furan has been studied, both experimentally and computationally. One combustion study reports on its ignition delay times over various temperature, pressure, and equivalence ratio test conditions.[301] A thermal decomposition showed production of acetylene, ketene, carbon monoxide, propyne, and propargyl radicals as important

products.[302] A detailed combustion model has been developed[303] and reaction pathways for both addition and abstraction with hydroxyl radicals[304] have been developed.

Furfural, which has also been converted from pentoses,[281] can be converted into 2MF by vapor-phase hydrogenation[305] or simultaneous furfural hydrogenation and cyclohexanol dehydrogenation.[280] 2MF hydrogenation has been shown to produce 2-methyltetrahydrofuran, 1- and 2-pentanol, and 2-pentanone,[282,283] and its reactions with hydroxyl radicals has been studied.[285,287,288] Lifshitz et al.[306] looked at the thermal decomposition of 2MF from 1070-1370 K and report hydrogen atom and methyl group migration as initiation steps to unimolecular decomposition. Corma et al.[279] detailed a two-step catalytic hydroxyalkylation/alkylation and hydrodeoxygenation process beginning from 2MF to create high-quality diesel fuels.

Studies on 25DMF include a detailed reaction mechanism for thermal decomposition from 1070-1370 K[307] and analysis of combustion intermediates from premixed laminar flames[284] have also been reported. Simmie and Metcalfe[291] studied 25DMF thermal breakdown to 2MF through hydrogen addition to the furan ring carbon at the methyl site followed by elimination of the methyl group. Their rate constant calculation showed H addition is faster than H abstractions, below 1500 K. Sirjean and Fournet[308] computationally studied the thermal breakdown of the methyl radical on 25DMF where the easiest decomposition pathway was predicted to be ring opening via a C–O bond with subsequent ring expansion. Computational studies on the thermochemical properties of furan-based species including substituted derivatives,[309] HMF,[310] and tetrahydrofurans[311] along with various species created during flash pyrolysis of

biomass[243] have been completed. The results from these studies aid in creating and predicting chemical kinetic models for larger related species.

This work reports on the reactions involving 2MF radicals plus O_2 in order to understand furan ring oxidation and further reactions of furan systems. Notation and heat of formations, in kcal mol^{-1}, for several important 2MF related species that are key for analysis are shown in Figure 10.1.

Simmie and Curran[45] determined $\Delta H_f^\circ{}_{298}$ for 2MF and 2MF5j of -19.3 and 49.0 kcal mol^{-1}, according to the numbering shown for 2MF in Figure 10.1. They also reported ring carbon-hydrogen bond dissociation energies (C–H BDEs) of approximately 120 kcal mol^{-1} for furan and 2MF, similar to those of 2- and 3-methoxyfuran.[292] They also calculated the 2MF methyl C–H BDE of 86.3 kcal mol^{-1} compared to higher energies of 98 kcal mol^{-1} for methoxy-methyl C–H bonds of 2- and 3-methoxyfuran.

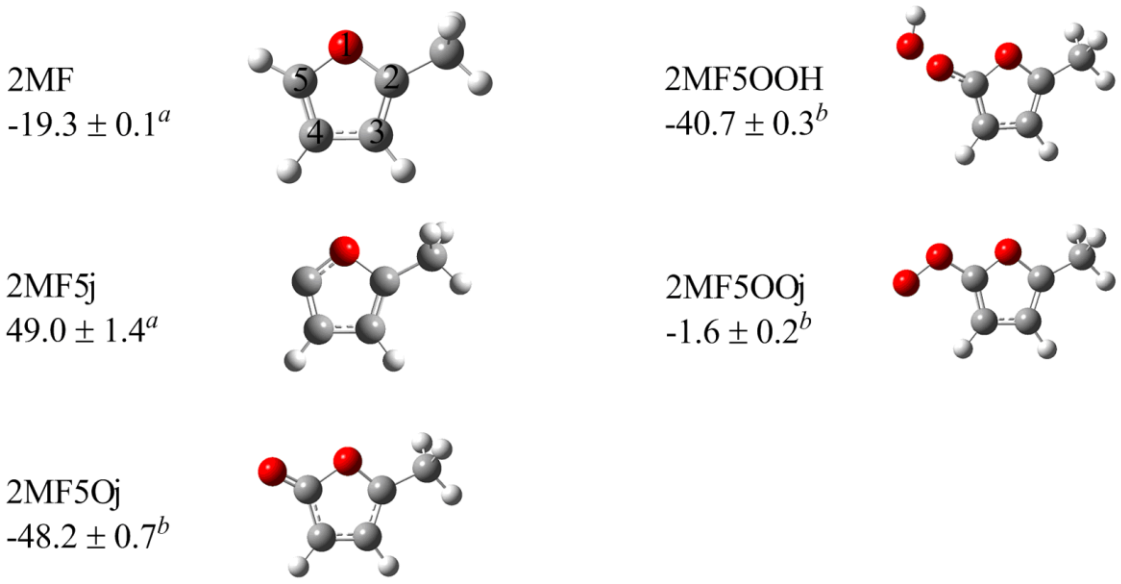

[a] Ref 45 [b] Our previously determined values

Figure 10.1 Nomenclature and heat of formation (units of kcal mol^{-1}) for important 2MF species in the 2MF5j + O_2 system.

Enthalpies for 2MF alcohol and hydroperoxide species, including radicals, from high level CBS-QB3 and G3MP2B3 calculations have recently been determined[312] and are illustrated in Figure 10.1. Calculated $\Delta H_f^\circ{}_{298}$ values for the 2MF peroxide radicals range from -0.9 to -1.6 kcal mol^{-1} which would produce well depths of over 50 kcal mol^{-1} for furan ring radical species (2MF3j, 2MF4j, and 2MF5j) plus O_2 compared to 15 kcal mol^{-1} for the 2MF2j location.

Important thermochemical properties, including enthalpies ($\Delta H_f^\circ{}_{298}$), entropies (S°_{298}), and heat capacities ($C_p(T)$), for the association of 2MF5j and O_2 forming the chemically active 2MF5OOj* radical along with 2MF, 2MF5j, 2MF5Oj, 2MF5OOH, and 2MF5OOj species, will aid in uncovering the reaction pathways of these representative furans.

10.2 Nomenclature

Abbreviations are utilized as illustrated below:

- – represents a bond between two atoms,
- = represents a double bond between two atoms,
- # or ≡ represents a triple bond between two atoms,
- Y represents a cyclic structure,
- j represents a radical site on the preceding carbon atom,
- Brackets () represents a substituent on the preceding carbon atom, CC(=O) is acetaldehyde,
- C_i or O_i denotes carbon or oxygen *i* according to numbering in Figure 10.1,
- TS denotes transition state,
- * denotes an activated adduct complex,
- 2MF or MF denotes 2-methylfuran.

10.3 Computational Methods

Optimized geometries are determined using the density functional theory (DFT) B3LYP[46,47] method with the 6-31G(d,p) basis set. In some cases, B3LYP either could not determine appropriate structures or for the transition states (TS) gave negative frequencies that did not correctly represent the desired species. For these situations, the MP2[66-70] or PM3[64,65] methods are used to determine more appropriate structures. Stable species are verified by having all positive vibrations while TS species all had a characteristic single imaginary (negative) frequency corresponding to the mode of vibration connecting the reactant and product.

High level DFT based composite calculations are performed with CBS-QB3[60,61] using the Gaussian 03[62] and Gaussian 09[63] program suites. This method uses geometries and frequencies from the B3LYP/6-311G(2d,d,p) level with single point energy calculations at the CCSD(T), MP4SDQ, and MP2 levels and a final CBS extrapolation. Single point energies are calculated from the MP2 and PM3 optimized geometries when the B3LYP method could not converge on acceptable geometries.

For calculation of $\Delta H^{\circ}_{f\ 298}$ values, isodesmic work reactions are used to cancel systematic CBS-QB3 calculation errors for all stable and TS species. The work reactions use standard reference species, which have well-established $\Delta H^{\circ}_{f\ 298}$ values. For six of these standard reference species, enthalpies from literature sources were not available so they are calculated from a set of work reactions, shown in Appendix I, where the assigned error is from the standard deviation of the work reaction values.

Atomization reactions are also included as a check on our calculated values. This type of reaction relies on simply the balancing of the target species with constituent

atoms, C, O, and H, in the gas phase. Although this allows for fast enthalpy estimation, there is not the same error cancelling capabilities as the work reaction method because the environment of the atoms is not the same as that of the molecule.

Entropy and heat capacities are calculated using the rigid-rotor harmonic-oscillator approximation for contributions from translations, vibrations, and external rotations using the Statistical Mechanics for Heat Capacity and Entropy (SMCPS) program.[98] The SMCPS program uses input including geometry, mass, electronic degeneracy, symmetry, frequencies, number of optical isomers, and moments of inertia for each species. Zero-point vibration energies are scaled by 0.9806 for B3LYP, 0.9608 for MP2, and 0.9761 for PM3 as recommended by Scott and Radom.[99]

Corrections for internal rotor torsion frequencies corresponding to single bond rotations are replaced with hindered rotor analysis from VIBIR which uses the Pitzer and Gwinn[85-87] approximation method. Reduced moments of inertia are calculated from the optimized structures using the mass and radius of rotation for the rotating group and barriers to single bond rotation are determined. Rotations which would substantially change the conformation of a species are not analyzed. Summing the SMCPS and VIBIR contributions gives the total entropy and heat capacities for the species.

High-pressure rate constants, k(T), are calculated for the 300–2000 K temperature range using canonical transition state theory (CTST) given in equation 2.19. Degeneracy is accounted for in the symmetry of reactants and products. These rate constants are then used to determine elementary rate parameters (A, n, E_a) using a modified form of the Arrhenius equation given in equation 2.20. Calculations for the 2MF5j + O_2 adduct, bond length scans are performed for energy and vibration frequencies and results are analyzed

and used in variational transition state theory to determine the rate parameters for this barrier-less reaction.

Temperature- and pressure-dependent rate constants are calculated using the multichannel, multifrequency quantum Rice-Ramsperger-Kassel (QRRK) analysis for *k*(E) with master equation for falloff and stabilization as implemented in the CHEMASTER code.[107,313] Energy dependence of the rate constant, *k*(E), must be considered to correctly account for product distribution from chemical activation reactions. The steady-state assumption is applied to the energized adduct where both forward and reverse reaction paths are calculated. In comparison, the formation of products is not reversible and only adjacent product formation is considered and subsequent dissociation needs to be handled separately. The required input for CHEMASTER includes temperature and pressure ranges of interest, the mass of the species, the Lennard-Jones transport parameters for the collider molecule, the third body bath gas, and reactants, and a reduced set of three representative vibrations and their degeneracies.

10.4 Results and Discussion

Optimized geometry parameters, symmetry values, optical isomers, moments of inertia, and vibrational frequencies for all species in the 2MF5j + O_2 system are presented in Appendix I.

10.4.1 Heat of Formation $\Delta H^{\circ}_{f\,298}$

Error cancelling isodesmic work reactions are used to determine $\Delta H_f{}^{\circ}{}_{298}$ values for stable and TS species from CBS-QB3 calculations. Enthalpies for each species are analyzed

using at least three reactions with standard reference species, presented in Table 10.1. Some of the species have hydrogens illustrated, while others do not for clarity. In selecting the work reactions, care is taken to ensure that similar environments, including aromaticity where applicable, in order to cancellation of error in the calculation. The work reactions, corresponding enthalpies, and error, reported as the standard deviation, along with the atomization reaction results are given in Appendix I. There is good agreement between the $\Delta H_f^\circ{}_{298}$ from the work reaction and atomization methods.

Optimized geometries for all of the stable species are shown in Figure 10.2 while the stable species are depicted in the potential energy (PE) diagrams, Figures 10.4- 10.6. The optimized structure parameters for all of the species are also included in Appendix I.

Table 10.1 Standard Enthalpies of Formation for Reference Species

Species	$\Delta H^{\circ}_{f\,298}$ (kcal mol^{-1})	Reference
CH_4	-17.8 ± 0.1	120
CH_3CH_3	-20.0 ± 0.1	120
$CH_3CH_2CH_3$	-25.0 ± 0.1	120
$CH_3CH_2CH_2CH_3$	-30.0 ± 0.1	120
$CH_3CH_2CH_2CH_2CH_3$	-35.1 ± 0.2	120
$CH_2=CH_2$	12.5 ± 0.1	120
$CH_2=CHCH_3$	4.8 ± 0.2	120
$CH_2=CHCH_2CH_3$	-0.15 ± 0.19	314
CH#CH	54.5 ± 0.2	120
$CH\#CCH_3$	44.2 ± 0.2	120
$CH\#CCH_2CH_3$	39.5 ± 0.2	120
CH_3OH	-48.2 ± 0.1	120
CH_3CH_2OH	-56.2 ± 0.1	120
$CH_3CH_2CH_2OH$	-61.0 ± 0.1	120
$CH_3CH_2CH_2CH_2OH$	-65.7 ± 0.1	120
CH_3OOH	-31.0 ± 0.2	241
CH_3CH_2OOH	-39.1 ± 0.2	241
$CH_3CH_2CH_2OOH$	-43.8 ± 0.2	241
CC(=O)	-39.7 ± 0.1	120
CC(=O)C	-51.9 ± 0.2	120
CC(=O)CC	-57.3 ± 0.2	315
n-CC(=O)CCC	-62.0 ± 0.2	315
CCC(=O)CC	-62.5 ± 0.2	315
CC(=O)C=C	-27.4 ± 2.6	316
$H_2C=C=O$	-11.3	317
$CH_3CH=C=O$	-15.1	317
$H_2C=CHCH=O$	-15.7 ± 0.1	*a*
$H_2C=C=C=O$	30.7 ± 0.2	*a*
$CH_3CH_2CH=C=O$	-20.7	317
HOCH=C=O	-35.8	317
$HOCH_2CH=C=O$	-51.6	317
CjH_3	35.1 ± 0.2	173
CH_3CjH_2	29.0 ± 0.4	121
$CH_3CH_2CjH_2$	23.9 ± 0.5	173
$CH_3CH_2CH_2CjH_2$	19.3 ± 0.5	239
$CH_3CH_2CH_2CH_2CjH_2$	14.3 ± 0.3	*a*
CH_3CH_2Oj	-3.6 ± 0.8	240
$CH_3CH_2CH_2Oj$	-8.7 ± 0.3	*a*
$CH_3CH_2CH_2CH_2Oj$	-13.5 ± 0.3	*a*

[a] See Appendix I for enthalpy calculation.
[b] From average of CBS-QB3 and G3MP2B3 calculation methods.[312]

Table 10.1 Standard Enthalpies of Formation for Reference Species (Continued)

Species	$\Delta H^{\circ}_{f\,298}$ (kcal mol^{-1})	Reference
CH_3OOj	2.9 ± 0.2	241
CH_3CH_2OOj	-5.6 ± 0.2	241
$CH_3CH_2CH_2OOj$	-10.5 ± 0.2	241
CC(=O)Cj	-8.3 ± 0.5	157
CC(=O)CCj	-7.8 ± 0.4	315
n-CC(=O)CCCj	-12.9 ± 0.4	315
CjCC(=O)CC	-13.1 ± 0.4	315
2MF5Oj	-48.2 ± 0.7	*b*
2MF5OOH	-40.7 ± 0.3	*b*
Y($C_4H_4O_2$) (Dioxin)	-20.0 ± 0.3	*a*
Y($C_4H_8O_2$) (1,3-Dioxane)	-81.4 ± 1.0	120

[a] See Appendix I for enthalpy calculation.
[b] From average of CBS-QB3 and G3MP2B3 calculation methods.[312]

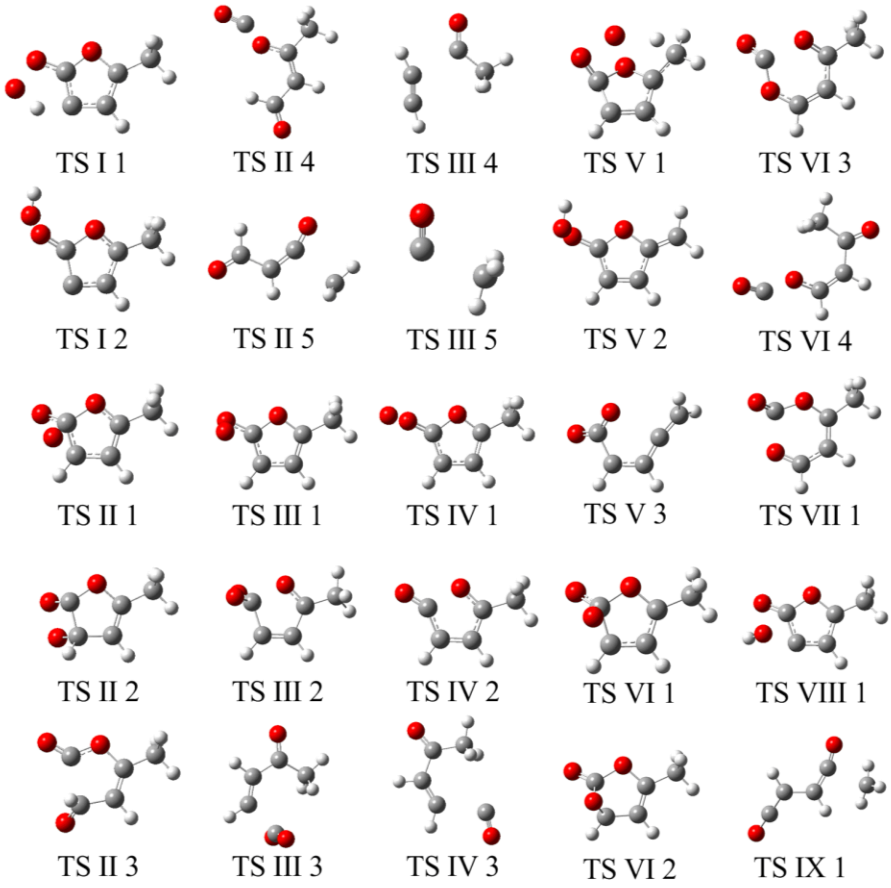

Figure 10.2 Optimized structures for transition state species studied in the 2MF5j + O_2 system.

10.4.2 Entropy ($S^{\circ}(T)$) and Heat Capacity ($C_p(T)$)

S°_{298} and $C_p(T)$, for 300 ≤ T ≤ 1500 K, are presented in Table 10.2. These values are the combination of the contributions from the translations, vibrations, and external rotations with corrections for single bond rotations with barriers below 5 kcal mol^{-1}. Geometries, moments of inertia, vibrational frequencies, and internal rotor potentials for these species are from the B3LYP/6-31G(d,p) method, unless otherwise noted. Other well-known small combustion species, which are not calculated in this study such as CjH3, CH#CH, CO, CO_2, O, and OH, are also listed in Table 10.2.

10.4.3 2MF5j + O_2 Reaction System

Variational transition state theory (VTST) is used to determine the rate constants for barrier-less reactions common to association reactions such as 2MF5j + O_2. A scan of the bond length for 2MF5OOj → 2MF5j + O_2 is shown in Figure 10.3 using unrestricted B3LYP/6-31G(d,p). Calculation of elementary rate parameters from VTST are given in Table 10.3.

Table 10.2 Recommended Enthalpies, Entropies, and Heat Capacities for Species in the 2MF5j + O_2 System[a]

Species	$\Delta H^\circ_{f\,298}$ [b]	S°_{298} [c]	$C_p(T)$ [c]							Method
			300 K	400 K	500 K	600 K	800 K	1000 K	1500 K	
CjH_3	35.1 ± 0.2	46.38	9.26	10.05	10.81	11.54	12.90	14.09	16.26	
CH#CH	54.5 ± 0.2	48.00	10.53	11.97	12.97	13.73	14.93	15.92	18.00	
CO	-26.42	47.21	6.96	7.02	7.13	7.27	7.61	7.94	8.41	
CO_2	-94.05	51.07	8.90	9.85	10.65	11.31	12.30	12.97	13.93	
O	59.55 ± 0.02	38.47	5.23	5.14	5.08	5.04	5.01	5.01	4.98	
OH	8.91 ± 0.1	43.88	7.16	7.08	7.05	7.05	7.15	7.33	7.87	
2MF5j	49.0 ± 1.4	73.77	20.72	26.36	31.31	35.39	41.48	45.74	52.06	
2MF5OOj	-1.6 ± 0.2	86.36	28.50	35.17	40.84	45.39	51.96	56.42	62.89	
TS 2MF5OOj	47.7 ± 0.2	89.45	27.84	33.77	39.03	43.41	50.00	54.62	61.42	M06-2X/6-31G(d,p)
TS I 1	35.9 ± 0.2	82.70	26.86	33.68	39.49	44.22	51.12	55.77	62.31	
MF4j5Q	27.8 ± 0.2	87.87	29.60	36.21	41.75	46.15	52.47	56.74	62.98	
TS I 2	47.2 ± 0.2	88.26	28.09	34.03	39.23	43.53	49.94	54.41	61.10	MP2/6-31G(d,p)
CC(=O)CH=C=C=O	-8.2 ± 0.5	86.28	25.88	30.76	34.91	38.33	43.49	47.13	52.50	
TS II 1	36.4 ± 0.2	81.51	24.10	30.49	36.15	40.88	48.01	53.01	60.43	MP2/6-31G(d,p)
MF45Y(CjCOOj)	23.3 ± 0.2	82.96	27.23	34.46	40.49	45.30	52.22	56.91	63.67	
TS II 2	22.6 ± 0.2	82.22	26.21	33.12	38.95	43.63	50.42	55.04	61.74	
MF4Oj5O	-52.1 ± 0.2	84.76	28.19	34.88	40.53	45.13	51.94	56.65	63.51	
TS II 3	-45.9 ± 0.2	85.44	28.45	34.51	39.66	43.92	50.40	54.96	61.69	
O=CjOC(C)=CHCH(=O)	-52.8 ± 0.1	92.67	31.12	36.76	41.57	45.58	51.75	56.17	62.75	
TS II 4	-41.6 ± 0.1	90.36	30.86	36.15	40.78	44.71	50.80	55.19	61.76	
n-CC(=O)CjHCH(=O)	-38.4 ± 0.2	81.25	23.38	28.31	32.72	36.43	42.13	46.20	52.33	
TS II 5	0.4 ± 0.2	84.77	25.40	29.78	33.46	36.53	41.34	44.92	50.55	
O=CHCH=C=O	-40.3 ± 0.2	70.68	17.31	20.26	22.75	24.81	27.98	30.22	33.51	
TS III 1	8.6 ± 0.2	82.90	26.62	33.31	38.99	43.59	50.32	54.93	61.64	
MF5Yj(COO)	-7.2 ± 0.2	82.77	28.10	35.13	40.98	45.65	52.41	57.02	63.70	
TS III 2	-6.4 ± 0.2	80.60	25.78	32.11	37.60	42.15	49.05	53.92	61.09	MP2/3-21G

[a] B3LYP/6-31G(d,p) method used unless otherwise noted.
[b] Units in kcal mol^{-1}.
[c] Units in cal mol^{-1} K^{-1}.

Table 10.2 Recommended Enthalpies, Entropies, and Heat Capacities for Species in the 2MF5j + O_2 System[a] (Continued)

Species	$\Delta H^\circ_{f\,298}$ [b]	S°_{298} [c]	$C_p(T)$[c]							Method
			300 K	400 K	500 K	600 K	800 K	1000 K	1500 K	
CC(=O)CH=CHCO2j	-50.6 ± 0.1	93.39	29.98	36.27	41.49	45.67	51.79	56.01	62.23	
TS III 3	-49.7 ± 0.1	96.11	31.82	37.17	41.45	44.93	50.29	54.20	60.21	
CC(=O)CH=CjH	29.8 ± 0.2	75.07	20.70	25.25	29.16	32.41	37.42	41.08	46.74	
TS III 4	56.7 ± 0.2	84.75	23.44	26.80	29.62	32.02	35.93	38.97	44.02	
CCj(=O)	-2.8 ± 0.1	62.92	12.12	14.11	16.04	17.76	20.57	22.71	26.07	
TS III 5	14.2 ± 0.1	66.89	14.35	15.78	17.00	18.09	19.99	21.60	24.39	
TS IV 1	18.3 ± 0.2	85.08	27.08	33.62	39.20	43.74	50.40	54.98	61.66	
2MF5Oj	-48.2 ± 0.7	78.33	24.09	30.38	35.74	40.11	46.59	51.10	57.72	
TS IV 2	-42.0 ± 0.4	77.64	22.47	28.26	33.29	37.47	43.82	48.36	55.19	MP2/3-21G
CC(=O)CHCjHC=O	-31.6 ± 0.1	80.06	24.51	30.22	35.05	39.07	45.27	49.80	56.79	MP2/6-31G(d)
TS IV 3	9.7 ± 0.1	93.17	27.84	32.30	36.27	39.65	45.01	48.98	55.10	
TS V 1	58.2 ± 0.2	80.41	27.41	34.65	40.63	45.40	52.31	56.95	63.46	PM3
MF2CjH25Q	-3.8 ± 0.2	87.35	29.64	36.78	42.45	46.82	52.98	57.15	63.39	MP2/6-31G(d,p)
TS V 2	-10.1 ± 0.2	82.31	27.97	35.01	40.73	45.17	51.37	55.50	61.62	MP2/6-31G(d,p)
MF2CH25O	-47.2 ± 0.2	74.93	22.71	29.05	34.20	38.26	44.11	48.09	53.87	
TS V 3	32.5 ± 0.2	78.80	24.39	29.98	34.51	38.11	43.37	47.01	52.38	
C=C=CHCHCO2	5.9 ± 0.5	83.03	25.67	31.34	35.93	39.53	44.74	48.31	53.56	
TS VI 1	-12.6 ± 0.2	84.27	27.72	34.41	40.03	44.55	51.14	55.64	62.14	PM3
MF45Y(CCO)5Oj	-28.1 ± 0.2	82.06	26.95	33.93	39.75	44.42	51.26	56.00	63.02	MP2/3-21G
TS VI 2	-36.9 ± 0.2	80.06	26.09	32.85	38.51	43.06	49.76	54.40	61.25	MP2/3-21G
Y(OC(C)=CCjOC(=O))	-79.5 ± 0.4	83.59	28.19	34.83	40.47	45.05	51.85	56.55	63.43	
TS VI 3	-37.5 ± 0.4	86.07	27.59	33.92	39.28	43.68	50.24	54.82	61.57	
CC(=O)CH=CHOCj=O	-53.4 ± 0.1	89.23	30.17	36.03	41.14	45.41	51.91	56.53	63.38	
TS VI 4	-39.3 ± 0.1	92.25	30.37	35.73	40.46	44.44	50.59	55.00	61.63	
CC(=O)CjHCH(=O)	-37.7 ± 0.2	79.55	23.40	28.34	32.74	36.45	42.14	46.22	52.34	
TS VII 1	-37.1 ± 0.4	85.32	28.03	34.12	39.38	43.73	50.28	54.88	61.63	

[a] B3LYP/6-31G(d,p) method used unless otherwise noted.
[b] Units in kcal mol^{-1}.
[c] Units in cal mol^{-1} K^{-1}.

Table 10.2 Recommended Enthalpies, Entropies, and Heat Capacities for Species in the 2MF5j + O_2 System[a] (Continued)

Species	$\Delta H^\circ_{f\,298}$ [b]	S°_{298} [c]	$C_p(T)$ [c]							Method
			300 K	400 K	500 K	600 K	800 K	1000 K	1500 K	
TS VIII 1	54.1 ± 0.2	84.30	28.10	34.62	40.06	44.45	50.86	55.27	61.74	PM3
MF4OH5Oj	-93.2 ± 0.2	83.43	28.22	34.83	40.43	44.98	51.72	56.38	63.23	
TS IX 1	31.4 ± 0.1	94.87	30.66	35.10	38.63	41.54	46.14	49.64	55.28	
O=C=CHCH=C=O	-10.5 ± 0.3	79.77	21.52	24.84	27.42	29.48	32.61	34.87	38.23	

[a] B3LYP/6-31G(d,p) method used unless otherwise noted.
[b] Units in kcal mol^{-1}.
[c] Units in cal mol^{-1} K^{-1}.

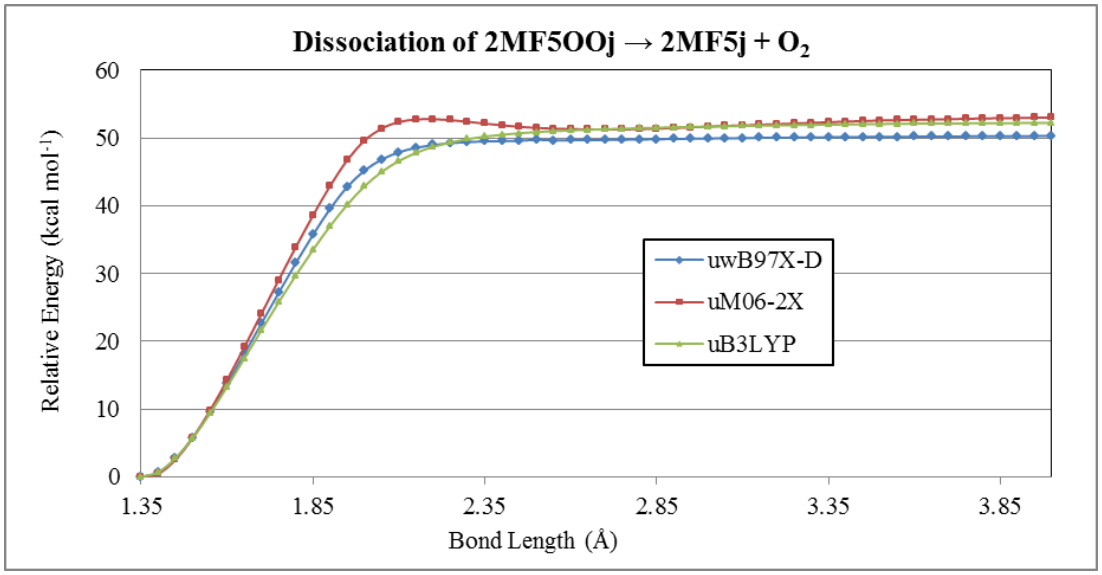

Figure 10.3 Scan of 2MF5OOj bond length for VTST calculation.

Table 10.3 Elementary Rate Parameters for 2MF5OOj

Method	Association 2MF5j + O_2→TS			Dissociation 2MF5OOj→TS		
	A	***n***	**E_a**	**A**	***n***	**E_a**
uB3LYP (VTST)	$7.28x10^{3}$	2.30	-0.1	$1.36x10^{14}$	-0.11	51.5
u*w*B97X-D (VTST)	$1.75x10^{3}$	2.37	-1.4	$3.27x10^{13}$	-0.04	50.2
uM06-2X (VTST)	$3.93x10^{2}$	2.52	1.7	$7.35x10^{12}$	0.11	53.3
uM06-2X (TS)	$2.11x10^{3}$	2.53	-1.8	$3.93x10^{13}$	0.11	49.9

Units: A (mol cm^{-3} s^{-1}), Ea (kcal mol^{-1})

To verify these rate parameters, calculations using unrestricted *w*B97X-D[53,54] with the 6-311+G(d,p) and M06-2X[55,56] with the 6-31G(d,p) basis sets are shown. The dissociation scans for B3YLP and *w*B97X-D are similar while M06-2X shows a saddle point at approximately 2.20 Å. An optimized geometry converged on a TS with a bond length of 2.18 Å. Similar elementary rate parameters are determined, using CTST,

denoted uM06-2X (TS), to those from VTST. Rate parameters from uM06-2X and the TS structure, denoted TS 2MF5OOj, are used in this study.

The focus of this analysis is on the initial reaction pathways of the 2MF5j + O_2 system given in Figure 10.4. Additional ring opening products of some furan-based species are determined. Values in the figure are calculated enthalpies of formation, kcal mol^{-1}, where values in parenthesis are the total enthalpies when more than one species is formed. Note that species in blue are optimized using either PM3 or MP2 methods. Pathways are denoted with roman numbers followed by sequential numbering.

10.4.4 Reaction Pathways

The initial reactions pathways of the 2MF5j + O_2 system, given in Figure 10.4, are separated based upon their type of reaction and are presented in more detail in the PE diagrams in Figures 10.5 and 10.6. In the subsequent analysis, the furan ring numbering also follows that in Figure 10.1.

The initial association of 2MF5j + O_2 creates a chemically activated 2MF5OOj* radical with 50.6 kcal mol^{-1} of chemical activation energy. The excited 2MF5OOj* can dissociate back to the original reactants, form new isomers via intramolecular abstraction of a hydrogen or a hydroxyl group transfer. The peroxy oxygen radical can also undergo oxygen addition to the furan ring, which initiates ring opening or expansion, Figure 10.6. The energized adduct can also dissociate to new products, as shown in Figure 10.5.

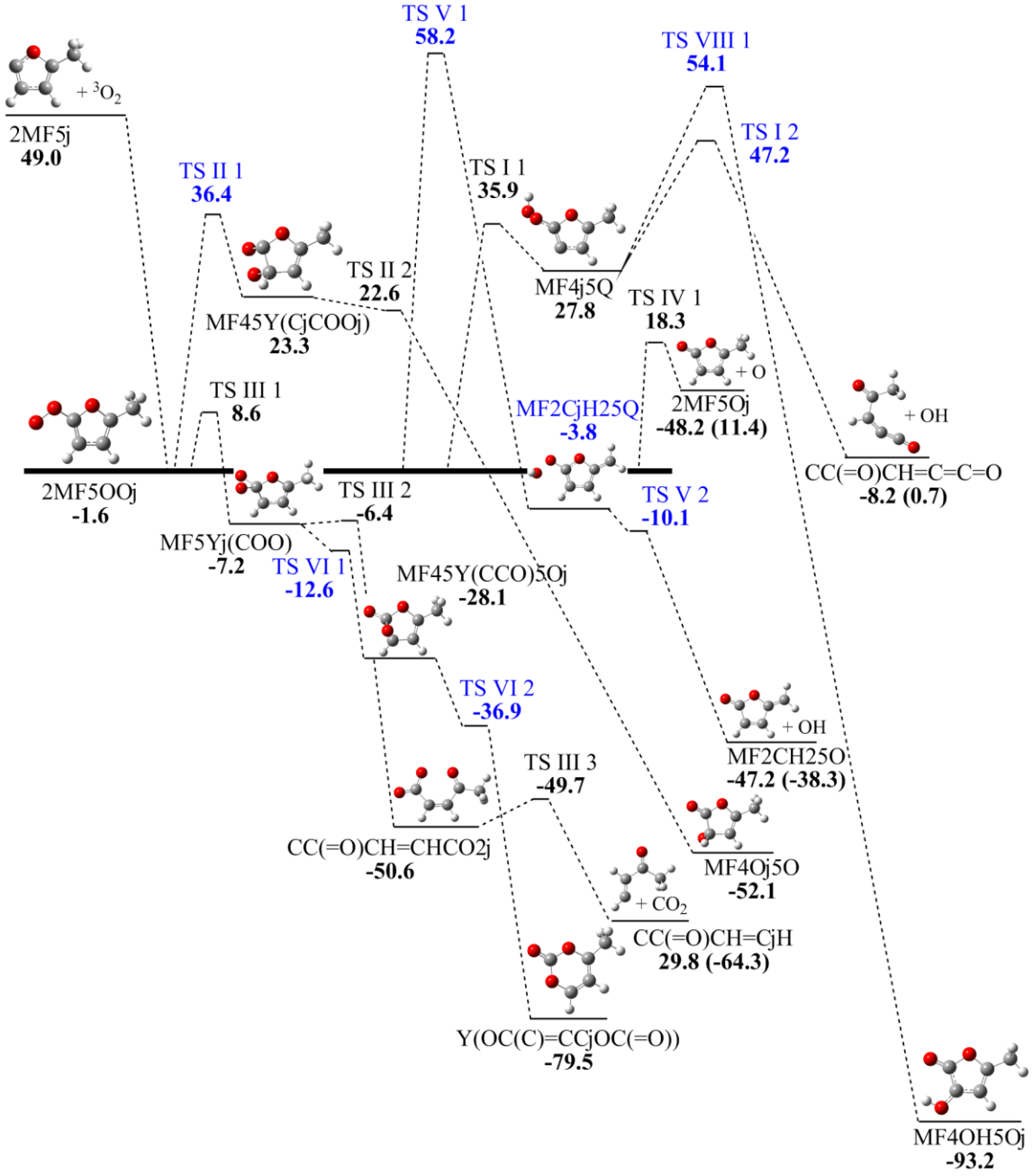

Figure 10.4 Chemical activation, isomerization, and dissociation pathways studied for the 2MF5j + O_2 → 2MF5OOj reaction system. Units are in kcal mol^{-1}.

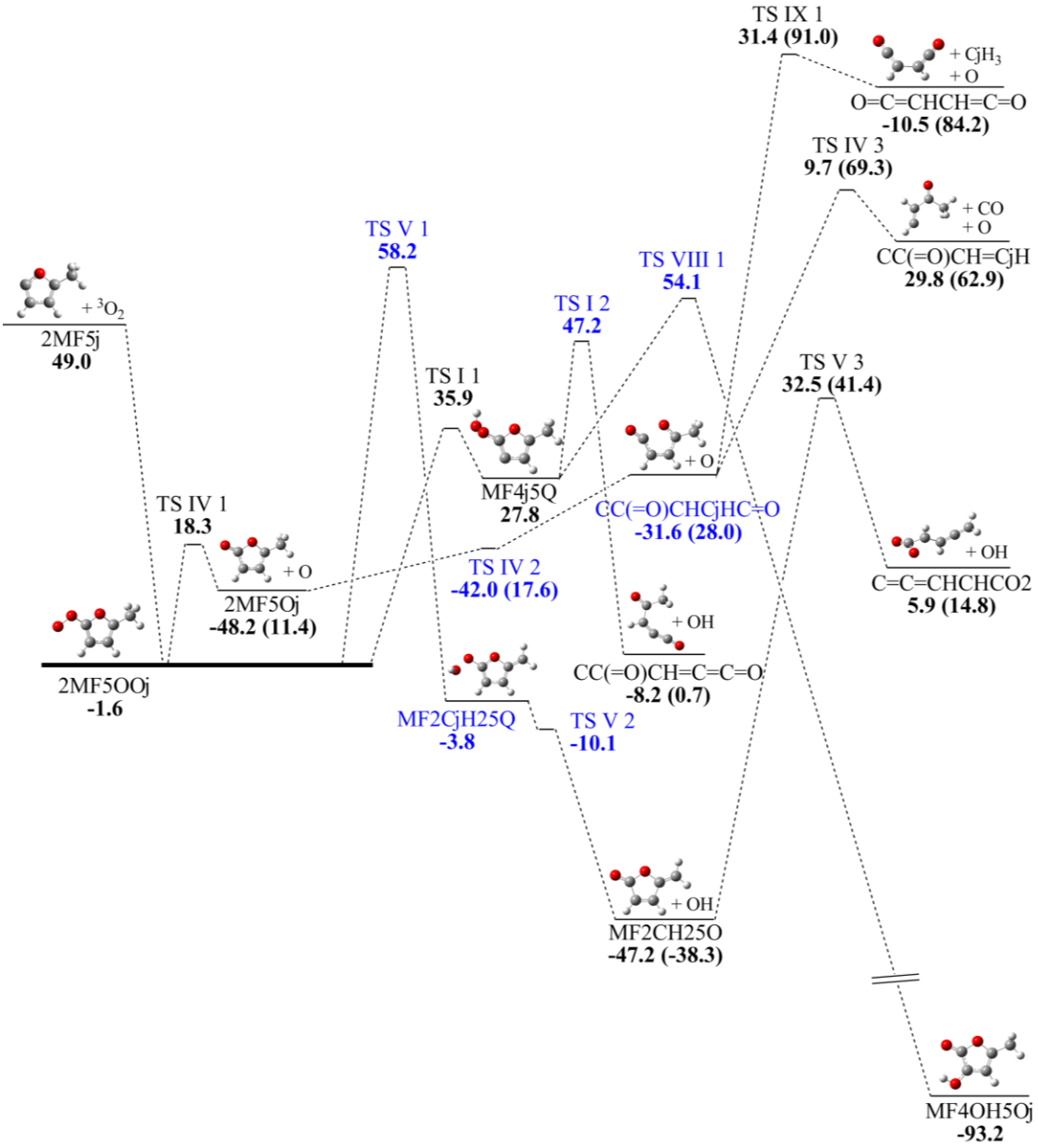

Figure 10.5 PE diagram for abstraction, dissociation, and group transfers studied in the 2MF5j + O_2 → 2MF5OOj reaction system. Units are in kcal mol^{-1}; overall these are higher barrier reaction paths.

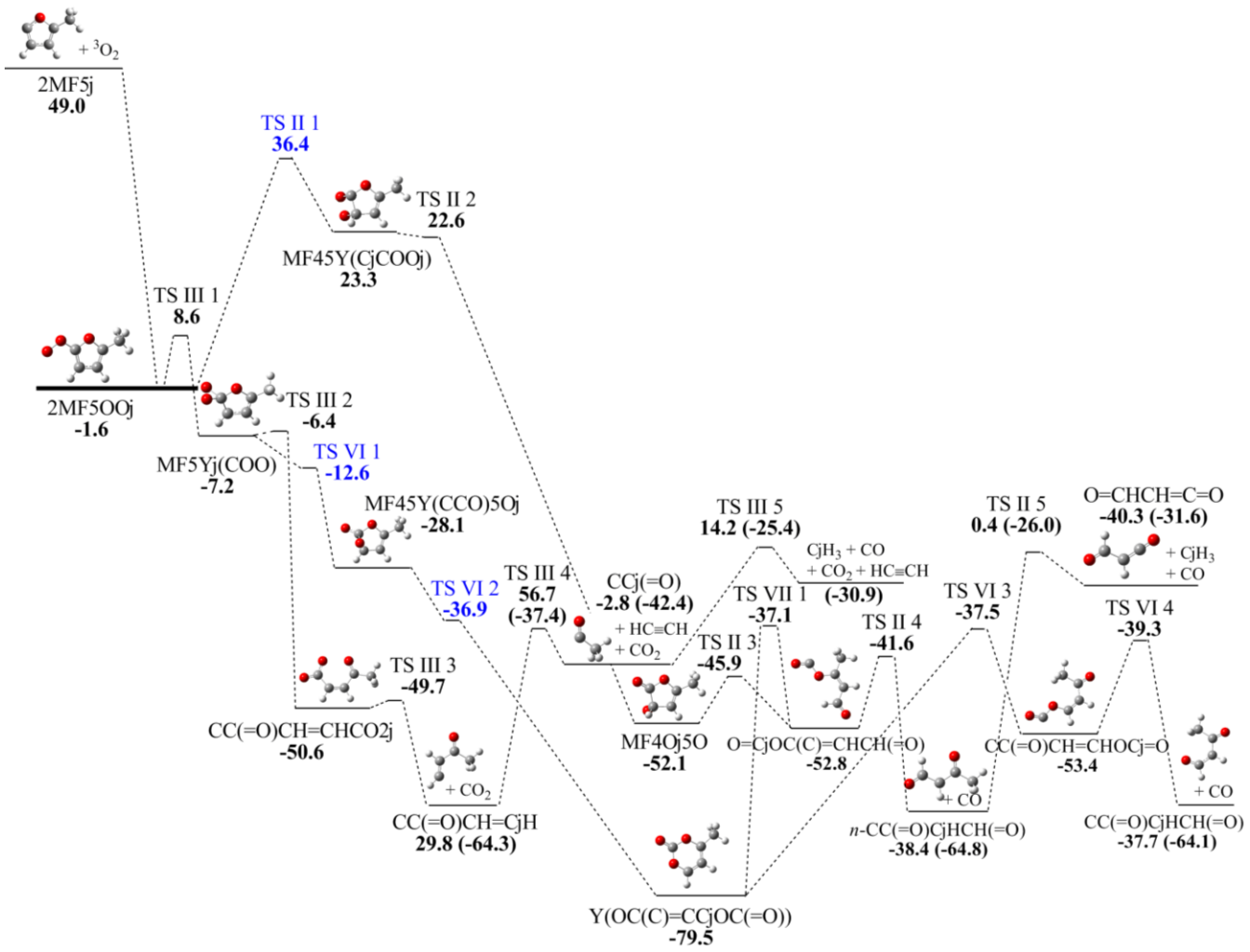

Figure 10.6 PE diagram for radical peroxy oxygen intramolecular addition initiating ring opening and expansion in the 2MF5j + O_2 → 2MF5OOj reaction system. Units are in kcal mol^{-1}.

10.4.4.1 Intramolecular Hydrogen Transfer (Abstraction) from C_4 by 2MF5OOj Radical Peroxy Oxygen (Pathway I). This pathway begins with an intramolecular hydrogen transfer from C_4 to the radical peroxy oxygen on 2MF5OOj with a 38 kcal mol^{-1} energy barrier (TS I 1) and an endothermicity of 29 kcal mol^{-1}, to form MF4j5Q. Further reaction of this MF4j5Q isomer, through a 20 kcal mol^{-1} barrier (TS I 2) to cleave the OH group via simple bond cleavage, results in ring opening via electron re-arrangement, after the separation to form the linear CC(=O)CH=C=C=O with no barrier other than ΔH_{rxn}. The very weak RO—OH bond is a result of electron rearrangement within the ring forming two carbonyl double bonds. A stable cyclic intermediate species could not be identified. It is observed that upon ring opening, the CC(=O)CH=C=C=O structure rotates around the CC(=O)–CH bond 180° over a 4.7 kcal mol^{-1} barrier to a more stable conformation which is 0.3 kcal mol^{-1} lower in energy.

10.4.4.2 Hydrogen Abstraction from Methyl Substituent by 2MF5OOj Radical Peroxy Oxygen (Pathway V). A high, 60 kcal mol^{-1}, barrier (TS V 1) is calculated for intramolecular hydrogen transfer from the methyl group to the radical peroxy oxygen on 2MF5OOj, due to the strain created in the TS structure. The resulting MF2CjH25Q (methyl radical) can then dissociate, via a TS which is calculated to have no barrier, to a substituted furan MF2CH25O and hydroxyl radical. The overall reaction is 87 kcal mol^{-1} exothermic from the initial entrance channel.

Ring opening of MF2CH25O requires surpassing a very large 80 kcal mol^{-1} barrier (TS V 3) to form C=C=CHCHCO2. The initial ring opened species rotates 180°

over a 2.1 kcal mol^{-1} barrier across the C–C bond to move the CO_2 group further away from the double bond.

10.4.4.3 Dissociation of O Atom from 2MF5OOj (Pathways IV and IX). 2MF5OOj dissociation of the terminal oxygen to form 2MF5Oj + O occurs over a 20 kcal mol^{-1} energy barrier, TS IV 1. A transition state (TS IV 2) and subsequent stable ring opened product (CC(=O)CHCjHC=O) could not be determined with the B3LYP method. Optimization of these structures reformed the C_5–O_1 bond back to the five-member furan ring. MP2 converged on appropriate structures, but the resulting energy for TS IV 2 is lower than that of CC(=O)CHCjHC=O. Simmie and Metcalfe[291] determined a 19.6 kcal mol^{-1} barrier for ring opening of 2MF5Oj with G3 calculations for this same system. The energy difference from 2MF5Oj and CC(=O)CHCjHC=O is calculated to be 16.6 kcal mol^{-1}, consistent with their findings.

As the terminal CO group in CC(=O)CHCjHC=O moved further from O_1, the rotational barrier for the CC(=O)–CH bond lowered to 4.9 kcal mol^{-1} allowing the 180° rotation depicted in TS IV 3. Loss of the terminal CO group generates CC(=O)CH=CjH which is further described in Pathway III. The reactions of this CC(=O)CH=CjH species are shown in Figure 10.6.

From CC(=O)CHCjHC=O, Simmie and Metcalfe[291] suggested that the methyl group could also be dissociated. Pathway IX, Figure 10.5, depicts this with an energy barrier of 63 kcal mol^{-1} (TS IX 1). There is bond rotation over the elongated C_3–C_4 bond in the center of the species created upon transition state formation leading to the stable O=C=CHCH=C=O species.

10.4.4.4 Hydroxyl Group Transfer to C_4 in 2MF5OOj (Pathway VIII). A hydroxyl group dissociation from the peroxide with simultaneous ring opening was previously described in Pathway V. It is also possible to have the OH group transfer to the original hydrogen abstraction site on C_4 from MF4j5Q with a 26 kcal mol^{-1} barrier of TS VIII 1. The resulting MF4OH5Oj species is calculated to be the most stable substituted furan, with over 120 kcal mol^{-1} of chemical activation energy relative to the entrance channel MF4j5Q*.

10.4.4.5 Intramolecular Addition of Peroxy Oxygen Radical to C_4 in 2MF5OOj and Subsequent Weak RO–OR' Bond Cleavage (Pathway II). The peroxy oxygen radical of 2MF5OOj attacks the unsaturated bond on C_4 forming a four-member peroxide ring over a 38 kcal mol^{-1} barrier of TS II 1. Formation of the strained bicyclic MF45Y(CjCOOj) species begins to break the O–O bond in the peroxide ring through TS II 2 which is calculated to be slightly lower in energy than MF45Y(CjCOOj). The resulting MF4Oj5O completes the oxygen transfer by forming a carbonyl bond and ring opening with a substantial 75 kcal mol^{-1} exothermicity.

Ring opening of MF4Oj5O through TS II 3 has a low 6 kcal mol^{-1} barrier with the resulting O=CjOC(C)=CHCH(=O) structure. Initial ring opening has the terminal CO group at the peak of its calculated rotational barrier where rotation by 180°, through a small 0.5 kcal mol^{-1} barrier, over the O=CjO–C bond to a 2 kcal mol^{-1} lower energy conformation. Elimination of CO can occur through a low 11 kcal mol^{-1} barrier, TS II 4, generating a straight chain *n*-CC(=O)CjHCH(=O) followed by beta scission (elimination) of the terminal methyl group requiring approximately 39 kcal mol^{-1} over TS II 5 yielding O=CHCH=C=O and a methyl radical.

10.4.4.6 Ring Opening from Three-Member Ring Formation, Ipso Addition of Radical Peroxy Oxygen in 2MF5OOj (Pathway III). The terminal peroxy radical oxygen can also undergo addition to the ipso carbon, C_5, forming a three-member ring over a 10 kcal mol^{-1} energy barrier, TS III 1. The stable bicyclic formed, MF5Yj(COO) has several low energy reaction paths in Pathway III.

Cleavage of the C_5–O_1 bond in MF5Yj(COO) requires surpassing a 1 kcal mol^{-1} energy barrier (TS III 2) for CC(=O)CH=CHCO2j formation which is 40 kcal mol^{-1} lower in energy. The overall reaction is 100 kcal mol^{-1} exothermic from the initial reactants with all barriers below the entrance channel.

Loss of CO_2 from CC(=O)CH=CHCO2j occurs over a 1 kcal mol^{-1} barrier (TS III 3). In this reaction step, the bond lengthening for the leaving CO_2 group lowers the CC(=O)–CH rotational barrier to 2.5 kcal mol^{-1}, allowing for a 180° rotation to a lower energy conformation. Complete removal of CO_2 results in CC(=O)CH=CjH formation, the same product created by the CO removal from CC(=O)CHCjHC=O in Pathway IV. A barrier of 27 kcal mol^{-1} is required for further reaction, beta scission of acetylene from CC(=O)CH=CjH via TS III 4 and further beta scission of CCj(=O) into a methyl radical and CO over TS III 5. The overall reaction is 80 kcal mol^{-1} exothermic from the entrance channel, with all barriers below the entrance channel.

10.4.4.7 Ring Expansion from Ipso Addition of Radical Peroxy Oxygen in 2MF5OOj (Pathways VI and VII). A second reaction path for ipso addition adduct, MF5Yj(COO), has one oxygen of the three-member ring move towards C_4 radical site, and the O–O bond of the COO ring cleaving with the new C_4–O bond forming MF45Y(CCO)5Oj. The oxygen on C_5 is a radical and forms a new double bond with C_5

and cleaves the ring C_4–C_5 carbon bond forming a new six-member ring, which is calculated to be 129 kcal mol^{-1} below than the entrance channel and 51 kcal mol^{-1} lower than MF45Y(CCO)5Oj.

The structure of this reaction path has the oxygen inserting between the C_4 and C_5 bond slightly elevated above the plane of the furan ring in MF45Y(CCO)5Oj. Bicyclic TS VI 2 has a negative frequency corresponding to the bond breaking between the C_4–C_5 furan carbons leading to the oxygen insertion into the furan ring and creating the six-member ring Y(OC(C)=CCjOC(=O)) some 78 kcal mol^{-1} below the 2MF5OOj radical. Formation and reaction through the equivalent of this Y(OC(C)=CCjOC(=O)) intermediate is the lowest energy channel in oxidation of benzene[318,319] and toluene rings[320] and is an important intermediate in this furan ring carbon oxidation path. This ring expansion to a stable six-member ring was also shown to be a favorable pathway for the thermal decomposition of 5-methyl-2-furanylmethyl radical by Sirjean and Fournet.[308]

Two locations for ring opening of this six-member ring Y(OC(C)=CCjOC(=O)) involve breaking the C(=O)–O bonds. Breaking the bond on the C_5 carbon and the newly inserted oxygen (further from the methyl substituent) generates the ring opening species O=CjOC(C)=CHCH(=O) through TS VII 1 species with a barrier of 42 kcal mol^{-1}. The ring opening allows for rotation of both the terminal CO and aldehyde groups by 180°. Upon initial ring opening, the terminal CO group is at the peak of the rotational barrier while the aldehyde group overcomes about a 6 kcal mol^{-1} energy barrier which could occur due to the large excess energy during this chemical activation process. The

resulting structure is O=CjOC(C)=CHCH(=O) which is the equivalent product from the ring opening of MF4Oj5O.

The second ring opening location has an almost equivalent 42 kcal mol^{-1} barrier for breaking the C(=O)–O bond to O_1 over TS VI 3. In the stable ring opened product, CC(=O)CH=CHOCj=O, there are two internal bond rotations, terminal CO group rotation over a 3.0 kcal mol^{-1} barrier and a 180° rotation across the CC(=O)–CH bond over the 4.2 kcal mol^{-1} barrier, to the most stable species. Elimination of CO occurs over a 14 kcal mol^{-1} TS VI 4 barrier to form CC(=O)CjHCH(=O).

CC(=O)CjHCH(=O) and *n*-CC(=O)CjHCH(=O) are within 1 kcal mol^{-1} of each other, where internal rotational of two bonds converts from one structure to the other. The rotational for the CC(=O)–Cj bond in CC(=O)CjHCH(=O) has an approximate 6.7 kcal mol^{-1} barrier and a larger 10 kcal mol^{-1} barrier for terminal CH(=O).

10.4.5 Kinetic Analysis

A summary of the elementary rate parameters for forward and reverse reactions studied in the 2MF5j + O_2 system are listed in Table 10.4. Rate parameters for all reactions are given in Appendix I.

Reactions of the chemically energized adduct 2MF5OOj*, formed from 2MF5j + O_2 association, have over 50 kcal mol^{-1} activation energy from the new bond formation. This 2MF5OOj*adduct can undergo unimolecular reactions, including isomerization or dissociation, or become deactivated through collisional stabilization.

The temperature- and pressure-dependent rate constants are calculated using the multichannel, multifrequency quantum Rice-Ramsperger-Kassel (QRRK) analysis for *k*(E) with master equation for falloff and stabilization as implemented in the

CHEMASTER code.[107] A reduced set of three representative vibrations, from the full set of 3*n*-6 vibrations that reproduces heat capacity plus energy levels of one external rotation, have been shown to compare well to direct count methods,[108] and are determined for each well species. These calculated vibrations are listed in Table 10.5 while the rest of the input data for CHEMASTER is tabulated in Table 10.6.

Table 10.4 Summary of Elementary Rate Parameters for Reactions Studied in the 2MF5j + O_2 System

Reactions	A	*n*	E_a
2MF5j + O_2 → TS 2MF5OOj	$2.11x10^{3}$	2.53	0.0
2MF5OOj → TS 2MF5OOj	$3.93x10^{13}$	0.11	49.9
2MF5OOj → TS I 1	$5.21x10^{10}$	0.57	37.7
MF4j5Q → TS I 1	$1.72x10^{10}$	0.58	8.1
MF4j5Q → TS I 2	$5.89x10^{12}$	0.17	19.8
MF4j5Q → TS VIII 1	$1.92x10^{10}$	0.71	26.3
2MF5OOj → TS II 1	$5.69x10^{14}$	-0.93	39.0
MF45Y(CjCOOj) → TS II 1	$8.02x10^{14}$	-0.71	14.0
MF45Y(CjCOOj) → TS II 2	$6.53x10^{11}$	0.43	1.0
2MF5OOj → TS III 1	$6.85x10^{12}$	-0.12	10.9
MF45Y(CCO)5Oj → TS III 1	$9.11x10^{11}$	0.51	37.1
CC(=O)CH=CHCO2j → TS III 1	$1.88x10^{10}$	0.18	59.5
CC(=O)CH=CHCO2j → TS III 3	$9.83x10^{11}$	0.68	1.3
MF45Y(CCO)5Oj → TS VI 2	$2.44x10^{11}$	0.48	1.0
2MF5OOj → TS IV 1	$1.21x10^{12}$	0.29	20.3
2MF5OOj → TS V 1	$7.73x10^{8}$	1.02	59.7

Units: A (mol cm^{-3} s^{-1}), Ea (kcal mol^{-1})

Table 10.5 Reduced Frequencies for Well Species in 2MF5j + O_2 System

Species	Frequency (cm^{-1})	Vibrational Modes
2MF5OOj	426.8	13.351
	1393.9	15.907
	3999.7	3.742
MF4j5Q	439.1	14.292
	1348.1	13.782
	3815.5	4.426
MF45Y(CCO)5Oj	441.3	11.660
	1230.2	14.850
	3110.9	5.990
CC(=O)CH=CHCO2j	360.0	12.184
	1191.7	13.912
	3051.1	5.403
MF45Y(CjCOOj)	434.3	11.506
	1212.8	15.675
	3086.5	5.319

Table 10.6 CHEMASTER Input Parameters for 2MF5j + O_2 System

CHEMASTER Input Parameters	
Temperatures (K)	300-2100
Pressures (ATM)	0.001-100
N_2 (Bath Gas):	
σ (A)	3.5
e/k (K)	98.3
2MF5OOj:	
Mass	113.02
σ (A)	6.3
e/k (K)	692.0
ΔE_{down} (cal mol^{-1})	900
Integration Interval (kcal)	1.0
E_{head} (kcal mol^{-1})	75

10.4.5.1 Chemical Activation Analysis: 2MF5OOj*. Figures 10.7 and 10.8 provide the rate constant versus pressure (1 and 100 atm) and temperature (300 and 1000 K) for the chemical activation reactions of the 2MF5j + O_2 system, Figure 10.4, forming the chemically activated 2MF5OOj* radical. Several modifications are made to these reactions systems. Species MF5Yj(COO) and MF2CjH25Q are removed from consideration as wells because further reaction had reaction barriers that were less than 1 kcal mol^{-1}. Comparison to calculations that included the wells showed this assumptions did not affect the calculate rate constants for chemical activation. Activation energies for TS II 2 and TS VI 2 are also set to 1.0 kcal mol^{-1} to include some type of barrier for reaction. MF45Y(CjCOOj), MF45Y(CCO)5Oj, and CC(=O)CH=CHCO2j are included in these calculations, but their rates are extremely low so they are not included in Figures 10.7 and 10.8.

Results of the chemical activation kinetic calculations show that favored product distributions are for loss of oxygen (2MF5Oj + O), ring opening and loss of CO_2 (CC(=O)CH=CjH), and ring expansion (Y(OC(C)=CCjOC(=O))) across the temperatures and pressures considered in Figures 10.7 and 10.8. This is consistent with the two lowest energy barriers described in the PE diagram in Figure 10.4.

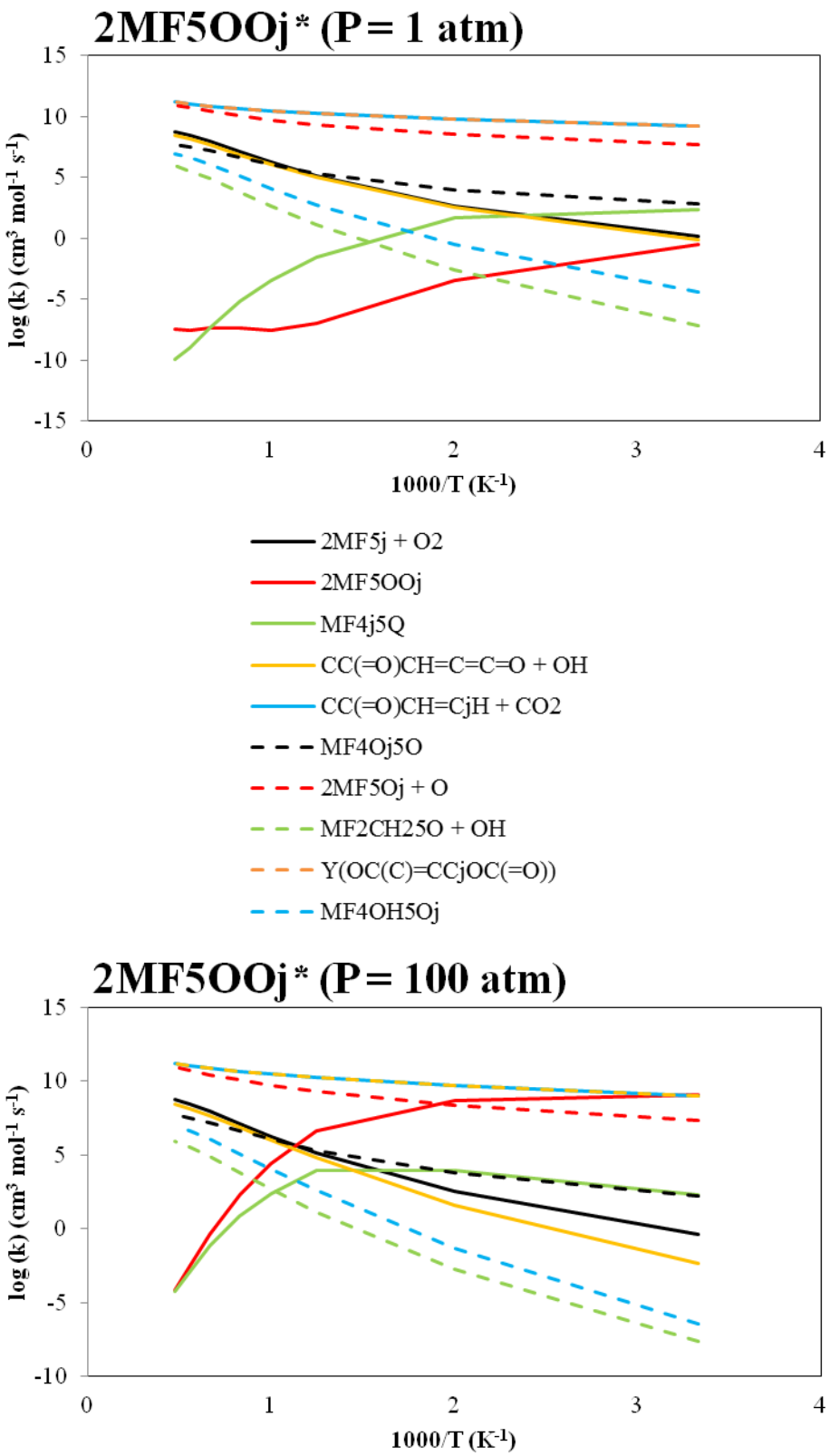

Figure 10.7 Chemical activation rate constants vs. temperature for chemically activated 2MF5OOj* radical at pressures of 1 and 100 atm.

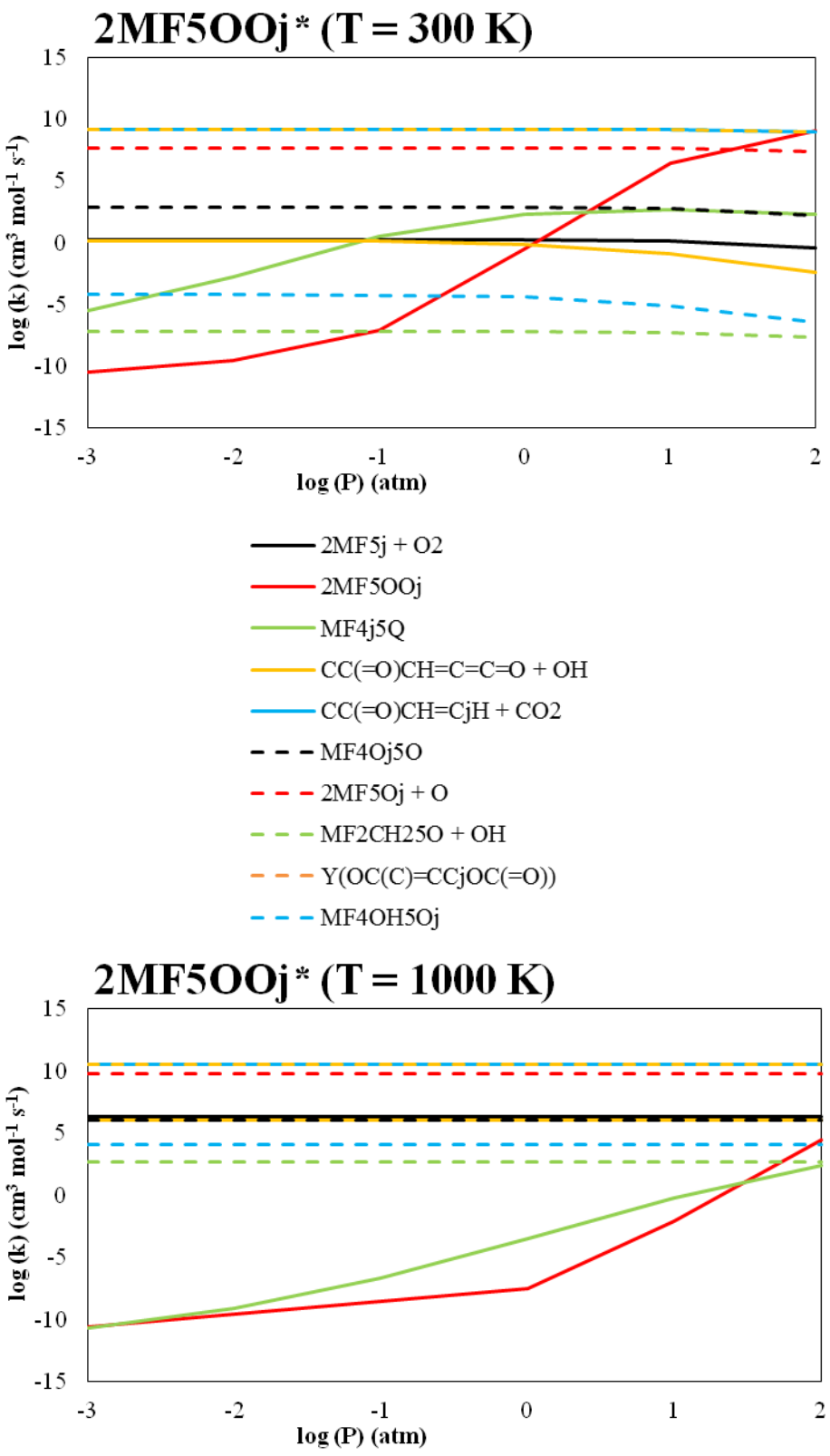

Figure 10.8 Chemical activation rate constants vs. pressure for chemically activated 2MF5OOj* radical at temperatures of 300 and 1000 K.

10.4.5.2 Isomerization and Dissociation Analysis: 2MF5OOj. Rate constants for isomerization and dissociation of the stabilized 2MF5OOj are illustrated in Figures 10.9 and 10.10. Under the conditions of constant pressure (1 and 100 atm) and temperature (300 and 1000 K), the important channels for 2MF5OOj reaction are CC(=O)CH=CHCO2j, 2MF5Oj + O, and MF45Y(CCO)5Oj. Formation of 2MF5Oj is the second lowest energy barrier in Figure 10.4 while the lowest (through TS III 1) generates the other two favored products CC(=O)CH=CHCO2j and MF45Y(CCO)5Oj. These will each generate CC(=O)CH=CjH and the six-member ring Y(OC(C)=CCjOC(=O)) depicted in Figures 10.11 and 10.12, which shows the rate constants for the channels described in this chemical activation analysis.

Reactions over the next highest energy barriers are for isomerization to MF4j5Q and MF45Y(CjCOOj) depicted in Figures 10.13 and 10.14. Figure 10.13 illustrates a slight preference for 2MF5OOj reformation and CC(=O)CH=C=C=O + OH product formation from MF4j5Q over hydroxyl group transfer and formation of MF4OH5Oj. In Figure 10.14, ring opening to MF4Oj5O is more important than ring opening back to 2MF5OOj for MF45Y(CjCOOj).

Dissociation of 2MF5OOj back to the original 2MF5j + O_2 reactants along with hydroxyl dissociation to MF2CH25O have the lowest rates at constant temperature and pressure. Formation of both products results in going through transition states with 50.6 and 58.2 kcal mol^{-1} barriers accounting for their relative decreased rates. Overall, both the chemical activation and isomerization and dissociation analysis conclude that Pathways III, IV, and VI are the major product channels for 2MF5OOj across the temperature and pressures considered in this analysis.

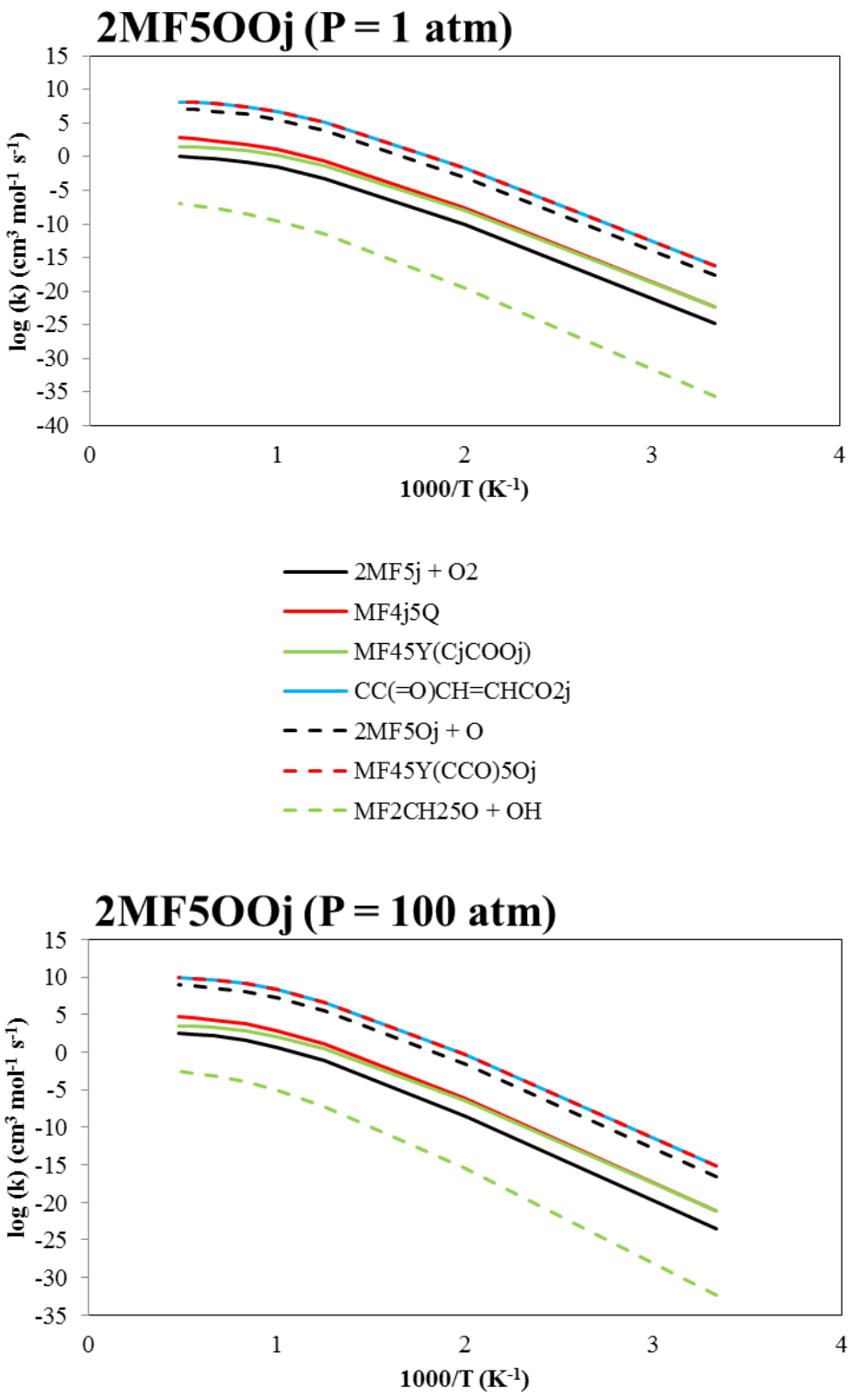

Figure 10.9 Rate constants vs. temperature for 2MF5OOj dissociation at pressures of 1 and 100 atm.

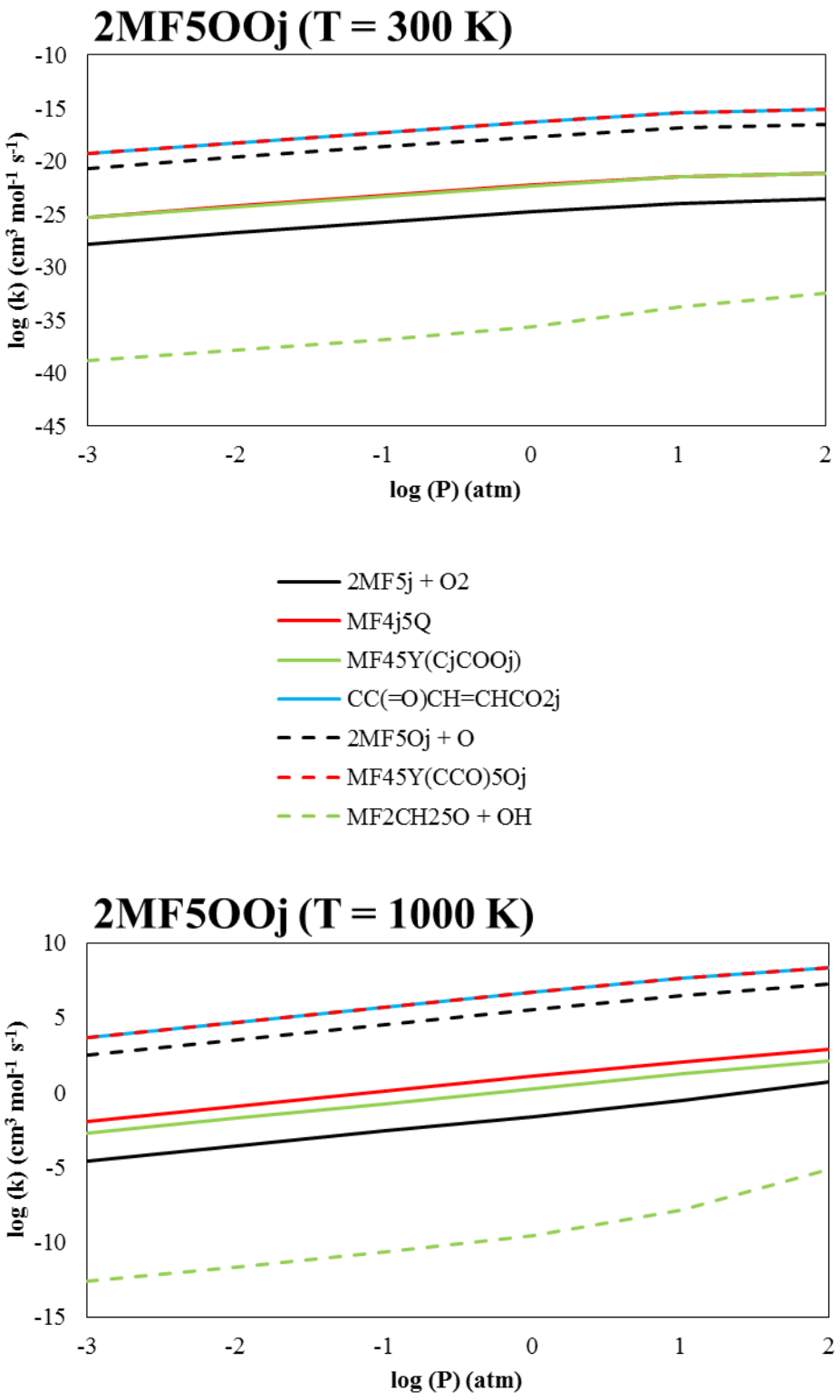

Figure 10.10 Rate constants vs. pressure for 2MF5OOj dissociation at temperatures of 300 and 1000 K.

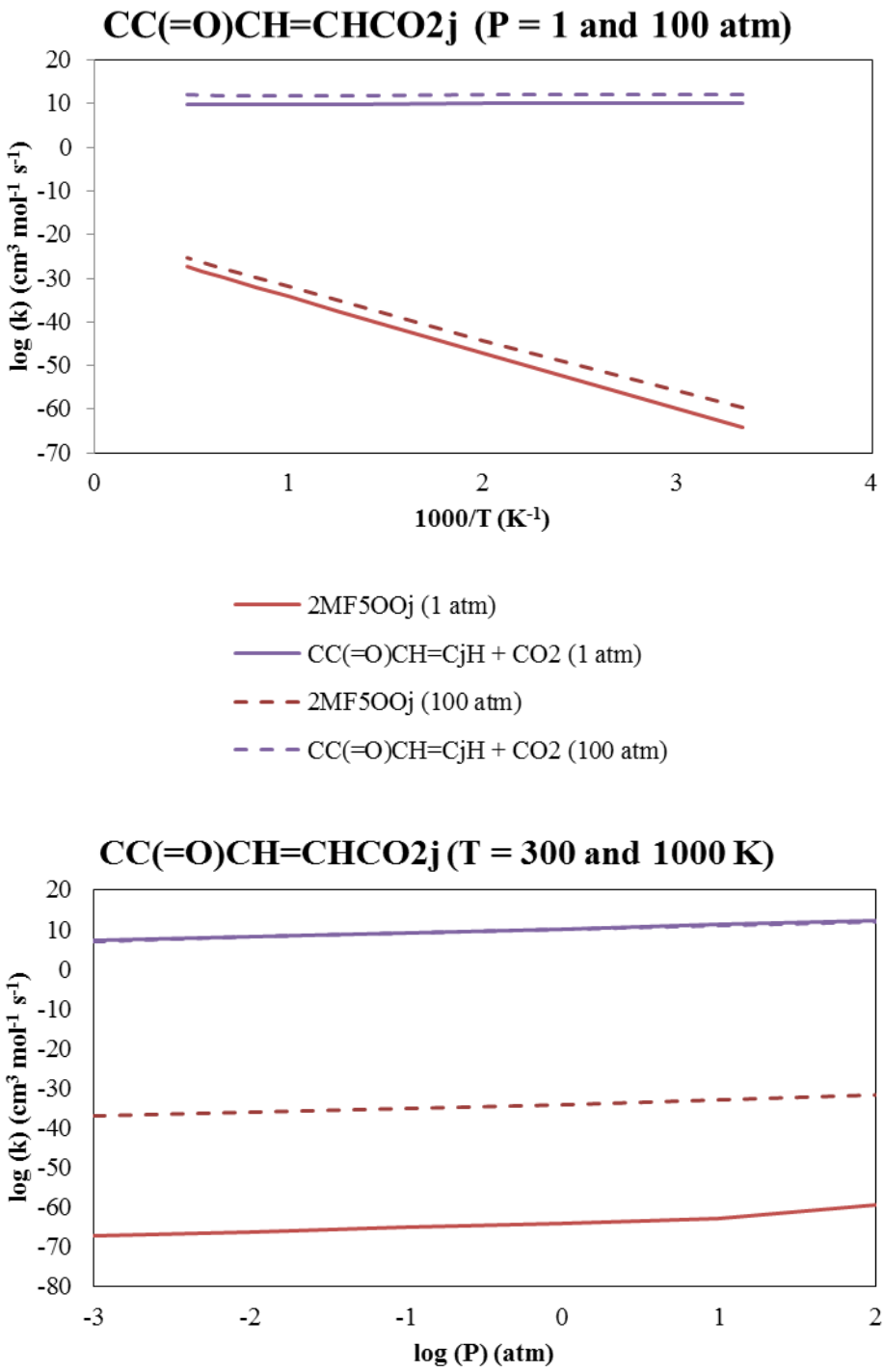

Figure 10.11 Dissociation rate constants of CC(=O)CH=CHCO2j at constant pressure and temperature.

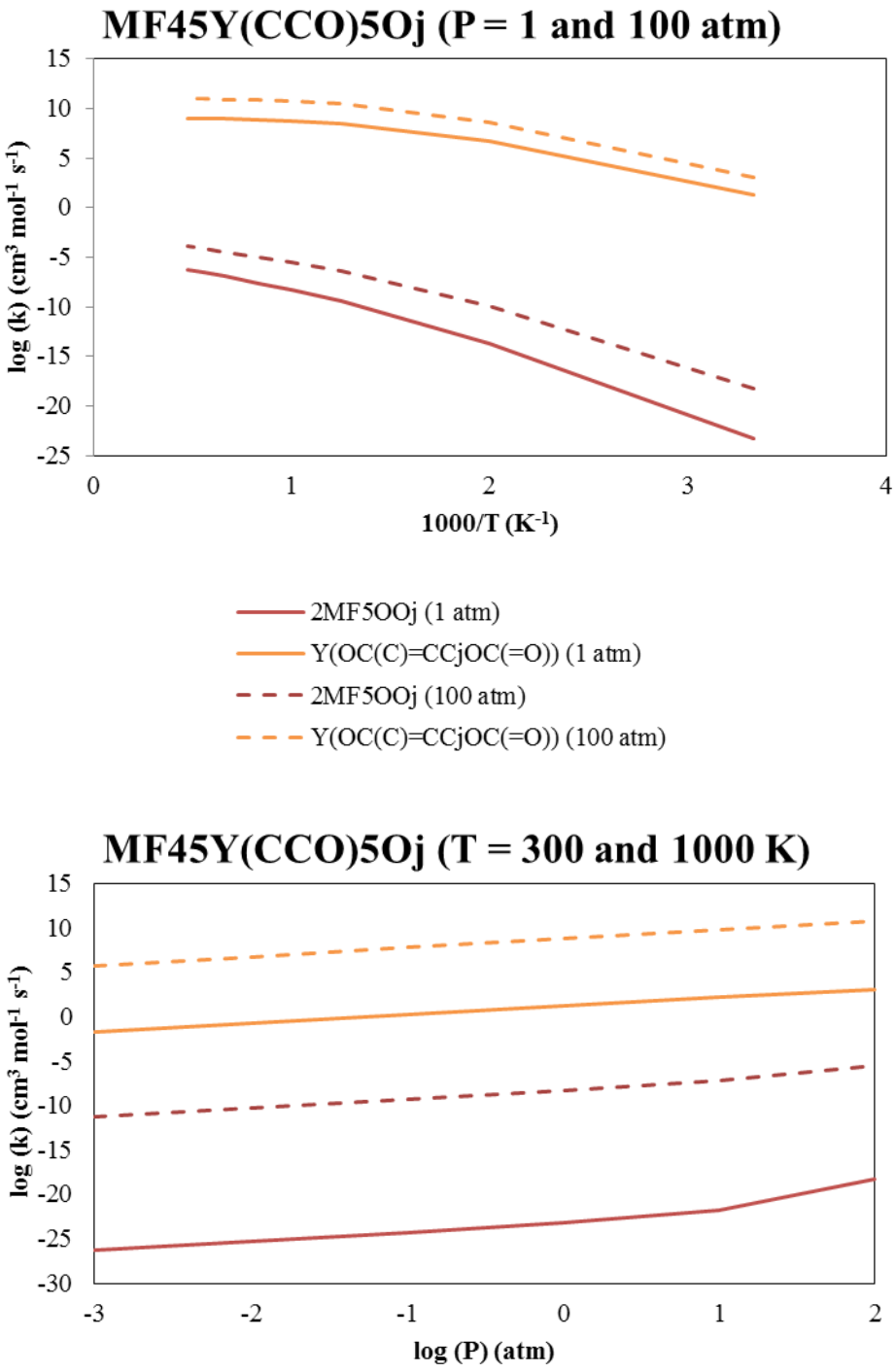

Figure 10.12 Dissociation rate constants of MF45Y(CCO)5Oj at constant pressure and temperature.

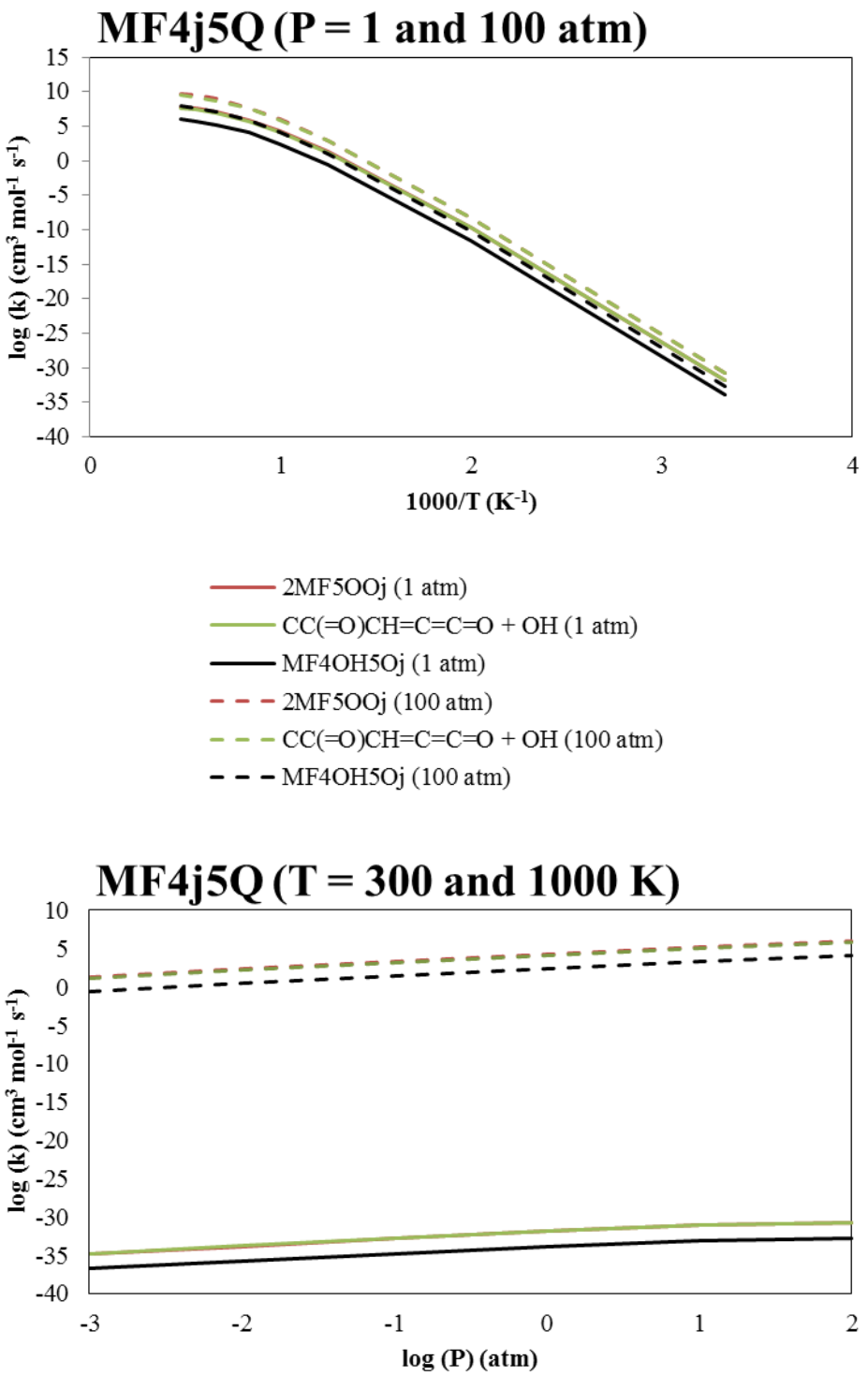

Figure 10.13 Dissociation rate constants of MF4j5Q at constant pressure and temperature.

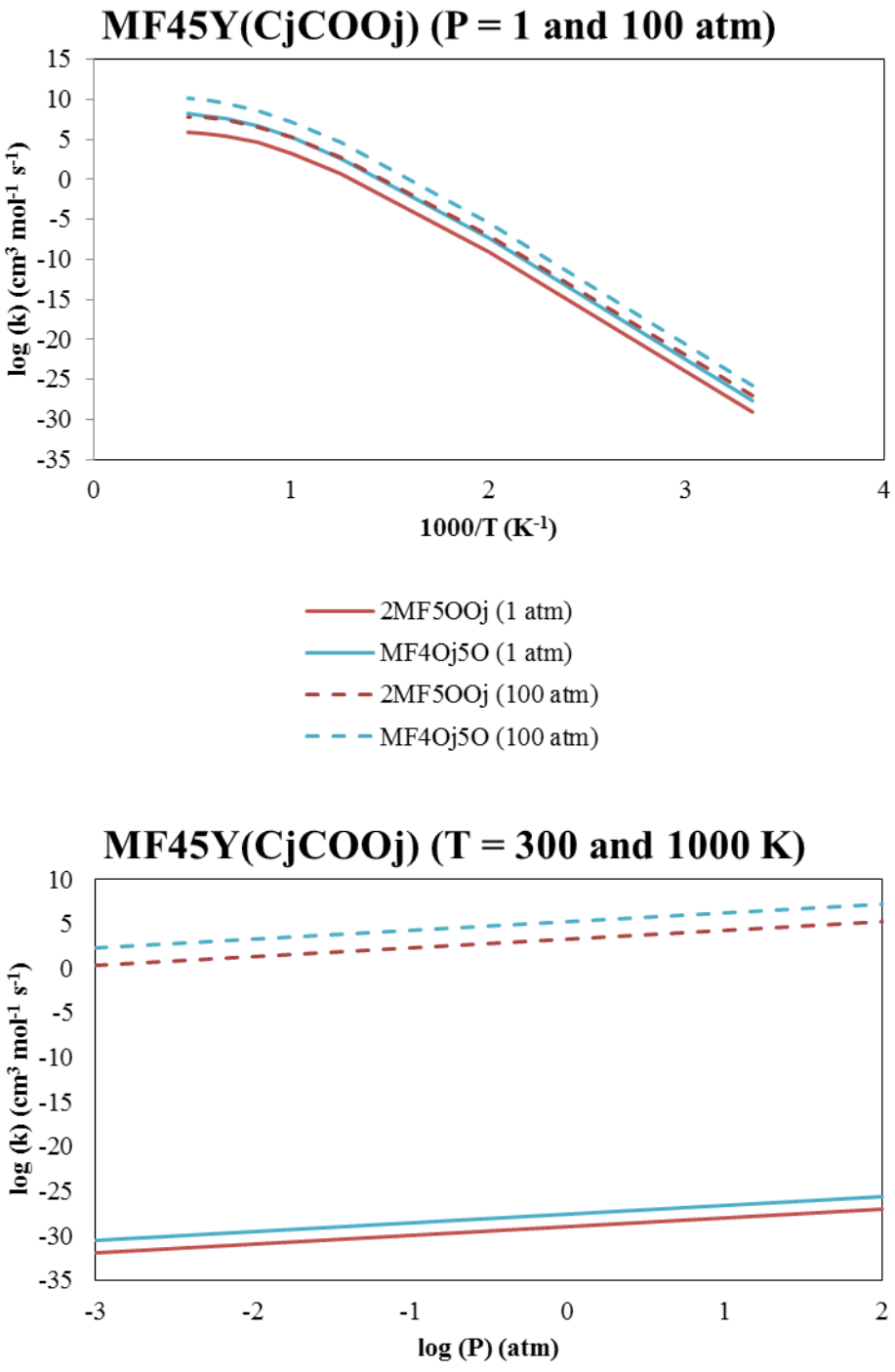

Figure 10.14 Dissociation rate constants of MF45Y(CjCOOj) at constant pressure and temperature.

10.5 Conclusions

A detailed study of the oxidation of 2MF5j including the thermochemistry and kinetics of stable and transition state species are analyzed using theoretical methods. Enthalpies, entropies, and heat capacities are determined for all species. Elementary rate parameters are fit to a three-parameter form of the Arrhenius equation and then a QRRK analysis, along with master equation for falloff and stabilization, is used to calculate temperature- and pressure-dependent rate constants.

The resulting 2MF5OOj radical has a well depth of 50.6 kcal mol^{-1} below the 2MF5j + O_2 entrance channel. Reaction pathways analyzed include intramolecular abstraction and group transfers, dissociations, and radical peroxy oxygen additions leading to ring opening or expansion. The important products formed from the chemical activation reaction to the 2MF5OOj* peroxy radical are: dissociation of a peroxy oxygen atom (2MF5Oj), ring opening and subsequent CO_2 loss (CC(=O)CH=CjH), and ring expansion (Y(OC(C)=CCjOC(=O))) from the three-member ring formed via ipso addition of the radical peroxy oxygen. 2MF5Oj, CC(=O)CH=CjH, and Y(OC(C)=CCjOC(=O)) are calculated to be 38, 113, and 129 kcal mol^{-1}, respectively, lower than the initial entrance channel. Isomerization and dissociation analysis of the stabilized 2MF5OOj radical confirm the chemical activation findings with formation of 2MF5Oj, CC(=O)CH=CHCO2j, and MF45Y(CCO)5Oj. The latter two species are shown to further dissociate to CC(=O)CH=CjH + CO_2 and isomerize to Y(OC(C)=CCjOC(=O)).

Overall, Pathways III, IV, and VI are the major product channels for 2MF5OOj across the temperatures and pressures considered. This initial set of thermochemical and kinetic parameters can serve as a basis for other furan-based oxidation systems.

APPENDIX A

CALCULATION OF HEAT OF FORMATIONS AND BOND DISSOCIATION ENERGIES

This appendix contains sample calculations for enthalpies of formation, $\Delta H^{\circ}_{f\ 298}$, and carbon-hydrogen bond dissociation energies (C–H BDE). An example of the work reactions used to calculate the $\Delta H^{\circ}_{f\ 298}$ for unknown target species, CJCCCCCC, is presented in Table A.1. These reactions relate the calculated energies for all four species to known literature $\Delta H^{\circ}_{f\ 298}$ values for the non-target species using Hess's Law, see equations 2.13 and 2.14. Due to the error cancelling in these isodesmic reactions, accurate $\Delta H^{\circ}_{f\,298}$ values can be calculated.

Table A.1 Calculation of $\Delta H^{\circ}_{f\,298}$ and C–H Bond Dissociation Energies for CJCCCCCC.

Isodesmic Work Reaction	CJCCCCCC	+	CH_3CH_3	→	*n*-C_7H_{16}	+	CH_3CJH_2
H_{298} B3LYP/6-31G(d,p) (Hartree)	-275.534013		-79.759382		-276.192833		-79.100870
$\Delta H^{\circ}_{f\,298}$ Literature (kcal mol^{-1})	X		-20.00		-45.05		29.00
ΔH°_{rxn} (kcal mol^{-1})	-0.19						
$\Delta H^{\circ}_{f\,298}$ (kcal mol^{-1})	**4.15**						
Bond Dissociation Reaction			*n*-C_7H_{16}	→	CJCCCCCC	+	H
$\Delta H^{\circ}_{f\,298}$ (kcal mol^{-1})			-45.05		4.15		52.10
C–H Bond Dissociation Energy (kcal mol^{-1})	**101.3**						

Based on the example in Table A.1, all of the species are first optimized using the same method and basis set, B3LYP/6-31G(d,p). Enthalpies, H_{298}, are calculated in Gaussian 03 or 09 according to equations in A.1 as the sum of the total electronic energy, E, and thermal enthalpy corrections, H_{Corr}, in units of Hartrees.

$$H_{298} = E + H_{Corr} \quad \text{(A.1)}$$
$$H_{Corr} = E_{Corr} + k_B T$$
$$E_{Corr} = E_{Trans} + E_{Rot} + E_{Vib} + E_{Elec} + E_{ZPVE}$$

H_{Corr} includes the sum of an energy correction, E_{Corr}, and the product of Boltzmann's constant and the temperature in Kelvin. E_{Corr} includes corrections from translational (E_{Trans}), rotational (E_{Rot}), vibrational (E_{Vib}), and electronic (E_{Elec}) motions along with the zero-point vibration energy (E_{ZPVE}). These quantities are derived from the molecular partition functions using standard statistical mechanics.

The difference in the H_{298} energies for the products and reactants, ΔH°_{rxn}, is calculated using Hess's Law and reported in units of kcal mol^{-1} using the conversion of one Hartree equal 627.509 kcal mol^{-1}. Combining the ΔH°_{rxn} with the known literature $\Delta H^{\circ}_{f\,298}$ values generates the $\Delta H^{\circ}_{f\,298}$ value for the target species.

The C–H bond dissociation reaction has the parent species and sets it equal to the radical and H atom. The difference between the literature $\Delta H^{\circ}_{f\,298}$ value for the parent, *n*-C_7H_{16}, species and the H atom with the previously calculated $\Delta H^{\circ}_{f\,298}$ value for radical, CJCCCCCC, species determines the energy needed to remove a H atom from *n*-C_7H_{16} to generate CJCCCCCC. Similar types of bond dissociation reactions can also be utilized to determine oxygen-hydrogen (O–H) and oxygen-oxygen (O–O) BDEs.

APPENDIX B

THERMOCHEMISTRY AND BOND DISSOCIATION ENERGIES OF C_7H_{16} ISOMERS

This appendix contains the optimized geometries with corresponding Gaussian atom numbering and symmetry values in parenthesis, moments of inertia, vibrational frequencies, internal rotor potential energy graphs, entropies, and heat capacities for all of the parent and radical species from B3LYP/6-31G(d,p) level of theory.

Table B.1 *n*-C_7H_{16} Optimized Species

n-C_7H_{16} (σ = 18)

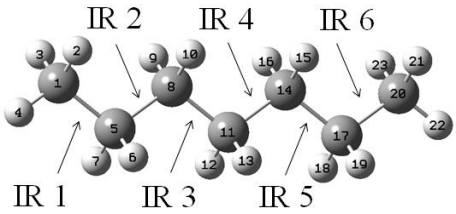

C,0,-0.0116195267,0.0712143561,-0.0094345107
H,0,0.0078003149,0.1178971467,1.0853907131
H,0,1.0262051398,0.1166917722,-0.3587917013
H,0,-0.5233380819,0.9690983197,-0.3710362823
C,0,-0.7042278432,-1.204949686,-0.4967812035
H,0,-1.750280862,-1.2050085734,-0.1612340939
H,0,-0.7393839031,-1.2062045858,-1.5947708654
C,0,-0.0192246039,-2.4888975601,-0.0126615611
H,0,1.0279424816,-2.4885228783,-0.3479849169
H,0,0.016518942,-2.4873249765,1.0863019051
C,0,-0.7057039542,-3.7722131331,-0.4956778958
H,0,-0.7412877712,-3.7728128087,-1.5945728526
H,0,-1.752753149,-3.7716130363,-0.1602314586
C,0,-0.0202364211,-5.0555292401,-0.0112281374
H,0,0.0155063491,-5.055902524,1.0877364182
H,0,1.0269298963,-5.0571040666,-0.3465503953
C,0,-0.7062519288,-6.3394765771,-0.4939137166
H,0,-0.7414071414,-6.3394204907,-1.5919041194
H,0,-1.7523045309,-6.3382180345,-0.1583676571
C,0,-0.0146500222,-7.6156411551,-0.0051412605
H,0,0.0047335475,-7.6611160107,1.089735442
H,0,-0.5270767094,-8.5135247177,-0.3657398342
H,0,1.0231382825,-7.6623273296,-0.3544470309

CJCCCCCC (σ = 3)

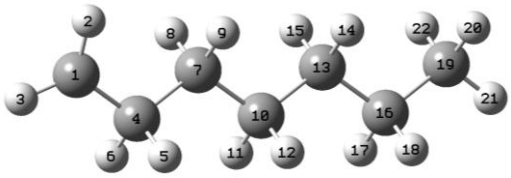

C,0,0.,0.,0.
H,0,0.,0.,1.08595119
H,0,0.9616820825,0.,-0.5021715176
C,0,-1.2653627845,0.2109312319,-0.7595078562
H,0,-1.4151705646,1.2902678673,-0.9552022417
H,0,-1.1829220669,-0.2448251602,-1.7569777726
C,0,-2.5164371608,-0.3282678635,-0.046396593
H,0,-2.3939036829,-1.4054877033,0.1277615178
H,0,-2.5882760058,0.1346056692,0.9478985398
C,0,-3.8153413596,-0.0769731559,-0.8205505589
H,0,-3.7395721195,-0.538276812,-1.8156686884
H,0,-3.9303562659,1.0023436842,-0.9962588513
C,0,-5.0652122026,-0.6104012413,-0.1102499771
H,0,-5.1428483404,-0.14853359,0.8844946708
H,0,-4.9501935558,-1.6894527263,0.0665210692
C,0,-6.3654362381,-0.3615994854,-0.8846953391
H,0,-6.2879756553,-0.8232090261,-1.8784907554
H,0,-6.4804259203,0.7166820055,-1.0605570118
C,0,-7.6084248655,-0.8977803861,-0.1682827408
H,0,-7.7313419732,-0.4301856867,0.8152841876
H,0,-8.5189467149,-0.7034515324,-0.7444288266
H,0,-7.5391262512,-1.9802507714,-0.0113586037

Table B.1 *n*-C_7H_{16} Optimized Species (Continued)

CCJCCCCC (σ = 9)

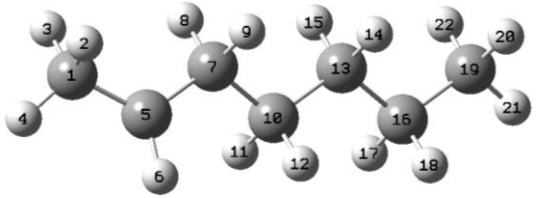

C,0,-0.0002837047,-0.0003127493,0.001452597
H,0,-0.0011558228,-0.0030082341,1.1063551728
H,0,1.0551919863,0.0009485517,-0.3013605356
H,0,-0.4432475058,0.9512049216,-0.310469027
C,0,-0.7329457102,-1.1691558347,-0.5669550345
H,0,-1.800546415,-1.0713133893,-0.7557569363
C,0,-0.1419622651,-2.5417187555,-0.5618591767
H,0,0.9204437847,-2.4862807735,-0.8476867265
H,0,-0.1322706712,-2.9496692938,0.4682560167
C,0,-0.8703555369,-3.539779172,-1.4748782747
H,0,-0.8618809657,-3.1565501668,-2.5040670597
H,0,-1.9274413787,-3.5905817019,-1.1780980639
C,0,-0.2670584725,-4.9483805454,-1.4467867218
H,0,-0.2726271227,-5.3262775489,-0.4141155701
H,0,0.7905446898,-4.8970460176,-1.7432856802
C,0,-0.9963977785,-5.947010515,-2.3538153042
H,0,-0.9911259384,-5.5687175402,-3.3851168763
H,0,-2.0526775342,-6.0002346934,-2.0568896822
C,0,-0.3860604203,-7.3513850536,-2.3218187853
H,0,-0.4102147483,-7.7709790248,-1.3096054483
H,0,-0.9274708366,-8.0393751954,-2.9793249691
H,0,0.6606159957,-7.3360026742,-2.6464910875

CCCJCCCC (σ = 9)

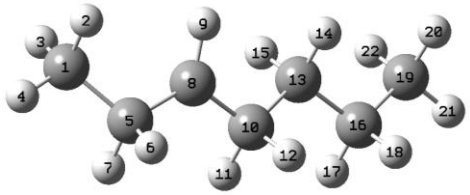

C,0,-0.0014842811,0.0004936108,0.0010939627
H,0,-0.002248668,-0.0004199333,1.096754984
H,0,1.0422930005,0.0021343547,-0.3292048221
H,0,-0.4636823453,0.9353361879,-0.3313604509
C,0,-0.7506932921,-1.2204881775,-0.5487300669
H,0,-1.813796493,-1.1478942226,-0.2488195922
H,0,-0.7688819791,-1.182225472,-1.6484075946
C,0,-0.1788439822,-2.5275833927,-0.103111416
H,0,0.3047595247,-2.5688280639,0.8728411224
C,0,-0.5387532701,-3.8179855109,-0.7652492574
H,0,-0.5599995894,-3.6799710823,-1.8577715692
H,0,-1.5747665163,-4.1081531921,-0.5005259318
C,0,0.3983663629,-4.9830222671,-0.4114779621
H,0,0.4105380805,-5.1153383645,0.6797099575
H,0,1.4254139732,-4.7173784311,-0.6961511437
C,0,0.0088724106,-6.3073364318,-1.0777952044
H,0,-0.0029434054,-6.1739318533,-2.1682077995
H,0,-1.0205700232,-6.5659555866,-0.7940975172
C,0,0.9446964368,-7.4641583047,-0.7152252888
H,0,0.9498082035,-7.6456423348,0.3655950394
H,0,0.6417573346,-8.39443217,-1.2067029309
H,0,1.9759708695,-7.2491798242,-1.0174365809

CCCCJCCC (σ = 9)

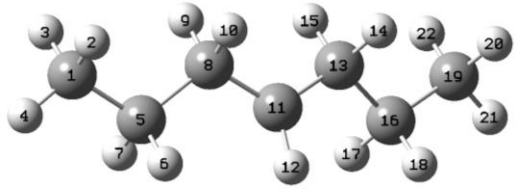

C,0,-0.0008352347,0.0001310648,0.0016448165
H,0,-0.0018551031,-0.0005803922,1.0977284315
H,0,1.044948405,0.0005576557,-0.326356544
H,0,-0.4526037097,0.9404622594,-0.3304014383
C,0,-0.7556944468,-1.2100827224,-0.5541962804
H,0,-1.8070890634,-1.1629910447,-0.2402116605
H,0,-0.7639056073,-1.1707991195,-1.6507954394
C,0,-0.1603014696,-2.5540760254,-0.1059139266
H,0,0.8962952557,-2.609069677,-0.4115941106
H,0,-0.1320446484,-2.5709056703,1.0016419796
C,0,-0.8953376294,-3.7479593485,-0.6230213796
H,0,-1.9706508646,-3.6599380514,-0.7782739522
C,0,-0.2980802748,-5.1176294883,-0.6050485117
H,0,-0.2905134231,-5.5194228662,0.4275533449
H,0,0.7644779909,-5.0617009454,-0.8891316803
C,0,-1.0199577198,-6.1270438481,-1.5115491841
H,0,-1.0101294771,-5.7521137374,-2.5427965638
H,0,-2.0766936494,-6.1793342287,-1.2169146668
C,0,-0.4054527782,-7.5283033985,-1.4641728724
H,0,-0.4284340591,-7.9376354341,-0.4476493938
H,0,-0.9451512608,-8.2240241016,-2.114765277
H,0,0.6410776314,-7.5139821842,-1.7894688917

Table B.2 C_2CCCCC Optimized Species

C_2CCCCC ($\sigma = 27$)

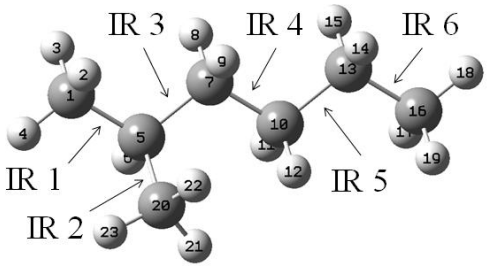

C,0,2.8188938156,-0.9056310946,-0.0518240442
H,0,2.9567712935,-1.0362625924,1.0243233923
H,0,2.6551716318,-1.8929308023,-0.4866488119
H,0,3.7515183345,-0.5111344321,-0.4583236238
C,0,1.643055496,0.0345403017,-0.3409381157
H,0,1.5463114274,0.1224517736,-1.4289277781
C,0,0.3300420061,-0.5624299674,0.1941222322
H,0,0.2513243832,-1.5957654698,-0.1581024914
H,0,0.3882994788,-0.6209276848,1.286927155
C,0,-0.944819917,0.1856612504,-0.2062227471
H,0,-0.9755392326,0.2888382756,-1.2960934337
H,0,-0.925568023,1.2025377846,0.1940672925
C,0,-2.2258061322,-0.5067811979,0.2676427768
H,0,-2.1929900569,-0.617956006,1.3553230468
H,0,-2.2572191508,-1.5219326472,-0.1383306043
C,0,-3.4996635251,0.2404315641,-0.1294439059
H,0,-3.5772194528,0.3386468664,-1.2139641373
H,0,-4.3927872918,-0.2786077031,0.2205363889
H,0,-3.5144777455,1.2468496832,0.2932004489
C,0,1.9241317049,1.4339811335,0.2195846099
H,0,1.1357649356,2.1427735188,-0.0321999311
H,0,2.0106737967,1.404158528,1.3087981514
H,0,2.8610142237,1.8311519176,-0.1743818701

CJ_2CCCCC ($\sigma = 9$, OI)

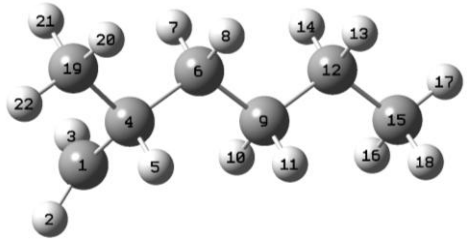

C,0,0.0001289134,-0.0006349579,0.0004069476
H,0,0.0015225806,-0.010210871,1.0858437648
H,0,0.964478739,0.0101844684,-0.50087091
C,0,-1.2504302017,-0.2841882377,-0.771493201
H,0,-2.1005892588,0.1519791518,-0.224302735
C,0,-1.2187970809,0.343585996,-2.1800203954
H,0,-0.3510268013,-0.0576087522,-2.724631392
H,0,-2.1058471583,0.0134443382,-2.737872316
C,0,-1.1606893938,1.8756782451,-2.1828603798
H,0,-0.2851949512,2.2074699678,-1.6085869876
H,0,-2.0375065027,2.2712743945,-1.6499101902
C,0,-1.1079238959,2.483442053,-3.589654278
H,0,-1.9831574073,2.1486350024,-4.1632719161
H,0,-0.2306490734,2.0895216829,-4.1208845705
C,0,-1.0562629828,4.0142383191,-3.5850098008
H,0,-0.173568276,4.3787457438,-3.0473230016
H,0,-1.0161360368,4.417918343,-4.6019992773
H,0,-1.9389865235,4.4389401036,-3.0934221876
C,0,-1.5089654216,-1.8097698099,-0.8610322053
H,0,-2.4558951467,-2.0149963072,-1.3740295529
H,0,-0.7069356532,-2.3072795095,-1.4173315159
H,0,-1.5563750207,-2.2626417058,0.1340875199

$C_2CJCCCC$ ($\sigma = 54$)

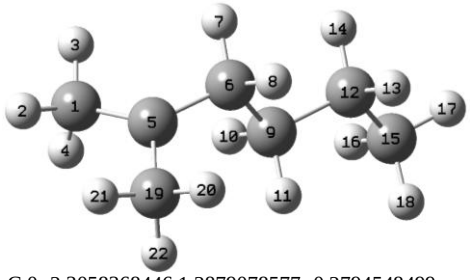

C,0,-2.3058368446,1.2879078577,-0.2794548499
H,0,-3.4029101764,1.2584632731,-0.2645566106
H,0,-1.9806711197,2.1396479473,0.3288950931
H,0,-2.0219097866,1.5181598925,-1.3223760857
C,0,-1.714043584,0.0000770025,0.2050344218
C,0,-0.347605371,-0.0012564153,0.8258425548
H,0,-0.2346502371,0.8789571156,1.4755024689
H,0,-0.2350551307,-0.8836496626,1.4726084548
C,0,0.8222110842,0.0001464454,-0.1915856242
H,0,0.733563603,0.8797049675,-0.8436761335
H,0,0.7331581031,-0.877221032,-0.8465662823
C,0,2.2021127874,-0.0012718689,0.476939957
H,0,2.2848294285,-0.8794847066,1.1318206527
H,0,2.2852341988,0.8747425786,1.1347075275
C,0,3.3605469013,0.0001090956,-0.5249270196
H,0,3.3251447811,0.8847452261,-1.1709717805
H,0,4.3304793477,-0.0009523496,-0.0167356539
H,0,3.3247351485,-0.8823789386,-1.1738805431
C,0,-2.306457123,-1.2858916372,-0.2836248583
H,0,-1.9816997818,-2.1397554891,0.3219595401
H,0,-3.403516238,-1.2559675464,-0.2686267564
H,0,-2.0226439908,-1.5128977558,-1.3272884729

Table B.2 C_2CCCCC Optimized Species (Continued)

$C_2CCJCCC$ ($\sigma = 27$)

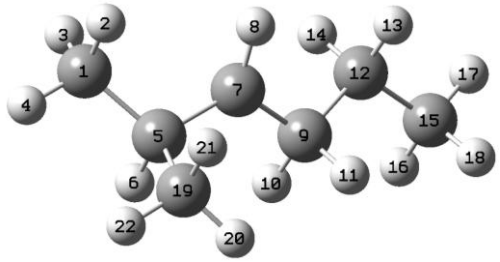

C,0,0.,0.,0.
H,0,0.,0.,1.09670875
H,0,1.0425168964,0.,-0.3332023113
H,0,-0.4643041422,0.935069055,-0.3315703083
C,0,-0.7588775751,-1.2219907453,-0.5434663677
H,0,-0.7335717588,-1.1795745459,-1.6436644634
C,0,-0.1134326661,-2.506925591,-0.1135315634
H,0,0.2821943608,-2.5582302592,0.9017627052
C,0,-0.2928983799,-3.790701157,-0.8576666195
H,0,-0.3205871872,-3.5910127376,-1.9399508111
H,0,-1.2797685675,-4.2383612292,-0.6276366091
C,0,0.7893077686,-4.8409707411,-0.5564966694
H,0,0.8107997529,-5.0307567139,0.5249948772
H,0,1.7719537023,-4.4245589422,-0.8115073788
C,0,0.5747037622,-6.1594518011,-1.3040861933
H,0,0.5806124795,-6.0058949774,-2.3892791635
H,0,1.359145087,-6.8856709519,-1.0678174101
H,0,-0.3880803,-6.6126872508,-1.0413317619
C,0,-2.2494118873,-1.1639159955,-0.1252211151
H,0,-2.8114154725,-2.0109482424,-0.5311816878
H,0,-2.3463979756,-1.1885095942,0.9661058179
H,0,-2.7211180569,-0.2420452516,-0.4852090314

$C_2CCCJCC$ ($\sigma = 27$)

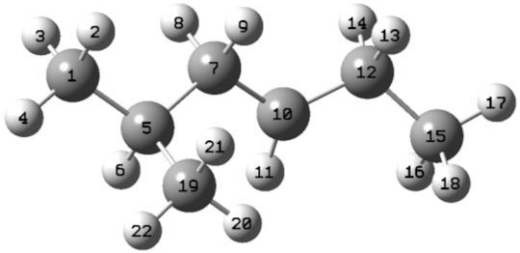

C,0,-0.0000767608,0.0000415726,0.0000195486
H,0,-0.0001921111,0.0000859405,1.097024044
H,0,1.0439714412,0.0000943301,-0.3320318508
H,0,-0.4570932189,0.939178045,-0.3298300346
C,0,-0.7635358538,-1.2130724783,-0.5471077885
H,0,-0.7244970757,-1.1690942705,-1.6460998017
C,0,-0.0873837061,-2.5328226206,-0.1166877886
H,0,0.99394956,-2.4546647199,-0.3428093337
H,0,-0.1405888156,-2.6263088015,0.9795910362
C,0,-0.6524231926,-3.7594687234,-0.7567270353
H,0,-0.9714709938,-3.6892588946,-1.7971587906
C,0,-0.4585098799,-5.1233263933,-0.1766977781
H,0,-0.5859209927,-5.0800853027,0.9152878853
H,0,0.5875813404,-5.454558581,-0.3236841924
C,0,-1.3958108696,-6.184818551,-0.7675346073
H,0,-1.2589432497,-6.2693746927,-1.8513358907
H,0,-1.20763744,-7.1705010031,-0.3304018452
H,0,-2.4442839298,-5.9276879396,-0.5852408516
C,0,-2.2384549254,-1.1735580425,-0.1241650183
H,0,-2.787717096,-2.0352055969,-0.5160973172
H,0,-2.3282588435,-1.1921755729,0.969183139
H,0,-2.7309607676,-0.2630230773,-0.4823398481

Table B.2 C_2CCCCC Optimized Species (Continued)

$C_2CCCCJC$ ($\sigma = 27$)

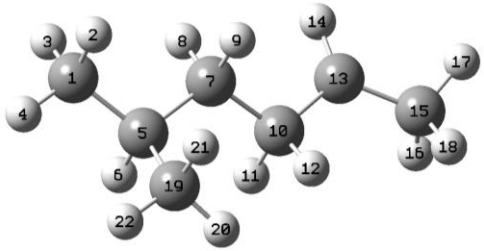

C,0,-0.0000793103,-0.0000491507,0.0001239915
H,0,-0.0002824753,-0.0000901505,1.0970821686
H,0,1.0440241935,-0.0000170092,-0.3313641899
H,0,-0.457009346,0.939132315,-0.3301187497
C,0,-0.7633515217,-1.2148659289,-0.5476326313
H,0,-0.7295396357,-1.1647742777,-1.646889103
C,0,-0.0723340593,-2.5238378389,-0.1207592059
H,0,0.9945742051,-2.4544173766,-0.3746028914
H,0,-0.1178079248,-2.616138007,0.9736303244
C,0,-0.6377856163,-3.8034533207,-0.7589097824
H,0,-0.6693277012,-3.6628406497,-1.8578967421
H,0,-1.6874295331,-3.947634202,-0.464764575
C,0,0.1402571008,-5.0341188142,-0.4206343236
H,0,1.2108571807,-4.9326151197,-0.2513163399
C,0,-0.4191039327,-6.399571515,-0.6411977605
H,0,-0.4259717681,-6.6815304303,-1.7095118584
H,0,0.1592081034,-7.1677666486,-0.1175178187
H,0,-1.4612921051,-6.4690743338,-0.3022603211
C,0,-2.2378175379,-1.1608293298,-0.1197583611
H,0,-2.8249180552,-1.9735394467,-0.557927455
H,0,-2.3293045209,-1.23368464,0.9711640822
H,0,-2.7011793961,-0.2172635524,-0.4279162485

$C_2CCCCCJ$ ($\sigma = 9$)

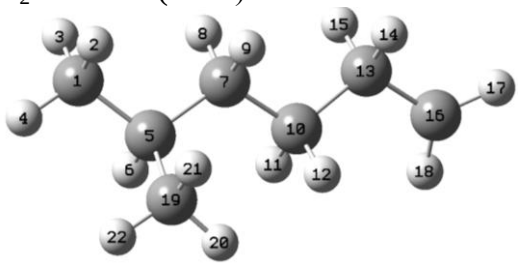

C,0,-0.0000149426,0.0000064494,-0.0000040299
H,0,-0.0000026665,0.0000050047,1.0969813361
H,0,1.0441508104,0.0000168325,-0.3313868928
H,0,-0.4569390689,0.9390937328,-0.3303806634
C,0,-0.7626160523,-1.2153079062,-0.5477416229
H,0,-0.723636734,-1.1678009785,-1.6468430757
C,0,-0.0740534322,-2.5245150342,-0.1145626843
H,0,0.995710237,-2.4521580512,-0.3572946904
H,0,-0.1291428035,-2.6090677336,0.9812917608
C,0,-0.6330360813,-3.8028059216,-0.7515716681
H,0,-0.6238853159,-3.699228868,-1.8460632569
H,0,-1.6818782413,-3.9459280907,-0.46627823
C,0,0.1587575391,-5.0635076013,-0.3636682883
H,0,0.1633464941,-5.175334538,0.7303095759
H,0,1.2202924961,-4.9043884059,-0.6346449324
C,0,-0.3493581523,-6.3130058157,-0.9984925309
H,0,-0.1464171394,-7.2857894562,-0.5631733901
H,0,-0.7933459689,-6.2886835378,-1.9892844476
C,0,-2.2389400661,-1.1591472683,-0.126714003
H,0,-2.823301692,-1.9749845449,-0.5623241763
H,0,-2.3353603601,-1.2247088106,0.9643100253
H,0,-2.7010673664,-0.2176215684,-0.4428739688

Table B.3 $C_2CC(C)CC$ Optimized Species

$C_2CC(C)CC$ ($\sigma = 81$, OI)

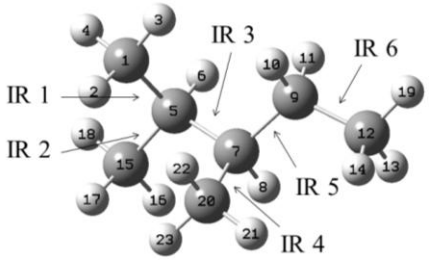

C,0,-0.0004782242,0.0001056662,0.0010125643
H,0,-0.0041728151,0.0021044855,1.0965691837
H,0,1.042428642,-0.0017818497,-0.3304212084
H,0,-0.4471803834,0.9451010951,-0.3266066021
C,0,-0.790034004,-1.1916654067,-0.5650872102
H,0,-0.771284542,-1.1013518574,-1.6614970429
C,0,-0.1604850878,-2.5774442786,-0.2435141572
H,0,-0.8527377773,-3.3249579831,-0.6620745766
C,0,1.1896020609,-2.7699242323,-0.9674387897
H,0,1.9508593249,-2.126826663,-0.5060853067
H,0,1.0844488831,-2.4203045154,-2.0034436798
C,0,1.7020818787,-4.2148700768,-0.9891698359
H,0,0.9686811292,-4.8877500915,-1.4486339992
H,0,1.913210569,-4.5925484398,0.0161570067
C,0,-2.2644688323,-1.1097788472,-0.1389572369
H,0,-2.845739367,-1.9448041914,-0.5459292706
H,0,-2.3766777536,-1.1253701807,0.9508218005
H,0,-2.7207804245,-0.1805881528,-0.4972868126
H,0,2.6290475545,-4.292428885,-1.5668453169
C,0,-0.0414056187,-2.8587798973,1.2637404534
H,0,0.2834046777,-3.8867154196,1.4497388665
H,0,0.6888760505,-2.1943765277,1.7390719065
H,0,-0.9976241353,-2.7265260811,1.7787592038

$CJ_2CC(C)CC$ ($\sigma = 27$, OI)

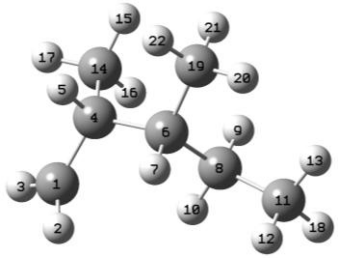

C,0,-0.0000724458,-0.0000388533,0.0000771575
H,0,-0.0002438839,0.0004887926,1.0862618556
H,0,0.9625065323,-0.0008289837,-0.5016309735
C,0,-1.2696367596,-0.2121163152,-0.7608316295
H,0,-1.5082165489,-1.2932681404,-0.7181355013
C,0,-2.4772983848,0.4997701614,-0.0743616061
H,0,-2.4408213307,0.1913503277,0.9820920496
C,0,-2.3469288913,2.036245769,-0.1023159355
H,0,-2.5093226796,2.3983038715,-1.1261771242
H,0,-1.3134362267,2.3009547822,0.1554126211
C,0,-3.2997044019,2.7696751163,0.8484032458
H,0,-3.1593193541,2.4362725757,1.8833154135
H,0,-4.3502820705,2.6050424121,0.5879841569
C,0,-1.0904921234,0.1375655332,-2.250165226
H,0,-1.9948957971,-0.0693689188,-2.8295497459
H,0,-0.8332357435,1.1925932107,-2.3863378924
H,0,-0.2793229733,-0.456739967,-2.6837401037
H,0,-3.1237349404,3.850153844,0.8229022524
C,0,-3.8216418544,0.018173004,-0.6408793507
H,0,-4.6628851766,0.403575837,-0.057200894
H,0,-3.9651720128,0.3469281974,-1.6762843168
H,0,-3.8873597,-1.0754901019,-0.626275557

$C_2CJC(C)CC$ ($\sigma = 81$, OI)

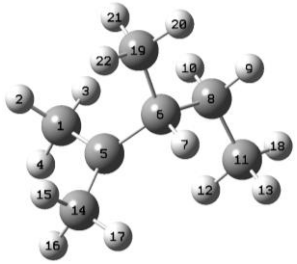

C,0,0.0000302583,0.0001273225,-0.0000754122
H,0,-0.0003867798,0.000404781,1.104575141
H,0,1.0487636475,-0.000101969,-0.313454782
H,0,-0.439278726,0.9593793892,-0.3026097169
C,0,-0.7722662598,-1.1549875582,-0.5642686881
C,0,-0.0732838072,-2.4583203207,-0.8835028932
H,0,-0.8333995454,-3.149012756,-1.277181483
C,0,1.0150528398,-2.32155522,-1.9749840169
H,0,1.4946905438,-3.3003940505,-2.107278167
H,0,1.8062336593,-1.6477928423,-1.6200709467
C,0,0.4849927545,-1.826754604,-3.3231747142
H,0,0.0238610673,-0.8382670757,-3.2289196262
H,0,-0.2755916558,-2.5077633726,-3.7225490168
C,0,-2.2619764728,-1.1344215908,-0.4087711345
H,0,-2.5816310578,-1.4166139823,0.6115228526
H,0,-2.6739830183,-0.1334254831,-0.588665121
H,0,-2.7545430515,-1.8330093605,-1.0944668367
H,0,1.2879466545,-1.7554125264,-4.0642289996
C,0,0.5228038091,-3.1126371606,0.3861878916
H,0,0.963581703,-4.0890356667,0.1545862275
H,0,1.3111765465,-2.4867335211,0.8188484535
H,0,-0.2435295283,-3.2629235248,1.1535790594

Table B.3 $C_2CC(C)CC$ Optimized Species (Continued)

$C_2CCJ(C)CC$ ($\sigma = 81$)

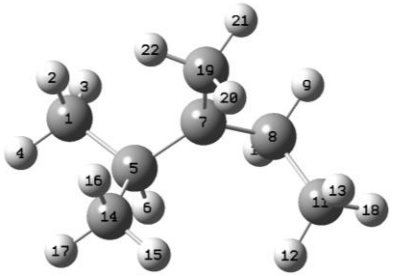

C,0,0.,0.,0.
H,0,0.,0.,1.09568026
H,0,1.0423224219,0.,-0.3337292076
H,0,-0.4638135153,0.9366045439,-0.3303488993
C,0,-0.7654703513,-1.2216124746,-0.5573550906
H,0,-0.7275045885,-1.1530988364,-1.6536384263
C,0,-0.1078607035,-2.5254862039,-0.1626570754
C,0,0.4154831214,-3.4504173369,-1.2241175874
H,0,1.2245627249,-4.0698241479,-0.8126526449
H,0,0.8576122049,-2.864480487,-2.0424714111
C,0,-0.6552714158,-4.3901713976,-1.8285928782
H,0,-1.4618503699,-3.8180014954,-2.2991145274
H,0,-1.1029187631,-5.0264300541,-1.0580894322
C,0,-2.2526673842,-1.1515468849,-0.1455809664
H,0,-2.8262867793,-1.9774157706,-0.5785853457
H,0,-2.3650532197,-1.2021174483,0.9430867798
H,0,-2.7065510873,-0.2118130874,-0.4803076405
H,0,-0.2184987381,-5.0436369982,-2.5921522373
C,0,-0.1670444734,-3.0043933653,1.2568935036
H,0,-1.0249051177,-3.673193496,1.4457420814
H,0,0.7303900372,-3.577447815,1.5228576446
H,0,-0.2579562563,-2.178624102,1.971166910

$C_2CC(CJ)CC$ ($\sigma = 27$, OI)

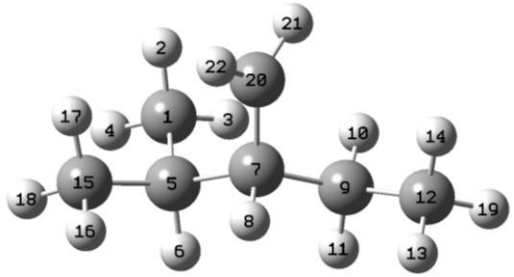

C,0,0.,0.,0.
H,0,0.,0.,1.09575891
H,0,1.0415487472,0.,-0.3355091716
H,0,-0.4520064794,0.9410219012,-0.3317957307
C,0,-0.7858052646,-1.199059327,-0.5501254611
H,0,-0.7402861828,-1.15641095,-1.6486610711
C,0,-0.162691643,-2.5838688377,-0.1504521767
H,0,-0.8322272892,-3.3359770111,-0.5991153619
C,0,1.2347696416,-2.7851987509,-0.7756661848
H,0,1.9573348085,-2.1299905488,-0.2718568246
H,0,1.2073400211,-2.4618848519,-1.8245827654
C,0,1.7311492699,-4.2327775894,-0.7035460734
H,0,1.0569744539,-4.9083719509,-1.242534743
H,0,1.786731091,-4.5820627225,0.3327388996
C,0,-2.2634372016,-1.1113494088,-0.1447960888
H,0,-2.8408199541,-1.9498764755,-0.5502906557
H,0,-2.3769049717,-1.1222851851,0.9447299778
H,0,-2.7154647231,-0.1849057053,-0.5152839632
H,0,2.727382495,-4.3340825165,-1.146445734
C,0,-0.1415323148,-2.8149191227,1.3277303131
H,0,0.7336822999,-2.560924839,1.9186598712
H,0,-1.0253554128,-3.1437510238,1.8637102768

Table B.3 $C_2CC(C)CC$ Optimized Species (Continued)

$C_2CC(C)CJC$ ($\sigma = 81$, OI)

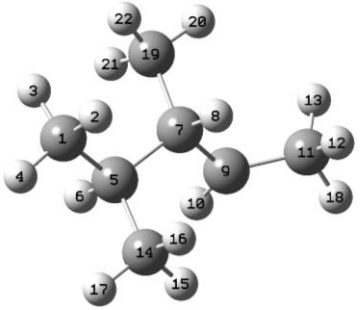

C,0,0.0001079055,-0.0000024294,-0.0001281673
H,0,0.0008014256,-0.0005267907,1.097141615
H,0,1.0407063396,0.0004121228,-0.335626755
H,0,-0.4492710735,0.9440106479,-0.3266426747
C,0,-0.7954811475,-1.193952138,-0.5493669651
H,0,-0.6948421945,-1.1892570851,-1.6462531375
C,0,-0.2576375831,-2.5639125374,-0.0512881078
H,0,-0.4095926687,-2.6013883527,1.0403199523
C,0,-1.010777753,-3.7094975103,-0.6667008209
H,0,-1.2213847129,-3.6541066082,-1.7346452326
C,0,-1.1354002469,-5.0354695001,0.0068120418
H,0,-1.3436784171,-4.9257264467,1.0788145677
H,0,-0.2114508474,-5.6366709416,-0.0675133424
C,0,-2.2853689683,-1.0311147053,-0.2099604406
H,0,-2.8817947419,-1.8564777114,-0.6094598286
H,0,-2.4346028503,-1.0096456606,0.8768408073
H,0,-2.6820511385,-0.094519838,-0.6164452705
H,0,-1.9345772795,-5.6412688618,-0.4336352641
C,0,1.2626000618,-2.7333423753,-0.3045136218
H,0,1.5972464312,-3.7283963939,0.0048709419
H,0,1.4941316434,-2.6212493582,-1.3701100939
H,0,1.8550233324,-1.9998962909,0.2509945226

$C_2CC(C)CCJ$ ($\sigma = 27$, OI)

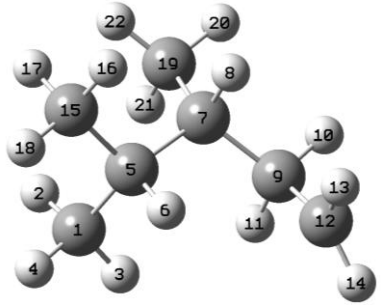

C,0,0.0005642392,-0.0003626242,0.0011172824
H,0,0.0021217558,-0.0021137764,1.0967388948
H,0,1.0422800976,0.0006097924,-0.3350243012
H,0,-0.447019328,0.9457015538,-0.3218230074
C,0,-0.7917551651,-1.1887599352,-0.5667002458
H,0,-0.7933780502,-1.0850017677,-1.6611398305
C,0,-0.1454702077,-2.572155335,-0.2745787312
H,0,-0.8615058886,-3.3269905974,-0.6347907951
C,0,1.161075925,-2.7913629786,-1.0768039624
H,0,1.5779715615,-3.768038785,-0.7663139525
H,0,1.9174001662,-2.0553199969,-0.7729564483
C,0,0.9925082079,-2.7699967534,-2.5577760794
H,0,0.130922489,-3.2445468042,-3.0190907993
H,0,1.7902871254,-2.4379157666,-3.2133464803
C,0,-2.2557852978,-1.1291994172,-0.1042844242
H,0,-2.8427972486,-1.9509602537,-0.5293862287
H,0,-2.3427796944,-1.1874587002,0.9867505993
H,0,-2.7246218031,-0.1894136616,-0.4158912799
C,0,0.0954782266,-2.8435966356,1.2183646782
H,0,0.432655021,-3.874209921,1.3729298183
H,0,0.8673726386,-2.1831414807,1.6283483923
H,0,0.8125389217,-2.702963866,1.812367282

Table B.4 Moments of Inertia[a]

Species	I_a	I_b	I_c
n-C_7H_{16}	149.58338	2509.17715	2580.87717
CJCCCCCC	142.72611	2440.64744	2514.26322
CCJCCCCC	137.80568	2490.14161	2555.29526
CCCJCCCC	159.65346	2456.92481	2535.13885
CCCCJCCC	146.35318	2489.69086	2546.02118
C_2CCCCC	296.78839	1825.56851	2006.56789
CJ_2CCCCC	282.39955	1800.63004	1963.78143
C_2CJCCCC	339.80474	1752.19184	1862.59800
C_2CCJCCC	292.60868	1846.28346	2020.68490
C_2CCCJCC	301.45487	1744.00999	1921.52743
C_2CCCCJC	286.73865	1801.90682	1989.36238
C_2CCCCCJ	290.62937	1771.43227	1947.67958
C_2CC(C)CC	458.24033	1223.93298	1315.69979
CJ_2CC(C)CC	529.28271	1056.92220	1245.89127
C_2CJC(C)CC	650.56073	955.76187	1147.90634
C_2CCJ(C)CC	539.15082	1117.88842	1192.40082
C_2CC(CJ)CC	439.31414	1198.33515	1301.90982
C_2CC(C)CJC	498.62236	1053.43236	1424.50165
C_2CC(C)CCJ	588.22509	995.55667	1145.85526

[a] AMU $Bohr^2$.

Table B.5 Vibrational Frequencies

Species	Frequencies (cm^{-1})									
n-C_7H_{16}	68.14	83.53	98.40	146.64	151.31	243.76	245.41	247.63	301.48	416.28
	481.10	737.04	742.83	778.31	852.33	884.77	920.90	944.90	999.98	1033.16
	1041.81	1068.75	1069.56	1093.08	1160.78	1213.32	1249.34	1264.74	1300.83	1325.96
	1332.49	1340.68	1346.51	1378.59	1411.28	1416.81	1427.13	1428.34	1499.42	1500.28
	1503.69	1509.63	1513.51	1513.58	1517.86	1525.00	1530.07	3008.87	3009.20	3015.60
	3023.77	3027.50	3031.50	3036.82	3037.04	3037.27	3049.02	3062.04	3072.90	3104.94
	3105.29	3109.89	3110.03							
CJCCCCCC	66.74	81.64	100.66	117.21	145.32	157.10	246.64	247.91	305.07	411.49
	461.75	490.87	732.38	740.81	784.38	862.79	894.17	921.20	993.18	1008.81
	1053.60	1059.14	1072.09	1089.33	1118.98	1164.86	1225.25	1259.37	1278.54	1316.74
	1324.35	1337.68	1342.52	1374.60	1406.67	1415.76	1427.29	1477.00	1482.89	1500.18
	1500.93	1509.12	1513.67	1519.75	1528.23	2927.85	3009.28	3012.36	3019.63	3024.51
	3028.72	3033.29	3037.26	3044.50	3061.75	3074.61	3105.38	3110.33	3153.65	3256.26
CCJCCCCC	45.17	69.81	96.58	110.62	123.13	151.09	249.02	252.17	306.03	401.82
	425.38	481.94	733.28	753.73	837.59	888.67	925.88	956.74	994.56	1006.12
	1049.68	1067.67	1081.28	1115.42	1142.48	1172.87	1230.58	1259.22	1291.34	1319.83
	1331.09	1337.17	1376.57	1410.89	1418.35	1426.67	1430.36	1481.06	1489.72	1499.12
	1500.20	1503.56	1514.29	1516.10	1526.30	2917.49	2955.34	3001.18	3009.38	3018.69
	3026.55	3035.07	3037.05	3043.04	3054.26	3071.38	3101.81	3105.28	3110.36	3163.39
CCCJCCCC	35.60	45.40	90.18	125.86	128.95	236.96	248.31	252.15	308.50	411.71
	416.83	482.59	733.20	766.96	793.11	888.31	918.67	934.08	1003.68	1040.11
	1046.88	1067.53	1083.23	1113.36	1142.89	1170.69	1238.33	1256.04	1276.99	1309.89
	1318.78	1333.87	1373.90	1409.50	1422.98	1428.09	1434.81	1477.61	1488.73	1501.00
	1511.44	1511.63	1514.52	1519.18	1525.09	2916.92	2927.98	3002.70	3014.91	3016.59
	3024.93	3037.69	3042.13	3043.95	3067.80	3105.84	3110.45	3110.75	3117.32	3146.60
CCCCJCCC	37.67	38.93	85.65	118.31	154.78	244.75	246.00	246.91	302.75	420.00
	424.37	482.25	733.09	746.47	851.14	874.96	885.35	918.26	1003.44	1048.55
	1055.16	1068.35	1091.40	1111.49	1142.48	1170.43	1248.17	1257.70	1261.51	1320.45
	1324.02	1328.88	1375.01	1406.66	1425.22	1426.09	1437.24	1476.96	1487.68	1505.58
	1505.97	1513.48	1513.50	1522.18	1522.63	2914.36	2919.45	3003.60	3008.52	3029.46
	3029.97	3036.78	3037.06	3064.72	3065.12	3104.99	3105.18	3111.15	3111.28	3145.90

Table B.5 Vibrational Frequencies (Continued A)

Species	Frequencies (cm^{-1})									
C_2CCCCC	58.60	81.26	127.78	144.14	224.32	246.02	254.57	300.25	303.09	406.85
	435.50	478.73	738.56	790.54	826.36	906.53	918.61	932.14	953.04	970.11
	1031.55	1046.75	1069.88	1093.20	1169.19	1196.82	1208.65	1258.51	1284.39	1323.84
	1338.25	1347.66	1377.17	1391.22	1412.81	1417.23	1427.14	1435.54	1492.65	1500.70
	1503.05	1508.55	1513.54	1514.38	1519.57	1524.42	1526.62	3000.41	3006.37	3015.07
	3024.86	3029.73	3035.58	3036.52	3038.71	3048.44	3071.97	3095.65	3101.78	3105.05
	3106.76	3110.10	3116.48							
CJ_2CCCCC	69.27	80.71	123.76	133.51	153.87	243.22	247.48	287.54	297.66	380.88
	428.65	469.87	547.23	739.53	794.09	843.14	906.95	911.01	937.02	964.93
	1018.32	1038.40	1047.55	1072.65	1117.43	1171.25	1201.48	1254.22	1280.26	1318.72
	1325.55	1337.26	1367.41	1387.34	1405.78	1416.04	1427.02	1475.55	1498.74	1501.40
	1508.06	1511.34	1513.64	1515.59	1526.07	2997.09	3009.12	3014.94	3024.44	3033.43
	3036.81	3039.25	3049.10	3070.35	3104.39	3105.09	3110.10	3116.28	3144.88	3248.30
$C_2CJCCCC$	35.39	81.32	97.88	114.11	127.20	130.50	237.57	252.21	320.22	391.13
	410.92	462.27	737.49	774.90	794.84	901.12	931.04	947.93	977.40	987.83
	1014.24	1050.41	1056.05	1082.84	1120.32	1231.87	1269.25	1290.48	1304.74	1333.76
	1349.56	1357.33	1395.63	1411.83	1427.14	1429.38	1482.31	1485.84	1492.64	1497.97
	1499.59	1510.09	1511.79	1515.29	1524.00	2948.50	2954.46	2998.55	3017.44	3025.90
	3034.94	3036.99	3040.99	3043.26	3046.63	3071.58	3092.71	3094.93	3105.27	3109.18
$C_2CCJCCC$	32.71	49.36	103.71	164.86	232.75	244.08	258.03	277.23	298.69	356.04
	415.84	477.40	534.14	741.55	829.82	867.63	901.72	929.28	943.34	963.21
	1045.37	1063.55	1087.99	1105.58	1131.73	1183.34	1195.78	1254.50	1271.77	1323.20
	1333.60	1342.65	1391.44	1407.36	1422.98	1425.94	1438.08	1482.45	1501.74	1503.94
	1505.50	1513.16	1516.17	1522.42	1524.22	2918.08	2994.68	3011.62	3030.45	3031.69
	3036.28	3036.92	3065.66	3099.47	3104.93	3105.22	3111.12	3113.90	3115.64	3137.46
$C_2CCCJCC$	42.53	46.54	104.93	170.28	228.25	245.74	254.11	291.99	308.57	404.64
	425.89	453.81	482.40	770.40	816.09	867.71	914.83	934.65	952.23	969.68
	1033.94	1049.70	1082.26	1121.42	1142.92	1184.33	1197.02	1245.81	1273.60	1278.82
	1343.17	1370.40	1387.54	1413.94	1424.15	1428.72	1436.90	1474.85	1486.97	1501.56
	1507.71	1512.07	1517.09	1519.63	1523.08	2919.65	2927.38	2999.63	3013.94	3018.43
	3029.90	3035.08	3042.25	3096.23	3101.84	3107.39	3110.53	3115.44	3117.33	3140.86
$C_2CCCCJC$	48.08	75.23	104.31	114.08	149.60	225.48	250.11	298.82	307.69	402.31
	416.13	441.94	477.27	754.97	823.55	910.18	930.78	933.32	958.33	971.30
	997.27	1046.13	1082.94	1122.55	1143.26	1177.21	1197.41	1232.45	1278.17	1314.10
	1343.95	1376.47	1389.61	1415.05	1418.61	1429.35	1435.17	1480.09	1489.66	1497.70
	1501.24	1503.67	1510.93	1519.82	1524.82	2912.43	2955.30	3001.46	3014.93	3023.23
	3030.50	3036.43	3042.46	3057.11	3096.41	3101.80	3102.44	3107.05	3115.15	3162.19

Table B.5 Vibrational Frequencies (Continued B)

Species	Frequencies (cm^{-1})									
$C_2CCCCCJ$	61.49	82.43	117.43	130.65	150.85	223.93	252.79	301.64	306.21	407.37
	434.63	455.46	491.82	732.54	805.20	831.34	897.73	931.96	948.98	968.29
	1003.64	1050.22	1063.23	1088.30	1125.34	1174.12	1196.75	1220.48	1275.12	1302.93
	1333.67	1343.76	1375.85	1389.14	1410.42	1416.82	1435.87	1475.94	1482.04	1492.89
	1502.99	1508.88	1515.72	1519.61	1525.77	2926.81	3000.72	3007.18	3019.12	3029.58
	3030.70	3036.17	3041.82	3079.35	3096.26	3102.24	3107.09	3117.21	3153.46	3256.15
$C_2CC(C)CC$	58.13	86.93	204.47	211.92	232.04	248.83	260.95	297.41	321.45	339.01
	432.53	461.95	560.27	753.02	791.32	857.65	925.93	934.12	969.29	976.95
	983.85	1039.79	1054.30	1079.50	1148.94	1187.61	1198.43	1216.99	1300.67	1318.33
	1344.20	1370.15	1392.93	1395.57	1417.50	1427.07	1430.90	1438.96	1498.56	1502.92
	1506.24	1512.18	1519.10	1521.70	1524.52	1526.39	1530.56	2990.73	3005.40	3022.43
	3035.74	3039.56	3042.01	3048.84	3058.37	3101.77	3105.11	3106.64	3107.90	3112.05
	3116.51	3118.26	3122.93							
$CJ_2CC(C)CC$	78.39	85.23	132.69	206.80	213.14	233.91	244.35	280.36	312.84	345.13
	424.12	449.62	503.30	592.65	746.44	793.44	863.38	910.86	956.90	975.06
	995.01	1018.58	1038.46	1065.10	1119.17	1155.57	1190.33	1213.52	1285.34	1301.08
	1310.86	1355.01	1375.52	1398.55	1418.80	1424.78	1429.19	1474.81	1497.92	1507.73
	1512.74	1515.50	1519.29	1523.84	1525.56	2906.11	2996.24	3026.95	3038.61	3040.90
	3048.29	3063.08	3103.94	3105.95	3111.25	3114.10	3118.97	3125.42	3147.25	3249.87
$C_2CJC(C)CC$	36.93	95.18	112.34	127.74	175.16	220.08	222.41	243.70	287.10	357.45
	404.50	464.92	510.22	696.56	806.36	849.27	945.42	948.87	979.72	985.32
	1004.96	1020.18	1049.52	1094.21	1102.13	1170.82	1241.58	1286.83	1306.90	1329.49
	1377.40	1396.15	1412.39	1412.79	1424.35	1431.41	1483.47	1487.97	1495.10	1501.33
	1508.76	1511.25	1512.84	1515.12	1522.49	2944.05	2957.50	3008.89	3026.35	3035.12
	3038.71	3043.84	3046.44	3059.28	3095.55	3102.99	3105.02	3106.90	3111.82	3114.95
$C_2CCJ(C)CC$	42.33	44.54	104.17	147.21	214.87	231.72	248.48	265.01	294.82	334.15
	413.77	477.07	528.58	697.30	788.58	862.56	927.81	928.88	955.06	985.72
	993.11	1035.35	1056.61	1094.19	1097.43	1178.07	1240.74	1257.89	1341.33	1345.77
	1348.93	1388.87	1405.08	1415.21	1419.48	1431.20	1484.98	1494.53	1498.56	1500.59
	1509.56	1511.54	1518.21	1519.65	1524.28	2960.64	3006.33	3019.92	3033.57	3036.83
	3038.17	3044.32	3047.75	3095.26	3100.71	3106.59	3107.31	3112.64	3115.15	3116.65
$C_2CC(CJ)CC$	80.48	106.73	153.98	194.94	229.70	235.90	251.83	276.79	311.81	340.25
	432.34	445.88	474.91	606.95	773.89	795.01	856.60	933.25	948.42	967.64
	974.41	996.69	1048.83	1080.94	1102.10	1180.53	1189.59	1201.49	1284.57	1297.66
	1319.75	1370.06	1384.11	1393.81	1415.25	1425.99	1433.33	1479.43	1503.49	1503.84
	1509.24	1512.08	1520.27	1521.99	1526.36	2979.44	3008.27	3027.26	3034.97	3039.01
	3041.72	3063.26	3103.89	3105.25	3107.19	3110.12	3114.86	3117.24	3152.65	3254.84

Table B.5 Vibrational Frequencies (Continued C)

Species	Frequencies (cm^{-1})									
$C_2CC(C)CJC$	54.49	78.71	118.77	201.75	220.21	222.87	259.97	275.95	338.78	367.23
	413.70	450.00	467.66	538.66	789.05	863.81	930.16	933.77	963.08	971.85
	993.75	1015.22	1045.49	1094.05	1140.02	1184.70	1192.54	1202.45	1281.96	1320.35
	1355.80	1373.43	1404.74	1412.32	1419.24	1425.08	1433.91	1488.84	1499.59	1501.68
	1503.52	1510.98	1513.47	1521.09	1531.66	2954.62	2980.32	2999.87	3032.23	3037.22
	3039.79	3046.63	3096.08	3099.06	3102.49	3109.84	3113.92	3119.14	3125.21	3148.05
$C_2CC(C)CCJ$	57.19	129.07	131.64	205.33	220.14	241.42	263.62	275.93	289.04	380.88
	423.91	459.74	496.42	555.25	724.85	821.77	887.26	928.85	936.62	968.76
	970.61	1012.98	1046.12	1084.01	1126.82	1167.31	1186.43	1207.29	1235.78	1313.83
	1347.00	1355.48	1390.83	1395.53	1417.08	1424.83	1438.48	1474.14	1483.10	1501.42
	1506.01	1513.81	1522.47	1525.51	1527.45	2932.36	2997.37	3016.11	3034.56	3040.82
	3043.62	3047.96	3100.92	3104.33	3105.90	3110.01	3114.60	3119.33	3151.55	3254.28

Internal Rotor (IR) notation and 0° dihedral angle corresponds to the structures from the Optimized Species.

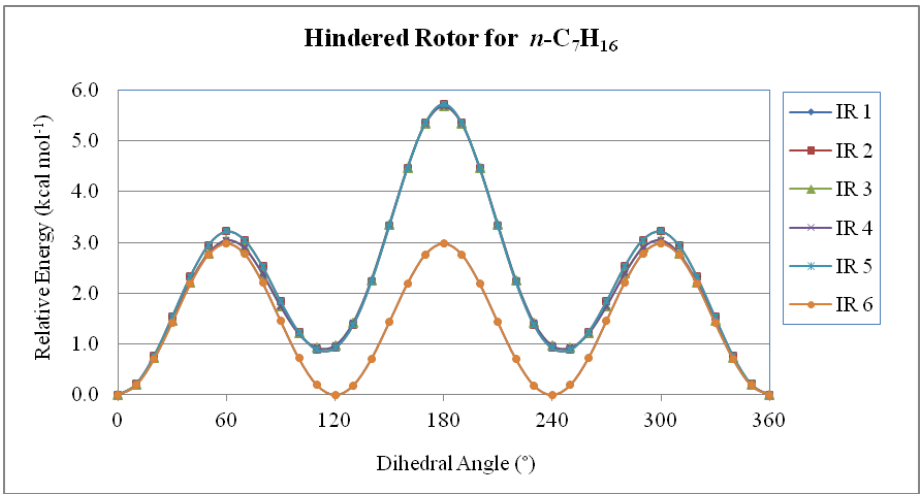

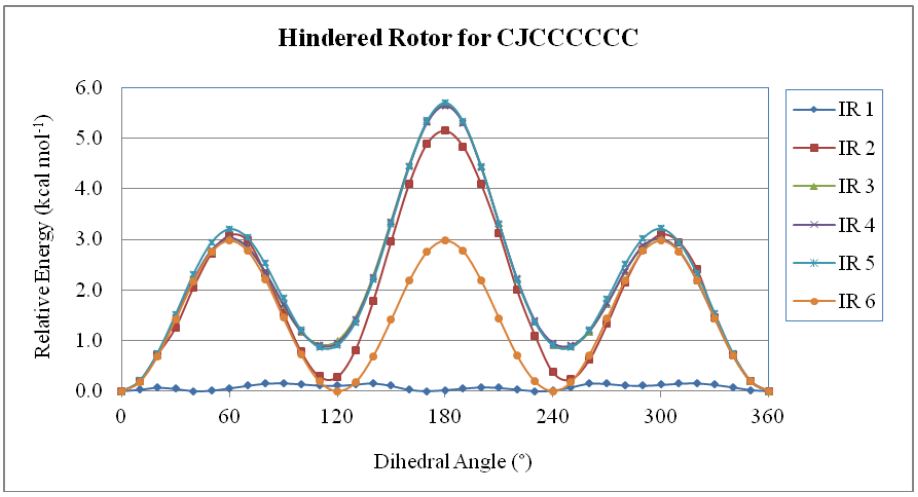

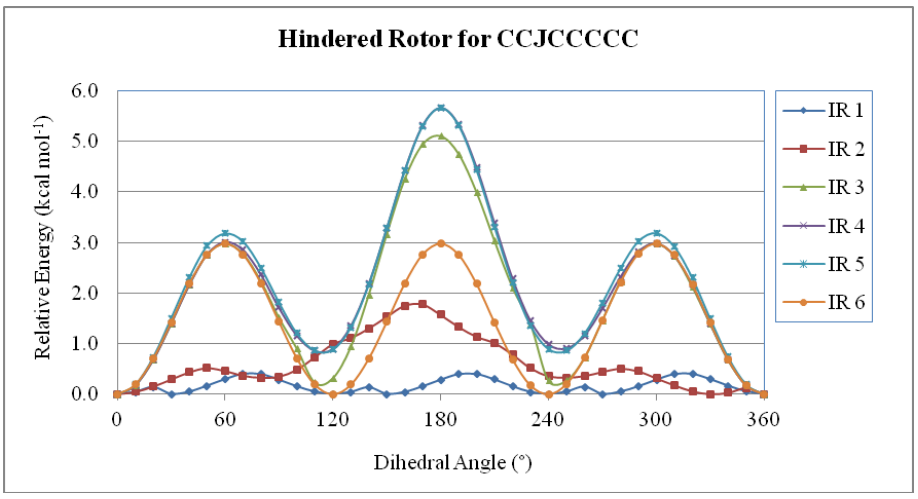

Figure B.1 Internal rotation of n-C_7H_{16} species.

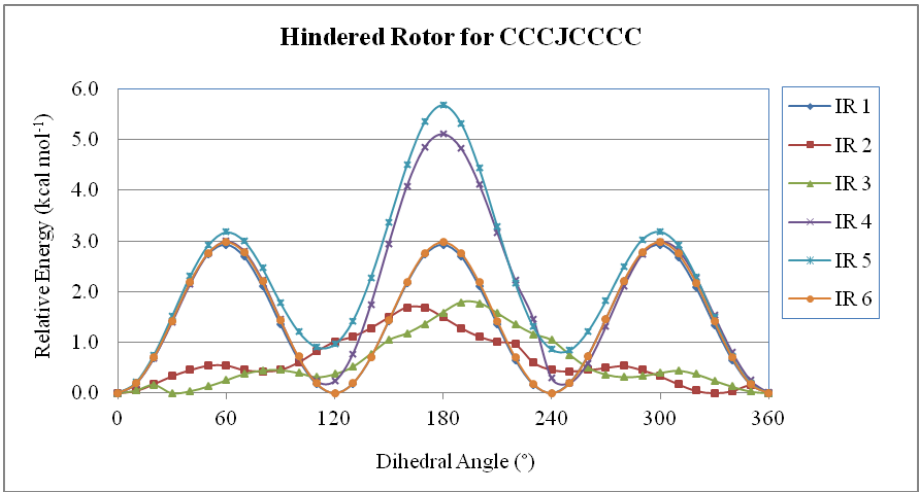

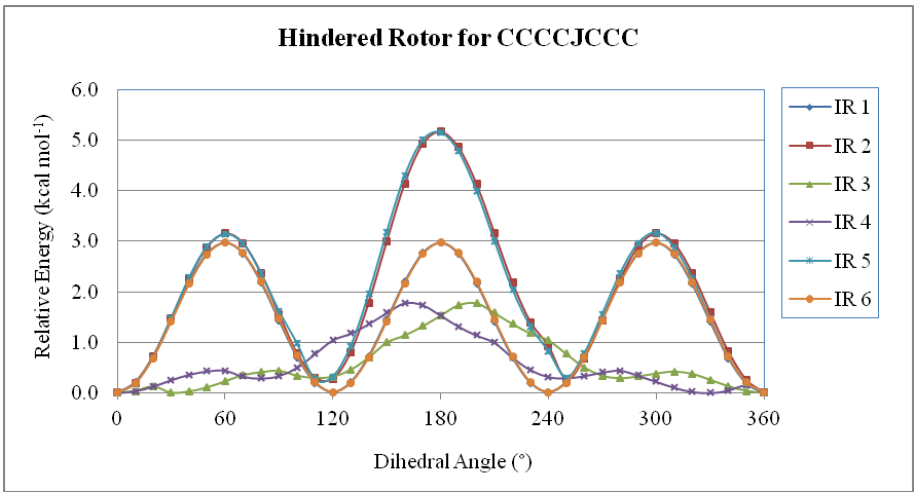

Figure B.1 Internal rotation of *n*-C_7H_{16} species. (Continued)

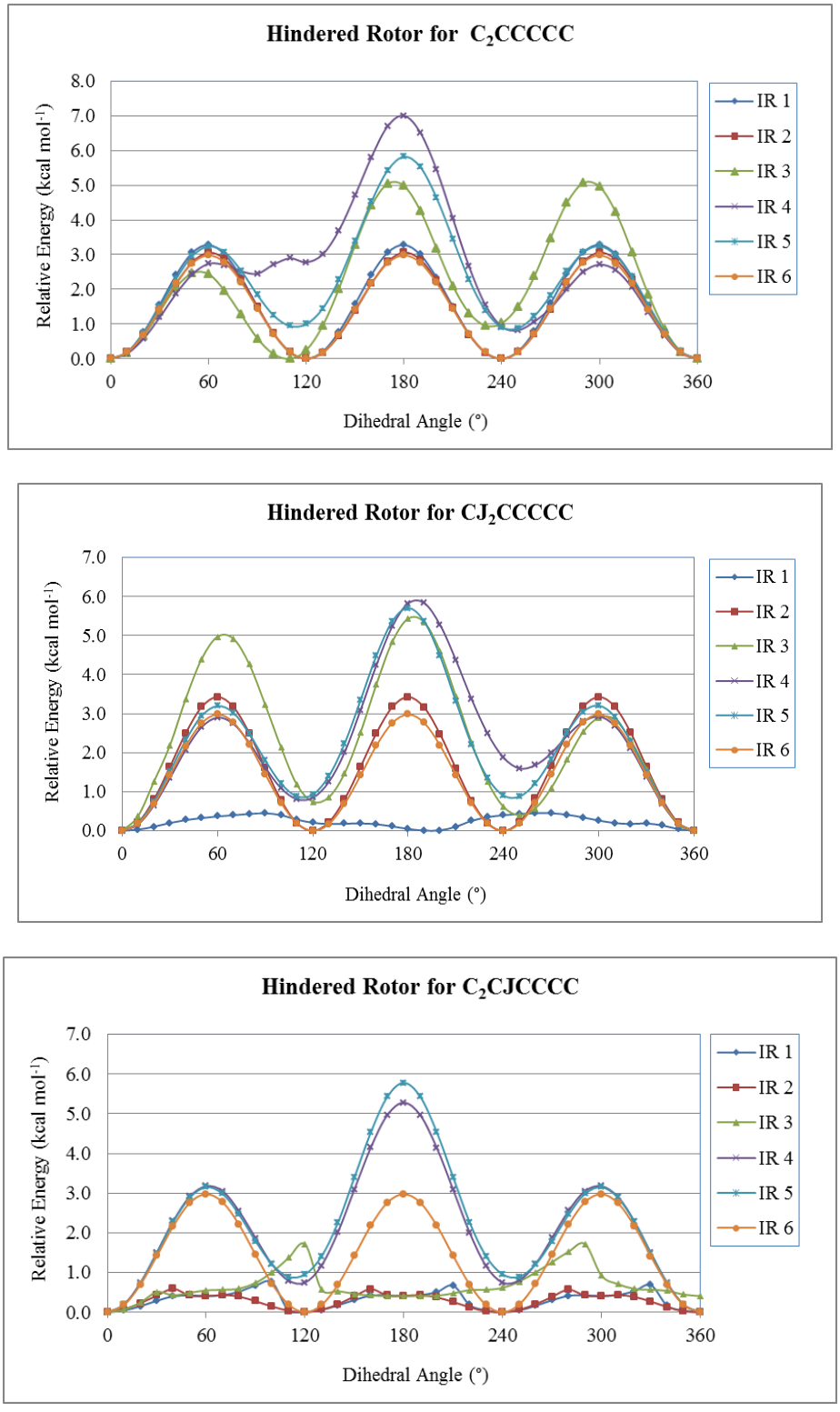

Figure B.2 Internal rotation of C_2CCCCC species.

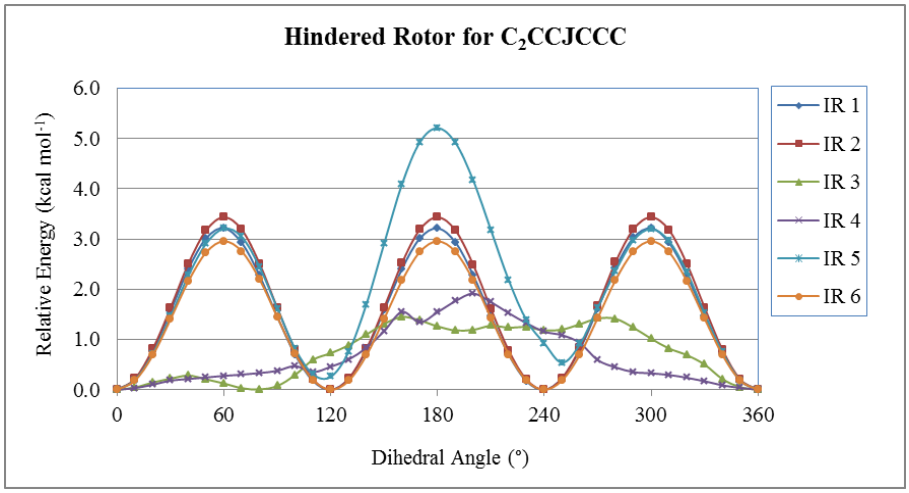

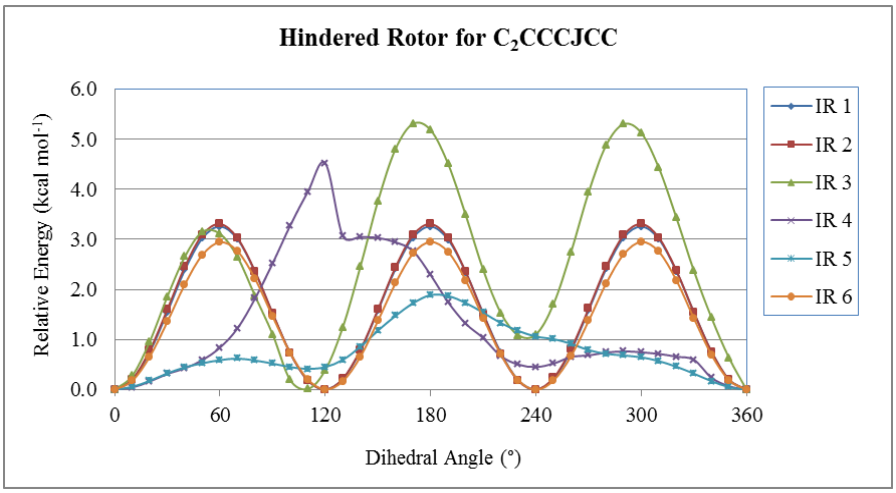

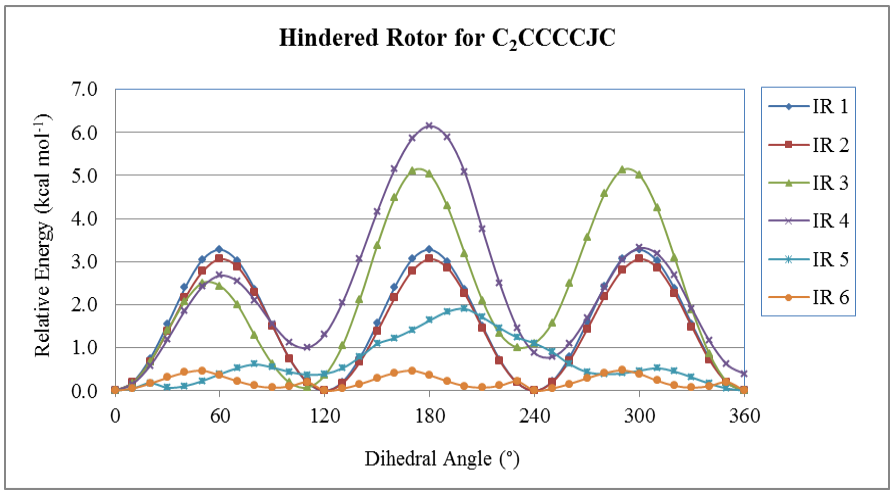

Figure B.2 Internal rotation of C_2CCCCC species. (Continued)

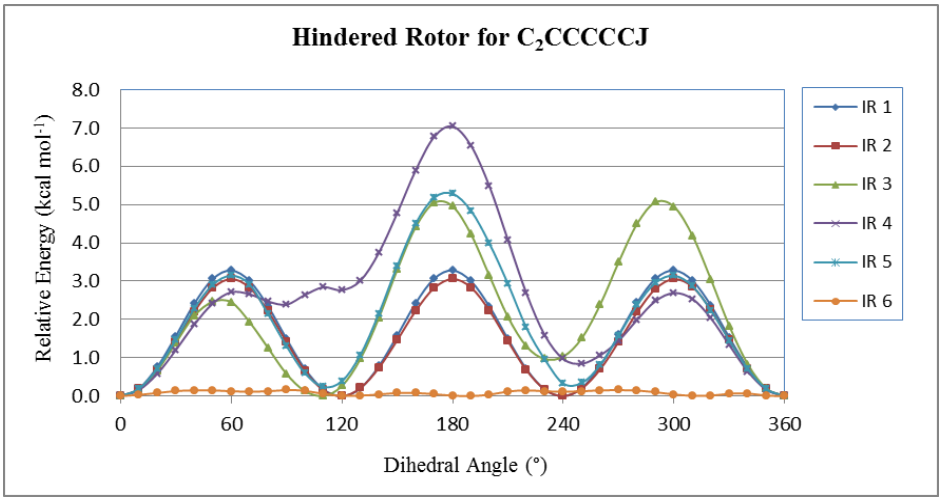

Figure B.2 Internal rotation of C_2CCCCC species. (Continued)

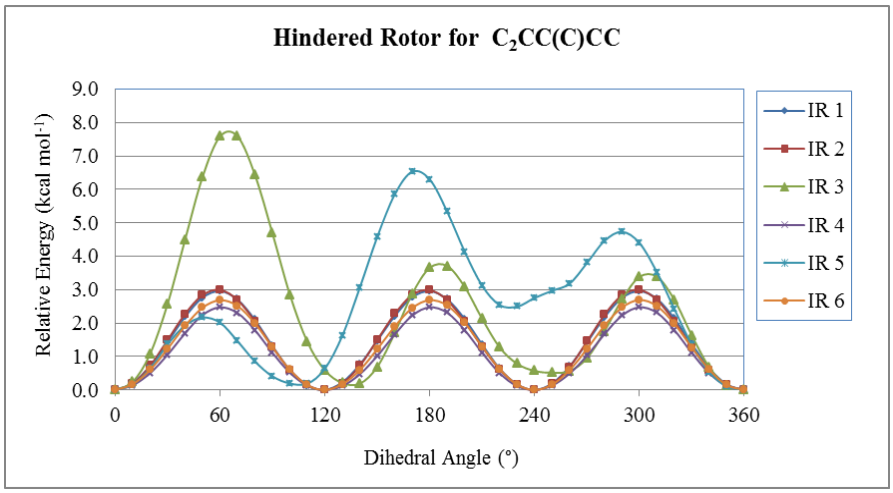

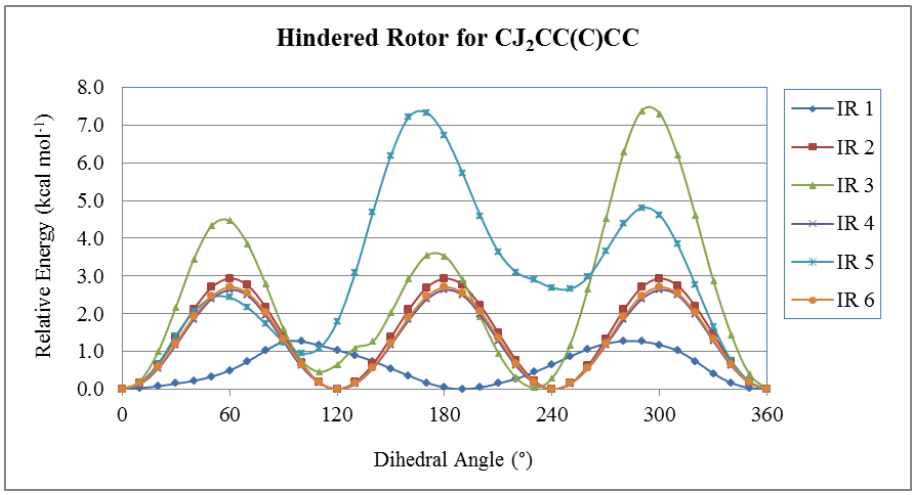

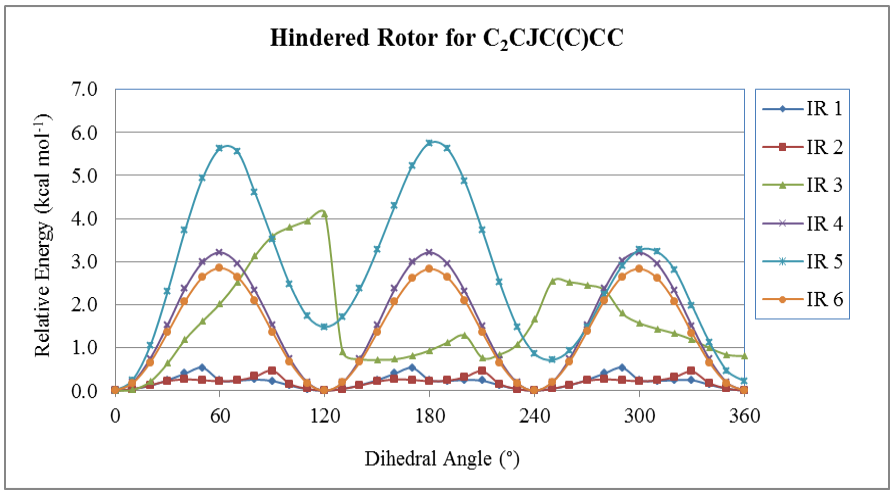

Figure B.3 Internal rotation of $C_2CC(C)CC$ species.

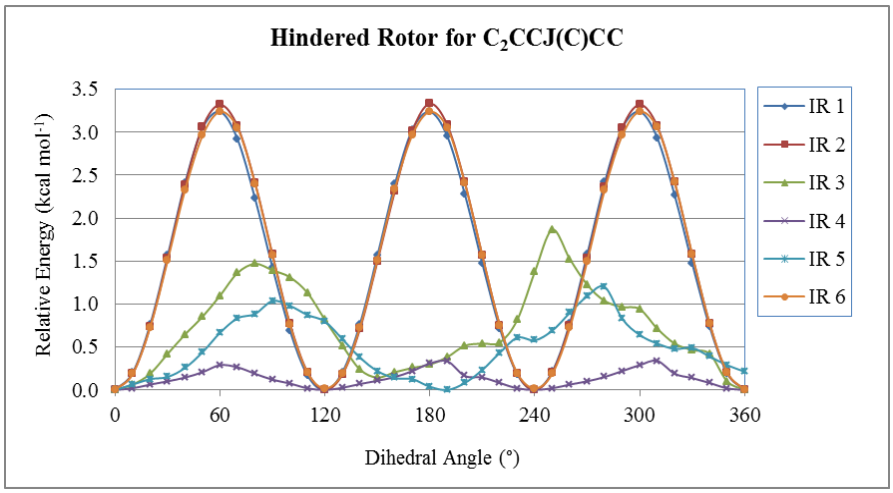

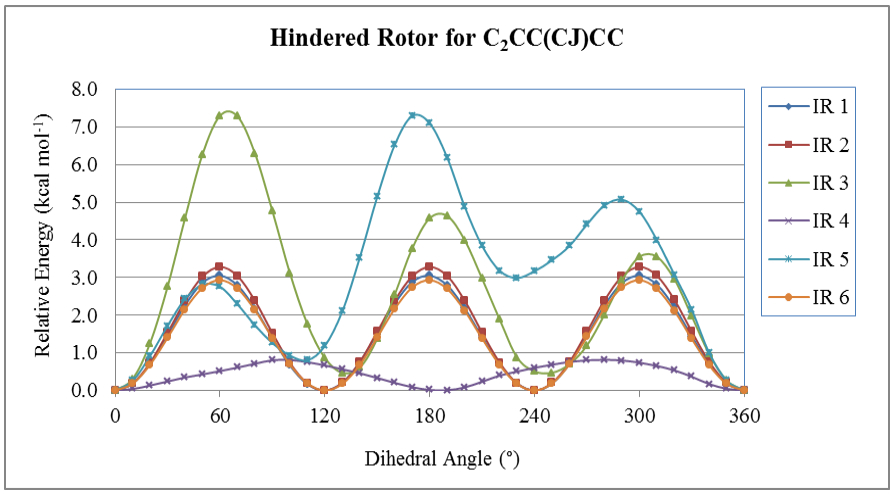

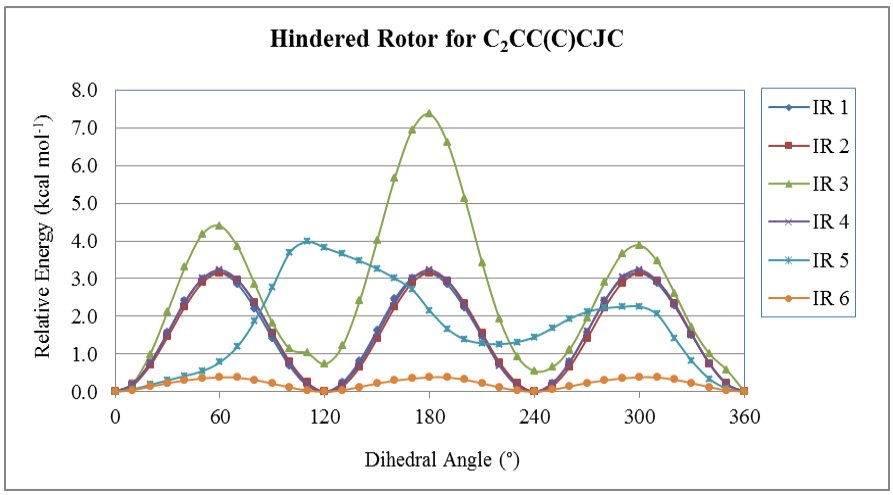

Figure B.3 Internal rotation of $C_2CC(C)CC$ species. (Continued)

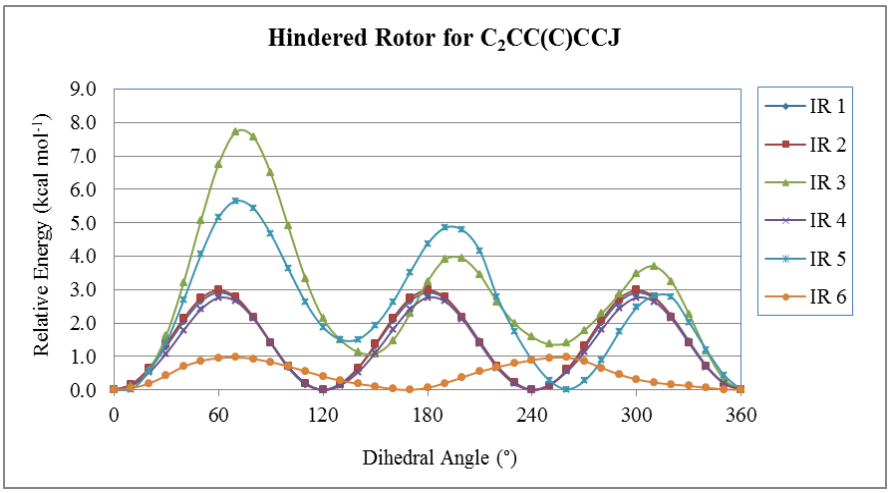

Figure B.3 Internal rotation of $C_2CC(C)CC$ species. (Continued)

Table B.6 Calculated Total Entropies[a] and Heat Capacities[a]

Temperature	*n*-C_7H_{16}		CJCCCCCC		CCJCCCCC		CCCJCCCC		CCCCJCCC	
(K)	Cp	S	Cp	S	Cp	S	Cp	S	Cp	S
50	14.68	56.97	17.04	62.72	18.87	63.02	18.78	64.65	19.64	65.10
100	23.15	69.59	23.80	76.53	23.95	77.70	23.09	79.02	23.15	79.98
150	29.70	80.34	29.11	87.26	27.94	88.21	26.78	89.09	25.94	89.87
200	33.58	89.44	32.73	96.14	31.13	96.67	30.17	97.25	29.25	97.77
250	37.18	97.30	36.35	103.81	34.64	103.98	33.98	104.37	33.24	104.70
298	41.08	104.14	40.28	110.52	38.56	110.37	38.13	110.68	37.59	110.89
400	50.32	117.49	49.36	123.61	47.78	122.98	47.63	123.20	47.38	123.30
500	59.19	129.66	57.85	135.53	56.48	134.57	56.42	134.77	56.32	134.83
600	67.06	141.13	65.29	146.73	64.12	145.53	64.09	145.73	64.06	145.78
700	73.91	151.98	71.69	157.27	70.71	155.91	70.68	156.10	70.69	156.14
800	79.86	162.23	77.21	167.19	76.39	165.71	76.37	165.90	76.39	165.95
1000	89.54	181.11	86.17	185.40	85.59	183.77	85.58	183.95	85.59	184.01
1500	104.56	220.57	100.04	223.26	99.76	221.45	99.77	221.63	99.75	221.69
2000	112.03	251.77	106.94	253.07	106.78	251.20	106.80	251.39	106.74	251.43
2500	115.97	277.22	110.58	277.35	110.49	275.46	110.49	275.65	110.42	275.68
3000	118.22	298.58	112.66	297.71	112.60	295.80	112.60	295.99	112.52	296.00
3500	119.60	316.91	113.93	315.17	113.89	313.26	113.88	313.45	113.81	313.45
4000	120.49	332.94	114.75	330.44	114.72	328.52	114.71	328.71	114.64	328.70
4500	121.09	347.16	115.30	343.99	115.28	342.06	115.27	342.25	115.21	342.24
5000	121.52	359.94	115.70	356.16	115.68	354.23	115.67	354.41	115.62	354.40
Zero Point Energy[b]	**133.050**		**123.781**		**123.859**		**123.869**		**123.879**	

[a] Units of cal mol^{-1} K^{-1}.

[b] Units of kcal mol^{-1}.

Table B.6 Calculated Total Entropies[a] and Heat Capacities[a] (Continued)

Temperature (K)	C_2CCCCC		CJ_2CCCCC		$C_2CJCCCC$		$C_2CCJCCC$		$C_2CCCJCC$		$C_2CCCCJC$		$C_2CCCCCJ$	
	Cp	**S**	**Cp**	**S**	**Cp**	**S**	**Cp**	**S**	**Cp**	**S**	**Cp**	**S**	**Cp**	**S**
50	13.63	58.60	15.55	60.60	18.35	60.74	16.25	63.12	17.06	60.15	16.16	62.36	15.56	62.54
100	20.80	70.14	21.77	73.21	23.38	75.04	21.07	75.81	22.48	73.88	21.44	75.17	20.56	74.80
150	27.12	79.83	27.56	83.17	27.02	85.25	25.76	85.25	26.17	83.68	26.13	84.77	25.87	84.15
200	31.98	88.31	32.28	91.75	29.94	93.41	29.91	93.23	30.11	91.73	30.21	92.85	30.71	92.25
250	36.56	95.93	36.73	99.42	33.33	100.44	34.18	100.34	34.54	98.91	34.37	100.02	35.45	99.60
298	41.11	102.72	41.07	106.23	37.22	106.60	38.59	106.71	39.12	105.35	38.65	106.40	40.09	106.21
400	50.97	116.18	50.34	119.60	46.47	118.81	48.28	119.40	48.97	118.23	48.17	119.09	49.86	119.37
500	59.94	128.51	58.71	131.72	55.27	130.12	57.04	131.11	57.74	130.09	56.91	130.77	58.50	131.42
600	67.77	140.12	65.97	143.06	63.04	140.88	64.60	142.17	65.26	141.28	64.52	141.81	65.92	142.73
700	74.52	151.07	72.22	153.70	69.76	151.09	71.08	152.61	71.68	151.82	71.05	152.24	72.25	153.36
800	80.37	161.40	77.63	163.69	75.57	160.78	76.67	162.46	77.22	161.74	76.69	162.09	77.70	163.36
1000	89.89	180.37	86.43	181.97	84.98	178.68	85.73	180.56	86.19	179.96	85.82	180.21	86.55	181.67
1500	104.75	219.94	100.20	219.90	99.52	216.19	99.84	218.28	100.17	217.84	99.97	217.97	100.34	219.65
2000	112.24	251.19	107.16	249.77	106.79	245.91	106.95	248.07	107.19	247.70	107.09	247.80	107.30	249.56
2500	116.28	276.70	110.91	274.11	110.68	270.19	110.77	272.37	110.96	272.06	110.91	272.13	111.04	273.93
3000	118.62	298.12	113.08	294.53	112.94	290.58	112.98	292.77	113.14	292.49	113.12	292.56	113.21	294.38
3500	120.09	316.52	114.44	312.07	114.34	308.09	114.36	310.30	114.50	310.04	114.49	310.10	114.55	311.94
4000	121.05	332.62	115.33	327.41	115.26	323.42	115.28	325.63	115.38	325.38	115.39	325.45	115.43	327.29
4500	121.71	346.91	115.95	341.03	115.89	337.03	115.90	339.24	115.99	339.01	116.00	339.08	116.04	340.92
5000	122.19	359.76	116.39	353.27	116.34	349.27	116.35	351.48	116.43	351.25	116.44	351.32	116.47	353.17
Zero Point Energy[b]	**132.602**		**123.497**		**123.912**		**123.644**		**123.475**		**123.450**		**123.361**	

[b] Units of kcal mol^{-1}.

Table B.6 Calculated Total Entropies[a] and Heat Capacities[a] (Continued)

Temperature (K)	$C_2CC(C)CC$		$CJ_2CC(C)CC$		$C_2CJC(C)CC$		$C_2CCJ(C)CC$		$C_2CC(CJ)CC$		$C_2CC(C)CJC$		$C_2CC(C)CCJ$	
	Cp	**S**	**Cp**	**S**	**Cp**	**S**	**Cp**	**S**	**Cp**	**S**	**Cp**	**S**	**Cp**	**S**
50	13.02	57.10	14.70	56.84	16.03	58.45	15.50	63.00	13.29	57.69	14.77	56.74	15.20	57.15
100	19.63	68.13	21.47	69.22	22.27	71.60	19.74	74.90	20.68	69.18	20.72	68.83	20.90	69.34
150	25.27	77.19	26.74	78.95	26.42	81.45	24.07	83.74	26.63	78.74	25.95	78.24	26.79	78.94
200	30.20	85.13	31.37	87.27	30.03	89.54	28.01	91.20	31.48	87.07	30.64	86.34	31.90	87.35
250	35.11	92.39	36.04	94.75	33.95	96.64	32.22	97.88	36.19	94.58	35.30	93.67	36.63	94.97
298	39.98	98.95	40.68	101.47	38.13	102.95	36.66	103.90	40.83	101.32	39.92	100.25	41.13	101.77
400	50.33	112.15	50.49	114.80	47.56	115.46	46.51	116.05	50.61	114.70	49.71	113.35	50.55	115.18
500	59.55	124.37	59.11	126.99	56.29	127.01	55.48	127.38	59.20	126.91	58.36	125.37	58.92	127.36
600	67.51	135.93	66.47	138.42	63.93	137.94	63.26	138.18	66.52	138.35	65.77	136.67	66.15	138.74
700	74.34	146.84	72.74	149.13	70.53	148.29	69.93	148.43	72.77	149.07	72.11	147.27	72.37	149.39
800	80.25	157.14	78.14	159.19	76.24	158.07	75.70	158.14	78.15	159.13	77.58	157.25	77.76	159.40
1000	89.89	176.11	86.94	177.59	85.52	176.10	85.06	176.06	86.92	177.53	86.49	175.54	86.57	177.72
1500	105.03	215.72	100.78	215.73	100.02	213.82	99.69	213.61	100.75	215.66	100.55	213.55	100.51	215.73
2000	112.74	247.09	107.84	245.78	107.37	243.69	107.14	243.40	107.83	245.71	107.74	243.55	107.67	245.72
2500	116.92	272.73	111.67	270.29	111.35	268.11	111.18	267.78	111.66	270.21	111.64	268.04	111.57	270.19
3000	119.36	294.27	113.90	290.85	113.67	288.63	113.54	288.27	113.90	290.77	113.92	288.61	113.84	290.74
3500	120.89	312.79	115.30	308.52	115.12	306.26	115.02	305.88	115.30	308.44	115.33	306.28	115.26	308.40
4000	121.89	329.00	116.22	323.97	116.08	321.70	116.00	321.31	116.22	323.90	116.26	321.74	116.20	323.86
4500	122.59	343.40	116.85	337.70	116.74	335.41	116.68	335.01	116.85	337.62	116.90	335.47	116.84	337.58
5000	123.09	356.34	117.31	350.04	117.22	347.73	117.16	347.33	117.31	349.96	117.35	347.81	117.31	349.91
Zero Point Energy[b]	**132.339**		**123.036**		**123.500**		**123.727**		**123.153**		**123.269**		**123.027**	

[b] Units of kcal mol^{-1}.

APPENDIX C

THERMOCHEMISTRY AND BOND DISSOCIATION ENERGIES OF KETONES

This appendix contains the optimized geometries with corresponding Gaussian atom numbering and symmetry values in parenthesis, moments of inertia, vibrational frequencies, internal rotor potential energy graphs, entropies, and heat capacities for all of the parent and radical species from B3LYP/6-31G(d,p) level of theory.

Table C.1 CC(=O)CC Optimized Species

CC(=O)CC (σ = 9)

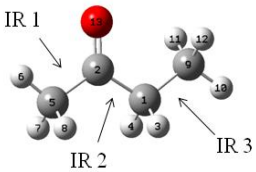

C,0,-0.1592355407,-0.0057947903,0.0750763104
C,0,-0.290041015,-0.0279296363,1.5941495478
H,0,0.8855833549,-0.2395214221,-0.1752479319
H,0,-0.7401418791,-0.8496629772,-0.324129195
C,0,0.1274294633,-1.3107458375,2.2944385139
H,0,-0.0112289814,-1.2047750882,3.3710800295
H,0,-0.4645486649,-2.1580695333,1.9296566433
H,0,1.1774314959,-1.5413412367,2.0804513843
C,0,-0.5962007961,1.3128356988,-0.5575231036
H,0,-0.4834443167,1.2776457974,-1.6449748642
H,0,-1.6418413601,1.5293287198,-0.3243238613
H,0,-0.0006623836,2.1452617722,-0.1740928812
O,0,-0.7069512245,0.9308301707,2.2163060747

CC(=O)CJC (σ = 9)

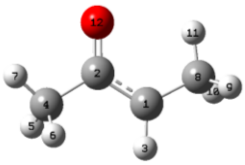

C,0,0.0000031744,0.0024166962,-0.0001212819
C,0,0.0000741453,-0.0014631889,1.4444035803
H,0,0.9550549092,0.0060315525,-0.5224525641
C,0,1.3435815983,-0.0177584375,2.1595397493
H,0,1.8209819414,-0.9987429318,2.0484283048
H,0,2.0308663972,0.7265961857,1.7438465725
H,0,1.1895343387,0.1775726644,3.2215591792
C,0,-1.2566646113,-0.0032422181,-0.7910298689
H,0,-1.3093502464,0.8693980626,-1.4567981679
H,0,-1.3088785068,-0.8861496558,-1.4435262495
H,0,-2.12080418,0.0006756888,-0.1244884746
O,0,-1.0620165427,-0.004538193,2.0844263996

CJC(=O)CC (σ = 3)

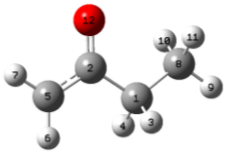

C,0,-0.1019265244,-0.0591026774,-0.0993921029
C,0,0.167943591,-0.028638714,1.4040927273
H,0,0.857383895,-0.2042087053,-0.6158175614
H,0,-0.6887837367,-0.9610203207,-0.3232589168
C,0,0.8312516224,-1.1607004192,1.9984336918
H,0,1.139928534,-2.0227585927,1.4149136417
H,0,1.027192017,-1.147873569,3.0648290039
C,0,-0.8108894615,1.1925337096,-0.6093454958
H,0,-0.9824184807,1.1279109721,-1.6877284922
H,0,-1.7751465575,1.3249883002,-0.1117754815
H,0,-0.2176001106,2.0876191959,-0.4051311578
O,0,-0.1691042752,0.9367794388,2.1037474266

CC(=O)CCJ (σ = 3)

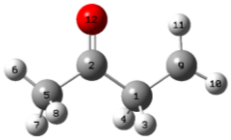

C,0,-0.001514437,-0.0011541164,-0.0000700276
C,0,-0.0001556463,-0.0002679035,1.5296278024
H,0,1.046530878,-0.0046766919,-0.3457732922
H,0,-0.3781706032,-0.9919960016,-0.3166791922
C,0,0.9027688583,-1.0211130631,2.1999456926
H,0,0.7016599122,-1.0439699377,3.2716333188
H,0,0.762100764,-2.0188889366,1.7704033397
H,0,1.9527982562,-0.7486664063,2.0383630051
C,0,-0.7849399649,1.1035734434,-0.6095551817
H,0,-0.8147789497,1.226901294,-1.6855611733
H,0,-1.355431212,1.770296724,0.0241860735
O,0,-0.6794846709,0.7731978488,2.1754569217

Table C.2 CCC(=O)CC Optimized Species

CCC(=O)CC (σ = 18)

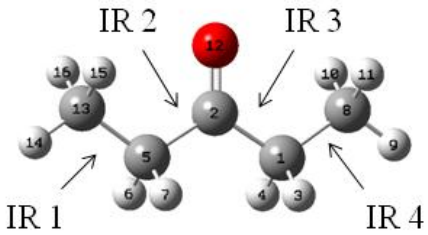

C,0,-0.1494745944,0.0181154996,0.0517110693
C,0,-0.4738311439,0.003989362,1.5423032592
H,0,0.9184943343,-0.2160620327,-0.0627410655
H,0,-0.6757290319,-0.8266376442,-0.4152339554
C,0,-0.1494745944,-1.2798382724,2.2998329483
H,0,-0.6757290319,-2.1066010978,1.8017277781
H,0,0.9184943343,-1.4960454947,2.1542553236
C,0,-0.5008780526,1.3339820711,-0.6382940876
H,0,-0.2495374922,1.2930408664,-1.702112333
H,0,-1.5676320955,1.5518520734,-0.5422097551
H,0,0.0411067526,2.1683269531,-0.1857681623
O,0,-0.9665722005,0.9678869166,2.0988097718
C,0,-0.5008780526,-1.2194669812,3.7844094056
H,0,-0.2495374922,-2.1612312091,4.2808624049
H,0,0.0411067526,-0.410395593,4.2807103062
H,0,-1.5676320955,-1.0273205072,3.9250481961

CJCC(=O)CC (σ = 3)

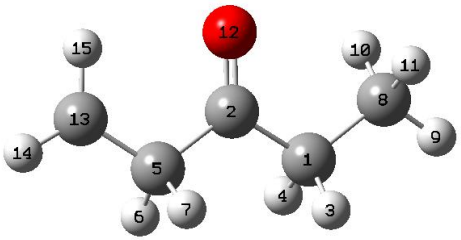

C,0,1.2248170458,-0.7360169236,-0.0536105799
C,0,-0.0575572787,0.0863488207,-0.0003228841
H,0,1.1900579093,-1.4794492263,0.7549168668
H,0,1.1987872049,-1.3251824222,-0.9819124633
C,0,-1.3662707689,-0.7054878005,0.0534672132
H,0,-1.3369803824,-1.4758798632,-0.7357870775
H,0,-1.3438711095,-1.2955521815,0.988836316
C,0,2.4955133167,0.1069223821,0.0212421009
H,0,3.3847423275,-0.5264990141,-0.0451810239
H,0,2.5260271895,0.8361932296,-0.7918605445
H,0,2.5394148824,0.6660360938,0.9597024796
O,0,-0.0405938609,1.3020977758,0.0027620453
C,0,-2.5898635626,0.1321507594,-0.0348038073
H,0,-3.5699270369,-0.3293115553,-0.0575292999
H,0,-2.5033238762,1.2110379253,-0.0442613416

CCJC(=O)CC (σ = 9)

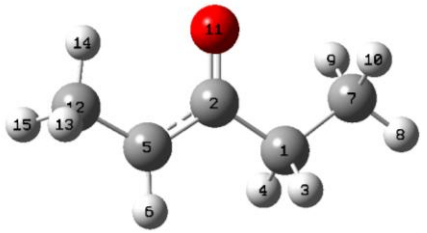

C,0,0.0979778579,0.1629735762,0.0531648259
C,0,0.1062555585,0.2374785382,1.5798525963
H,0,1.1309592399,0.28562737,-0.3020350381
H,0,-0.1874376501,-0.8575060111,-0.23910257
C,0,0.9494826903,-0.6958469918,2.2922164719
H,0,1.5395922024,-1.4080771603,1.7179223857
C,0,-0.8245225687,1.1911750388,-0.5959802644
H,0,-0.7987480357,1.1014453906,-1.6859817818
H,0,-1.8561810923,1.0564039993,-0.2606831505
H,0,-0.5283972936,2.2076764794,-0.324059225
O,0,-0.5849661503,1.0681379123,2.18706777
C,0,1.0359768773,-0.7139850527,3.7746184413
H,0,2.0677498319,-0.5444492857,4.1130987642
H,0,0.3890677353,0.055511833,4.1995155751
H,0,0.7421281224,-1.6938343588,4.1763825009

Table C.3 *n*-CC(=O)CCC Optimized Species

n-CC(=O)CCC (σ = 9)

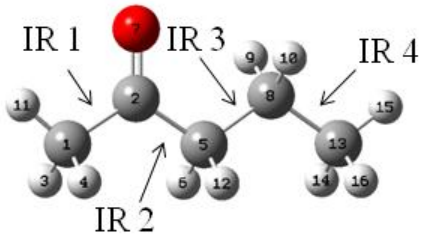

C,0,0.1723886725,0.0028585389,0.0357563224
C,0,-0.2919697233,0.043177066,1.4827100722
H,0,1.2172841458,-0.3230848743,-0.0232451252
H,0,-0.4186743862,-0.7206129075,-0.5375845809
C,0,-0.2206110291,-1.2672625966,2.2581424362
H,0,0.8170969038,-1.6308173959,2.212932275
O,0,-0.6988504498,1.0708560373,1.991608332
C,0,-0.6987117911,-1.1624074804,3.7066139557
H,0,-0.1046849959,-0.4001499533,4.2225552751
H,0,-1.7283100257,-0.7883264026,3.7147032747
H,0,0.0724382583,0.9928562312,-0.4110124642
H,0,-0.8046544634,-2.0188985379,1.705858235
C,0,-0.6148491583,-2.4942770627,4.456662693
H,0,0.4140274766,-2.870893101,4.4916233411
H,0,-0.9630421455,-2.3882622858,5.488910585
H,0,-1.2306180228,-3.2641051745,3.977243141

n-CJC(=O)CCC (σ = 3)

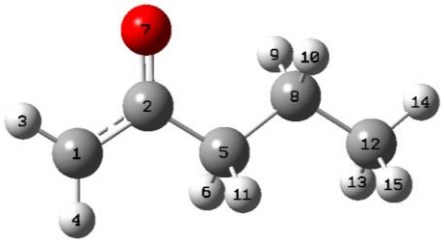

C,0,0.106923829,-0.1386298603,0.0214921723
C,0,0.1620191641,-0.0754330128,1.4594172218
H,0,-0.2875365559,0.7129400842,-0.5217032826
H,0,0.4463760745,-1.0081492878,-0.5331499355
C,0,0.719691644,-1.2818204266,2.2118606341
H,0,1.7341080344,-1.4825628127,1.8365001444
O,0,-0.2355347804,0.9358872008,2.0553991778
C,0,0.7326638341,-1.1068536742,3.7303309303
H,0,1.315868282,-0.2137572122,3.980677741
H,0,-0.2865672338,-0.8968112005,4.0730591732
H,0,0.1298444227,-2.1663327531,1.9290545419
C,0,1.2952899858,-2.3277005267,4.4625015546
H,0,2.3284779315,-2.535369718,4.1607623797
H,0,1.2921876748,-2.1738110271,5.5461478577
H,0,0.7047595666,-3.2274892574,4.254402834

n-CC(=O)CJCC (σ = 9)

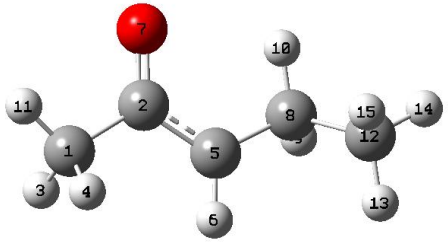

C,0,0.,0.,0.
C,0,0.,0.,1.52225494
H,0,1.027388361,0.,-0.3830344425
H,0,-0.4942493593,-0.8921271323,-0.3996245226
C,0,0.4796329042,-1.1815743154,2.2006268173
H,0,0.8075103172,-2.0307845343,1.6017949701
O,0,-0.3910653942,0.9902612527,2.1585279499
C,0,0.5422389561,-1.2865791746,3.6840212579
H,0,1.598434717,-1.3564710126,3.9902608497
H,0,0.1448851195,-0.3626957429,4.1132768889
H,0,-0.5109072188,0.8935168654,-0.3609333071
C,0,-0.2053489064,-2.5156734881,4.2369572662
H,0,0.1876675686,-3.4471926235,3.8155212148
H,0,-0.1010056017,-2.5694219404,5.3248641469
H,0,-1.2725554525,-2.4640307701,4.0016254369

Table C.3 *n*-CC(=O)CCC Optimized Species (Continued)

n-CC(=O)CCJC (σ = 9)

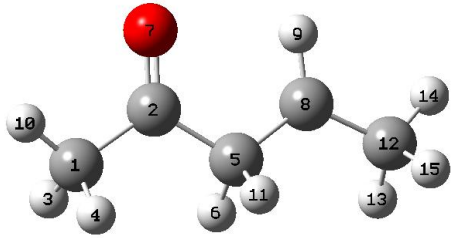

C,0,0.,0.,0.
C,0,0.,0.,1.51907517
H,0,1.0326762582,0.,-0.3694383347
H,0,-0.4811852363,-0.9004236392,-0.3968991564
C,0,0.4728641382,-1.2873484218,2.1941767751
H,0,1.4034676273,-1.6184295737,1.7006591829
O,0,-0.3582018105,0.9715185719,2.1560167953
C,0,0.6349696095,-1.1890522673,3.6704676632
H,0,0.2671140886,-0.2923766208,4.1561605474
H,0,-0.5105107734,0.8903588482,-0.3691784596
H,0,-0.256839804,-2.0734992095,1.9148841166
C,0,1.1280626399,-2.3473442178,4.4675861627
H,0,2.0444842024,-2.7806773231,4.0403209558
H,0,1.3422765426,-2.0655008367,5.502398051
H,0,0.3947011376,-3.1719302739,4.5023784067

n-CC(=O)CCCJ (σ = 3)

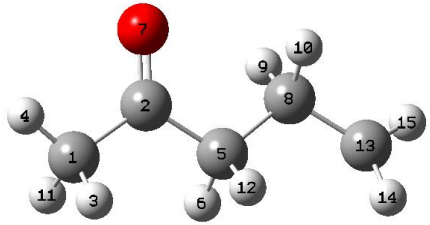

C,0,-0.0021166166,0.0018717439,0.0000885036
C,0,0.0020229182,-0.0012853676,1.519690149
H,0,1.0193243375,0.0383399885,-0.3946903403
H,0,-0.5109962455,-0.8893684434,-0.3693114773
C,0,0.7934847458,1.1092136947,2.1999053889
H,0,0.4932003861,2.072672408,1.7655616887
O,0,-0.597186931,-0.8473047574,2.1568023516
C,0,0.6488600084,1.1269591122,3.7256878729
H,0,-0.4063930944,1.2678812154,3.9898562595
H,0,0.892228887,0.1180363881,4.1010605011
H,0,-0.5189941594,0.8946305934,-0.3715239116
H,0,1.8492617868,0.9862917935,1.914553833
C,0,1.4947001004,2.1605165956,4.3861351448
H,0,2.4760661853,2.4112284473,3.9940049651
H,0,1.2310383651,2.55330426,5.3620957238

Table C.4 CC(=O)C(C)C Optimized Species

CC(=O)C(C)C (σ = 27)

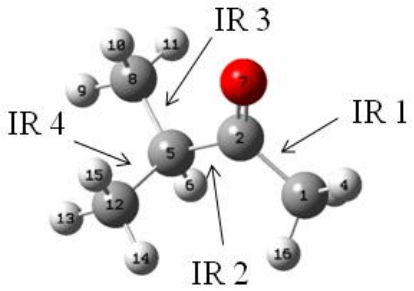

C,0,-0.0020451387,0.0022486545,-0.0000841247
C,0,0.0048212766,-0.0010989216,1.5187174991
H,0,1.0322803269,-0.0200560409,-0.3655412678
H,0,-0.5309130261,-0.8756963859,-0.3735330181
C,0,0.4606221701,1.2868479453,2.2153244224
H,0,1.1762323849,1.7947091173,1.5541508219
O,0,-0.3485533867,-0.9771377018,2.1540685025
C,0,1.1254233983,0.9846035445,3.5617808321
H,0,1.4053045811,1.91207434,4.0710943892
H,0,0.4417064537,0.4232374141,4.2034413466
H,0,2.0286764622,0.3803009244,3.4332057547
C,0,-0.7645251907,2.2115647574,2.3873650547
H,0,-0.46365846,3.156945439,2.8494195896
H,0,-1.243997471,2.4451933102,1.431116578
H,0,-1.5102048386,1.7380076593,3.0339437746
H,0,-0.4582327901,0.9149365347,-0.397933546

CJC(=O)C(C)C (σ = 9)

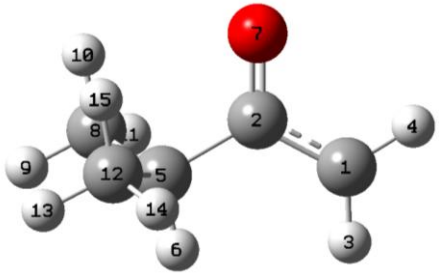

C,0,0.3325801323,-0.3166112614,0.1917624436
C,0,-0.1413627582,0.033512096,1.4988956887
H,0,1.0167096407,0.3148902973,-0.3658034521
H,0,-0.0068232312,-1.2462684813,-0.2523638745
C,0,0.3223254452,1.3388600884,2.1561191095
H,0,0.9866770021,1.8681528774,1.4612278095
O,0,-0.9256498913,-0.7222405302,2.1001859342
C,0,1.1031649182,1.014249003,3.4414907081
H,0,1.4136215193,1.9341467782,3.9469447081
H,0,0.4727762483,0.4373818902,4.1244695647
H,0,2.0011318278,0.4243228618,3.2297822358
C,0,-0.8976046111,2.2263791279,2.4550225713
H,0,-0.5906275636,3.1456728237,2.9637187237
H,0,-1.4261411895,2.5068594312,1.5379244093
H,0,-1.5997854386,1.6890778648,3.0989626467

Table C.4 CC(=O)C(C)C Optimized Species (Continued)

CC(=O)CJ(C)C (σ = 27)

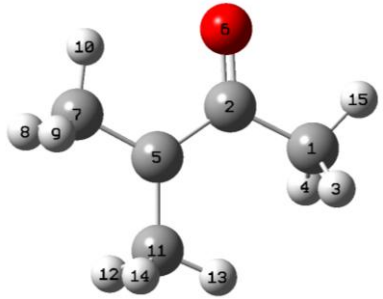

C,0,0.054004464,-0.0188720238,0.00565626
C,0,-0.1893566295,-0.0789936648,1.509393213
H,0,1.089182399,0.2552043466,-0.226629572
H,0,-0.143542129,-0.9832304557,-0.4756498711
C,0,0.5713997053,-1.0016063745,2.3314912137
O,0,-1.0411966192,0.666123207,2.0208657553
C,0,0.3113691366,-1.038526367,3.80228291
H,0,-0.0007018141,-2.0435833267,4.1196160354
H,0,1.2262476862,-0.8109851306,4.3674800326
H,0,-0.4637559244,-0.3211788365,4.0719433956
C,0,1.6118492683,-1.9273474216,1.7845163758
H,0,1.3596285411,-2.9723454186,2.0152900383
H,0,1.7465717463,-1.8442468402,0.7053785336
H,0,2.5843378603,-1.7422012902,2.2629233599
H,0,-0.6144541252,0.7315765504,-0.4174154937

CC(=O)C(C)CJ (σ = 9, OI)

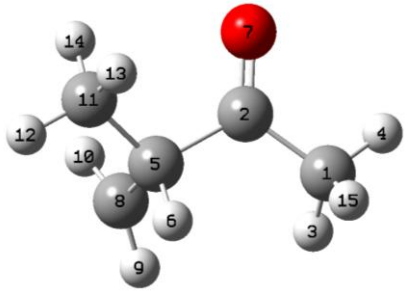

C,0,0.0001542686,0.0008650046,-0.0002156266
C,0,-0.0007149476,0.0013127456,1.5173730279
H,0,1.0203827723,0.0169282622,-0.3956859029
H,0,-0.5336358837,-0.8746749839,-0.3724460503
C,0,0.953382228,1.0129071942,2.2115897401
H,0,0.9359082023,1.9334403454,1.6112905023
O,0,-0.6983180996,-0.756219105,2.1613977629
C,0,2.3287248752,0.4288412842,2.1597101136
H,0,2.9932425406,0.6088571772,1.3218549003
H,0,2.6177269091,-0.3225682283,2.8876348478
C,0,0.4879734319,1.3022998046,3.6440083583
H,0,1.1672746509,2.0068606588,4.1313938043
H,0,-0.5205623122,1.7261721497,3.6510670515
H,0,0.4600358973,0.3781985067,4.2264914239
H,0,-0.5021176967,0.9062995776,-0.363099292

Table C.5 CC(C)C(=O)CC Optimized Species

CC(C)C(=O)CC (σ = 27)

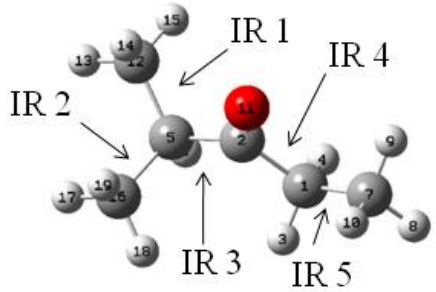

C,0,0.0722543856,0.1543265123,0.0712513956
C,0,0.0740385253,0.2131539206,1.5928833142
H,0,1.1053471137,0.2859863851,-0.2801466396
H,0,-0.1885949649,-0.8778552223,-0.2075196689
C,0,1.1329334869,-0.625071922,2.3202371278
H,0,1.4586478784,-1.4289028787,1.6464784669
C,0,-0.8752010611,1.1548795644,-0.5846318222
H,0,-0.8633509472,1.0467284537,-1.6730644428
H,0,-1.898536049,1.00828257,-0.2306087682
H,0,-0.5918196033,2.1816043432,-0.3370799569
O,0,-0.7125708135,0.9092752394,2.209180126
C,0,0.5647776832,-1.2313195579,3.6086899024
H,0,1.341028601,-1.7769168104,4.1543960622
H,0,0.1704136924,-0.4415921987,4.2531358373
H,0,-0.2531210026,-1.9270461839,3.3959210087
C,0,2.3502240868,0.2779211961,2.6128564114
H,0,3.1402282788,-0.2964283779,3.106822732
H,0,2.7716951658,0.7083205869,1.6981723331
H,0,2.0604907337,1.1014326774,3.2730043529

CJC(C)C(=O)CC (σ = 9, OI)

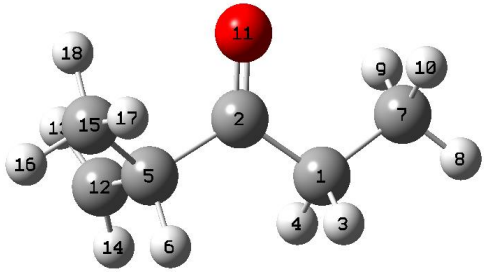

C,0,0.,0.,0.
C,0,0.,0.,1.52276922
H,0,1.0535162865,0.,-0.3182083134
H,0,-0.4030910419,-0.9613252736,-0.344261263
C,0,0.5448954008,-1.2811116667,2.2139436535
H,0,1.3536855506,-1.6720548611,1.5814359667
C,0,-0.7530026139,1.1772772088,-0.6144663054
H,0,-0.6883628367,1.1517900135,-1.7061176084
H,0,-1.8090669378,1.156341989,-0.3314953733
H,0,-0.3419339765,2.1266456358,-0.2629807529
O,0,-0.4192611386,0.9383603759,2.1713715316
C,0,-0.573883372,-2.2725734231,2.2366277363
H,0,-1.3474207295,-2.1875971088,2.9932504644
H,0,-0.7317099117,-2.9709141714,1.422108523
C,0,1.0757399906,-0.956338512,3.616535383
H,0,1.4400731573,-1.8631284259,4.1068549985
H,0,1.8945317191,-0.2320362156,3.5685490002
H,0,0.2831424925,-0.5178562905,4.227649926

CCJ(C)C(=O)CC (σ = 27)

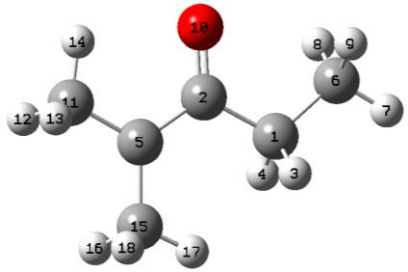

C,0,0.2722185636,0.6577222219,0.2422183014
C,0,-0.1211694762,0.0873614054,1.6076966062
H,0,0.8850804207,1.5566921763,0.3955511651
H,0,0.9306967992,-0.0598051732,-0.2665198277
C,0,0.9108797117,-0.2750810457,2.5636928361
C,0,-0.936591669,0.9821334935,-0.6331377537
H,0,-0.6153548443,1.3863312176,-1.5978824307
H,0,-1.5398210611,0.0888289448,-0.8134947021
H,0,-1.5857122253,1.7150316615,-0.1474363377
O,0,-1.3205204912,-0.0628585174,1.891870717
C,0,0.5004584662,-0.8295992682,3.8892893154
H,0,0.9275237072,-1.8305703491,4.044159253
H,0,0.8817301593,-0.2053801791,4.7098317666
H,0,-0.5855917499,-0.8893339685,3.9604031525
C,0,2.3762156668,-0.1249578415,2.298214425
H,0,2.8859944744,-1.0949753318,2.3880182437
H,0,2.6041128177,0.2846552844,1.3135854066
H,0,2.8401352109,0.5271028305,3.0521885579

Table C.5 CC(C)C(=O)CC Optimized Species (Continued)

CC(C)C(=O)CJC (σ = 27)

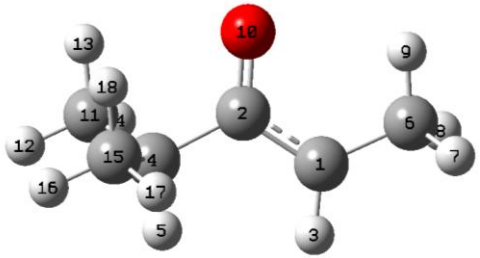

C,0,-1.4711174763,0.1031032083,-0.6831655617
C,0,-0.3018358691,-0.0323320978,0.1468495474
H,0,-1.3381351997,0.2731377986,-1.749627866
C,0,1.0888065608,0.0692689544,-0.4905793054
H,0,0.9725680939,0.20769389,-1.573314782
C,0,-2.8480930551,0.0195774231,-0.1332796587
H,0,-3.4076993128,0.9446611197,-0.3302957622
H,0,-3.416785848,-0.7875303098,-0.6156206599
H,0,-2.8149197922,-0.1573316562,0.9430731669
O,0,-0.4077957073,-0.2262696795,1.3711704371
C,0,1.8707319777,-1.2301603495,-0.2353028502
H,0,2.8831001229,-1.1600954527,-0.6459701961
H,0,1.9423300369,-1.4159761953,0.8401617583
H,0,1.3776093734,-2.0930791597,-0.6951585588
C,0,1.8301611354,1.2870846801,0.0882143642
H,0,2.8411394339,1.357308871,-0.3257747963
H,0,1.3062178822,2.2219837386,-0.1372109917
H,0,1.9048086433,1.1953292168,1.1757217149

CC(C)C(=O)CCJ (σ = 9)

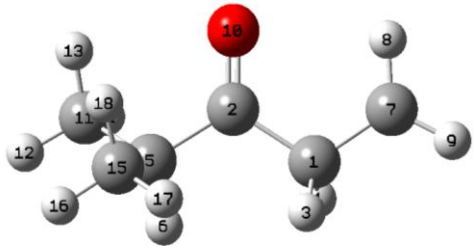

C,0,0.,0.,0.
C,0,0.,0.,1.52782316
H,0,1.0468772171,0.,-0.3480635913
H,0,-0.3693328762,-0.997600469,-0.3069231143
C,0,0.9665323986,-0.9714852921,2.2138036392
H,0,1.2035513681,-1.777469881,1.5063071658
C,0,-0.7944689037,1.0927360071,-0.6152825699
H,0,-1.3930138442,1.7399117577,0.0130411504
H,0,-0.8112618544,1.2220809299,-1.6909397494
O,0,-0.7152336881,0.7436466383,2.1723749261
C,0,0.3424901884,-1.565928747,3.4816641543
H,0,1.0585884002,-2.2137648951,3.9968339725
H,0,0.0387840802,-0.7663522228,4.1620233078
H,0,-0.5464914831,-2.1603463771,3.2482888703
C,0,2.2733713899,-0.2132873897,2.5315701326
H,0,3.0002241746,-0.8875514034,2.9951104257
H,0,2.7333672762,0.2073476928,1.6311514246
H,0,2.0750817134,0.6085830511,3.2265456048

Table C.6 Moments of Inertia[a]

Species	I_a	I_b	I_c
CC(=O)CC	189.39105	505.35910	661.52402
CJC(=O)CC	180.91563	477.27129	636.07929
CC(=O)CJC	179.55491	498.43809	655.69499
CC(=O)CCJ	185.60218	478.32019	641.15294
CCC(=O)CC	202.67834	930.49092	1089.01852
CJCC(=O)CC	198.12991	894.57144	1058.89429
CCJC(=O)CC	192.38548	917.16050	1076.34979
n-CC(=O)CCC	216.24129	1015.05276	1187.00608
n-CJC(=O)CCC	203.41448	981.49519	1151.73784
n-CC(=O)CJCC	229.45174	964.34632	1098.88524
n-CC(=O)CCJC	205.77428	1006.95001	1178.16998
n-CC(=O)CCCJ	209.98594	972.69340	1144.47572
CC(=O)C(C)C	381.81433	649.01129	807.21600
CJC(=O)C(C)C	365.29318	688.72204	716.87563
CC(=O)CJ(C)C	382.83975	564.99730	914.45275
CC(=O)C(C)CJ	370.37465	612.04143	801.78333
CC(C)C(=O)CC	393.15883	1157.50038	1280.89312
CJC(C)C(=O)CC	382.14385	1101.73291	1275.41623
CCJ(C)C(=O)CC	399.04154	1041.86771	1396.62496
CC(C)C(=O)CJC	380.61463	1196.31226	1221.60735
CC(C)C(=O)CCJ	389.72724	1115.50489	1242.54386

[a] AMU Bohr^2.

Table C.7 Vibrational Frequencies

Species	Frequencies (cm^{-1})									
CC(=O)CC	32.08	106.20	196.58	248.24	400.84	472.75	588.48	759.35	763.43	943.49
	954.86	1003.08	1111.09	1135.26	1193.56	1288.84	1378.93	1399.78	1428.27	1466.59
	1480.28	1491.69	1507.07	1513.25	1814.88	3023.19	3045.70	3051.26	3061.04	3106.38
	3133.15	3140.10	3164.47							
CJC(=O)CC	53.70	196.56	250.05	375.14	406.05	493.91	586.36	723.10	773.22	811.52
	980.71	1016.50	1078.50	1103.15	1215.07	1281.20	1385.22	1427.78	1473.95	1476.87
	1505.60	1511.83	1612.65	3024.88	3054.14	3059.99	3132.44	3138.25	3160.21	3277.26
CC(=O)CJC	37.64	114.25	157.41	259.61	414.68	522.72	597.96	665.51	796.16	962.43
	984.65	1034.84	1044.55	1141.51	1222.15	1393.08	1398.66	1434.38	1480.31	1490.27
	1493.26	1499.67	1622.44	3014.65	3044.64	3055.31	3107.01	3151.24	3162.39	3171.98
CC(=O)CCJ	47.46	106.35	180.29	267.98	405.00	415.86	474.16	587.12	748.64	806.19
	945.07	1014.90	1023.69	1120.76	1186.18	1192.04	1372.53	1399.08	1437.11	1452.45
	1478.63	1491.24	1819.93	2950.72	2983.79	3045.14	3107.17	3165.44	3179.57	3294.81
CCC(=O)CC	30.40	66.97	174.89	194.41	200.22	308.74	407.64	465.49	623.60	715.39
	783.28	825.14	968.49	1004.64	1013.63	1021.93	1118.75	1142.54	1143.28	1267.71
	1309.76	1361.65	1394.46	1427.68	1428.59	1463.47	1476.05	1506.26	1506.44	1512.49
	1512.70	1808.85	3020.60	3030.50	3047.86	3059.38	3060.26	3060.73	3132.41	3132.72
	3139.38	3139.75								
CJCC(=O)CC	22.70	62.12	179.45	197.24	204.54	323.02	409.43	417.04	467.66	617.49
	729.42	774.19	875.93	981.02	1001.00	1036.81	1062.19	1125.37	1138.36	1186.72
	1291.66	1355.87	1391.57	1427.77	1437.49	1452.80	1469.76	1507.41	1513.46	1813.84
	2951.36	2985.65	3024.88	3054.48	3061.28	3132.72	3141.62	3179.33	3294.58	
CCJC(=O)CC	45.75	117.11	136.70	198.53	206.87	319.06	424.04	514.22	630.17	653.52
	801.56	806.28	975.75	992.12	1029.27	1064.40	1080.28	1135.69	1186.22	1280.89
	1359.52	1400.40	1427.20	1440.08	1475.42	1490.96	1497.74	1505.29	1511.85	1629.07
	3014.22	3022.92	3051.81	3054.54	3059.09	3131.07	3137.79	3150.47	3170.02	
n-CC(=O)CCC	24.80	91.73	108.62	174.84	247.93	340.59	394.59	476.40	593.01	727.65
	824.48	838.67	907.34	964.25	981.09	1054.60	1132.90	1145.41	1187.94	1257.70
	1328.77	1329.62	1395.95	1409.95	1429.58	1465.62	1479.94	1491.95	1501.88	1514.97
	1521.71	1812.78	3013.17	3036.24	3040.09	3045.25	3060.09	3086.57	3106.16	3110.58
	3113.61	3163.61								
n-CJC(=O)CCC	37.12	94.74	177.05	250.71	342.75	375.58	398.81	496.18	591.27	715.97
	760.19	828.28	881.31	928.15	1000.30	1055.48	1098.81	1127.43	1202.82	1251.61
	1326.13	1335.42	1408.61	1429.91	1471.66	1476.21	1500.36	1515.56	1521.43	1609.53
	3013.58	3036.41	3041.89	3058.26	3085.65	3109.60	3113.74	3160.09	3277.22	

Table C.7 Vibrational Frequencies (Continued)

Species	Frequencies (cm^{-1})									
n-CC(=O)CJCC	39.26	47.18	115.61	201.57	272.95	348.21	417.06	521.67	593.84	684.97
	765.58	872.36	928.12	979.11	1021.18	1049.40	1067.31	1159.42	1220.97	1277.88
	1332.62	1396.69	1419.93	1454.91	1484.69	1487.95	1492.99	1512.79	1519.12	1621.10
	2992.99	3044.54	3045.80	3104.30	3106.16	3121.97	3126.71	3158.52	3163.09	
n-CC(=O)CCJC	49.61	71.70	98.83	121.25	180.88	337.33	352.54	392.65	463.93	594.23
	802.40	825.60	919.29	969.86	984.02	1035.90	1114.99	1163.41	1185.82	1194.40
	1309.15	1395.23	1413.38	1429.21	1444.45	1478.79	1487.50	1491.17	1498.49	1817.13
	2924.19	2965.12	2976.23	3022.31	3044.93	3107.23	3113.24	3164.61	3222.92	
n-CC(=O)CCCJ	50.12	95.60	110.30	135.14	179.87	348.16	391.56	475.16	479.46	594.16
	723.91	820.11	880.09	924.39	967.52	1040.00	1094.31	1128.31	1174.70	1196.58
	1295.72	1327.63	1394.16	1404.49	1464.91	1477.52	1479.34	1483.46	1491.54	1812.34
	2971.41	3018.81	3045.29	3051.97	3066.62	3107.20	3154.38	3164.17	3257.42	
CC(=O)C(C)C	44.87	133.39	203.84	228.66	235.98	288.11	327.84	434.46	593.21	601.64
	732.58	889.92	936.93	960.53	974.24	1008.31	1123.51	1130.62	1170.34	1214.05
	1332.01	1375.91	1397.79	1411.68	1430.67	1476.59	1490.11	1500.79	1503.91	1517.22
	1526.12	1811.33	3029.80	3043.01	3044.73	3052.72	3105.37	3116.22	3120.29	3123.55
	3140.05	3163.17								
CJC(=O)C(C)C	18.23	217.69	237.30	241.75	287.79	321.63	391.40	445.86	602.51	628.53
	740.23	806.41	907.26	937.11	975.64	1001.36	1113.72	1122.93	1185.02	1225.71
	1348.73	1388.69	1405.37	1425.27	1476.73	1500.47	1507.29	1515.96	1527.52	1569.23
	3040.61	3044.08	3047.63	3114.07	3116.37	3129.11	3133.77	3162.01	3276.98	
CC(=O)CJ(C)C	66.92	98.64	105.81	152.65	280.36	307.94	363.55	449.59	552.05	566.28
	692.34	939.13	950.06	962.01	990.27	1008.44	1055.94	1158.69	1284.27	1369.25
	1400.46	1404.80	1423.58	1474.42	1479.27	1487.69	1496.67	1505.10	1513.29	1605.73
	3008.64	3015.47	3044.52	3048.59	3053.66	3105.25	3149.37	3163.32	3165.18	
CC(=O)C(C)CJ	57.07	109.77	193.09	213.06	228.35	276.40	333.16	426.26	523.58	578.48
	600.65	729.58	900.13	926.30	950.61	1012.05	1057.98	1131.70	1168.38	1190.93
	1282.13	1357.71	1393.26	1417.96	1472.51	1476.78	1490.61	1506.82	1508.66	1811.56
	3025.30	3045.07	3057.64	3112.04	3130.04	3143.09	3159.02	3164.00	3267.29	
CC(C)C(=O)CC	33.24	74.73	184.38	194.48	210.68	243.60	258.09	309.37	329.01	448.89
	567.82	629.12	765.11	809.87	880.52	938.40	974.87	992.92	1031.38	1053.60
	1122.57	1128.39	1142.24	1204.28	1280.98	1336.53	1360.97	1392.48	1409.38	1426.96
	1428.96	1464.70	1500.81	1504.93	1507.21	1513.11	1516.72	1526.70	1805.77	3018.01
	3034.74	3043.16	3049.52	3050.86	3060.06	3113.74	3117.82	3124.96	3130.68	3139.53
	3140.42									

Table C.7 Vibrational Frequencies (Continued)

Species	Frequencies (cm^{-1})									
CJC(C)C(=O)CC	54.96	61.79	180.78	186.98	203.78	220.09	242.32	310.43	335.07	436.58
	522.58	563.92	628.27	759.93	809.64	894.01	925.44	984.45	1018.45	1040.58
	1084.76	1122.12	1147.34	1179.32	1267.77	1298.45	1354.90	1376.89	1415.89	1427.00
	1466.44	1472.30	1506.57	1506.93	1509.18	1513.58	1805.45	3019.25	3031.52	3056.47
	3059.94	3062.58	3128.28	3130.89	3141.55	3143.56	3158.83	3267.27		
CCJ(C)C(=O)CC	45.18	76.88	107.34	111.21	206.41	218.27	308.82	324.04	359.05	463.85
	551.77	558.76	733.91	804.65	922.63	950.06	961.97	1005.36	1035.45	1056.26
	1082.91	1130.37	1283.14	1283.36	1324.96	1398.37	1402.68	1423.92	1427.46	1472.46
	1480.97	1482.83	1502.22	1507.05	1512.29	1514.60	1609.68	3008.17	3014.95	3023.24
	3048.06	3052.87	3053.82	3059.20	3131.00	3140.68	3151.57	3164.68		
CC(C)C(=O)CJC	18.07	113.50	131.06	206.16	227.48	264.84	267.49	303.91	338.93	467.40
	606.88	640.08	738.41	787.33	885.95	936.38	974.91	997.11	1017.76	1082.26
	1114.26	1129.32	1183.64	1206.85	1348.19	1365.83	1398.31	1404.58	1422.73	1437.87
	1490.09	1493.53	1500.19	1507.52	1515.88	1528.06	1594.01	3015.90	3037.43	3043.01
	3046.60	3056.98	3112.44	3114.71	3128.30	3133.16	3152.13	3176.78		
CC(C)C(=O)CCJ	31.93	84.39	178.83	201.62	209.76	230.23	258.02	311.22	342.57	428.77
	454.01	559.99	622.68	755.13	878.46	890.57	940.41	975.59	1004.44	1033.46
	1097.98	1126.54	1131.48	1179.80	1204.35	1333.08	1356.23	1391.09	1410.78	1428.92
	1434.52	1453.50	1501.02	1504.79	1516.41	1526.12	1809.98	2941.51	2987.83	3033.41
	3044.35	3051.64	3115.19	3118.98	3125.67	3140.01	3178.66	3293.55		

Internal Rotor (IR) notation and 0° dihedral angle corresponds to the structures from the Optimized Species.

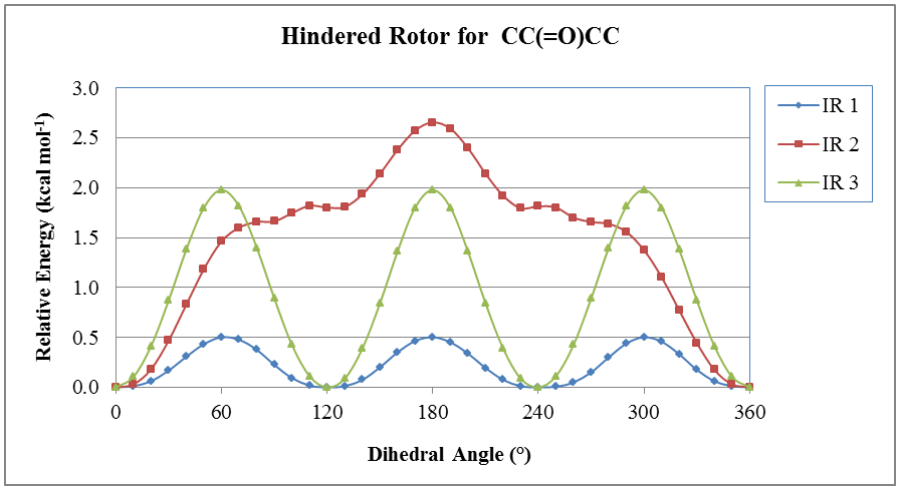

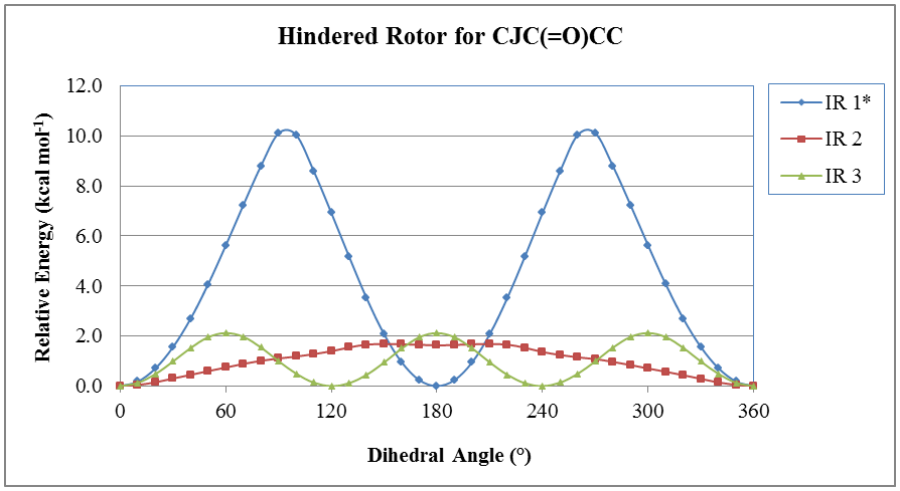

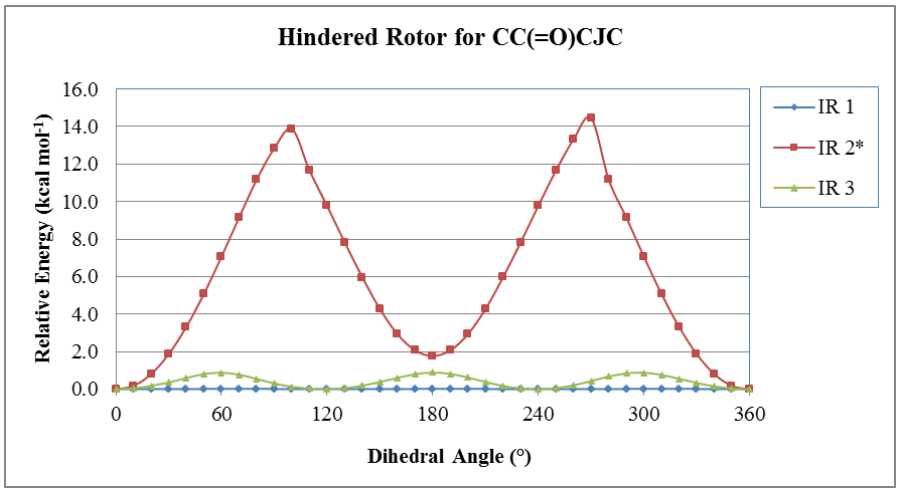

Figure C.1 Internal rotation of CC(=O)CC species.

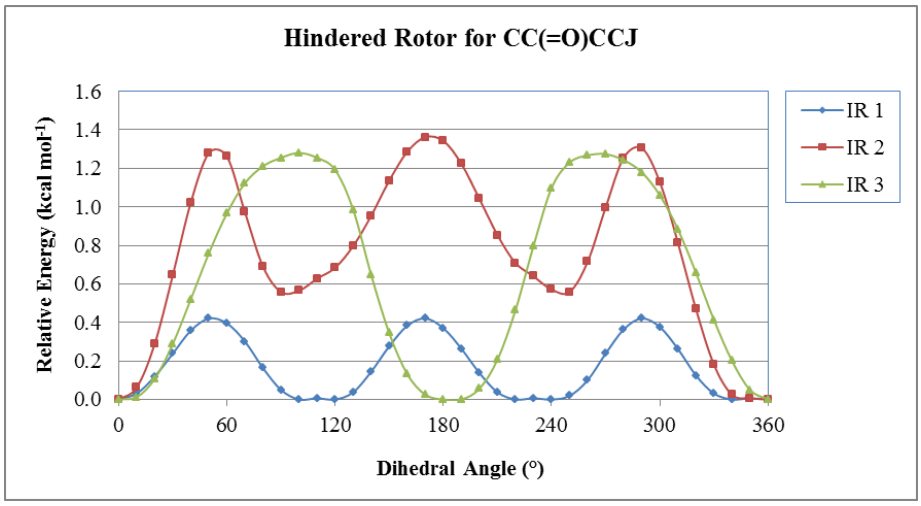

Figure C.1 Internal rotation of CC(=O)CC species. (Continued)

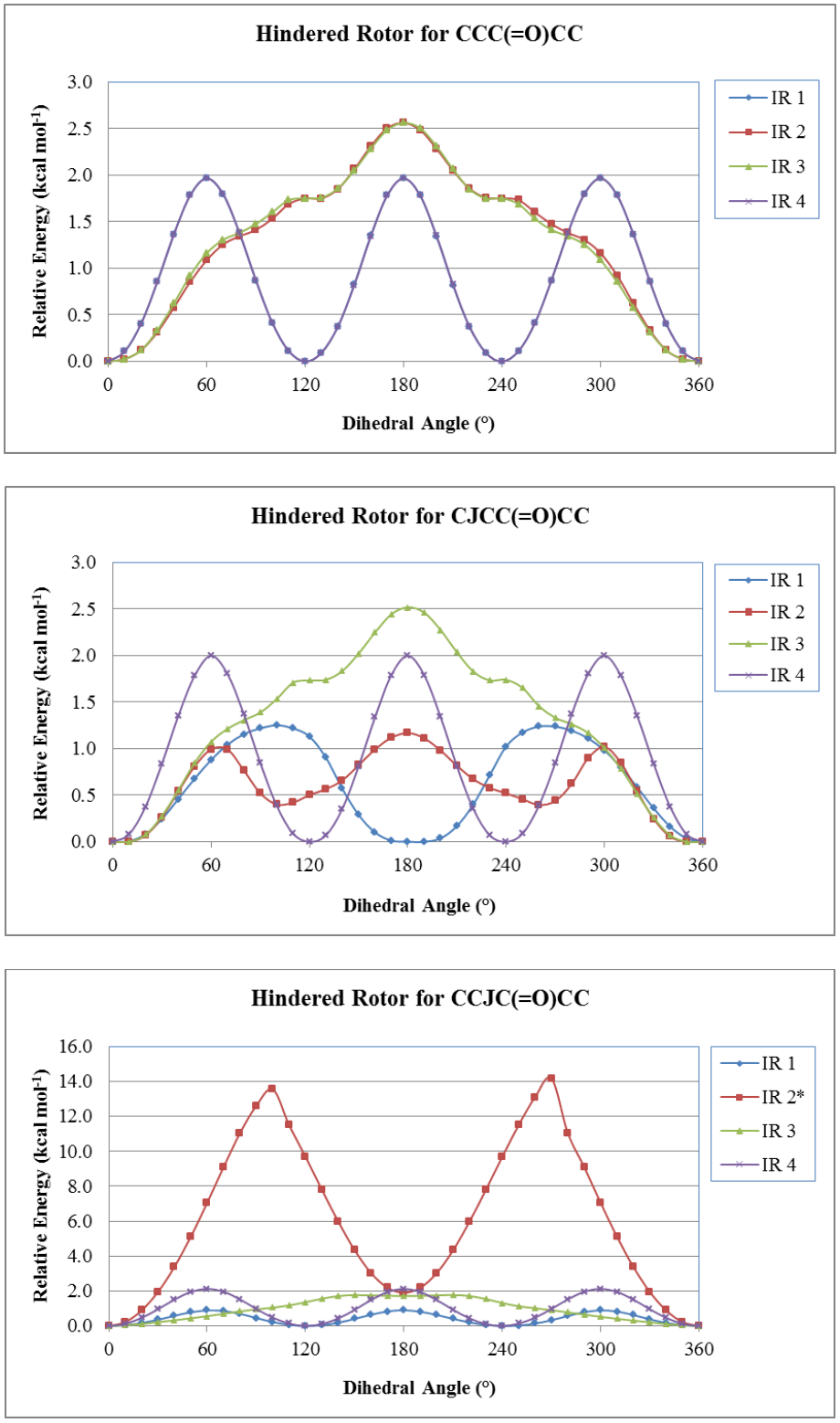

Figure C.2 Internal rotation of CCC(=O)CC species.

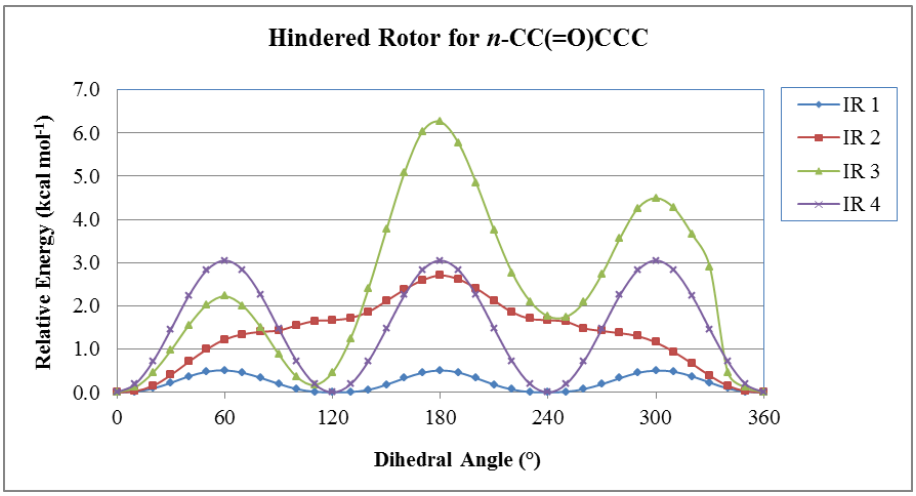

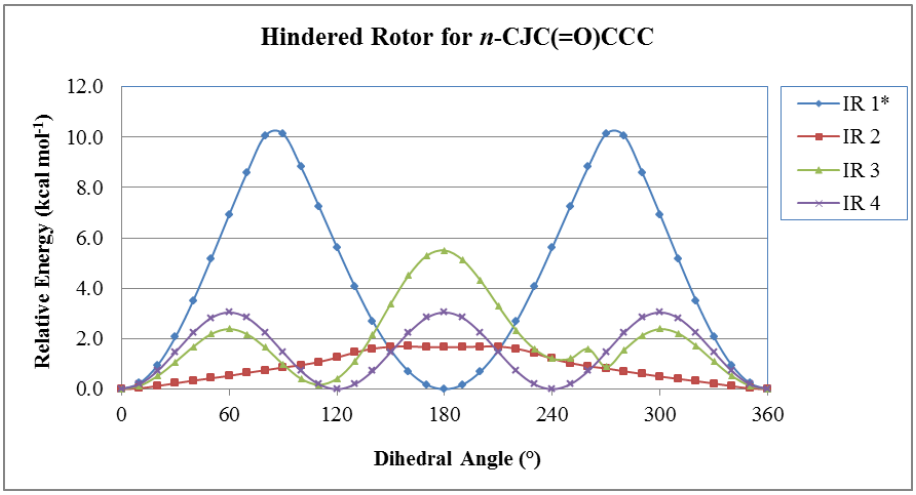

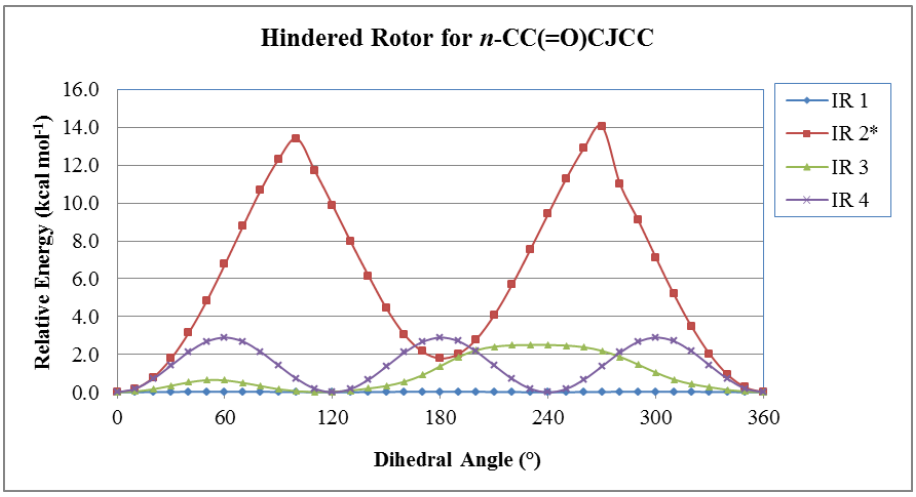

Figure C.3 Internal rotation of *n*-CC(=O)CCC species.

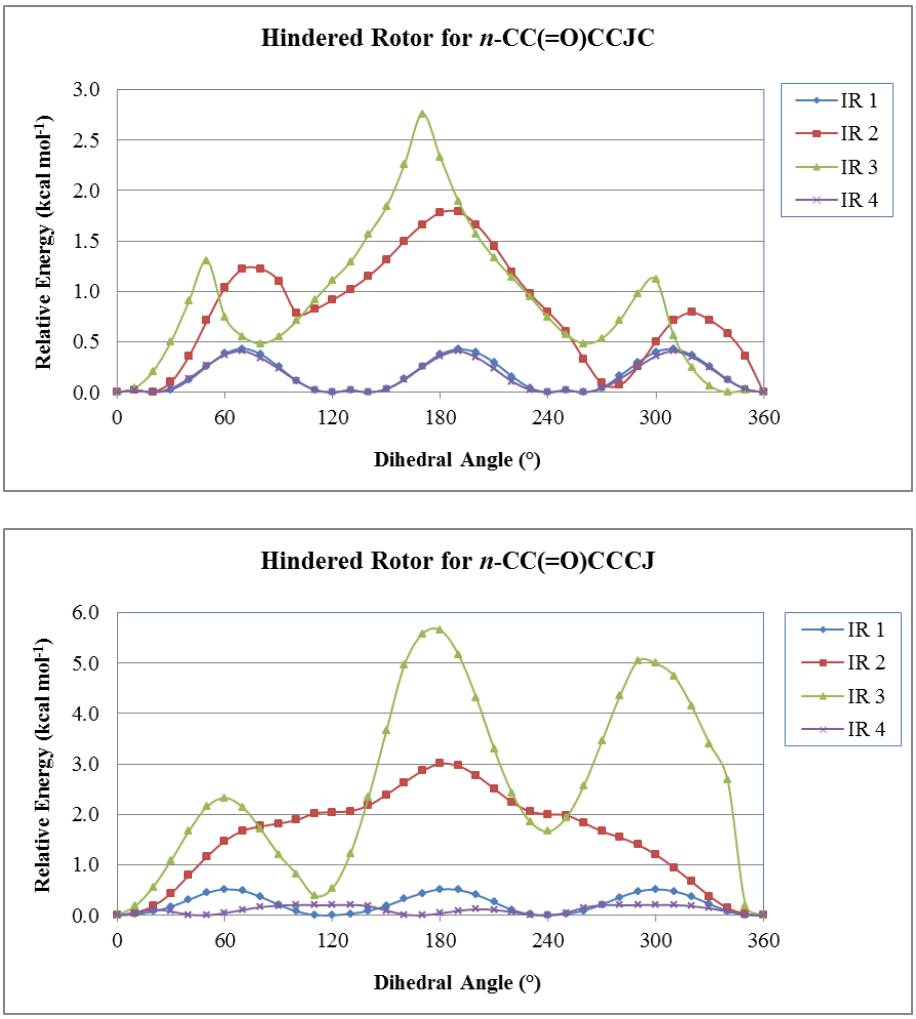

Figure C.3 Internal rotation of *n*-CC(=O)CCC species. (Continued)

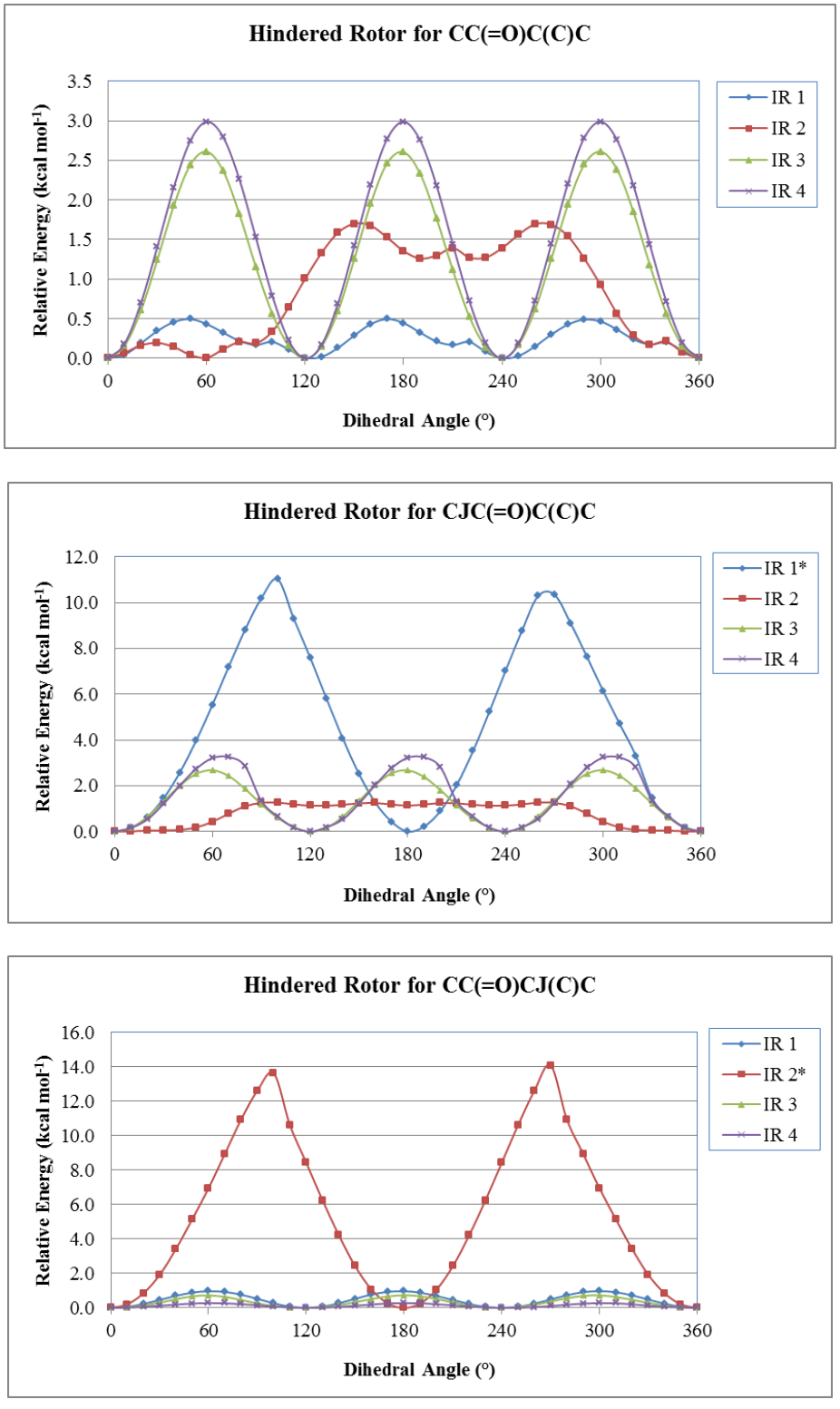

Figure C.4 Internal rotation of CC(=O)C(C)C species.

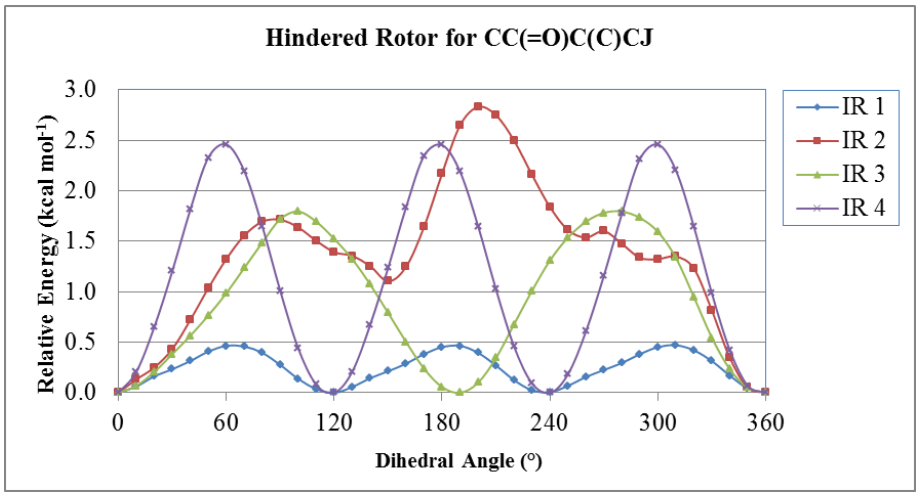

Figure C.4 Internal rotation of CC(=O)C(C)C species. (Continued)

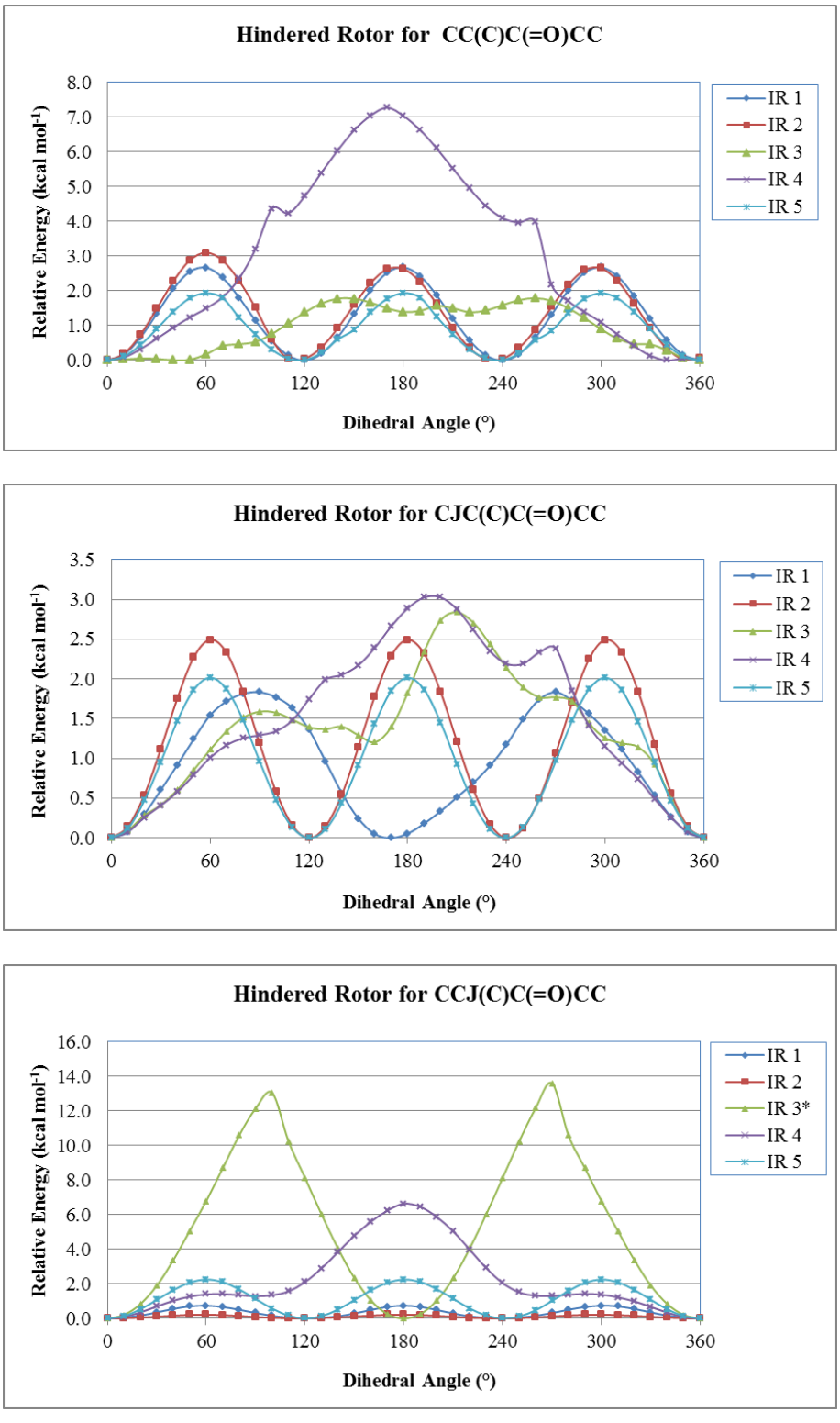

Figure C.5 Internal rotation of CC(C)C(=O)CC species.

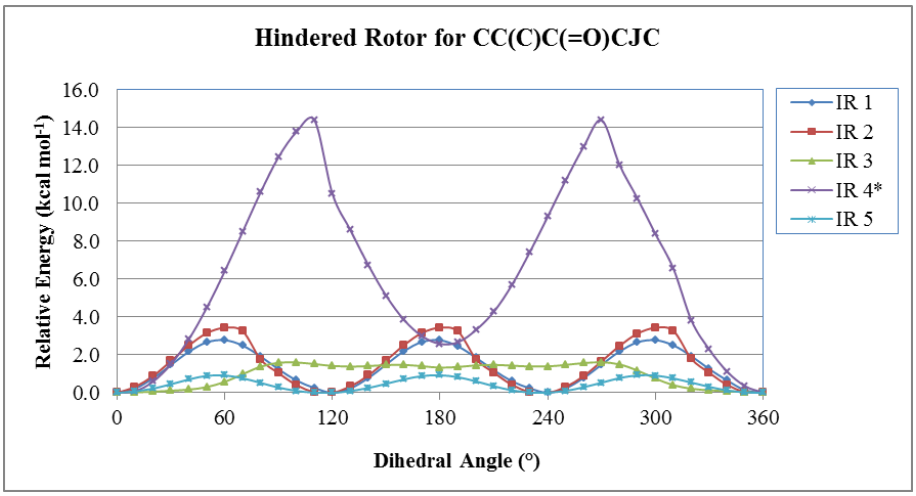

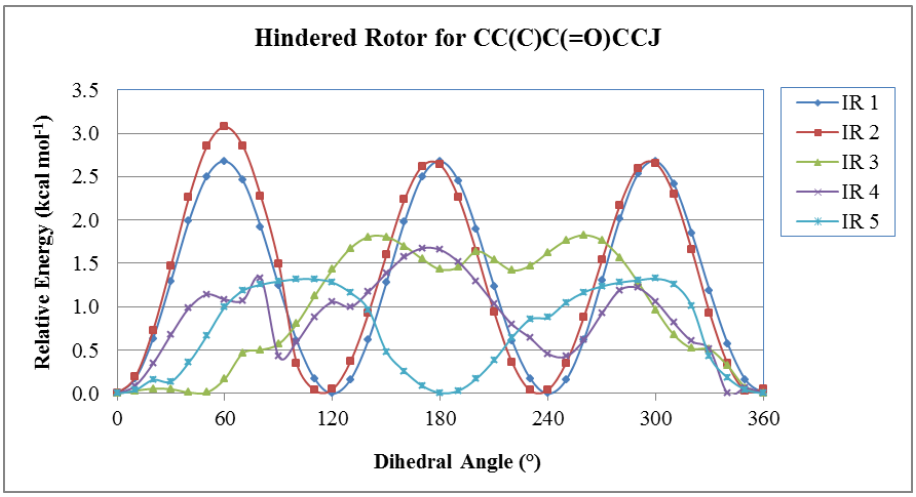

Figure C.5 Internal rotation of CC(C)C(=O)CC species. (Continued)

Table C.8 Calculated Total Entropies[a] and Heat Capacities[a]

Temperature	CC(=O)CC		CJC(=O)CC		CC(=O)CJC		CC(=O)CCJ	
(K)	Cp	S	Cp	S	Cp	S	Cp	S
100	14.060	65.551	12.709	62.790	13.106	62.641	14.570	68.274
150	16.178	70.431	15.577	67.672	15.065	67.517	16.873	73.404
200	18.459	74.524	18.347	71.960	17.098	71.549	18.985	77.688
250	20.883	78.239	21.000	75.888	19.396	75.156	21.141	81.483
298	23.362	81.585	23.516	79.437	21.804	78.413	23.338	84.850
400	28.753	88.323	28.686	86.489	27.105	84.973	28.163	91.505
500	33.675	94.601	33.223	92.933	31.899	91.094	32.548	97.590
600	37.996	100.574	37.115	98.969	36.036	96.912	36.345	103.316
700	41.746	106.250	40.433	104.631	39.559	102.423	39.606	108.704
800	45.000	111.631	43.285	109.947	42.578	107.635	42.423	113.776
1000	50.304	121.592	47.903	119.672	47.436	117.226	47.012	123.081
1500	58.682	142.531	55.188	139.811	54.991	137.237	54.262	142.448
2000	63.028	159.202	58.978	155.681	58.875	153.066	58.034	157.760
2500	65.435	172.878	61.086	168.640	61.023	166.007	60.128	170.284
3000	66.875	184.397	62.349	179.532	62.306	176.889	61.378	180.819
3500	67.791	194.317	63.154	188.898	63.124	186.250	62.177	189.884
4000	68.409	203.011	63.695	197.102	63.673	194.450	62.717	197.823
4500	68.841	210.742	64.075	204.392	64.058	201.738	63.095	204.880
5000	69.155	217.698	64.352	210.948	64.339	208.292	63.371	211.228
Zero Point Energy[b]	68.787		60.749		60.733		59.389	

[a] Units of cal mol^{-1} K^{-1}.

[b] Units of kcal mol^{-1}.

Table C.8 Calculated Total Entropies[a] and Heat Capacities[a] (Continued A)

Temperature	CCC(=O)CC		CJCC(=O)CC		CCJC(=O)CC	
(K)	Cp	S	Cp	S	Cp	S
100	16.571	69.926	17.302	74.185	15.983	67.786
150	20.039	75.704	20.739	80.260	19.230	73.685
200	23.244	80.756	23.643	85.478	22.077	78.751
250	26.397	85.387	26.493	90.156	24.960	83.310
298	29.487	89.583	29.312	94.345	27.882	87.413
400	36.100	97.996	35.405	102.638	34.276	95.613
500	42.102	105.809	40.899	110.238	40.127	103.225
600	47.374	113.218	45.667	117.389	45.232	110.447
700	51.962	120.245	49.783	124.122	49.619	117.284
800	55.952	126.905	53.349	130.464	53.397	123.750
1000	62.472	139.221	59.163	142.119	59.504	135.676
1500	72.794	165.098	68.365	166.420	69.056	160.594
2000	78.157	185.695	73.157	185.657	73.979	180.337
2500	81.127	202.590	75.815	201.400	76.700	196.492
3000	82.905	216.820	77.406	214.645	78.327	210.082
3500	84.038	229.073	78.424	226.042	79.364	221.775
4000	84.800	239.813	79.108	236.027	80.059	232.021
4500	85.333	249.365	79.587	244.903	80.545	241.127
5000	85.720	257.957	79.935	252.888	80.900	249.318
Zero Point Energy[b]	86.273		76.874		78.262	

[b] Units of kcal mol^{-1}.

Table C.8 Calculated Total Entropies[a] and Heat Capacities[a] (Continued B)

Temperature (K)	*n*-CC(=O)CCC		*n*-CJC(=O)CCC		*n*-CC(=O)CJCC		*n*-CC(=O)CCJC		*n*-CC(=O)CCCJ	
	Cp	S	Cp	S	Cp	S	Cp	S	Cp	S
100	14.107	75.068	12.783	72.020	14.297	68.197	17.457	75.329	14.806	78.633
150	18.681	77.458	18.088	74.433	17.615	73.406	19.832	81.229	18.901	81.195
200	21.752	82.101	21.647	79.261	20.922	78.062	22.279	86.113	21.797	85.872
250	25.086	86.418	25.179	83.793	24.312	82.415	24.965	90.485	25.001	90.182
298	28.514	90.408	28.614	87.981	27.634	86.440	27.802	94.399	28.279	94.149
400	35.844	98.651	35.700	96.516	34.526	94.656	34.100	102.276	35.182	102.267
500	42.320	106.453	41.794	104.467	40.543	102.339	39.847	109.612	41.164	109.872
600	47.833	113.930	46.885	111.995	45.661	109.639	44.849	116.592	46.166	117.096
700	52.506	121.039	51.141	119.078	50.007	116.539	49.152	123.214	50.360	123.912
800	56.511	127.774	54.752	125.741	53.734	123.057	52.861	129.483	53.933	130.334
1000	62.984	140.207	60.551	137.932	59.757	135.041	58.879	141.054	59.679	142.113
1500	73.123	166.255	69.616	163.172	69.171	160.038	68.295	165.286	68.684	166.582
2000	78.368	186.927	74.312	183.039	74.042	179.805	73.142	184.510	73.360	185.891
2500	81.273	203.862	76.919	199.256	76.741	195.971	75.818	200.251	75.952	201.672
3000	83.010	218.113	78.481	212.880	78.352	209.569	77.412	213.496	77.506	214.937
3500	84.113	230.384	79.474	224.596	79.380	221.268	78.427	224.896	78.496	226.349
4000	84.859	241.133	80.143	234.855	80.072	231.514	79.112	234.881	79.163	236.343
4500	85.384	250.688	80.615	243.969	80.558	240.622	79.592	243.758	79.632	245.225
5000	85.763	259.285	80.958	252.166	80.910	248.813	79.940	251.743	79.972	253.213
Zero Point Energy[b]	86.259		78.218		78.459		76.852		76.942	

[b] Units of kcal mol^{-1}.

Table C.8 Calculated Total Entropies[a] and Heat Capacities[a] (Continued C)

Temperature (K)	CC(=O)C(C)C		CJC(=O)C(C)C		CC(=O)CJ(C)C		CC(=O)C(C)CJ	
	Cp	S	Cp	S	Cp	S	Cp	S
100	15.857	69.781	14.483	66.899	15.865	67.017	16.434	72.435
150	19.373	75.267	18.561	72.343	18.565	72.761	20.102	78.181
200	22.572	80.132	22.142	77.321	21.094	77.584	23.504	83.280
250	25.751	84.615	25.594	81.957	23.834	81.907	26.766	87.990
298	28.915	88.704	28.903	86.202	26.720	85.801	29.857	92.251
400	35.708	96.983	35.671	94.778	33.207	93.679	36.125	100.739
500	41.862	104.716	41.523	102.695	39.215	101.069	41.574	108.496
600	47.217	112.095	46.470	110.161	44.471	108.140	46.232	115.764
700	51.841	119.099	50.662	117.176	48.989	114.869	50.234	122.569
800	55.851	125.747	54.262	123.773	52.873	121.262	53.692	128.967
1000	62.396	138.042	60.098	135.855	59.142	133.085	59.357	140.681
1500	72.737	163.894	69.300	160.940	68.886	157.898	68.396	165.025
2000	78.116	184.475	74.103	180.732	73.881	177.603	73.153	184.265
2500	81.101	201.362	76.772	196.910	76.638	193.740	75.807	200.004
3000	82.884	215.588	78.373	210.511	78.283	207.321	77.398	213.247
3500	84.020	227.840	79.393	222.213	79.331	219.009	78.413	224.643
4000	84.785	238.578	80.082	232.460	80.034	229.250	79.099	234.628
4500	85.322	248.126	80.566	241.568	80.528	238.354	79.579	243.503
5000	85.714	256.716	80.918	249.760	80.886	246.543	79.929	251.486
Zero Point Energy[b]	85.982		78.033		77.981		76.899	

[b] Units of kcal mol^{-1}.

Table C.8 Calculated Total Entropies[a] and Heat Capacities[a] (Continued D)

Temperature (K)	CC(C)C(=O)CC		CJC(C)C(=O)CC		CCJ(C)C(=O)CC		CC(C)C(=O)CJC		CC(C)C(=O)CCJ	
	Cp	S	Cp	S	Cp	S	Cp	S	Cp	S
100	16.126	77.827	18.827	77.753	15.546	75.256	17.259	71.206	18.858	77.751
150	20.937	83.695	23.838	84.346	19.397	81.092	21.991	77.529	23.956	84.387
200	27.047	86.172	28.189	90.371	24.959	83.426	25.881	83.244	28.003	90.415
250	30.963	91.523	32.247	95.984	28.619	88.488	29.668	88.531	31.680	95.949
298	34.824	96.404	36.039	101.092	32.339	93.123	33.425	93.356	35.225	100.927
400	43.090	106.325	43.669	111.296	40.504	102.592	41.451	103.131	42.671	110.859
500	50.591	115.633	50.252	120.639	47.968	111.546	48.588	112.256	49.318	119.979
600	57.142	124.528	55.865	129.387	54.447	120.140	54.730	120.930	55.073	128.571
700	62.784	132.988	60.680	137.586	59.970	128.327	59.968	129.142	60.028	136.665
800	67.638	141.011	64.854	145.288	64.679	136.106	64.469	136.907	64.319	144.286
1000	75.461	155.860	71.681	159.404	72.184	150.480	71.765	151.208	71.336	158.298
1500	87.580	186.989	82.596	188.731	83.654	180.547	83.202	181.090	82.461	187.535
2000	93.767	211.674	88.335	211.916	89.465	204.338	89.118	204.762	88.270	210.690
2500	97.169	231.882	91.531	230.886	92.659	223.778	92.398	224.139	91.497	229.648
3000	99.198	248.875	93.454	246.843	94.553	240.122	94.361	240.440	93.428	245.602
3500	100.478	263.502	94.677	260.577	95.756	254.179	95.607	254.471	94.656	259.336
4000	101.343	276.312	95.502	272.610	96.565	266.488	96.447	266.762	95.489	271.364
4500	101.947	287.699	96.082	283.305	97.132	277.426	97.039	277.685	96.073	282.058
5000	102.388	297.937	96.503	292.926	97.544	287.262	97.470	287.512	96.497	291.678
Zero Point Energy[b]	103.497		94.409		95.534		95.599		94.096	

[b] Units of kcal mol^{-1}.

APPENDIX D

THERMOCHEMICAL PROPERTIES OF *EXO*-TRICYCLO[5.2.1.0^{2,6}]DECANE (JP-10 JET FUEL) AND DERIVED TRICYCLODECYL RADICALS

This appendix contains the optimized geometries with corresponding Gaussian atom numbering, moments of inertia, vibrational frequencies, entropies, and heat capacities for all of the parent and radical species from B3LYP/6-31G(d,p) level of theory. Enthalpies of formation for 2-norbornyl radical and TCD isomers, small molecule work reactions that do not provide acceptable results, reaction enthalpies for tricyclodecyl radicals, and NASA polynomial thermodynamic data for TCD and radicals are also presented.

Table D.1 TCD Optimized Species

TCD

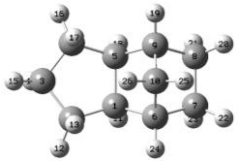

C,0,-0.009936876,-0.0454603529,0.0379517511
C,0,0.0222885028,-0.0729379786,1.5845590761
C,0,1.4968749666,0.1763335726,1.9480299357
C,0,2.268117951,-0.6122856752,0.8747565882
C,0,1.4584178383,-0.398099485,-0.426126579
C,0,-0.8624667339,-1.1362541719,-0.6550440384
C,0,-0.8901879465,-0.8330200385,-2.1730641133
C,0,0.5649050899,-1.1824630788,-2.6329449535
C,0,1.2478221695,-1.6430705993,-1.3219963221
C,0,0.0782845622,-2.3609743294,-0.6123658083
H,0,-0.3090291634,0.9514017703,-0.3057230136
H,0,-0.658860967,0.6592928665,2.0304491421
H,0,-0.285495562,-1.0593424885,1.9551396349
H,0,1.7259861906,1.2464392125,1.8598176764
H,0,1.7478184305,-0.1247746002,2.9708162495
H,0,3.311146217,-0.2941259396,0.7757080367
H,0,2.285183703,-1.6767013886,1.1426767422
H,0,1.9020553835,0.4203870496,-1.0045454973
H,0,2.1550308282,-2.2345818433,-1.4787624379
H,0,0.5598921187,-1.989832061,-3.3728356121
H,0,1.0807258031,-0.3299487901,-3.0870365055
H,0,-1.6255552045,-1.4650224287,-2.6821049477
H,0,-1.1598401138,0.2081067641,-2.3789582341
H,0,-1.8537536064,-1.271814847,-0.2118014366
H,0,-0.3060204524,-3.2175876574,-1.177378613
H,0,0.3168831213,-2.7002016817,0.4003618345

TCD-R1

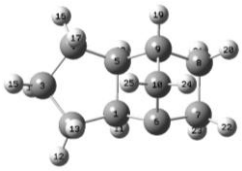

C,0,-0.0283445637,-0.0633797186,0.0423488369
C,0,0.0222099751,-0.0589748357,1.5885825883
C,0,1.5035945775,0.1809588621,1.9308382874
C,0,2.2580428642,-0.6462840885,0.8746395895
C,0,1.4476202023,-0.4594171789,-0.4283494379
C,0,-0.8323534336,-1.1535404298,-0.6415941182
C,0,-0.9444595659,-0.9200745232,-2.1386496039
C,0,0.512224488,-1.3148101614,-2.6096879551
C,0,1.2076644743,-1.7334186851,-1.2852373429
C,0,0.0246330457,-2.4099163262,-0.5317870006
H,0,-0.3084937087,0.9283898572,-0.3280008044
H,0,-0.6452917674,0.6926072537,2.0216864662
H,0,-0.2970094303,-1.0314909012,1.982116048
H,0,1.7456988414,1.2452191246,1.8121487863
H,0,1.7597525642,-0.0960364112,2.9590255797
H,0,3.3039311105,-0.3425744312,0.7602996257
H,0,2.2643911369,-1.7029148539,1.1712524572
H,0,1.8933032689,0.3368591646,-1.0351865407
H,0,2.1063876293,-2.342023808,-1.4309691628
H,0,0.4825629999,-2.1512806837,-3.3156548751
H,0,1.0291734384,-0.4855825715,-3.1036423679
H,0,-1.6920294818,-1.573549909,-2.6007523585
H,0,-1.2026684707,0.1130246908,-2.3896177613
H,0,-0.3836335608,-3.273646372,-1.0660889295
H,0,0.2686377734,-2.7114510041,0.490119056

Table D.1 TCD Optimized Species (Continued)

TCD-R2

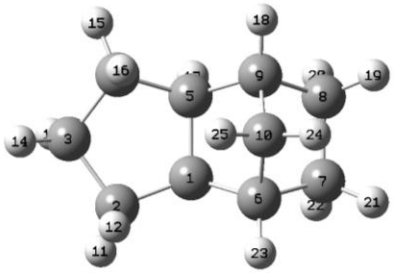

C,0,-0.0044629229,0.0245452199,0.011773605
C,0,0.0251823975,-0.1129263915,1.5119222333
C,0,1.5073666603,0.1529728787,1.8786062875
C,0,2.2969156269,-0.3182232377,0.6381232454
C,0,1.412195367,0.1297559395,-0.5496156587
C,0,-0.7957340367,-0.8217932034,-0.9549868889
C,0,-0.964042562,-0.0297220586,-2.2825897617
C,0,0.4869228882,0.0001088995,-2.8689617923
C,0,1.3183604993,-0.7707354137,-1.8120342533
C,0,0.3009897049,-1.8504712874,-1.3698348472
H,0,-0.6644868143,0.5651189231,2.0331320611
H,0,-0.2723816619,-1.1321018852,1.8116126904
H,0,1.6630068498,1.2287425504,2.0258164324
H,0,1.8162593179,-0.3480994112,2.8014839847
H,0,3.3122980347,0.0901347976,0.5967888099
H,0,2.3860642165,-1.4122203958,0.6499635301
H,0,1.6890462848,1.1571499956,-0.8328196146
H,0,2.2812783503,-1.1336523823,-2.1832104734
H,0,0.5290723292,-0.507227095,-3.8385154734
H,0,0.8584919146,1.0188901771,-3.0192683382
H,0,-1.6512062522,-0.5537744588,-2.9556893107
H,0,-1.3704337992,0.9705590817,-2.1094258786
H,0,-1.7260477514,-1.2376576425,-0.5593879998
H,0,-0.010269921,-2.5093495429,-2.1892973498
H,0,0.6459900818,-2.470656526,-0.536336413

TCD-R3

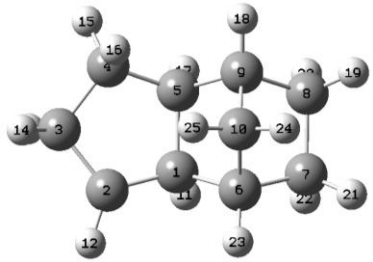

C,0,-0.0162016665,-0.0903685413,0.0523436858
C,0,0.0128575792,-0.0894006901,1.5461139578
C,0,1.3794096051,0.1983627519,2.0798509853
C,0,2.3271263968,-0.2245075139,0.9311864858
C,0,1.500985179,-0.1241246451,-0.3798746506
C,0,-0.6097558381,-1.3511977646,-0.6475745842
C,0,-0.6909271368,-1.0541007853,-2.1635366018
C,0,0.8102433302,-1.0641013423,-2.6061105378
C,0,1.5657754223,-1.3751247514,-1.2909164877
C,0,0.576737449,-2.3350546081,-0.5917262809
H,0,-0.5357140812,0.8054888246,-0.3275198565
H,0,-0.8843109983,-0.0867626729,2.1586993935
H,0,1.4978597586,1.2757418664,2.2993765384
H,0,1.596421912,-0.3190292702,3.0236381051
H,0,3.2337024023,0.3876367913,0.8916314379
H,0,2.6522172769,-1.2590221137,1.0899247501
H,0,1.7811535329,0.7771667112,-0.9360082026
H,0,2.581335539,-1.7532580593,-1.4434716315
H,0,0.9951034262,-1.8430863638,-3.3532404287
H,0,1.1272652308,-0.1123230288,-3.04529411
H,0,-1.259170483,-1.8338186212,-2.681677758
H,0,-1.1870237618,-0.0998682506,-2.3701414114
H,0,-1.5493804672,-1.6962106864,-0.2070752431
H,0,0.4006910433,-3.2566304922,-1.1576532431
H,0,0.8655709574,-2.6029625718,0.429319952

TCD-R4

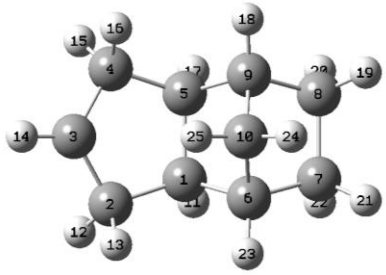

C,0,-0.0085860189,0.01170965,-0.002081102
C,0,-0.0091288282,0.0302936032,1.5503841134
C,0,1.4124919502,-0.1691699014,1.9637781886
C,0,2.3697581937,-0.01868456,0.8268182823
C,0,1.5044815168,-0.0194717391,-0.462300869
C,0,-0.5834518128,-1.2817019671,-0.6329577233
C,0,-0.6792291128,-1.0782209699,-2.1636062981
C,0,0.8169011011,-1.1090951093,-2.618659563
C,0,1.5816624587,-1.326325483,-1.2914951078
C,0,0.6119450001,-2.2548802619,-0.5267736683
H,0,-0.536721316,0.8885458838,-0.3909422797
H,0,-0.4090918044,0.9884659137,1.9262324875
H,0,-0.6770176526,-0.7390066853,1.9681473298
H,0,1.7256298574,-0.2602901226,2.9994742776
H,0,2.9469978801,0.9193579247,0.9054349368
H,0,3.1275879462,-0.8173556718,0.810913129
H,0,1.7594092769,0.8411976896,-1.0893886986
H,0,2.6026333867,-1.6961052553,-1.4264297447
H,0,1.0010985668,-1.9364611737,-3.3121413537
H,0,1.12505735,-0.1881374225,-3.1247080125
H,0,-1.2494377675,-1.8898771908,-2.6277784635
H,0,-1.1817474244,-0.1404281389,-2.4228829296
H,0,-1.5198602174,-1.6111526251,-0.1725992471
H,0,0.4375826191,-3.2096991499,-1.0354487727
H,0,0.9210633631,-2.4586632968,0.5034064003

Table D.1 TCD Optimized Species (Continued)

TCD-R9

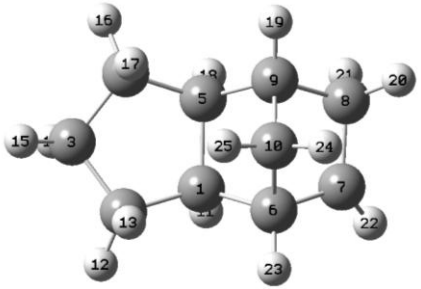

C,0,-0.0232542262,-0.0476539328,0.0461655647
C,0,0.0194728642,-0.0913542014,1.5931042743
C,0,1.4945012843,0.1757415462,1.9438639369
C,0,2.2685120496,-0.5915128456,0.8563914077
C,0,1.4425959929,-0.385271312,-0.4356672898
C,0,-0.8746354384,-1.1527688346,-0.6644502363
C,0,-0.8380911258,-0.8482244269,-2.1371179277
C,0,0.5435311234,-1.1892137994,-2.640322266
C,0,1.2451104465,-1.6378826305,-1.329375139
C,0,0.0887844343,-2.3663038835,-0.6075017969
H,0,-0.3358566188,0.9470990392,-0.2873652204
H,0,-0.6670270107,0.6287846154,2.0500195667
H,0,-0.2720906211,-1.0848159993,1.9569425255
H,0,1.7064165805,1.2498445313,1.8635436399
H,0,1.7600644959,-0.131097056,2.9613112779
H,0,3.3041322914,-0.2526385746,0.7493745947
H,0,2.308892986,-1.6569449399,1.1173429038
H,0,1.8695017924,0.4383053975,-1.0190860614
H,0,2.1583360476,-2.2187229542,-1.4883892365
H,0,0.5270894408,-2.008422019,-3.3778588754
H,0,1.0551877983,-0.346819699,-3.1278157664
H,0,-1.544754398,-0.2084274914,-2.6551898726
H,0,-1.8703439284,-1.289616904,-0.2329948514
H,0,-0.2873280613,-3.232650382,-1.1608673464
H,0,0.3374126095,-2.6850553575,0.4092838508

TCD-R10

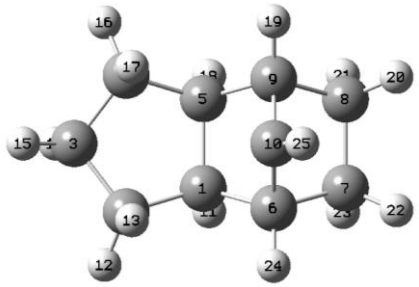

C,0,-0.0032478505,-0.0369644392,0.045925464
C,0,0.0326448265,-0.0504655963,1.5912318369
C,0,1.5054179382,0.2115354347,1.9486818117
C,0,2.2700667539,-0.601803203,0.8907192486
C,0,1.4667822519,-0.3992257579,-0.4143320496
C,0,-0.8592320231,-1.1505754446,-0.6150856812
C,0,-0.8901069111,-0.876487357,-2.1513927525
C,0,0.5660658033,-1.2353675603,-2.6073415595
C,0,1.257344267,-1.6721652297,-1.2777829196
C,0,0.0927945907,-2.3230154802,-0.5683253756
H,0,-0.3059304616,0.9523183021,-0.3160629165
H,0,-0.6563920309,0.675246533,2.0359335808
H,0,-0.2578044708,-1.0434534777,1.9576128737
H,0,1.7343799733,1.2799052986,1.8391079021
H,0,1.7577537619,-0.0704511267,2.976571253
H,0,3.3192687184,-0.3043879514,0.791178459
H,0,2.2566340266,-1.6630405183,1.1703874648
H,0,1.9116841251,0.4058161908,-1.0104013848
H,0,2.1593823268,-2.27234684,-1.4216986076
H,0,0.559745906,-2.0594942399,-3.3275623828
H,0,1.0836163383,-0.3923187572,-3.0787664807
H,0,-1.6253002776,-1.5209575684,-2.6434206908
H,0,-1.1619745453,0.161128182,-2.3756225629
H,0,-1.8471363495,-1.2850192383,-0.1672325022
H,0,-0.1881685217,-3.3694980108,-0.6420297783

exo-TCD boat

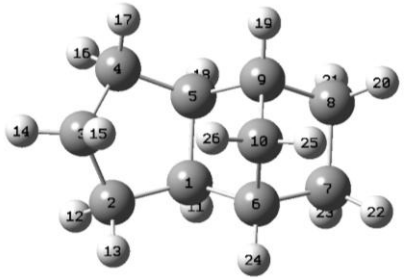

C,0,0.3261078927,0.7880784319,-0.6557988601
C,0,1.7510856722,1.2190868907,-0.2361422678
C,0,2.4104094301,-0.0000841123,0.4352958924
C,0,1.750952794,-1.2191524414,-0.2362250566
C,0,0.3260736378,-0.7879243391,-0.6560733951
C,0,-0.8174881944,1.130222533,0.3291048831
C,0,-2.1562324286,0.7820851608,-0.3614154461
C,0,-2.1563155832,-0.7815873137,-0.3619469593
C,0,-0.817698487,-1.1303590246,0.3285062693
C,0,-0.7279069615,-0.0003547586,1.3750522397
H,0,0.0929863846,1.1983330026,-1.638510762
H,0,2.3172547383,1.4916572173,-1.1291395043
H,0,1.7440728481,2.0985424287,0.4097075576
H,0,3.49413063,-0.000135509,0.3145151573
H,0,2.2181598856,-0.0001069441,1.5081016476
H,0,2.3171987234,-1.4918689512,-1.1291246529
H,0,1.743686087,-2.0985740297,0.4096675021
H,0,0.0931562879,-1.1978266483,-1.6389800093
H,0,-0.7731839996,-2.1488511532,0.7121115324
H,0,-2.9990321227,-1.1734091065,0.2082005701
H,0,-2.2204625353,-1.2012530808,-1.3658812476
H,0,-2.9988153386,1.1735972189,0.2091447059
H,0,-2.2204987587,1.2024589287,-1.3650451184
H,0,-0.7727367112,2.1485034363,0.713243296
H,0,-1.5703201262,-0.0004506599,2.0688047483
H,0,0.1913452355,-0.0006079983,1.9552662779

Table D.1 TCD Optimized Species (Continued)

exo-TCD TS

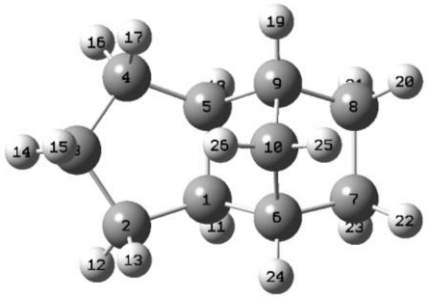

C,0,-0.0101723399,0.0012531259,-0.0005240507
C,0,-0.0083095075,0.0122681845,1.5498460581
C,0,1.4637177013,-0.004962711,2.0422600344
C,0,2.3829829779,-0.0227661545,0.7915536046
C,0,1.4909622926,-0.0208656297,-0.4765383034
C,0,-0.5931310188,-1.2850402989,-0.6400474355
C,0,-0.7071776365,-1.066615151,-2.1672597439
C,0,0.7835759245,-1.0886795583,-2.639916764
C,0,1.5643244605,-1.3168957274,-1.3240748439
C,0,0.6057088299,-2.2561955806,-0.558739789
H,0,-0.5400508933,0.8812808689,-0.3811988865
H,0,-0.5323594118,0.8975187634,1.9245619952
H,0,-0.5585845966,-0.8519233377,1.9392084687
H,0,1.6742073928,0.8701048794,2.6655969913
H,0,1.6515306746,-0.8787178612,2.6749158102
H,0,3.0504484447,0.8450988121,0.7883594871
H,0,3.033929881,-0.9044849124,0.8000741754
H,0,1.7280217225,0.8477984049,-1.1005251101
H,0,2.5849388687,-1.6819064316,-1.4740029078
H,0,0.9615800811,-1.9081725383,-3.3443808661
H,0,1.083644599,-0.161520412,-3.1394032439
H,0,-1.2804861938,-1.874943729,-2.6335695943
H,0,-1.2151050526,-0.1274684741,-2.4105003413
H,0,-1.5230988436,-1.6212598481,-0.1715589789
H,0,0.4284249324,-3.2071287902,-1.0736286778
H,0,0.9271680545,-2.474690886,0.4653354214

endo-TCD chair

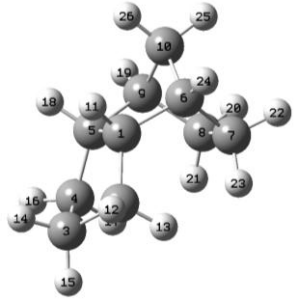

C,0,-0.0479213909,-0.0422240996,-0.0551270221
C,0,0.0618741379,-0.332073774,1.457069256
C,0,1.5233107435,0.0226850915,1.8001453921
C,0,1.7999457998,1.2874175854,0.9615646431
C,0,1.0834864618,1.0119005832,-0.3776896464
C,0,-1.3175006986,0.6123089139,-0.6649677633
C,0,-1.7561450328,1.8614556997,0.1339810667
C,0,-0.6364642592,2.9046643926,-0.1853597093
C,0,0.3124654908,2.1308517807,-1.1297442731
C,0,-0.7068502615,1.276452327,-1.9247445432
H,0,0.1472426365,-0.9704877053,-0.6056083729
H,0,-0.194295539,-1.3664512205,1.708268743
H,0,-0.6109016202,0.3102199012,2.0363557014
H,0,2.1878217933,-0.7893956054,1.4768989826
H,0,1.691637739,0.1701182367,2.8724642869
H,0,2.8688277517,1.4877754742,0.835028989
H,0,1.3727500746,2.1585834069,1.4707981029
H,0,1.804793367,0.573734383,-1.0780621632
H,0,0.9568706294,2.7824300744,-1.7276061479
H,0,-1.0486253402,3.7759390902,-0.7055332475
H,0,-0.1400781594,3.2835526607,0.7121059586
H,0,-2.7305201975,2.2089911563,-0.2257316115
H,0,-1.8685048635,1.6730392659,1.2050893459
H,0,-2.1320259196,-0.0953148105,-0.8468155856
H,0,-1.4274412849,1.8760590955,-2.4928206268
H,0,-0.2335779759,0.5601098583,-2.6054155294

endo-TCD boat

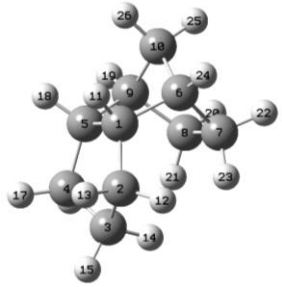

C,0,-0.3614002459,-1.2725384566,0.7338301578
C,0,-0.028905934,0.0739055859,1.4185443086
C,0,1.4033559452,0.443365745,0.9748310727
C,0,2.1122245012,-0.913170284,0.7690018175
C,0,1.0194868282,-1.9091019777,0.3149808385
C,0,-1.1571992857,-1.2659290086,-0.6017861312
C,0,-0.5809090639,-0.2319700759,-1.5970612863
C,0,0.7881495751,-0.863399955,-2.0124982092
C,0,0.8272170566,-2.181078554,-1.2038024271
C,0,-0.6644505425,-2.5887196296,-1.2339580729
H,0,-0.8950586213,-1.9236791505,1.4351308182
H,0,-0.7573808631,0.860283896,1.1914620056
H,0,-0.0479192542,-0.0635878744,2.5062711693
H,0,1.3795925049,1.0083245037,0.0375912308
H,0,1.9167418317,1.0747773625,1.7078367115
H,0,2.9505997975,-0.8489764223,0.0663979455
H,0,2.5313725149,-1.2524574628,1.7237746553
H,0,1.1696858813,-2.8755695726,0.808824788
H,0,1.5343045224,-2.9147837926,-1.6028468613
H,0,0.8096577276,-1.0816552443,-3.0856702558
H,0,1.641884342,-0.2119756606,-1.8074610476
H,0,-1.2458082081,-0.1337006591,-2.4619507241
H,0,-0.4799181014,0.7666097014,-1.1635862515
H,0,-2.2382865767,-1.1749980498,-0.4584935076
H,0,-1.048890031,-2.7560840248,-2.2467916468
H,0,-0.8861319418,-3.4710737041,-0.6235099069

Table D.2 Moments of Inertia[a]

Species	I_a	I_b	I_c
TCD	672.31522	1530.45148	1762.53870
TCD-R1	650.72306	1529.05623	1745.13222
TCD-R2	662.54177	1538.11739	1770.09036
TCD-R3	657.49978	1505.22653	1737.18458
TCD-R4	683.21973	1439.51857	1682.64090
TCD-R9	662.27117	1496.79953	1725.44953
TCD-R10	657.11600	1508.65548	1755.84933
exo-TCD boat	693.14502	1476.55079	1694.38846
exo-TCD TS	686.16885	1505.27558	1749.59314
endo-TCD chair	768.68843	1435.33096	1573.05455
endo-TCD boat	820.03888	1330.42622	1421.85720

[a] AMU Bohr^2.

Table D.3 Vibrational Frequencies

Species	Frequencies (cm^{-1})									
TCD	140.07	178.67	270.76	318.67	319.57	398.09	495.09	533.36	551.22	670.38
	740.94	754.14	794.24	831.05	867.96	868.52	893.40	898.14	917.44	919.92
	929.18	962.04	966.39	995.06	1003.67	1045.77	1053.99	1055.31	1056.57	1078.61
	1141.88	1158.27	1173.98	1199.19	1211.43	1216.60	1237.76	1257.45	1267.57	1295.12
	1305.36	1311.09	1319.35	1325.08	1336.41	1339.50	1353.76	1359.70	1375.45	1381.22
	1502.14	1504.82	1506.41	1513.31	1524.72	1536.28	3034.63	3036.37	3040.06	3044.40
	3049.68	3057.64	3058.00	3060.82	3085.07	3087.50	3089.46	3090.57	3094.30	3097.43
	3106.03	3107.57								
TCD-R1	140.33	176.78	269.88	315.69	318.91	395.73	492.25	521.85	549.43	661.61
	716.94	750.67	774.71	826.73	838.38	859.75	876.30	887.77	913.44	917.01
	931.68	951.19	971.46	996.80	1007.22	1041.20	1050.59	1062.44	1087.91	1101.19
	1146.35	1169.00	1195.50	1201.79	1215.71	1221.89	1242.44	1260.11	1266.70	1293.69
	1306.50	1314.74	1320.95	1324.76	1340.88	1352.59	1364.83	1378.34	1499.88	1500.29
	1504.69	1510.16	1521.98	1531.83	3035.86	3040.42	3048.59	3050.68	3052.52	3060.55
	3066.44	3069.60	3083.34	3089.62	3093.38	3094.29	3102.68	3113.00	3122.98	
TCD-R2	114.80	156.33	233.10	281.80	313.56	382.68	484.07	535.71	554.87	616.62
	719.45	738.49	796.07	826.10	845.76	876.18	885.16	891.90	893.13	907.44
	919.50	958.97	965.91	992.05	1017.68	1040.75	1046.29	1061.67	1096.32	1127.32
	1134.94	1155.90	1167.39	1197.81	1213.17	1228.08	1239.10	1252.04	1259.09	1288.78
	1310.16	1315.40	1320.22	1331.92	1344.78	1348.45	1358.80	1372.55	1483.89	1499.91
	1501.71	1510.83	1517.39	1531.60	2974.51	2991.16	3029.89	3038.13	3049.56	3050.28
	3050.62	3061.42	3089.76	3091.24	3095.77	3100.53	3103.11	3105.94	3113.40	
TCD-R3	118.83	133.35	263.56	281.82	315.56	395.02	418.75	497.90	534.07	625.30
	738.54	751.87	764.36	798.65	832.63	848.40	871.84	892.03	910.53	927.74
	930.04	952.85	965.17	981.88	1005.67	1020.94	1051.00	1053.38	1067.59	1078.48
	1124.41	1145.32	1164.64	1192.23	1215.09	1224.39	1238.04	1249.46	1286.91	1290.77
	1298.57	1303.70	1316.73	1324.95	1330.19	1341.03	1355.91	1369.90	1379.25	1485.08
	1503.98	1504.74	1517.39	1531.14	2937.17	2962.75	3040.50	3049.27	3054.90	3058.27
	3058.64	3061.14	3084.74	3090.46	3097.07	3099.21	3105.88	3109.46	3191.85	
TCD-R4	76.04	92.78	252.02	252.66	326.41	385.85	401.83	492.86	512.89	722.71
	723.33	744.79	758.35	800.60	820.61	834.36	889.20	894.48	913.41	926.51
	933.62	935.94	966.42	978.46	1013.81	1021.39	1045.80	1052.37	1067.40	1092.67
	1123.11	1148.51	1148.86	1174.07	1208.01	1221.11	1240.32	1255.86	1276.97	1293.54
	1302.91	1309.05	1312.14	1328.88	1332.99	1354.91	1363.40	1371.81	1389.01	1480.26
	1485.55	1500.84	1512.39	1531.40	2952.10	2954.75	3001.18	3002.14	3048.13	3055.75
	3058.44	3059.36	3073.37	3083.72	3088.98	3094.54	3103.79	3106.63	3197.37	

Table D.3 Vibrational Frequencies (Continued)

Species	Frequencies (cm^{-1})									
TCD-R9	149.10	175.63	271.53	299.78	319.15	370.01	441.31	496.92	546.51	564.79
	669.79	745.28	764.59	794.56	865.57	867.44	894.28	907.55	909.26	916.79
	935.66	937.86	961.30	982.37	999.71	1015.26	1035.98	1043.43	1052.05	1074.77
	1123.75	1148.93	1159.21	1191.84	1198.57	1217.75	1242.34	1257.24	1274.46	1286.29
	1301.84	1309.41	1321.54	1332.90	1345.20	1351.41	1353.50	1366.07	1375.65	1483.63
	1502.60	1505.99	1516.14	1530.05	2979.20	3024.00	3035.99	3038.30	3041.79	3050.82
	3065.38	3067.92	3087.90	3092.21	3093.58	3097.90	3099.69	3113.26	3207.52	
TCD-R10	108.16	183.19	254.33	301.87	316.15	349.55	432.96	530.57	538.70	667.46
	685.49	739.64	764.92	793.71	833.54	855.96	873.63	877.89	914.83	919.98
	923.34	953.07	955.25	992.16	997.20	1000.17	1038.99	1050.62	1059.17	1077.17
	1158.16	1169.20	1196.90	1196.92	1212.44	1212.70	1242.94	1248.75	1266.32	1284.47
	1301.03	1313.19	1314.82	1338.15	1338.42	1353.85	1354.69	1371.73	1375.83	1497.19
	1501.25	1502.09	1518.68	1521.28	3032.95	3035.65	3039.61	3044.39	3047.83	3055.77
	3060.74	3086.67	3087.80	3091.14	3098.34	3104.63	3104.81	3108.72	3197.87	
exo-TCD boat	81.72	213.44	258.26	261.33	320.24	397.95	484.39	499.28	617.10	710.17
	738.82	783.76	801.72	805.31	838.29	848.30	888.05	890.08	903.57	929.68
	930.20	956.56	963.74	988.15	989.94	1039.96	1043.40	1066.91	1093.94	1094.87
	1129.88	1144.73	1159.47	1202.58	1208.10	1213.94	1232.69	1256.24	1284.48	1290.75
	1302.51	1307.35	1316.09	1327.52	1333.81	1343.24	1346.27	1366.65	1378.93	1381.39
	1500.73	1501.32	1502.51	1512.97	1525.11	1541.24	3038.09	3039.79	3048.56	3054.57
	3055.07	3058.07	3062.12	3069.74	3078.10	3082.06	3084.54	3089.34	3093.77	3100.49
	3105.98	3130.93								
exo-TCD TS	-163.16	85.00	236.12	248.54	319.29	390.38	494.18	521.27	685.27	722.70
	730.94	740.15	773.06	800.88	834.28	835.24	891.82	894.06	908.36	930.32
	939.88	955.47	967.21	996.55	1006.32	1055.26	1057.72	1066.08	1083.09	1102.26
	1138.66	1155.53	1165.28	1214.66	1219.82	1233.03	1257.16	1266.05	1278.16	1286.84
	1294.46	1313.46	1313.84	1315.00	1327.99	1332.25	1347.61	1366.83	1371.49	1375.85
	1500.86	1503.46	1511.25	1513.00	1530.86	1536.57	3044.45	3044.95	3048.29	3051.31
	3054.97	3057.43	3059.59	3064.23	3076.60	3083.47	3086.65	3090.02	3094.44	3099.84
	3105.31	3106.88								
endo-TCD chair	87.45	189.40	299.21	317.26	384.30	444.62	489.00	521.63	543.88	592.33
	717.07	776.25	790.31	817.06	833.15	867.56	883.89	885.77	912.68	928.33
	929.36	971.21	974.81	995.86	1003.25	1031.73	1035.59	1072.30	1076.36	1113.21
	1149.69	1151.56	1157.86	1193.67	1210.06	1210.41	1246.15	1258.58	1285.44	1288.43
	1306.60	1314.39	1320.33	1335.05	1341.18	1349.11	1352.63	1363.44	1378.02	1386.82
	1496.07	1504.33	1513.55	1515.35	1523.33	1539.31	3030.09	3035.28	3046.30	3050.01
	3051.11	3052.63	3056.03	3065.48	3087.03	3087.76	3091.91	3094.47	3098.53	3098.91
	3102.23	3113.52								

Table D.3 Vibrational Frequencies (Continued)

Species	**Frequencies (cm^{-1})**									
endo-TCD boat	160.30	228.48	278.38	288.66	381.67	445.61	455.60	503.30	624.01	669.37
	705.70	754.04	798.42	826.04	828.46	852.45	874.19	889.64	902.71	932.63
	942.78	969.65	972.26	986.33	990.17	1041.91	1044.48	1069.79	1084.53	1126.18
	1138.87	1148.87	1162.08	1190.25	1205.78	1208.43	1246.51	1261.40	1281.14	1288.03
	1308.06	1318.81	1325.31	1334.76	1340.99	1345.63	1352.88	1366.87	1375.42	1380.45
	1501.76	1507.69	1511.54	1517.43	1523.45	1545.97	3036.86	3040.83	3048.41	3050.54
	3054.09	3059.30	3065.11	3066.38	3081.92	3085.02	3086.87	3093.70	3097.97	3100.90
	3106.19	3117.24								

Table D.4 Calculated Total Entropies[a] and Heat Capacities[a]

Temperature	TCD		TCD-R1		TCD-R2		TCD-R3EX		TCD-R3EN		TCD-R4EX	
(K)	Cp	S	Cp	S	Cp	S	Cp	S	Cp	S	Cp	S
1	7.949	24.334	7.949	25.647	7.949	25.685	7.949	25.637	7.949	25.637	7.949	25.599
50	8.945	55.693	8.956	57.008	9.442	57.253	9.546	57.255	9.545	57.255	10.610	58.044
100	12.502	62.918	12.550	64.251	13.235	64.930	13.282	64.973	13.281	64.973	13.980	66.385
150	16.700	68.748	16.811	70.112	17.375	71.049	17.565	71.136	17.564	71.135	18.013	72.782
200	21.931	74.223	22.080	75.625	22.516	76.706	22.826	76.866	22.825	76.865	23.102	78.615
250	28.537	79.785	28.628	81.217	28.974	82.385	29.368	82.623	29.367	82.622	29.541	84.422
298	35.827	85.390	35.759	86.827	36.048	88.050	36.499	88.362	36.499	88.361	36.615	90.187
300	36.142	85.630	36.066	87.066	36.353	88.291	36.806	88.606	36.805	88.605	36.921	90.432
400	51.917	98.162	51.301	99.507	51.525	100.806	52.025	101.259	52.025	101.258	52.090	103.110
500	65.987	111.266	64.763	112.410	64.954	113.755	65.435	114.319	65.435	114.318	65.484	116.182
600	77.637	124.332	75.848	125.203	76.022	126.581	76.452	127.229	76.451	127.227	76.499	129.100
700	87.205	137.017	84.920	137.576	85.084	138.979	85.455	139.689	85.455	139.688	85.507	141.568
800	95.158	149.176	92.443	149.402	92.601	150.827	92.915	151.583	92.915	151.581	92.972	153.469
900	101.856	160.764	98.768	160.649	98.921	162.093	99.186	162.883	99.186	162.881	99.247	164.776
1000	107.552	171.783	104.140	171.327	104.288	172.786	104.511	173.602	104.511	173.601	104.575	175.502
1100	112.425	182.256	108.733	181.461	108.875	182.935	109.064	183.770	109.064	183.769	109.129	185.676
1200	116.614	192.211	112.678	191.086	112.814	192.571	112.974	193.422	112.974	193.420	113.039	195.333
1300	120.227	201.682	116.080	200.233	116.209	201.730	116.346	202.592	116.346	202.591	116.410	204.509
1400	123.353	210.701	119.024	208.939	119.145	210.444	119.264	211.316	119.264	211.315	119.325	213.237
1500	126.069	219.299	121.580	217.233	121.693	218.746	121.797	219.626	121.796	219.625	121.855	221.552
2000	135.333	256.954	130.298	253.515	130.379	255.056	130.436	255.959	130.436	255.957	130.480	257.899
2500	140.398	287.736	135.064	283.139	135.123	284.696	135.158	285.608	135.158	285.607	135.191	287.557
3000	143.404	313.614	137.893	308.027	137.936	309.594	137.960	310.511	137.960	310.510	137.985	312.466
3500	145.314	335.868	139.689	329.423	139.723	330.996	139.740	331.917	139.740	331.915	139.759	333.875
4000	146.595	355.358	140.895	348.157	140.921	349.733	140.934	350.656	140.934	350.655	140.950	352.616
4500	147.493	372.677	141.740	364.801	141.762	366.381	141.772	367.305	141.772	367.303	141.784	369.267
5000	148.146	388.250	142.354	379.767	142.372	381.348	142.380	382.273	142.380	382.272	142.390	384.236
Zero Point Energy[b]	149.018		140.906		140.337		139.795		139.795		139.448	

[a] Units of cal mol^{-1} K^{-1}.
[b] Units of kcal mol^{-1}.

Table D.4 Calculated Total Entropies[a] and Heat Capacities[a] (Continued)

Temperature (K)	TCD-R4EN		TCD-R9EX		TCD-R9EN		TCD-R10EX		TCD-R10EN	
	Cp	S	Cp	S	Cp	S	Cp	S	Cp	S
1	7.949	25.599	7.949	25.632	7.949	25.632	7.949	25.649	7.949	25.649
50	10.607	58.040	8.895	56.963	8.895	56.963	9.302	57.204	9.301	57.204
100	13.978	66.378	12.722	64.216	12.722	64.216	13.041	64.727	13.040	64.726
150	18.011	72.774	17.296	70.208	17.296	70.208	17.409	70.810	17.409	70.809
200	23.100	78.607	22.755	75.890	22.755	75.890	22.725	76.502	22.725	76.501
250	29.539	84.414	29.402	81.644	29.402	81.644	29.307	82.241	29.307	82.241
298	36.615	90.178	36.581	87.394	36.581	87.394	36.458	87.972	36.459	87.971
300	36.920	90.423	36.889	87.638	36.889	87.638	36.766	88.216	36.766	88.215
400	52.089	103.101	52.130	100.320	52.130	100.320	51.993	100.859	51.993	100.859
500	65.484	116.173	65.525	113.402	65.526	113.402	65.394	113.911	65.394	113.910
600	76.499	129.091	76.519	126.326	76.519	126.326	76.396	126.812	76.396	126.811
700	85.507	141.559	85.500	138.795	85.500	138.795	85.383	139.262	85.383	139.262
800	92.972	153.460	92.941	150.693	92.941	150.693	92.830	151.146	92.831	151.145
900	99.247	164.767	99.197	161.995	99.197	161.995	99.091	162.435	99.092	162.434
1000	104.575	175.493	104.510	172.715	104.510	172.716	104.411	173.144	104.411	173.143
1100	109.129	185.667	109.055	182.883	109.055	182.883	108.961	183.303	108.961	183.302
1200	113.039	195.324	112.960	192.533	112.960	192.534	112.871	192.945	112.872	192.944
1300	116.410	204.500	116.328	201.703	116.328	201.703	116.245	202.107	116.245	202.107
1400	119.325	213.229	119.243	210.425	119.243	210.425	119.166	210.824	119.166	210.823
1500	121.855	221.543	121.775	218.734	121.775	218.734	121.703	219.127	121.703	219.127
2000	130.480	257.890	130.415	255.060	130.415	255.060	130.364	255.436	130.365	255.435
2500	135.191	287.548	135.142	284.706	135.142	284.706	135.105	285.072	135.105	285.071
3000	137.985	312.457	137.947	309.606	137.947	309.606	137.920	309.966	137.920	309.966
3500	139.759	333.866	139.730	331.010	139.730	331.010	139.709	331.366	139.709	331.366
4000	140.950	352.607	140.926	349.748	140.926	349.748	140.910	350.102	140.910	350.102
4500	141.784	369.258	141.765	366.396	141.765	366.396	141.752	366.748	141.752	366.748
5000	142.390	384.227	142.375	381.364	142.375	381.364	142.364	381.715	142.364	381.714
Zero Point Energy[b]	139.449		139.904		139.903		140.153		140.152	

[b] Units of kcal mol^{-1}.

Table D.5 Enthalpy of Formation Calculation for 2-Norbornyl Radical

No literature value currently exists for the gas phase heat of formation for the 2-Norbornyl radical. A $\Delta H^{\circ}_{f\,298}$ of 33.9 kcal mol^{-1} for 2-Norbornyl was calculated using the norbornane gas phase heat of formation[120] value of -13.1 kcal mol^{-1}, hydrogen atom gas phase heat of formation[83] value of 52.10 kcal mol^{-1}, and the bond dissociation energy[203] of 99.09 kcal mol^{-1}.

Enthalpy of Formation 2-Norbornyl					
	Norbornane		2-Norbornyl		
	YYC_7H_{12}	$\rightarrow$	$YYCJ_7H_{11}$	+	H
ΔH°_{f} (kcal mol^{-1})	-13.1		X		52.10
ΔH°_{rxn} Bond Energy	**99.09 kcal mol^{-1}**				
$\Delta H^{\circ}_{f\,298}$ 2-Norbornyl	**33.9 kcal mol^{-1}**				

Table D.6 Calculations of $\Delta H^{\circ}_{f\,298}$ for TCD Using Small Molecule Work Reactions Which Show Unacceptable Results

Isodesmic Reactions	$\Delta H^{\circ}_{f\,298}$ (kcal mol^{-1})						
	B3LYP		BB1K	MPWB1K	BMK	CBS-QB3	G3MP2B3
	6-31G(d,p)	6-311G(2d,2p)	6-31G(d,p)	6-31G(d,p)	6-31G(d,p)		
TCD System							
TCD + 14 CH_4 → 12 CH_3CH_3	0.34	-1.60	-10.18	-8.89	-11.66	-20.08	-19.48
TCD + 4 CH_4 → 2 YC_5H_{10} + 2 CH_3CH_3	-9.91	-9.90	-15.31	-15.11	-14.08	-20.78	-20.51
Average	**-4.78**	**-5.75**	**-12.75**	**-12.00**	**-12.87**	**-20.43**	**-19.99**

Table D.7 Reaction Enthalpies for Tricyclodecyl Radicals

Isodesmic Reactions							ΔH°_{rxn}						
							B3LYP		BB1K	MPWB1K	BMK	CBS-QB3	G3MP2B3
							6-31G(d,p)	6-311G(2d,2p)	6-31G(d,p)	6-31G(d,p)	6-31G(d,p)		
TCD-R1 System													
TCD-R1	+	CH_3CH_3	→	TCD	+	CH_3CJH_2	-4.90	-5.27	-3.25	-3.36	-4.74	-5.92	-6.48
TCD-R1	+	$CH_3CH_2CH_3$	→	TCD	+	CH_3CJHCH_3	-8.80	-9.07	-8.04	-8.11	-7.83	-8.67	-8.80
TCD-R1	+	$(CH_3)_3CH$	→	TCD	+	$(CH_3)_3CJ$	-11.89	-12.00	-11.72	-11.69	-10.60	-10.40	-10.17
TCD-R1	+	$CH_3CH_2CH_2CH_3$	→	TCD	+	$CH_3CJHCH_2CH_3$	-8.57	-8.94	-7.76	-7.78	-7.94	-8.45	-8.55
TCD-R1	+	YYC_7H_{12}	→	TCD	+	$YYCJ_7H_{11}$	-8.55	-8.68	-8.26	-8.30	-8.01	-8.79	-8.76
TCD-R2 System													
TCD-R2	+	CH_3CH_3	→	TCD	+	CH_3CJH_2	3.43	3.05	4.81	4.64	2.40	1.41	0.50
TCD-R2	+	$CH_3CH_2CH_3$	→	TCD	+	CH_3CJHCH_3	-0.47	-0.75	0.02	-0.11	-0.69	-1.35	-1.82
TCD-R2	+	$(CH_3)_3CH$	→	TCD	+	$(CH_3)_3CJ$	-3.56	-3.68	-3.66	-3.70	-3.46	-3.07	-3.19
TCD-R2	+	$CH_3CH_2CH_2CH_3$	→	TCD	+	$CH_3CJHCH_2CH_3$	-0.24	-0.62	0.30	0.21	-0.80	-1.12	-1.57
TCD-R2	+	YYC_7H_{12}	→	TCD	+	$YYCJ_7H_{11}$	-0.22	-0.37	-0.20	-0.30	-0.87	-1.46	-1.77
TCD-R3 System													
TCD-R3	+	CH_3CH_3	→	TCD	+	CH_3CJH_2	4.95	4.82	5.80	5.70	3.69	3.30	2.73
TCD-R3	+	$CH_3CH_2CH_3$	→	TCD	+	CH_3CJHCH_3	1.04	1.02	1.01	0.95	0.60	0.54	0.41
TCD-R3	+	$(CH_3)_3CH$	→	TCD	+	$(CH_3)_3CJ$	-2.04	-1.91	-2.67	-2.63	-2.17	-1.18	-0.96
TCD-R3	+	$CH_3CH_2CH_2CH_3$	→	TCD	+	$CH_3CJHCH_2CH_3$	1.28	1.15	1.29	1.28	0.49	0.76	0.66
TCD-R3	+	YYC_7H_{12}	→	TCD	+	$YYCJ_7H_{11}$	1.29	1.41	0.79	0.76	0.42	0.43	0.45

Table D.7 Reaction Enthalpies for Tricyclodecyl Radicals (Continued)

Isodesmic Reactions							ΔH°_{rxn}						
							B3LYP		BB1K	MPWB1K	BMK	CBS-QB3	G3MP2B3
							6-31G(d,p)	6-311G(2d,2p)	6-31G(d,p)	6-31G(d,p)	6-31G(d,p)		
TCD-R4 System													
TCD-R4	+	CH_3CH_3	→	TCD	+	CH_3CJH_2	4.40	4.30	5.19	5.17	3.10	2.74	2.22
TCD-R4	+	$CH_3CH_2CH_3$	→	TCD	+	CH_3CJHCH_3	0.50	0.50	0.40	0.42	0.01	-0.02	-0.10
TCD-R4	+	$(CH_3)_3CH$	→	TCD	+	$(CH_3)_3CJ$	-2.59	-2.43	-3.27	-3.17	-2.76	-1.75	-1.46
TCD-R4	+	$CH_3CH_2CH_2CH_3$	→	TCD	+	$CH_3CJHCH_2CH_3$	0.73	0.63	0.69	0.74	-0.09	0.20	0.15
TCD-R4	+	YYC_7H_{12}	→	TCD	+	$YYCJ_7H_{11}$	0.75	0.88	0.19	0.23	-0.17	-0.13	-0.05
TCD-R9 System													
TCD-R9	+	CH_3CH_3	→	TCD	+	CH_3CJH_2	3.45	3.20	4.71	4.63	3.01	2.61	2.02
TCD-R9	+	$CH_3CH_2CH_3$	→	TCD	+	CH_3CJHCH_3	-0.46	-0.60	-0.08	-0.12	-0.08	-0.15	-0.30
TCD-R9	+	$(CH_3)_3CH$	→	TCD	+	$(CH_3)_3CJ$	-3.54	-3.53	-3.76	-3.71	-2.85	-1.88	-1.67
TCD-R9	+	$CH_3CH_2CH_2CH_3$	→	TCD	+	$CH_3CJHCH_2CH_3$	-0.23	-0.48	0.20	0.20	-0.19	0.07	-0.05
TCD-R9	+	YYC_7H_{12}	→	TCD	+	$YYCJ_7H_{11}$	-0.21	-0.22	-0.30	-0.32	-0.26	-0.26	-0.25
TCD-R10 System													
TCD-R10	+	CH_3CH_3	→	TCD	+	CH_3CJH_2	-1.52	-1.66	-0.88	-1.04	-2.21	-2.83	-3.35
TCD-R10	+	$CH_3CH_2CH_3$	→	TCD	+	CH_3CJHCH_3	-5.43	-5.46	-5.67	-5.79	-5.29	-5.59	-5.67
TCD-R10	+	$(CH_3)_3CH$	→	TCD	+	$(CH_3)_3CJ$	-8.51	-8.39	-9.35	-9.37	-8.06	-7.31	-7.04
TCD-R10	+	$CH_3CH_2CH_2CH_3$	→	TCD	+	$CH_3CJHCH_2CH_3$	-5.20	-5.33	-5.39	-5.46	-5.40	-5.36	-5.42
TCD-R10	+	YYC_7H_{12}	→	TCD	+	$YYCJ_7H_{11}$	-5.18	-5.07	-5.89	-5.98	-5.48	-5.70	-5.62

Table D.8 Isodesmic and Isomerization Reactions for Enthalpies of Formation Calculations of TCD Isomers

Work Reactions									$\Delta H^{\circ}_{f\,298}$ (kcal mol^{-1})		
									B3LYP 6-31G(d,p)	**CBS-QB3**	**G3MP2B3**
***exo*-TCD boat System**											
exo-TCD boat	+	YC_4H_8	→	YYC_7H_{12}	+	YYC_7H_{12}			-17.40	-15.46	-15.55
exo-TCD boat	+	YC_5H_{10}	→	YYC_7H_{12}	+	YYC_8H_{14}			-17.06	-16.52	-16.55
exo-TCD boat	+	YC_6H_{12}	→	YYC_8H_{14}	+	YYC_8H_{14}			-18.01	-18.15	-18.22
exo-TCD boat	+	3 CH_3CH_3	→	3 YC_4H_8	+	$CH_3CH_2CH_2CH_3$				-18.19	-17.96
exo-TCD boat	+	4 CH_3CH_3	→	2 $CH_3CH_2CH_2CH_3$	+	YC_4H_8	+	2 YC_3H_6		-18.92	-18.69
								Average	**-17.49**	**-17.45**	**-17.39**
		exo-TCD boat	→	*exo*-TCD chair					**-17.5**	**-17.4**	**-17.4**
***exo*-TCD TS System**											
exo-TCD TS	+	YC_4H_8	→	YYC_7H_{12}	+	YYC_7H_{12}			-15.93	-13.48	-13.50
exo-TCD TS	+	YC_5H_{10}	→	YYC_7H_{12}	+	YYC_8H_{14}			-15.60	-14.54	-14.51
exo-TCD TS	+	YC_6H_{12}	→	YYC_8H_{14}	+	YYC_8H_{14}			-16.54	-16.17	-16.18
exo-TCD TS	+	3 CH_3CH_3	→	3 YC_4H_8	+	$CH_3CH_2CH_2CH_3$				-16.20	-15.92
exo-TCD TS	+	4 CH_3CH_3	→	2 $CH_3CH_2CH_2CH_3$	+	YC_4H_8	+	2 YC_3H_6		-16.94	-16.65
								Average	**-16.02**	**-15.47**	**-15.35**
		exo-TCD TS	→	*exo*-TCD chair					**-16.0**	**-15.4**	**-15.4**
***endo*-TCD chair System**											
endo-TCD chair	+	YC_4H_8	→	YYC_7H_{12}	+	YYC_7H_{12}			-15.44	-13.38	-13.42
endo-TCD chair	+	YC_5H_{10}	→	YYC_7H_{12}	+	YYC_8H_{14}			-15.11	-14.44	-14.42
endo-TCD chair	+	YC_6H_{12}	→	YYC_8H_{14}	+	YYC_8H_{14}			-16.05	-16.07	-16.09
endo-TCD chair	+	3 CH_3CH_3	→	3 YC_4H_8	+	$CH_3CH_2CH_2CH_3$				-16.10	-15.83
endo-TCD chair	+	4 CH_3CH_3	→	2 $CH_3CH_2CH_2CH_3$	+	YC_4H_8	+	2 YC_3H_6		-16.84	-16.56
								Average	**-15.53**	**-15.37**	**-15.26**
		endo-TCD chair	→	*exo*-TCD chair					**-15.6**	**-15.3**	**-15.3**

Table D.8 Isodesmic and Isomerization Reactions for Enthalpies of Formation Calculations of TCD Isomers (Continued)

Work Reactions									$\Delta H^{\circ}_{f\,298}$ (kcal mol^{-1})		
									B3LYP 6-31G(d,p)	**CBS-QB3**	**G3MP2B3**
***endo*-TCD boat System**											
endo-TCD boat	+	YC_4H_8	→	YYC_7H_{12}	+	YYC_7H_{12}			-15.65	-14.45	-14.62
endo-TCD boat	+	YC_5H_{10}	→	YYC_7H_{12}	+	YYC_8H_{14}			-15.31	-15.51	-15.62
endo-TCD boat	+	YC_6H_{12}	→	YYC_8H_{14}	+	YYC_8H_{14}			-16.26	-17.14	-17.29
endo-TCD boat	+	3 CH_3CH_3	→	3 YC_4H_8	+	$CH_3CH_2CH_2CH_3$				-17.17	-17.03
endo-TCD boat	+	4 CH_3CH_3	→	2 $CH_3CH_2CH_2CH_3$	+	YC_4H_8	+	2 YC_3H_6		-17.91	-17.76
								Average	**-15.74**	**-16.44**	**-16.46**
		endo-TCD boat	→	*exo*-TCD chair					**-15.8**	**-16.4**	**-16.5**

Table D.9 NASA Polynomial Thermodynamic Data for TCD and Radicals

```
THERMO
   300.000  1500.000  5000.000
TCD       TCD  level b31C  10H  16    0    0G   300.000  5000.000 1399.000    01
 2.53375963E+01 4.25886209E-02-1.46060943E-05 2.27210376E-09-1.32014524E-13    2
-2.44260117E+04-1.24605712E+02-1.53764567E+01 1.39751131E-01-1.03279999E-04    3
 3.90654702E-08-5.98179812E-12-1.05825722E+04 9.31735320E+01                   4
TCDR1     TCDR1  level bC  10H  15    0    0G   300.000  5000.000 1400.000    01
 2.53123286E+01 4.00950652E-02-1.37528205E-05 2.13959548E-09-1.24325465E-13    2
 3.65718455E+03-1.22553148E+02-1.44509225E+01 1.36547754E-01-1.03618762E-04    3
 4.03365675E-08-6.35748628E-12 1.70197975E+04 8.95845780E+01                   4
TCDR2     TCDR2  level bC  10H  15    0    0G   300.000  5000.000 1399.000    01
 2.54631943E+01 4.00001915E-02-1.37275021E-05 2.13641905E-09-1.24172025E-13    2
 1.17442318E+01-1.22780303E+02-1.41510324E+01 1.35730762E-01-1.02494553E-04    3
 3.96580050E-08-6.21112045E-12 1.33596480E+04 8.86892406E+01                   4
TCDR3     TCDR3  level bC  10H  15    0    0G   300.000  5000.000 1400.000    01
 2.57424908E+01 3.97397049E-02-1.36322871E-05 2.12098146E-09-1.23249333E-13    2
-1.06337134E+03-1.24080662E+02-1.41306407E+01 1.37076545E-01-1.05062791E-04    3
 4.13506895E-08-6.58949623E-12 1.22765374E+04 8.84277689E+01                   4
TCDR4     TCDR4  level bC  10H  15    0    0G   300.000  5000.000 1400.000    01
 2.57953688E+01 3.97259905E-02-1.36344735E-05 2.12204453E-09-1.23340486E-13    2
-8.22267458E+02-1.23474058E+02-1.39224548E+01 1.36247575E-01-1.03784416E-04    3
 4.05512073E-08-6.41437299E-12 1.25082485E+04 8.83596514E+01                   4
TCDR9     TCDR9  level bC  10H  15    0    0G   300.000  5000.000 1400.000    01
 2.57504044E+01 3.97126122E-02-1.36182334E-05 2.11828140E-09-1.23071121E-13    2
-6.90364925E+02-1.24563613E+02-1.41655013E+01 1.37576636E-01-1.06059188E-04    3
 4.20389502E-08-6.74838149E-12 1.26245115E+04 8.80276354E+01                   4
TCDR10    TCDR10 level bC  10H  15    0    0G   300.000  5000.000 1400.000    01
 2.56614518E+01 3.97557725E-02-1.36261206E-05 2.11879623E-09-1.23072512E-13    2
 2.05577520E+03-1.23770506E+02-1.41801156E+01 1.37296733E-01-1.05556053E-04    3
 4.17025900E-08-6.67015781E-12 1.53551570E+04 8.84667068E+01                   4
END
```

APPENDIX E

BOND ENERGIES AND THERMOCHEMICAL PROPERTIES OF RING OPENED DIRADICALS AND CARBENES OF *EXO*-TRICYCLO[5.2.1.0^{2,6}]DECANE

This appendix contains the optimized geometries with symmetry values in parenthesis, moments of inertia, vibrational frequencies, internal rotor potential energy graphs, entropies, and heat capacities for all of the TCD species from B3LYP/6-31G(d,p) level of theory. Data provided for the diradical and carbene species are from the triplet state. Enthapies for parent and radical species with bond dissociation energies are provided.

Table E.1 TCD-H2 1-2 Optimized Species

TCD-H2 1-2 (σ = 1)

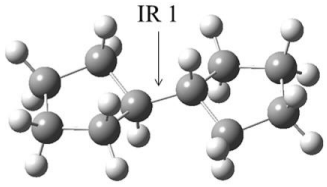

C,0,-0.0018879393,0.0038578668,-0.0000801723
C,0,0.0008751935,1.5460616935,0.0248804195
C,0,1.4937603655,1.9434332166,-0.028914934
C,0,2.2776421401,0.7206810343,0.538087055
C,0,1.2064142596,-0.3344070658,0.8969182555
C,0,-1.321534916,-0.6484211206,0.4176687306
C,0,-2.5298367203,-0.3101560055,-0.4793301165
C,0,-3.6010647376,-1.3652413912,-0.1204945745
C,0,-2.8171814097,-2.5880022871,0.4464860652
C,0,-1.3242955346,-2.1906261502,0.3927071961
H,0,0.2299598288,-0.3237901262,-1.0271338117
H,0,-0.5844953354,1.990851206,-0.7860667542
H,0,-0.4481525719,1.8857215208,0.9684337648
H,0,1.7977802875,2.1425537739,-1.0621842058
H,0,1.6902598196,2.8604739648,0.5351029724
H,0,2.9627763327,0.3252491047,-0.2195057495
H,0,2.891718997,0.9864036114,1.4041088702
H,0,1.5642079838,-1.3608357337,0.7682343092
H,0,-3.1212073226,-2.7871481672,1.4797485471
H,0,-4.2861852928,-0.969812099,0.6371120626
H,0,-4.2151556853,-1.6309529693,-0.9865096929
H,0,-2.8876281905,0.7162733967,-0.3506468093
H,0,-2.230609139,-0.4161830876,-1.5312368881
H,0,-1.5533815094,-0.3207729369,1.4447222574
H,0,-0.7389345838,-2.6354124129,1.2036625802
H,0,-0.8752564448,-2.5302836775,-0.5508409397
H,0,0.9071861864,-0.2283841837,1.9488256071
H,0,-3.0136740613,-3.5050309751,-0.1175540444

TCD-H2 1J-2 (σ = 1)

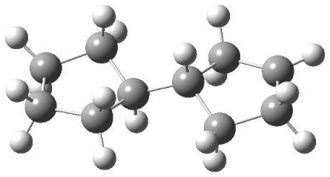

C,0,0.0027709412,0.0029506622,-0.004177843
C,0,-0.0004251154,0.0122338901,1.542502672
C,0,1.4928759311,-0.0096220681,1.9747151794
C,0,2.3040398284,-0.3171484873,0.684804088
C,0,1.2637549362,-0.8210246778,-0.3302292989
C,0,-1.2908106069,-0.5045533631,-0.6441335314
C,0,-2.5522660132,0.3249101785,-0.3084552966
C,0,-3.5834946254,-0.0723185703,-1.3888566452
C,0,-2.7316316079,-0.4303464957,-2.5689279924
C,0,-1.2848869856,-0.5271488418,-2.1962164562
H,0,0.1739617305,1.0329800083,-0.3575015999
H,0,-0.5455267974,0.8668343996,1.9549291308
H,0,-0.5105556566,-0.8904899826,1.9031236582
H,0,1.8000098386,0.9450921792,2.4131821397
H,0,1.6629831119,-0.7717065857,2.7419407866
H,0,2.768015396,0.6010347621,0.305480093
H,0,3.1137738242,-1.0335445522,0.8549276618
H,0,1.5942303014,-0.714903881,-1.3686624231
H,0,-3.1160210339,-0.6001454288,-3.5690255511
H,0,-4.1853277205,-0.9349586538,-1.0510481369
H,0,-4.3077852492,0.7267080439,-1.6000741166
H,0,-2.9126162666,0.1578417935,0.7111943737
H,0,-2.316489041,1.3936907779,-0.4007561677
H,0,-1.4618887288,-1.5351436705,-0.2953926307
H,0,-0.7878239767,-1.4174005733,-2.6054558904
H,0,-0.7104684905,0.3362931957,-2.5817770058
H,0,1.0530153506,-1.8868829275,-0.1625528751

Table E.1 TCD-H2 1-2 Optimized Species (Continued)

TCD-H2 1-2J (σ = 1)

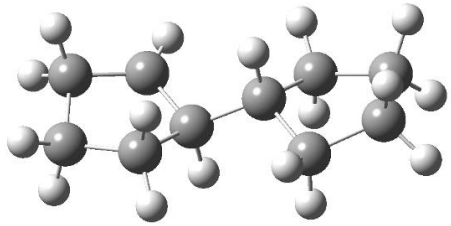

C,0,-0.0002598343,0.0000641607,0.0003498684
C,0,0.0000346074,-0.0004680231,1.5522016627
C,0,1.4891154632,-0.0003205912,1.9432595647
C,0,2.1556161532,-0.8983624368,0.8746623959
C,0,1.2801030869,-0.71794932,-0.3276658007
C,0,-1.2694482761,-0.5903724178,-0.6394284139
C,0,-2.5735100298,0.1536754659,-0.2921978938
C,0,-3.598958432,-0.385100636,-1.3085391699
C,0,-2.7754710728,-0.7286916341,-2.5853193088
C,0,-1.2852841273,-0.5742734381,-2.1828905979
H,0,0.0667233735,1.0505730278,-0.3484159076
H,0,-0.5550663044,0.8399763033,1.9800604355
H,0,-0.4772783361,-0.9229727698,1.9096972676
H,0,1.8913992802,1.0174617752,1.8695514521
H,0,1.6636621338,-0.3460958135,2.9669050454
H,0,3.2072759686,-0.6373834135,0.6920333191
H,0,2.1654567546,-1.9513284654,1.2088035764
H,0,1.5513456098,-1.0429248538,-1.3265103004
H,0,-2.9894152496,-1.7491924725,-2.9190071052
H,0,-4.0722393586,-1.2902982343,-0.9115586287
H,0,-4.4044632892,0.3287944021,-1.5068783511
H,0,-2.8899240391,0.0124249506,0.7463149507
H,0,-2.4196418135,1.2319311331,-0.4404449558
H,0,-1.3660390958,-1.6333562439,-0.2999884613
H,0,-0.6480883107,-1.3480349759,-2.6219463024
H,0,-0.8988348931,0.3927320444,-2.531614457
H,0,-3.0287133093,-0.0697693011,-3.4217311562

TCD-H2 1J-2J (σ = 1)

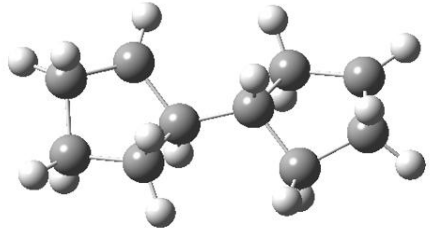

C,0,-0.0106083663,0.0250354637,-0.0144766193
C,0,0.0398078434,0.1335822653,1.5324539254
C,0,1.5218834295,-0.0814524665,1.8901280335
C,0,1.998302707,-1.1509667307,0.879500959
C,0,1.1227295231,-0.9175444886,-0.3136476695
C,0,-1.3777850252,-0.3909388667,-0.5843018885
C,0,-2.5321723419,0.5839556572,-0.2567801118
C,0,-3.6396702196,0.2371063352,-1.2771035636
C,0,-2.8746668166,-0.2697022137,-2.4619955874
C,0,-1.4322971597,-0.4985883378,-2.1313030303
H,0,0.2172514965,1.0225823587,-0.441864156
H,0,-0.3584062331,1.0811541233,1.9082092869
H,0,-0.5674222452,-0.6717692017,1.9676553241
H,0,2.0803165666,0.848948004,1.7299680318
H,0,1.6727901484,-0.3763516363,2.9332540745
H,0,3.0713991162,-1.0786199845,0.6542010113
H,0,1.8501249946,-2.1646320907,1.2929159098
H,0,1.3008137678,-1.3571657021,-1.2894257174
H,0,-3.3124752905,-0.4528776568,-3.4374584622
H,0,-4.3113110884,-0.5396708343,-0.8698291091
H,0,-4.2874649207,1.0938417535,-1.5098021465
H,0,-2.8675669158,0.5133144535,0.7824780385
H,0,-2.1903931882,1.6148136719,-0.4210778355
H,0,-1.6327356656,-1.3769773043,-0.1688511575
H,0,-1.0475062297,-1.4583108424,-2.5025303838
H,0,-0.7866108412,0.2765173602,-2.5856331698

Table E.1 TCD-H2 1-2 Optimized Species (Continued)

TCD-H2 1JJ-2 (σ = 1)

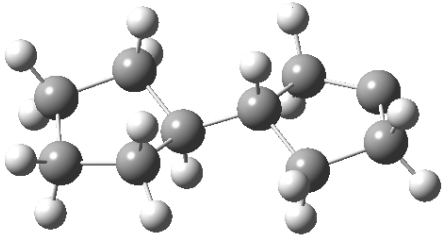

C,0,-0.0047066526,-0.0029447241,0.0087446561
C,0,0.0058746721,-0.0676478667,1.5491492893
C,0,1.4822969392,0.1655174824,1.9250261312
C,0,2.3094159771,-0.4263063347,0.7454320498
C,0,1.2797128622,-0.7769086123,-0.3602249679
C,0,-1.2801077092,-0.5262649455,-0.6541104439
C,0,-2.5732085059,0.2367569592,-0.2649316189
C,0,-3.6153018316,-0.1277758729,-1.3617424158
C,0,-2.721214873,-0.3865930079,-2.5246129418
C,0,-1.267978789,-0.4687293169,-2.2174404044
H,0,0.1261682291,1.0503049485,-0.2886833625
H,0,-0.6703386557,0.6541200629,2.0182494623
H,0,-0.315494579,-1.0689484421,1.868716719
H,0,1.6740615962,1.2405932178,2.0162387471
H,0,1.7428708367,-0.2828594735,2.8886326378
H,0,3.0425074895,0.3022376146,0.3846307478
H,0,2.8763853616,-1.3111827203,1.0507797465
H,0,1.6430167099,-0.5421082033,-1.3655666454
H,0,-4.1940230023,-1.0214024735,-1.0739908409
H,0,-4.3466238769,0.67361141,-1.5290402034
H,0,-2.9201053932,-0.007609347,0.7440233956
H,0,-2.379829612,1.3165093883,-0.2962082972
H,0,-1.4103804569,-1.5806747314,-0.3676686656
H,0,-0.7643454202,-1.3358203322,-2.6636558768
H,0,-0.7174147256,0.4236422045,-2.5642674735
H,0,1.060631147,-1.8528356489,-0.3446543058

TCD-H2 1-2JJ (σ = 1)

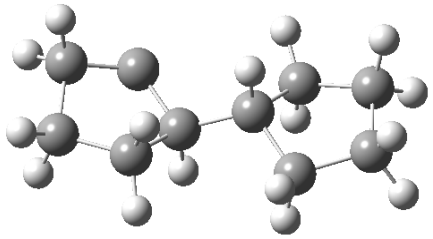

C,0,-0.0290260281,0.0463612611,0.0114420815
C,0,0.0088159249,-0.028436751,1.5709417172
C,0,1.5078868689,-0.043344315,1.945080969
C,0,2.1859555219,-0.8883937141,0.825712879
C,0,1.2630156945,-0.6326200903,-0.314290177
C,0,-1.2816051048,-0.5670057674,-0.6333602662
C,0,-2.6037985332,0.1467095717,-0.2811310715
C,0,-3.6102283104,-0.2832008616,-1.3814382345
C,0,-2.7491755984,-0.8604114062,-2.5447637484
C,0,-1.2897107937,-0.5368910885,-2.1721036391
H,0,0.0092399823,1.1088531731,-0.2965336109
H,0,-0.5387905688,0.7922500456,2.0451734089
H,0,-0.4621106364,-0.9676207573,1.8881058246
H,0,1.9074906193,0.9767391,1.9168467919
H,0,1.6916393902,-0.4430180858,2.9474989669
H,0,3.2238858086,-0.5845788731,0.6379962914
H,0,2.2188672825,-1.9550655482,1.1037540017
H,0,-2.8827401146,-1.9463703392,-2.6074466286
H,0,-4.3068322839,-1.0390581264,-1.0046829162
H,0,-4.2204213751,0.5641385988,-1.7095340259
H,0,-2.9577063609,-0.083501437,0.7288004146
H,0,-2.4412777939,1.2321149274,-0.3218223695
H,0,-1.3483522048,-1.6171916573,-0.3105677137
H,0,-0.5653986502,-1.2278286406,-2.6145701253
H,0,-1.0240814722,0.4735134504,-2.5131458362
H,0,-3.0324589907,-0.4523738816,-3.5198598405

Table E.2 TCD-H2 2-3 Optimized Species

TCD-H2 2-3 (σ = 3)

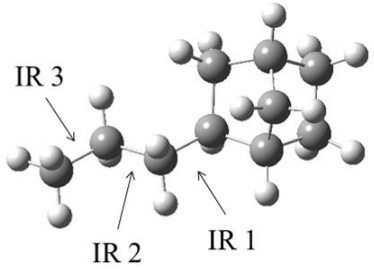

C,0,-0.0020239032,0.0092154414,-0.0017088219
C,0,-0.0008480935,0.0134369177,1.5347907949
C,0,1.4014537959,-0.0159362981,2.1572904539
C,0,1.3798312137,-0.00801648,3.6889141098
C,0,0.5128087321,-1.3314953424,-0.6344048759
C,0,-1.4193973675,0.1418553966,-0.6274236718
C,0,-1.2600179907,0.5288949714,-2.1170713136
C,0,-0.7011807038,-0.7807317895,-2.7659741682
C,0,-0.6391656734,-1.761920843,-1.5713265024
C,0,-1.8725576672,-1.3303893913,-0.7495486766
H,0,0.6204789402,0.8508612251,-0.3341280122
H,0,-0.5254756568,0.9121498796,1.889275555
H,0,-0.579587402,-0.8435254283,1.9082085969
H,0,1.9435319363,-0.903537856,1.8060809275
H,0,1.9721752193,0.8499109979,1.7943630623
H,0,2.3926486715,-0.0210064155,4.104738023
H,0,0.8740515574,0.8849165697,4.0737880269
H,0,1.4614374708,-1.2141815967,-1.1688275977
H,0,-0.5968043021,-2.8146239723,-1.8654391299
H,0,-1.3749189008,-1.1550315886,-3.5440748444
H,0,0.2804349603,-0.6374361362,-3.2297146943
H,0,-2.2281119481,0.8004424686,-2.5517334711
H,0,-0.5931416663,1.3869507612,-2.2510736642
H,0,-2.0827377678,0.8084172061,-0.0679202263
H,0,-2.8179320891,-1.4445403638,-1.2916055952
H,0,-1.9571762212,-1.8486247241,0.211413245
H,0,0.8478879897,-0.8818726912,4.0821813075
H,0,0.6723016351,-2.0882620318,0.1432407563

TCD-H2 2J-3 (σ = 3)

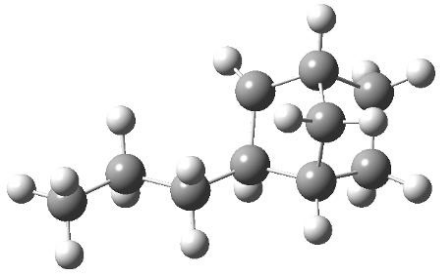

C,0,-0.0639484123,-0.1948683442,0.076747836
C,0,0.0294680315,-0.0374200394,1.6129029626
C,0,1.4679953393,0.0343848794,2.1386211678
C,0,1.5441957146,0.2341635256,3.6552752759
C,0,0.5030295259,-1.4876377084,-0.4694763864
C,0,-1.5240911313,-0.279290676,-0.4600841123
C,0,-1.4918458565,-0.0826556722,-1.9983557367
C,0,-0.8660378236,-1.4160285613,-2.5240761129
C,0,-0.5931020516,-2.2082443675,-1.2026913818
C,0,-1.8255994569,-1.7925215303,-0.3625030292
H,0,0.4484968595,0.6783095006,-0.3614299785
H,0,-0.5060597598,0.8786220818,1.9010920798
H,0,-0.4929011698,-0.8694869657,2.1027474162
H,0,1.9996099391,-0.8852596843,1.8634434485
H,0,1.9964855243,0.8555391337,1.6346332035
H,0,2.5818901772,0.2837075378,4.0013235198
H,0,1.0480443425,1.1630819941,3.9591196522
H,0,1.5614730419,-1.6851112441,-0.6070400488
H,0,-0.4337345985,-3.2787860877,-1.3570227676
H,0,-1.569401074,-1.9659097958,-3.1607377068
H,0,0.0477043363,-1.2584241194,-3.1043129459
H,0,-2.5048325792,0.0568120287,-2.3899701812
H,0,-0.9093281074,0.7986467665,-2.2860455465
H,0,-2.2206291463,0.3873891005,0.0567288945
H,0,-2.7783501019,-2.0694094576,-0.8273390367
H,0,-1.8028994743,-2.184671629,0.6584754093
H,0,1.0553236674,-0.5891320513,4.1884994307

TCD-H2 2-3J (σ = 1)

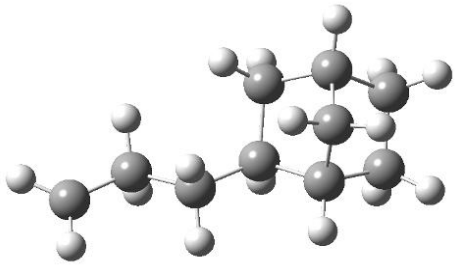

C,0,-0.0014574557,-0.0004644327,0.000765389
C,0,-0.0018574134,-0.0028306548,1.5364488409
C,0,1.4068705457,-0.0009598734,2.1559838011
C,0,1.4053020368,0.039207013,3.6462175867
C,0,0.5477886253,-1.3254946827,-0.6361563623
C,0,-1.4216854406,0.0983722889,-0.6245613294
C,0,-1.2713054275,0.4978447611,-2.1118847812
C,0,-0.67611507,-0.7927804037,-2.7668298147
C,0,-0.5912223788,-1.7793419675,-1.5775995675
C,0,-1.8360817626,-1.3844257193,-0.7553306652
H,0,0.5998834705,0.8578930858,-0.3282022244
H,0,-0.542374626,0.8835385991,1.8967527506
H,0,-0.5562646306,-0.8736209268,1.9106287227
H,0,1.9740006612,-0.8755131175,1.8082749814
H,0,1.9578741379,0.8710487349,1.7533528078
H,0,2.2578572334,-0.3120235952,4.2179362018
H,0,1.4944484423,-1.182535789,-1.1678278924
H,0,-0.5214748313,-2.8287704169,-1.8779136405
H,0,-1.3375064447,-1.1800604935,-3.5491018924
H,0,0.3026353668,-0.6206528828,-3.2267375517
H,0,-2.2462645418,0.7447127656,-2.5458224381
H,0,-0.6282080026,1.3747000058,-2.2405175626
H,0,-2.1024656258,0.744321324,-0.061877825
H,0,-2.7775566846,-1.5203265862,-1.2991113661
H,0,-1.9084829695,-1.9099374756,0.2026919155
H,0,0.6220613576,0.5651883664,4.1841626826
H,0,0.7233790526,-2.0814559364,0.13886088

Table E.2 TCD-H2 2-3 Optimized Species (Continued)

TCD-H2 2J-3J (σ = 1)

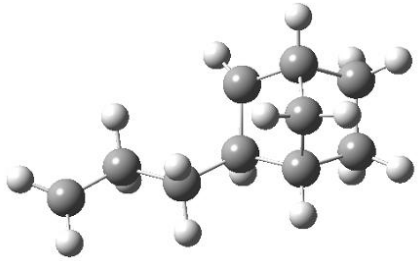

C,0,0.,0.,0.
C,0,0.,0.,1.54614973
C,0,1.4098396857,0.,2.1593217355
C,0,1.4151075702,0.0916214619,3.6472303236
C,0,0.6056409215,-1.2311610874,-0.6395260684
C,0,-1.4258107058,-0.0296712002,-0.6268591003
C,0,-1.3054546728,0.3207600602,-2.1329056018
C,0,-0.642589722,-0.9531011528,-2.7524763159
C,0,-0.4419615232,-1.8743537834,-1.5037744111
C,0,-1.723371443,-1.5452089986,-0.6989835664
H,0,0.5328726992,0.912854558,-0.3161899952
H,0,-0.5407760754,0.8910470551,1.8949915465
H,0,-0.5534675063,-0.8689583159,1.9211211272
H,0,1.9525396651,-0.8993032188,1.8377475044
H,0,1.9775965868,0.8463777151,1.7258128752
H,0,2.2656295107,-0.2517269762,4.2267662912
H,0,1.6715208083,-1.412788008,-0.7356888003
H,0,-0.2676536694,-2.9239311779,-1.7550960076
H,0,-1.3048857576,-1.4360476782,-3.4808383076
H,0,0.3021362149,-0.7381229735,-3.2601775052
H,0,-2.2949028409,0.4987235217,-2.566662206
H,0,-0.7123281187,1.2264385395,-2.2963446194
H,0,-2.1549939611,0.5816644139,-0.0871648063
H,0,-2.6460335414,-1.7740234749,-1.2437807862
H,0,-1.7575608957,-2.0377754838,0.2771247541
H,0,0.6413287737,0.6456444613,4.1705059624

TCD-H2 2JJ-3 (σ = 3)

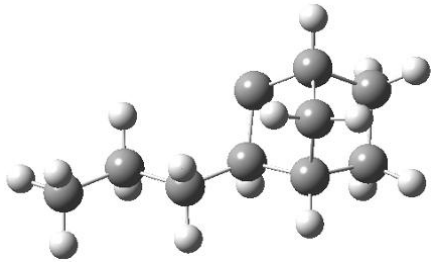

C,0,-0.1897420145,-0.2488182009,-0.4656320296
C,0,-1.5583866425,-0.5411840374,0.1824307832
C,0,-2.7056863414,0.2536612301,-0.4522424381
C,0,-4.0665704334,-0.0380952314,0.1863047061
C,0,0.3146723102,1.1577513501,-0.3110505277
C,0,1.0219514488,-0.9836360686,0.2187450281
C,0,2.2562844687,-0.8758689375,-0.7129849926
C,0,2.7013127973,0.6175252447,-0.5752875137
C,0,1.6322533977,1.2027654632,0.3994061114
C,0,1.4193008478,-0.0085763002,1.3551494398
H,0,-0.2541567606,-0.5485179214,-1.5243398972
H,0,-1.765304684,-1.6174369628,0.0943602631
H,0,-1.5141188428,-0.3177842514,1.2561266396
H,0,-2.4800100138,1.3247940625,-0.3726033537
H,0,-2.7487938993,0.0306117278,-1.5271415632
H,0,-4.8638689743,0.5434917835,-0.2879535183
H,0,-4.3298727698,-1.0982641865,0.0954882199
H,0,1.9065006396,2.15568295,0.856899632
H,0,3.7029887108,0.6979020264,-0.1363413526
H,0,2.7146698383,1.1470430185,-1.5312903026
H,0,3.0473125657,-1.5535924937,-0.3754867642
H,0,2.0135283373,-1.1489638408,-1.7448693504
H,0,0.780290407,-2.0075160134,0.5208271997
H,0,2.335432652,-0.3119193855,1.8759516419
H,0,0.6302294424,0.161280241,2.0924153201
H,0,-4.0645224874,0.2100977334,1.2538076191

TCD-H2 2-3JJ (σ = 1)

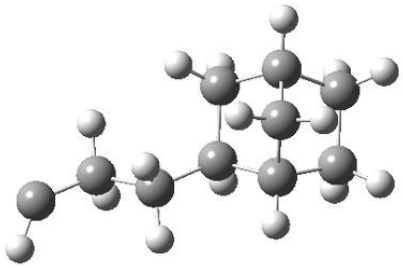

C,0,0.0014008379,-0.0002519392,-0.0003319859
C,0,0.002763736,0.0008185936,1.5362209385
C,0,1.429912435,0.0019660564,2.1434425967
C,0,1.4575391458,0.0112188536,3.6138699846
C,0,0.5428837226,-1.3292677889,-0.6345389773
C,0,-1.4215822819,0.1023350358,-0.6194482951
C,0,-1.2752611958,0.4938943778,-2.1093651083
C,0,-0.6905000017,-0.8029819153,-2.7610344273
C,0,-0.6033627405,-1.7835924938,-1.567333711
C,0,-1.8424992864,-1.3794417734,-0.7407167982
H,0,0.6042555289,0.855565486,-0.3327218703
H,0,-0.5317449797,0.8881701305,1.8989942702
H,0,-0.5434464141,-0.8703371529,1.918210202
H,0,1.9786021445,-0.8781116142,1.7781707631
H,0,1.9806974482,0.874624075,1.745906291
H,0,1.0801974067,0.7032579279,4.360378402
H,0,1.4866368889,-1.1913325903,-1.172527752
H,0,-0.5390078273,-2.8348749782,-1.8620082735
H,0,-1.3587316464,-1.1911718071,-3.5369390459
H,0,0.2861334586,-0.6382194468,-3.2279931737
H,0,-2.250846197,0.7444503864,-2.5396487218
H,0,-0.6279392667,1.366531179,-2.2450905625
H,0,-2.0967023862,0.7542651008,-0.0570057622
H,0,-2.7870021317,-1.5138676974,-1.2794298398
H,0,-1.9127995625,-1.8998904684,0.2201643548
H,0,0.7205917419,-2.0832080983,0.1420808781

Table E.3 TCD-H2 3-4 Optimized Species

TCD-H2 3-4 (σ = 9)

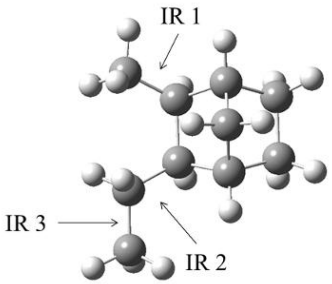

C,0,0.0000090434,-0.0005055046,-0.0001271979
C,0,0.0001159137,-0.0009481645,1.5395662791
C,0,1.4077785894,0.0005940602,2.1485729292
C,0,-2.6136683268,-0.4145297693,0.2257196954
C,0,-1.4038527515,-0.2423228971,-0.7020147384
C,0,0.454546617,1.3532240415,-0.6200803014
C,0,0.8488129359,1.1176474705,-2.0970212607
C,0,-0.5286714125,0.8667366182,-2.7926673437
C,0,-1.5372517222,0.9992341135,-1.6280248684
C,0,-0.8824687958,2.1070934304,-0.7773595048
H,0,0.6924866507,-0.7925866195,-0.3156697627
H,0,-0.5598241179,0.863005826,1.9205518336
H,0,-0.5320927772,-0.8879519882,1.9027139355
H,0,1.9787176327,0.8894395103,1.8612056041
H,0,1.3630476624,-0.0207004954,3.2424761096
H,0,-3.5216566634,-0.5595882261,-0.3698347992
H,0,-2.7775701122,0.4578728899,0.8664556546
H,0,-1.3414269972,-1.1477615243,-1.3188799738
H,0,-2.5649920848,1.1835326507,-1.9561092273
H,0,-0.7241253924,1.6198603793,-3.563535686
H,0,-0.5871348015,-0.1137790259,-3.2767867339
H,0,1.3447711349,2.0014627811,-2.5125940745
H,0,1.540325354,0.27602189,-2.2085501045
H,0,1.2280878458,1.8645382472,-0.0408665118
H,0,-0.780864134,3.0598002102,-1.309262415
H,0,-1.3960302891,2.2958680595,0.170662084
H,0,-2.5096520422,-1.287806544,0.8770322488
H,0,1.9789146464,-0.8762889389,1.822492991

TCD-H2 3J-4 (σ = 3)

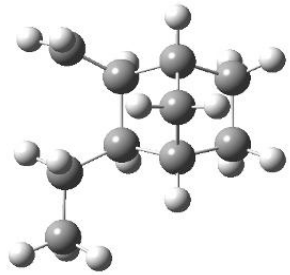

C,0,0.,0.,0.
C,0,0.,0.,1.53708346
C,0,1.4061720884,0.,2.1486829352
C,0,-2.5924889532,-0.3679207493,0.2495502145
C,0,-1.4375960663,-0.241193842,-0.6818142793
C,0,0.4449865473,1.3460630297,-0.6352140436
C,0,0.8259121394,1.0976679193,-2.1131740577
C,0,-0.557395786,0.8356133159,-2.7920728851
C,0,-1.5587180332,0.9933020613,-1.6243629116
C,0,-0.8918780672,2.1020929628,-0.7857480671
H,0,0.6758749372,-0.80162192,-0.326169528
H,0,-0.563744856,0.8637603872,1.9123942795
H,0,-0.5422196658,-0.8843239401,1.8927427391
H,0,1.9788107781,0.8882289232,1.8619744533
H,0,1.3594840394,-0.0203111815,3.2425572814
H,0,-2.8895862922,-1.3310755915,0.6511431174
H,0,-3.1086402502,0.5089822068,0.6288725472
H,0,-1.378782969,-1.1628605788,-1.2750183726
H,0,-2.5863839036,1.1801283423,-1.9478174603
H,0,-0.7591118298,1.5740262251,-3.5752989316
H,0,-0.6219180026,-0.1534782232,-3.2574037912
H,0,1.3142024991,1.9792812439,-2.5421731323
H,0,1.5192687708,0.2575357066,-2.2236388219
H,0,1.2234165603,1.8611978516,-0.0655288371
H,0,-0.792629906,3.0520289847,-1.3229449085
H,0,-1.3962644968,2.2951075726,0.1665506719
H,0,1.9773788843,-0.8777157519,1.8247964208

TCD-H2 3-4J (σ = 3)

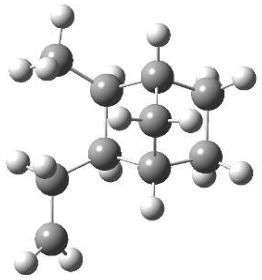

C,0,0.,0.,0.
C,0,0.,0.,1.54298644
C,0,1.3713420198,0.,2.1303153067
C,0,-2.6329760509,-0.2331251767,0.2229745637
C,0,-1.4139475655,-0.1336732161,-0.7035765292
C,0,0.556593994,1.321357781,-0.6012540277
C,0,0.932351896,1.0754855181,-2.0808449157
C,0,-0.4602574924,0.9391202752,-2.7796701665
C,0,-1.4564055212,1.1279914663,-1.6117811047
C,0,-0.7209439433,2.1743628564,-0.7484914968
H,0,0.6371016253,-0.8384312385,-0.3115793012
H,0,-0.5671369886,0.8556611278,1.9333719941
H,0,-0.5505822249,-0.890260162,1.8969176011
H,0,2.182422058,-0.5297791248,1.6392171294
H,0,1.5517895323,0.375565839,3.1320395002
H,0,-3.5484302478,-0.3178052421,-0.3726229788
H,0,-2.7416453494,0.6455085221,0.8671827912
H,0,-1.4151533115,-1.032539484,-1.3329705276
H,0,-2.4683043732,1.3912522415,-1.9352370748
H,0,-0.5990951351,1.7175352609,-3.5375369569
H,0,-0.5914302101,-0.026072589,-3.2801411364
H,0,1.4950161378,1.9237654344,-2.4852721973
H,0,1.557535128,0.1849039409,-2.2039154265
H,0,1.3652137076,1.7538579429,-0.0054069117
H,0,-0.5496248147,3.1227371615,-1.2699191665
H,0,-1.2192975029,2.3905858187,0.2018236881
H,0,-2.5837417176,-1.1139107,0.8709487177

Table E.3 TCD-H2 3-4 Optimized Species (Continued)

TCD-H2 3J-4J (σ = 1)

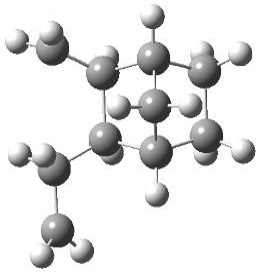

C,0,0.0042882069,0.0330494846,-0.0002314222
C,0,0.0053255717,0.050994574,1.5390582193
C,0,1.3732537862,-0.002720768,2.1319807
C,0,-2.6126361651,0.0322065527,0.242059741
C,0,-1.447636127,-0.0115839904,-0.6850940698
C,0,0.635082529,1.3019656538,-0.6336664892
C,0,0.9886374268,0.9975264938,-2.1073773692
C,0,-0.4133776429,0.921691361,-2.7952297893
C,0,-1.3915719844,1.220610793,-1.6352871682
C,0,-0.5843871577,2.2334157764,-0.7974774214
H,0,0.5692642546,-0.8549113615,-0.3125400984
H,0,-0.5300486165,0.9346718078,1.9137416489
H,0,-0.5925595176,-0.80554597,1.8988682053
H,0,1.5485569023,0.3050363253,3.1576377896
H,0,2.184759285,-0.5054352685,1.6140678308
H,0,-3.0560435395,0.9757120187,0.5458671711
H,0,-2.9926850454,-0.8694933186,0.7111120385
H,0,-1.515491331,-0.9382473378,-1.2706915603
H,0,-2.3821381026,1.5441407118,-1.9669258609
H,0,-0.5081366893,1.6761756208,-3.5832852802
H,0,-0.6085566281,-0.0521173228,-3.2564217405
H,0,1.5945744681,1.8029969994,-2.5359873359
H,0,1.5627649235,0.0708959474,-2.2105810663
H,0,1.4710074479,1.6964755234,-0.0488240841
H,0,-0.3527072556,3.1573198722,-1.3390127476
H,0,-1.0642108879,2.4994844377,0.1499229987

TCD-H2 3JJ-4 (σ = 3)

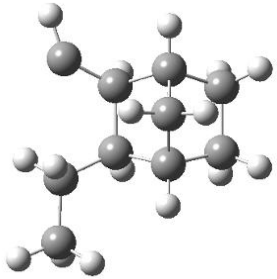

C,0,0.0564109634,-0.019653373,0.010712007
C,0,0.0695492425,-0.030468086,1.5483349498
C,0,1.4784590342,0.02196101,2.1496977531
C,0,-2.4655252446,-0.4785337228,0.3161064161
C,0,-1.3653090485,-0.3125006933,-0.6427237602
C,0,0.4384665874,1.3478884105,-0.6224162699
C,0,0.8103008654,1.1216974437,-2.10651811
C,0,-0.5674856228,0.7980346234,-2.769384863
C,0,-1.5611372364,0.9252403677,-1.5915999498
C,0,-0.9293603962,2.0508140464,-0.7528255741
H,0,0.7614245117,-0.7898839178,-0.3278658993
H,0,-0.5284965185,0.8062039934,1.9313785684
H,0,-0.4362471687,-0.9391103519,1.8965340071
H,0,2.0124091867,0.9357065287,1.8680822495
H,0,1.439738626,-0.0100792512,3.2434774585
H,0,-3.516721557,-0.7216576964,0.1971111611
H,0,-1.2999664913,-1.2296231947,-1.2545467815
H,0,-2.6006529512,1.0670068161,-1.8982079544
H,0,-0.8093008346,1.5204137505,-3.5561490196
H,0,-0.5959489912,-0.1970472919,-3.2259201797
H,0,1.250225327,2.0270881943,-2.5381509634
H,0,1.5407024324,0.3154597104,-2.2301612714
H,0,1.2034269145,1.889626558,-0.0599311867
H,0,-0.8727087998,3.0079124926,-1.2833097113
H,0,-1.4385914518,2.2077973238,0.2028964796
H,0,2.0831270375,-0.8287609422,1.8144759891

TCD-H2 3-4JJ (σ = 3)

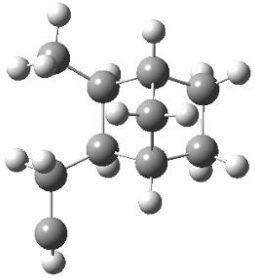

C,0,0.0008582978,0.0006045345,-0.0017144752
C,0,0.0025029553,0.000143813,1.5537269927
C,0,1.3518262136,0.0013537722,2.1409324999
C,0,-2.6405233858,-0.1384877528,0.2452286862
C,0,-1.4252570076,-0.0847972221,-0.6902094769
C,0,0.5948303556,1.3041033439,-0.6017430072
C,0,0.9516373995,1.048097505,-2.0842940569
C,0,-0.449584172,0.9559625415,-2.7733607621
C,0,-1.4308144084,1.1771890059,-1.5985461405
C,0,-0.6555595143,2.1986092425,-0.7398761893
H,0,0.6064141661,-0.8584812085,-0.3147774952
H,0,-0.5508297956,0.8725019989,1.9284664339
H,0,-0.5567423014,-0.8791026869,1.9170127966
H,0,2.1828236015,-0.6957826629,2.0942869646
H,0,-3.5615446244,-0.1918076275,-0.34527814
H,0,-1.4618055071,-0.9844577247,-1.3171576344
H,0,-2.4358836578,1.4734829757,-1.9145711959
H,0,-0.5692387637,1.737783152,-3.5309024786
H,0,-0.6150740483,-0.0049200092,-3.2719628325
H,0,1.5370922854,1.879615165,-2.4908909112
H,0,1.5485833534,0.1393084614,-2.2135782509
H,0,1.4213712249,1.7066425255,-0.0098942319
H,0,-0.4561487985,3.1407709154,-1.2622178966
H,0,-1.141045405,2.4310710339,0.2133094207
H,0,-2.7151388105,0.7459786036,0.8863252831
H,0,-2.6208310248,-1.0183572872,0.896041225

Table E.4 TCD-H2 2-6 Optimized Species

TCD-H2 2-6 (σ = 1)

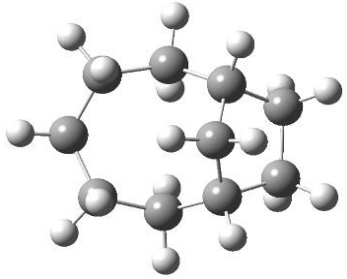

C,0,-0.7063668508,0.3275254684,0.2036911825
C,0,-0.1939712252,0.114503313,1.6462603494
C,0,1.3247840314,-0.1194663855,1.7896734526
C,0,1.9759629197,-1.3576487634,1.1377917606
C,0,1.886592388,-1.4300657543,-0.403459685
C,0,-1.2656793555,-0.9180001399,-0.5396346362
C,0,-1.0377237306,-0.8365229054,-2.0752834513
C,0,0.2400112014,-1.6893183815,-2.3752102703
C,0,0.7172232122,-2.2577233036,-1.0082969667
C,0,-0.5846502726,-2.2515041679,-0.1894249754
H,0,-1.5053685513,1.0789638723,0.216637373
H,0,-0.4235151971,1.0142836586,2.2307965905
H,0,-0.7522520525,-0.6954469096,2.1329918405
H,0,1.8359570781,0.7705471092,1.3942880344
H,0,1.5599920974,-0.1432573136,2.8620968346
H,0,3.0357766262,-1.332914333,1.4209754529
H,0,1.5794796353,-2.2776257675,1.5861550343
H,0,0.0983863231,0.7821913335,-0.3858606854
H,0,1.0714991259,-3.2891063346,-1.1237308797
H,0,-0.0107837265,-2.5067318245,-3.0595596341
H,0,1.0253345275,-1.1042614184,-2.8651481648
H,0,-1.8977159254,-1.2562349039,-2.6080030897
H,0,-0.9369129165,0.1995257967,-2.4152456538
H,0,-2.3366059969,-0.9824955301,-0.3122674099
H,0,-1.2227018368,-3.071139384,-0.5451901401
H,0,-0.4420523672,-2.4148828752,0.8807330592
H,0,2.818008741,-1.8582091114,-0.7938282001
H,0,1.8606054036,-0.4070040173,-0.7966578007

TCD-H2 2J-6 (σ = 1)

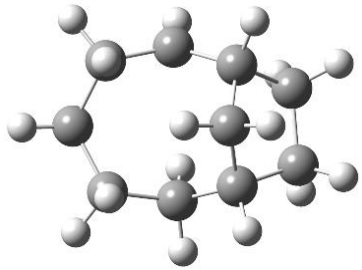

C,0,-0.2038819031,-0.1340913342,0.0710685959
C,0,0.0363044394,-0.1935930898,1.5977322198
C,0,1.4764795278,0.1324813776,2.0366515595
C,0,2.5960926511,-0.8313613409,1.5520207519
C,0,2.7814114285,-0.9064047325,0.0677178952
C,0,-0.2232055297,-1.4787263646,-0.7028163763
C,0,0.1684903906,-1.262134017,-2.1838576721
C,0,1.7247967089,-1.3558757274,-2.2157149587
C,0,2.1572301811,-1.9406735807,-0.8271195348
C,0,0.8347821185,-2.506532557,-0.2650703849
H,0,-1.163554705,0.3594462103,-0.1280171245
H,0,-0.6202816195,0.536094408,2.0874926687
H,0,-0.2663050461,-1.1710411972,1.9959816755
H,0,1.7215888356,1.1460254482,1.691126696
H,0,1.5121753315,0.1659115598,3.1338881753
H,0,3.5329015201,-0.4883996965,2.0129483919
H,0,2.4018120307,-1.8283504436,1.9695738936
H,0,3.4188982774,-0.1583482163,-0.401493333
H,0,2.8797586756,-2.7606201191,-0.9842828575
H,0,2.0549922168,-2.0042432916,-3.0334579253
H,0,2.1874938546,-0.3784717112,-2.3843851215
H,0,-0.2657826808,-2.0568515221,-2.8009192931
H,0,-0.2045599545,-0.3117392496,-2.5800394298
H,0,-1.2277110135,-1.9112467662,-0.6161267087
H,0,0.61373014,-3.466148377,-0.7492064287
H,0,0.8575562545,-2.6972835465,0.8101218025
H,0,0.5556520657,0.5250227991,-0.3682186641

TCD-H2 2-6J (σ = 1)

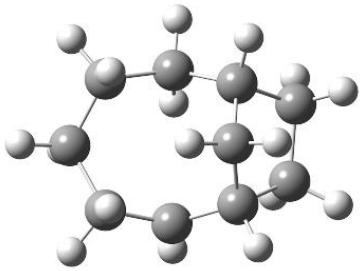

C,0,-0.6558865222,-0.0004718794,0.1556376245
C,0,-0.2649532282,-0.1482890875,1.5938413117
C,0,1.2556519024,-0.0139495789,1.8888993614
C,0,2.1867868059,-1.0575793501,1.2431891148
C,0,2.212229122,-1.0332782118,-0.3029937575
C,0,-0.8505252417,-1.1398259156,-0.8056056377
C,0,-0.3542842147,-0.8000110064,-2.2532070419
C,0,0.9717554442,-1.5949134291,-2.4574020118
C,0,1.3665178086,-2.0990490404,-1.0489408152
C,0,-0.0167953371,-2.3872670819,-0.4400838255
H,0,-0.8163789112,1.0074469191,-0.2244192409
H,0,-0.7735391781,0.6262889223,2.1846540255
H,0,-0.6134075489,-1.109954418,1.9936445091
H,0,1.58149566,0.9848544897,1.5680529886
H,0,1.3916967867,-0.0452965708,2.9783092572
H,0,3.1987640092,-0.8577773272,1.6165313657
H,0,1.9352823449,-2.0625384655,1.6070146835
H,0,1.9062680772,-0.0326703531,-0.6336356605
H,0,1.9530548135,-3.0243343448,-1.1074084452
H,0,0.7958017896,-2.4498624871,-3.1199849028
H,0,1.7585966371,-0.9900458399,-2.9204305302
H,0,-1.0981270726,-1.0931342695,-3.0008073522
H,0,-0.203638279,0.2780372134,-2.3669780795
H,0,-1.9227823424,-1.4011292488,-0.838278023
H,0,-0.4423188016,-3.2686299667,-0.9363119456
H,0,0.0006705781,-2.6091424739,0.6292166943
H,0,3.2460673902,-1.1485530538,-0.6524056698

Table E.4 TCD-H2 2-6 Optimized Species (Continued)

TCD-H2 2J-6J (σ = 1)

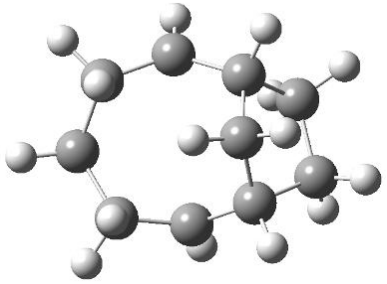

C,0,-0.169773155,-1.5697510303,-0.3776304177
C,0,-1.5949426333,-1.4437369529,0.0597053194
C,0,-2.3362149493,-0.1729235557,-0.438594418
C,0,-1.8642373551,1.1746713451,0.1758635585
C,0,-0.5155789874,1.6672401033,-0.2508613322
C,0,1.0233135798,-1.156784161,0.4368270472
C,0,2.1852046874,-0.6603748538,-0.4536141879
C,0,1.8313746603,0.8123049651,-0.7802273281
C,0,0.8157236655,1.2777000831,0.3312920212
C,0,0.7761408667,0.0860443146,1.3201365059
H,0,0.0175864015,-1.9787945735,-1.3694456835
H,0,-2.1599771155,-2.3114873908,-0.3088127216
H,0,-1.6673840487,-1.4782716095,1.1557659597
H,0,-2.2612026836,-0.1168699727,-1.5315922955
H,0,-3.4020143153,-0.2925345832,-0.2020827995
H,0,-2.6101938186,1.9315370377,-0.0991101759
H,0,-1.9204941538,1.0838154737,1.2706664811
H,0,1.2349008536,2.1605636454,0.8413902074
H,0,2.7245075227,1.4447872479,-0.801841362
H,0,1.3630841492,0.8887271986,-1.766464563
H,0,3.1221291821,-0.709407194,0.1140526056
H,0,2.3203817828,-1.2718465513,-1.3519416485
H,0,1.3554082581,-2.0056498685,1.0617764778
H,0,1.6016748378,0.1768002129,2.0361488234
H,0,-0.143074357,0.0364973765,1.9085129354
H,0,-0.4813798745,2.3557202932,-1.0943070092

TCD-H2 2JJ-6 (σ = 1)

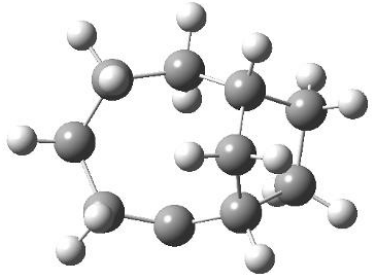

C,0,-0.4226482962,-1.6233298872,-0.2590617094
C,0,-1.8270643735,-1.3422933598,0.109856534
C,0,-2.410454456,0.0143303093,-0.373391004
C,0,-1.6790670405,1.2876971301,0.0908198086
C,0,-0.2514163396,1.451141901,-0.4844526528
C,0,0.8883035919,-1.3192859955,0.3610368733
C,0,1.9684357962,-0.8289409707,-0.6719956082
C,0,2.1729332626,0.689703385,-0.3980651823
C,0,0.9476404675,1.1158408679,0.4425067468
C,0,0.7662920635,-0.1178970581,1.3418257086
H,0,-2.4726115752,-2.1382693988,-0.2895105085
H,0,-1.9385466828,-1.4031517932,1.2080392302
H,0,-2.4325540761,0.0076886194,-1.4709085631
H,0,-3.4567429107,0.0625295086,-0.0433451331
H,0,-2.2882322534,2.1422236534,-0.2278907639
H,0,-1.6636485113,1.3345044645,1.1876731372
H,0,-0.1814244917,0.8411248769,-1.3933217304
H,0,1.1705362022,1.9973809997,1.05631206
H,0,3.0902922933,0.8454650076,0.1813789625
H,0,2.2737964334,1.2731938387,-1.3193418613
H,0,2.9053074603,-1.3803231508,-0.5466334087
H,0,1.6237725267,-1.0158175559,-1.692508151
H,0,1.2638086402,-2.2079559172,0.8945495077
H,0,1.5921363156,-0.1563867584,2.0638906863
H,0,-0.1608375552,-0.1258561351,1.920170964
H,0,-0.110500491,2.4862234191,-0.8196569424

Table E.5 TCD-H2 1-10 Optimized Species

TCD-H2 1-10 (σ = 3)

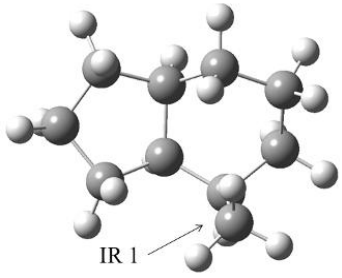

C,0,-0.0000015599,0.000104128,0.0000170713
C,0,-0.0000521173,-0.0001226831,1.5416740575
C,0,1.4944984674,0.0000232966,1.8939147389
C,0,2.0859723363,-1.0166121209,0.8991256305
C,0,1.2519232715,-0.8630594031,-0.4037855882
C,0,-1.3180798089,-0.3818099148,-0.7318920547
C,0,-0.9600973766,-0.7814613899,-2.1781017595
C,0,-0.0652695608,-2.0413468302,-2.2631326545
C,0,0.8661503748,-2.2048499689,-1.0395702514
C,0,-2.1989231709,-1.4367431952,-0.0392703778
H,0,0.2251073126,1.0295790377,-0.3115209202
H,0,-0.5497869964,0.8468009048,1.9672231015
H,0,-0.4627997695,-0.9154504151,1.9307712997
H,0,1.9185270882,0.9971189418,1.7174839018
H,0,1.6958415284,-0.257844379,2.9388959896
H,0,3.1587392327,-0.8761884875,0.731907234
H,0,1.9588130463,-2.0314790413,1.2984924611
H,0,1.8353321133,-0.2997099491,-1.1434994557
H,0,1.7705725379,-2.7563524177,-1.3248700944
H,0,-0.6866649282,-2.938904954,-2.3608913614
H,0,0.5304973215,-1.9883538327,-3.1820531619
H,0,-1.8724853311,-0.9302625361,-2.768203918
H,0,-0.4353225245,0.0657118457,-2.6391655037
H,0,-1.9283746946,0.5301920637,-0.7878912174
H,0,-3.0892403792,-1.634588112,-0.6471089311
H,0,-2.5438124997,-1.0903565184,0.9397420177
H,0,0.3742207512,-2.8211554734,-0.276857417
H,0,-1.6883783959,-2.3925206336,0.1113601786

TCD-H2 1J-10 (σ = 3)

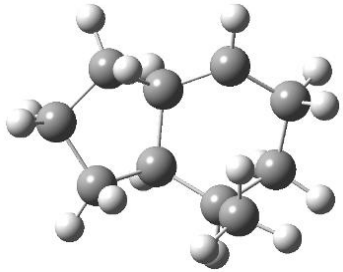

C,0,0.0045745446,0.0736927087,-0.0537934998
C,0,0.0180962104,0.2108420055,1.488930418
C,0,1.4840267726,-0.0202676346,1.8899864806
C,0,1.9108549982,-1.1690575858,0.9657603734
C,0,1.2702910504,-0.8112541433,-0.4002813325
C,0,-1.3126053138,-0.4176236861,-0.7078550498
C,0,-1.0166094563,-0.7375482034,-2.1881115846
C,0,-0.07210044,-1.94662159,-2.3396762602
C,0,0.9905766148,-1.9803795004,-1.2855023994
C,0,-1.9954972605,-1.6012098105,-0.0018096589
H,0,0.1888179482,1.0700481142,-0.4757446497
H,0,-0.3779979181,1.1747907716,1.8259576129
H,0,-0.5981564061,-0.5680715502,1.9511287406
H,0,2.0827059305,0.8755437174,1.6780811868
H,0,1.6075255548,-0.2511112105,2.9531944433
H,0,2.9962262711,-1.2984590948,0.8997142457
H,0,1.4903460775,-2.1140633786,1.3330964607
H,0,1.985833439,-0.1432404284,-0.9170691116
H,0,1.6809791508,-2.8216850866,-1.2691278362
H,0,-0.6522856292,-2.8819486944,-2.3012613716
H,0,0.3718576914,-1.9408371877,-3.350521022
H,0,-1.9492759174,-0.9238463368,-2.7336850078
H,0,-0.5585260219,0.1470734218,-2.6500231186
H,0,-2.0201344899,0.4231567217,-0.685029001
H,0,-2.8506394192,-1.952146635,-0.5906774239
H,0,-2.3755312275,-1.3206178283,0.9846526084
H,0,-1.3139316048,-2.4474448048,0.1322531447

TCD-H2 1-10J (σ = 1)

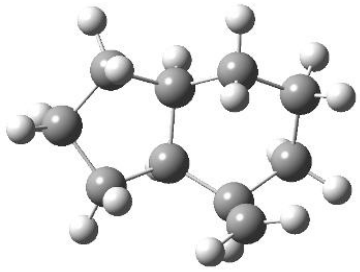

C,0,-0.0000496102,-0.0000774084,0.0000071289
C,0,0.0000132818,0.0002114195,1.5431861439
C,0,1.4929981764,0.000206766,1.9058164272
C,0,2.0876373259,-1.003891677,0.9033006412
C,0,1.3091029068,-0.768420725,-0.4169262822
C,0,-1.2814733747,-0.5182559977,-0.7249411295
C,0,-0.9375707105,-0.7015875973,-2.2190197263
C,0,0.1563243076,-1.7775125879,-2.4573393153
C,0,1.0059357763,-2.0502055784,-1.1998968449
C,0,-1.9178128683,-1.7378968135,-0.1390681514
H,0,0.1179670347,1.0425084862,-0.3246462278
H,0,-0.554057653,0.8452359902,1.966294969
H,0,-0.4589115007,-0.9174746417,1.9289835848
H,0,1.9200155893,0.9985104356,1.742837886
H,0,1.6851157747,-0.2690697366,2.9496759601
H,0,3.1705034958,-0.9002587281,0.778905456
H,0,1.9036507482,-2.0256905314,1.2614980395
H,0,1.900972658,-0.1096013218,-1.0664775345
H,0,1.9385721326,-2.5573246332,-1.4772955558
H,0,-0.2993122773,-2.717390487,-2.7891111331
H,0,0.8052220473,-1.4513192375,-3.2790791183
H,0,-1.843384566,-0.9477550908,-2.7848208911
H,0,-0.591279389,0.2656422045,-2.6035556402
H,0,-2.0207717299,0.3013109123,-0.6529581004
H,0,-2.2793774922,-2.5373598732,-0.7781505482
H,0,-2.1991698247,-1.7782815897,0.9076279747
H,0,0.4636550322,-2.7387657967,-0.5394950327

Table E.5 TCD-H2 1-10 Optimized Species (Continued)

TCD-H2 1J-10J (σ = 1)

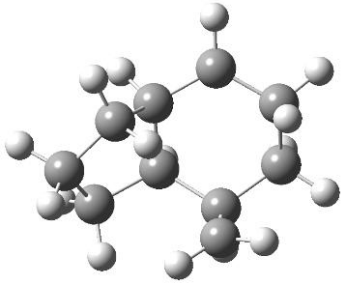

C,0,-0.0003126367,-0.000012167,-0.0002237726
C,0,-0.0002592761,0.0001938574,1.5516256578
C,0,1.4913499596,-0.0021788596,2.0043987369
C,0,2.3264422764,-0.1488719686,0.7162005621
C,0,1.4266674188,0.4779549514,-0.388676654
C,0,-0.3799758788,-1.3653419045,-0.6509969595
C,0,-0.1958335094,-1.2688521225,-2.179440941
C,0,1.267026865,-0.9716823162,-2.5585514907
C,0,1.822968866,0.1927772028,-1.8007991253
C,0,0.3119953426,-2.5644526124,-0.0847547618
H,0,-0.7357016965,0.7207321139,-0.3781588079
H,0,-0.5101964594,0.8922925449,1.9289632472
H,0,-0.5523719928,-0.8565438247,1.9516088573
H,0,1.7327076686,0.9435554054,2.502041972
H,0,1.7064244315,-0.7982285337,2.7243866436
H,0,3.3046368959,0.338803013,0.7808177704
H,0,2.4983447471,-1.2057560708,0.4861987208
H,0,1.4618905365,1.5677603705,-0.2294648293
H,0,2.6796226364,0.7224396409,-2.2120295818
H,0,1.8703309489,-1.8785455949,-2.3663929731
H,0,1.3494740536,-0.7960523205,-3.6390449023
H,0,-0.5273607273,-2.1987954671,-2.6569546713
H,0,-0.8380581632,-0.4668411452,-2.5646617409
H,0,-1.4634271443,-1.4884209982,-0.4553347752
H,0,0.3960540961,-2.7149882849,0.9861920642
H,0,0.5644948508,-3.4067694672,-0.7215460654

TCD-H2 1JJ-10 (σ = 3)

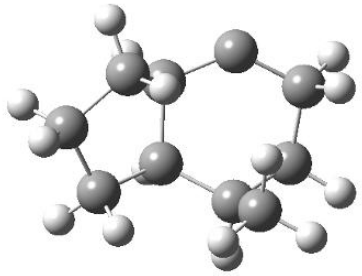

C,0,0.0025128755,0.112122835,-0.0771974329
C,0,0.00069615,0.2739036568,1.4722537469
C,0,1.400163897,-0.1629632071,1.967381467
C,0,1.8982555292,-1.1445942444,0.8977978882
C,0,1.4313655921,-0.4763326596,-0.4232918831
C,0,-1.1695222282,-0.7127849917,-0.6754986366
C,0,-0.9544097452,-0.8543030641,-2.1967869056
C,0,0.3096836571,-1.6956620476,-2.5274694593
C,0,1.4268170128,-1.2970180806,-1.646187912
C,0,-1.4230832177,-2.0848411584,-0.0263111608
H,0,-0.0653320279,1.1001554846,-0.5475124267
H,0,-0.2325484899,1.3015349586,1.768391031
H,0,-0.7689306281,-0.358157731,1.9256013298
H,0,2.0726202953,0.7030764036,2.0078771019
H,0,1.3753082856,-0.5959742576,2.9724439117
H,0,2.9809665592,-1.3023941879,0.9216224845
H,0,1.4199518131,-2.1235164788,1.0164236939
H,0,2.1010750888,0.3897740487,-0.5679845552
H,0,0.0749532198,-2.7677433592,-2.4141214361
H,0,0.5685733477,-1.5686098981,-3.5893322545
H,0,-1.8322652733,-1.3131924408,-2.6680372597
H,0,-0.8418001315,0.1446955381,-2.6358099408
H,0,-2.0800380996,-0.1141568901,-0.5263050601
H,0,-2.2644063012,-2.583680728,-0.5204008593
H,0,-1.677470206,-1.9991304748,1.0336825985
H,0,-0.556407329,-2.7479389637,-0.104725654

TCD-H2 1-10JJ (σ = 1)

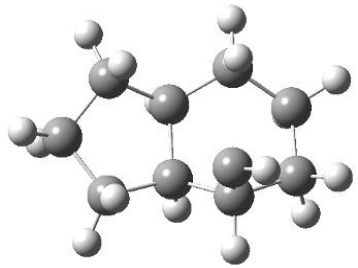

C,0,-0.2974983426,-0.5445490696,-0.690662855
C,0,-1.6401681981,-1.2458836647,-0.3452207596
C,0,-2.6418274292,-0.1068483112,-0.0783786679
C,0,-1.7729001039,0.9789911089,0.573218358
C,0,-0.4746342551,0.9550198535,-0.2565876261
C,0,0.9546883683,-1.2046477407,-0.0551607047
C,0,2.2317070487,-0.3897504434,-0.4402721361
C,0,2.043299228,1.1484063962,-0.3299933039
C,0,0.767237127,1.5360131722,0.4323693016
C,0,0.8383205992,-1.395599276,1.4047364594
H,0,-0.1365742772,-0.578090095,-1.7751471072
H,0,-1.9705603427,-1.9298630509,-1.1338026659
H,0,-1.5144538817,-1.8416487004,0.5667793458
H,0,-3.0570691949,0.2663811293,-1.0238549687
H,0,-3.4862017292,-0.4203152519,0.5442947859
H,0,-2.2475401111,1.9661263002,0.5917668798
H,0,-1.5525573312,0.7005796256,1.6125082659
H,0,-0.6503446926,1.5391027383,-1.1713526108
H,0,0.6857562326,2.6278722456,0.4996939289
H,0,2.9193119771,1.6009540357,0.1472292511
H,0,1.9890851319,1.5823216386,-1.3366764155
H,0,3.0636330389,-0.7213510524,0.1903307238
H,0,2.5041127897,-0.6573757471,-1.4686272219
H,0,1.0589094959,-2.2073728159,-0.5110375206
H,0,1.4938413037,-1.8413629711,2.146593735
H,0,0.8268695487,1.1610379462,1.4619375286

Table E.6 TCD-H2 1-9 Optimized Species

TCD-H2 1-9 (σ = 3)

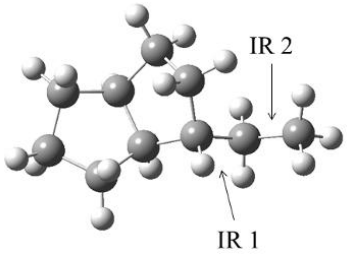

C,0,0.0029189169,-0.0027523873,-0.0062524158
C,0,-0.0093563637,-0.0036255941,1.5430591622
C,0,1.472970351,-0.0000612705,1.9462443355
C,0,2.1018701781,-0.9580421194,0.9232672302
C,0,1.3899395969,-0.6292003054,-0.4130536778
C,0,-1.094265257,-0.8783420772,-0.6728336877
C,0,-1.6249482603,-0.2523111113,-1.9780570493
C,0,-2.7969578407,-1.0075393298,-2.6132683808
C,0,1.0540124785,-1.8552981872,-1.2911784225
C,0,-0.3815059996,-2.2354011075,-0.8858633759
H,0,-0.0712056423,1.0314014245,-0.3622677133
H,0,-0.5775434313,0.8342983696,1.9604822293
H,0,-0.4819104338,-0.9243170648,1.9115795874
H,0,1.8937873506,1.0070337161,1.8267110812
H,0,1.6411332036,-0.30224678,2.9855463471
H,0,3.1909837759,-0.8685098201,0.8530289984
H,0,1.8849247009,-1.9944242352,1.2165104917
H,0,1.9931422163,0.0950735583,-0.9710558939
H,0,1.7656974091,-2.6770720163,-1.1546138135
H,0,-3.63733777,-1.0899541725,-1.9141859103
H,0,-3.1597832085,-0.4912646433,-3.5081923646
H,0,-1.9432634481,0.7756568762,-1.7594289641
H,0,-0.8072547219,-0.1623803934,-2.7060404007
H,0,-1.9491064201,-0.9960311211,0.0074581936
H,0,-0.8784077267,-2.8800845044,-1.6178206527
H,0,-0.3637876089,-2.7902668181,0.0608562637
H,0,1.0843239768,-1.5853255326,-2.3532851965
H,0,-2.5178061515,-2.0229911768,-2.9127370743

TCD-H2 1J-9 (σ = 3)

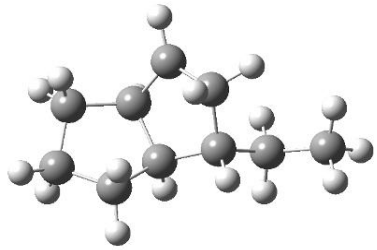

C,0,0.102737823,-0.0876795312,-0.1350590559
C,0,0.0291082677,0.1999071978,1.3787387184
C,0,1.4690717573,-0.01681042,1.8648167068
C,0,1.9204332036,-1.2846957562,1.112828837
C,0,1.1627252666,-1.2369016354,-0.2606439914
C,0,-1.2040361639,-0.6112080809,-0.7842346388
C,0,-1.3032258436,-0.2208306578,-2.2718224119
C,0,-2.6489761507,-0.551710942,-2.9253826327
C,0,0.3395866787,-2.4468876591,-0.5793442257
C,0,-1.1270120739,-2.1504126218,-0.5826577428
H,0,0.4496923314,0.8187970706,-0.6460282512
H,0,-0.3603857943,1.1992202158,1.6007464501
H,0,-0.6385397583,-0.5235139536,1.8666004845
H,0,2.0900462576,0.8381124472,1.5670042803
H,0,1.5515977922,-0.1131417253,2.9527011209
H,0,3.0063567783,-1.3384951164,0.987505575
H,0,1.6177637476,-2.1780082268,1.6712198262
H,0,1.8871508729,-1.0278338821,-1.0618602241
H,0,0.7523742903,-3.4489385991,-0.6499161316
H,0,-3.4717417817,-0.038918751,-2.4137216839
H,0,-2.6647615849,-0.2391612155,-3.9746705038
H,0,-1.1236138764,0.8586111633,-2.3620418375
H,0,-0.4923654317,-0.7119656007,-2.8275270524
H,0,-2.0781017682,-0.1941573892,-0.2655528478
H,0,-1.6779035312,-2.7101763287,-1.3497795531
H,0,-1.5976158025,-2.4361717716,0.3757153121
H,0,-2.8649497257,-1.6249812399,-2.9012925572

TCD-H2 1-9J (σ = 1)

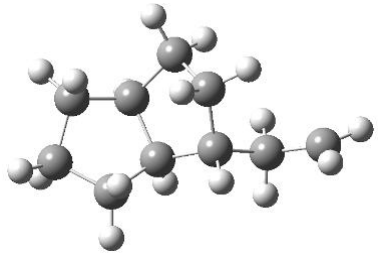

C,0,0.0624647539,-0.0713666529,-0.1248189987
C,0,0.061552723,0.3170084407,1.374966835
C,0,1.4802303079,-0.010833361,1.864530178
C,0,1.7870648989,-1.3332225223,1.1454991298
C,0,1.1966602109,-1.154830878,-0.2759029508
C,0,-1.2472847395,-0.7312457924,-0.6322197479
C,0,-1.5733232828,-0.3373863096,-2.0905685204
C,0,-2.851222003,-0.9043253571,-2.6068949739
C,0,0.5047359782,-2.4090744416,-0.8574115869
C,0,-0.9766651022,-2.2448622232,-0.4730149578
H,0,0.29577448,0.8174716466,-0.7229177875
H,0,-0.2274404751,1.3602727892,1.540022885
H,0,-0.6616018538,-0.3044633991,1.9203793002
H,0,2.1815708608,0.7676108899,1.5362667692
H,0,1.557894241,-0.0806475937,2.9548400502
H,0,2.8526923101,-1.5847386111,1.129836367
H,0,1.2726118698,-2.1546742987,1.6627569307
H,0,1.9847288631,-0.798918238,-0.9483550236
H,0,0.941056121,-3.340861783,-0.480965433
H,0,-3.7110855236,-1.0106686617,-1.9516317409
H,0,-1.6070354429,0.767725979,-2.1378297633
H,0,-0.7431900366,-0.6201989036,-2.7528106066
H,0,-2.0986731078,-0.4218260759,-0.0109621355
H,0,-1.6524353622,-2.8592996733,-1.0770011712
H,0,-1.1231433224,-2.5375256742,0.5744913241
H,0,0.6079874746,-2.4314306566,-1.9486005296
H,0,-3.0086491792,-1.0646797828,-3.6682464017

Table E.6 TCD-H2 1-9 Optimized Species (Continued)

TCD-H2 1J-9J (σ = 1)

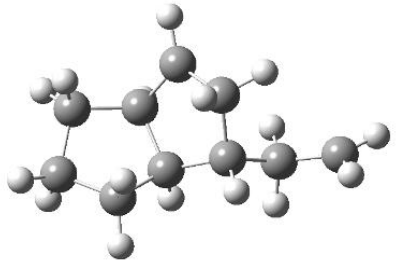

C,0,0.,0.,0.
C,0,0.,0.,1.54268604
C,0,1.4904360765,0.,1.9108554452
C,0,2.1090442052,-1.0019229597,0.9165112124
C,0,1.253316995,-0.8601085914,-0.3913465946
C,0,-1.224816177,-0.6694438174,-0.6714001208
C,0,-1.5281041777,-0.0536737985,-2.055792596
C,0,-2.7500714558,-0.5946336131,-2.7162693871
C,0,0.6656531968,-2.1347415515,-0.9151254683
C,0,-0.8247577852,-2.1653342421,-0.7828672546
H,0,0.1134265223,1.0337653806,-0.3492979767
H,0,-0.5539442637,0.8450321015,1.9653580336
H,0,-0.4728538273,-0.917737977,1.9184579443
H,0,1.9100083464,1.0011141477,1.7466937483
H,0,1.6804449538,-0.2632176191,2.9568763107
H,0,3.1738397011,-0.8215842863,0.7391000766
H,0,2.017446802,-2.0213040667,1.3088946533
H,0,1.8589012319,-0.3578180186,-1.1603572904
H,0,1.2638710932,-2.9903723018,-1.2138255377
H,0,-3.6388645142,-0.816237907,-2.1321041303
H,0,-1.6304177383,1.039828968,-1.9215674567
H,0,-0.6576204749,-0.1832137807,-2.7138608486
H,0,-2.1197687183,-0.5486980625,-0.0464677086
H,0,-1.3296297778,-2.669370862,-1.6169438308
H,0,-1.1353394187,-2.7133057264,0.1255480907
H,0,-2.8414639972,-0.6249814945,-3.7967183515

TCD-H2 1JJ-9 (σ = 3)

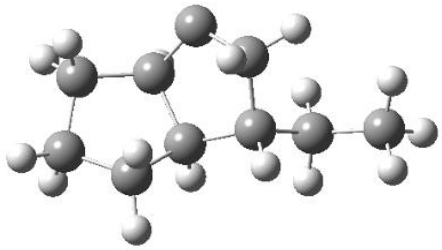

C,0,0.0045217042,-0.0069513324,-0.000740978
C,0,0.0029436946,-0.0087990963,1.5400366207
C,0,1.4915060166,0.0077219232,1.9144743871
C,0,2.1323760696,-0.9838810957,0.9222748759
C,0,1.2683876139,-0.8791029584,-0.3797957031
C,0,-1.2342923869,-0.6620411655,-0.6753805245
C,0,-1.5279655879,-0.0493659254,-2.0568191846
C,0,-2.8424583262,-0.515575588,-2.6908240357
C,0,0.6166406199,-2.1343435623,-0.8366728574
C,0,-0.8680241193,-2.1816192715,-0.7690669127
H,0,0.1343706726,1.0228824914,-0.3557335249
H,0,-0.5614304356,0.8315107557,1.9587242769
H,0,-0.4636049933,-0.9307165349,1.9130657913
H,0,1.8984575618,1.0149411972,1.7565018123
H,0,1.6780988333,-0.2555031805,2.960932044
H,0,3.188582651,-0.7685968169,0.7343051712
H,0,2.0769154698,-2.0039176305,1.3167206942
H,0,1.8548639604,-0.406179864,-1.1801664221
H,0,-3.6977028819,-0.2677453237,-2.0515725126
H,0,-3.0028626235,-0.0345975817,-3.6611507859
H,0,-1.5543260792,1.0434564734,-1.9523467468
H,0,-0.6913867921,-0.270378952,-2.7339376156
H,0,-2.1217950658,-0.5238608491,-0.042405245
H,0,-1.3325871627,-2.6739297148,-1.632303513
H,0,-1.2271420493,-2.7277853442,0.1197007355
H,0,-2.8578939632,-1.5978107976,-2.8566938163

TCD-H2 1-9JJ (σ = 1)

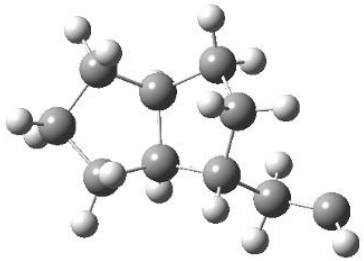

C,0,-0.2784895791,-0.6429850644,-0.4176902118
C,0,-1.3715438292,-1.3514297733,0.4214105431
C,0,-2.6812876683,-0.6525561773,0.0259023312
C,0,-2.2583371245,0.8202565188,-0.0817545576
C,0,-0.8635045204,0.7807717183,-0.7548553371
C,0,1.061881751,-0.4005554037,0.3271369137
C,0,2.2827487546,-0.5353456546,-0.6319735874
C,0,3.5912054499,-0.3291119406,0.004617469
C,0,0.1585149808,1.7988976071,-0.19951909
C,0,0.9159503098,1.0271194373,0.8960997875
H,0,-0.1052407193,-1.2168160926,-1.3357604732
H,0,-1.3889710459,-2.4346395077,0.262162655
H,0,-1.1840692204,-1.1891651723,1.4914413604
H,0,-3.0235925408,-1.0181748574,-0.951156298
H,0,-3.4947050478,-0.8202095992,0.7398969992
H,0,-2.973130795,1.4407935745,-0.6321393314
H,0,-2.1740017388,1.2478685346,0.9266991627
H,0,-0.9852046325,0.9024719317,-1.8366521691
H,0,-0.3197071732,2.7100424493,0.1762168746
H,0,2.2442689746,-1.5363263807,-1.0989739379
H,0,2.1668008355,0.1752578297,-1.4636301658
H,0,1.1959951475,-1.1331633742,1.1325174226
H,0,1.8805232219,1.474901756,1.1565076512
H,0,0.314954551,0.9972563402,1.813795555
H,0,0.85451762,2.1109906113,-0.9869249928
H,0,4.1279536785,-0.856211871,0.7873766466

Table E.7 TCD-H2 9-8 Optimized Species

TCD-H2 9-8 (σ = 9)

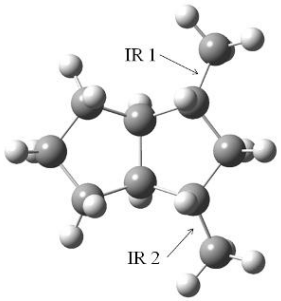

C,0,0.3826132044,-0.7857890846,0.421530224
C,0,1.7365880988,-1.2086391532,-0.1942371926
C,0,2.659717041,-0.0000018164,0.0472956506
C,0,1.73658976,1.208636901,-0.1942366801
C,0,0.3826142199,0.785788394,0.4215304054
C,0,-0.9084201192,-1.2145792382,-0.3212648833
C,0,-1.4988643132,-2.5472775948,0.1410836045
C,0,-1.4988608161,2.5472795233,0.1410835462
C,0,-0.908418424,1.2145803347,-0.3212648317
C,0,-1.8394854719,0.0000011956,-0.1471399272
H,0,0.3275330839,-1.1488141871,1.4560584551
H,0,2.1315560696,-2.138666971,0.2277071622
H,0,1.6220520631,-1.3700744411,-1.2747555251
H,0,3.0101569941,-0.0000022788,1.08792768
H,0,3.5488369011,-0.0000022858,-0.5927197536
H,0,2.131558973,2.1386639624,0.2277081752
H,0,1.6220540483,1.3700728908,-1.274754942
H,0,0.3275343208,1.1488133292,1.4560587074
H,0,-0.6708910002,1.2964235859,-1.3928403163
H,0,-2.4120017042,2.7948571016,-0.4116309895
H,0,-0.7910682776,3.3710673466,-0.0034666993
H,0,-2.4120055704,-2.7948539667,-0.4116308595
H,0,-0.7910729015,-3.3710663889,-0.0034666287
H,0,-0.6708929169,-1.2964228686,-1.3928403856
H,0,-2.2651153756,0.0000014743,0.8679075818
H,0,-2.6820983515,0.0000018028,-0.8490375977
H,0,-1.7546345756,2.5126306855,1.2070384733
H,0,-1.7546379598,-2.512628348,1.2070385465

TCD-H2 9J-8 (σ = 3)

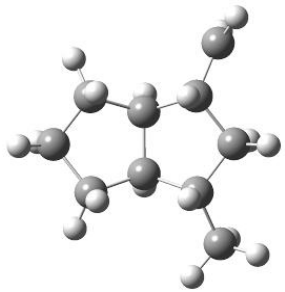

C,0,0.2102354184,-0.81117477,0.4134820947
C,0,1.453256316,-1.4765940618,-0.2210916371
C,0,2.5954385122,-0.477333012,0.0407888097
C,0,1.9269448353,0.8932583861,-0.1734642801
C,0,0.5145259726,0.729098416,0.4324791782
C,0,-1.1445572786,-0.9753050178,-0.319481557
C,0,-1.9804913903,-2.1690302822,0.1448716902
C,0,-0.9642231734,2.802182897,0.1279987895
C,0,-0.6631747589,1.4158002766,-0.3181166834
C,0,-1.823783094,0.3939973353,-0.131718508
H,0,0.0966577837,-1.1704598823,1.4446231819
H,0,1.6591451959,-2.4754880168,0.1772785496
H,0,1.3062314638,-1.5865575179,-1.3039856821
H,0,2.9399361222,-0.5677118561,1.0794251465
H,0,3.4665261893,-0.6383655509,-0.6035657556
H,0,2.4907107671,1.7206277613,0.2689260487
H,0,1.8501629719,1.0974757812,-1.2496976939
H,0,0.5186372747,1.0887825027,1.4688478112
H,0,-0.4245084473,1.4321795642,-1.3915782202
H,0,-1.2583245798,3.5776609715,-0.5709097574
H,0,-2.9278011939,-2.2325128575,-0.4018386439
H,0,-1.4466431833,-3.1137619057,-0.006856055
H,0,-0.9377072464,-1.0965155903,-1.3936982714
H,0,-2.226669626,0.4783735259,0.8873469884
H,0,-2.6538347696,0.5672827843,-0.8254383748
H,0,-1.0299984753,3.0309147146,1.1884721055
H,0,-2.2167716062,-2.088884595,1.2127507258

TCD-H2 9-8J (σ = 3)

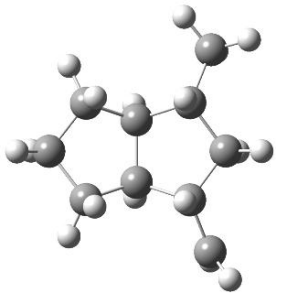

C,0,0.3385739712,-0.7648779693,0.4343997274
C,0,1.6862433236,-1.2251151714,-0.1664431711
C,0,2.6319177087,-0.0308851922,0.0589986731
C,0,1.7320584244,1.1913915781,-0.2017249797
C,0,0.3717863575,0.8048900655,0.4234497138
C,0,-0.9548395788,-1.1792369222,-0.3254174582
C,0,-1.5486434373,-2.4710095572,0.1109613881
C,0,-1.4752714809,2.602336399,0.153687684
C,0,-0.9122369134,1.259446631,-0.3143172615
C,0,-1.8703289952,0.0667628153,-0.1378031007
H,0,0.2597458183,-1.1222612928,1.4685722917
H,0,2.0570196097,-2.1563488598,0.2733409391
H,0,1.5733803997,-1.4027242866,-1.2442166143
H,0,2.9820592614,-0.0216955284,1.0996373852
H,0,3.5208065232,-0.0572054875,-0.5806121159
H,0,2.1451752336,2.1208762685,0.2035785483
H,0,1.6179948807,1.3357448427,-1.2845543884
H,0,0.3322327686,1.1750034836,1.4562562831
H,0,-0.6782997769,1.3388590967,-1.3868785946
H,0,-2.383906562,2.8702587625,-0.3966922513
H,0,-0.7504201811,3.4113345301,0.01000117
H,0,-1.9983091997,-3.1618705369,-0.5939120381
H,0,-0.7193309811,-1.2410383846,-1.3979217986
H,0,-2.2875382099,0.0656503305,0.878989368
H,0,-2.7144004994,0.0790180984,-0.8361253826
H,0,-1.7291123788,2.5693771063,1.2200346875
H,0,-1.6678061062,-2.685613789,1.1697312659

Table E.7 TCD-H2 9-8 Optimized Species (Continued)

TCD-H2 9J-8J (σ = 1)

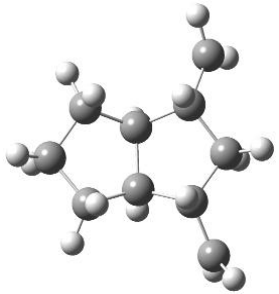

C,0,0.2940520169,-0.8025432618,0.4258299255
C,0,1.6134003422,-1.3151988196,-0.195285093
C,0,2.6135785521,-0.1660261235,0.0311842291
C,0,1.7672979242,1.098185574,-0.2084695404
C,0,0.4000116317,0.7641086661,0.4274440998
C,0,-1.0250179146,-1.154429659,-0.3185534241
C,0,-1.6666852528,-2.4237277668,0.1189383194
C,0,-1.3629058047,2.6178574222,0.1402254841
C,0,-0.8816847643,1.2842123436,-0.3117425513
C,0,-1.8837591712,0.1266140841,-0.1145281779
H,0,0.2137510015,-1.1617485434,1.4591469668
H,0,1.9474065441,-2.2660106892,0.2318127973
H,0,1.4809186183,-1.4772739012,-1.2733137795
H,0,2.9739943533,-0.1827731465,1.0681577959
H,0,3.4940285954,-0.225750436,-0.6178081046
H,0,2.2224987458,2.004849114,0.2026461918
H,0,1.6499002503,1.2590106232,-1.2887337572
H,0,0.3772405307,1.1318872185,1.4596336229
H,0,-0.6373169203,1.3384424201,-1.3829643912
H,0,-1.9230000742,2.7121059275,1.0667242021
H,0,-1.0228522864,3.5325359729,-0.3339819545
H,0,-1.7838996793,-2.6386728933,1.1777978984
H,0,-2.1393891296,-3.0992795269,-0.5855048749
H,0,-0.8055588206,-1.2205122013,-1.394123192
H,0,-2.2819327884,0.1464627733,0.9093165974
H,0,-2.7374624902,0.1777691391,-0.7978723496

TCD-H2 9JJ-8 (σ = 3)

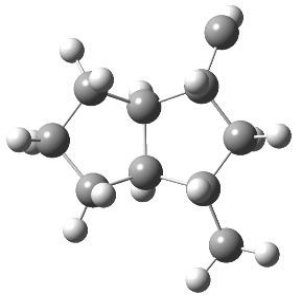

C,0,0.1096078129,-0.7718190196,0.4241943384
C,0,1.2708334887,-1.5857087277,-0.1859785363
C,0,2.5156317476,-0.7117938751,0.0410702275
C,0,2.0002176573,0.7168587845,-0.1959922771
C,0,0.5912493032,0.7186890893,0.4268503862
C,0,-1.2459323045,-0.7948534196,-0.3199535889
C,0,-2.2059343745,-1.8873100728,0.1443619629
C,0,-0.6658179381,2.916145801,0.0932521711
C,0,-0.5175192352,1.5249444286,-0.3258425031
C,0,-1.7803390639,0.6350533861,-0.1527202109
H,0,-0.0552717277,-1.0964865933,1.4542340553
H,0,1.3672674141,-2.5812867128,0.2473690048
H,0,1.1093084958,-1.7173126253,-1.2594568992
H,0,2.8622546633,-0.8169665481,1.0725060409
H,0,3.3500265913,-0.9792601585,-0.6082529675
H,0,2.652100639,1.4823227197,0.2237869037
H,0,1.9333651189,0.9070220604,-1.2705462719
H,0,0.6470189309,1.0853798962,1.4524979704
H,0,-0.2633937444,1.5159562191,-1.3929844695
H,0,-0.8821617822,3.3894944196,1.0414385107
H,0,-3.1457662394,-1.8546181373,-0.4093853146
H,0,-1.7754890261,-2.8805602361,0.0050687437
H,0,-1.0429391702,-0.9466417582,-1.3857837577
H,0,-2.1893386795,0.7698216909,0.8529009393
H,0,-2.5664151714,0.8907698681,-0.8635152881
H,0,-2.440226406,-1.7727434791,1.2050848299

Table E.8 Moments of Inertia[a]

Species	I_a	I_b	I_c
TCD	672.31522	1530.45148	1762.53870
TCD-H2 1-2	556.57898	2545.23805	2953.37296
TCD-H2 1J-2	546.07458	2483.81594	2895.01121
TCD-H2 1-2J	544.58460	2512.73229	2904.71840
TCD-H2 1J-2J	532.28774	2455.91706	2853.19185
TCD-H2 1JJ-2	541.42139	2425.36028	2830.75335
TCD-H2 1-2JJ	526.00565	2517.25687	2889.91061
TCD-H2 2-3	567.77291	2589.84255	2680.28277
TCD-H2 2J-3	548.24699	2577.90161	2660.87866
TCD-H2 2-3J	562.61503	2510.80094	2606.34807
TCD-H2 2J-3J	542.75323	2496.76131	2586.64945
TCD-H2 2JJ-3	529.44792	2579.94974	2651.82955
TCD-H2 2-3JJ	559.85735	2428.45932	2522.09129
TCD-H2 3-4	964.81891	1531.85441	2059.86372
TCD-H2 3J-4	929.77157	1530.31636	2022.69907
TCD-H2 3-4J	957.37328	1473.14772	1998.48922
TCD-H2 3J-4J	923.04754	1468.74637	1961.10940
TCD-H2 3JJ-4	893.19987	1525.14711	1990.67016
TCD-H2 3-4JJ	947.20105	1427.67551	1946.54626
TCD-H2 2-6	926.38204	1447.21432	1939.62173
TCD-H2 2J-6	888.59422	1447.71538	1895.18160
TCD-H2 2-6J	888.45315	1447.86242	1895.21512
TCD-H2 2J-6J	904.01126	1413.19012	1864.33101
TCD-H2 2JJ-6	869.17561	1448.16265	1882.73041
TCD-H2 1-10	883.31274	1554.93476	2023.27298
TCD-H2 1J-10	853.84757	1548.31935	1971.68852
TCD-H2 1-10J	845.20486	1551.26968	1973.08358
TCD-H2 1J-10J	863.32835	1441.73802	1790.75400
TCD-H2 1JJ-10	831.77466	1528.26055	1876.34175
TCD-H2 1-10JJ	826.92986	1522.80270	1897.59870
TCD-H2 1-9	682.15272	2065.00546	2396.14332
TCD-H2 1J-9	652.22907	2106.15017	2378.27371
TCD-H2 1-9J	673.25397	2001.46655	2324.71955
TCD-H2 1J-9J	644.68890	2040.20555	2308.77493
TCD-H2 1JJ-9	621.53226	2120.59593	2355.90256
TCD-H2 1-9JJ	671.69610	1935.03104	2261.71108
TCD-H2 9-8	1206.01155	1322.73512	2341.05024
TCD-H2 9J-8	1172.60286	1310.20148	2294.58348
TCD-H2 9-8J	1172.60269	1310.20164	2294.58329
TCD-H2 9J-8J	1144.71017	1290.82239	2250.56067
TCD-H2 9JJ-8	1126.40463	1304.45754	2247.18680

[a] AMU Bohr^2.

Table E.9 Vibrational Frequencies

Species	Frequencies (cm^{-1})									
TCD	140.07	178.67	270.76	318.67	319.57	398.09	495.09	533.36	551.22	670.38
	740.94	754.14	794.24	831.05	867.96	868.52	893.40	898.14	917.44	919.92
	929.18	962.04	966.39	995.06	1003.67	1045.77	1053.99	1055.31	1056.57	1078.61
	1141.88	1158.27	1173.98	1199.19	1211.43	1216.60	1237.76	1257.45	1267.57	1295.12
	1305.36	1311.09	1319.35	1325.08	1336.41	1339.50	1353.76	1359.70	1375.45	1381.22
	1502.14	1504.82	1506.41	1513.31	1524.72	1536.28	3034.63	3036.37	3040.06	3044.40
	3049.68	3057.64	3058.00	3060.82	3085.07	3087.50	3089.46	3090.57	3094.30	3097.43
	3106.03	3107.57								
TCD-H2 1-2	17.08	25.00	92.41	94.11	130.19	182.83	313.91	365.37	385.01	515.55
	622.70	632.08	637.22	766.41	786.70	823.76	823.90	878.29	886.74	896.04
	901.97	945.57	957.76	968.32	978.77	986.29	992.58	1048.62	1058.00	1072.46
	1122.05	1129.31	1137.01	1207.78	1208.60	1223.77	1236.18	1248.77	1256.05	1267.05
	1290.41	1300.64	1304.90	1329.45	1335.09	1339.78	1340.82	1343.07	1352.05	1356.92
	1376.71	1412.04	1498.39	1499.13	1509.08	1509.59	1509.74	1510.84	1533.62	1534.28
	2978.90	2989.44	3024.88	3024.91	3030.70	3033.17	3049.92	3050.15	3061.81	3062.79
	3081.28	3083.10	3091.02	3093.86	3094.99	3097.53	3110.31	3110.39		
TCD-H2 1J-2	23.18	83.55	102.23	129.25	179.54	187.87	315.35	340.44	360.19	389.29
	523.51	611.35	640.78	684.52	775.75	822.43	833.79	867.36	888.28	899.32
	910.33	922.40	941.63	962.59	963.82	991.52	1006.99	1047.84	1051.55	1062.61
	1098.47	1118.52	1133.76	1136.28	1211.16	1221.26	1227.09	1239.71	1271.55	1277.34
	1290.99	1299.83	1313.16	1330.95	1334.28	1343.79	1350.33	1352.37	1364.37	1376.50
	1409.82	1482.04	1485.78	1498.59	1506.70	1510.06	1510.75	1533.44	2932.73	2951.42
	2985.15	3000.53	3023.64	3024.70	3033.52	3036.21	3039.36	3046.41	3062.16	3083.08
	3092.15	3095.64	3099.01	3110.17	3208.20					
TCD-H2 1-2J	32.37	80.50	83.84	137.26	162.75	225.21	310.97	341.44	376.33	403.83
	552.28	593.64	628.55	684.42	776.07	825.71	842.40	875.26	881.63	894.18
	906.81	917.02	944.71	964.78	972.93	986.31	1014.23	1036.87	1051.33	1075.38
	1091.68	1109.45	1138.77	1176.29	1211.13	1216.41	1231.88	1234.49	1264.35	1278.68
	1294.12	1299.47	1305.84	1329.47	1335.42	1341.21	1345.91	1347.71	1357.98	1379.46
	1395.41	1483.78	1498.98	1503.39	1508.56	1510.44	1518.23	1534.13	2898.97	2951.52
	3001.17	3024.34	3028.28	3032.60	3034.27	3049.25	3049.68	3062.88	3083.02	3092.54
	3095.60	3096.53	3102.49	3110.62	3209.73					
TCD-H2 1J-2J	75.46	77.22	132.17	147.20	178.93	223.33	311.16	338.15	343.28	373.53
	406.52	559.31	597.93	660.45	693.26	824.21	841.94	864.97	876.83	904.47
	911.63	916.24	924.05	942.18	964.08	990.74	1016.50	1036.73	1051.57	1067.48
	1083.50	1101.11	1112.55	1140.77	1170.80	1214.47	1233.09	1234.13	1261.52	1284.00
	1296.09	1302.34	1310.90	1332.40	1335.39	1346.81	1349.40	1365.04	1378.68	1394.01
	1481.73	1483.12	1484.16	1503.01	1510.99	1517.78	2898.94	2934.20	2951.72	2952.10
	3012.20	3024.60	3028.04	3032.29	3034.71	3039.58	3049.52	3095.05	3098.99	3102.32
	3207.80	3208.35								

Table E.9 Vibrational Frequencies (Continued A)

Species	Frequencies (cm^{-1})									
TCD-H2 1JJ-2	22.55	86.51	98.46	135.48	176.56	206.07	314.85	357.16	389.28	519.37
	614.75	639.88	675.08	775.36	820.68	827.52	850.55	884.28	895.61	904.02
	923.69	935.64	956.97	970.07	986.41	1006.87	1044.99	1052.68	1096.56	1108.65
	1122.76	1132.33	1199.24	1210.81	1212.36	1226.86	1233.41	1259.83	1271.09	1284.13
	1303.52	1304.43	1323.14	1331.09	1341.88	1347.18	1353.26	1367.43	1406.22	1484.07
	1489.33	1498.60	1507.05	1508.92	1509.63	1533.94	2955.39	2972.32	2988.19	3010.77
	3025.65	3034.49	3036.21	3046.32	3048.63	3050.16	3063.98	3084.59	3094.52	3097.19
	3100.46	3111.91								
TCD-H2 1-2JJ	18.88	81.59	84.71	129.12	171.97	223.54	313.98	375.47	396.49	549.00
	589.71	623.85	680.46	773.85	823.30	830.86	861.86	881.81	892.54	895.60
	905.31	935.50	962.02	977.07	989.13	1004.09	1032.05	1048.38	1087.85	1109.49
	1121.10	1171.36	1193.70	1205.61	1211.60	1221.14	1230.01	1266.96	1271.19	1289.68
	1299.42	1305.16	1328.14	1332.52	1341.93	1346.58	1350.10	1357.64	1393.55	1485.54
	1497.74	1497.99	1508.16	1509.54	1512.01	1533.48	2921.16	2972.36	3005.09	3026.30
	3034.54	3040.74	3041.50	3049.59	3056.00	3062.85	3083.05	3094.35	3096.32	3098.27
	3106.77	3110.94								
TCD-H2 2-3	73.58	97.79	109.41	161.31	247.40	268.21	298.79	331.29	401.93	464.88
	496.56	585.44	741.52	760.51	770.98	810.06	839.73	844.44	876.05	892.14
	912.38	931.60	939.19	956.11	962.67	965.64	1015.73	1028.87	1046.22	1056.72
	1074.70	1122.07	1132.56	1145.00	1170.74	1194.13	1200.55	1243.87	1249.69	1271.60
	1284.55	1298.65	1304.01	1313.03	1327.82	1336.09	1347.84	1352.32	1360.23	1387.17
	1407.89	1426.21	1496.33	1502.22	1507.71	1508.68	1513.15	1513.98	1524.36	1534.61
	3009.59	3021.70	3026.29	3036.41	3041.56	3043.98	3048.52	3055.43	3059.21	3066.21
	3084.47	3088.55	3090.92	3097.57	3103.48	3105.20	3106.52	3109.63		
TCD-H2 2J-3	72.95	78.82	117.99	170.92	242.11	257.42	296.13	324.76	328.25	456.72
	486.26	529.04	650.27	744.39	763.56	774.90	815.51	846.40	850.50	881.70
	907.47	917.30	923.76	950.58	956.29	962.17	1012.48	1025.89	1040.28	1051.76
	1068.34	1107.16	1120.05	1139.92	1153.52	1182.85	1210.64	1243.93	1247.49	1265.24
	1286.43	1291.53	1305.05	1315.20	1330.10	1333.89	1353.59	1357.99	1370.27	1400.71
	1426.16	1496.76	1501.60	1507.36	1509.84	1512.99	1524.12	1528.48	2968.22	3013.63
	3024.24	3036.39	3043.69	3050.88	3057.65	3060.37	3070.26	3089.67	3094.51	3101.73
	3105.04	3108.97	3109.16	3113.59	3200.66					
TCD-H2 2-3J	73.11	92.79	107.57	126.99	164.09	264.39	301.96	330.65	400.30	458.37
	467.32	505.47	585.14	741.27	757.34	771.45	810.09	842.39	845.44	882.28
	901.99	919.26	933.35	956.53	963.24	966.23	995.81	1014.11	1042.61	1052.41
	1087.52	1098.57	1121.35	1142.00	1154.26	1170.97	1197.40	1209.23	1248.54	1252.90
	1283.61	1297.31	1298.90	1309.67	1317.25	1327.11	1346.04	1351.50	1359.20	1384.15
	1403.76	1475.75	1482.10	1499.86	1503.94	1509.39	1513.86	1533.95	2925.21	3018.59
	3022.22	3034.95	3042.76	3048.64	3055.10	3059.18	3064.80	3084.60	3088.51	3091.15
	3098.20	3103.79	3106.66	3152.48	3255.15					

Table E.9 Vibrational Frequencies (Continued B)

Species	Frequencies (cm^{-1})									
TCD-H2 2J-3J	75.99	85.89	120.99	141.82	171.49	254.71	299.51	326.16	329.90	453.76
	462.02	495.05	531.05	649.39	747.97	762.52	776.15	814.96	846.01	854.06
	883.31	911.43	923.60	951.35	956.67	962.68	1000.11	1011.23	1031.90	1043.11
	1079.16	1088.24	1105.67	1139.06	1145.63	1166.98	1186.00	1211.65	1242.86	1254.86
	1286.32	1290.19	1301.28	1306.63	1315.01	1332.49	1352.62	1355.74	1370.81	1394.88
	1476.16	1483.33	1500.73	1502.51	1510.36	1528.45	2922.12	2967.73	3020.69	3039.82
	3044.07	3057.77	3060.55	3076.36	3089.73	3094.71	3102.24	3109.13	3114.35	3152.32
	3200.25	3254.96								
TCD-H2 2JJ-3	76.30	87.63	115.00	174.57	243.87	263.88	293.73	325.43	439.10	482.04
	521.67	632.54	741.79	756.71	762.39	810.06	840.63	858.16	882.18	899.50
	909.23	918.90	933.60	948.78	965.47	1012.61	1039.25	1050.17	1061.40	1107.51
	1116.59	1127.02	1139.23	1161.67	1177.26	1209.81	1231.74	1246.41	1261.23	1284.75
	1296.91	1302.29	1321.27	1329.29	1335.57	1342.67	1368.43	1399.82	1426.59	1496.33
	1500.37	1506.44	1509.42	1513.50	1523.29	1526.63	2978.30	3015.49	3026.45	3036.28
	3044.40	3051.59	3053.82	3059.83	3072.15	3088.28	3096.39	3104.80	3109.85	3115.77
	3116.82	3120.45								
TCD-H2 2-3JJ	77.73	105.36	110.38	156.76	203.08	266.28	311.37	352.82	402.40	467.06
	505.33	585.78	724.29	750.63	771.11	806.88	825.95	844.73	877.65	884.66
	922.10	933.18	956.64	960.70	965.94	982.98	1006.03	1034.12	1051.70	1070.42
	1099.26	1116.84	1142.98	1157.02	1167.63	1193.46	1211.94	1246.07	1250.55	1276.25
	1290.88	1298.65	1304.82	1316.73	1324.98	1342.37	1349.01	1356.00	1369.84	1391.43
	1464.60	1499.45	1503.23	1509.45	1513.87	1534.32	2942.10	3023.90	3027.43	3035.21
	3041.88	3049.35	3056.36	3060.00	3077.82	3085.43	3089.34	3092.35	3099.34	3104.84
	3107.39	3213.37								
TCD-H2 3-4	71.05	104.96	190.68	217.18	229.48	268.07	284.87	300.43	388.44	421.71
	440.99	493.83	658.83	726.67	733.89	779.60	800.03	829.37	851.00	891.37
	904.17	933.36	942.01	960.41	967.53	988.24	1019.26	1036.73	1052.31	1062.18
	1074.70	1102.35	1110.57	1148.15	1165.54	1186.86	1201.37	1237.53	1256.74	1257.47
	1291.69	1298.10	1317.52	1321.26	1334.31	1340.71	1353.63	1369.64	1385.00	1403.98
	1425.36	1428.49	1496.96	1503.37	1509.80	1512.94	1516.16	1519.04	1522.70	1532.13
	3015.88	3033.37	3038.27	3040.31	3043.23	3047.67	3056.18	3058.82	3070.51	3083.43
	3087.82	3100.38	3102.74	3105.37	3107.11	3108.09	3114.46	3117.75		
TCD-H2 3J-4	73.69	99.60	138.18	183.58	215.88	260.72	279.71	286.15	385.51	420.74
	424.86	495.48	516.67	675.52	727.31	738.27	770.43	796.97	827.97	845.57
	890.94	909.00	930.92	939.63	962.93	965.88	994.60	1015.10	1049.02	1053.93
	1070.29	1075.07	1109.13	1146.14	1159.06	1183.08	1197.51	1213.75	1251.31	1254.26
	1287.98	1295.06	1304.26	1314.24	1331.39	1334.69	1338.22	1364.98	1376.43	1402.42
	1427.25	1482.15	1496.87	1502.75	1511.75	1514.05	1521.27	1530.76	3018.61	3033.83
	3037.72	3040.20	3048.82	3056.56	3059.99	3068.62	3084.92	3096.54	3100.41	3103.83
	3106.70	3107.16	3113.19	3151.16	3251.42					

Table E.9 Vibrational Frequencies (Continued C)

Species	Frequencies (cm^{-1})									
TCD-H2 3-4J	72.31	106.67	137.61	186.69	231.75	261.33	269.63	299.47	390.61	416.29
	441.83	475.36	493.15	658.92	732.77	738.17	787.86	806.71	828.25	864.05
	898.06	905.612	934.77	943.98	966.89	988.47	998.36	1028.20	1035.80	1061.48
	1064.82	1093.08	1101.94	1146.02	1158.97	1171.88	1189.05	1210.59	1249.44	1255.39
	1263.30	1294.81	1313.14	1316.77	1328.97	1338.57	1349.68	1359.94	1384.49	1401.26
	1427.39	1471.81	1477.66	1502.82	1509.99	1514.95	1518.71	1532.36	2947.82	3018.75
	3037.12	3042.01	3046.08	3047.87	3056.81	3059.32	3083.26	3087.9	3099.01	3102.64
	3105.45	3108.01	3114.70	3151.19	3254.23					
TCD-H2 3J-4J	72.87	114.29	132.19	150.39	180.35	258.64	262.12	281.37	391.24	415.88
	423.53	468.92	493.33	509.54	678.40	738.02	738.30	776.25	809.17	827.15
	862.95	900.78	910.69	932.85	940.37	966.41	989.15	996.78	1027.26	1054.70
	1059.38	1073.70	1091.81	1141.67	1153.01	1162.04	1185.05	1206.94	1219.82	1251.87
	1262.08	1295.42	1302.41	1310.84	1321.59	1332.85	1337.27	1354.77	1374.68	1400.67
	1469.86	1476.73	1480.98	1502.17	1511.44	1530.65	2950.93	3015.88	3027.91	3041.69
	3048.97	3056.97	3060.13	3084.69	3095.16	3099.04	3103.79	3106.66	3150.61	3150.97
	3250.86	3253.09								
TCD-H2 3JJ-4	73.61	107.16	171.32	186.41	219.76	268.63	289.03	300.77	398.15	421.51
	449.39	504.71	669.20	722.22	746.28	775.74	800.02	830.61	861.51	871.39
	895.66	920.81	938.50	951.65	965.13	967.54	1005.52	1036.85	1056.83	1059.52
	1098.15	1107.70	1144.71	1153.36	1178.88	1181.87	1211.64	1237.16	1248.85	1285.65
	1288.13	1294.78	1307.88	1318.72	1333.86	1337.47	1347.79	1366.62	1401.01	1426.27
	1496.36	1502.51	1509.44	1513.13	1520.22	1528.91	2942.92	3030.20	3037.39	3039.84
	3049.06	3057.87	3061.09	3069.46	3084.89	3100.63	3103.39	3105.95	3107.94	3111.98
	3113.18	3211.00								
TCD-H2 3-4JJ	74.71	115.25	169.56	223.45	244.03	262.99	270.19	298.37	397.50	439.87
	443.72	497.54	658.56	731.29	732.59	773.55	789.16	826.29	840.81	890.61
	905.96	931.53	939.98	964.14	984.45	993.72	1007.21	1034.10	1061.31	1063.25
	1096.97	1104.56	1134.60	1145.01	1176.47	1189.46	1215.52	1245.52	1253.91	1264.43
	1292.08	1299.26	1312.93	1327.76	1334.83	1347.92	1353.67	1380.94	1384.80	1427.35
	1460.53	1501.90	1509.25	1516.85	1518.32	1532.69	2963.95	3026.89	3036.92	3043.07
	3048.78	3051.39	3058.29	3061.15	3084.03	3088.66	3100.54	3104.52	3106.78	3108.79
	3115.96	3212.21								
TCD-H2 2-6	36.51	180.73	235.32	250.79	253.92	332.19	345.47	389.43	459.21	461.83
	501.55	682.87	701.74	735.60	755.28	778.89	809.44	851.31	871.39	889.84
	902.78	927.84	933.65	990.29	991.16	1028.49	1032.84	1083.13	1089.71	1101.11
	1104.90	1110.48	1167.79	1191.48	1220.56	1224.31	1244.24	1267.89	1282.29	1285.20
	1294.74	1317.13	1321.47	1337.73	1353.62	1368.70	1382.23	1388.89	1394.56	1396.20
	1397.21	1404.83	1495.13	1499.47	1502.57	1503.99	1506.27	1521.31	1526.43	1533.78
	3009.63	3026.19	3027.52	3030.84	3035.10	3037.06	3037.13	3047.50	3051.20	3053.55
	3064.38	3064.40	3068.69	3070.55	3079.44	3083.05	3104.66	3123.94		

Table E.9 Vibrational Frequencies (Continued D)

Species	Frequencies (cm^{-1})									
TCD-H2 2J-6	85.62	163.68	218.24	241.48	260.58	336.08	339.59	362.78	424.68	462.01
	483.70	518.48	683.15	718.45	746.68	771.81	801.91	822.07	861.34	884.51
	895.60	923.04	935.40	973.84	992.01	999.66	1036.10	1059.63	1087.34	1090.65
	1098.52	1135.12	1163.78	1187.70	1194.59	1216.74	1231.52	1247.89	1273.46	1285.17
	1297.34	1311.52	1327.15	1343.91	1350.12	1355.69	1370.01	1384.67	1389.93	1402.92
	1410.81	1490.22	1498.07	1500.89	1503.56	1509.90	1518.17	1531.89	2945.21	3010.39
	3019.19	3025.59	3031.42	3035.42	3045.29	3049.93	3052.32	3058.94	3063.37	3069.88
	3070.37	3085.39	3106.36	3119.89	3151.72					
TCD-H2 2-6J	85.72	163.71	218.24	241.47	260.45	336.00	339.53	362.71	424.55	462.02
	483.69	518.50	683.30	718.46	746.70	771.79	801.84	822.11	861.30	884.48
	895.59	923.01	935.38	973.85	992.00	999.61	1036.10	1059.63	1087.33	1090.63
	1098.49	1135.12	1163.75	1187.68	1194.61	1216.78	1231.47	1247.86	1273.44	1285.13
	1297.29	1311.55	1327.15	1343.86	1350.12	1355.69	1370.00	1384.65	1389.91	1402.81
	1410.78	1490.22	1498.06	1500.89	1503.56	1509.88	1518.17	1531.89	2945.11	3010.41
	3019.25	3025.67	3031.59	3035.52	3045.32	3050.00	3052.40	3059.03	3063.44	3069.93
	3070.55	3085.40	3106.41	3119.91	3151.86					
TCD-H2 2J-6J	67.01	127.89	210.67	225.60	265.22	324.16	336.64	347.41	409.56	436.28
	468.45	509.53	530.93	647.28	746.81	753.12	785.21	819.54	822.21	883.19
	891.83	907.77	933.93	956.17	985.27	996.85	1009.88	1054.07	1079.67	1090.45
	1129.32	1146.16	1152.11	1183.36	1190.54	1209.73	1224.66	1242.42	1268.51	1291.97
	1303.68	1326.54	1332.44	1343.37	1347.47	1353.88	1359.75	1380.04	1412.95	1418.47
	1490.03	1494.81	1498.15	1504.26	1515.54	1528.99	2940.08	2964.02	3004.68	3006.19
	3023.89	3043.75	3046.45	3052.08	3053.39	3061.11	3073.88	3087.35	3106.62	3117.45
	3149.12	3151.86								
TCD-H2 2JJ-6	101.39	153.80	205.08	230.35	290.96	321.25	343.82	388.28	450.91	478.29
	496.17	664.26	709.99	737.09	755.99	810.44	822.92	844.57	877.77	894.26
	913.10	928.40	953.89	990.43	1000.58	1031.79	1053.95	1078.26	1089.54	1096.06
	1153.56	1163.76	1181.43	1210.87	1221.37	1241.64	1253.11	1279.45	1285.13	1298.11
	1312.40	1333.41	1337.72	1349.85	1358.22	1368.86	1383.49	1391.45	1404.83	1462.18
	1493.68	1499.74	1501.60	1507.23	1515.78	1528.62	2944.76	2962.98	3014.99	3026.11
	3029.71	3033.92	3035.74	3042.58	3053.14	3060.88	3069.76	3071.92	3073.68	3088.92
	3113.90	3115.54								
TCD-H2 1-10	62.68	156.92	171.87	217.47	235.22	277.15	330.14	338.54	388.64	447.36
	519.26	545.51	609.27	667.73	743.72	769.97	818.25	857.51	875.56	886.55
	915.11	928.84	966.85	985.71	997.66	1021.46	1035.32	1042.97	1059.69	1091.66
	1110.43	1126.11	1138.34	1184.50	1204.82	1223.48	1252.77	1257.97	1287.20	1310.56
	1317.86	1335.47	1337.17	1342.67	1349.45	1355.63	1376.69	1379.90	1387.90	1395.89
	1402.35	1428.82	1496.88	1502.00	1504.80	1505.29	1514.29	1519.80	1522.86	1527.41
	3000.35	3017.05	3025.06	3028.99	3033.58	3036.52	3038.07	3041.64	3043.43	3047.20
	3058.94	3068.33	3085.97	3087.66	3089.80	3098.72	3107.06	3122.22		

Table E.9 Vibrational Frequencies (Continued E)

Species	Frequencies (cm^{-1})									
TCD-H2 1J-10	29.89	118.63	198.82	217.59	251.58	293.05	320.24	351.69	389.84	442.29
	497.15	503.19	569.13	602.64	685.98	721.66	820.49	855.45	871.39	876.18
	907.78	926.28	939.52	965.86	998.20	1020.66	1025.54	1041.65	1061.38	1084.90
	1098.91	1111.32	1156.01	1177.12	1197.86	1210.15	1242.38	1250.03	1284.50	1299.82
	1317.26	1330.71	1334.49	1345.84	1351.82	1358.67	1371.20	1377.61	1399.18	1412.57
	1428.02	1482.58	1503.28	1505.47	1507.42	1516.36	1520.67	1525.84	2901.05	2958.24
	2993.57	3010.71	3025.86	3034.07	3036.40	3038.53	3042.14	3055.77	3072.51	3089.39
	3092.58	3101.80	3107.59	3120.73	3159.70					
TCD-H2 1-10J	49.00	93.00	159.60	189.15	227.99	285.00	319.28	333.86	396.16	446.60
	479.37	529.32	548.64	610.89	707.26	748.12	775.55	822.27	868.44	879.97
	883.83	915.88	928.02	972.11	985.95	1009.63	1020.33	1040.18	1045.51	1067.54
	1098.91	1120.64	1129.37	1176.00	1199.90	1212.58	1245.76	1255.64	1273.86	1282.20
	1306.30	1315.01	1331.35	1338.11	1350.21	1353.80	1361.66	1375.99	1377.89	1391.89
	1400.69	1478.08	1495.03	1502.13	1504.42	1507.01	1522.87	1523.45	2923.56	3007.94
	3025.73	3028.68	3032.64	3035.02	3037.50	3046.10	3050.10	3061.88	3072.40	3088.30
	3089.46	3091.24	3100.62	3156.82	3255.93					
TCD-H2 1J-10J	50.11	117.84	139.59	187.28	229.60	271.18	301.34	367.29	382.54	423.88
	481.98	519.01	542.63	611.02	678.06	720.17	738.21	782.46	835.62	866.26
	881.91	898.05	930.48	959.17	966.11	984.45	998.53	1036.99	1059.06	1071.74
	1091.83	1104.10	1141.25	1163.61	1199.82	1206.18	1226.80	1251.66	1272.42	1292.89
	1307.61	1312.79	1327.45	1339.42	1343.57	1354.88	1368.34	1383.77	1390.45	1410.37
	1477.35	1480.46	1499.89	1506.35	1509.77	1530.17	2904.39	2935.23	2981.09	3031.85
	3040.54	3047.31	3049.80	3055.04	3065.04	3075.28	3083.08	3098.15	3110.02	3155.43
	3164.77	3254.10								
TCD-H2 1JJ-10	41.50	98.41	202.75	225.36	255.49	298.18	322.74	363.11	408.21	470.13
	516.51	578.67	621.68	697.25	703.57	815.57	829.57	857.96	870.20	896.54
	912.68	945.56	947.75	980.06	1000.34	1023.20	1039.34	1059.67	1075.05	1079.50
	1114.65	1166.00	1186.30	1197.74	1233.18	1236.35	1267.73	1286.25	1300.34	1313.83
	1318.77	1327.51	1340.52	1347.00	1353.84	1362.54	1370.86	1395.07	1430.92	1484.41
	1498.75	1504.22	1505.26	1518.05	1524.70	1530.95	2940.52	2961.43	3005.61	3008.81
	3035.69	3041.73	3044.12	3047.90	3057.00	3066.96	3076.94	3090.77	3103.80	3107.85
	3113.70	3126.17								
TCD-H2 1-10JJ	37.42	136.58	152.41	174.57	246.51	273.11	319.38	345.97	422.03	456.54
	496.54	552.11	619.45	692.73	721.42	817.53	833.20	859.33	864.97	883.59
	904.63	917.85	925.74	986.65	993.87	1027.23	1039.50	1055.37	1056.57	1096.43
	1107.18	1123.05	1181.28	1194.65	1204.28	1230.89	1249.42	1256.25	1271.38	1304.38
	1313.69	1327.17	1341.63	1346.99	1352.26	1359.82	1373.51	1377.31	1385.86	1396.52
	1498.19	1498.86	1502.33	1505.99	1521.05	1522.46	2921.34	3003.99	3027.71	3029.83
	3033.15	3036.48	3039.49	3043.35	3044.36	3068.58	3072.96	3088.41	3089.71	3091.04
	3098.96	3209.79								

Table E.9 Vibrational Frequencies (Continued F)

Species	Frequencies (cm^{-1})									
TCD-H2 1-9	63.95	90.04	150.34	186.83	247.23	262.13	306.24	328.23	372.95	453.09
	547.58	577.86	641.91	690.60	765.25	779.77	828.39	850.36	890.18	900.86
	914.27	924.12	929.35	963.84	993.66	1017.42	1028.58	1041.70	1056.52	1060.28
	1073.85	1100.28	1154.99	1168.90	1199.04	1208.97	1222.62	1235.28	1270.50	1294.58
	1295.05	1313.44	1319.13	1335.92	1342.53	1349.06	1350.97	1355.26	1375.64	1378.89
	1405.71	1427.73	1497.86	1499.99	1503.93	1506.18	1513.40	1517.19	1522.67	1526.55
	3020.28	3025.55	3027.55	3029.19	3036.65	3038.63	3042.56	3044.57	3046.32	3059.47
	3063.82	3086.60	3088.32	3089.41	3095.26	3099.25	3106.28	3113.48		
TCD-H2 1J-9	61.10	86.93	126.98	158.77	231.51	257.49	297.36	319.43	339.15	433.92
	448.95	548.69	605.59	689.40	709.82	781.97	803.28	830.00	861.88	897.56
	907.65	920.49	933.45	947.94	969.83	1018.15	1028.35	1038.54	1056.70	1061.76
	1072.74	1101.38	1120.80	1155.83	1193.16	1203.93	1230.92	1244.31	1271.34	1292.46
	1297.68	1305.98	1317.35	1322.72	1344.05	1347.19	1355.36	1367.14	1390.77	1402.43
	1427.97	1483.98	1501.09	1504.87	1506.88	1515.15	1520.22	1524.43	2942.17	2993.98
	3020.40	3027.04	3031.75	3037.42	3038.15	3043.51	3047.47	3048.88	3059.08	3087.74
	3091.03	3102.17	3106.65	3111.62	3194.22					
TCD-H2 1-9J	68.93	97.80	126.38	155.29	209.47	253.62	300.35	329.03	372.98	443.46
	486.77	547.03	579.05	640.98	691.72	775.92	800.46	838.33	848.32	893.31
	901.07	915.74	926.19	938.55	988.08	996.86	1028.28	1033.52	1042.40	1059.62
	1075.52	1090.15	1138.28	1153.07	1185.46	1200.20	1220.22	1222.93	1243.63	1273.14
	1291.95	1312.51	1318.09	1328.25	1341.34	1342.13	1349.58	1354.74	1370.98	1375.35
	1403.23	1472.55	1481.25	1499.08	1503.88	1506.32	1514.21	1525.98	2929.74	3023.26
	3028.45	3029.52	3036.93	3038.73	3041.73	3045.32	3047.60	3063.19	3086.27	3088.57
	3089.63	3094.75	3099.00	3151.37	3253.72					
TCD-H2 1J-9J	58.82	90.66	112.19	142.98	166.96	250.23	291.90	316.51	340.00	429.66
	444.28	487.05	547.46	605.54	689.29	710.60	796.52	821.42	830.18	863.74
	903.24	907.48	922.27	938.51	963.89	989.87	1021.83	1029.50	1039.75	1061.91
	1077.87	1088.33	1115.56	1139.74	1180.76	1199.62	1205.38	1233.66	1262.10	1273.61
	1296.10	1297.82	1309.93	1321.74	1334.76	1344.67	1355.26	1366.14	1383.63	1400.98
	1472.74	1482.46	1486.75	1504.26	1506.54	1523.57	2931.85	2940.22	2994.30	3027.00
	3032.16	3037.49	3045.09	3045.75	3048.57	3049.15	3088.18	3091.38	3102.42	3151.51
	3196.12	3254.43								
TCD-H2 1JJ-9	66.41	91.43	127.42	158.27	228.52	256.04	294.94	327.41	402.16	438.41
	547.02	600.94	679.11	695.79	775.64	800.03	829.66	859.09	879.89	900.91
	916.81	934.68	945.50	953.08	1011.07	1026.60	1052.93	1054.36	1060.24	1085.55
	1117.47	1142.14	1177.70	1197.04	1209.28	1225.14	1231.65	1261.05	1288.85	1296.85
	1304.87	1319.12	1326.37	1337.92	1348.10	1353.88	1377.14	1397.20	1428.21	1486.15
	1500.12	1504.44	1506.47	1514.84	1519.64	1524.39	2964.52	3005.14	3020.89	3026.66
	3032.78	3038.41	3039.69	3047.49	3051.65	3058.73	3059.37	3088.67	3092.53	3108.06
	3108.08	3113.01								

Table E.9 Vibrational Frequencies (Continued G)

Species	Frequencies (cm^{-1})									
TCD-H2 1-9JJ	70.86	100.85	154.22	183.92	231.60	263.30	299.20	343.71	373.45	471.67
	548.11	581.22	639.18	690.82	760.46	787.36	809.42	847.83	885.79	900.89
	910.60	925.55	938.69	977.59	991.37	1012.66	1030.49	1035.55	1057.43	1076.28
	1098.14	1129.65	1144.60	1188.44	1200.40	1214.06	1222.24	1245.36	1273.00	1275.41
	1311.74	1317.32	1324.94	1332.32	1342.14	1349.77	1354.40	1361.30	1374.88	1384.16
	1460.08	1498.99	1504.24	1506.48	1514.25	1526.10	2947.10	3024.12	3028.74	3030.38
	3037.57	3038.82	3041.92	3047.24	3053.92	3063.66	3087.90	3089.45	3090.68	3096.20
	3100.09	3212.40								
TCD-H2 9-8	42.21	130.12	196.77	225.47	229.78	243.30	255.99	326.29	341.39	444.80
	472.17	511.26	526.63	545.72	664.65	757.98	853.83	862.85	884.62	907.28
	916.66	924.75	935.20	978.53	979.39	1004.13	1025.24	1040.63	1070.59	1076.84
	1106.36	1125.07	1156.67	1165.87	1190.90	1198.07	1239.78	1243.55	1282.16	1282.48
	1308.89	1315.15	1326.80	1343.97	1347.83	1352.70	1362.62	1370.82	1393.57	1399.87
	1425.49	1427.84	1503.78	1504.96	1505.10	1510.92	1511.60	1514.20	1514.60	1521.43
	2999.56	3000.72	3014.89	3020.54	3029.25	3029.59	3031.26	3031.40	3035.79	3043.16
	3073.24	3086.11	3088.69	3095.63	3098.59	3099.61	3103.30	3103.63		
TCD-H2 9J-8	46.97	108.05	136.61	200.83	223.19	233.02	251.43	329.42	343.14	429.99
	451.33	511.44	526.02	533.82	549.11	663.66	757.63	855.01	862.61	894.07
	902.83	916.78	930.00	939.83	979.41	982.46	1017.75	1025.83	1056.49	1073.64
	1095.92	1120.96	1121.81	1150.21	1173.30	1198.41	1235.38	1242.57	1271.69	1279.35
	1307.63	1314.18	1323.64	1334.81	1344.87	1347.46	1352.92	1364.64	1388.68	1395.93
	1424.66	1480.78	1503.30	1505.11	1506.41	1510.91	1513.57	1523.57	2997.99	3008.16
	3023.45	3028.37	3030.75	3032.41	3033.66	3037.39	3047.47	3087.82	3088.42	3091.65
	3098.83	3100.65	3104.20	3148.25	3252.97					
TCD-H2 9-8J	46.98	108.05	136.61	200.83	223.19	233.02	251.43	329.42	343.14	429.99
	451.33	511.44	526.02	533.81	549.11	663.66	757.63	855.01	862.61	894.07
	902.83	916.78	930.00	939.83	979.41	982.47	1017.75	1025.83	1056.49	1073.64
	1095.92	1120.96	1121.81	1150.21	1173.30	1198.41	1235.38	1242.57	1271.69	1279.35
	1307.63	1314.18	1323.64	1334.81	1344.87	1347.46	1352.92	1364.64	1388.68	1395.93
	1424.66	1480.78	1503.30	1505.11	1506.41	1510.91	1513.57	1523.57	2997.99	3008.17
	3023.44	3028.36	3030.76	3032.41	3033.67	3037.39	3047.47	3087.83	3088.42	3091.65
	3098.83	3100.65	3104.21	3148.25	3252.98					
TCD-H2 9J-8J	46.17	87.73	123.75	142.29	203.08	227.24	240.10	323.45	338.48	424.77
	451.51	491.51	519.59	525.90	537.75	549.47	668.90	760.48	854.92	861.47
	887.86	903.62	919.03	938.67	940.97	977.94	1006.98	1024.25	1042.64	1055.40
	1077.52	1115.27	1117.91	1136.87	1147.76	1195.51	1228.59	1239.60	1262.17	1266.66
	1302.16	1310.78	1320.83	1329.40	1337.95	1346.11	1351.33	1360.30	1384.39	1391.09
	1478.07	1481.71	1503.53	1504.48	1505.29	1521.33	3006.67	3011.48	3028.52	3032.03
	3033.01	3037.13	3038.88	3057.36	3088.44	3094.18	3097.41	3100.27	3147.21	3149.09
	3250.90	3254.20								

Table E.9 Vibrational Frequencies (Continued H)

Species	Frequencies (cm^{-1})									
TCD-H2 9JJ-8	43.59	131.02	170.92	201.87	224.33	247.27	298.02	328.89	350.65	442.98
	489.57	511.17	524.97	548.83	661.93	756.33	854.00	857.33	873.53	902.89
	917.45	924.47	939.07	963.09	980.33	1008.56	1024.31	1049.92	1064.16	1101.93
	1115.52	1119.22	1149.42	1164.27	1195.65	1224.43	1240.83	1260.27	1270.23	1302.89
	1311.45	1315.57	1328.06	1342.22	1348.08	1352.87	1359.33	1369.75	1394.06	1424.58
	1503.60	1503.75	1505.03	1510.40	1513.69	1522.65	2988.08	3001.34	3026.32	3030.64
	3031.79	3033.41	3036.18	3038.73	3056.51	3088.87	3093.30	3095.43	3101.24	3101.78
	3105.25	3205.50								

Table E.10 Isodesmic Reactions and Calculated $\Delta H^{\circ}_{f\,298}$ for TCD-H2 *m-n* Parent Species

Isodesmic Reactions							$\Delta H^{\circ}_{f\,298}$ (kcal mol^{-1})			
							B3LYP		CBS-QB3	G3MP2B3
							6-31G(d,p)	6-311G(2d,2p)		
TCD-H2 1-2 System										
TCD-H2 1-2	+	YC_4H_8	→	YYC_7H_{12}	+	YC_7H_{14}	-33.77	-34.39	-30.07	-30.07
TCD-H2 1-2	+	YC_5H_{10}	→	YYC_7H_{12}	+	YC_8H_{16}	-32.91	-33.68	-29.26	-29.23
TCD-H2 1-2	+	YC_6H_{12}	→	YYC_8H_{14}	+	YC_8H_{16}	-33.90	-34.46	-30.94	-30.95
TCD-H2 1-2	+	3 CH_3CH_3	→	2 YC_4H_8	+	2 $CH_3CH_2CH_2CH_3$			-31.62	-31.47
						Average	**-33.5**	**-34.2**	**-30.5**	**-30.4**
TCD-H2 1-2	+	YYC_7H_{12}	→	YC_7H_{14}	+	TCD	-33.90	-34.59	-32.05	-31.97
TCD-H2 1-2	+	YYC_8H_{14}	→	YC_8H_{16}	+	TCD	-33.36	-33.76	-30.16	-30.10
TCD-H2 1-2	+	YC_5H_{10}	→	$CH_3CH_2CH_2CH_2CH_3$	+	TCD	-34.15	-34.75	-30.48	-30.52
TCD-H2 1-2	+	YC_4H_8	→	$CH_3CH_2CH_2CH_3$	+	TCD			-30.74	-30.82
						Average	**-33.8**	**-34.4**	**-30.9**	**-30.9**
TCD-H2 2-3 System										
TCD-H2 2-3	+	YC_4H_8	→	YYC_7H_{12}	+	YC_7H_{14}	-31.49	-31.78	-30.47	-30.44
TCD-H2 2-3	+	YC_5H_{10}	→	YYC_7H_{12}	+	YC_8H_{16}	-30.63	-31.07	-29.67	-29.59
TCD-H2 2-3	+	YC_6H_{12}	→	YYC_8H_{14}	+	YC_8H_{16}	-31.63	-31.85	-31.35	-31.31
TCD-H2 2-3	+	3 CH_3CH_3	→	2 YC_4H_8	+	2 $CH_3CH_2CH_2CH_3$			-32.02	-31.83
						Average	**-31.2**	**-31.6**	**-30.9**	**-30.8**
TCD-H2 2-3	+	YYC_7H_{12}	→	YC_7H_{14}	+	TCD	-31.63	-31.98	-32.45	-32.33
TCD-H2 2-3	+	YYC_8H_{14}	→	YC_8H_{16}	+	TCD	-31.08	-31.14	-30.57	-30.46
TCD-H2 2-3	+	YC_5H_{10}	→	$CH_3CH_2CH_2CH_2CH_3$	+	TCD	-31.87	-32.13	-30.88	-30.88
TCD-H2 2-3	+	YC_4H_8	→	$CH_3CH_2CH_2CH_3$	+	TCD			-31.15	-31.18
						Average	**-31.5**	**-31.7**	**-31.3**	**-31.2**

Table E.10 Isodesmic Reactions and Calculated $\Delta H^{\circ}_{f\,298}$ for TCD-H2 *m-n* Parent Species (Continued A)

Isodesmic Reactions							$\Delta H^{\circ}_{f\,298}$ (kcal mol^{-1})			
							B3LYP		CBS-QB3	G3MP2B3
							6-31G(d,p)	6-311G(2d,2p)		
TCD-H2 3-4 System										
TCD-H2 3-4	+	YC_4H_8	→	YYC_7H_{12}	+	YC_7H_{14}	-29.22	-29.35	-30.02	-30.03
TCD-H2 3-4	+	YC_5H_{10}	→	YYC_7H_{12}	+	YC_8H_{16}	-28.36	-28.64	-29.22	-29.19
TCD-H2 3-4	+	YC_6H_{12}	→	YYC_8H_{14}	+	YC_8H_{16}	-29.36	-29.42	-30.89	-30.91
TCD-H2 3-4	+	3 CH_3CH_3	→	2 YC_4H_8	+	2 $CH_3CH_2CH_2CH_3$			-31.57	-31.43
						Average	**-29.0**	**-29.1**	**-30.4**	**-30.4**
TCD-H2 3-4	+	YYC_7H_{12}	→	YC_7H_{14}	+	TCD	-29.35	-29.55	-32.00	-31.93
TCD-H2 3-4	+	YYC_8H_{14}	→	YC_8H_{16}	+	TCD	-28.81	-28.71	-30.11	-30.06
TCD-H2 3-4	+	YC_5H_{10}	→	$CH_3CH_2CH_2CH_2CH_3$	+	TCD	-29.60	-29.71	-30.43	-30.48
TCD-H2 3-4	+	YC_4H_8	→	$CH_3CH_2CH_2CH_3$	+	TCD			-30.69	-30.78
						Average	**-29.3**	**-29.3**	**-30.8**	**-30.8**
TCD-H2 2-6 System										
TCD-H2 2-6	+	YC_4H_8	→	YYC_7H_{12}	+	YC_7H_{14}	-25.27	-25.40	-23.50	-23.85
TCD-H2 2-6	+	YC_5H_{10}	→	YYC_7H_{12}	+	YC_8H_{16}	-24.41	-24.69	-22.69	-23.01
TCD-H2 2-6	+	YC_6H_{12}	→	YYC_8H_{14}	+	YC_8H_{16}	-25.41	-25.47	-24.37	-24.72
TCD-H2 2-6	+	3 CH_3CH_3	→	2 YC_4H_8	+	2 $CH_3CH_2CH_2CH_3$			-25.05	-25.24
						Average	**-25.0**	**-25.2**	**-23.9**	**-24.2**
TCD-H2 2-6	+	YYC_7H_{12}	→	YC_7H_{14}	+	TCD	-25.41	-25.60	-25.48	-25.75
TCD-H2 2-6	+	YYC_8H_{14}	→	YC_8H_{16}	+	TCD	-24.86	-24.76	-23.59	-23.88
TCD-H2 2-6	+	YC_5H_{10}	→	$CH_3CH_2CH_2CH_2CH_3$	+	TCD	-25.65	-25.75	-23.91	-24.30
TCD-H2 2-6	+	YC_4H_8	→	$CH_3CH_2CH_2CH_3$	+	TCD			-24.17	-24.60
						Average	**-25.3**	**-25.4**	**-24.3**	**-24.6**

Table E.10 Isodesmic Reactions and Calculated $\Delta H^{\circ}_{f\,298}$ for TCD-H2 *m-n* Parent Species (Continued B)

Isodesmic Reactions							$\Delta H^{\circ}_{f\,298}$ (kcal mol^{-1})			
							B3LYP		CBS-QB3	G3MP2B3
							6-31G(d,p)	6-311G(2d,2p)		
TCD-H2 1-10 System										
TCD-H2 1-10	+	YC_4H_8	→	YYC_7H_{12}	+	YC_7H_{14}	-32.35	-32.47	-31.01	-31.14
TCD-H2 1-10	+	YC_5H_{10}	→	YYC_7H_{12}	+	YC_8H_{16}	-31.49	-31.76	-30.20	-30.30
TCD-H2 1-10	+	YC_6H_{12}	→	YYC_8H_{14}	+	YC_8H_{16}	-32.49	-32.54	-31.88	-32.02
TCD-H2 1-10	+	3 CH_3CH_3	→	2 YC_4H_8	+	2 $CH_3CH_2CH_2CH_3$			-32.56	-32.54
						Average	**-32.1**	**-32.3**	**-31.4**	**-31.5**
TCD-H2 1-10	+	YYC_7H_{12}	→	YC_7H_{14}	+	TCD	-32.48	-32.67	-32.99	-33.04
TCD-H2 1-10	+	YYC_8H_{14}	→	YC_8H_{16}	+	TCD	-31.94	-31.84	-31.10	-31.17
TCD-H2 1-10	+	YC_5H_{10}	→	$CH_3CH_2CH_2CH_2CH_3$	+	TCD	-32.73	-32.83	-31.42	-31.59
TCD-H2 1-10	+	YC_4H_8	→	$CH_3CH_2CH_2CH_3$	+	TCD			-31.68	-31.89
						Average	**-32.4**	**-32.4**	**-31.8**	**-31.9**
TCD-H2 1-9 System										
TCD-H2 1-9	+	YC_4H_8	→	YYC_7H_{12}	+	YC_7H_{14}	-35.79	-36.16	-33.74	-33.82
TCD-H2 1-9	+	YC_5H_{10}	→	YYC_7H_{12}	+	YC_8H_{16}	-34.93	-35.45	-32.94	-32.98
TCD-H2 1-9	+	YC_6H_{12}	→	YYC_8H_{14}	+	YC_8H_{16}	-35.93	-36.23	-34.62	-34.69
TCD-H2 1-9	+	3 CH_3CH_3	→	2 YC_4H_8	+	2 $CH_3CH_2CH_2CH_3$			-35.29	-35.21
						Average	**-35.6**	**-35.9**	**-34.1**	**-34.2**
TCD-H2 1-9	+	YYC_7H_{12}	→	YC_7H_{14}	+	TCD	-35.93	-36.36	-35.73	-35.72
TCD-H2 1-9	+	YYC_8H_{14}	→	YC_8H_{16}	+	TCD	-35.39	-35.52	-33.84	-33.85
TCD-H2 1-9	+	YC_5H_{10}	→	$CH_3CH_2CH_2CH_2CH_3$	+	TCD	-36.18	-36.51	-34.15	-34.26
TCD-H2 1-9	+	YC_4H_8	→	$CH_3CH_2CH_2CH_3$	+	TCD			-34.42	-34.56
						Average	**-35.8**	**-36.1**	**-34.5**	**-34.6**

Table E.10 Isodesmic Reactions and Calculated $\Delta H^{\circ}_{f\,298}$ for TCD-H2 *m-n* Parent Species (Continued C)

Isodesmic Reactions							$\Delta H^{\circ}_{f\,298}$ (kcal mol^{-1})			
							B3LYP		CBS-QB3	G3MP2B3
							6-31G(d,p)	6-311G(2d,2p)		
TCD-H2 9-8 System										
TCD-H2 9-8	+	YC_4H_8	→	YYC_7H_{12}	+	YC_7H_{14}	-38.22	-38.59	-35.95	-35.94
TCD-H2 9-8	+	YC_5H_{10}	→	YYC_7H_{12}	+	YC_8H_{16}	-37.37	-37.88	-35.15	-35.10
TCD-H2 9-8	+	YC_6H_{12}	→	YYC_8H_{14}	+	YC_8H_{16}	-38.36	-38.66	-36.83	-36.82
TCD-H2 9-8	+	3 CH_3CH_3	→	2 YC_4H_8	+	2 $CH_3CH_2CH_2CH_3$			-37.50	-37.33
						Average	**-38.0**	**-38.4**	**-36.4**	**-36.3**
TCD-H2 9-8	+	YYC_7H_{12}	→	YC_7H_{14}	+	TCD	-38.36	-38.79	-37.93	-37.84
TCD-H2 9-8	+	YYC_8H_{14}	→	YC_8H_{16}	+	TCD	-37.82	-37.96	-36.04	-35.97
TCD-H2 9-8	+	YC_5H_{10}	→	$CH_3CH_2CH_2CH_2CH_3$	+	TCD	-38.61	-38.95	-36.36	-36.39
TCD-H2 9-8	+	YC_4H_8	→	$CH_3CH_2CH_2CH_3$	+	TCD			-36.63	-36.69
						Average	**-38.3**	**-38.6**	**-36.7**	**-36.7**

Table E.11 Isodesmic Reactions, Calculated $\Delta H^{\circ}_{f\,298}$, and C–H Bond Dissociation Energies for TCD-H2 *m-n* Radical Species

Isodesmic Reactions							$\Delta H^{\circ}_{f\,298}$ (kcal mol^{-1})			
							B3LYP		CBS-QB3	G3MP2B3
							6-31G(d,p)	6-311G(2d,2p)		
TCD-H2 1J-2 System										
TCD-H2 1J-2	+	CH_3CH_3	→	TCD-H2 1-2	+	CH_3CJH_2	12.17	12.48	13.25	13.75
TCD-H2 1J-2	+	$CH_3CH_2CH_3$	→	TCD-H2 1-2	+	CH_3CJHCH_3	13.57	13.78	13.51	13.57
TCD-H2 1J-2	+	$(CH_3)_3CH$	→	TCD-H2 1-2	+	$(CH_3)_3CJ$	14.55	14.61	13.13	12.84
TCD-H2 1J-2	+	$CH_3CH_2CH_2CH_3$	→	TCD-H2 1-2	+	$CH_3CJHCH_2CH_3$	12.94	13.25	12.88	12.92
TCD-H2 1J-2	+	YYC_7H_{12}	→	TCD-H2 1-2	+	$YYCJ_7H_{11}$	13.82	13.90	14.12	14.03
						Average	**13.4**	**13.6**	**13.4**	**13.4**
						Bond Energy	**96.0**	**96.2**	**95.9**	**96.0**
TCD-H2 1-2J System										
TCD-H2 1-2J	+	CH_3CH_3	→	TCD-H2 1-2	+	CH_3CJH_2	12.56	12.82	13.70	14.26
TCD-H2 1-2J	+	$CH_3CH_2CH_3$	→	TCD-H2 1-2	+	CH_3CJHCH_3	13.95	14.12	13.96	14.08
TCD-H2 1-2J	+	$(CH_3)_3CH$	→	TCD-H2 1-2	+	$(CH_3)_3CJ$	14.94	14.95	13.58	13.35
TCD-H2 1-2J	+	$CH_3CH_2CH_2CH_3$	→	TCD-H2 1-2	+	$CH_3CJHCH_2CH_3$	13.32	13.60	13.34	13.43
TCD-H2 1-2J	+	YYC_7H_{12}	→	TCD-H2 1-2	+	$YYCJ_7H_{11}$	14.21	14.24	14.57	14.54
						Average	**13.8**	**13.9**	**13.8**	**13.9**
						Bond Energy	**96.3**	**96.5**	**96.4**	**96.5**
TCD-H2 2J-3 System										
TCD-H2 2J-3	+	CH_3CH_3	→	TCD-H2 2-3	+	CH_3CJH_2	14.62	14.83	15.67	16.31
TCD-H2 2J-3	+	$CH_3CH_2CH_3$	→	TCD-H2 2-3	+	CH_3CJHCH_3	16.02	16.13	15.93	16.13
TCD-H2 2J-3	+	$(CH_3)_3CH$	→	TCD-H2 2-3	+	$(CH_3)_3CJ$	17.00	16.95	15.55	15.39
TCD-H2 2J-3	+	$CH_3CH_2CH_2CH_3$	→	TCD-H2 2-3	+	$CH_3CJHCH_2CH_3$	15.39	15.60	15.30	15.48
TCD-H2 2J-3	+	YYC_7H_{12}	→	TCD-H2 2-3	+	$YYCJ_7H_{11}$	16.27	16.24	16.54	16.58
						Average	**15.9**	**16.0**	**15.8**	**16.0**
						Bond Energy	**98.8**	**98.9**	**98.7**	**98.9**

Table E.11 Isodesmic Reactions, Calculated $\Delta H^{\circ}_{f\,298}$, and C–H Bond Dissociation Energies for TCD-H2 *m-n* Radical Species (Continued A)

Isodesmic Reactions							$\Delta H^{\circ}_{f\,298}$ (kcal mol^{-1})			
							B3LYP		CBS-QB3	G3MP2B3
							6-31G(d,p)	6-311G(2d,2p)		
TCD-H2 2-3J System										
TCD-H2 2-3J	+	CH_3CH_3	→	TCD-H2 2-3	+	CH_3CJH_2	18.31	18.23	18.38	18.44
TCD-H2 2-3J	+	$CH_3CH_2CH_3$	→	TCD-H2 2-3	+	CH_3CJHCH_3	19.71	19.53	18.64	18.26
TCD-H2 2-3J	+	$(CH_3)_3CH$	→	TCD-H2 2-3	+	$(CH_3)_3CJ$	20.69	20.36	18.27	17.53
TCD-H2 2-3J	+	$CH_3CH_2CH_2CH_3$	→	TCD-H2 2-3	+	$CH_3CJHCH_2CH_3$	19.08	19.00	18.02	17.61
TCD-H2 2-3J	+	YYC_7H_{12}	→	TCD-H2 2-3	+	$YYCJ_7H_{11}$	19.96	19.65	19.25	18.72
						Average	**19.6**	**19.4**	**18.5**	**18.1**
						Bond Energy	**102.5**	**102.3**	**101.4**	**101.0**
TCD-H2 3J-4 System										
TCD-H2 3J-4	+	CH_3CH_3	→	TCD-H2 3-4	+	CH_3CJH_2	17.61	17.57	18.16	18.39
TCD-H2 3J-4	+	$CH_3CH_2CH_3$	→	TCD-H2 3-4	+	CH_3CJHCH_3	19.01	18.87	18.41	18.21
TCD-H2 3J-4	+	$(CH_3)_3CH$	→	TCD-H2 3-4	+	$(CH_3)_3CJ$	19.99	19.70	18.04	17.48
TCD-H2 3J-4	+	$CH_3CH_2CH_2CH_3$	→	TCD-H2 3-4	+	$CH_3CJHCH_2CH_3$	18.38	18.34	17.79	17.56
TCD-H2 3J-4	+	YYC_7H_{12}	→	TCD-H2 3-4	+	$YYCJ_7H_{11}$	19.26	18.98	19.03	18.66
						Average	**18.8**	**18.7**	**18.3**	**18.1**
						Bond Energy	**101.4**	**101.2**	**100.8**	**100.6**
TCD-H2 3-4J System										
TCD-H2 3-4J	+	CH_3CH_3	→	TCD-H2 3-4	+	CH_3CJH_2	18.08	18.04	18.32	18.42
TCD-H2 3-4J	+	$CH_3CH_2CH_3$	→	TCD-H2 3-4	+	CH_3CJHCH_3	19.48	19.34	18.58	18.25
TCD-H2 3-4J	+	$(CH_3)_3CH$	→	TCD-H2 3-4	+	$(CH_3)_3CJ$	20.46	20.16	18.20	17.51
TCD-H2 3-4J	+	$CH_3CH_2CH_2CH_3$	→	TCD-H2 3-4	+	$CH_3CJHCH_2CH_3$	18.85	18.81	17.95	17.60
TCD-H2 3-4J	+	YYC_7H_{12}	→	TCD-H2 3-4	+	$YYCJ_7H_{11}$	19.73	19.45	19.19	18.70
						Average	**19.3**	**19.2**	**18.4**	**18.1**
						Bond Energy	**101.8**	**101.7**	**101.0**	**100.6**

Table E.11 Isodesmic Reactions, Calculated $\Delta H^{\circ}_{f\,298}$, and C–H Bond Dissociation Energies for TCD-H2 *m-n* Radical Species (Continued B)

Isodesmic Reactions							$\Delta H^{\circ}_{f\,298}$ (kcal mol^{-1}) B3LYP 6-31G(d,p)	B3LYP 6-311G(2d,2p)	CBS-QB3	G3MP2B3
TCD-H2 2J-6 System										
TCD-H2 2J-6	+	CH_3CH_3	→	TCD-H2 2-6	+	CH_3CJH_2	15.85	16.12	16.80	17.52
TCD-H2 2J-6	+	$CH_3CH_2CH_3$	→	TCD-H2 2-6	+	CH_3CJHCH_3	17.25	17.42	17.06	17.34
TCD-H2 2J-6	+	$(CH_3)_3CH$	→	TCD-H2 2-6	+	$(CH_3)_3CJ$	18.23	18.25	16.69	16.60
TCD-H2 2J-6	+	$CH_3CH_2CH_2CH_3$	→	TCD-H2 2-6	+	$CH_3CJHCH_2CH_3$	16.62	16.89	16.44	16.69
TCD-H2 2J-6	+	YYC_7H_{12}	→	TCD-H2 2-6	+	$YYCJ_7H_{11}$	17.50	17.54	17.67	17.79
						Average	**17.1**	**17.2**	**16.9**	**17.2**
						Bond Energy	**93.2**	**93.4**	**93.1**	**93.3**
TCD-H2 2-6J System										
TCD-H2 2-6J	+	CH_3CH_3	→	TCD-H2 2-6	+	CH_3CJH_2	15.85	16.12	16.81	17.52
TCD-H2 2-6J	+	$CH_3CH_2CH_3$	→	TCD-H2 2-6	+	CH_3CJHCH_3	17.25	17.42	17.07	17.34
TCD-H2 2-6J	+	$(CH_3)_3CH$	→	TCD-H2 2-6	+	$(CH_3)_3CJ$	18.23	18.25	16.69	16.61
TCD-H2 2-6J	+	$CH_3CH_2CH_2CH_3$	→	TCD-H2 2-6	+	$CH_3CJHCH_2CH_3$	16.62	16.89	16.44	16.69
TCD-H2 2-6J	+	YYC_7H_{12}	→	TCD-H2 2-6	+	$YYCJ_7H_{11}$	17.50	17.54	17.68	17.79
						Average	**17.1**	**17.2**	**16.9**	**17.2**
						Bond Energy	**93.2**	**93.4**	**93.1**	**93.3**
TCD-H2 1J-10 System										
TCD-H2 1J-10	+	CH_3CH_3	→	TCD-H2 1-10	+	CH_3CJH_2	10.31	10.46	11.79	12.42
TCD-H2 1J-10	+	$CH_3CH_2CH_3$	→	TCD-H2 1-10	+	CH_3CJHCH_3	11.70	11.76	12.05	12.24
TCD-H2 1J-10	+	$(CH_3)_3CH$	→	TCD-H2 1-10	+	$(CH_3)_3CJ$	12.69	12.59	11.67	11.50
TCD-H2 1J-10	+	$CH_3CH_2CH_2CH_3$	→	TCD-H2 1-10	+	$CH_3CJHCH_2CH_3$	11.07	11.23	11.42	11.59
TCD-H2 1J-10	+	YYC_7H_{12}	→	TCD-H2 1-10	+	$YYCJ_7H_{11}$	11.95	11.88	12.66	12.69
						Average	**11.5**	**11.6**	**11.9**	**12.1**
						Bond Energy	**95.1**	**95.1**	**95.5**	**95.6**

Table E.11 Isodesmic Reactions, Calculated $\Delta H^{\circ}_{f\,298}$, and C–H Bond Dissociation Energies for TCD-H2 *m-n* Radical Species (Continued C)

Isodesmic Reactions							$\Delta H^{\circ}_{f\,298}$ (kcal mol^{-1})			
							B3LYP		CBS-QB3	G3MP2B3
							6-31G(d,p)	6-311G(2d,2p)		
TCD-H2 1-10J System										
TCD-H2 1-10J	+	CH_3CH_3	→	TCD-H2 1-10	+	CH_3CJH_2	15.99	15.99	16.51	16.73
TCD-H2 1-10J	+	$CH_3CH_2CH_3$	→	TCD-H2 1-10	+	CH_3CJHCH_3	17.39	17.29	16.77	16.55
TCD-H2 1-10J	+	$(CH_3)_3CH$	→	TCD-H2 1-10	+	$(CH_3)_3CJ$	18.37	18.12	16.39	15.82
TCD-H2 1-10J	+	$CH_3CH_2CH_2CH_3$	→	TCD-H2 1-10	+	$CH_3CJHCH_2CH_3$	16.76	16.76	16.14	15.90
TCD-H2 1-10J	+	YYC_7H_{12}	→	TCD-H2 1-10	+	$YYCJ_7H_{11}$	17.64	17.41	17.38	17.01
						Average	**17.2**	**17.1**	**16.6**	**16.4**
						Bond Energy	**100.8**	**100.7**	**100.2**	**100.0**
TCD-H2 1J-9 System										
TCD-H2 1J-9	+	CH_3CH_3	→	TCD-H2 1-9	+	CH_3CJH_2	9.69	9.74	11.29	11.90
TCD-H2 1J-9	+	$CH_3CH_2CH_3$	→	TCD-H2 1-9	+	CH_3CJHCH_3	11.09	11.04	11.55	11.73
TCD-H2 1J-9	+	$(CH_3)_3CH$	→	TCD-H2 1-9	+	$(CH_3)_3CJ$	12.07	11.87	11.18	10.99
TCD-H2 1J-9	+	$CH_3CH_2CH_2CH_3$	→	TCD-H2 1-9	+	$CH_3CJHCH_2CH_3$	10.46	10.51	10.93	11.08
TCD-H2 1J-9	+	YYC_7H_{12}	→	TCD-H2 1-9	+	$YYCJ_7H_{11}$	11.34	11.16	12.16	12.18
						Average	**10.9**	**10.9**	**11.4**	**11.6**
						Bond Energy	**97.2**	**97.1**	**97.7**	**97.8**
TCD-H2 1-9J System										
TCD-H2 1-9J	+	CH_3CH_3	→	TCD-H2 1-9	+	CH_3CJH_2	14.30	14.27	14.54	14.62
TCD-H2 1-9J	+	$CH_3CH_2CH_3$	→	TCD-H2 1-9	+	CH_3CJHCH_3	15.70	15.57	14.80	14.45
TCD-H2 1-9J	+	$(CH_3)_3CH$	→	TCD-H2 1-9	+	$(CH_3)_3CJ$	16.68	16.40	14.42	13.71
TCD-H2 1-9J	+	$CH_3CH_2CH_2CH_3$	→	TCD-H2 1-9	+	$CH_3CJHCH_2CH_3$	15.07	15.04	14.17	13.80
TCD-H2 1-9J	+	YYC_7H_{12}	→	TCD-H2 1-9	+	$YYCJ_7H_{11}$	15.95	15.69	15.41	14.90
						Average	**15.5**	**15.4**	**14.7**	**14.3**
						Bond Energy	**101.8**	**101.7**	**100.9**	**100.6**

Table E.11 Isodesmic Reactions, Calculated $\Delta H^{\circ}_{f\,298}$, and C–H Bond Dissociation Energies for TCD-H2 *m-n* Radical Species (Continued D)

Isodesmic Reactions							$\Delta H^{\circ}_{f\,298}$ (kcal mol^{-1})			
							B3LYP		CBS-QB3	G3MP2B3
							6-31G(d,p)	6-311G(2d,2p)		
TCD-H2 9J-8 System										
TCD-H2 9J-8	+	CH_3CH_3	→	TCD-H2 9-8	+	CH_3CJH_2	12.66	12.58	12.75	12.99
TCD-H2 9J-8	+	$CH_3CH_2CH_3$	→	TCD-H2 9-8	+	CH_3CJHCH_3	14.05	13.88	13.00	12.81
TCD-H2 9J-8	+	$(CH_3)_3CH$	→	TCD-H2 9-8	+	$(CH_3)_3CJ$	15.04	14.71	12.63	12.08
TCD-H2 9J-8	+	$CH_3CH_2CH_2CH_3$	→	TCD-H2 9-8	+	$CH_3CJHCH_2CH_3$	13.42	13.35	12.38	12.17
TCD-H2 9J-8	+	YYC_7H_{12}	→	TCD-H2 9-8	+	$YYCJ_7H_{11}$	14.30	13.99	13.62	13.27
						Average	**13.9**	**13.7**	**12.9**	**12.7**
						Bond Energy	**102.3**	**102.1**	**101.3**	**101.1**
TCD-H2 9-8J System										
TCD-H2 9-8J	+	CH_3CH_3	→	TCD-H2 9-8	+	CH_3CJH_2	12.66	12.58	12.75	12.99
TCD-H2 9-8J	+	$CH_3CH_2CH_3$	→	TCD-H2 9-8	+	CH_3CJHCH_3	14.05	13.88	13.00	12.81
TCD-H2 9-8J	+	$(CH_3)_3CH$	→	TCD-H2 9-8	+	$(CH_3)_3CJ$	15.04	14.71	12.63	12.08
TCD-H2 9-8J	+	$CH_3CH_2CH_2CH_3$	→	TCD-H2 9-8	+	$CH_3CJHCH_2CH_3$	13.42	13.35	12.38	12.17
TCD-H2 9-8J	+	YYC_7H_{12}	→	TCD-H2 9-8	+	$YYCJ_7H_{11}$	14.30	13.99	13.62	13.27
						Average	**13.9**	**13.7**	**12.9**	**12.7**
						Bond Energy	**102.3**	**102.1**	**101.3**	**101.1**

Internal Rotor (IR) notation and 0° dihedral angle corresponds to the structures from the Optimized Species.

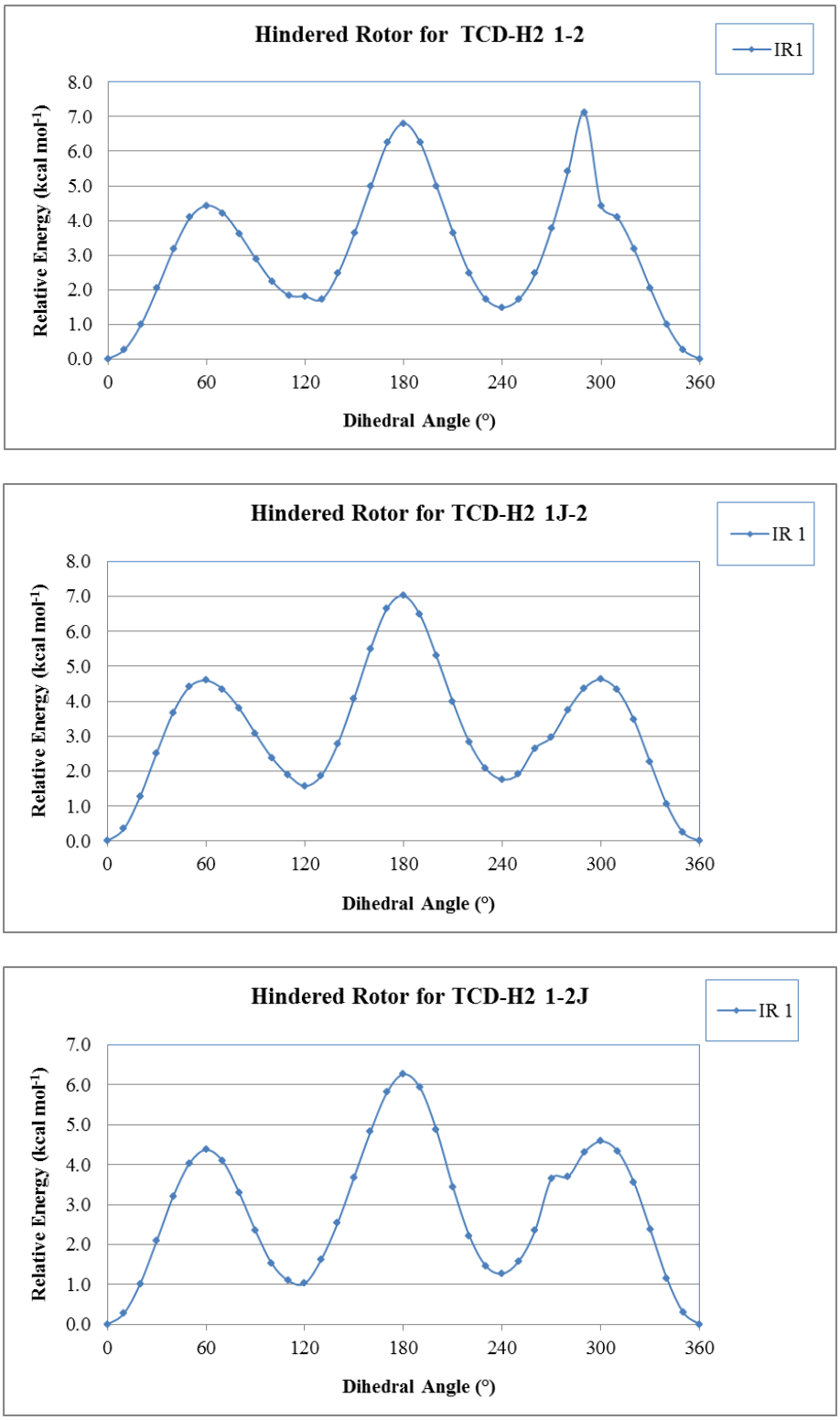

Figure E.1 Internal rotation of TCD-H2 1-2 species.

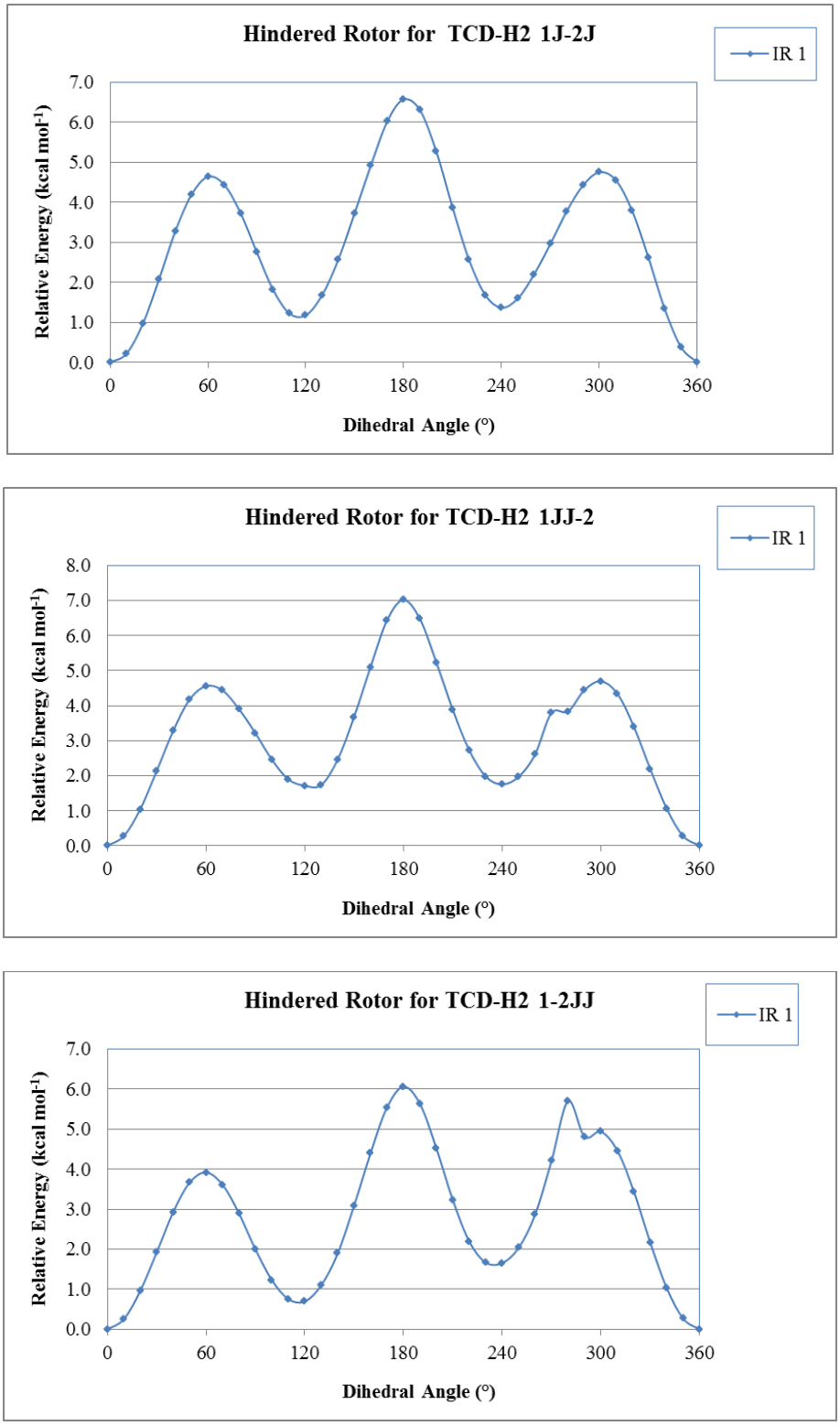

Figure E.1 Internal rotation of TCD-H2 1-2 species. (Continued)

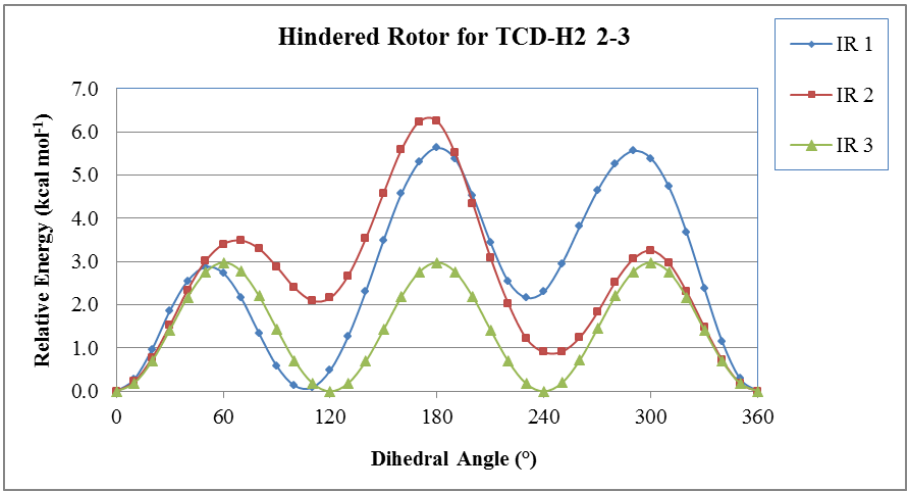

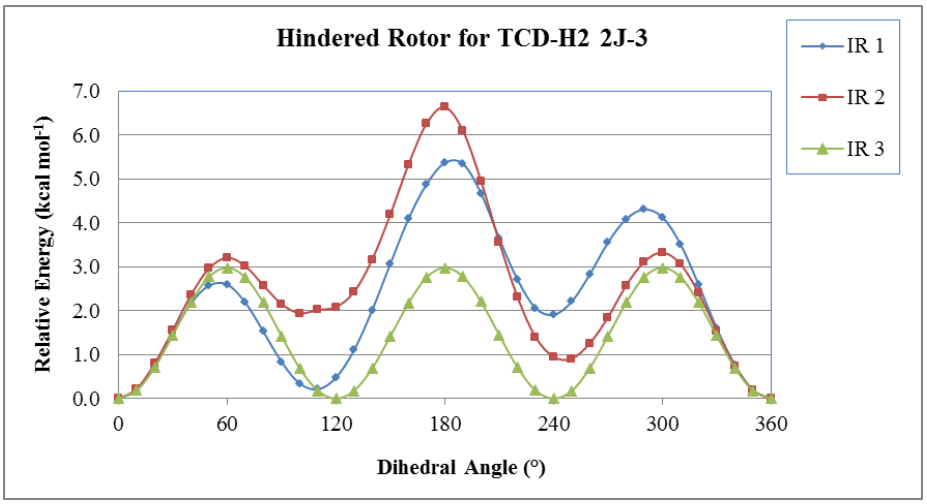

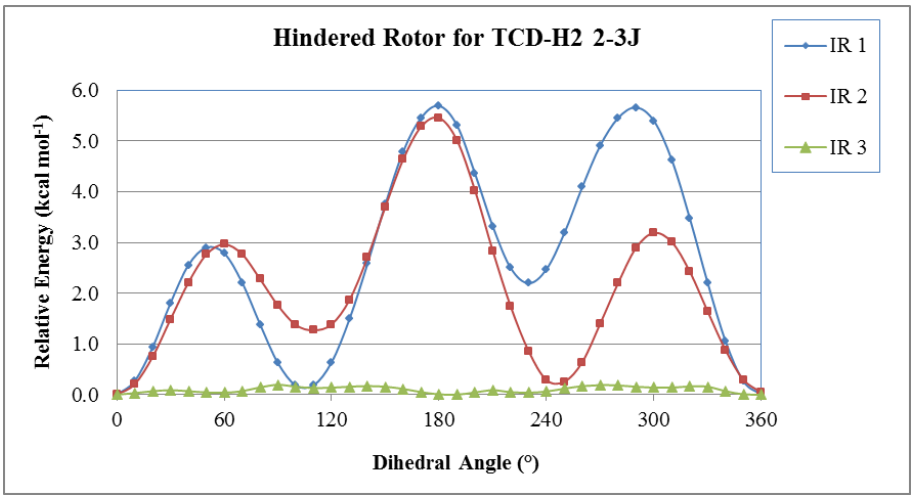

Figure E.2 Internal rotation of TCD-H2 2-3 species.

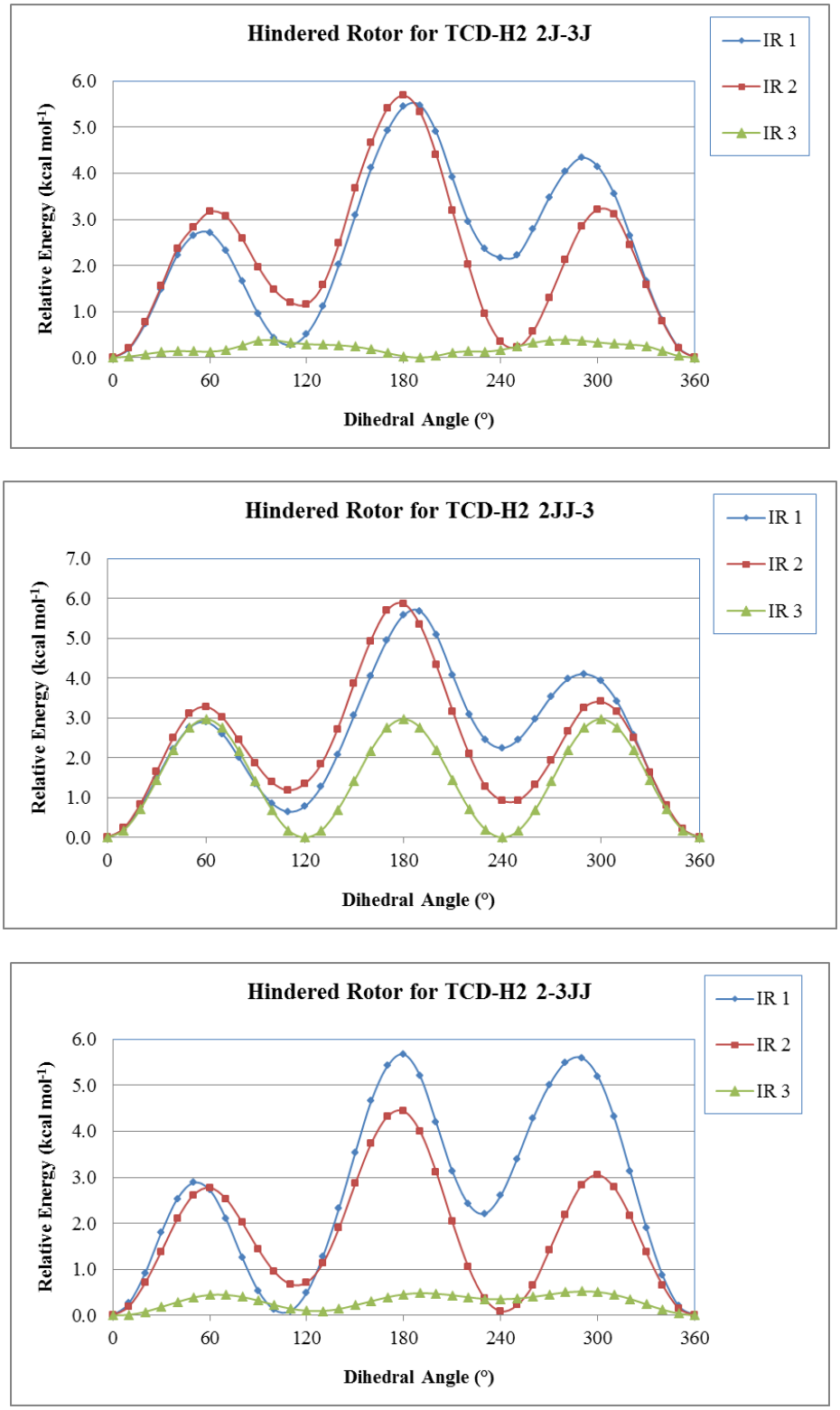

Figure E.2 Internal rotation of TCD-H2 2-3 species. (Continued)

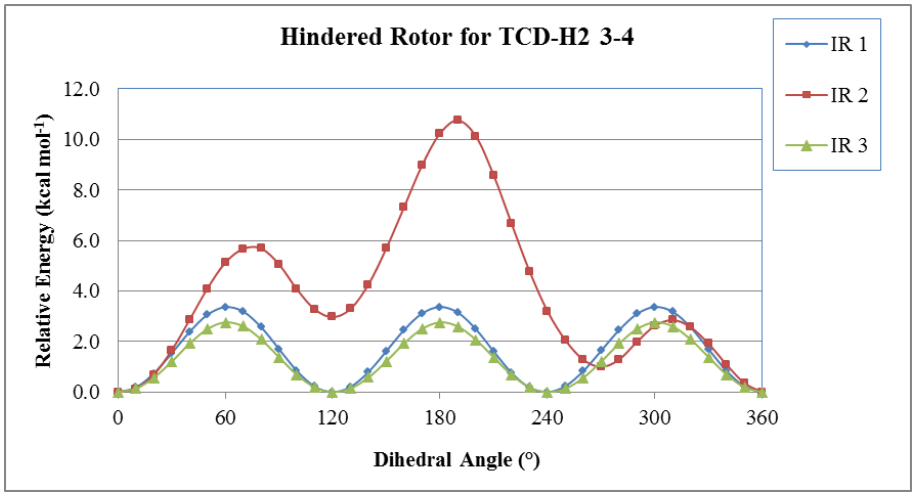

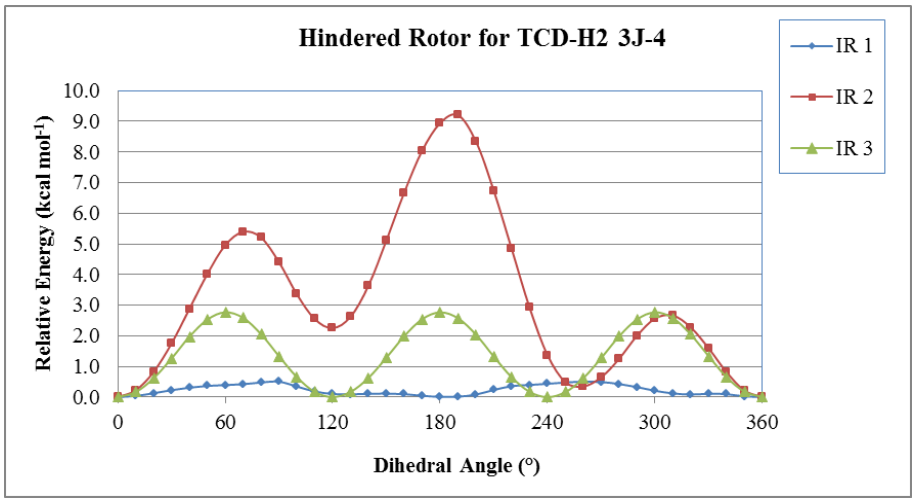

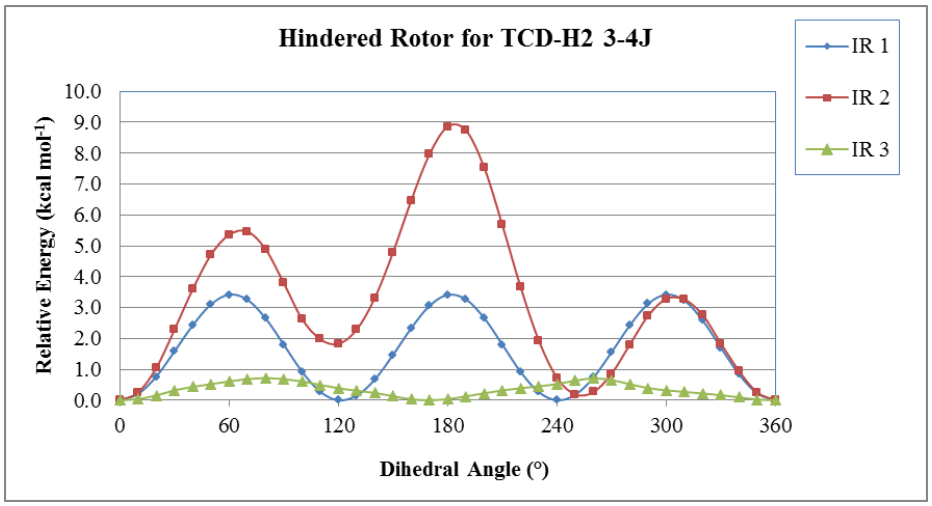

Figure E.3 Internal rotation of TCD-H2 3-4 species.

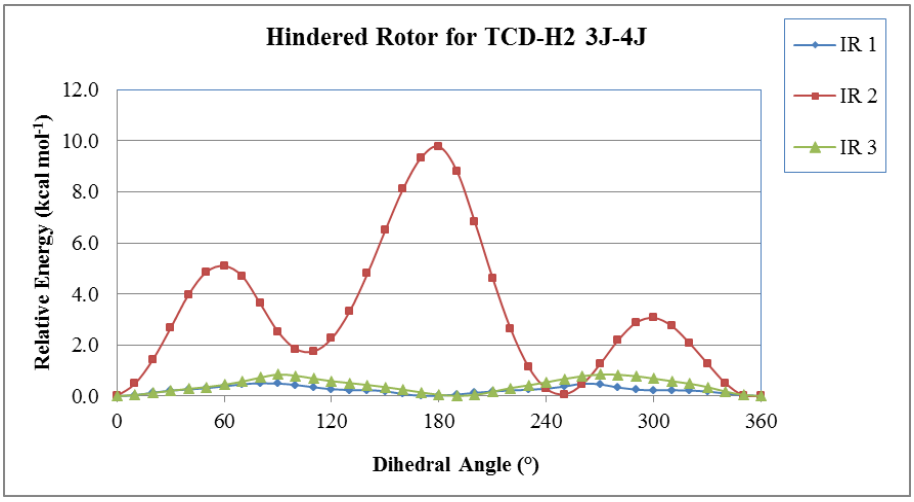

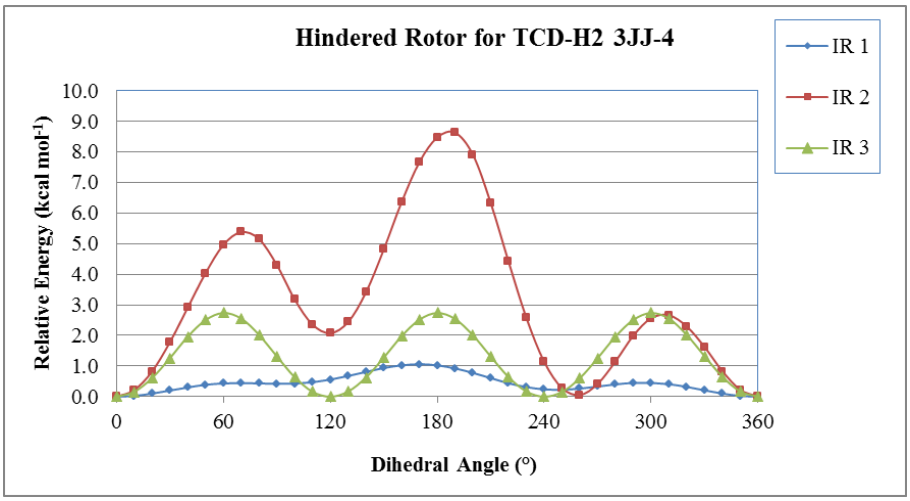

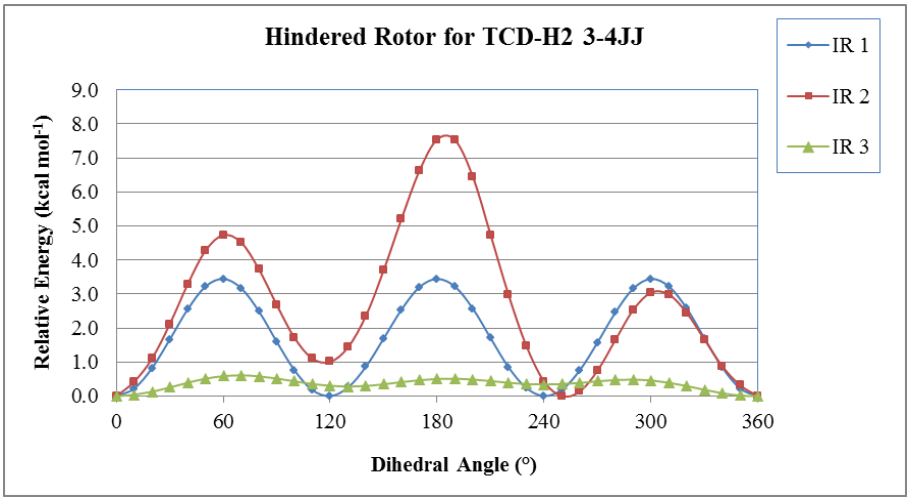

Figure E.3 Internal rotation of TCD-H2 3-4 species. (Continued)

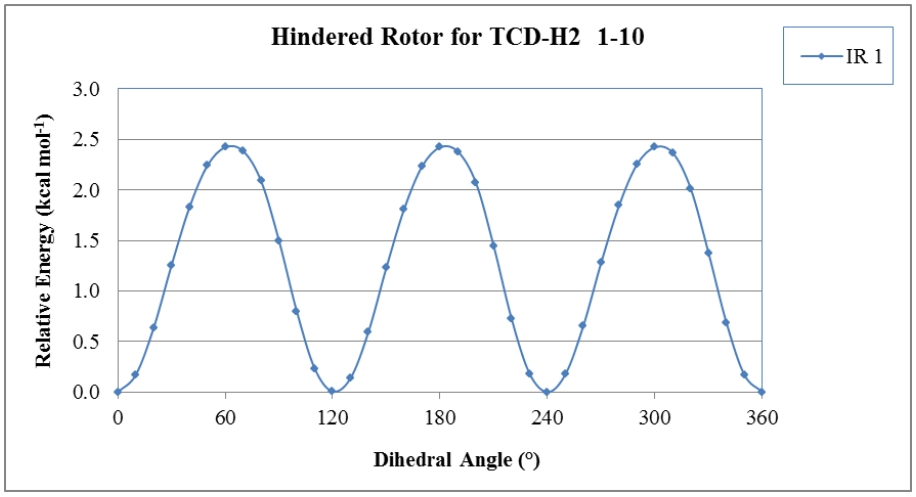

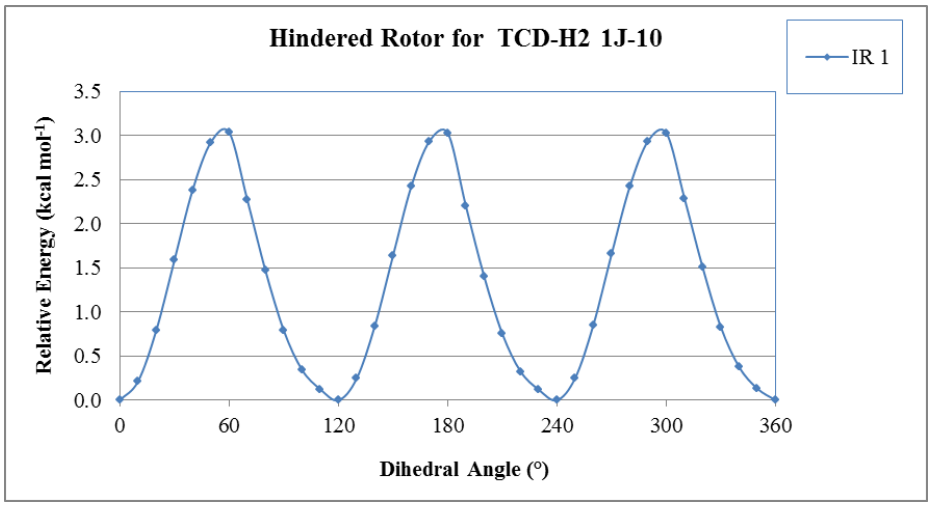

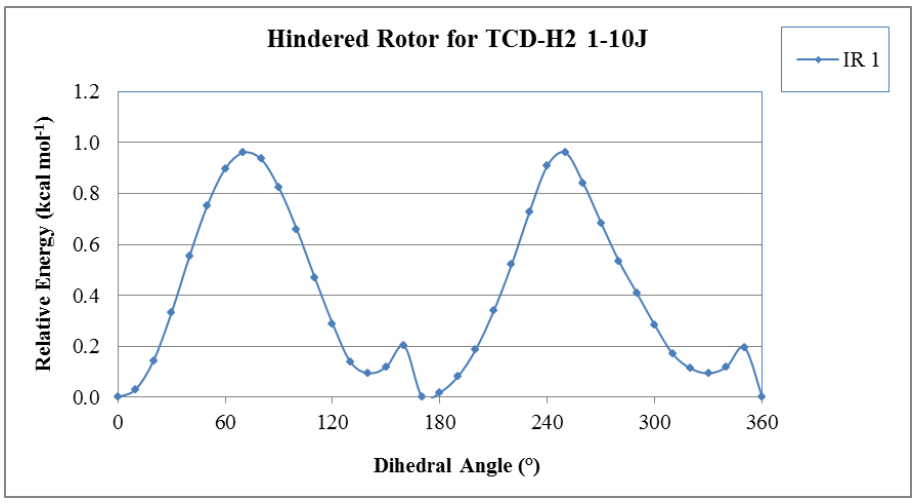

Figure E.4 Internal rotation of TCD-H2 1-10 species.

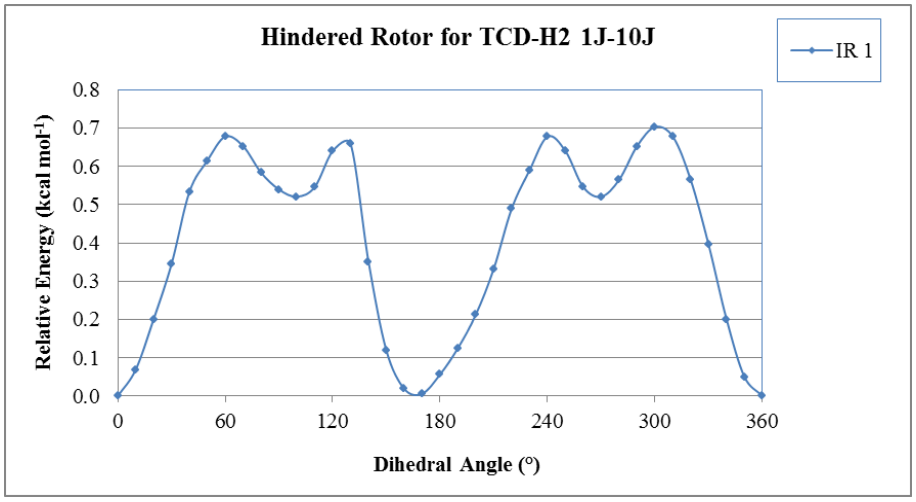

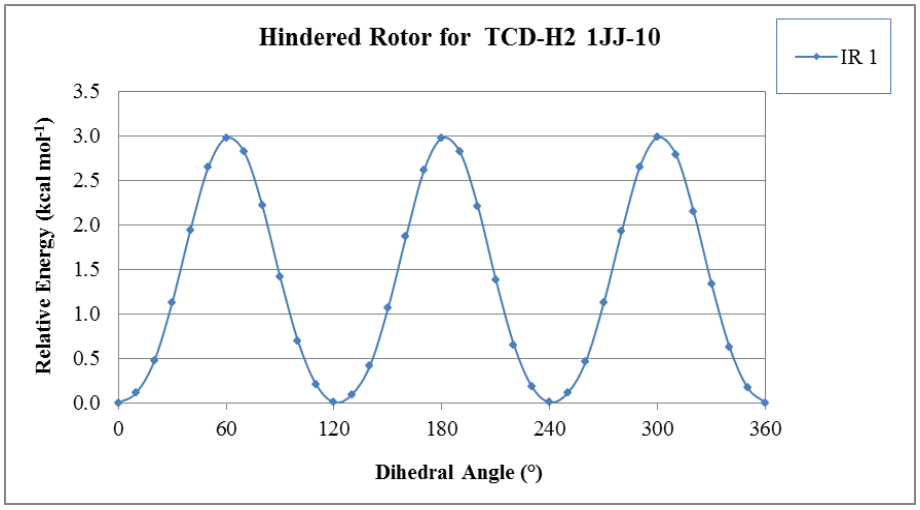

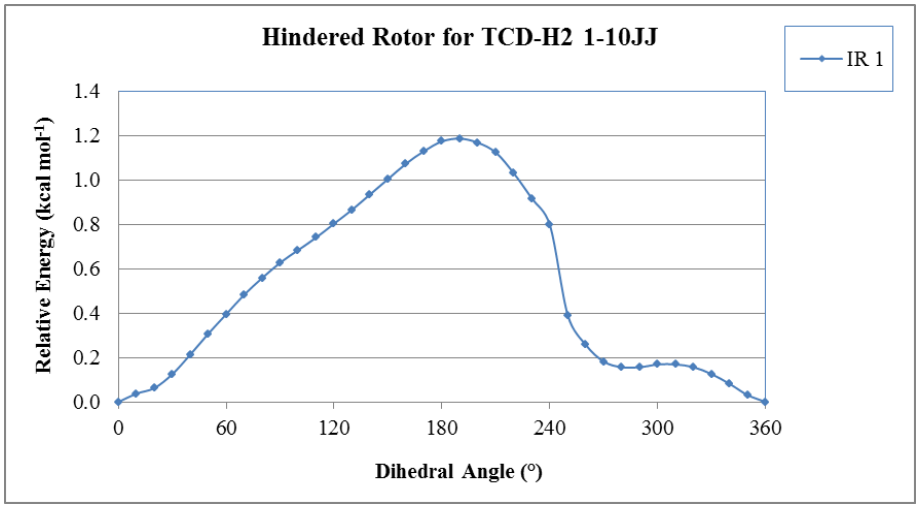

Figure E.4 Internal rotation of TCD-H2 1-10 species. (Continued)

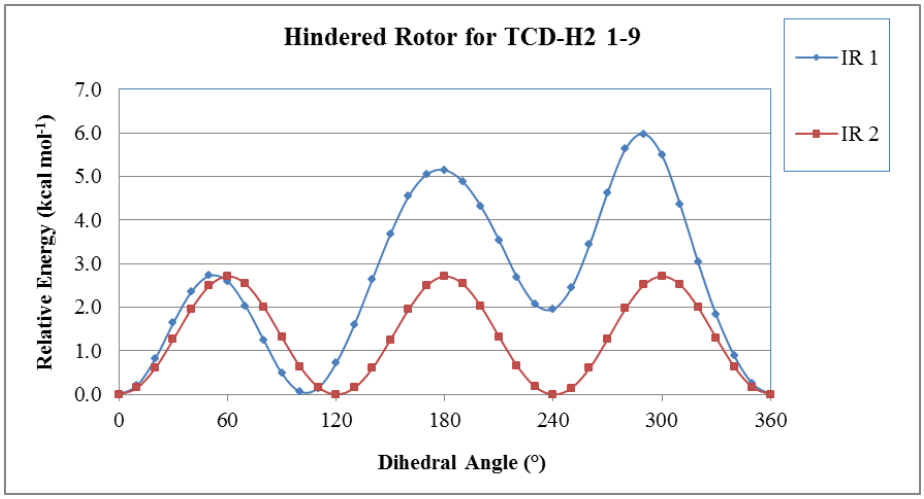

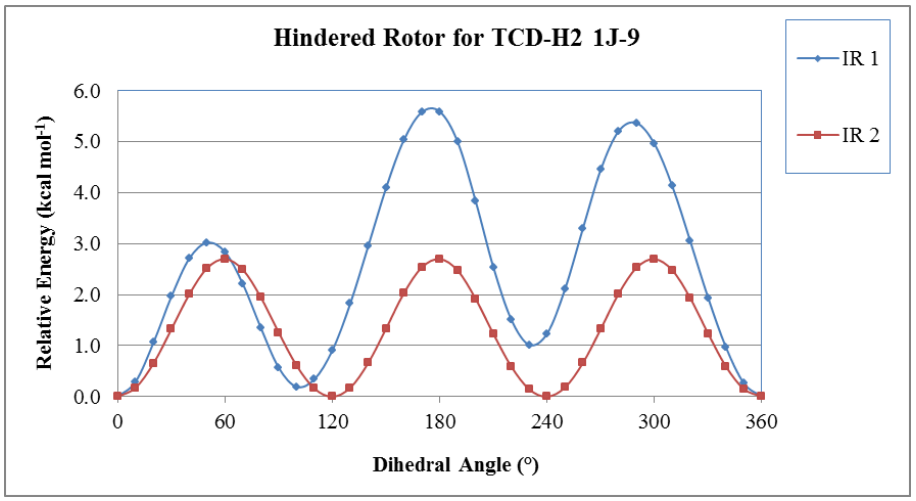

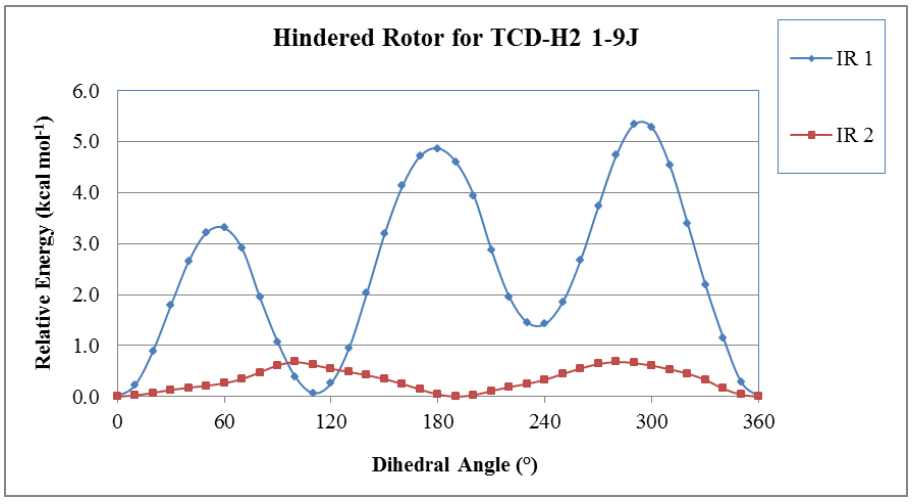

Figure E.5 Internal rotation of TCD-H2 1-9 species.

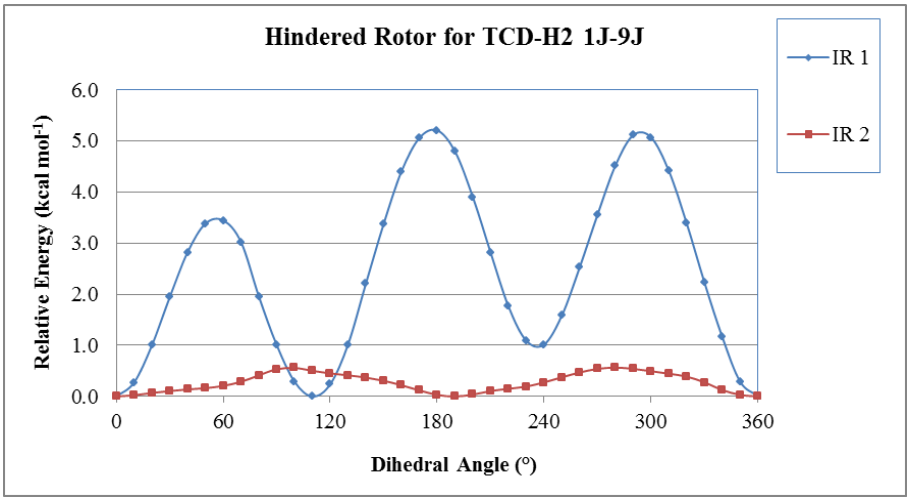

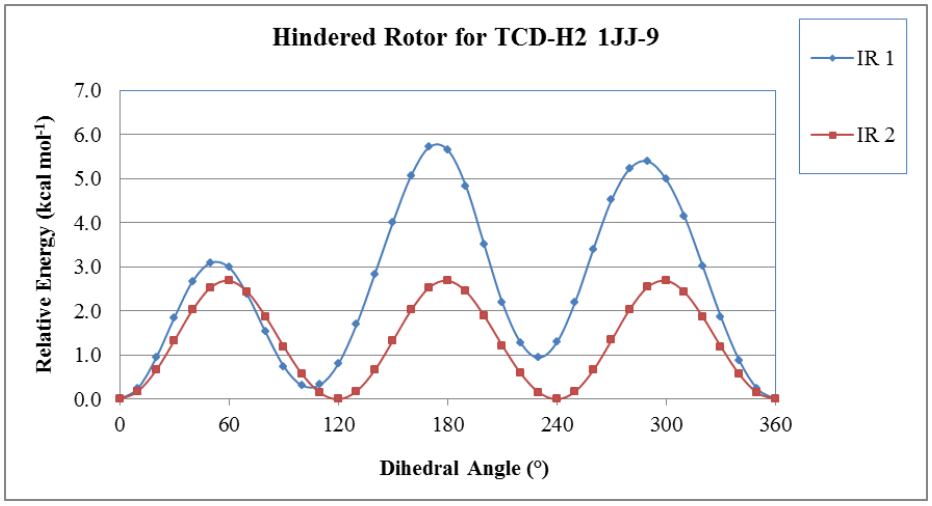

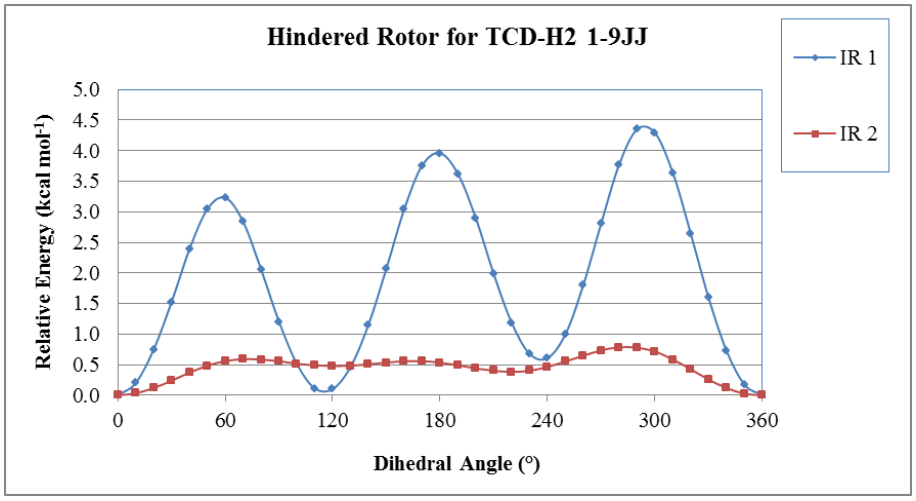

Figure E.5 Internal rotation of TCD-H2 1-9 species. (Continued)

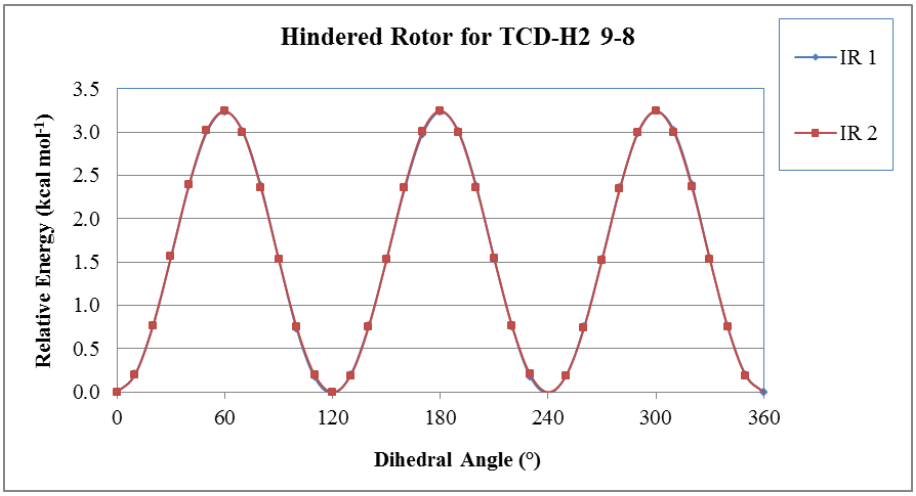

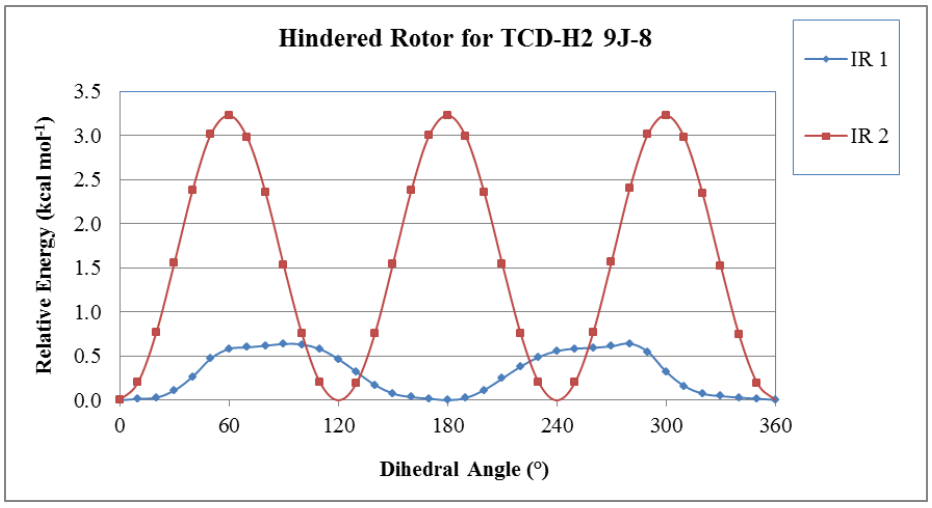

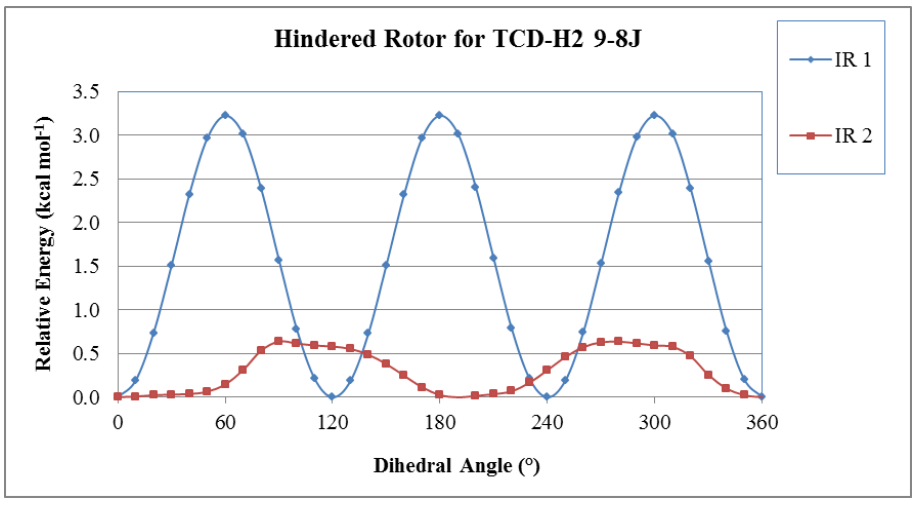

Figure E.6 Internal rotation of TCD-H2 9-8 species.

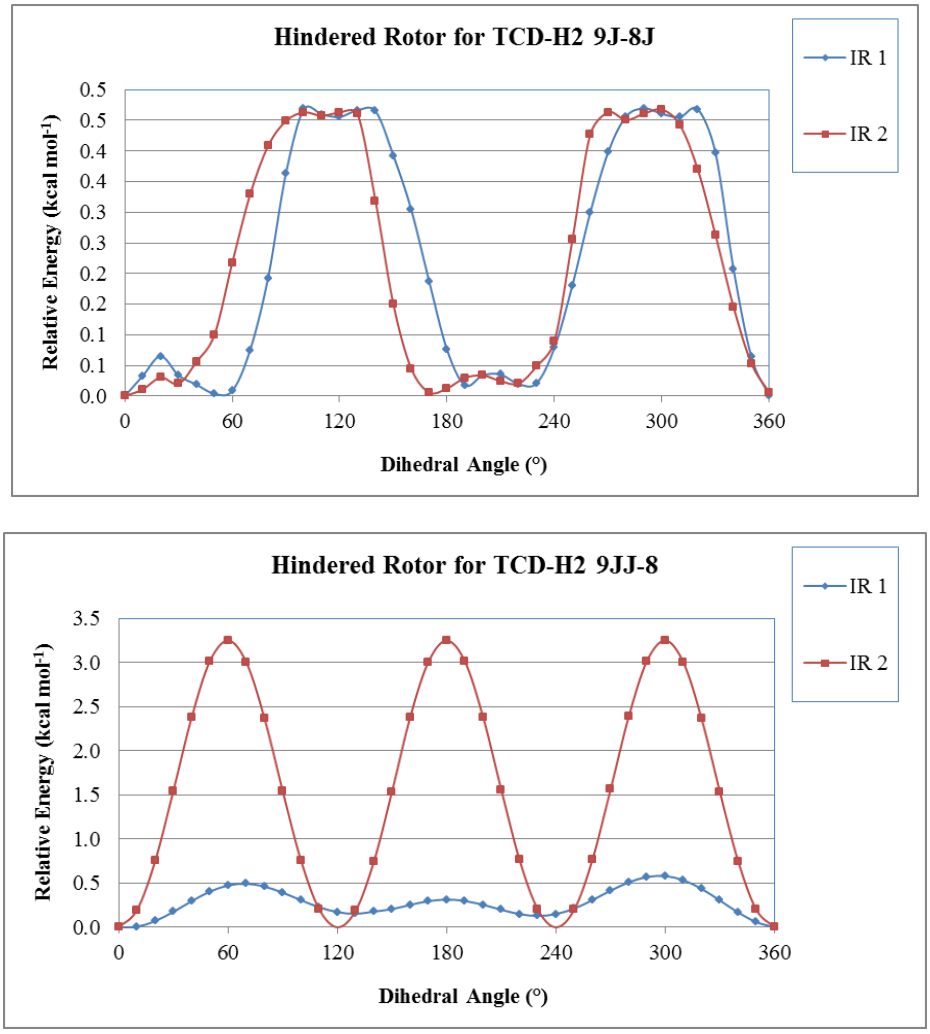

Figure E.6 Internal rotation of TCD-H2 9-8 species. (Continued)

Table E.12 Calculated Total Entropies[a] and Heat Capacities[a]

Temperature	TCD-H2 1-2		TCD-H2 1J-2		TCD-H2 1-2J		TCD-H2 1J-2J		TCD-H2 1JJ-2		TCD-H2 1-2JJ	
(K)	Cp	S	Cp	S	Cp	S	Cp	S	Cp	S	Cp	S
50	15.07	65.13	13.45	64.06	13.55	63.68	12.35	63.11	13.33	62.61	13.62	63.25
100	19.10	76.90	18.62	75.04	18.47	74.64	18.25	73.53	18.14	73.41	18.14	74.16
150	22.77	85.31	23.09	83.42	22.91	82.95	23.38	81.90	22.17	81.51	22.09	82.24
200	27.49	92.46	28.16	90.72	27.99	90.20	28.76	89.33	26.91	88.50	26.84	89.20
250	33.69	99.21	34.41	97.64	34.27	97.08	35.07	96.39	32.92	95.11	32.87	95.80
298	40.71	105.70	41.31	104.24	41.20	103.66	41.88	103.10	39.62	101.44	39.59	102.12
400	56.66	119.87	56.74	118.53	56.65	117.92	56.79	117.49	54.64	115.17	54.63	115.85
500	71.02	134.06	70.45	132.67	70.38	132.04	69.86	131.58	67.98	128.80	67.98	129.48
600	83.14	148.08	81.96	146.53	81.89	145.89	80.75	145.28	79.15	142.18	79.14	142.86
700	93.26	161.66	91.52	159.88	91.46	159.23	89.76	158.40	88.41	155.08	88.40	155.75
800	101.76	174.66	99.55	172.62	99.48	171.96	97.29	170.87	96.15	167.38	96.14	168.06
1000	115.17	198.85	112.16	196.23	112.10	195.56	109.12	193.89	108.29	190.18	108.27	190.85
1500	135.43	249.81	131.20	245.72	131.14	245.02	126.93	241.89	126.51	237.93	126.47	238.59
2000	145.63	290.30	140.76	284.89	140.72	284.18	135.87	279.75	135.62	275.69	135.59	276.34
2500	151.21	323.44	146.00	316.91	145.97	316.19	140.76	310.63	140.60	306.53	140.58	307.17
3000	154.53	351.32	149.11	343.81	149.08	343.09	143.66	336.56	143.55	332.44	143.53	333.08
3500	156.64	375.30	151.08	366.95	151.06	366.23	145.51	358.85	145.42	354.71	145.41	355.35
4000	158.05	396.31	152.41	387.22	152.39	386.49	146.75	378.36	146.68	374.21	146.67	374.85
4500	159.05	414.98	153.33	405.22	153.32	404.49	147.61	395.70	147.56	391.54	147.55	392.18
5000	159.77	431.78	154.01	421.41	154.00	420.68	148.24	411.28	148.20	407.12	148.20	407.76
Zero Point Energy[b]	161.321		152.201		152.443		143.197		145.454		145.555	

[a] Units of cal mol^{-1} K^{-1}.

[b] Units of kcal mol^{-1}.

Table E.12 Calculated Total Entropies[a] and Heat Capacities[a] (Continued A)

Temperature	TCD-H2 2-3		TCD-H2 2J-3		TCD-H2 2-3J		TCD-H2 2J-3J		TCD-H2 2JJ-3		TCD-H2 2-3JJ	
(K)	Cp	S	Cp	S	Cp	S	Cp	S	Cp	S	Cp	S
50	10.54	60.76	10.67	62.25	12.93	63.45	12.92	63.54	10.54	58.52	12.36	59.85
100	16.37	67.51	16.66	69.09	17.39	73.21	17.86	73.54	16.23	67.37	17.21	69.39
150	21.60	74.73	22.17	76.48	22.05	80.72	22.75	81.28	21.30	74.50	21.59	76.76
200	27.22	81.39	27.94	83.33	27.43	87.47	28.24	88.26	26.77	81.06	26.68	83.31
250	33.91	87.93	34.66	90.02	33.94	94.03	34.75	95.00	33.25	87.47	32.96	89.68
298	41.17	94.30	41.83	96.53	41.03	100.40	41.70	101.50	40.20	93.71	39.77	95.89
400	57.21	108.35	57.38	110.70	56.60	114.34	56.72	115.56	55.32	107.35	54.89	109.44
500	71.39	122.42	70.93	124.75	70.26	128.22	69.71	129.41	68.48	120.89	68.18	122.90
600	83.30	136.31	82.19	138.50	81.64	141.86	80.45	142.89	79.40	134.16	79.19	136.13
700	93.21	149.74	91.51	151.71	91.07	154.99	89.29	155.80	88.41	146.92	88.28	148.86
800	101.54	162.58	99.33	164.30	98.96	167.53	96.67	168.06	95.95	159.08	95.86	161.00
1000	114.70	186.48	111.64	187.60	111.39	190.77	108.27	190.70	107.79	181.58	107.74	183.49
1500	134.67	236.79	130.35	236.40	130.22	239.49	125.87	237.90	125.68	228.65	125.65	230.54
2000	144.76	276.75	139.82	275.03	139.75	278.09	134.79	275.15	134.69	265.87	134.68	267.76
2500	150.30	309.47	145.02	306.61	144.98	309.66	139.69	305.57	139.63	296.27	139.63	298.15
3000	153.59	336.99	148.12	333.16	148.09	336.20	142.61	331.13	142.57	321.82	142.57	323.70
3500	155.68	360.68	150.09	355.99	150.06	359.03	144.46	353.10	144.44	343.79	144.44	345.67
4000	157.09	381.43	151.41	375.99	151.39	379.02	145.71	372.34	145.69	363.03	145.69	364.91
4500	158.08	399.87	152.34	393.76	152.33	396.79	146.59	389.44	146.57	380.12	146.57	382.00
5000	158.79	416.46	153.02	409.74	153.00	412.77	147.22	404.81	147.21	395.49	147.21	397.38
Zero Point Energy[b]	161.296		152.385		151.865		143.034		145.543		144.633	

[b] Units of kcal mol^{-1}.

Table E.12 Calculated Total Entropies[a] and Heat Capacities[a] (Continued B)

Temperature	TCD-H2 3-4		TCD-H2 3J-4		TCD-H2 3-4J		TCD-H2 3J-4J		TCD-H2 3JJ-4		TCD-H2 3-4JJ	
(K)	Cp	S	Cp	S	Cp	S	Cp	S	Cp	S	Cp	S
50	8.59	63.18	10.93	64.87	10.64	64.54	12.82	65.55	10.40	62.13	10.41	62.22
100	15.26	66.34	16.83	71.50	16.77	70.95	18.43	75.41	16.48	68.31	16.01	68.11
150	21.61	72.93	22.45	78.57	22.51	78.04	23.55	83.03	21.95	75.22	21.53	74.83
200	27.86	79.40	28.36	85.23	28.40	84.71	29.10	89.95	27.61	81.69	27.26	81.18
250	34.81	85.89	35.09	91.82	35.11	91.29	35.54	96.67	34.13	88.06	33.85	87.48
298	42.12	92.26	42.18	98.21	42.21	97.69	42.37	103.12	41.04	94.25	40.79	93.66
400	57.97	106.26	57.47	112.16	57.58	111.67	57.07	117.04	55.77	107.89	55.74	107.23
500	71.88	120.25	70.75	125.98	70.94	125.51	69.77	130.71	68.69	121.29	68.78	120.63
600	83.51	134.03	81.81	139.49	82.03	139.07	80.26	144.00	79.38	134.40	79.53	133.76
700	93.19	147.32	90.98	152.48	91.21	152.09	88.92	156.71	88.22	146.99	88.37	146.38
800	101.34	160.02	98.67	164.86	98.90	164.50	96.16	168.79	95.60	158.98	95.76	158.39
1000	114.24	183.61	110.83	187.78	111.04	187.47	107.58	191.06	107.23	181.16	107.37	180.60
1500	133.91	233.26	129.38	235.81	129.53	235.57	124.98	237.53	124.86	227.54	124.95	227.03
2000	143.89	272.71	138.82	273.87	138.92	273.67	133.83	274.24	133.79	264.23	133.85	263.73
2500	149.38	305.00	144.02	305.00	144.09	304.82	138.72	304.22	138.70	294.20	138.74	293.72
3000	152.65	332.18	147.12	331.19	147.17	331.01	141.63	329.42	141.62	319.40	141.64	318.92
3500	154.73	355.57	149.09	353.71	149.13	353.54	143.48	351.09	143.47	341.07	143.50	340.59
4000	156.13	376.06	150.41	373.44	150.44	373.28	144.72	370.06	144.72	360.04	144.74	359.57
4500	157.11	394.27	151.34	390.98	151.37	390.82	145.60	386.92	145.60	376.91	145.61	376.44
5000	157.82	410.65	152.02	406.75	152.04	406.59	146.23	402.09	146.23	392.07	146.24	391.60
Zero Point Energy[b]	160.970		151.647		151.528		142.180		144.183		144.270	

[b] Units of kcal mol^{-1}.

Table E.12 Calculated Total Entropies[a] and Heat Capacities[a] (Continued C)

Temperature	TCD-H2 2-6		TCD-H2 2J-6		TCD-H2 2-6J		TCD-H2 2J-6J		TCD-H2 2JJ-6	
(K)	Cp	S	Cp	S	Cp	S	Cp	S	Cp	S
50	10.35	57.92	9.92	57.91	9.92	57.91	10.53	59.15	9.82	56.33
100	14.67	66.28	14.91	66.22	14.91	66.21	15.57	67.90	14.74	64.58
150	19.88	73.19	20.46	73.29	20.46	73.29	21.30	75.27	19.94	71.53
200	25.62	79.66	26.40	79.96	26.40	79.96	27.36	82.20	25.56	78.00
250	32.37	86.06	33.17	86.54	33.17	86.54	34.10	89.00	32.07	84.37
298	39.66	92.34	40.34	92.95	40.34	92.95	41.11	95.56	39.02	90.57
400	55.84	106.25	56.01	107.00	56.01	107.00	56.17	109.75	54.23	104.16
500	70.31	120.26	69.83	120.98	69.83	120.98	69.30	123.70	67.63	117.70
600	82.53	134.16	81.42	134.74	81.42	134.74	80.23	137.31	78.84	131.03
700	92.74	147.65	91.05	148.01	91.05	148.01	89.28	150.35	88.14	143.88
800	101.33	160.59	99.13	160.69	99.13	160.69	96.85	162.76	95.92	156.15
1000	114.85	184.69	111.84	184.22	111.84	184.22	108.75	185.69	108.12	178.90
1500	135.28	235.57	131.00	233.60	131.00	233.61	126.69	233.57	126.41	226.60
2000	145.54	276.02	140.64	272.73	140.64	272.74	135.71	271.36	135.56	264.34
2500	151.16	309.14	145.91	304.72	145.91	304.73	140.65	302.22	140.56	295.16
3000	154.49	337.01	149.05	331.62	149.05	331.62	143.58	328.13	143.52	321.06
3500	156.61	360.99	151.04	354.75	151.04	354.75	145.45	350.41	145.40	343.33
4000	158.03	382.00	152.37	375.01	152.37	375.01	146.70	369.92	146.66	362.83
4500	159.03	400.67	153.31	393.01	153.31	393.01	147.58	387.25	147.55	380.16
5000	159.75	417.47	153.99	409.20	153.99	409.20	148.21	402.83	148.19	395.74
Zero Point Energy[b]	162.844		153.714		153.715		144.605		146.478	

[b] Units of kcal mol^{-1}.

Table E.12 Calculated Total Entropies[a] and Heat Capacities[a] (Continued D)

Temperature	TCD-H2 1-10		TCD-H2 1J-10		TCD-H2 1-10J		TCD-H2 1J-10J		TCD-H2 1JJ-10		TCD-H2 1-10JJ	
(K)	Cp	S	Cp	S	Cp	S	Cp	S	Cp	S	Cp	S
50	9.08	59.70	9.27	61.11	11.22	61.11	11.41	61.87	9.46	59.80	10.66	58.38
100	15.31	65.52	15.11	66.85	16.87	70.25	16.94	71.09	14.93	65.56	16.57	66.91
150	21.20	72.43	21.24	73.72	22.23	77.70	22.22	78.54	20.61	72.28	21.81	74.22
200	27.18	79.04	27.49	80.38	27.85	84.54	27.95	85.40	26.53	78.71	27.21	80.92
250	33.89	85.57	34.36	87.00	34.31	91.20	34.50	92.08	33.16	85.08	33.45	87.40
298	41.01	91.93	41.49	93.44	41.23	97.61	41.39	98.53	40.10	91.30	40.16	93.65
400	56.73	105.88	56.88	107.50	56.46	111.56	56.23	112.48	55.06	104.89	54.94	107.22
500	70.77	119.82	70.37	121.42	69.94	125.39	69.15	126.20	68.15	118.36	68.00	120.66
600	82.67	133.60	81.68	135.07	81.28	138.96	79.91	139.58	79.07	131.57	78.94	133.85
700	92.64	146.93	91.08	148.21	90.72	152.04	88.82	152.42	88.12	144.29	88.02	146.54
800	101.05	159.71	98.99	160.75	98.65	164.54	96.28	164.63	95.72	156.41	95.63	158.66
1000	114.35	183.50	111.46	184.00	111.17	187.71	108.02	187.19	107.66	178.87	107.58	181.10
1500	134.51	233.71	130.33	232.76	130.13	236.38	125.79	234.33	125.65	225.91	125.60	228.11
2000	144.68	273.64	139.84	271.39	139.70	274.96	134.76	271.57	134.70	263.13	134.66	265.32
2500	150.25	306.34	145.05	302.98	144.95	306.52	139.68	301.98	139.65	293.53	139.62	295.71
3000	153.56	333.87	148.15	329.53	148.07	333.05	142.60	327.54	142.59	319.08	142.56	321.26
3500	155.66	357.55	150.11	352.37	150.05	355.88	144.46	349.51	144.45	341.06	144.44	343.23
4000	157.07	378.29	151.43	372.37	151.39	375.87	145.71	368.75	145.70	360.30	145.69	362.47
4500	158.06	396.73	152.36	390.14	152.32	393.64	146.59	385.85	146.58	377.39	146.57	379.56
5000	158.78	413.32	153.03	406.12	153.00	409.62	147.22	401.22	147.22	392.76	147.21	394.93
Zero Point Energy[b]	161.957		152.823		152.554		143.726		145.847		145.114	

[b] Units of kcal mol^{-1}.

Table E.12 Calculated Total Entropies[a] and Heat Capacities[a] (Continued E)

Temperature	TCD-H2 1-9		TCD-H2 1J-9		TCD-H2 1-9J		TCD-H2 1J-9J		TCD-H2 1JJ-9		TCD-H2 1-9JJ	
(K)	Cp	S	Cp	S	Cp	S	Cp	S	Cp	S	Cp	S
50	10.08	60.43	10.56	61.96	12.09	61.82	12.81	63.02	10.50	60.46	10.54	66.19
100	16.08	66.88	16.84	68.85	17.63	71.55	18.32	73.27	16.54	67.26	16.90	71.53
150	21.56	74.03	22.48	76.34	22.47	79.20	23.26	81.22	21.76	74.54	21.70	78.47
200	27.32	80.70	28.29	83.29	27.85	86.08	28.71	88.33	27.24	81.24	27.00	84.82
250	34.01	87.26	34.91	90.07	34.29	92.73	35.09	95.17	33.60	87.75	33.37	91.03
298	41.22	93.65	41.94	96.59	41.26	99.14	41.90	101.72	40.41	94.03	40.27	97.09
400	57.11	107.68	57.23	110.76	56.62	113.12	56.70	115.81	55.26	107.69	55.18	110.52
500	71.22	121.72	70.67	124.76	70.18	126.99	69.59	129.63	68.29	121.20	68.33	123.82
600	83.11	135.58	81.92	138.46	81.53	140.61	80.31	143.09	79.19	134.44	79.21	136.88
700	93.04	148.98	91.27	151.63	90.96	153.73	89.17	155.98	88.22	147.17	88.17	149.46
800	101.40	161.81	99.13	164.19	98.87	166.26	96.59	168.23	95.80	159.30	95.64	161.45
1000	114.60	185.67	111.54	187.46	111.33	189.48	108.26	190.85	107.71	181.77	107.35	183.64
1500	134.63	235.95	130.34	236.25	130.21	238.19	125.91	238.06	125.68	228.83	125.00	230.07
2000	144.74	275.91	139.84	274.88	139.74	276.79	134.83	275.33	134.71	266.05	133.90	266.80
2500	150.29	308.62	145.04	306.46	144.98	308.35	139.73	305.76	139.65	296.46	138.78	296.79
3000	153.59	336.15	148.14	333.01	148.09	334.89	142.64	331.33	142.59	322.01	141.68	322.00
3500	155.68	359.83	150.10	355.85	150.07	357.72	144.49	353.30	144.45	343.99	143.52	343.68
4000	157.09	380.58	151.43	375.84	151.40	377.72	145.73	372.55	145.71	363.23	144.76	362.66
4500	158.08	399.03	152.35	393.62	152.33	395.49	146.60	389.65	146.58	380.32	145.63	379.52
5000	158.79	415.61	153.02	409.60	153.01	411.46	147.24	405.02	147.22	395.69	146.26	394.69
Zero Point Energy[b]	161.462		152.263		152.047		142.868		145.350		144.632	

[b] Units of kcal mol^{-1}.

Table E.12 Calculated Total Entropies[a] and Heat Capacities[a] (Continued F)

Temperature	TCD-H2 9-8		TCD-H2 9J-8		TCD-H2 9-8J		TCD-H2 9J-8J		TCD-H2 9JJ-8	
(K)	Cp	S	Cp	S	Cp	S	Cp	S	Cp	S
50	8.60	63.38	10.75	63.48	10.76	63.59	13.41	64.26	10.60	62.62
100	15.29	66.48	16.98	70.03	17.01	70.13	18.30	74.21	16.18	68.57
150	21.89	73.14	22.87	77.23	22.89	77.33	23.44	81.76	21.89	75.38
200	28.25	79.70	28.86	84.02	28.86	84.13	29.14	88.68	27.73	81.85
250	35.17	86.28	35.50	90.70	35.51	90.81	35.58	95.40	34.22	88.27
298	42.38	92.71	42.45	97.16	42.45	97.27	42.32	101.86	40.98	94.52
400	58.08	106.76	57.51	111.15	57.51	111.27	56.81	115.74	55.69	108.07
500	71.91	120.77	70.70	124.96	70.70	125.08	69.42	129.33	68.56	121.44
600	83.53	134.54	81.75	138.47	81.75	138.58	79.91	142.56	79.26	134.53
700	93.24	147.84	90.93	151.45	90.93	151.57	88.59	155.22	88.12	147.10
800	101.42	160.55	98.66	163.83	98.66	163.94	95.88	167.25	95.54	159.09
1000	114.35	184.16	110.87	186.75	110.87	186.86	107.37	189.47	107.22	181.25
1500	134.05	233.86	129.46	234.81	129.46	234.92	124.88	235.88	124.90	227.64
2000	144.00	273.35	138.89	272.89	138.89	273.00	133.78	272.56	133.83	264.34
2500	149.47	305.66	144.07	304.03	144.07	304.14	138.68	302.54	138.73	294.32
3000	152.71	332.85	147.16	330.22	147.16	330.33	141.60	327.73	141.64	319.52
3500	154.78	356.25	149.12	352.75	149.12	352.86	143.46	349.40	143.50	341.19
4000	156.16	376.75	150.44	372.49	150.44	372.60	144.71	368.37	144.74	360.17
4500	157.14	394.96	151.36	390.03	151.36	390.14	145.59	385.23	145.61	377.04
5000	157.85	411.34	152.04	405.80	152.04	405.91	146.23	400.39	146.24	392.20
Zero Point Energy[b]	160.708		151.570		151.570		142.406		144.250	

[b] Units of kcal mol^{-1}.

APPENDIX F

HYDROGEN ABSTRACTION FROM *EXO*-TRICYCLO[5.2.1.0^{2,6}]DECANE (TCD) BY HYDROGEN AND OXYGEN ATOMS AND METHYL, HYDROXYL, AND HYDROPEROXYL RADICALS

This appendix contains the optimized geometries with corresponding Gaussian atom numbering and symmetry values in parenthesis, moments of inertia, vibrational frequencies, internal rotor potential energy graphs, entropies, and heat capacities for all of the transition state species from B3LYP/6-31G(d,p), except for TS-TCD R*i*-OH species which are from MP2/6-31G(d,p). Calculated enthalpies of formation are also included.

Table F.1 TS-TCD R*i*-H Optimized Species

TS-TCD R1-H (σ = 1)

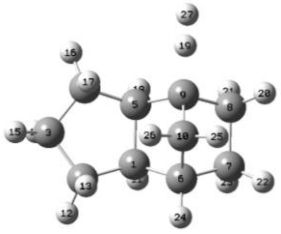

C,0,-0.0225418666,0.0150541182,0.0133553739
C,0,-0.0075805985,-0.0187182776,1.5594236115
C,0,1.4837458298,0.0136926453,1.9389539993
C,0,2.1468145175,-0.8774492758,0.8735791051
C,0,1.3981050838,-0.5413485972,-0.4374336117
C,0,-1.0144662902,-0.9492596533,-0.6904870021
C,0,-0.9898428545,-0.6539124211,-2.2131366277
C,0,0.4172595107,-1.1978265079,-2.6600414058
C,0,0.9837712935,-1.7092569716,-1.3333443515
C,0,-0.2482741976,-2.2981466171,-0.6375838504
H,0,-0.1718988538,1.042881125,-0.3359599562
H,0,-0.5797425841,0.8049651748,1.9988269434
H,0,-0.4594977008,-0.9498194856,1.924477229
H,0,1.8663445631,1.0394488167,1.8577655578
H,0,1.6759109092,-0.3231398219,2.9630757788
H,0,3.2255933033,-0.7147653061,0.7877963723
H,0,2.0047844323,-1.9333946414,1.1336607835
H,0,1.9582681049,0.2079687294,-1.0066715144
H,0,2.0213066748,-2.6392368452,-1.5320080431
H,0,0.313225967,-2.0090136228,-3.3880191885
H,0,1.046335727,-0.4253578551,-3.1123168294
H,0,-1.7966615647,-1.1877866737,-2.725795803
H,0,-1.1141261071,0.4123315233,-2.4284457103
H,0,-2.0186521736,-0.9446376441,-0.25486295
H,0,-0.7350498137,-3.0925481982,-1.2122797889
H,0,-0.0619369229,-2.6631804268,0.3756996605
H,0,2.670771534,-3.2537469005,-1.6663843598

TS-TCD R2-H (σ = 1)

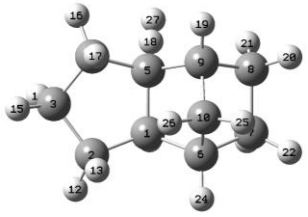

C,0,0.0315974488,-0.0224800246,-0.002087512
C,0,0.0216592039,-0.0003692653,1.5448407186
C,0,1.5110904522,-0.0151459169,1.9387504134
C,0,2.1500416708,-0.9725977857,0.9131869382
C,0,1.3749861368,-0.7135503336,-0.3808726926
C,0,-1.0122351619,-0.9247275306,-0.7087100706
C,0,-0.9198608833,-0.6637245422,-2.2322727552
C,0,0.4415267719,-1.3253591319,-2.6283240813
C,0,0.970638341,-1.8845300055,-1.2829855615
C,0,-0.3561185352,-2.3220397546,-0.6053226174
H,0,-0.0205801208,1.0045890999,-0.3849479356
H,0,-0.5200083203,0.8610088136,1.9488592471
H,0,-0.4711701932,-0.9008702656,1.9334151198
H,0,1.936753817,0.9893075463,1.8220193688
H,0,1.6803821878,-0.3212861158,2.9761636918
H,0,3.2290535947,-0.8213803711,0.7966105072
H,0,2.0095464581,-2.0157332104,1.2313639465
H,0,2.098303916,0.113463571,-1.0734415031
H,0,1.7387962231,-2.6552872033,-1.3896914262
H,0,0.2901195809,-2.1399526169,-3.3439421133
H,0,1.1407929947,-0.6169919669,-3.0810215025
H,0,-1.7555346924,-1.1379300218,-2.7575364629
H,0,-0.9532891058,0.4047560327,-2.4682646445
H,0,-2.0241166239,-0.8338483289,-0.3027405721
H,0,-0.8902024969,-3.0920817415,-1.1734543477
H,0,-0.2269734071,-2.6778658868,0.4214907078
H,0,2.6461511747,0.7393681179,-1.5977940971

Table F.1 TS-TCD R*i*-H Optimized Species (Continued)

TS-TCD R3-H (σ = 1)

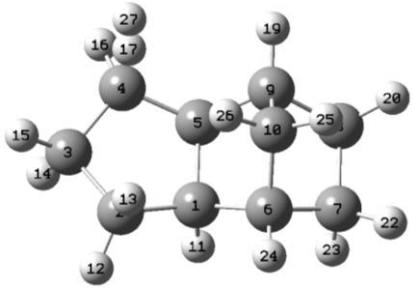

C,0,0.0009788539,-0.002602366,0.0020470659
C,0,0.0117362592,-0.035992606,1.5494269361
C,0,1.5021063408,-0.0156787889,1.939441902
C,0,2.172041231,-0.8341414604,0.8442852455
C,0,1.3941009119,-0.5923572931,-0.4480819051
C,0,-1.0122001259,-0.9413867568,-0.6941563046
C,0,-0.9574668228,-0.6695499289,-2.218019848
C,0,0.4158127857,-1.289784811,-2.6427804164
C,0,0.988707851,-1.8228659376,-1.3069683531
C,0,-0.2988408373,-2.3091105797,-0.606547283
H,0,-0.1234012866,1.0298500702,-0.3442210872
H,0,-0.5527889633,0.7925901209,1.9885910287
H,0,-0.4471283697,-0.963185718,1.913085229
H,0,1.8869950111,1.014898958,1.9164882877
H,0,1.6940470353,-0.4041953229,2.9458261195
H,0,3.2598797765,-0.7574434101,0.7730234599
H,0,2.0485770199,-2.0914791445,1.2099444915
H,0,1.9567661588,0.1182946103,-1.0685569293
H,0,1.785937423,-2.5617596439,-1.4255603471
H,0,0.2731250754,-2.1096573751,-3.3544294717
H,0,1.0811029882,-0.560907072,-3.1172467524
H,0,-1.7881751823,-1.1657800178,-2.7305334374
H,0,-1.0282562229,0.3988530181,-2.4478025213
H,0,-2.0203975285,-0.8935474127,-0.2716185491
H,0,-0.8146036135,-3.0963369284,-1.1677295355
H,0,-0.138327954,-2.665989543,0.4140505335
H,0,2.0032816357,-3.0028253721,1.5483353176

TS-TCD R4-H (σ = 1)

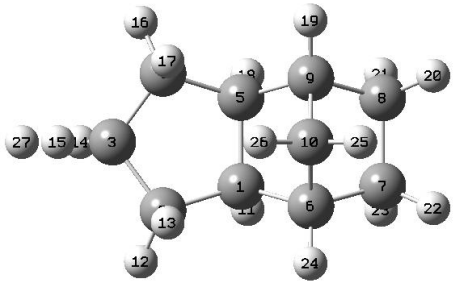

C,0,0.011805866,0.0638111177,-0.0548154938
C,0,0.0407629065,0.1473925506,1.4949050889
C,0,1.5225836049,0.1305609455,1.8489657541
C,0,2.1881901146,-0.7907348252,0.8342749128
C,0,1.4057367212,-0.5451466391,-0.4836434943
C,0,-1.0030407929,-0.9319628735,-0.6679742945
C,0,-0.9929067697,-0.7416727654,-2.2044960735
C,0,0.3878041472,-1.3448568255,-2.6292555733
C,0,0.9995272192,-1.8068116212,-1.2840405099
C,0,-0.2614019186,-2.2798910221,-0.5270346807
H,0,-0.1308667225,1.0666459327,-0.47196082
H,0,-0.4822320486,1.0282058753,1.8787862399
H,0,-0.4528004746,-0.7318485311,1.9306377338
H,0,1.9849229539,1.1159846724,1.9526995496
H,0,1.6745336213,-0.3828760309,3.0720840174
H,0,3.2612978865,-0.6072072683,0.7271380777
H,0,2.073465626,-1.8354812418,1.1534569611
H,0,1.9669901284,0.1501694072,-1.1173416233
H,0,1.8043818328,-2.5402389675,-1.390915598
H,0,0.2540821987,-2.1948953827,-3.3065177164
H,0,1.0263908779,-0.6186798408,-3.1428983898
H,0,-1.8204981122,-1.2885824316,-2.6682992132
H,0,-1.1001203112,0.3103198158,-2.48869978
H,0,-2.0000523864,-0.8782194973,-0.2205278542
H,0,-0.7767055784,-3.1081146843,-1.0259436877
H,0,-0.0705201634,-2.5732704917,0.5100565057
H,0,1.7501044251,-0.8057642465,3.9190917864

Table F.1 TS-TCD R*i*-H Optimized Species (Continued)

TS-TCD R9-H (σ = 1)

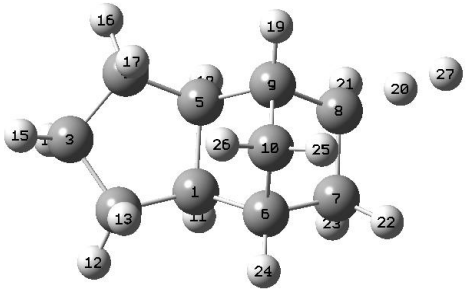

C,0,-0.0008519009,0.005481256,0.004421865
C,0,-0.015521224,-0.0334573864,1.5509505789
C,0,1.4695526197,-0.0232404146,1.9557404812
C,0,2.1369663554,-0.9195141253,0.8971512856
C,0,1.40533819,-0.5733309168,-0.4223655377
C,0,-0.9971428956,-0.9339574048,-0.7193670139
C,0,-0.9260685736,-0.6294997489,-2.238285395
C,0,0.454168787,-1.1962849295,-2.6261238744
C,0,1.0221710357,-1.7765599499,-1.3305204036
C,0,-0.2672422393,-2.2948184754,-0.6541016083
H,0,-0.1281214615,1.0383620287,-0.3391662286
H,0,-0.583282304,0.7961399936,1.9845877308
H,0,-0.4863278727,-0.9595386693,1.9050236714
H,0,1.8679150167,0.9971498854,1.8838524568
H,0,1.6410505695,-0.3660903308,2.9816723413
H,0,3.2188396188,-0.7678747909,0.8263607909
H,0,1.979501015,-1.9743695991,1.1557904677
H,0,1.9891357847,0.1639711936,-0.9845426923
H,0,1.8289147257,-2.5012633004,-1.473355258
H,0,0.2677772962,-2.1946133939,-3.4528481275
H,0,1.1170615945,-0.5446196399,-3.2005685545
H,0,-1.7315829135,-1.1425316083,-2.7784867446
H,0,-1.020475539,0.4397575523,-2.4583276584
H,0,-2.0113990591,-0.9091147401,-0.3100410442
H,0,-0.7652572321,-3.0798826042,-1.2325181643
H,0,-0.1120370517,-2.6634571324,0.3639107822
H,0,0.1029278748,-2.9441245428,-4.0517404336

TS-TCD R10-H (σ = 1)

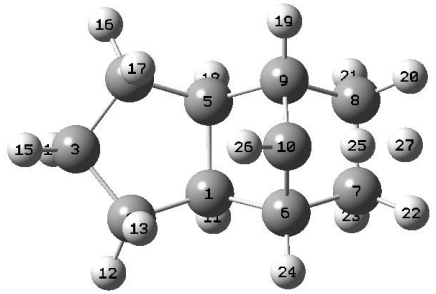

C,0,-0.0005531148,0.0006684026,0.0024280697
C,0,0.0030201757,0.0054195085,1.5490215524
C,0,1.4929285541,0.0106885665,1.9346577039
C,0,2.1345595287,-0.9262933853,0.8959346653
C,0,1.3957407754,-0.6096802122,-0.4253867799
C,0,-1.021315435,-0.9516305924,-0.6841336828
C,0,-0.9689854754,-0.6869880139,-2.2098830095
C,0,0.4117771205,-1.290582656,-2.632931814
C,0,0.9884453256,-1.8301512512,-1.2998900789
C,0,-0.2834704581,-2.2859890381,-0.5865160133
H,0,-0.1231213065,1.0233087738,-0.3729345777
H,0,-0.5514958765,0.8522679124,1.966034194
H,0,-0.4719085784,-0.9066787236,1.9329618962
H,0,1.9023594405,1.0234452765,1.826126285
H,0,1.6729433856,-0.3022474242,2.9686302023
H,0,3.2181726786,-0.7954748518,0.8110304538
H,0,1.9614150829,-1.9702995293,1.1874193643
H,0,1.9807023974,0.1036746653,-1.0175506367
H,0,1.7795860796,-2.575248675,-1.4190065798
H,0,0.2788428362,-2.1040805167,-3.3524810951
H,0,1.0740664277,-0.5501805499,-3.0928716694
H,0,-1.7916560384,-1.1989420406,-2.7181325477
H,0,-1.0530695802,0.3797047918,-2.4411056301
H,0,-2.0253253602,-0.91202057,-0.2532537291
H,0,-0.9338352465,-3.2518636136,-1.3312636594
H,0,-0.1959436126,-2.768889361,0.3881288328
H,0,-1.3665689024,-3.8861063237,-1.8383128008

Table F.2 TS-TCD R*i*-CH_3 Optimized Species

TS-TCD R1-CH_3 (σ = 3)

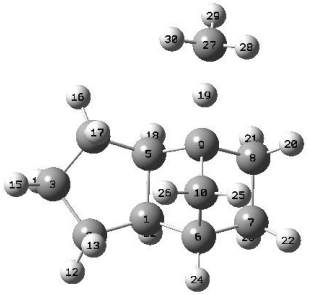

C,0,-0.0973986189,0.0151230996,0.0543625761
C,0,-0.0483947824,-0.0718200839,1.5977467475
C,0,1.4371027743,0.1182850602,1.9537139062
C,0,2.1730483241,-0.6554333292,0.8451597298
C,0,1.3639320561,-0.3626069137,-0.4406345442
C,0,-0.9889769822,-1.0275368331,-0.6682363327
C,0,-1.030802172,-0.6724296427,-2.176408039
C,0,0.4170434749,-1.0360767224,-2.6673119332
C,0,1.080658378,-1.5438230659,-1.3783868953
C,0,-0.0755058844,-2.2808777352,-0.6844525559
H,0,-0.3684708464,1.0322098854,-0.2510774611
H,0,-0.7019598552,0.6637413039,2.0781380146
H,0,-0.3819320319,-1.0618739424,1.9342158836
H,0,1.6992287404,1.1831535645,1.9021797109
H,0,1.6876847159,-0.2282411047,2.9620311142
H,0,3.2256143743,-0.3705476432,0.7488107062
H,0,2.153362558,-1.7287693138,1.071154806
H,0,1.825293001,0.4668101925,-0.9880192638
H,0,2.1519778044,-2.2997137469,-1.6281252091
H,0,0.386733577,-1.8197181715,-3.4321215332
H,0,0.9453250946,-0.1790202693,-3.0968857704
H,0,-1.784373777,-1.2733474189,-2.696457081
H,0,-1.2801325499,0.380357204,-2.3455219217
H,0,-1.9774869856,-1.1523232605,-0.2145319923
H,0,-0.4869330641,-3.1028398789,-1.2799770517
H,0,0.1689536287,-2.6625666348,0.3108264934
C,0,3.223037132,-3.1006723078,-1.9127267921
H,0,2.8194368604,-3.9287825039,-2.4945774939
H,0,3.9106984719,-2.4743848852,-2.4801806598
H,0,3.6235928903,-3.4111024047,-0.9483822608

TS-TCD R2-CH_3 (σ = 3)

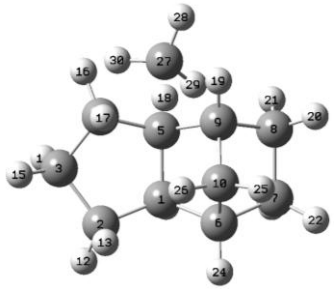

C,0,0.1166681267,-0.007686761,-0.0370957309
C,0,0.0611304592,0.0620045473,1.5079624684
C,0,1.5296361873,-0.0732813918,1.9534040902
C,0,2.1143482988,-1.1064671005,0.9710508591
C,0,1.4211666459,-0.8007630963,-0.361809081
C,0,-0.973561641,-0.8535677964,-0.7452364626
C,0,-0.8266226095,-0.6462534052,-2.2726504089
C,0,0.4902861104,-1.4196662871,-2.6142302458
C,0,0.9463131401,-1.9688197949,-1.2383878834
C,0,-0.4241753469,-2.2906752686,-0.5863443768
H,0,0.1422343702,1.0091772954,-0.4500621518
H,0,-0.4139950827,0.9792739131,1.8712639661
H,0,-0.522571551,-0.7788577332,1.9041281076
H,0,2.0448263087,0.8879187374,1.8301553277
H,0,1.6376060735,-0.3662897496,3.0029887573
H,0,3.2071904563,-1.0580710339,0.8996995308
H,0,1.8665598793,-2.1244503076,1.3052895028
H,0,2.2380211491,-0.0499097252,-1.0278733632
H,0,1.6570481457,-2.7976986635,-1.3036799295
H,0,0.2925027024,-2.2449497445,-3.3064246546
H,0,1.2482225543,-0.7816907143,-3.0761653699
H,0,-1.6829136658,-1.0722610244,-2.8061108122
H,0,-0.7742497229,0.4145394054,-2.539167762
H,0,-1.9858809816,-0.6774616148,-0.3689337584
H,0,-1.0006037785,-3.0360693775,-1.1464930866
H,0,-0.348329179,-2.6248725171,0.4528672509
C,0,3.1808378999,0.7917947611,-1.6816423491
H,0,3.8521498279,0.1122729887,-2.2044058587
H,0,2.5940323841,1.4237052866,-2.3462234697
H,0,3.6610760203,1.3406942767,-0.8728509423

TS-TCD R3-CH_3 (σ = 3)

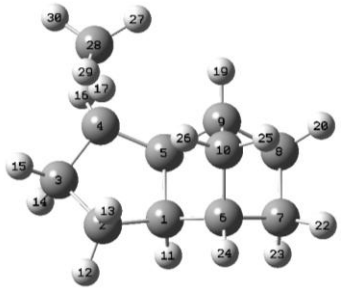

C,0,-0.0471630711,-0.0004795991,-0.0140655473
C,0,-0.079761885,-0.0606892266,1.531243057
C,0,1.3996183142,-0.0520384267,1.9602987345
C,0,2.0993734327,-0.8671298922,0.8758651222
C,0,1.3548683341,-0.5920262142,-0.4345600099
C,0,-1.0476315177,-0.9160549469,-0.7577636151
C,0,-0.9494749004,-0.6121919575,-2.2729992252
C,0,0.4315618965,-1.2320452898,-2.6721817941
C,0,0.9642277757,-1.7976329446,-1.3328264104
C,0,-0.3457984893,-2.2902884671,-0.6796830778
H,0,-0.1540333847,1.0393533994,-0.3440205687
H,0,-0.6534264021,0.7629543879,1.9685892089
H,0,-0.5540519698,-0.9911475169,1.8672558
H,0,1.7845896349,0.9788257591,1.9606417502
H,0,1.5593562931,-0.4488717168,2.9696390088
H,0,3.1847896256,-0.7415518456,0.8233620078
H,0,2.0193318014,-2.1203137775,1.2334286807
H,0,1.9343427777,0.1294547613,-1.0264250319
H,0,1.75871841,-2.5400834798,-1.4488054447
H,0,0.3040628394,-2.0343629783,-3.4066038129
H,0,1.1146721289,-0.4969177918,-3.1104416559
H,0,-1.7686633344,-1.0917858329,-2.8190252097
H,0,-1.007082291,0.4614378282,-2.481134541
H,0,-2.0668661317,-0.8702701405,-0.3619561771
H,0,-0.8516484584,-3.063536072,-1.2688888253
H,0,-0.2168919482,-2.663247289,0.3391334147
H,0,2.1098474624,-4.0893917012,0.8819467092
C,0,2.096334898,-3.4371334622,1.7533505096
H,0,1.2106168131,-3.5582440425,2.3753291883
H,0,3.0272817622,-3.4462175646,2.3182902252

Table F.2 TS-TCD R*i*-CH_3 Optimized Species (Continued)

TS-TCD R4-CH_3 (σ = 3)

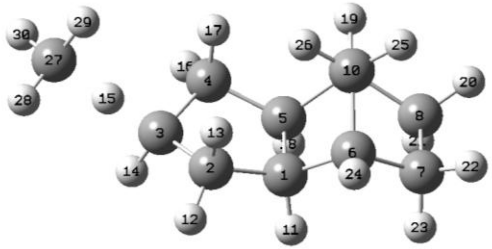

C,0,-0.0626077439,0.0284601458,-0.051943804
C,0,-0.1430488815,0.065541513,1.4974978983
C,0,1.3110965682,0.0453121879,1.9625981038
C,0,2.0419109038,-0.8531998186,0.9676899432
C,0,1.3587760941,-0.5691982104,-0.3965978549
C,0,-1.0296579294,-0.9469317342,-0.7664049289
C,0,-0.9102451121,-0.7153552977,-2.2923070664
C,0,0.4975936574,-1.307305496,-2.6336835675
C,0,1.0127700974,-1.8057149676,-1.261660093
C,0,-0.2993738931,-2.3004787225,-0.6113182528
H,0,-0.1759407825,1.043654205,-0.4481785284
H,0,-0.7003388095,0.9319321039,1.8670675394
H,0,-0.6636877175,-0.8281066739,1.8687949003
H,0,1.7547432912,1.0411190923,2.0653737341
H,0,1.3935309351,-0.4552051119,3.1705031552
H,0,3.1214040247,-0.6750556305,0.940374234
H,0,1.9014933117,-1.9067274182,1.2467862475
H,0,1.9643218751,0.1437293669,-0.9671365805
H,0,1.8237714635,-2.5370521896,-1.3316880429
H,0,0.413205204,-2.1388609039,-3.3413842389
H,0,1.1698433458,-0.5683642757,-3.0822901151
H,0,-1.7017589377,-1.249591985,-2.8285377262
H,0,-0.9992993041,0.3436869234,-2.5563163763
H,0,-2.0566178931,-0.9054553316,-0.3907532358
H,0,-0.7765363177,-3.1124397629,-1.1711779021
H,0,-0.1833318777,-2.6236608558,0.4276377099
C,0,1.4563932683,-1.0367588224,4.4367998811
H,0,0.8786165971,-0.3751872131,5.0805435011
H,0,1.0122209615,-2.0242173579,4.3188271803
H,0,2.516927472,-1.0645749226,4.6825607292

TS-TCD R9-CH_3 (σ = 3)

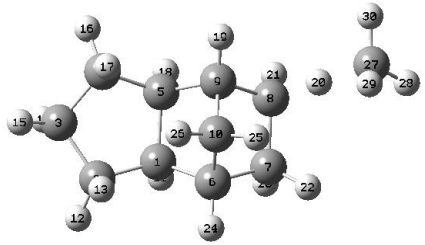

C,0,-0.0248172308,-0.0129352249,0.0288162684
C,0,-0.0045900203,-0.1393578263,1.5707544995
C,0,1.487482286,-0.0943786981,1.9459084836
C,0,2.1630281512,-0.905349617,0.8256182028
C,0,1.3925393216,-0.5118800766,-0.4578620154
C,0,-1.0014596374,-0.9463260792,-0.7278050791
C,0,-0.9791437852,-0.5520990777,-2.2270735098
C,0,0.4150332933,-1.037551601,-2.6840749138
C,0,1.0337125039,-1.668497549,-1.432102739
C,0,-0.2183639492,-2.2786004943,-0.7600236568
H,0,-0.1980599903,1.0321814486,-0.2522045305
H,0,-0.5938452687,0.6416930064,2.0622654569
H,0,-0.432163498,-1.1017854958,1.8802858726
H,0,1.8459708538,0.9429854221,1.9220544716
H,0,1.6940148973,-0.4853209075,2.9480067428
H,0,3.2376305647,-0.712114463,0.7440285601
H,0,2.0466031886,-1.9779077841,1.0271351825
H,0,1.9363505103,0.2795794494,-0.9854340386
H,0,1.863973379,-2.3529711482,-1.6318745648
H,0,0.2726088304,-1.9608804163,-3.5866416888
H,0,1.0389958471,-0.2956805612,-3.1908870963
H,0,-1.7800547864,-1.0650560137,-2.7754758332
H,0,-1.1258134862,0.5233473612,-2.3785951616
H,0,-2.0053858932,-0.9858059618,-0.2941162878
H,0,-0.7015721432,-3.046310589,-1.3732799052
H,0,-0.025400117,-2.7014565215,0.2302633336
C,0,0.1244642506,-2.9490330419,-4.5841182874
H,0,-0.4274743931,-2.4551145687,-5.3823573781
H,0,-0.4265603484,-3.7597375362,-4.1098945189
H,0,1.1429593689,-3.2176067524,-4.8599974538

TS-TCD R10-CH_3 (σ = 3)

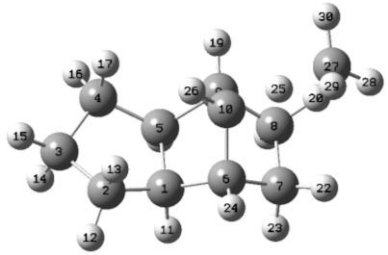

C,0,-0.0012495902,0.0177218978,-0.000114905
C,0,-0.0034069437,-0.0190542994,1.5458368631
C,0,1.4854127257,-0.0327540949,1.9371549743
C,0,2.1254714085,-0.9437971777,0.8740334007
C,0,1.3917050225,-0.587341272,-0.4396871781
C,0,-1.0230410836,-0.9096200906,-0.7158138576
C,0,-0.9643709621,-0.5985907377,-2.2325801119
C,0,0.4144512807,-1.1974604471,-2.6676995292
C,0,0.980227802,-1.7797703987,-1.3480083836
C,0,-0.3006133622,-2.2601458638,-0.6566274773
H,0,-0.1162769455,1.0519053899,-0.3457870217
H,0,-0.5547644708,0.8194521532,1.9836161039
H,0,-0.4838921609,-0.9388363768,1.90336277
H,0,1.9008801769,0.9804658086,1.8590170485
H,0,1.6600223103,-0.375746744,2.9626114854
H,0,3.2100090723,-0.8158862017,0.7955751676
H,0,1.9458226627,-1.9942541604,1.136630212
H,0,1.9833246795,0.1399031891,-1.0083330784
H,0,1.7709916089,-2.5223779241,-1.4882128715
H,0,0.2822617611,-1.9869698671,-3.4139986201
H,0,1.0825927697,-0.4468609625,-3.1025405389
H,0,-1.789345117,-1.0872412685,-2.7602169556
H,0,-1.0404587129,0.4752326096,-2.4326154441
H,0,-2.0293760186,-0.8716261585,-0.2888741247
H,0,-0.9302465178,-3.1974090562,-1.3617173819
H,0,-0.1909614674,-2.7227720196,0.3275884158
C,0,-1.5814720027,-4.2094346719,-2.0323061109
H,0,-1.7435335626,-3.8468061144,-3.0464145256
H,0,-2.5067518554,-4.364711255,-1.4786912299
H,0,-0.9041048774,-5.0612393689,-1.9838748909

Table F.3 TS-TCD R*i*-O Optimized Species

TS-TCD R1-O (σ = 1)

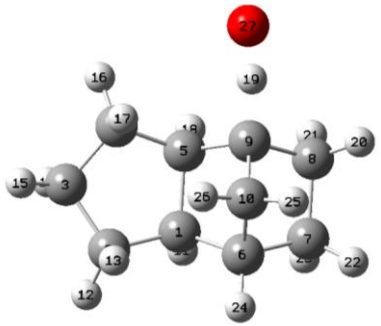

C,0,0.0007335447,-0.011704505,-0.0014121989
C,0,-0.0003672495,0.0052457995,1.544675696
C,0,1.4871538149,0.0217719519,1.9393902036
C,0,2.1476350273,-0.9148050849,0.9118516775
C,0,1.4145404437,-0.6131417562,-0.4158066371
C,0,-1.0049867417,-0.9766831105,-0.683329237
C,0,-0.9502297968,-0.7475153665,-2.2174766249
C,0,0.4461594727,-1.350528523,-2.6253276363
C,0,0.9771155009,-1.8067848566,-1.2653415671
C,0,-0.2759127527,-2.341710147,-0.5602568287
H,0,-0.1197867053,1.0067975165,-0.3868361915
H,0,-0.5608497749,0.8547876783,1.9483073578
H,0,-0.4755171026,-0.9034273033,1.9356989006
H,0,1.8887875273,1.0375567247,1.830638478
H,0,1.6607221815,-0.2855155499,2.9758205811
H,0,3.2283595045,-0.7682868871,0.8278237135
H,0,1.995857885,-1.9609358335,1.2008654025
H,0,1.9922626568,0.0984955385,-1.0143972646
H,0,1.9501638167,-2.7202196545,-1.3533255355
H,0,0.3263541952,-2.1945875267,-3.3110058699
H,0,1.1019606592,-0.6191051089,-3.1058379292
H,0,-1.7638996283,-1.2803455933,-2.7195531554
H,0,-1.0386084766,0.3111983699,-2.480681391
H,0,-2.0150155762,-0.9311582322,-0.2648314605
H,0,-0.7730666336,-3.1478100126,-1.1081267568
H,0,-0.1073201802,-2.6653182798,0.4694014369
O,0,2.8077642184,-3.5303671564,-1.3020073184

TS-TCD R2-O (σ = 1)

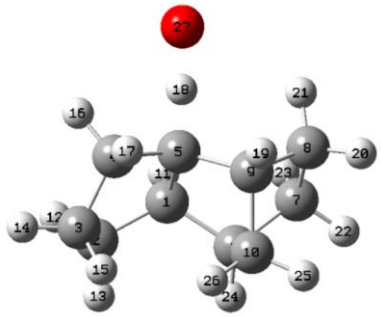

C,0,-0.3676781872,-0.3493371817,-0.943362781
C,0,-1.8592217528,-0.775117388,-1.0171087491
C,0,-2.5303223669,-0.2975896402,0.2906973552
C,0,-1.7159605512,0.942549398,0.7246692276
C,0,-0.2920986759,0.6901184853,0.2194046755
C,0,0.6602572131,-1.4183217039,-0.4818067223
C,0,2.0781782937,-0.8210849602,-0.6594206575
C,0,2.1617799536,0.2501621982,0.4779440226
C,0,0.7789390345,0.1366355748,1.1705636021
C,0,0.5187095301,-1.3898726817,1.0571749636
H,0,-0.0530294676,0.0732094747,-1.9038597315
H,0,-2.3302521148,-0.2806927361,-1.8739643458
H,0,-1.9732839267,-1.8532696385,-1.1739655191
H,0,-3.5917035886,-0.0671408478,0.1537259158
H,0,-2.4734452762,-1.0744784464,1.0602310291
H,0,-2.1149621208,1.8385237688,0.233793816
H,0,-1.7517476207,1.1254687351,1.8037698843
H,0,0.1204332739,1.7808811339,-0.2337116609
H,0,0.7430901881,0.5647941077,2.1756183124
H,0,2.960630771,0.012432254,1.1875124862
H,0,2.3367022883,1.2588598848,0.09739826
H,0,2.8409668925,-1.5958728779,-0.5300840354
H,0,2.2205130036,-0.3883099612,-1.6546760114
H,0,0.5244495855,-2.3904953413,-0.9646054483
H,0,1.2861542044,-1.9805940007,1.5700550234
H,0,-0.4609735957,-1.7045269071,1.424471572
O,0,0.519117013,2.8811692975,-0.7584514834

TS-TCD R3-O (σ = 1)

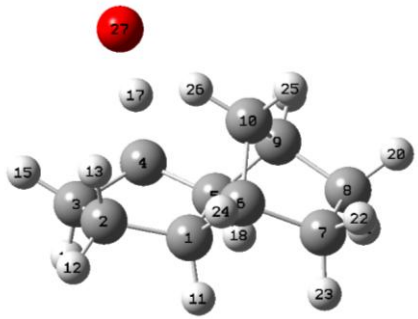

C,0,-0.1229376261,-1.211109603,0.0196939221
C,0,1.2534935949,-1.5241681883,-0.6153061059
C,0,2.2857924977,-0.9936687827,0.3970891095
C,0,1.6289181734,0.2619652021,0.954428968
C,0,0.1242282971,0.0019043044,0.9977479873
C,0,-1.2122277292,-0.6661411111,-0.9349411565
C,0,-2.5372912572,-0.5511964424,-0.1410455769
C,0,-2.2798353983,0.6652235487,0.8095653079
C,0,-0.836382457,1.0935498699,0.4498243911
C,0,-0.8123820281,0.8202632859,-1.0713048304
H,0,-0.4860796635,-2.0901282668,0.564586615
H,0,1.3815693084,-2.5891905586,-0.8313293576
H,0,1.3686508512,-0.9849334397,-1.5622750489
H,0,2.4236093934,-1.7150435933,1.2170711918
H,0,3.2756744649,-0.8124369143,-0.0347707142
H,0,2.0741009747,0.6946001125,1.8547425235
H,0,1.8809624618,1.166628749,0.1023005987
H,0,-0.1469155821,-0.2403219129,2.0345701455
H,0,-0.579374164,2.1081421218,0.767003203
H,0,-2.9822896632,1.4796637698,0.6049895153
H,0,-2.3847420743,0.4060380121,1.8683359158
H,0,-3.3761632659,-0.351533745,-0.8156283589
H,0,-2.7726246245,-1.4712278034,0.4043960415
H,0,-1.3018685913,-1.2310115614,-1.867548094
H,0,-1.5563960938,1.4119695489,-1.6161702819
H,0,0.1655249025,0.9893467643,-1.5277778631
O,0,2.2570002985,1.9847026335,-0.7934320477

Table F.3 TS-TCD R*i*-O Optimized Species (Continued)

TS-TCD R4-O (σ = 1)

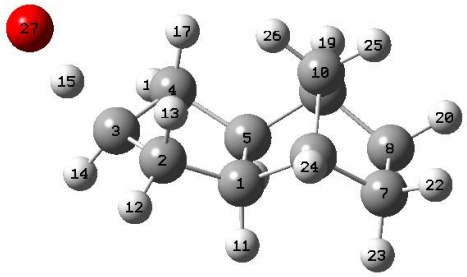

C,0,0.0039536724,-0.0091730362,-0.0067044401
C,0,0.0043971219,0.0478349382,1.5448755464
C,0,1.4809745076,0.089948537,1.9170533749
C,0,2.2009192224,-0.7897478586,0.9029496907
C,0,1.428996573,-0.5526883407,-0.4231745739
C,0,-0.9584988439,-1.0379143618,-0.6482730001
C,0,-0.9343973288,-0.8266713741,-2.1815989185
C,0,0.4760631109,-1.364785503,-2.5937569101
C,0,1.088212403,-1.8186094087,-1.2463196531
C,0,-0.1624046762,-2.3559824597,-0.5140097152
H,0,-0.1747996002,0.9941499588,-0.4079619222
H,0,-0.5618405203,0.8962177935,1.9392278467
H,0,-0.4472888794,-0.8629508625,1.9582777184
H,0,1.9012653975,1.0920850708,2.0475596925
H,0,1.6247761401,-0.4304040408,3.0878320644
H,0,3.2677135003,-0.5640030639,0.8200051545
H,0,2.11526247,-1.8400781381,1.2094287996
H,0,1.9718783919,0.1753321645,-1.0354508068
H,0,1.9251843675,-2.5153001995,-1.3510344226
H,0,0.3882861284,-2.2115658829,-3.2823230876
H,0,1.08971625,-0.6065018269,-3.0911937004
H,0,-1.7313858669,-1.4027692982,-2.6630385202
H,0,-1.0838495652,0.2228196588,-2.4559006867
H,0,-1.9630234336,-1.0322153536,-0.2149571885
H,0,-0.6348500537,-3.1963361698,-1.0338783508
H,0,0.0249450029,-2.6577252606,0.5210591715
O,0,1.6739315652,-1.0962234749,4.1212272308

TS-TCD R9-O (σ = 1)

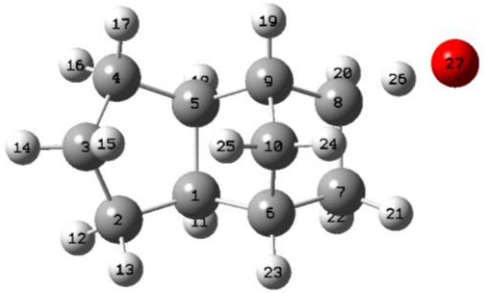

C,0,-0.0041122574,-0.0102041797,-0.0113037988
C,0,-0.065142348,0.2166675098,1.5213940783
C,0,1.3648267919,0.0137109143,2.0650382975
C,0,2.2863631761,0.4223910127,0.8983882351
C,0,1.5178549315,0.1024289142,-0.4093512247
C,0,-0.3861392649,-1.4277078127,-0.5122151141
C,0,-0.3992469784,-1.3861582731,-2.0633679996
C,0,1.1025720118,-1.2989125197,-2.4023644077
C,0,1.8105609048,-1.2926085799,-1.0479403093
C,0,0.8955609842,-2.2497109199,-0.2519953549
H,0,-0.6203574406,0.7375972253,-0.5219293119
H,0,-0.3866136731,1.2463701031,1.7170281115
H,0,-0.796385781,-0.4372927801,2.009689803
H,0,1.5527869864,0.6059804151,2.9667318842
H,0,1.5311179998,-1.032138468,2.3416050291
H,0,2.4733760187,1.5019876497,0.9411592514
H,0,3.2651338113,-0.0681038755,0.9399659503
H,0,1.698875957,0.8903184652,-1.1479897633
H,0,2.8742991469,-1.5411212463,-1.0907209628
H,0,1.4113562089,-0.543059836,-3.1297058602
H,0,-0.845851105,-2.2996109323,-2.4739704038
H,0,-0.9682678181,-0.5404646513,-2.4654406263
H,0,-1.3106336741,-1.8171967245,-0.0767413556
H,0,0.8642667167,-3.2470402094,-0.7010935278
H,0,1.1582525007,-2.3462757574,0.8024939728
H,0,1.4185798053,-2.385338667,-2.9657645284
O,0,1.6372492952,-3.5618162549,-3.3784353851

TS-TCD R10-O (σ = 1)

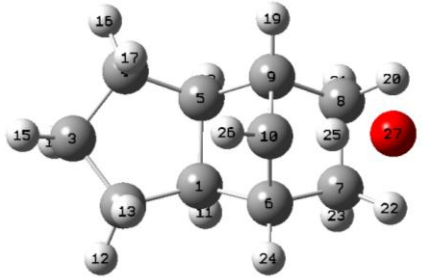

C,0,0.0024246343,0.0058295424,0.004417627
C,0,0.0051537242,0.0060966047,1.550752689
C,0,1.495782144,0.006305791,1.9355672677
C,0,2.1347486663,-0.9301959456,0.8940569437
C,0,1.3958616997,-0.6068103646,-0.4252727241
C,0,-1.0228509767,-0.9357317202,-0.6902238314
C,0,-0.968287876,-0.6664522325,-2.2153152103
C,0,0.4106345665,-1.272709401,-2.6405284969
C,0,0.9870190605,-1.8193947929,-1.3100013856
C,0,-0.2857736513,-2.2715146472,-0.5941718961
H,0,-0.1189114105,1.0291841783,-0.368385216
H,0,-0.5466041005,0.8539808158,1.9687282293
H,0,-0.4727441686,-0.9046088223,1.9340884009
H,0,1.9078237124,1.0181398624,1.8291396279
H,0,1.6752522683,-0.3098559736,2.9683534938
H,0,3.2182515719,-0.8012602017,0.8077716359
H,0,1.9606635593,-1.9744711922,1.1837159338
H,0,1.9828557187,0.1051145749,-1.0165072846
H,0,1.7749882585,-2.5672590349,-1.4298371188
H,0,0.2655382288,-2.0858398018,-3.3565873254
H,0,1.0774759608,-0.5356670236,-3.0986961052
H,0,-1.7858726501,-1.1839139481,-2.7240062849
H,0,-1.0528942234,0.4009679521,-2.4417714861
H,0,-2.0258444369,-0.8961764894,-0.2577926678
H,0,-0.9095937365,-3.1784656609,-1.3240207264
H,0,-0.2021564452,-2.7629985727,0.3777391633
O,0,-1.4708409607,-3.9221532598,-2.0844684702

Table F.4 TS-TCD R*i*-OH Optimized Species

TS-TCD R1-OH (σ = 1)

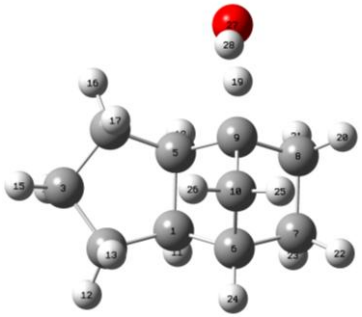

C,0,-0.0141084279,0.003498079,0.0086514109
C,0,-0.0036620579,-0.0311640521,1.5465263359
C,0,1.4791779347,0.0479241813,1.9175160998
C,0,2.1464278311,-0.851013153,0.8743635852
C,0,1.3992226962,-0.5303456567,-0.4299582874
C,0,-0.9842497681,-0.9730309711,-0.6792705091
C,0,-0.952447939,-0.6972545598,-2.1946792088
C,0,0.4453126117,-1.2356350934,-2.6306674142
C,0,1.0268054923,-1.7263697816,-1.3036871048
C,0,-0.2071883684,-2.2995503706,-0.6033670386
H,0,-0.1807230542,1.0258847837,-0.3406662151
H,0,-0.6029312417,0.7696232259,1.981891588
H,0,-0.4192703669,-0.977052731,1.9048775343
H,0,1.8329251659,1.0752025963,1.7974384638
H,0,1.6850434052,-0.2541307643,2.945416725
H,0,3.2207239077,-0.6920333128,0.7820643458
H,0,2.0020522411,-1.9002000829,1.1433261253
H,0,1.9525099,0.2136954967,-1.0077346662
H,0,1.9406871661,-2.4625582828,-1.4495984949
H,0,0.347482491,-2.0585057841,-3.3397909806
H,0,1.0719727751,-0.4716332782,-3.090980022
H,0,-1.7523062026,-1.2384403035,-2.7026791681
H,0,-1.0801847701,0.3632581017,-2.4159988487
H,0,-1.9871356492,-0.9755723711,-0.2489615637
H,0,-0.6842426927,-3.1034578297,-1.1675948104
H,0,-0.0225223636,-2.6415745398,0.4150541624
O,0,2.8361374222,-3.4496307658,-1.3706954932
H,0,2.2821888188,-4.0729229217,-0.8722408746

TS-TCD R2-OH (σ = 1)

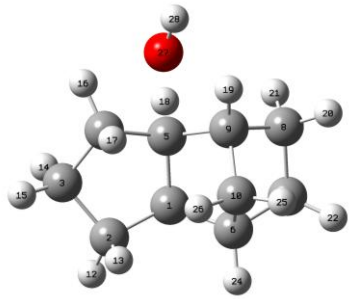

C,0,-0.3681064421,-0.5683784173,-0.8279538592
C,0,-1.7445700238,-1.2362787527,-0.6733596851
C,0,-2.6313820528,-0.135616481,-0.0848471327
C,0,-1.7129843213,0.5350199892,0.9399672365
C,0,-0.347718663,0.5597495384,0.2488106259
C,0,0.8559465806,-1.4162795464,-0.4431659187
C,0,2.1187779108,-0.6209378684,-0.8158283191
C,0,2.1377800334,0.5311317275,0.2291914875
C,0,0.8916632804,0.2477295287,1.0884167178
C,0,0.8669594373,-1.2913561118,1.0885196581
H,0,-0.2617066402,-0.1621400137,-1.8373159385
H,0,-2.1192033758,-1.6364485619,-1.6162707565
H,0,-1.6802445485,-2.0695340025,0.0320409628
H,0,-2.891337271,0.5838655911,-0.8648338165
H,0,-3.5599381331,-0.5111314217,0.3472206562
H,0,-2.0460917473,1.5302024661,1.2367432756
H,0,-1.6575168112,-0.076852638,1.8457178018
H,0,-0.2370529775,1.5844348409,-0.2932765446
H,0,0.9002627571,0.731584449,2.0667195614
H,0,3.0408254874,0.4906478538,0.8405925325
H,0,2.0861509034,1.5153672836,-0.234281543
H,0,3.0078880522,-1.2469697207,-0.7227295186
H,0,2.0796097149,-0.2545950005,-1.8424044093
H,0,0.8332336076,-2.4301785805,-0.8458776629
H,0,1.7594053184,-1.7258829611,1.5440764921
H,0,-0.0136810245,-1.7150252195,1.5726270109
O,0,-0.0834606439,2.893253073,-0.754488866
H,0,0.1572855925,3.2747179563,0.1068519516

TS-TCD R3-OH (σ = 1)

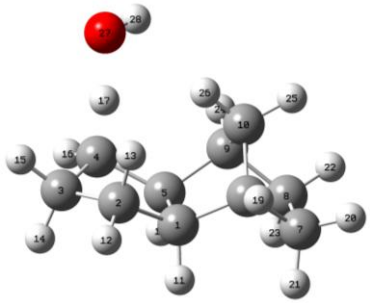

C,0,-0.2027024736,-1.232555958,-0.0325111437
C,0,1.1557167134,-1.5651698559,-0.6731673194
C,0,2.1837954371,-1.1639025591,0.3873581109
C,0,1.6018416761,0.1266636312,0.9480706327
C,0,0.0885613998,-0.0871575362,0.9978278391
C,0,-1.248349586,-0.5991506477,-0.9628371002
C,0,-2.5645681514,-0.4634884756,-0.1768614385
C,0,-2.2641520192,0.6883754671,0.8253484915
C,0,-0.8073907355,1.0615195127,0.5009358162
C,0,-0.7812452533,0.862509575,-1.0229880918
H,0,-0.6061109439,-2.1203890348,0.4622362426
H,0,1.2282092156,-2.6126746991,-0.968166885
H,0,1.309717243,-0.9598623211,-1.5695344034
H,0,2.2201846938,-1.9187532541,1.1790731153
H,0,3.1937643817,-1.040875723,-0.0044588161
H,0,2.0442187653,0.4760560801,1.8808613815
H,0,1.878843149,0.9485696738,0.1561444761
H,0,-0.1925034148,-0.3741775341,2.0161029064
H,0,-1.3534565682,-1.1127171836,-1.9198054261
H,0,-3.3859357996,-0.1955016897,-0.843439184
H,0,-2.838075545,-1.3948777171,0.3214589477
H,0,-2.9247708672,1.5392874792,0.6507326915
H,0,-2.3864315587,0.3866939894,1.8667755854
H,0,-0.5124167496,2.0451367035,0.8731867229
H,0,-1.4940041747,1.5090795204,-1.5403623168
H,0,0.2047220886,1.0015306459,-1.4614387685
O,0,2.3579063062,1.9264003435,-0.6834419679
H,0,1.7889617711,2.6391335677,-0.3456430978

Table F.4 TS-TCD R*i*-OH Optimized Species (Continued)

TS-TCD R4-OH (σ = 1)

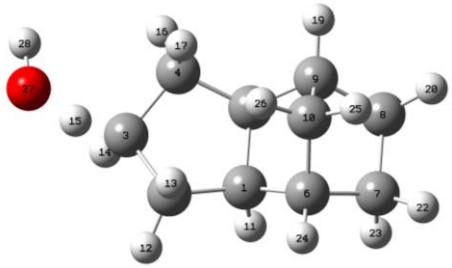

C,0,0.0057648628,0.0425073617,-0.0118856862
C,0,-0.0056958567,0.0816912425,1.5286336123
C,0,1.4691284683,0.1062115188,1.9050674176
C,0,2.1248061062,-0.8465142223,0.9152732276
C,0,1.3973749726,-0.5630134974,-0.4124285743
C,0,-0.9924778853,-0.931439421,-0.6583444607
C,0,-0.9428763857,-0.7201117946,-2.1812880269
C,0,0.4370115751,-1.319280813,-2.5784427703
C,0,1.0102594019,-1.8023173589,-1.2350819375
C,0,-0.2634026331,-2.2761312649,-0.5190091072
H,0,-0.1222810744,1.0528739508,-0.4088191536
H,0,-0.5667116364,0.9285692017,1.9234669996
H,0,-0.4598346916,-0.8283352016,1.9285186188
H,0,1.8973717326,1.1098640977,1.8704845004
H,0,1.5974668737,-0.2633329104,3.0195904032
H,0,3.2049909528,-0.7174310732,0.8339399399
H,0,1.9377740018,-1.8743098775,1.2365621582
H,0,1.9831339593,0.1372150408,-1.0135966301
H,0,1.8135014767,-2.5345868655,-1.3321486555
H,0,0.3150459853,-2.1563237845,-3.2679312168
H,0,1.0911256249,-0.5910575011,-3.0604424671
H,0,-1.7568526002,-1.2572523468,-2.6710276527
H,0,-1.0388033173,0.333443809,-2.4482038238
H,0,-1.9963442337,-0.8776367278,-0.2341950984
H,0,-0.7682677145,-3.0880217877,-1.0467517391
H,0,-0.1002218631,-2.5837560727,0.5143692743
O,0,1.8611749377,-0.9845744159,4.1219429753
H,0,2.7999571612,-1.1480118126,3.9316443177

TS-TCD R9-OH (σ = 1)

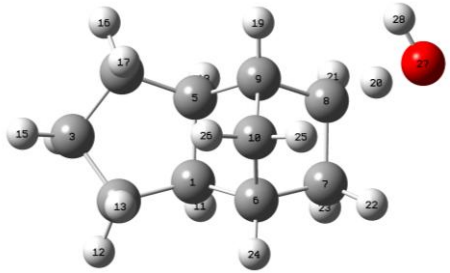

C,0,0.006559977,0.034687985,0.0153600198
C,0,0.0273313757,-0.0073223511,1.5525823756
C,0,1.5152342887,-0.0456775926,1.9083250335
C,0,2.0953067883,-0.993939821,0.8565028873
C,0,1.3590629874,-0.6154923145,-0.4406264787
C,0,-1.0482013081,-0.8489160758,-0.669063796
C,0,-0.9949282699,-0.5596027661,-2.1805789334
C,0,0.3320200075,-1.2248631157,-2.6071974312
C,0,0.8970153696,-1.8000049607,-1.3091383534
C,0,-0.3961442564,-2.2390384223,-0.6054630854
H,0,-0.0747833524,1.070505643,-0.3250970922
H,0,-0.5025669532,0.8361421472,1.9970445519
H,0,-0.4568377476,-0.9195111556,1.91172562
H,0,1.9486228035,0.9500948986,1.7840558385
H,0,1.7087197882,-0.3652124427,2.9333735321
H,0,3.1788742889,-0.919585666,0.7555863341
H,0,1.8650205873,-2.0269757528,1.1312670047
H,0,1.9665606525,0.0820906901,-1.0235488124
H,0,1.6643909266,-2.5640031109,-1.4493356881
H,0,0.0531506134,-2.1031437528,-3.3312552431
H,0,1.022117366,-0.5904992976,-3.164716429
H,0,-1.8381596698,-1.020039967,-2.6981598014
H,0,-1.015093463,0.5100844652,-2.3958239753
H,0,-2.0464385434,-0.7626824522,-0.237363614
H,0,-0.9404609225,-2.9905841441,-1.1786130445
H,0,-0.2410074602,-2.6050720373,0.4095651746
O,0,-0.3237194869,-3.3032007952,-3.8816511995
H,0,0.4641532007,-3.7998751692,-3.6036289847

TS-TCD R10-OH (σ = 1)

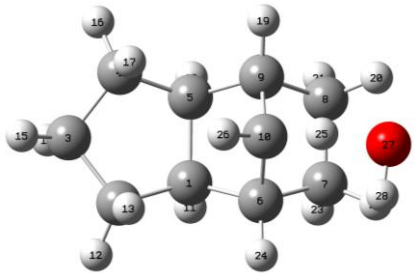

C,0,-0.0231920058,-0.0623515112,-0.0032384355
C,0,-0.0182772823,-0.080159972,1.5346601176
C,0,1.4621185644,0.0233837666,1.9078568968
C,0,2.1396411877,-0.8820369049,0.8769827117
C,0,1.3915003869,-0.5893201156,-0.4345031273
C,0,-0.9846629101,-1.054364588,-0.6828142621
C,0,-0.9529291651,-0.7892584012,-2.1984837327
C,0,0.4467331656,-1.3177585902,-2.6245215691
C,0,1.056211308,-1.8161148788,-1.3030290306
C,0,-0.1844660242,-2.35317245,-0.589491645
H,0,-0.2027107809,0.9538615148,-0.3642296096
H,0,-0.6298482388,0.7162960469,1.9606378221
H,0,-0.42046118,-1.0285668247,1.9020404523
H,0,1.8036260407,1.0530701551,1.7739052518
H,0,1.6701516264,-0.2625916383,2.939900722
H,0,3.21325724,-0.7111555553,0.7887537657
H,0,2.0011596264,-1.9282193443,1.1639658153
H,0,1.9381897989,0.15548132,-1.0190666289
H,0,1.8850116183,-2.5140434421,-1.4249383223
H,0,0.3442791889,-2.1412329901,-3.3309319913
H,0,1.0670206615,-0.5493123539,-3.0880547459
H,0,-1.7388609051,-1.3506414858,-2.7026296046
H,0,-1.095079359,0.2687537156,-2.4231443784
H,0,-1.9854915363,-1.0628640003,-0.2473072326
H,0,-0.6674095766,-3.2167965622,-1.2398348527
H,0,-0.0356523374,-2.7647767181,0.408534956
O,0,-1.425798243,-4.0210150027,-1.9967814445
H,0,-2.2726031267,-3.8270242593,-1.5607389155

Table F.5 TS-TCD R*i*-OOH Optimized Species

TS-TCD R1-OOH (σ = 1, OI)

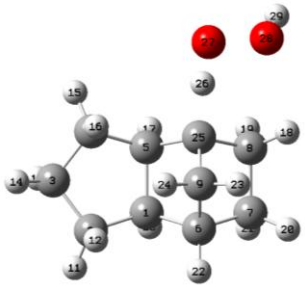

C,0,-0.0006298059,-0.0002705644,0.000595284
C,0,-0.0011583704,-0.0021689443,1.5466427801
C,0,1.4858316024,-0.0001248544,1.9432266344
C,0,2.1379821521,-0.9312277124,0.9056540153
C,0,1.4144095991,-0.6032631949,-0.4214319662
C,0,-1.0116942822,-0.9547221673,-0.6912141011
C,0,-0.9663824885,-0.7004810546,-2.2216109746
C,0,0.4346454094,-1.2870701963,-2.6405149972
C,0,-0.2812789718,-2.3229226035,-0.5971485114
H,0,-0.1166213817,1.0228144733,-0.3738829725
H,0,-0.5565063049,0.8456126674,1.9610663415
H,0,-0.4817175118,-0.913022716,1.9255906998
H,0,1.8961378226,1.0133972054,1.8457322642
H,0,1.6565890728,-0.3203642186,2.9762500184
H,0,3.221367701,-0.7984695026,0.8287918715
H,0,1.9651811521,-1.9773340047,1.1849107315
H,0,1.9983458935,0.1184911491,-1.0017928275
H,0,0.3246007041,-2.1198166337,-3.3419666828
H,0,1.0856219912,-0.5383333326,-3.1019214648
H,0,-1.778378712,-1.2310064338,-2.7288340067
H,0,-1.062010349,0.3619938596,-2.4673266425
H,0,-2.0190748342,-0.9131870714,-0.2654120202
H,0,-0.7773275796,-3.1191771055,-1.1594538972
H,0,-0.1120308228,-2.6664199222,0.4260683768
C,0,0.966263735,-1.7715178813,-1.2930121731
H,0,1.97911509,-2.7724277358,-1.511653819
O,0,2.7328521814,-3.5588556541,-1.744266047
O,0,2.235712424,-4.1446790376,-2.9473834821
H,0,2.7904298449,-3.7097421607,-3.6162275605

TS-TCD R2-OOH (σ = 1, OI)

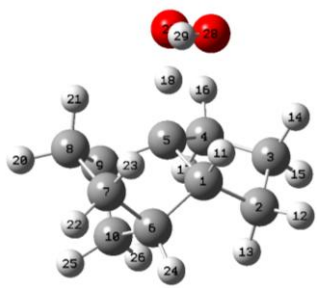

C,0,0.0080914514,0.0026228024,0.018338042
C,0,0.0006722436,-0.0121914287,1.565570142
C,0,1.4933574003,-0.0216506032,1.9506978291
C,0,2.1347612737,-0.959273015,0.9074614815
C,0,1.33601825,-0.6964777,-0.366454633
C,0,-1.0406745342,-0.8626644485,-0.7277051242
C,0,-0.9258635969,-0.553240508,-2.2413166764
C,0,0.4314013161,-1.2205648347,-2.6448426993
C,0,0.9381962751,-1.8299039254,-1.3109800514
C,0,-0.4047229059,-2.2715350142,-0.6626947742
H,0,-0.0161403709,1.0423873254,-0.3328478781
H,0,-0.5464782676,0.8349971558,1.9907886448
H,0,-0.4817971604,-0.9271951999,1.9329058838
H,0,1.9103050263,0.9863414233,1.8408809847
H,0,1.6712690895,-0.3415787374,2.9822553064
H,0,3.2098742394,-0.7922387162,0.7800744813
H,0,2.0124291139,-2.0110025475,1.2089170581
H,0,2.0748985113,0.2320400272,-1.0461167203
H,0,1.6981808076,-2.6059429783,-1.4328622293
H,0,0.2764301959,-2.0098333969,-3.3873172793
H,0,1.1521055645,-0.5118555013,-3.060076874
H,0,-1.761567829,-0.9968849335,-2.7921876817
H,0,-0.9442397918,0.5236453954,-2.4403532697
H,0,-2.056164129,-0.7704795687,-0.3316346523
H,0,-0.9391833716,-3.0180946301,-1.2610710453
H,0,-0.2915358984,-2.6606833687,0.3538333823
O,0,2.6952053276,1.0419112982,-1.6240817091
O,0,1.9321968746,2.2337121577,-1.4888256336
H,0,1.4758711081,2.2759967854,-2.3461329486

TS-TCD R3-OOH (σ = 1, OI)

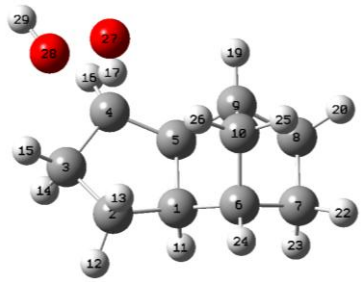

C,0,-0.0001211621,0.0001053528,0.0000348458
C,0,-0.0017412555,-0.0006175857,1.5481248969
C,0,1.4847588858,-0.0030157418,1.9559288815
C,0,2.1561658446,-0.8206641755,0.8697283774
C,0,1.389933268,-0.6098461707,-0.4279459812
C,0,-1.0150417426,-0.9470506507,-0.6838208013
C,0,-0.9490291559,-0.7073522476,-2.2127197847
C,0,0.4236859223,-1.3424379081,-2.616039436
C,0,0.9821545327,-1.8554009464,-1.2670544185
C,0,-0.3124146516,-2.3179117016,-0.5617412795
H,0,-0.1120388502,1.0256531787,-0.3704794716
H,0,-0.5511307368,0.849497744,1.9641858265
H,0,-0.4796865986,-0.9099728353,1.9293624239
H,0,1.8926607338,1.0209417853,1.9440722994
H,0,1.6566352339,-0.4035588889,2.9610161746
H,0,3.2479776437,-0.7915897007,0.8134144398
H,0,1.9923780346,-2.114599174,1.3107481877
H,0,1.9678216734,0.0795715234,-1.0602342793
H,0,1.7757315768,-2.6012692407,-1.36545995
H,0,0.2821148191,-2.1746621478,-3.3132572853
H,0,1.0966288215,-0.6261620502,-3.0992699304
H,0,-1.7785750573,-1.2114082974,-2.7193277752
H,0,-1.0133531615,0.3560714729,-2.4665435169
H,0,-2.0253106683,-0.8821453171,-0.2688327477
H,0,-0.8308563329,-3.1112643902,-1.1117252942
H,0,-0.1486615904,-2.6586182548,0.4626595635
O,0,1.9016656342,-3.1886304379,1.7748900018
O,0,1.8407756578,-2.9692487502,3.1754326998
H,0,2.764962282,-3.1130418146,3.4415081809

Table F.5 TS-TCD R*i*-OOH Optimized Species (Continued)

TS-TCD R4-OOH (σ = 1, OI)

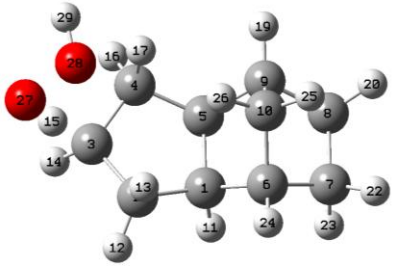

C,0,0.0953650407,0.2201542681,-0.0781467565
C,0,0.0939504341,0.5015084534,1.4497099112
C,0,1.5363082655,0.3135199546,1.8916752286
C,0,2.1655809751,-0.7223768814,0.9766215803
C,0,1.4291444244,-0.5691621677,-0.3830000245
C,0,-1.0020092883,-0.7497970491,-0.57985031
C,0,-0.9553494929,-0.7765152738,-2.1260717038
C,0,0.366720329,-1.5568677235,-2.4288470646
C,0,0.9138585426,-1.883765245,-1.0182874749
C,0,-0.3948574709,-2.1283551294,-0.2326724836
H,0,0.0582068753,1.1678277243,-0.6261176176
H,0,-0.2963549025,1.4932430701,1.6964863728
H,0,-0.546561842,-0.2268697081,1.9648484678
H,0,2.1175513436,1.2188129299,2.0851568139
H,0,1.4787259095,-0.256487147,3.1428478796
H,0,3.2499948547,-0.6073208446,0.8864775143
H,0,1.9813575149,-1.7271093561,1.3837756041
H,0,2.0675542182,-0.0210577521,-1.0842703063
H,0,1.6471440983,-2.6959526755,-1.0049933117
H,0,0.1618407949,-2.4766993411,-2.9865513838
H,0,1.0779209872,-0.9713367783,-3.0209168641
H,0,-1.8252041016,-1.3049675154,-2.5300045651
H,0,-0.9608674017,0.2305717524,-2.5562356477
H,0,-1.9940797214,-0.5406710273,-0.1688237521
H,0,-0.9807303328,-2.9661118096,-0.6265867363
H,0,-0.2452156627,-2.2874957944,0.8396697988
O,0,1.3668492515,-0.8449823428,4.1384261756
O,0,0.9375294395,-2.1325566664,3.7206540946
H,0,1.7661080993,-2.6402382961,3.7549454067

TS-TCD R9-OOH (σ = 1, OI)

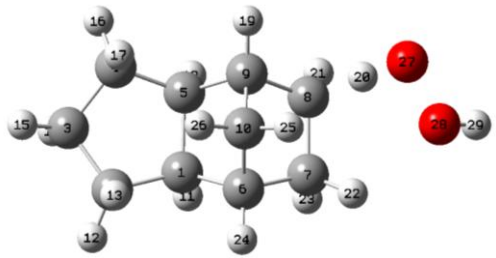

C,0,0.0014447089,0.0130844084,0.0189916567
C,0,-0.001300108,0.0107745491,1.5657424928
C,0,1.4873831785,0.0186141504,1.9578358533
C,0,2.1381485684,-0.9097463516,0.9162948834
C,0,1.3978578275,-0.5863257441,-0.4047469297
C,0,-1.0091180155,-0.9342821769,-0.6743090517
C,0,-0.9416687544,-0.6643312925,-2.2013542563
C,0,0.4220947905,-1.2541488491,-2.5751703793
C,0,0.9960315387,-1.8131773692,-1.2801362161
C,0,-0.2946584104,-2.3017056094,-0.5825288248
H,0,-0.1199808169,1.0389140247,-0.3472073357
H,0,-0.5584366093,0.8554982808,1.9835172416
H,0,-0.476481927,-0.9026305041,1.945420125
H,0,1.8933757443,1.0334522063,1.8561407922
H,0,1.6651015006,-0.2994449618,2.9906248463
H,0,3.2205549363,-0.7700189413,0.8320128368
H,0,1.9723121794,-1.9563895554,1.2008262785
H,0,1.9845824278,0.1307701269,-0.9893389097
H,0,1.7973277317,-2.5456929098,-1.4098802405
H,0,0.1401762956,-2.3567955148,-3.3537784939
H,0,1.0842194118,-0.6739544964,-3.2228616081
H,0,-1.7514916437,-1.1906956462,-2.7260202418
H,0,-1.0272591782,0.3993059249,-2.4550547492
H,0,-2.0214353954,-0.88843082,-0.2628069213
H,0,-0.7991428168,-3.0931235242,-1.1440338363
H,0,-0.1349179182,-2.6475645793,0.4427537787
O,0,-0.1400099512,-3.3091816406,-3.9621447682
O,0,-1.5432582335,-3.205696612,-4.156302711
H,0,-1.5947719654,-2.824713519,-5.0494882204

TS-TCD R10-OOH (σ = 1, OI)

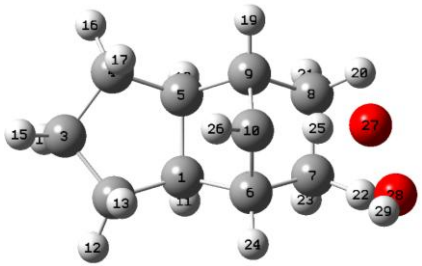

C,0,-0.0483664074,-0.0823057863,0.0363027679
C,0,-0.0155246947,-0.1058034367,1.5817697651
C,0,1.4774240676,0.0028111434,1.9389468483
C,0,2.1653327334,-0.8691907258,0.8731253899
C,0,1.3787276718,-0.5869299553,-0.4281007687
C,0,-1.0157418488,-1.0861546764,-0.6594929668
C,0,-0.9985613142,-0.7845444109,-2.1803737885
C,0,0.4068165514,-1.3019642373,-2.6355261702
C,0,1.0409865591,-1.8193757887,-1.3193643017
C,0,-0.1838514639,-2.361915182,-0.590940091
H,0,-0.2491066549,0.9357507201,-0.3163927611
H,0,-0.6222317189,0.6904470969,2.0247747517
H,0,-0.4141334432,-1.0565990269,1.9582791983
H,0,1.809653843,1.0442493644,1.8392620241
H,0,1.7005584006,-0.3115018581,2.9639774889
H,0,3.2341756577,-0.6568075785,0.7693921048
H,0,2.0770089475,-1.9273909256,1.1513240457
H,0,1.9004340168,0.1729893323,-1.0210708623
H,0,1.8781114118,-2.5081711499,-1.4587854852
H,0,0.3003172916,-2.1194591574,-3.353280785
H,0,1.0177814837,-0.5225311646,-3.1018645796
H,0,-1.7990059735,-1.3289066295,-2.6867145156
H,0,-1.1409866843,0.2826154622,-2.3789174648
H,0,-2.0141167572,-1.1231530677,-0.2168234845
H,0,-0.8017916171,-3.362686919,-1.3875635864
H,0,-0.0618516206,-2.8800882542,0.3628014617
O,0,-1.2708885757,-4.1506212455,-2.0509212076
O,0,-2.6475320713,-3.7922678364,-2.1018025302
H,0,-3.0297066065,-4.3776246406,-1.4265088507

Table F.6 Moments of Inertia[a]

Species	I_a	I_b	I_c
TS-TCD R1-H	716.93551	1541.57819	1809.38731
TS-TCD R2-H	706.03316	1560.93786	1780.25230
TS-TCD R3-H	700.94624	1562.39707	1785.92290
TS-TCD R4-H	682.21119	1602.23884	1829.54172
TS-TCD R9-H	680.24804	1587.98571	1825.47196
TS-TCD R10-H	695.74856	1586.26428	1796.70712
TS-TCD R1-CH_3	1307.11036	1724.04928	2537.71353
TS-TCD R2-CH_3	1275.90320	1710.73569	2231.79456
TS-TCD R3-CH_3	1092.50941	1963.55848	2354.77256
TS-TCD R4-CH_3	758.67795	2729.54872	2890.74347
TS-TCD R9-CH_3	761.40671	2570.32583	2860.58812
TS-TCD R10-CH_3	954.99829	2403.91867	2441.91048
TS-TCD R1-O	1289.73932	1640.24558	2440.89535
TS-TCD R2-O	1260.73027	1639.17692	2129.50929
TS-TCD R3-O	1033.58473	1916.72930	2232.51220
TS-TCD R4-O	758.76497	2611.20314	2762.19693
TS-TCD R9-O	786.72059	2383.43197	2617.38688
TS-TCD R10-O	884.38507	2352.93118	2375.35914
TS-TCD R1-OH	1303.59626	1641.08217	2443.27505
TS-TCD R2-OH	1268.12192	1652.93705	2207.60034
TS-TCD R3-OH	1058.62190	1912.86641	2262.10424
TS-TCD R4-OH	736.53871	2681.75144	2849.70762
TS-TCD R9-OH	754.26873	2472.84505	2741.69280
TS-TCD R10-OH	892.84988	2353.46332	2393.68852
TS-TCD R1-OOH	1322.18120	2628.77198	3456.89305
TS-TCD R2-OOH	1726.75323	1891.48006	2646.14299
TS-TCD R3-OOH	1144.39655	2736.04270	3094.47826
TS-TCD R4-OOH	987.24254	3265.22685	3355.24071
TS-TCD R9-OOH	773.27725	3573.13699	3840.42861
TS-TCD R10-OOH	1022.29369	3215.60622	3338.30412

[a] AMU $Bohr^2$.

Table F.7 Vibrational Frequencies

Species	Frequencies (cm^{-1})									
TS-TCD R1-H	-1082.95	134.96	176.47	234.74	256.03	286.78	321.07	330.09	397.03	493.60
	523.38	551.24	664.13	723.86	747.24	780.24	829.78	835.72	865.73	883.97
	893.47	914.85	918.67	927.05	957.28	971.79	993.98	1004.49	1043.72	1051.96
	1060.83	1067.26	1082.96	1135.96	1146.57	1156.95	1187.73	1198.48	1207.01	1223.61
	1237.21	1256.76	1268.51	1275.23	1300.57	1308.31	1320.93	1322.74	1327.28	1344.77
	1352.66	1364.52	1378.45	1500.17	1502.64	1504.74	1511.34	1523.55	1532.95	1834.39
	3036.63	3040.12	3049.53	3051.06	3054.09	3063.46	3067.71	3071.74	3087.64	3091.54
	3094.47	3095.55	3104.37	3114.26	3124.79					
TS-TCD R2-H	-1097.82	132.50	170.90	257.96	293.30	303.85	329.79	354.66	396.46	488.57
	535.13	553.98	652.83	728.46	749.01	795.27	829.59	862.63	871.65	890.83
	894.72	908.37	914.04	923.15	961.54	965.91	995.16	1019.95	1046.75	1053.62
	1064.52	1083.99	1092.15	1139.08	1149.35	1172.55	1184.14	1198.13	1222.23	1232.72
	1254.53	1258.18	1268.78	1288.48	1291.37	1311.58	1320.92	1322.05	1335.17	1348.87
	1352.07	1355.02	1371.57	1460.78	1492.01	1502.35	1506.73	1510.53	1521.46	1532.65
	3018.91	3036.87	3041.19	3045.07	3054.24	3058.49	3065.88	3078.46	3091.85	3093.28
	3095.58	3101.09	3102.72	3110.01	3116.24					
TS-TCD R3-H	-1207.35	134.88	157.04	263.89	282.68	306.57	340.00	388.30	400.83	501.28
	533.39	590.23	713.55	740.67	753.51	794.75	830.39	864.92	870.35	891.52
	903.25	919.27	926.88	931.49	959.49	965.30	995.24	1002.31	1042.15	1051.24
	1056.65	1058.64	1072.53	1138.80	1147.46	1170.28	1198.51	1203.90	1214.09	1231.19
	1247.61	1252.91	1293.05	1298.16	1299.65	1306.14	1319.62	1323.39	1330.62	1334.91
	1343.83	1360.42	1361.95	1376.11	1482.74	1495.27	1505.26	1506.97	1518.99	1534.03
	3010.99	3020.16	3048.55	3050.60	3054.24	3060.15	3063.29	3081.21	3086.29	3092.69
	3099.38	3102.16	3107.65	3112.39	3119.09					
TS-TCD R4-H	-1190.18	129.15	133.94	264.46	276.90	280.90	335.27	361.03	395.41	499.22
	534.42	581.97	677.70	740.37	761.55	794.31	829.07	860.84	880.84	892.09
	894.24	922.69	929.65	938.71	958.30	966.01	1001.07	1025.76	1037.69	1048.87
	1054.21	1065.41	1071.55	1141.88	1155.91	1169.87	1182.22	1210.33	1215.60	1231.46
	1252.48	1259.81	1274.78	1286.40	1296.08	1304.89	1309.88	1315.05	1327.58	1335.40
	1352.57	1355.94	1370.87	1371.03	1501.90	1503.92	1503.96	1517.85	1534.45	1580.24
	3030.46	3034.34	3049.50	3052.58	3059.30	3061.15	3065.83	3086.14	3091.63	3091.99
	3096.61	3100.52	3105.72	3108.42	3114.92					
TS-TCD R9-H	-1180.88	136.38	171.30	222.59	277.12	301.04	332.83	382.14	413.10	496.16
	543.64	567.15	669.34	739.40	764.70	796.05	861.57	870.22	885.68	896.17
	897.90	917.13	920.00	929.11	958.06	961.75	992.05	1014.52	1037.79	1041.49
	1046.79	1053.63	1092.96	1136.64	1156.95	1172.77	1188.48	1200.73	1211.15	1228.86
	1241.37	1264.91	1280.70	1293.67	1301.85	1307.24	1311.78	1323.92	1333.98	1334.86
	1351.63	1354.43	1370.70	1376.07	1488.05	1499.57	1505.59	1506.03	1518.47	1532.01
	3036.62	3038.60	3039.00	3042.43	3047.15	3061.09	3067.67	3080.59	3089.86	3093.31
	3093.83	3097.93	3100.42	3114.14	3116.18					

Table F.7 Vibrational Frequencies (Continued A)

Species	Frequencies (cm^{-1})									
TS-TCD R10-H	-1156.06	131.65	172.37	248.87	266.51	285.11	317.29	317.61	406.15	527.02
	541.96	581.42	663.49	743.33	745.77	787.88	833.96	860.67	867.79	890.80
	896.69	917.16	917.62	933.89	945.25	989.76	992.77	1002.87	1038.35	1041.05
	1049.07	1057.05	1077.44	1126.59	1155.97	1171.32	1197.90	1199.89	1209.94	1234.93
	1249.49	1259.23	1263.64	1271.41	1295.46	1302.25	1311.88	1316.85	1333.64	1339.27
	1352.13	1352.46	1370.84	1374.06	1502.63	1503.72	1504.63	1521.40	1523.22	1720.64
	3035.95	3036.55	3041.31	3043.45	3056.84	3057.42	3066.84	3089.87	3092.90	3094.93
	3099.64	3102.46	3103.21	3114.88	3132.11					
TS-TCD R1-CH_3	-1614.29	40.00	72.10	78.71	139.65	177.23	269.34	307.46	317.65	361.83
	396.39	480.50	515.35	528.11	544.73	558.57	665.62	733.66	753.52	802.13
	831.12	865.04	868.72	886.33	903.23	915.03	917.09	945.03	957.71	990.27
	994.86	1007.67	1044.24	1051.86	1059.96	1086.64	1091.32	1149.35	1164.12	1174.13
	1196.90	1198.83	1216.38	1227.92	1247.29	1264.69	1267.94	1300.80	1308.58	1314.76
	1320.00	1331.32	1341.27	1352.34	1356.09	1374.12	1379.74	1394.95	1463.13	1466.14
	1500.57	1502.15	1503.79	1510.34	1523.15	1532.27	3035.54	3038.92	3044.07	3046.75
	3049.59	3058.22	3061.51	3065.16	3074.13	3084.96	3088.72	3089.67	3092.96	3100.19
	3108.08	3115.43	3205.93	3207.30						
TS-TCD R2-CH_3	-1527.03	50.33	80.35	91.77	157.55	171.96	267.75	303.42	312.30	372.45
	395.30	499.27	510.81	527.86	544.47	567.28	691.15	744.33	760.29	800.55
	835.26	865.98	872.15	891.84	894.86	915.04	917.24	928.14	961.98	965.97
	996.76	1022.03	1049.59	1051.50	1071.81	1083.44	1105.74	1135.74	1146.00	1156.54
	1187.37	1200.90	1204.59	1231.49	1243.57	1255.31	1267.75	1291.15	1309.46	1321.01
	1322.67	1334.39	1337.91	1346.48	1353.72	1367.89	1376.78	1415.30	1455.85	1461.75
	1499.15	1503.26	1504.31	1512.21	1522.95	1533.82	3013.75	3029.05	3039.13	3042.50
	3051.92	3054.68	3063.32	3070.82	3077.93	3088.72	3090.10	3093.14	3097.67	3097.96
	3106.07	3117.04	3212.51	3215.44						
TS-TCD R3-CH_3	-1599.45	67.86	77.49	100.07	143.47	192.80	271.68	302.65	317.90	394.83
	409.77	493.45	518.17	544.00	565.11	617.61	736.47	751.58	754.85	795.53
	830.69	866.68	872.74	892.50	908.01	920.49	928.62	954.12	965.73	970.22
	998.68	1009.38	1049.89	1053.47	1058.81	1061.71	1086.23	1139.20	1144.03	1168.09
	1171.10	1205.25	1210.73	1220.35	1233.87	1255.02	1279.56	1293.44	1299.32	1307.63
	1317.66	1325.06	1334.80	1344.00	1354.05	1360.22	1376.22	1401.44	1432.48	1460.18
	1472.78	1496.81	1504.87	1508.98	1519.75	1535.29	3007.47	3018.52	3043.85	3048.80
	3052.65	3058.86	3063.64	3073.10	3078.02	3084.47	3090.63	3094.25	3095.99	3100.24
	3105.85	3125.97	3212.37	3217.03						

Table F.7 Vibrational Frequencies (Continued B)

Species	Frequencies (cm^{-1})									
TS-TCD R4-CH_3	-1580.06	50.55	52.30	78.76	142.76	198.53	267.27	304.01	318.75	364.61
	446.87	488.25	526.64	526.76	538.72	655.45	674.87	740.69	765.38	792.79
	829.33	861.83	889.36	893.01	895.63	925.56	939.84	952.32	964.86	975.14
	1004.08	1029.72	1038.48	1053.66	1053.74	1077.28	1080.91	1138.33	1153.62	1157.63
	1171.28	1208.61	1215.37	1234.25	1247.90	1264.28	1265.82	1292.00	1303.59	1314.55
	1315.33	1326.38	1330.05	1338.22	1356.26	1367.96	1370.39	1387.66	1419.47	1459.49
	1468.29	1502.22	1502.92	1506.28	1520.02	1533.75	3024.42	3027.56	3047.31	3049.69
	3058.02	3059.56	3062.41	3076.16	3077.76	3084.51	3089.57	3094.07	3094.31	3101.53
	3105.82	3108.54	3212.44	3214.25						
TS-TCD R9-CH_3	-1559.02	31.68	71.14	77.61	145.12	178.66	264.52	305.93	318.94	364.31
	439.97	495.22	526.22	545.67	561.32	615.46	672.29	744.35	769.11	796.32
	865.56	873.06	895.46	900.49	906.26	917.11	925.21	932.34	962.54	969.89
	994.00	1017.60	1041.83	1048.48	1053.99	1059.41	1098.37	1139.58	1145.54	1156.88
	1180.58	1198.49	1206.78	1222.80	1236.81	1265.62	1268.41	1293.96	1303.19	1310.26
	1322.40	1327.14	1334.25	1351.30	1354.73	1366.34	1376.16	1390.61	1426.08	1459.13
	1466.63	1498.00	1503.99	1505.22	1517.87	1531.52	3029.73	3035.53	3037.08	3040.72
	3045.99	3059.87	3067.30	3072.87	3078.54	3086.76	3088.15	3091.56	3091.82	3097.76
	3100.15	3115.45	3214.60	3215.54						
TS-TCD R10-CH_3	-1629.31	24.54	81.78	84.57	128.49	179.60	265.32	286.57	317.28	369.31
	424.60	466.36	503.36	548.22	562.87	665.40	685.53	746.11	753.80	795.65
	837.16	861.46	869.08	889.56	896.88	918.56	918.60	935.58	989.91	990.44
	1001.45	1010.00	1042.28	1050.84	1059.18	1076.28	1078.88	1156.75	1159.40	1174.15
	1198.16	1200.36	1207.28	1223.23	1234.75	1263.10	1263.53	1298.74	1303.53	1312.11
	1318.52	1330.16	1334.16	1353.30	1353.79	1367.39	1372.06	1377.18	1429.78	1460.95
	1477.42	1500.06	1502.59	1505.78	1522.92	1523.15	3035.45	3036.58	3040.19	3040.88
	3052.68	3054.21	3063.59	3075.96	3088.33	3089.54	3092.01	3093.75	3095.11	3099.19
	3109.78	3112.16	3209.06	3210.09						
TS-TCD R1-O	-1217.66	61.90	79.78	144.47	177.54	268.22	311.97	318.62	377.27	401.57
	493.66	527.21	551.94	665.61	725.21	753.86	792.70	828.17	861.52	872.08
	878.71	899.10	913.64	914.54	926.02	945.89	961.65	988.58	997.71	1008.34
	1040.37	1044.45	1051.69	1065.96	1094.60	1113.37	1152.34	1182.58	1198.48	1205.23
	1217.56	1235.21	1253.68	1264.84	1272.19	1300.88	1310.49	1318.68	1322.54	1330.57
	1343.28	1352.70	1366.31	1377.35	1499.96	1502.61	1504.13	1512.32	1522.99	1535.35
	3038.20	3041.95	3054.55	3058.70	3060.39	3069.82	3072.66	3079.05	3092.19	3094.53
	3098.16	3100.53	3111.12	3121.50	3133.52					

Table F.7 Vibrational Frequencies (Continued C)

Species	Frequencies (cm^{-1})									
TS-TCD R2-O	-874.04	67.88	88.55	118.23	198.20	255.41	273.59	322.93	398.25	453.24
	492.41	506.43	616.34	712.42	736.76	791.96	800.09	826.65	841.58	857.58
	887.27	890.44	901.09	919.54	937.10	956.18	961.59	985.69	996.51	1042.24
	1046.52	1070.26	1082.44	1090.03	1096.14	1139.67	1149.15	1166.56	1190.14	1206.97
	1211.51	1231.74	1257.53	1263.34	1281.87	1290.06	1300.65	1319.16	1327.08	1331.26
	1340.81	1348.39	1355.75	1369.33	1496.10	1499.46	1506.57	1510.43	1523.92	1537.11
	3045.73	3047.53	3056.38	3057.71	3062.40	3064.24	3069.43	3087.56	3092.66	3095.61
	3099.92	3106.73	3108.05	3128.06	3130.95					
TS-TCD R3-O	-1094.94	62.07	130.89	166.67	202.84	266.11	307.24	318.24	401.28	503.99
	520.96	564.58	577.48	689.76	738.93	749.22	794.48	828.96	857.27	864.71
	890.43	900.45	912.58	922.24	928.76	963.22	966.52	995.56	1001.58	1034.90
	1051.18	1053.32	1057.33	1081.72	1141.40	1156.61	1169.15	1176.62	1199.18	1210.15
	1219.58	1235.47	1245.86	1261.48	1291.67	1298.76	1306.13	1310.18	1320.69	1333.20
	1339.99	1349.56	1360.44	1371.72	1390.39	1489.43	1501.46	1513.75	1519.43	1540.00
	3008.75	3019.80	3051.07	3053.73	3058.97	3061.24	3069.38	3086.75	3089.22	3094.45
	3100.15	3106.90	3108.19	3108.41	3184.22					
TS-TCD R4-O	-1238.00	49.87	79.55	143.53	186.09	266.51	299.20	321.07	382.94	483.24
	492.43	529.98	654.13	672.70	738.53	753.48	792.13	828.91	844.47	857.97
	893.06	893.44	923.41	928.05	934.15	959.42	965.28	997.99	1018.42	1035.13
	1045.32	1052.17	1061.74	1063.53	1134.17	1141.70	1164.93	1186.62	1189.92	1217.84
	1228.07	1238.81	1252.71	1269.15	1291.93	1302.89	1308.93	1317.61	1325.09	1331.04
	1336.26	1354.55	1357.36	1369.56	1483.06	1500.48	1502.61	1506.75	1519.61	1534.34
	3045.01	3048.17	3051.44	3055.08	3060.78	3063.19	3068.23	3087.29	3089.32	3093.64
	3098.28	3107.00	3109.91	3112.49	3116.15					
TS-TCD R9-O	-1078.46	66.44	81.14	101.78	216.35	249.84	267.75	318.15	376.39	486.06
	509.89	615.14	625.31	716.04	744.43	784.56	805.40	809.68	845.30	851.72
	892.93	903.04	904.53	920.69	932.27	948.76	957.35	984.46	999.56	1023.42
	1038.60	1057.91	1085.53	1096.26	1125.31	1131.75	1148.69	1165.13	1191.68	1202.36
	1224.25	1234.31	1242.60	1277.70	1286.02	1297.63	1300.82	1305.45	1326.55	1328.18
	1339.38	1344.71	1365.36	1374.22	1378.12	1492.09	1500.33	1503.95	1519.01	1538.32
	3041.19	3042.96	3044.70	3057.93	3059.87	3073.19	3081.32	3084.32	3084.38	3087.05
	3099.42	3102.64	3105.88	3111.03	3148.86					
TS-TCD R10-O	-1285.96	84.21	96.22	133.89	175.38	267.72	282.62	313.23	367.03	431.73
	535.42	550.23	621.03	660.37	738.95	752.18	790.67	834.32	859.46	866.36
	888.89	894.74	912.85	917.06	927.40	939.69	974.19	991.28	997.61	1031.16
	1031.86	1041.97	1052.66	1075.31	1080.83	1155.62	1163.24	1188.87	1199.93	1205.74
	1220.90	1237.18	1245.91	1264.63	1270.91	1294.28	1306.99	1316.94	1317.77	1334.43
	1339.40	1352.44	1353.77	1369.28	1374.00	1490.13	1504.03	1506.02	1522.24	1522.91
	3036.73	3037.79	3043.09	3048.22	3061.23	3062.70	3071.87	3094.10	3095.95	3102.36
	3103.61	3106.68	3108.85	3122.50	3125.33					

Table F.7 Vibrational Frequencies (Continued D)

Species	Frequencies (cm^{-1})									
TS-TCD R1-OH	-1531.90	60.03	69.68	96.32	142.89	180.49	265.46	322.71	328.81	402.91
	481.51	500.21	551.59	558.24	672.88	749.22	771.78	809.01	839.13	850.56
	891.54	899.48	917.23	941.10	948.82	951.98	989.12	1005.15	1021.65	1034.70
	1045.61	1076.28	1079.48	1086.74	1097.82	1132.31	1146.81	1181.16	1219.90	1226.42
	1228.58	1248.00	1270.44	1272.27	1294.36	1305.53	1326.59	1334.25	1341.62	1348.18
	1359.39	1374.17	1384.20	1384.97	1402.39	1445.00	1536.55	1538.73	1540.99	1548.50
	1559.85	1570.99	3121.88	3125.92	3128.45	3132.41	3133.39	3140.74	3143.78	3145.75
	3167.85	3185.60	3189.95	3192.65	3201.56	3208.29	3209.86	3836.30		
TS-TCD R2-OH	-1057.58	66.71	84.08	136.45	169.34	179.61	264.60	319.99	330.01	403.75
	483.90	536.09	552.18	591.30	690.93	746.98	776.91	820.17	856.22	893.04
	901.03	914.31	927.98	942.27	950.54	957.78	992.30	997.73	1018.05	1039.19
	1060.84	1075.20	1086.59	1102.26	1109.00	1114.21	1168.74	1181.88	1217.41	1225.16
	1234.76	1250.79	1266.80	1274.78	1287.62	1303.50	1316.14	1338.79	1345.13	1352.65
	1359.60	1370.13	1382.17	1384.39	1391.88	1403.03	1531.92	1538.48	1540.66	1548.03
	1558.63	1569.66	3115.12	3121.76	3131.33	3132.10	3133.63	3136.73	3142.54	3164.38
	3170.41	3186.28	3189.17	3191.47	3198.87	3203.21	3214.54	3827.90		
TS-TCD R3-OH	-1373.21	60.16	107.20	130.71	157.77	194.34	266.91	320.37	335.33	405.82
	499.78	529.90	553.79	633.57	733.25	758.49	776.02	818.58	840.35	851.65
	891.97	894.09	926.93	932.01	948.84	959.56	979.59	996.60	999.81	1032.81
	1046.15	1074.89	1077.47	1083.59	1086.10	1118.40	1171.83	1196.19	1202.74	1232.90
	1235.64	1248.23	1263.94	1282.69	1313.61	1318.17	1321.82	1333.47	1343.16	1355.37
	1365.05	1369.84	1384.58	1390.74	1397.97	1406.63	1444.87	1535.04	1540.17	1546.66
	1557.29	1574.84	3112.16	3116.25	3128.33	3130.85	3132.64	3136.99	3139.21	3154.35
	3169.75	3182.30	3188.02	3192.17	3199.35	3200.37	3228.82	3825.33		
TS-TCD R4-OH	-1576.50	47.72	74.23	115.50	138.85	188.66	260.84	315.57	323.38	392.48
	497.13	512.28	536.50	657.75	694.94	762.88	770.80	817.98	850.93	866.97
	889.45	919.89	927.29	954.48	961.14	965.26	983.79	996.34	998.36	1049.15
	1065.37	1073.38	1074.52	1084.27	1110.14	1118.71	1164.80	1185.06	1197.75	1234.43
	1242.03	1262.92	1265.44	1288.84	1292.39	1315.15	1324.27	1335.32	1342.50	1355.65
	1362.08	1365.16	1376.10	1390.96	1397.00	1399.41	1421.16	1539.70	1540.62	1541.79
	1558.64	1570.74	3125.56	3126.67	3129.01	3131.63	3137.46	3138.64	3139.96	3164.00
	3165.99	3171.63	3182.56	3192.70	3199.33	3201.52	3205.66	3833.46		
TS-TCD R9-OH	-1407.58	62.66	80.94	118.43	145.51	182.26	251.70	314.06	330.54	387.23
	497.60	539.84	554.57	671.47	702.27	759.63	774.23	812.04	834.14	894.13
	904.42	923.63	927.30	940.18	950.18	960.67	994.07	1000.65	1025.30	1039.72
	1054.23	1076.25	1078.25	1084.25	1098.26	1136.04	1171.93	1183.74	1202.92	1228.69
	1237.68	1252.01	1266.24	1288.54	1296.14	1318.85	1325.42	1332.59	1348.33	1353.94
	1359.59	1366.84	1384.63	1386.78	1400.37	1404.52	1418.59	1536.29	1542.33	1543.36
	1554.87	1567.49	3121.41	3123.14	3124.03	3125.75	3133.24	3136.04	3147.69	3158.78
	3171.33	3177.55	3185.13	3188.61	3194.53	3197.39	3215.67	3832.19		

Table F.7 Vibrational Frequencies (Continued E)

Species	Frequencies (cm^{-1})									
TS-TCD R10-OH	-1555.07	76.33	93.15	130.48	143.08	180.62	263.65	309.39	320.38	383.34
	459.08	536.66	556.95	655.66	679.41	760.54	772.43	816.07	852.39	890.58
	892.38	919.14	925.84	928.92	947.20	951.54	976.84	998.37	1026.69	1035.37
	1048.83	1072.72	1076.34	1083.59	1086.67	1110.76	1182.54	1199.14	1225.00	1229.17
	1238.48	1247.21	1264.84	1287.48	1292.01	1322.41	1330.55	1340.65	1343.42	1351.40
	1359.25	1379.73	1384.07	1386.54	1389.38	1401.44	1408.50	1534.30	1542.43	1543.43
	1559.47	1560.35	3120.28	3122.13	3124.44	3126.06	3137.27	3138.72	3146.08	3163.44
	3177.51	3185.15	3188.25	3193.03	3198.37	3198.98	3214.07	3829.40		
TS-TCD R1-OOH	-1182.51	26.73	54.10	73.03	146.08	165.00	189.20	267.80	317.27	325.49
	370.95	396.33	442.98	500.71	537.32	552.32	665.12	723.20	757.29	791.04
	829.08	862.22	867.71	882.64	885.08	914.13	917.77	919.07	950.87	962.44
	979.16	996.55	1007.33	1036.80	1045.03	1053.47	1066.09	1094.62	1102.90	1150.41
	1183.52	1197.09	1204.43	1217.24	1233.35	1250.34	1261.75	1269.06	1299.36	1307.03
	1316.99	1322.49	1328.02	1341.85	1353.14	1364.69	1373.06	1377.14	1491.93	1498.84
	1502.32	1507.73	1513.04	1522.34	1537.16	3037.73	3042.00	3052.26	3053.92	3056.48
	3065.02	3070.89	3080.56	3090.80	3093.05	3096.75	3097.72	3107.36	3117.19	3135.17
	3731.57									
TS-TCD R2-OOH	-1553.81	22.89	84.06	91.72	145.90	159.75	212.19	277.67	297.65	326.91
	384.94	388.15	407.73	502.33	534.21	552.40	691.21	741.10	766.76	803.75
	837.74	863.67	878.09	887.61	892.60	911.04	916.69	927.57	961.42	965.59
	984.98	992.61	1021.23	1045.31	1050.57	1060.28	1072.44	1086.85	1135.41	1150.59
	1160.40	1190.81	1202.00	1208.37	1233.50	1242.56	1257.28	1267.95	1291.59	1312.37
	1318.42	1320.91	1334.67	1346.32	1351.36	1354.25	1368.79	1371.66	1454.76	1487.17
	1500.59	1504.08	1510.87	1519.29	1532.63	3005.24	3033.82	3041.02	3052.96	3053.37
	3057.73	3067.38	3081.21	3091.07	3096.63	3097.41	3105.64	3106.98	3109.50	3122.22
	3724.09									
TS-TCD R3-OOH	-1615.83	32.77	65.74	102.45	133.28	185.28	249.30	268.99	308.41	326.61
	395.62	401.94	499.75	514.41	548.24	590.32	711.64	740.47	751.01	795.69
	828.69	855.65	865.59	892.22	897.93	917.16	927.44	939.72	963.91	966.05
	986.47	997.48	1005.28	1037.31	1052.90	1055.18	1059.98	1082.49	1138.32	1145.96
	1170.63	1179.19	1210.60	1213.02	1223.82	1235.27	1254.53	1283.44	1294.62	1297.82
	1308.57	1318.48	1326.97	1334.68	1343.14	1355.96	1361.61	1375.54	1376.81	1479.38
	1487.38	1503.43	1509.98	1520.16	1541.36	2989.95	3007.75	3049.98	3052.91	3057.46
	3060.14	3065.47	3084.04	3085.63	3093.38	3100.55	3104.10	3105.78	3107.25	3137.57
	3719.79									

Table F.7 Vibrational Frequencies (Continued F)

Species	Frequencies (cm^{-1})									
TS-TCD R4-OOH	-1565.10	31.56	36.62	84.12	134.20	149.94	258.56	275.06	314.98	342.12
	386.35	413.64	476.26	499.06	530.15	631.52	678.59	736.41	757.72	793.12
	829.13	851.81	876.51	892.53	893.53	925.70	933.67	952.20	964.64	971.25
	982.17	990.29	1009.96	1033.08	1036.59	1055.60	1055.98	1079.94	1084.15	1141.69
	1162.74	1168.38	1210.68	1216.72	1231.16	1251.87	1260.47	1278.21	1296.70	1300.08
	1312.06	1313.12	1322.77	1332.17	1346.40	1356.80	1364.22	1369.25	1372.69	1486.04
	1493.09	1499.90	1503.85	1518.16	1536.65	3018.01	3034.16	3049.33	3053.70	3059.27
	3062.33	3067.11	3085.04	3090.28	3092.48	3096.92	3098.53	3106.31	3112.28	3117.83
	3720.96									
TS-TCD R9-OOH	-1550.91	33.74	66.75	80.84	148.97	169.43	199.73	289.16	315.29	361.11
	375.98	410.23	496.45	533.76	555.88	565.15	671.66	743.54	760.64	793.86
	849.85	869.18	874.54	895.15	904.96	913.32	916.16	930.48	957.60	962.51
	986.73	989.62	1013.01	1030.51	1037.36	1044.98	1052.26	1088.92	1131.76	1138.97
	1158.04	1187.90	1198.69	1204.96	1220.43	1234.99	1262.50	1273.97	1291.01	1304.10
	1311.65	1322.36	1330.61	1334.07	1350.40	1353.54	1367.58	1372.94	1376.08	1472.81
	1494.40	1503.60	1505.66	1518.57	1533.61	3019.93	3036.73	3041.11	3044.45	3047.19
	3060.90	3067.50	3075.07	3090.75	3094.61	3097.89	3101.53	3102.75	3114.46	3125.82
	3719.78									
TS-TCD R10-OOH	-1426.93	30.08	66.00	87.71	128.70	159.55	207.29	269.01	306.46	314.40
	356.74	400.18	445.89	536.44	551.59	600.87	663.44	741.14	750.05	794.29
	842.37	855.99	867.60	888.46	891.09	915.28	916.01	931.47	964.02	983.29
	987.59	996.65	1002.62	1031.00	1041.20	1049.97	1059.90	1079.64	1129.63	1154.59
	1179.52	1198.50	1205.27	1210.49	1232.20	1234.55	1261.88	1264.51	1289.72	1303.44
	1313.94	1315.40	1334.74	1337.81	1351.75	1352.08	1367.23	1372.52	1375.93	1463.35
	1503.33	1504.47	1506.68	1524.27	1525.46	3035.87	3038.18	3042.60	3046.59	3059.49
	3062.43	3071.82	3091.42	3094.38	3101.11	3105.05	3107.55	3111.98	3127.03	3129.71
	3725.24									

Internal Rotor (IR) notation and 0° dihedral angle corresponds to the structures from the Optimized Species.

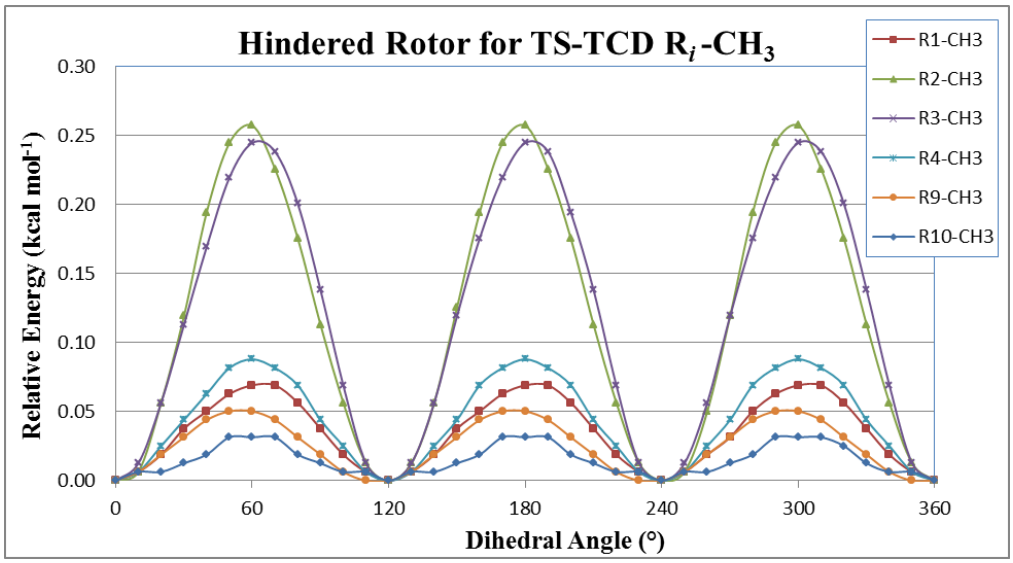

Figure F.1 Internal rotation of TS-TCD R*i*-CH_3 species.

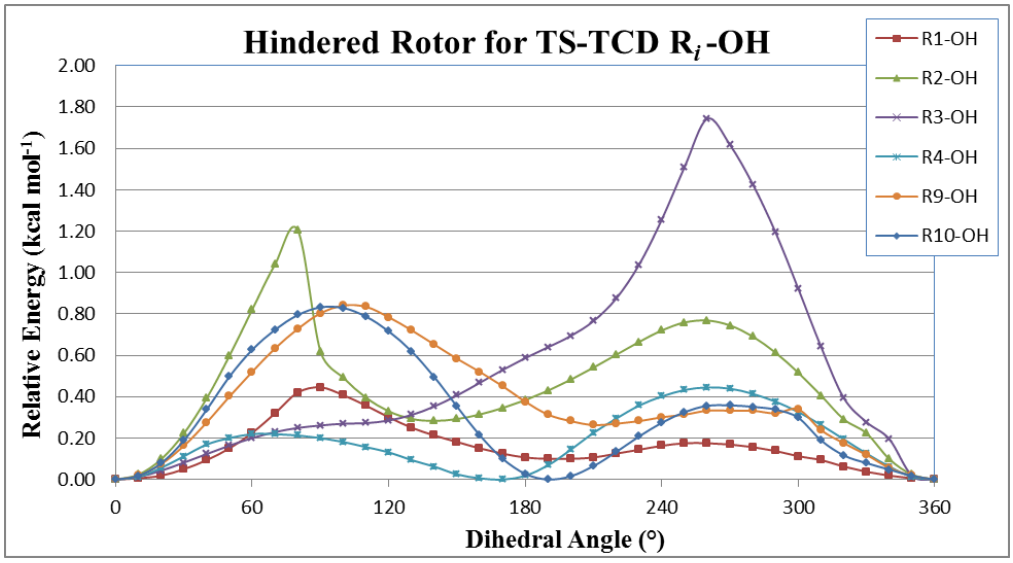

Figure F.2 Internal rotation of TS-TCD R*i*-OH species.

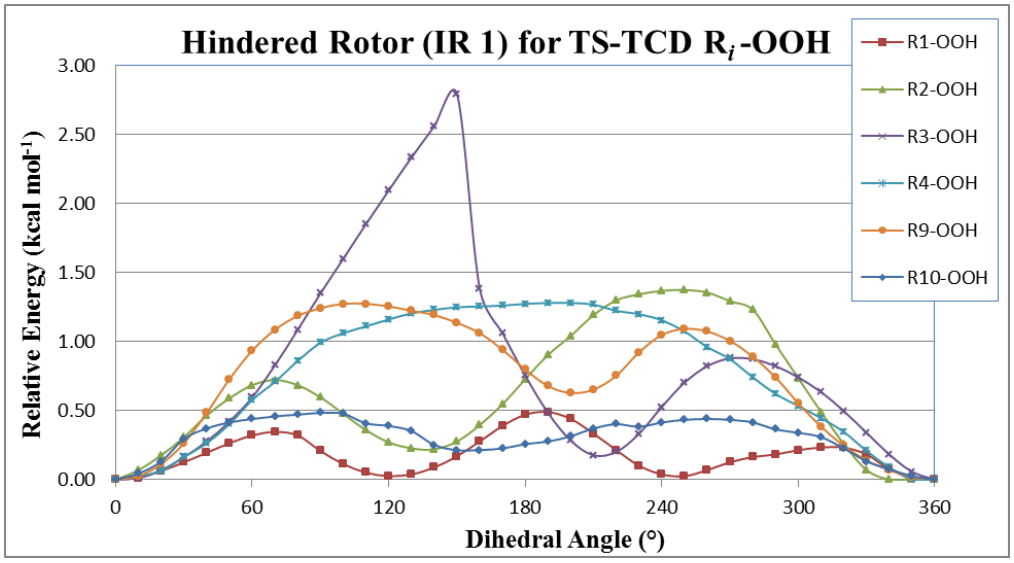

Figure F.3 Internal rotation for terminal OH rotation of TS-TCD R*i*-OOH species.

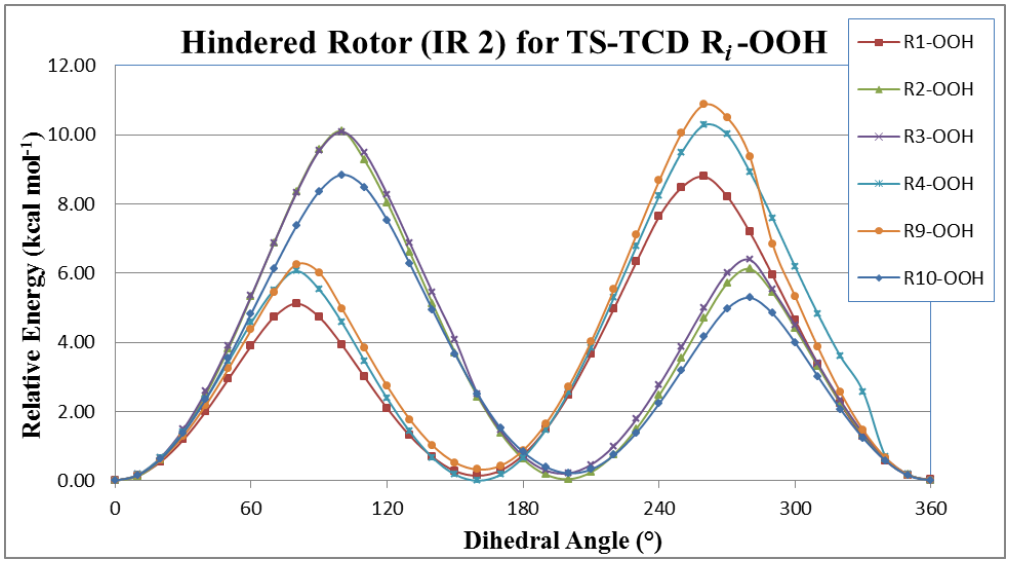

Figure F.4 Internal rotation for terminal H rotation of TS-TCD R*i*-OOH species.

Table F.8 Isodesmic Work Reactions and Calculated $\Delta H^{\circ}_{f\,298}$ for TS-TCD R*i*-H Species

Isodesmic Reactions							$\Delta H^{\circ}_{f\,298}$ (kcal mol^{-1})			
							B3LYP		CBS-QB3	G3MP2B3
							6-31G(d,p)	6-311G(2d,2p)		
TS-TCD R1-H System										
TS-TCD R1-H	+	CJH_3	→	TCD	+	CH_4	38.02	37.29	42.50	42.01
TS-TCD R1-H	+	CH_3CJH_2	→	TCD	+	CH_3CH_3	36.86	36.19	42.41	42.36
TS-TCD R1-H	+	$CH_3CH_2CJH_2$	→	TCD	+	$CH_3CH_2CH_3$	37.25	36.50	42.79	42.78
TS-TCD R1-H	+	$CH_3CH_2CH_2CJH_2$	→	TCD	+	$CH_3CH_2CH_2CH_3$	37.07	36.02	42.64	42.70
						Average	**37.30**	**36.50**	**42.58**	**42.46**
						Calculation Method Average	**36.90**		**42.52**	
TS-TCD R2-H System										
TS-TCD R2-H	+	CJH_3	→	TCD	+	CH_4	33.87	32.86	37.79	37.44
TS-TCD R2-H	+	CH_3CJH_2	→	TCD	+	CH_3CH_3	32.72	31.75	37.70	37.80
TS-TCD R2-H	+	$CH_3CH_2CJH_2$	→	TCD	+	$CH_3CH_2CH_3$	33.10	32.07	38.08	38.22
TS-TCD R2-H	+	$CH_3CH_2CH_2CJH_2$	→	TCD	+	$CH_3CH_2CH_2CH_3$	32.93	31.59	37.93	38.14
						Average	**33.16**	**32.07**	**37.87**	**37.90**
						Calculation Method Average	**32.61**		**37.89**	
TS-TCD R3-H System										
TS-TCD R3-H	+	CJH_3	→	TCD	+	CH_4	35.19	34.26	39.54	38.97
TS-TCD R3-H	+	CH_3CJH_2	→	TCD	+	CH_3CH_3	34.04	33.15	39.45	39.33
TS-TCD R3-H	+	$CH_3CH_2CJH_2$	→	TCD	+	$CH_3CH_2CH_3$	34.43	33.47	39.83	39.75
TS-TCD R3-H	+	$CH_3CH_2CH_2CJH_2$	→	TCD	+	$CH_3CH_2CH_2CH_3$	34.25	32.99	39.68	39.67
						Average	**34.48**	**33.47**	**39.63**	**39.43**
						Calculation Method Average	**33.97**		**39.53**	

Table F.8 Isodesmic Work Reactions and Calculated $\Delta H^{\circ}_{f\,298}$ for TS-TCD R*i*-H Species (Continued)

Isodesmic Reactions							$\Delta H^{\circ}_{f\,298}$ (kcal mol^{-1})			
							B3LYP		CBS-QB3	G3MP2B3
							6-31G(d,p)	6-311G(2d,2p)		
TS-TCD R4-H System										
TS-TCD R4-H	+	CJH_3	→	TCD	+	CH_4	36.16	35.14	41.02	40.46
TS-TCD R4-H	+	CH_3CJH_2	→	TCD	+	CH_3CH_3	35.00	34.03	40.93	40.81
TS-TCD R4-H	+	$CH_3CH_2CJH_2$	→	TCD	+	$CH_3CH_2CH_3$	35.39	34.35	41.31	41.23
TS-TCD R4-H	+	$CH_3CH_2CH_2CJH_2$	→	TCD	+	$CH_3CH_2CH_2CH_3$	35.21	33.87	41.16	41.15
						Average	**35.44**	**34.35**	**41.10**	**40.91**
						Calculation Method Average	**34.89**		**41.01**	
TS-TCD R9-H System										
TS-TCD R9-H	+	CJH_3	→	TCD	+	CH_4	34.68	33.73	39.11	38.55
TS-TCD R9-H	+	CH_3CJH_2	→	TCD	+	CH_3CH_3	33.52	32.63	39.02	38.91
TS-TCD R9-H	+	$CH_3CH_2CJH_2$	→	TCD	+	$CH_3CH_2CH_3$	33.91	32.94	39.40	39.33
TS-TCD R9-H	+	$CH_3CH_2CH_2CJH_2$	→	TCD	+	$CH_3CH_2CH_2CH_3$	33.73	32.46	39.25	39.25
						Average	**33.96**	**32.94**	**39.19**	**39.01**
						Calculation Method Average	**33.45**		**39.10**	
TS-TCD R10-H System										
TS-TCD R10-H	+	CJH_3	→	TCD	+	CH_4	37.51	36.77	42.07	41.43
TS-TCD R10-H	+	CH_3CJH_2	→	TCD	+	CH_3CH_3	36.36	35.66	41.98	41.79
TS-TCD R10-H	+	$CH_3CH_2CJH_2$	→	TCD	+	$CH_3CH_2CH_3$	36.75	35.97	42.36	42.21
TS-TCD R10-H	+	$CH_3CH_2CH_2CJH_2$	→	TCD	+	$CH_3CH_2CH_2CH_3$	36.57	35.50	42.21	42.13
						Average	**36.80**	**35.98**	**42.15**	**41.89**
						Calculation Method Average	**36.39**		**42.02**	

Table F.9 Isodesmic Work Reactions and Calculated $\Delta H^{\circ}_{f\,298}$ for TS-TCD R*i*-CH_3 Species

Isodesmic Reactions							$\Delta H^{\circ}_{f\,298}$ (kcal mol^{-1})			
							B3LYP		CBS-QB3	G3MP2B3
							6-31G(d,p)	6-311G(2d,2p)		
TS-TCD R1-CH_3 System										
TS-TCD R1-CH_3	+	CJH_3	→	TCD	+	CH_3CH_3	25.04	23.93	28.33	28.30
TS-TCD R1-CH_3	+	CH_3CJH_2	→	TCD	+	$CH_3CH_2CH_3$	22.73	21.72	28.16	28.58
TS-TCD R1-CH_3	+	$CH_3CH_2CJH_2$	→	TCD	+	$CH_3CH_2CH_2CH_3$	23.07	21.91	28.63	29.09
						Average	**23.61**	**22.52**	**28.37**	**28.66**
						Calculation Method Average	**23.07**		**28.52**	
TS-TCD R2-CH_3 System										
TS-TCD R2-CH_3	+	CJH_3	→	TCD	+	CH_3CH_3	22.45	21.30	24.96	24.86
TS-TCD R2-CH_3	+	CH_3CJH_2	→	TCD	+	$CH_3CH_2CH_3$	20.14	19.09	24.79	25.14
TS-TCD R2-CH_3	+	$CH_3CH_2CJH_2$	→	TCD	+	$CH_3CH_2CH_2CH_3$	20.48	19.28	25.26	25.64
						Average	**21.02**	**19.89**	**25.00**	**25.21**
						Calculation Method Average	**20.46**		**25.11**	
TS-TCD R3-CH_3 System										
TS-TCD R3-CH_3	+	CJH_3	→	TCD	+	CH_3CH_3	23.78	22.62	26.95	26.62
TS-TCD R3-CH_3	+	CH_3CJH_2	→	TCD	+	$CH_3CH_2CH_3$	21.47	20.41	26.77	26.89
TS-TCD R3-CH_3	+	$CH_3CH_2CJH_2$	→	TCD	+	$CH_3CH_2CH_2CH_3$	21.81	20.61	27.24	27.40
						Average	**22.35**	**21.21**	**26.99**	**26.97**
						Calculation Method Average	**21.78**		**26.98**	

Table F.9 Isodesmic Work Reactions and Calculated $\Delta H^{\circ}_{f\,298}$ for TS-TCD R*i*-CH_3 Species (Continued)

Isodesmic Reactions							$\Delta H^{\circ}_{f\,298}$ (kcal mol^{-1})			
							B3LYP		CBS-QB3	G3MP2B3
							6-31G(d,p)	6-311G(2d,2p)		
TS-TCD R4-CH_3 System										
TS-TCD R4-CH_3	+	CJH_3	→	TCD	+	CH_3CH_3	23.85	22.56	28.06	27.87
TS-TCD R4-CH_3	+	CH_3CJH_2	→	TCD	+	$CH_3CH_2CH_3$	21.54	20.35	27.88	28.15
TS-TCD R4-CH_3	+	$CH_3CH_2CJH_2$	→	TCD	+	$CH_3CH_2CH_2CH_3$	21.88	20.55	28.36	28.66
						Average	**22.42**	**21.16**	**28.10**	**28.23**
						Calculation Method Average	**21.79**		**28.16**	
TS-TCD R9-CH_3 System										
TS-TCD R9-CH_3	+	CJH_3	→	TCD	+	CH_3CH_3	22.74	21.54	26.48	26.28
TS-TCD R9-CH_3	+	CH_3CJH_2	→	TCD	+	$CH_3CH_2CH_3$	20.43	19.33	26.30	26.55
TS-TCD R9-CH_3	+	$CH_3CH_2CJH_2$	→	TCD	+	$CH_3CH_2CH_2CH_3$	20.77	19.53	26.78	27.06
						Average	**21.31**	**20.13**	**26.52**	**26.63**
						Calculation Method Average	**20.72**		**26.57**	
TS-TCD R10-CH_3 System										
TS-TCD R10-CH_3	+	CJH_3	→	TCD	+	CH_3CH_3	25.09	23.99	28.61	28.34
TS-TCD R10-CH_3	+	CH_3CJH_2	→	TCD	+	$CH_3CH_2CH_3$	22.78	21.78	28.43	28.62
TS-TCD R10-CH_3	+	$CH_3CH_2CJH_2$	→	TCD	+	$CH_3CH_2CH_2CH_3$	23.12	21.98	28.91	29.13
						Average	**23.66**	**22.58**	**28.65**	**28.70**
						Calculation Method Average	**23.12**		**28.67**	

Table F.10 Isodesmic Work Reactions and Calculated $\Delta H^{\circ}_{f\,298}$ for TS-TCD R*i*-O Species

Isodesmic Reactions							$\Delta H^{\circ}_{f\,298}$ (kcal mol^{-1})			
							B3LYP		CBS-QB3	G3MP2B3
							6-31G(d,p)	6-311G(2d,2p)		
TS-TCD R1-O System										
TS-TCD R1-O	+	CJH_3	→	TCD	+	CH_3OJ	40.95	39.50	43.36	42.48
TS-TCD R1-O	+	CH_3CJH_2	→	TCD	+	CH_3CH_2OJ	40.01	39.31	44.13	42.92
TS-TCD R1-O	+	$CH_3CH_2CJH_2$	→	TCD	+	$CH_3CH_2CH_2OJ$	40.59	39.26	43.95	43.44
TS-TCD R1-O	+	$CH_3CH_2CH_2CJH_2$	→	TCD	+	$CH_3CH_2CH_2CH_2OJ$	40.61	39.03	43.99	43.54
						Average	**40.54**	**39.28**	**43.86**	**43.10**
						Calculation Method Average		**39.91**		**43.48**
TS-TCD R2-O System										
TS-TCD R2-O	+	CJH_3	→	TCD	+	CH_3OJ	38.90	37.52	42.69	41.55
TS-TCD R2-O	+	CH_3CJH_2	→	TCD	+	CH_3CH_2OJ	37.96	37.33	43.46	41.99
TS-TCD R2-O	+	$CH_3CH_2CJH_2$	→	TCD	+	$CH_3CH_2CH_2OJ$	38.54	37.28	43.29	42.51
TS-TCD R2-O	+	$CH_3CH_2CH_2CJH_2$	→	TCD	+	$CH_3CH_2CH_2CH_2OJ$	38.56	37.05	43.32	42.62
						Average	**38.49**	**37.29**	**43.19**	**42.17**
						Calculation Method Average		**37.89**		**42.68**
TS-TCD R3-O System										
TS-TCD R3-O	+	CJH_3	→	TCD	+	CH_3OJ	38.67	36.85	41.70	40.24
TS-TCD R3-O	+	CH_3CJH_2	→	TCD	+	CH_3CH_2OJ	37.72	36.66	42.47	40.68
TS-TCD R3-O	+	$CH_3CH_2CJH_2$	→	TCD	+	$CH_3CH_2CH_2OJ$	38.31	36.61	42.30	41.20
TS-TCD R3-O	+	$CH_3CH_2CH_2CJH_2$	→	TCD	+	$CH_3CH_2CH_2CH_2OJ$	38.32	36.38	42.33	41.31
						Average	**38.26**	**36.63**	**42.20**	**40.86**
						Calculation Method Average		**37.44**		**41.53**

Table F.10 Isodesmic Work Reactions and Calculated $\Delta H^{\circ}_{f\,298}$ for TS-TCD R*i*-O Species (Continued)

Isodesmic Reactions							$\Delta H^{\circ}_{f\,298}$ (kcal mol^{-1})			
							B3LYP		CBS-QB3	G3MP2B3
							6-31G(d,p)	6-311G(2d,2p)		
TS-TCD R4-O System										
TS-TCD R4-O	+	CJH_3	→	TCD	+	CH_3OJ	40.75	38.91	44.10	42.57
TS-TCD R4-O	+	CH_3CJH_2	→	TCD	+	CH_3CH_2OJ	39.81	38.72	44.87	43.00
TS-TCD R4-O	+	$CH_3CH_2CJH_2$	→	TCD	+	$CH_3CH_2CH_2OJ$	40.40	38.67	44.70	43.53
TS-TCD R4-O	+	$CH_3CH_2CH_2CJH_2$	→	TCD	+	$CH_3CH_2CH_2CH_2OJ$	40.41	38.44	44.73	43.63
						Average	**40.34**	**38.68**	**44.60**	**43.18**
						Calculation Method Average		**39.51**		**43.89**
TS-TCD R9-O System										
TS-TCD R9-O	+	CJH_3	→	TCD	+	CH_3OJ	40.39	38.87	44.23	42.80
TS-TCD R9-O	+	CH_3CJH_2	→	TCD	+	CH_3CH_2OJ	39.44	38.69	45.00	43.24
TS-TCD R9-O	+	$CH_3CH_2CJH_2$	→	TCD	+	$CH_3CH_2CH_2OJ$	40.03	38.64	44.82	43.76
TS-TCD R9-O	+	$CH_3CH_2CH_2CJH_2$	→	TCD	+	$CH_3CH_2CH_2CH_2OJ$	40.04	38.41	44.86	43.87
						Average	**39.98**	**38.65**	**44.73**	**43.42**
						Calculation Method Average		**39.31**		**44.07**
TS-TCD R10-O System										
TS-TCD R10-O	+	CJH_3	→	TCD	+	CH_3OJ	40.95	39.59	43.99	42.72
TS-TCD R10-O	+	CH_3CJH_2	→	TCD	+	CH_3CH_2OJ	40.01	39.40	44.76	43.16
TS-TCD R10-O	+	$CH_3CH_2CJH_2$	→	TCD	+	$CH_3CH_2CH_2OJ$	40.60	39.35	44.58	43.68
TS-TCD R10-O	+	$CH_3CH_2CH_2CJH_2$	→	TCD	+	$CH_3CH_2CH_2CH_2OJ$	40.61	39.12	44.62	43.79
						Average	**40.54**	**39.37**	**44.49**	**43.34**
						Calculation Method Average		**39.95**		**43.91**

Table F.11 Isodesmic Work Reactions and Calculated $\Delta H^{\circ}_{f\,298}$ for TS-TCD R*i*-OH Species

Isodesmic Reactions							$\Delta H^{\circ}_{f\,298}$ (kcal mol^{-1})			
							B3LYP		CBS-QB3	G3MP2B3
							6-31G(d,p)	6-311G(2d,2p)		
TS-TCD R1-OH System										
TS-TCD R1-OH	+	CJH_3	→	TCD	+	CH_3OH	-15.46	-17.93	-10.25	-11.70
TS-TCD R1-OH	+	CH_3CJH_2	→	TCD	+	CH_3CH_2OH	-16.92	-19.24	-10.48	-11.48
TS-TCD R1-OH	+	$CH_3CH_2CJH_2$	→	TCD	+	$CH_3CH_2CH_2OH$	-16.19	-18.50	-9.92	-10.91
TS-TCD R1-OH	+	$CH_3CH_2CH_2CJH_2$	→	TCD	+	$CH_3CH_2CH_2CH_2OH$	-16.11	-18.70	-9.84	-10.76
						Average	**-16.17**	**-18.59**	**-10.12**	**-11.22**
						Calculation Method Average		**-17.38**		**-10.67**
TS-TCD R2-OH System										
TS-TCD R2-OH	+	CJH_3	→	TCD	+	CH_3OH	-18.03	-20.51	-12.12	-12.60
TS-TCD R2-OH	+	CH_3CJH_2	→	TCD	+	CH_3CH_2OH	-19.49	-21.82	-12.36	-12.38
TS-TCD R2-OH	+	$CH_3CH_2CJH_2$	→	TCD	+	$CH_3CH_2CH_2OH$	-18.76	-21.08	-11.79	-11.81
TS-TCD R2-OH	+	$CH_3CH_2CH_2CJH_2$	→	TCD	+	$CH_3CH_2CH_2CH_2OH$	-18.67	-21.28	-11.71	-11.66
						Average	**-18.74**	**-21.17**	**-11.99**	**-12.11**
						Calculation Method Average		**-19.95**		**-12.05**
TS-TCD R3-OH System										
TS-TCD R3-OH	+	CJH_3	→	TCD	+	CH_3OH	-17.26	-19.65	-11.02	-12.27
TS-TCD R3-OH	+	CH_3CJH_2	→	TCD	+	CH_3CH_2OH	-18.71	-20.96	-11.26	-12.04
TS-TCD R3-OH	+	$CH_3CH_2CJH_2$	→	TCD	+	$CH_3CH_2CH_2OH$	-17.98	-20.22	-10.69	-11.48
TS-TCD R3-OH	+	$CH_3CH_2CH_2CJH_2$	→	TCD	+	$CH_3CH_2CH_2CH_2OH$	-17.90	-20.42	-10.61	-11.33
						Average	**-17.96**	**-20.31**	**-10.90**	**-11.78**
						Calculation Method Average		**-19.14**		**-11.34**

Table F.11 Isodesmic Work Reactions and Calculated $\Delta H^{\circ}_{f\,298}$ for TS-TCD R*i*-OH Species (Continued)

Isodesmic Reactions							$\Delta H^{\circ}_{f\,298}$ (kcal mol^{-1})			
							B3LYP		CBS-QB3	G3MP2B3
							6-31G(d,p)	6-311G(2d,2p)		
TS-TCD R4-OH System										
TS-TCD R4-OH	+	CJH_3	→	TCD	+	CH_3OH	-15.45	-17.94	-9.67	-11.27
TS-TCD R4-OH	+	CH_3CJH_2	→	TCD	+	CH_3CH_2OH	-16.91	-19.24	-9.90	-11.05
TS-TCD R4-OH	+	$CH_3CH_2CJH_2$	→	TCD	+	$CH_3CH_2CH_2OH$	-16.18	-18.50	-9.34	-10.48
TS-TCD R4-OH	+	$CH_3CH_2CH_2CJH_2$	→	TCD	+	$CH_3CH_2CH_2CH_2OH$	-16.09	-18.70	-9.25	-10.33
						Average	**-16.16**	**-18.60**	**-9.54**	**-10.78**
						Calculation Method Average		**-17.38**		**-10.16**
TS-TCD R9-OH System										
TS-TCD R9-OH	+	CJH_3	→	TCD	+	CH_3OH	-16.86	-19.38	-10.86	-11.95
TS-TCD R9-OH	+	CH_3CJH_2	→	TCD	+	CH_3CH_2OH	-18.32	-20.69	-11.09	-11.73
TS-TCD R9-OH	+	$CH_3CH_2CJH_2$	→	TCD	+	$CH_3CH_2CH_2OH$	-17.59	-19.95	-10.53	-11.16
TS-TCD R9-OH	+	$CH_3CH_2CH_2CJH_2$	→	TCD	+	$CH_3CH_2CH_2CH_2OH$	-17.50	-20.14	-10.44	-11.01
						Average	**-17.57**	**-20.04**	**-10.73**	**-11.46**
						Calculation Method Average		**-18.80**		**-11.10**
TS-TCD R10-OH System										
TS-TCD R10-OH	+	CJH_3	→	TCD	+	CH_3OH	-15.34	-17.72	-9.80	-10.90
TS-TCD R10-OH	+	CH_3CJH_2	→	TCD	+	CH_3CH_2OH	-16.80	-19.03	-10.04	-10.68
TS-TCD R10-OH	+	$CH_3CH_2CJH_2$	→	TCD	+	$CH_3CH_2CH_2OH$	-16.07	-18.29	-9.47	-10.11
TS-TCD R10-OH	+	$CH_3CH_2CH_2CJH_2$	→	TCD	+	$CH_3CH_2CH_2CH_2OH$	-15.98	-18.48	-9.39	-9.96
						Average	**-16.05**	**-18.38**	**-9.67**	**-10.42**
						Calculation Method Average		**-17.21**		**-10.04**

Table F.12 Isodesmic Work Reactions and Calculated $\Delta H^{\circ}_{f\,298}$ for TS-TCD R*i*-OOH Species

Isodesmic Reactions							$\Delta H^{\circ}_{f\,298}$ (kcal mol^{-1})			
							B3LYP		CBS-QB3	G3MP2B3
							6-31G(d,p)	6-311G(2d,2p)		
TS-TCD R1-OOH System										
TS-TCD R1-OOH	+	CJH_3	→	TCD	+	CH_3OOH	-4.00	-5.99	0.05	-0.27
TS-TCD R1-OOH	+	CH_3CJH_2	→	TCD	+	CH_3CH_2OOH	-5.84	-7.69	-0.26	-0.19
TS-TCD R1-OOH	+	$CH_3CH_2CJH_2$	→	TCD	+	$CH_3CH_2CH_2OOH$	-5.18	-7.12	0.51	0.59
TS-TCD R1-OOH	+	$CH_3CH_2CH_2CJH_2$	→	TCD	+	$CH_3CH_2CH_2CH_2OOH$	-5.03	-7.25	0.74	0.89
						Average	**-5.01**	**-7.01**	**0.26**	**0.26**
						Calculation Method Average	**-6.01**		**0.26**	
TS-TCD R2-OOH System										
TS-TCD R2-OOH	+	CJH_3	→	TCD	+	CH_3OOH	-9.42	-11.13	-4.87	-4.67
TS-TCD R2-OOH	+	CH_3CJH_2	→	TCD	+	CH_3CH_2OOH	-11.27	-12.82	-5.18	-4.60
TS-TCD R2-OOH	+	$CH_3CH_2CJH_2$	→	TCD	+	$CH_3CH_2CH_2OOH$	-10.61	-12.26	-4.41	-3.82
TS-TCD R2-OOH	+	$CH_3CH_2CH_2CJH_2$	→	TCD	+	$CH_3CH_2CH_2CH_2OOH$	-10.45	-12.39	-4.18	-3.51
						Average	**-10.44**	**-12.15**	**-4.66**	**-4.15**
						Calculation Method Average	**-11.29**		**-4.40**	
TS-TCD R3-OOH System										
TS-TCD R3-OOH	+	CJH_3	→	TCD	+	CH_3OOH	-8.00	-9.82	-2.40	-2.82
TS-TCD R3-OOH	+	CH_3CJH_2	→	TCD	+	CH_3CH_2OOH	-9.85	-11.52	-2.72	-2.74
TS-TCD R3-OOH	+	$CH_3CH_2CJH_2$	→	TCD	+	$CH_3CH_2CH_2OOH$	-9.19	-10.95	-1.94	-1.96
TS-TCD R3-OOH	+	$CH_3CH_2CH_2CJH_2$	→	TCD	+	$CH_3CH_2CH_2CH_2OOH$	-9.03	-11.08	-1.71	-1.65
						Average	**-9.02**	**-10.84**	**-2.20**	**-2.29**
						Calculation Method Average	**-9.93**		**-2.24**	

Table F.12 Isodesmic Work Reactions and Calculated $\Delta H^{\circ}_{f\,298}$ for TS-TCD R*i*-OOH Species (Continued)

Isodesmic Reactions							$\Delta H^{\circ}_{f\,298}$ (kcal mol^{-1})			
							B3LYP		CBS-QB3	G3MP2B3
							6-31G(d,p)	6-311G(2d,2p)		
TS-TCD R4-OOH System										
TS-TCD R4-OOH	+	CJH_3	→	TCD	+	CH_3OOH	-6.28	-8.28	-0.71	-1.16
TS-TCD R4-OOH	+	CH_3CJH_2	→	TCD	+	CH_3CH_2OOH	-8.12	-9.98	-1.02	-1.08
TS-TCD R4-OOH	+	$CH_3CH_2CJH_2$	→	TCD	+	$CH_3CH_2CH_2OOH$	-7.46	-9.41	-0.25	-0.30
TS-TCD R4-OOH	+	$CH_3CH_2CH_2CJH_2$	→	TCD	+	$CH_3CH_2CH_2CH_2OOH$	-7.31	-9.54	-0.02	0.01
						Average	**-7.29**	**-9.30**	**-0.50**	**-0.63**
						Calculation Method Average		**-8.30**		**-0.56**
TS-TCD R9-OOH System										
TS-TCD R9-OOH	+	CJH_3	→	TCD	+	CH_3OOH	-8.35	-10.15	-3.17	-3.52
TS-TCD R9-OOH	+	CH_3CJH_2	→	TCD	+	CH_3CH_2OOH	-10.20	-11.85	-3.48	-3.45
TS-TCD R9-OOH	+	$CH_3CH_2CJH_2$	→	TCD	+	$CH_3CH_2CH_2OOH$	-9.54	-11.28	-2.71	-2.66
TS-TCD R9-OOH	+	$CH_3CH_2CH_2CJH_2$	→	TCD	+	$CH_3CH_2CH_2CH_2OOH$	-9.38	-11.41	-2.48	-2.36
						Average	**-9.36**	**-11.17**	**-2.96**	**-3.00**
						Calculation Method Average		**-10.27**		**-2.98**
TS-TCD R10-OOH System										
TS-TCD R10-OOH	+	CJH_3	→	TCD	+	CH_3OOH	-4.15	-6.11	0.47	-0.28
TS-TCD R10-OOH	+	CH_3CJH_2	→	TCD	+	CH_3CH_2OOH	-6.00	-7.81	0.15	-0.21
TS-TCD R10-OOH	+	$CH_3CH_2CJH_2$	→	TCD	+	$CH_3CH_2CH_2OOH$	-5.34	-7.25	0.93	0.58
TS-TCD R10-OOH	+	$CH_3CH_2CH_2CJH_2$	→	TCD	+	$CH_3CH_2CH_2CH_2OOH$	-5.19	-7.37	1.16	0.88
						Average	**-5.17**	**-7.14**	**0.67**	**0.24**
						Calculation Method Average		**-6.15**		**0.46**

Table F.13 Calculated Total Entropies[a] and Heat Capacities[a]

Temperature (K)	TS-TCD R1-H		TS-TCD R2-H		TS-TCD R3-H		TS-TCD R4-H		TS-TCD R9-H		TS-TCD R10-H	
	Cp	S	Cp	S	Cp	S	Cp	S	Cp	S	Cp	S
50	9.162	57.242	9.121	57.228	9.185	57.246	9.470	57.389	9.160	57.230	9.185	57.251
100	13.988	64.978	13.554	64.801	13.477	64.836	13.898	65.231	13.673	64.879	13.901	64.972
150	19.230	71.622	18.768	71.257	18.502	71.222	18.906	71.788	18.725	71.354	19.016	71.556
200	25.093	77.917	24.688	77.426	24.341	77.302	24.677	77.975	24.536	77.494	24.810	77.779
250	32.101	84.230	31.751	83.654	31.416	83.453	31.675	84.193	31.572	83.685	31.823	84.028
298	39.659	90.484	39.369	89.852	39.087	89.596	39.280	90.376	39.212	89.852	39.431	90.237
400	56.127	104.440	55.990	103.743	55.843	103.423	55.929	104.244	55.920	103.709	56.047	104.146
500	70.443	118.511	70.440	117.799	70.385	117.456	70.408	118.289	70.435	117.756	70.477	118.213
600	82.261	132.405	82.347	131.700	82.342	131.352	82.329	132.186	82.376	131.660	82.359	132.118
700	91.933	145.811	92.067	145.123	92.087	144.777	92.055	145.607	92.110	145.089	92.058	145.542
800	99.937	158.605	100.093	157.937	100.123	157.594	100.082	158.419	100.139	157.908	100.068	158.353
1000	112.326	182.280	112.485	181.648	112.519	181.313	112.472	182.128	112.527	181.630	112.445	182.057
1500	130.633	231.696	130.745	231.119	130.769	230.796	130.732	231.594	130.770	231.115	130.705	231.511
2000	139.713	270.637	139.787	270.088	139.803	269.770	139.776	270.558	139.802	270.089	139.757	270.469
2500	144.658	302.383	144.710	301.847	144.721	301.533	144.702	302.316	144.720	301.851	144.688	302.223
3000	147.588	329.030	147.626	328.503	147.633	328.190	147.619	328.970	147.633	328.508	147.609	328.875
3500	149.447	351.926	149.476	351.403	149.481	351.091	149.471	351.870	149.481	351.410	149.463	351.773
4000	150.694	371.965	150.716	371.446	150.720	371.135	150.712	371.912	150.720	371.453	150.706	371.814
4500	151.567	389.765	151.585	389.248	151.589	388.938	151.582	389.714	151.588	389.256	151.577	389.616
5000	152.202	405.767	152.217	405.252	152.219	404.942	152.214	405.717	152.219	405.260	152.210	405.619
Zero Point Energy[b]	**147.607**		**147.381**		**147.400**		**147.410**		**147.335**		**147.449**	

[a] Units of cal mol^{-1} K^{-1}.

[b] Units of kcal mol^{-1}.

Table F.13 Calculated Total Entropies[a] and Heat Capacities[a] (Continued A)

Temperature (K)	TS-TCD R1-CH_3		TS-TCD R2-CH_3		TS-TCD R3-CH_3		TS-TCD R4-CH_3		TS-TCD R9-CH_3		TS-TCD R10-CH_3	
	Cp	**S**	**Cp**	**S**	**Cp**	**S**	**Cp**	**S**	**Cp**	**S**	**Cp**	**S**
50	12.825	63.427	13.106	62.502	13.018	62.534	13.054	64.070	12.745	63.672	12.639	63.477
100	17.622	73.305	17.674	72.406	17.427	72.323	17.443	73.761	17.460	73.257	17.597	73.071
150	23.058	81.037	23.029	80.148	22.635	79.936	22.680	81.380	22.678	80.881	22.871	80.765
200	29.417	88.212	29.339	87.308	28.886	86.973	28.955	88.431	28.937	87.928	29.106	87.866
250	36.947	95.322	36.863	94.401	36.438	93.965	36.503	95.440	36.485	94.932	36.613	94.904
298	44.996	102.294	44.928	101.359	44.568	100.855	44.625	102.339	44.615	101.829	44.703	101.819
400	62.508	117.672	62.486	116.723	62.284	116.135	62.314	117.633	62.319	117.122	62.345	117.130
500	77.795	133.049	77.800	132.099	77.704	131.478	77.721	132.979	77.733	132.471	77.726	132.480
600	90.490	148.178	90.507	147.231	90.470	146.598	90.480	148.102	90.497	147.596	90.474	147.602
700	100.954	162.757	100.976	161.814	100.970	161.178	100.976	162.682	100.993	162.180	100.964	162.182
800	109.683	176.669	109.707	175.728	109.716	175.092	109.718	176.598	109.735	176.098	109.704	176.096
1000	123.348	202.436	123.370	201.500	123.389	200.867	123.385	202.372	123.402	201.877	123.371	201.868
1500	143.911	256.380	143.926	255.451	143.940	254.825	143.935	256.329	143.947	255.839	143.923	255.818
2000	154.264	299.043	154.273	298.117	154.282	297.494	154.277	298.998	154.287	298.511	154.270	298.485
2500	159.941	333.898	159.949	332.973	159.955	332.352	159.950	333.855	159.957	333.370	159.944	333.341
3000	163.317	363.192	163.321	362.268	163.325	361.648	163.322	363.150	163.327	362.666	163.318	362.635
3500	165.463	388.381	165.466	387.458	165.470	386.838	165.467	388.340	165.471	387.857	165.463	387.825
4000	166.903	410.439	166.907	409.517	166.909	408.898	166.907	410.399	166.909	409.916	166.904	409.883
4500	167.914	430.040	167.917	429.118	167.919	428.499	167.917	430.000	167.918	429.517	167.914	429.483
5000	168.649	447.664	168.650	446.743	168.652	446.124	168.651	447.625	168.652	447.142	168.649	447.108
Zero Point Energy[b]	**166.214**		**166.243**		**166.341**		**166.269**		**166.235**		**166.277**	

[b] Units of kcal mol^{-1}.

Table F.13 Calculated Total Entropies[a] and Heat Capacities[a] (Continued B)

Temperature (K)	TS-TCD R1-O		TS-TCD R2-O		TS-TCD R3-O		TS-TCD R4-O		TS-TCD R9-O		TS-TCD R10-O	
	Cp	S	Cp	S	Cp	S	Cp	S	Cp	S	Cp	S
50	11.764	58.850	11.775	58.538	10.852	58.095	11.877	59.251	12.042	58.911	11.390	58.205
100	16.426	68.420	16.462	68.147	15.615	67.064	16.310	68.831	16.510	68.635	16.377	67.659
150	21.333	75.980	21.166	75.685	20.458	74.284	20.958	76.293	20.990	76.149	21.148	75.178
200	27.108	82.864	26.782	82.497	26.214	80.912	26.578	83.046	26.492	82.892	26.806	81.990
250	34.135	89.627	33.731	89.179	33.281	87.480	33.536	89.683	33.438	89.507	33.808	88.683
298	41.727	96.242	41.304	95.721	40.942	93.950	41.114	96.191	41.056	96.001	41.430	95.242
400	58.174	110.808	57.795	110.166	57.568	108.309	57.616	110.581	57.669	110.390	57.992	109.736
500	72.336	125.321	72.028	124.603	71.888	122.705	71.871	124.980	71.987	124.809	72.250	124.220
600	83.938	139.542	83.691	138.772	83.608	136.854	83.561	139.124	83.699	138.976	83.911	138.430
700	93.384	153.190	93.185	152.386	93.139	150.458	93.081	152.719	93.218	152.593	93.389	152.077
800	101.180	166.164	101.017	165.336	100.996	163.404	100.935	165.657	101.062	165.548	101.203	165.053
1000	113.239	190.081	113.122	189.221	113.127	187.288	113.073	189.527	113.173	189.444	113.271	188.976
1500	131.095	239.768	131.034	238.874	131.053	236.946	131.020	239.168	131.072	239.115	131.121	238.676
2000	139.982	278.813	139.945	277.905	139.961	275.982	139.941	278.197	139.972	278.155	140.000	277.727
2500	144.834	310.608	144.809	309.693	144.821	307.773	144.807	309.984	144.827	309.948	144.846	309.525
3000	147.711	337.282	147.693	336.363	147.702	334.445	147.693	336.654	147.707	336.621	147.720	336.201
3500	149.538	360.194	149.524	359.273	149.532	357.356	149.525	359.564	149.535	359.533	149.545	359.115
4000	150.763	380.244	150.753	379.321	150.759	377.406	150.753	379.612	150.761	379.583	150.769	379.165
4500	151.622	398.052	151.614	397.128	151.619	395.213	151.615	397.419	151.621	397.390	151.627	396.973
5000	152.247	414.059	152.240	413.134	152.244	411.220	152.240	413.425	152.245	413.397	152.250	412.981
Zero Point Energy[b]	**144.904**		**145.271**		**145.453**		**145.398**		**145.210**		**144.946**	

[b] Units of kcal mol^{-1}.

Table F.13 Calculated Total Entropies[a] and Heat Capacities[a] (Continued C)

Temperature (K)	TS-TCD R1-OH		TS-TCD R2-OH		TS-TCD R3-OH		TS-TCD R4-OH		TS-TCD R9-OH		TS-TCD R10-OH	
	Cp	S	Cp	S	Cp	S	Cp	S	Cp	S	Cp	S
50	13.364	61.837	11.744	60.261	11.376	59.677	13.074	61.658	12.579	60.749	12.317	60.517
100	17.674	71.734	17.230	69.627	17.125	68.649	17.557	71.413	17.931	70.472	17.859	70.109
150	21.991	79.228	21.970	77.340	22.127	76.072	21.809	78.854	22.250	78.090	22.335	77.729
200	27.279	85.881	27.282	84.001	27.642	82.805	26.971	85.439	27.268	84.788	27.443	84.464
250	33.853	92.336	33.782	90.444	34.283	89.348	33.478	91.818	33.660	91.216	33.872	90.935
298	41.133	98.629	41.009	96.718	41.562	95.717	40.755	98.044	40.863	97.469	41.086	97.226
400	57.298	112.457	57.148	110.503	57.677	109.662	57.003	111.770	57.031	111.213	57.236	111.036
500	71.628	126.395	71.495	124.411	71.958	123.675	71.431	125.652	71.430	125.098	71.601	124.962
600	83.545	140.189	83.440	138.183	83.829	137.526	83.420	139.415	83.414	138.859	83.550	138.752
700	93.326	153.530	93.244	151.508	93.572	150.904	93.250	152.740	93.238	152.184	93.346	152.096
800	101.440	166.286	101.375	164.255	101.650	163.691	101.394	165.488	101.385	164.930	101.471	164.856
1000	114.085	189.949	114.045	187.904	114.243	187.396	114.071	189.144	114.066	188.585	114.120	188.526
1500	133.199	239.591	133.183	237.535	133.285	237.088	133.205	238.785	133.205	238.224	133.224	238.180
2000	142.968	278.963	142.960	276.905	143.022	276.480	142.975	278.159	142.975	277.599	142.983	277.559
2500	148.389	311.201	148.382	309.142	148.426	308.728	148.395	310.399	148.395	309.839	148.399	309.800
3000	151.634	338.336	151.630	336.276	151.661	335.869	151.639	337.535	151.640	336.974	151.642	336.936
3500	153.708	361.694	153.706	359.632	153.728	359.230	153.712	360.893	153.713	360.333	153.715	360.295
4000	155.105	382.162	155.104	380.100	155.119	379.701	155.108	381.361	155.109	380.801	155.110	380.763
4500	156.087	400.360	156.087	398.297	156.098	397.901	156.090	399.560	156.091	398.998	156.092	398.961
5000	156.802	416.728	156.801	414.665	156.811	414.270	156.804	415.929	156.804	415.368	156.805	415.331
Zero Point Energy[b]	**152.966**		**153.323**		**153.194**		**153.101**		**153.216**		**153.082**	

[b] Units of kcal mol^{-1}.

Table F.13 Calculated Total Entropies[a] and Heat Capacities[a] (Continued D)

Temperature (K)	TS-TCD R1-OOH		TS-TCD R2-OOH		TS-TCD R3-OOH		TS-TCD R4-OOH		TS-TCD R9-OOH		TS-TCD R10-OOH	
	Cp	S	Cp	S	Cp	S	Cp	S	Cp	S	Cp	S
50	14.413	68.791	13.604	66.157	13.410	65.894	14.372	67.600	13.849	66.647	14.348	67.876
100	19.362	79.582	19.816	76.823	19.148	76.255	19.616	78.448	19.512	77.308	19.572	78.762
150	24.726	88.009	25.513	85.522	24.924	84.688	25.119	87.015	25.013	85.837	24.765	87.248
200	30.936	95.646	31.596	93.371	31.323	92.408	31.281	94.759	31.159	93.547	30.836	94.868
250	38.342	103.082	38.813	100.934	38.794	99.940	38.624	102.265	38.504	101.025	38.190	102.278
298	46.296	110.313	46.631	108.233	46.775	107.253	46.553	109.541	46.448	108.282	46.161	109.482
400	63.427	125.997	63.615	123.990	63.902	123.077	63.698	125.302	63.621	124.016	63.391	125.141
500	78.243	141.531	78.375	139.561	78.693	138.714	78.534	140.895	78.480	139.594	78.289	140.675
600	90.416	156.696	90.526	154.750	90.825	153.960	90.700	156.116	90.659	154.809	90.500	155.854
700	100.346	171.226	100.446	169.296	100.718	168.547	100.612	170.689	100.586	169.374	100.446	170.397
800	108.553	185.023	108.648	183.106	108.887	182.391	108.797	184.522	108.780	183.203	108.654	184.208
1000	121.273	210.436	121.360	208.538	121.539	207.873	121.475	209.984	121.468	208.663	121.358	209.642
1500	140.219	263.202	140.282	261.335	140.380	260.726	140.341	262.816	140.342	261.494	140.265	262.434
2000	149.722	304.676	149.766	302.824	149.827	302.237	149.801	304.318	149.806	302.997	149.749	303.919
2500	154.936	338.464	154.966	336.621	155.008	336.045	154.990	338.120	154.993	336.801	154.954	337.711
3000	158.037	366.819	158.060	364.981	158.090	364.411	158.076	366.485	158.078	365.166	158.050	366.069
3500	160.011	391.181	160.029	389.345	160.051	388.780	160.040	390.851	160.042	389.534	160.021	390.432
4000	161.337	412.503	161.351	410.670	161.367	410.107	161.360	412.177	161.362	410.859	161.344	411.757
4500	162.266	431.443	162.279	429.611	162.290	429.051	162.286	431.120	162.287	429.802	162.273	430.697
5000	162.943	448.469	162.954	446.639	162.963	446.080	162.959	448.148	162.961	446.830	162.948	447.724
Zero Point Energy[b]	**154.905**		**154.903**		**154.949**		**154.802**		**154.835**		**154.830**	

[b] Units of kcal mol^{-1}.

Table F.14 Calculated $\Delta H^{\circ}_{f\,298}$ for Alcohol Radical Reference Species in TS-TCD Isodesmic Work Reactions

Isodesmic Reactions							$\Delta H^{\circ}_{f\,298}$ (kcal mol^{-1})	
							CBS-QB3	G3MP2B3
$CH_3CH_2CH_2OJ$ System								
$CH_3CH_2CH_2OJ$	+	CH_4	→	$CH_3CH_2CH_2OH$	+	CJH_3	-8.70	-7.97
$CH_3CH_2CH_2OJ$	+	CH_3CH_3	→	$CH_3CH_2CH_2OH$	+	CH_3CJH_2	-8.61	-8.33
$CH_3CH_2CH_2OJ$	+	$CH_3CH_2CH_3$	→	$CH_3CH_2CH_2OH$	+	$CH_3CH_2CJH_2$	-8.99	-8.75
$CH_3CH_2CH_2OJ$	+	$CH_3CH_2CH_2CH_3$	→	$CH_3CH_2CH_2OH$	+	$CH_3CH_2CH_2CJH_2$	-8.84	-8.67
						Method Average	**-8.8**	**-8.4**
						Average	**-8.6 ± 0.3**	
$CH_3CH_2CH_2CH_2OJ$ System								
$CH_3CH_2CH_2CH_2OJ$	+	CH_4	→	$CH_3CH_2CH_2CH_2OH$	+	CJH_3	-13.44	-12.73
$CH_3CH_2CH_2CH_2OJ$	+	CH_3CH_3	→	$CH_3CH_2CH_2CH_2OH$	+	CH_3CJH_2	-13.35	-13.09
$CH_3CH_2CH_2CH_2OJ$	+	$CH_3CH_2CH_3$	→	$CH_3CH_2CH_2CH_2OH$	+	$CH_3CH_2CJH_2$	-13.73	-13.50
$CH_3CH_2CH_2CH_2OJ$	+	$CH_3CH_2CH_2CH_3$	→	$CH_3CH_2CH_2CH_2OH$	+	$CH_3CH_2CH_2CJH_2$	-13.58	-13.43
						Method Average	**-13.5**	**-13.2**
						Average	**-13.4 ± 0.3**	

APPENDIX G

STRUCTURE AND THERMOCHEMICAL PROPERTIES OF 2-METHOXYFURAN, 3-METHOXYFURAN, AND THEIR CARBON-CENTERED RADICALS

This appendix contains the optimized geometries with corresponding Gaussian atom numbering, moments of inertia, vibrational frequencies, internal rotor potential energy graphs, entropies, and heat capacities for the methoxyfuran species from B3LYP/ 6-31G(d,p). Comparison of bond lengths and angles of 2-methoxyfuran are also included.

Table G.1 2-Methoxyfuran Optimized Species

Y(OC[OCH_3]CCC)

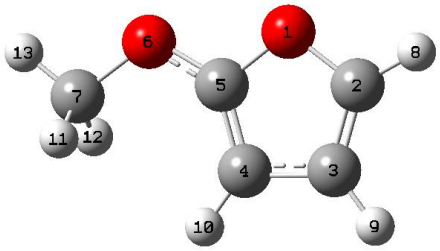

O,0,0.7686436825,-1.114968905,0.0001231098
C,0,1.9742723225,-0.4453986825,0.0001908655
C,0,1.7625683075,0.8941542989,0.0000159268
C,0,0.3362880869,1.0913084263,-0.0002138242
C,0,-0.1948835694,-0.167867927,-0.0001597679
O,0,-1.4379355315,-0.6729048005,-0.0003761104
C,0,-2.4737906284,0.3042175765,0.0004086892
H,0,2.8512230319,-1.0714771119,0.0003617826
H,0,2.5221997063,1.6627262991,0.0000363782
H,0,-0.1993650562,2.0273032218,-0.0004034976
H,0,-2.4168854722,0.9372330231,-0.8935332254
H,0,-2.4158698993,0.9368555613,0.894546489
H,0,-3.4134969807,-0.24795198,0.0008011842

Y(OC[OCH_3]CCC•)

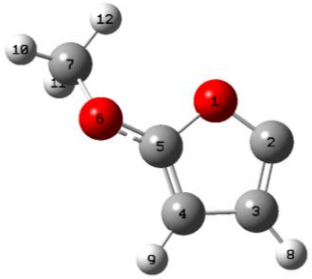

O,0,-0.0728185702,-0.0839672594,0.146232169
C,0,0.1183288229,-0.1531120396,1.4767739811
C,0,1.4196293445,-0.024144302,1.8367426316
C,0,2.1359073815,0.0577973434,0.5814290701
C,0,1.1972080424,0.0267131898,-0.40390692
O,0,1.3062246027,-0.0436693577,-1.733535766
C,0,0.4448674964,0.8335096482,-2.4796087824
H,0,1.8316312685,-0.004871887,2.8333590587
H,0,3.2044230328,0.1174946349,0.4374104626
H,0,0.6988252748,0.6798156839,-3.5285296485
H,0,0.6228562305,1.87783178,-2.2004929011
H,0,-0.6060086279,0.5819393573,-2.3120687865

Table G.1 2-Methoxyfuran Optimized Species (Continued)

Y(OC[OCH_3]CC$^{\bullet}$C)

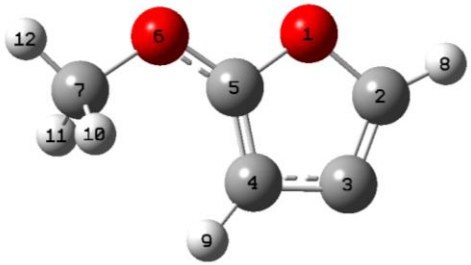

O,0,-0.0277316263,0.0014223483,0.0341976736
C,0,0.030055759,-0.0006751367,1.4281228963
C,0,1.3305068921,-0.0016428969,1.7763255617
C,0,2.1614454811,-0.0000332054,0.6151836761
C,0,1.2490405741,0.0019766725,-0.4089823778
O,0,1.3404776416,0.0042493876,-1.7457118325
C,0,2.6714313882,0.0046588437,-2.2562016469
H,0,-0.9158678196,-0.0012024509,1.9404633795
H,0,3.2368443279,-0.0002575106,0.548445029
H,0,3.2149474059,-0.8907338935,-1.9319322372
H,0,3.2156576705,0.8984333637,-1.9286720847
H,0,2.5793125818,0.0066955029,-3.342025398

Y(OC[OCH_3]C$^{\bullet}$CC)

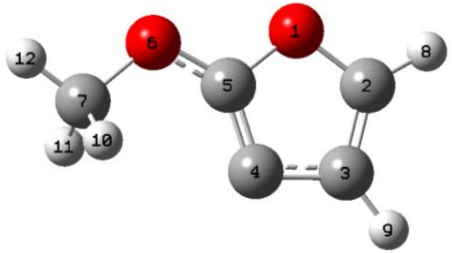

O,0,-0.0384313852,0.0014179,0.0238014078
C,0,0.0209476361,0.0007331221,1.403519814
C,0,1.3117736772,0.000040808,1.8351733221
C,0,2.0906385344,0.0003126599,0.6389541635
C,0,1.2459576237,0.0011427222,-0.4240253885
O,0,1.3727002082,0.0016889085,-1.7556983876
C,0,2.7293647595,0.0023382728,-2.2008666533
H,0,-0.9337378573,0.0008701727,1.904292362
H,0,1.6542661625,-0.0005652584,2.8590649816
H,0,3.2557448969,-0.8909098262,-1.8446093682
H,0,3.2550326619,0.8958217769,-1.8441763521
H,0,2.6917792761,0.0025469562,-3.2900388623

Y(OC[O$C^{\bullet}H_2$]CCC)

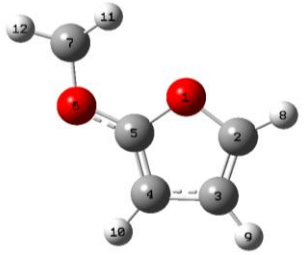

O,0,-0.0684482403,-0.0330343624,0.1188936922
C,0,0.0050453444,0.0114258735,1.4974316448
C,0,1.3047629878,0.0331927328,1.8909184527
C,0,2.1056685713,0.001401635,0.6997373342
C,0,1.209815093,-0.038475784,-0.3280503715
O,0,1.4328604221,-0.0890198341,-1.651040543
C,0,0.3908704766,-0.0644933442,-2.5413185631
H,0,-0.9418550571,0.0245157705,2.0111885562
H,0,1.6616615558,0.0691401581,2.9101378307
H,0,3.1805257219,0.0064457684,0.6123477345
H,0,-0.595943916,-0.323919017,-2.1830675292
H,0,0.7200403701,-0.2537005304,-3.5527119493

Table G.2 3-Methoxyfuran Optimized Species

Y(OCC[OCH_3]CC)

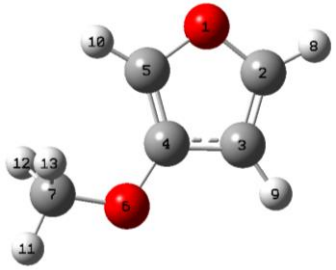

O,0,0.032706187,-0.0004468944,-0.0014041848
C,0,0.009180326,-0.0026430182,1.35714268
C,0,1.2687742885,0.0001137401,1.8687534387
C,0,2.1452901495,0.0035779083,0.73278781
C,0,1.3524993084,0.0035417532,-0.3826512647
O,0,3.4966856125,0.0064551785,0.8484462724
C,0,4.2046278645,0.0110687717,-0.3828148782
H,0,-0.9693592469,-0.0058530529,1.8116971832
H,0,1.5614514912,-0.0005228168,2.907894638
H,0,1.5423169855,0.005649555,-1.4422114387
H,0,5.2663997238,0.0141076671,-0.1335209628
H,0,3.964737028,0.90514545,-0.973810564
H,0,3.9706841305,-0.8823909226,-0.9771331397

Y(OCC[OCH_3]CC$^{\bullet}$)

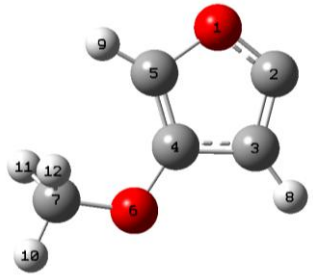

O,0,-0.0788694126,-0.0012558227,0.0456896453
C,0,0.0951024117,-0.0065157191,1.3595884199
C,0,1.3913252212,-0.0030539674,1.7569384628
C,0,2.1164806648,0.0055849955,0.505203566
C,0,1.2017754334,0.0065009686,-0.5129170537
O,0,3.468178038,0.0112648717,0.460603316
C,0,4.0291251763,0.0201137883,-0.8470150161
H,0,1.8029161672,-0.0059011212,2.7528096143
H,0,1.247634144,0.0116159473,-1.5876610751
H,0,5.1122357503,0.0242890353,-0.7207870814
H,0,3.7200895408,0.9158301793,-1.4014889361
H,0,3.7280245208,-0.8728670756,-1.4102048703

Y(OCC[OCH_3]C$^{\bullet}$C)

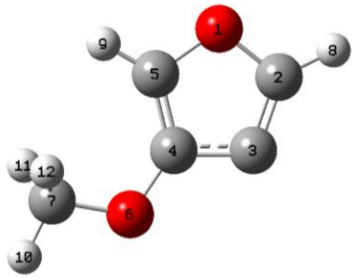

O,0,-0.0494378666,0.0066729174,0.0200600081
C,0,0.0248679218,0.0012538772,1.3892431332
C,0,1.3257094133,-0.0072313541,1.7495122609
C,0,2.1364529048,-0.0074311853,0.5755132645
C,0,1.2394370317,0.001224263,-0.4617306855
O,0,3.4888422693,-0.0149989694,0.5784951523
C,0,4.0898438164,-0.0127214916,-0.7097241599
H,0,-0.9109462037,0.0043855561,1.9227811893
H,0,1.3408138583,0.0049274789,-1.5341564545
H,0,5.168281106,-0.0189553385,-0.5489827031
H,0,3.808703655,0.8852777906,-1.2756168655
H,0,3.7995078286,-0.9030429648,-1.2830626442

Table G.2 3-Methoxyfuran Optimized Species (Continued)

Y(OC•C[OCH$_3$]CC)

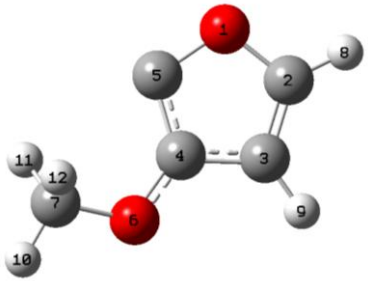

O,0,0.0088791704,-0.0891876998,0.0254241346
C,0,-0.0044487851,-0.0218415967,1.3937732211
C,0,1.2662546931,0.0191536121,1.8909881836
C,0,2.1267911183,-0.0751484482,0.7536226273
C,0,1.30483488,0.0112875416,-0.3711766928
O,0,3.4683074453,-0.0941515488,0.8160641627
C,0,4.116378939,-0.3889875636,-0.4225360977
H,0,-0.9767540524,0.0690101642,1.8544261994
H,0,1.5630382664,0.0857222626,2.9275430765
H,0,5.1847546842,-0.254703501,-0.252103918
H,0,3.7643936841,0.2957507287,-1.2041335937
H,0,3.9151012517,-1.4199071336,-0.7343608722

Y(OCC[OC•H$_2$]CC)

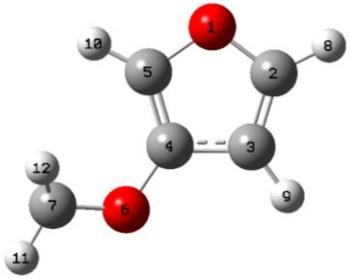

O,0,-0.0429376815,0.0340257655,0.0203565483
C,0,0.0117854182,-0.0387019815,1.3780803857
C,0,1.2982095929,0.0016922845,1.8168756644
C,0,2.0978879016,0.1074228218,0.6334413533
C,0,1.2453963541,0.1270187521,-0.4346361238
O,0,3.4593263601,0.1819137593,0.6617013792
C,0,4.131445844,-0.0678622891,-0.5014510643
H,0,-0.9376085256,-0.1177839116,1.8840095145
H,0,1.6523962208,-0.040920112,2.8356768885
H,0,1.3791290607,0.225394063,-1.4982100533
H,0,5.2024321792,0.0417780514,-0.3936219698
H,0,3.7012868612,-0.8024912781,-1.1774767628

Table G.3 Moments of Inertia[a]

Species	I_a	I_b	I_c
Y(OC[OCH_3]CCC)	236.17827	862.58837	1087.25973
Y(OC[OCH_3]CCC$^{\bullet}$)	231.47982	842.29108	1022.77366
Y(OC[OCH_3]CC$^{\bullet}$C)	225.31719	839.04616	1052.84245
Y(OC[OCH_3]C$^{\bullet}$CC)	220.02912	865.58312	1074.12269
Y(OC[OC$^{\bullet}H_2$]CCC)	229.47844	815.08735	1043.93010
Y(OCC[OCH_3]CC)	238.91785	890.48036	1117.89812
Y(OCC[OCH_3]CC$^{\bullet}$)	238.23631	854.74256	1081.46354
Y(OCC[OCH_3]C$^{\bullet}$C)	216.63119	899.03817	1104.15887
Y(OC$^{\bullet}$C[OCH_3]CC)	229.47133	880.50565	1094.02764
Y(OCC[OC$^{\bullet}H_2$]CC)	229.77952	868.67896	1087.95088

[a] AMU $Bohr^2$

Table G.4 Vibrational Frequencies

Species	Frequencies (cm^{-1})									
Y(OC[OCH_3]CCC)	97.64	201.97	241.60	314.92	495.90	607.20	658.43	670.34	709.24	753.64
	853.28	895.03	967.67	1034.33	1093.01	1106.25	1185.06	1187.78	1217.49	1273.79
	1305.66	1446.79	1482.76	1499.29	1520.53	1582.34	1656.75	3024.63	3088.04	3164.15
	3261.82	3286.77	3307.31							
Y(OC[OCH_3]CCC˙)	41.58	153.48	193.58	350.43	399.92	476.78	628.25	684.45	768.45	816.82
	862.84	921.91	1016.16	1023.81	1113.28	1169.03	1182.14	1219.96	1272.18	1344.99
	1467.15	1498.36	1500.77	1516.36	1672.53	3043.72	3123.02	3166.81	3273.16	3291.37
Y(OC[OCH_3]CC˙C)	94.69	194.15	243.19	305.41	496.26	522.95	630.03	663.12	692.70	727.58
	875.54	961.34	1049.16	1087.70	1126.56	1183.82	1210.64	1227.93	1286.07	1411.66
	1476.51	1499.12	1519.07	1559.75	1624.22	3027.92	3093.31	3167.14	3296.45	3324.59
Y(OC[OCH_3]C˙CC)	91.03	170.51	222.66	262.06	493.30	519.87	627.43	645.18	675.14	827.38
	874.47	961.69	1070.35	1083.53	1164.55	1183.17	1185.29	1228.01	1284.55	1397.88
	1477.17	1494.91	1516.96	1544.03	1659.00	3030.53	3094.90	3166.85	3272.70	3301.11
Y(OC[OC˙H_2]CCC)	75.11	235.68	254.01	325.70	509.20	544.58	604.41	639.90	658.21	697.54
	775.42	862.12	894.32	960.01	1030.42	1092.36	1160.92	1185.79	1203.09	1265.74
	1345.43	1433.15	1482.91	1565.88	1661.01	3179.26	3264.24	3291.48	3309.95	3326.50
Y(OCC[OCH_3]CC)	107.66	221.18	235.94	347.57	473.12	607.42	640.04	665.78	685.44	760.36
	837.94	881.11	990.60	1043.23	1084.61	1106.76	1182.69	1213.06	1229.39	1273.67
	1328.56	1437.10	1484.70	1499.11	1521.20	1559.32	1662.73	3010.41	3068.95	3153.48
	3273.54	3296.15	3313.63							
Y(OCC[OCH_3]CC˙)	105.81	218.49	235.81	330.17	473.63	492.48	615.76	639.44	661.77	772.00
	859.96	969.68	1046.01	1059.74	1115.82	1181.23	1209.41	1235.23	1309.06	1390.63
	1476.46	1498.99	1511.30	1521.44	1645.91	3014.73	3075.68	3157.02	3303.11	3322.14
Y(OCC[OCH_3]C˙C)	105.65	220.09	234.75	337.82	484.10	548.76	605.10	658.36	678.71	761.35
	857.99	981.68	1040.59	1097.63	1162.93	1182.09	1221.10	1244.62	1317.18	1399.01
	1481.53	1499.69	1520.50	1541.98	1632.54	3012.97	3072.72	3157.56	3302.93	3310.23
Y(OC˙C[OCH_3]CC)	114.31	168.40	223.85	315.19	410.57	515.60	596.01	642.99	739.07	809.21
	840.67	875.66	1028.12	1074.25	1087.96	1137.82	1178.16	1214.21	1265.42	1332.37
	1452.70	1493.26	1513.90	1528.12	1589.31	3027.50	3095.23	3162.26	3266.60	3289.03
Y(OCC[OC˙H_2]CC)	106.33	232.73	271.28	385.86	479.12	610.32	632.65	658.84	681.83	700.79
	765.53	841.62	880.82	995.07	1047.15	1092.66	1193.58	1206.79	1224.05	1266.64
	1344.23	1442.13	1479.58	1554.82	1650.01	3129.96	3276.35	3284.97	3299.59	3316.43

Internal Rotor (IR) notation and 0° dihedral angle corresponds to the structures from the Optimized Species.

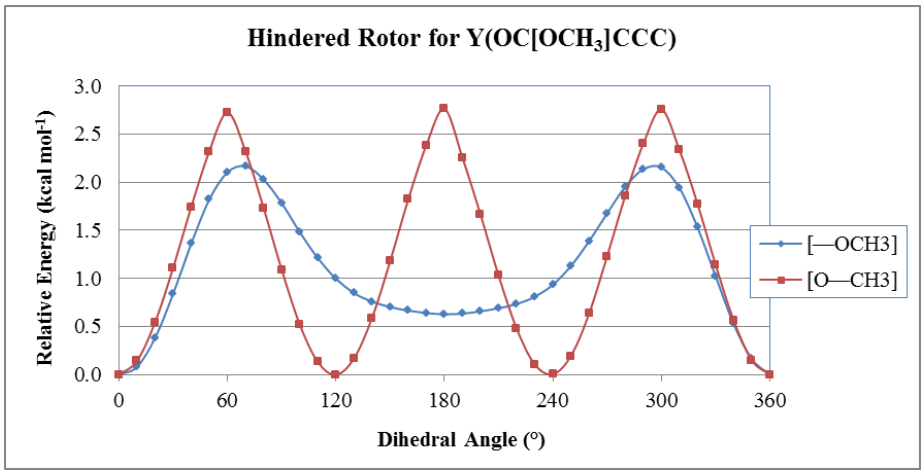

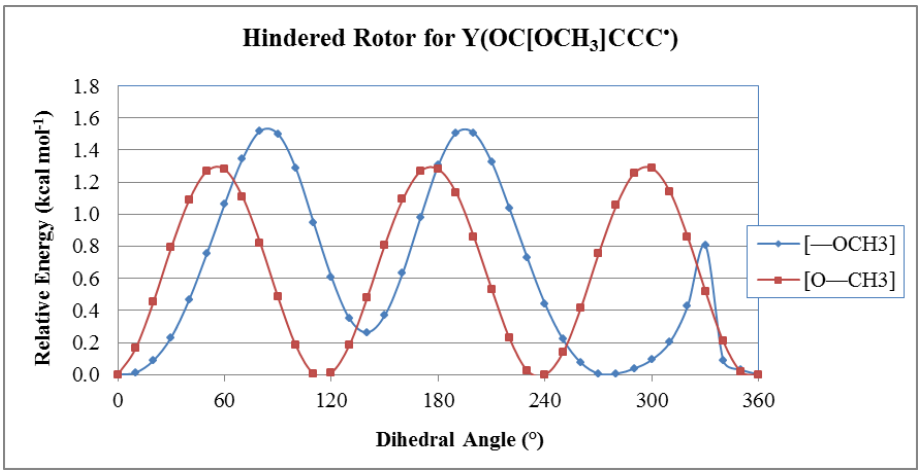

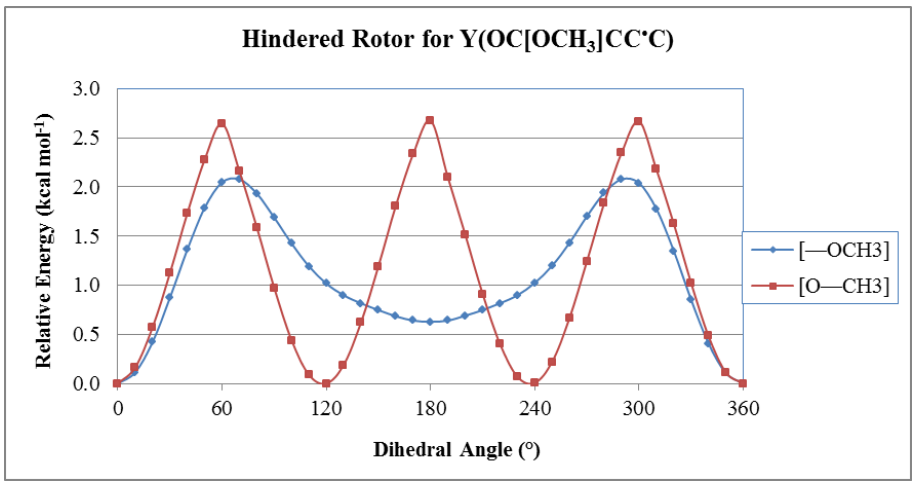

Figure G.1 Internal rotation of 2-methoxyfuran species.

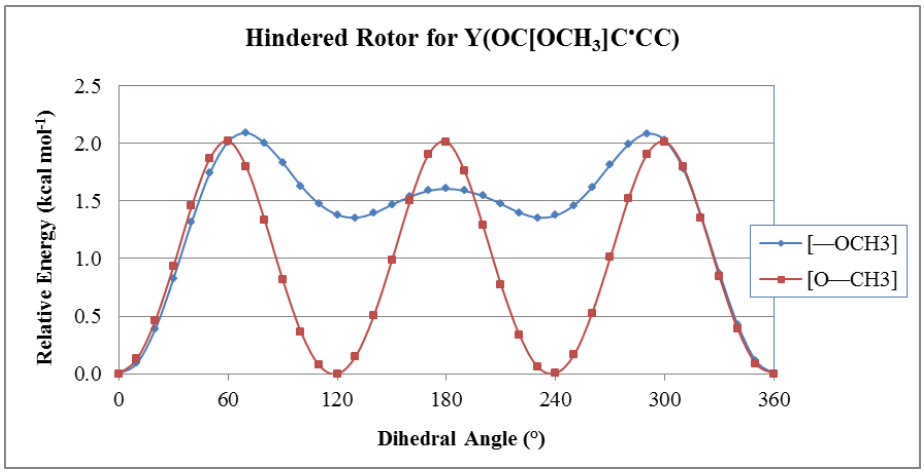

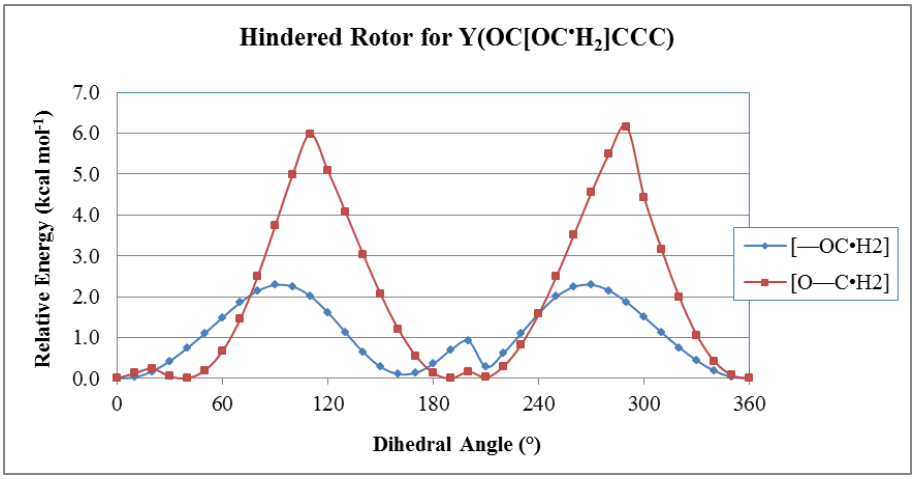

Figure G.1 Internal rotation of 2-methoxyfuran species. (Continued)

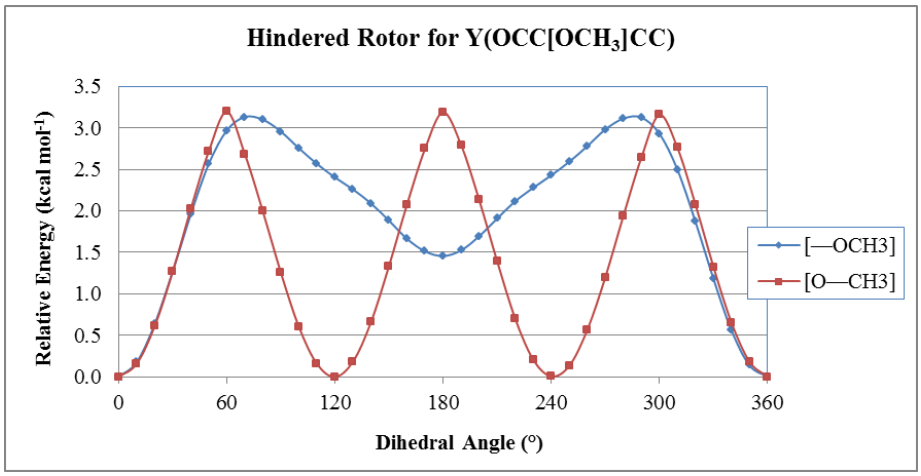

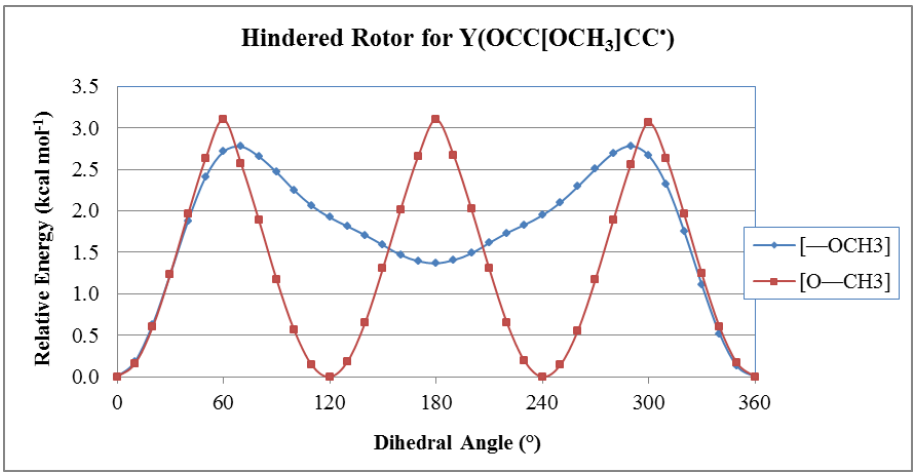

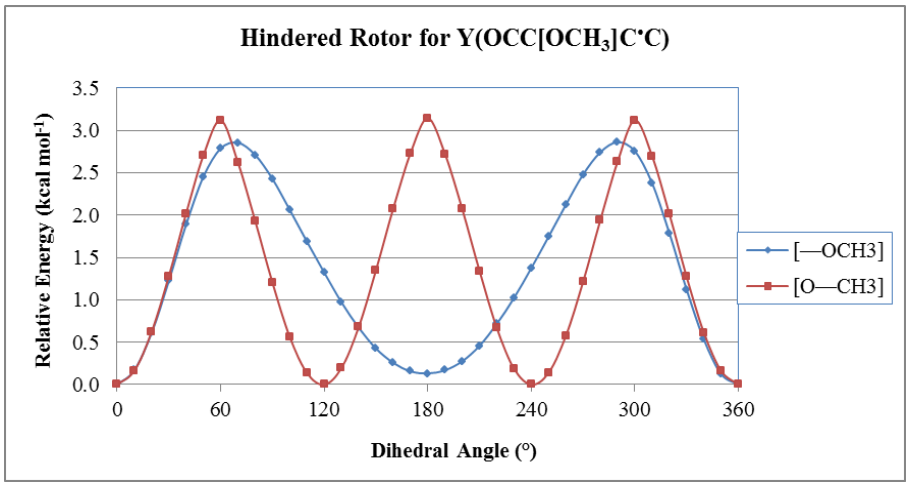

Figure G.2 Internal rotation of 3-methoxyfuran species.

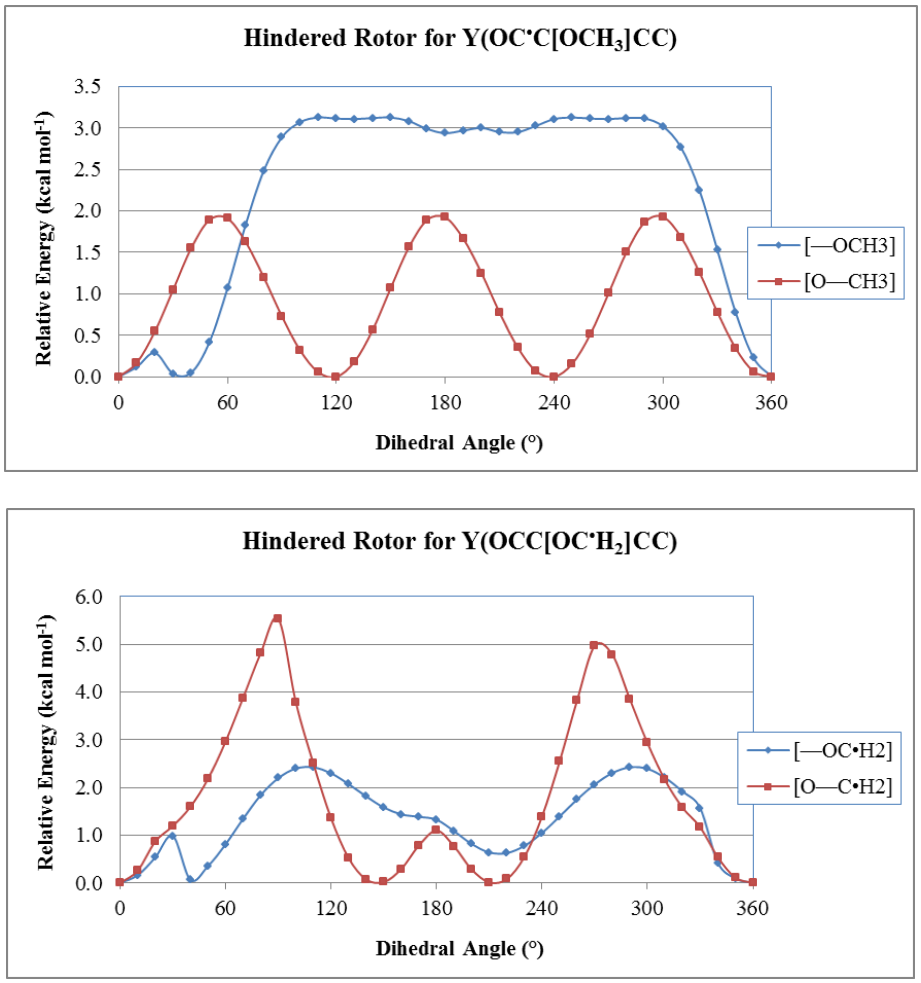

Figure G.2 Internal rotation of 3-methoxyfuran species. (Continued)

Table G.5 Calculated Total Entropies[a] and Heat Capacities[a]

Temperature (K)	Y(OC[OCH$_3$]CCC)		Y(OC[OCH$_3$]CCC$^{\bullet}$)		Y(OC[OCH$_3$]CC$^{\bullet}$C)		Y(OC[OCH$_3$]C$^{\bullet}$CC)		Y(OC[OC$^{\bullet}$H$_2$]CCC)	
	Cp	S	Cp	S	Cp	S	Cp	S	Cp	S
100	12.41	65.04	13.56	69.66	12.52	68.53	13.07	68.91	11.29	69.94
150	15.18	69.78	16.20	74.86	15.41	73.34	15.90	73.93	13.76	74.55
200	18.32	74.00	18.73	79.29	18.51	77.63	18.81	78.33	18.49	76.14
250	21.73	78.01	21.43	83.32	21.68	81.66	21.77	82.41	22.15	80.22
298	25.09	81.76	24.19	86.97	24.72	85.37	24.62	86.12	25.60	84.05
400	31.87	89.53	30.07	94.33	30.74	92.92	30.46	93.61	32.27	91.97
500	37.54	96.83	35.19	101.16	35.79	99.90	35.47	100.52	37.60	99.32
600	42.19	103.74	39.44	107.60	39.93	106.44	39.63	107.00	41.80	106.20
700	46.00	110.23	42.91	113.65	43.32	112.55	43.05	113.08	45.10	112.59
800	49.15	116.31	45.78	119.31	46.12	118.25	45.90	118.74	47.76	118.53
1000	54.05	127.39	50.21	129.58	50.45	128.59	50.28	129.05	51.77	129.20
1500	61.41	150.08	56.76	150.54	56.87	149.62	56.80	150.02	57.61	150.64
2000	65.14	167.74	60.03	166.79	60.09	165.89	60.05	166.28	60.53	167.08
2500	67.19	182.07	61.82	179.95	61.85	179.07	61.83	179.45	62.15	180.33
3000	68.41	194.08	62.88	190.96	62.91	190.08	62.89	190.46	63.11	191.39
3500	69.19	204.38	63.55	200.40	63.57	199.53	63.56	199.90	63.72	200.86
4000	69.72	213.39	64.01	208.65	64.02	207.78	64.01	208.15	64.14	209.14
4500	70.09	221.39	64.33	215.98	64.34	215.11	64.33	215.48	64.43	216.47
5000	70.36	228.58	64.56	222.56	64.57	221.69	64.56	222.06	64.64	223.06
Zero Point Energy[b]	62.893		53.971		55.044		55.009		54.636	

[a] Units of cal mol^{-1} K^{-1}.
[b] Units of kcal mol^{-1}.

Table G.5 Calculated Total Entropies[a] and Heat Capacities[a] (Continued)

Temperature	Y(OCC[OCH_3]CC)		Y(OCC[OCH_3]CC$^{\bullet}$)		Y(OCC[OCH_3]C$^{\bullet}$C)		Y(OC$^{\bullet}$C[OCH_3]CC)		Y(OCC[OC$^{\bullet}H_2$]CC)	
(K)	**Cp**	**S**	**Cp**	**S**	**Cp**	**S**	**Cp**	**S**	**Cp**	**S**
100	12.14	64.62	12.31	68.24	12.23	68.17	12.88	68.51	11.00	69.88
150	14.92	69.25	15.28	72.98	15.08	72.85	15.83	73.48	14.66	71.78
200	18.14	73.40	18.50	77.24	18.23	77.04	18.89	77.88	18.09	75.89
250	21.70	77.39	21.82	81.29	21.53	81.02	22.07	81.99	21.76	79.88
298	25.21	81.16	25.00	85.04	24.70	84.73	25.15	85.79	25.25	83.65
400	32.32	88.66	31.34	92.38	31.06	91.98	31.47	93.19	32.04	91.17
500	38.31	95.87	36.66	99.31	36.41	98.85	36.75	100.16	37.51	98.28
600	43.02	103.03	40.80	106.10	40.61	105.60	40.84	106.95	41.77	105.25
700	46.77	109.70	44.10	112.39	43.94	111.87	44.12	113.24	45.12	111.70
800	49.83	115.92	46.79	118.23	46.66	117.69	46.81	119.08	47.79	117.67
1000	54.39	127.29	50.78	128.83	50.69	128.27	50.83	129.66	51.64	128.54
1500	61.60	150.07	57.06	149.96	57.02	149.38	57.09	150.80	57.51	149.93
2000	65.25	167.78	60.20	166.28	60.18	165.69	60.23	167.14	60.47	166.35
2500	67.27	182.13	61.93	179.48	61.92	178.88	61.95	180.33	62.10	179.59
3000	68.47	194.15	62.96	190.50	62.95	189.90	62.97	191.36	63.07	190.65
3500	69.24	204.46	63.61	199.96	63.61	199.35	63.63	200.82	63.70	200.11
4000	69.75	213.48	64.05	208.21	64.05	207.61	64.06	209.08	64.12	208.38
4500	70.11	221.48	64.36	215.54	64.36	214.94	64.37	216.41	64.41	215.72
5000	70.38	228.67	64.59	222.13	64.59	221.52	64.59	222.99	64.63	222.31
Zero Point Energy[b]	62.859		54.813		55.124		54.225		54.236	

[b] Units of kcal mol^{-1}.

Table G.6 Comparison of Bond Lengths of 2-Methoxyfuran[a]

Bond Length (Å)	Beukes' Work[b]			This Work				
	MP2/ 6-311++G**	B3LYP/ 6-311++G**	B3LYP/ cc-pVTZ	B3LYP/ 6-31G(d,p)	B3LYP/ 6-311G(2d,2p)	G3	CBS-QB3	G3MP2B3
O_1–C_2	1.373	1.379	1.378	1.379	1.378	1.376	1.379	1.379
C_2–C_3	1.366	1.354	1.350	1.356	1.350	1.361	1.353	1.356
C_3–C_4	1.438	1.440	1.437	1.440	1.438	1.432	1.439	1.440
C_4–C_5	1.374	1.365	1.361	1.367	1.362	1.368	1.364	1.367
C_5–O_1	1.348	1.349	1.348	1.351	1.348	1.354	1.348	1.351
C_5–O_6	1.340	1.337	1.336	1.342	1.337	1.346	1.337	1.342
O_6–C_7	1.425	1.427	1.424	1.424	1.425	1.428	1.425	1.424
C_2–H_8	1.078	1.075	1.077	1.078	1.073	1.079	1.075	1.078
C_3–H_9	1.081	1.079	1.076	1.081	1.076	1.081	1.079	1.081
C_4–H_{10}	1.078	1.077	1.074	1.078	1.074	1.079	1.076	1.079
C_7–H_{11}	1.088	1.088	1.086	1.090	1.085	1.088	1.088	1.091
C_7–H_{12}	1.095	1.095	1.093	1.097	1.092	1.094	1.095	1.097
C_7–H_{13}	1.095	1.095	1.092	1.097	1.092	1.094	1.095	1.098

[a] Numbering followings the convention in Table G.1.
[b] Ref. 261.

Table G.7 Comparison of Bond Angles of 2-Methoxyfuran[a]

Angle (°)	Beukes' Work[b]		This Work					
	MP2/ 6-311++G**	B3LYP/ 6-311++G**	B3LYP/ cc-pVTZ	B3LYP/ 6-31G(d,p)	B3LYP/ 6-311G(2d,2p)	G3	CBS-QB3	G3MP2B3
C_4–C_3–C_2	106.6	106.9	106.9	106.9	106.9	106.9	106.9	106.8
C_3–C_4–C_5	104.9	105.0	105.1	105.0	105.0	105.1	105.0	105.0
C_3–C_2–O_1	110.3	109.9	110.0	110.1	110.1	110.2	110.0	110.1
C_4–C_5–O_1	111.8	111.5	111.5	111.6	111.7	111.7	111.6	111.6
C_2–O_1–C_5	106.5	106.6	106.5	106.5	106.4	106.2	106.5	106.5
C_4–C_5–O_6	134.8	135.0	135.0	135.0	135.0	135.3	135.1	135.0
O_1–C_5–O_6	113.4	113.4	113.4	113.4	113.3	113.1	113.4	113.4
C_5–O_6–C_7	112.7	115.2	115.1	114.6	114.8	112.8	115.0	114.5
C_4–C_3–H_9	127.3	126.9	126.8	126.8	126.9	126.9	126.8	126.8
C_2–C_3–H_9	126.1	126.3	126.3	126.4	126.2	126.2	126.3	126.4
C_3–C_4–H_{10}	127.9	127.6	127.6	127.7	127.7	127.5	127.6	127.6
C_5–C_4–H_{10}	127.2	127.4	127.3	127.3	127.3	127.4	127.4	127.4
C_3–C_2–H_8	134.3	134.5	134.4	134.5	134.3	134.6	134.6	134.7
O_1–C_2–H_8	115.5	115.5	115.6	115.4	115.6	115.3	115.4	115.3
O_6–C_7–H_{13}	106.0	106.0	106.2	106.2	106.1	105.7	106.1	106.1
O_6–C_7–H_{12}	110.5	110.7	110.8	111.0	110.8	110.6	110.9	110.9
H_{13}–C_7–H_{12}	110.0	109.8	109.8	109.7	109.8	110.1	109.8	109.8
O_6–C_7–H_{11}	110.5	110.7	110.8	111.0	110.8	110.6	110.9	110.9
H_{13}–C_7–H_{11}	110.0	109.8	109.8	109.7	109.8	110.1	109.8	109.8
H_{12}–C_7–H_{11}	109.7	109.7	109.4	109.2	109.4	109.6	109.5	109.3

[a] Numbering followings the convention in Table G.1.
[b] Ref. 261.

APPENDIX H

THERMOCHEMISTRY OF 2-METHYLFURAN HYDROPEROXIDE AND ALCOHOL SPECIES

This appendix contains the optimized geometries with symmetry values in parenthesis, moments of inertia, and vibrational frequencies for all of the substituted methylfuran species from B3LYP/6-31G(d,p).

Table H.1 Substituted Methylfuran Optimized Species

Y(OC[CH_3]CCC[OOH]) (σ = 3,OI)

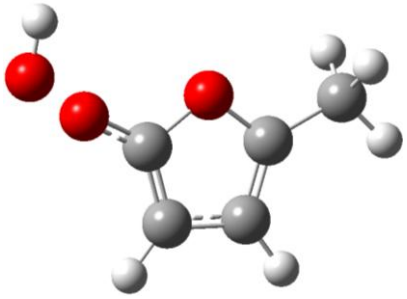

O,0,0.0286894412,-0.0168458337,0.1286313593
C,0,0.0663059368,-0.0062719572,1.5039452056
C,0,1.3592051084,0.0276301448,1.9439484558
C,0,2.1722008652,0.0575760187,0.7708764219
C,0,1.3240146506,0.0178743127,-0.3026988853
C,0,1.5426403509,0.0124852962,-1.7738750939
H,0,3.2509080539,0.0998068617,0.7229739654
H,0,1.6711006843,0.0364103486,2.9772921875
O,0,-1.0909333029,0.0346394064,2.1486013955
O,0,-1.6709249346,-1.3738151288,2.2004223811
H,0,-2.3990983989,-1.2458670268,1.5687633349
H,0,2.6128367837,0.044158424,-1.9896517751
H,0,1.1245034234,-0.8889630258,-2.2360344719
H,0,1.0687313963,0.8771603324,-2.2521545011

Y(OC[CH_3]CCC[OOJ]) (σ = 3)

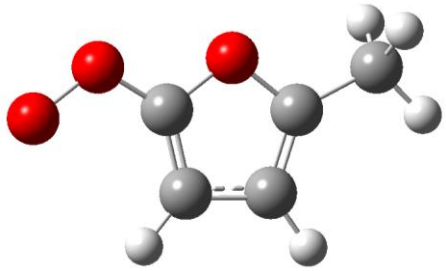

O,0,0.4051971965,-0.8434243248,0.0000093733
C,0,-0.7045972714,-0.0751208395,0.0000075697
C,0,-0.4133136289,1.2557640717,-0.0000061431
C,0,1.0141808935,1.308995859,-0.0000207398
C,0,1.4740656958,0.0235457012,-0.0000039704
C,0,2.8242213018,-0.5907053423,0.0000122935
H,0,1.626430271,2.1968841093,-0.0000377335
H,0,-1.1264500455,2.0609168058,-0.0000109493
O,0,-1.8449190422,-0.7982207269,0.0000180568
O,0,-2.9524130209,-0.0512880599,0.0000194348
H,0,3.5852898946,0.1902856593,-0.0001046694
H,0,2.97340193,-1.2194205925,0.8831810805
H,0,2.9733288258,-1.2196173205,-0.8830275183

Table H.1 Substituted Methylfuran Optimized Species (Continued A)

Y(OC[CH_3]CCC[OH]) (σ = 3)

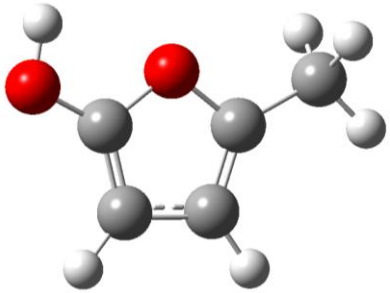

O,0,0.,0.,0.
C,0,0.,0.,1.35808915
C,0,1.2624603081,0.,1.8603539799
C,0,2.1221182047,0.,0.703929642
C,0,1.332906161,0.0000796324,-0.4023502261
C,0,1.5816994762,-0.0000699193,-1.867335698
H,0,3.2031736393,0.0000919151,0.7047762244
H,0,1.5403581573,0.0000793713,2.902275813
O,0,-1.2029838691,-0.0001922759,1.9647929303
H,0,2.6586152685,0.0002795097,-2.0524312444
H,0,1.1543546675,-0.884322092,-2.3557534591
H,0,1.1536958911,0.8836819101,-2.3560643821
H,0,-1.8849654941,0.0008105072,1.2785561655

Y(OC[CH3]CCC[OJ]) (σ = 3)

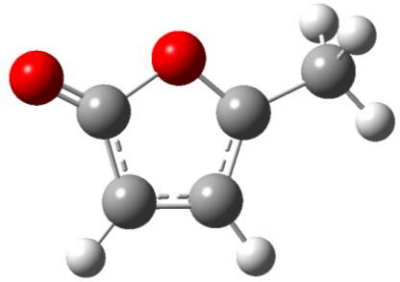

O,0,-0.0223755896,-0.0000216885,-0.0487744299
C,0,-0.0958990503,-0.0000238951,1.3833981439
C,0,1.2727942275,0.0000085961,1.8485792381
C,0,2.1029182768,0.000027018,0.7357496608
C,0,1.2850438213,0.0000084678,-0.3946659678
C,0,1.6060598999,-0.0000014573,-1.8427652404
H,0,3.1840415869,0.0000536419,0.7154140499
H,0,1.5394877193,0.000017227,2.894886519
O,0,-1.1705852207,-0.000046926,1.9404630582
H,0,2.6870057706,0.0001006339,-1.996679984
H,0,1.1788073497,-0.8815027632,-2.335196328
H,0,1.1786280958,0.8813830478,-2.3352471169

Y(OC[CH_3]CC[OOH]C) (σ = 3,OI)

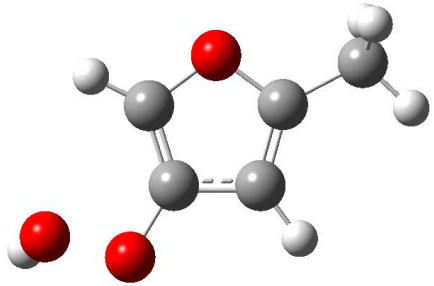

C,0,-0.0003269649,0.0027116812,-0.0002428025
C,0,-0.0004597221,0.0033250548,1.3600399299
C,0,1.3646682081,0.0013882012,1.7967429231
C,0,2.1137617058,-0.0015798694,0.6557983313
O,0,1.3037839433,-0.0008031475,-0.4403345308
C,0,3.5811432268,-0.0056310493,0.4066950795
O,0,-1.0403133802,0.004940317,2.2509701174
O,0,-2.284753892,0.0290946498,1.5043049541
H,0,-0.7737919215,0.0222187386,-0.7461687364
H,0,1.7224607288,0.0026063132,2.8152254282
H,0,3.8903170557,0.8754406925,-0.1668187795
H,0,3.8875109346,-0.8915130013,-0.1610129786
H,0,4.120804741,-0.0032750542,1.3562257928
H,0,-2.5910666633,-0.8802145267,1.6628252713

Table H.1 Substituted Methylfuran Optimized Species (Continued B)

Y(OC[CH_3]CC[OOJ]C) (σ = 3)

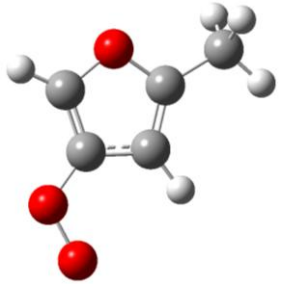

C,0,-3.5815018922,1.0757787603,-0.2222453931
C,0,-3.7127154213,-0.2655099668,0.0012163878
C,0,-2.4045122159,-0.823803975,0.1340998247
C,0,-1.5494071924,0.226028776,-0.0187931262
O,0,-2.2550546239,1.3854392376,-0.2359160548
C,0,-0.0677910498,0.3486617006,0.0037727122
O,0,-4.9303976041,-0.8957839746,0.07240373
O,0,-4.8353238045,-2.2075347773,0.2974829066
H,0,-4.2837910071,1.8773244445,-0.37862596
H,0,-2.1625892088,-1.8579255745,0.316421214
H,0,0.2623120812,1.031233886,0.7945973201
H,0,0.3132755543,0.7360630227,-0.9475338548
H,0,0.3823963845,-0.6297715594,0.1827202935

Y(OC[CH_3]CC[OH]C) (σ = 3)

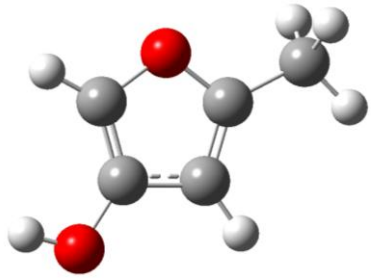

C,0,0.0000225287,-0.0018100938,0.0001330198
C,0,0.0001671282,0.0004313217,1.3642651823
C,0,1.3712620921,0.001345386,1.7808484848
C,0,2.1157206352,-0.0004123121,0.6378315096
O,0,1.2989049916,-0.0023434448,-0.4549238458
C,0,3.5810030571,-0.0006049881,0.3764876865
O,0,-1.0420093892,0.001707322,2.243888072
H,0,-0.7743632286,-0.0031693135,-0.7500673514
H,0,1.7343514423,0.0030766513,2.7978369541
H,0,3.8850087873,0.881901425,-0.1978992834
H,0,3.8853021862,-0.8849187443,-0.1949569878
H,0,4.127859955,0.0010601675,1.3219360209
H,0,-1.8711001451,0.000716092,1.7485598379

Y(OC[CH_3]CC[OJ]C) (σ = 3)

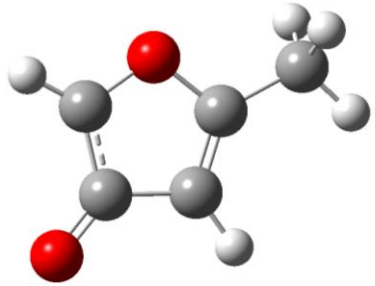

C,0,0.0124676285,0.0000045009,-0.0297536439
C,0,-0.0593363477,-0.0000083926,1.4115891042
C,0,1.3575478456,0.0000011828,1.8194887365
C,0,2.1044161921,0.0000018311,0.6992003043
O,0,1.2910916486,0.0000055929,-0.4450979043
C,0,3.5624542422,0.000005949,0.4206673421
O,0,-1.0892642746,-0.0000095258,2.1082191159
H,0,-0.7588667821,0.0000093086,-0.7857506615
H,0,1.7174276067,0.0000027001,2.8375392994
H,0,3.8493015416,0.8831797128,-0.1609357587
H,0,3.8493021725,-0.8831534766,-0.1609571931
H,0,4.1235997885,-0.00000502,1.3568020867

Table H.1 Substituted Methylfuran Optimized Species (Continued C)

Y(OC[CH_3]C[OOH]CC) (σ = 3,OI)

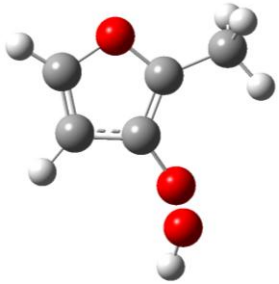

O,0,-1.8320646427,-0.1764777241,0.1739548326
C,0,-1.4249056917,-1.4837237347,0.0912085557
C,0,-0.0983551831,-1.5563762403,-0.1612181407
C,0,0.3467389342,-0.1914541346,-0.2355474274
C,0,-0.7361452201,0.6115306119,-0.0078722698
H,0,-2.1973779168,-2.2196318944,0.2344819261
H,0,0.4998250512,-2.4452404608,-0.276008903
C,0,-0.9050689491,2.0830761057,0.0310035485
H,0,0.0707401665,2.555866775,-0.0828030814
H,0,-1.5591658259,2.4336053934,-0.7736734556
H,0,-1.3435723887,2.4023337123,0.9809820284
O,0,1.579075756,0.2721241158,-0.5629228439
O,0,2.5012674149,-0.02975374,0.5785218505
H,0,3.2586934953,-0.3482517852,0.06752938

Y(OC[CH_3]C[OOJ]CC) (σ = 3)

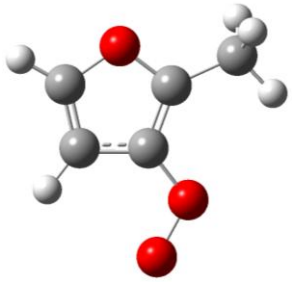

O,0,-0.0067264593,-0.0000012282,0.0061028816
C,0,-0.0070524617,-0.0000002,1.3758554061
C,0,1.2588385138,0.0000005913,1.8657191395
C,0,2.0914077676,-0.0000004175,0.7042389406
C,0,1.2944152143,-0.0000013025,-0.411708314
H,0,-0.979630926,0.0000000975,1.8417745227
H,0,1.5847274675,0.0000016569,2.892780608
C,0,1.5732658638,-0.0000032015,-1.8690869089
H,0,2.6525352097,0.0000040976,-2.0343877026
H,0,1.1476056874,-0.8847066166,-2.355629576
H,0,1.1475930681,0.8846918047,-2.3556337745
O,0,3.4628839326,-0.0000002799,0.6275135071
O,0,4.0648893128,0.0000011737,1.8179720514

Y(OC[CH_3]C[OH]CC) (σ = 3)

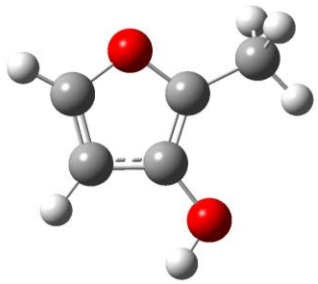

O,0,-0.0038697008,0.0000000141,0.0197964747
C,0,-0.0287034383,0.0000000119,1.3779704645
C,0,1.2353450196,0.0000000002,1.8833815373
C,0,2.1041584668,-0.0000000052,0.7410388802
C,0,1.3157701445,0.0000000035,-0.3751546222
H,0,-1.0054574571,0.0000000194,1.8359000199
H,0,1.5170790757,-0.0000000041,2.9274895423
C,0,1.6163745071,0.0000000036,-1.8293102099
H,0,2.6999718724,-0.0000000054,-1.9683704542
H,0,1.2068666632,-0.8846196074,-2.3315677058
H,0,1.2068666783,0.8846196233,-2.3315677026
O,0,3.4726660205,-0.0000000168,0.7123618915
H,0,3.80023618,-0.0000000212,1.6193118696

Table H.1 Substituted Methylfuran Optimized Species (Continued D)

Y(OC[CH_3]C[OJ]CC) (σ = 3)

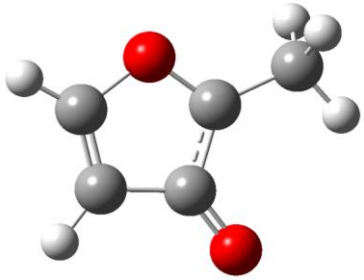

O,0,-0.0104453526,-0.0000026997,-0.0055686605
C,0,0.0250538492,-0.0000008991,1.3858995358
C,0,1.2810846296,0.0000005728,1.8616273761
C,0,2.1747966119,0.0000030471,0.6888610126
C,0,1.2695401135,-0.0000008818,-0.4386759951
H,0,-0.9479801158,-0.0000021869,1.8535337705
H,0,1.5913548158,0.0000010531,2.8956159277
C,0,1.5568527467,-0.0000036988,-1.8866773051
H,0,2.6408614774,-0.0000023263,-2.0186006214
H,0,1.134857553,-0.8838884931,-2.3803552842
H,0,1.1348548974,0.8838777217,-2.3803590195
O,0,3.4194708399,0.0000048874,0.6281742776

Y(OC[CH_2OOH]CCC) (σ = 1,OI)

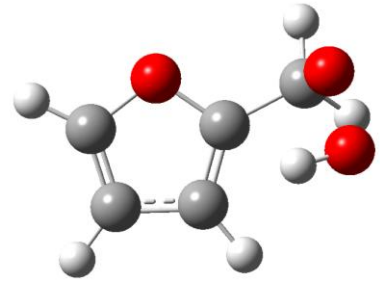

C,0,0.0998298705,0.1236724931,0.0220964558
C,0,0.1004853324,0.1419972635,1.3836580481
C,0,1.4741600931,0.0433602948,1.7775591809
C,0,2.2083126441,-0.0317885643,0.6277871819
O,0,1.3697734023,0.0211968251,-0.4565884284
C,0,3.6701680422,-0.0846271236,0.3532768549
O,0,4.2553972132,1.2035318902,0.111559152
O,0,4.2566238839,1.9110551608,1.3773824126
H,0,-0.6814083371,0.1653610536,-0.7209387422
H,0,-0.7649361002,0.2121454552,2.0264405812
H,0,1.8701332074,0.0229693931,2.7827957414
H,0,4.194230389,-0.5726945403,1.1812638189
H,0,3.8690255311,-0.6301835557,-0.5751383929
H,0,3.4199850413,2.4030518008,1.3124718972

Y(OC[CH_2OOJ]CCC) (σ = 1)

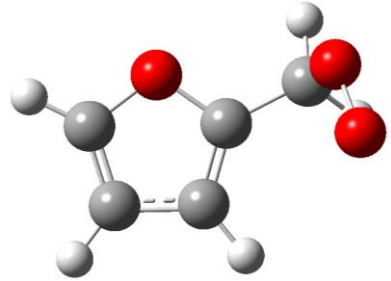

C,0,0.015723647,-0.0606389626,0.01289292
C,0,0.0287220115,0.0710833197,1.3690293219
C,0,1.4069139892,0.0784750042,1.7513845148
C,0,2.1303414857,-0.0515962532,0.6006352853
O,0,1.2827668585,-0.13590602,-0.4744525995
C,0,3.5780571449,-0.0579721582,0.3149462975
O,0,4.1044981457,1.2946748044,0.0092167073
O,0,4.1804795352,2.0269146485,1.1042576647
H,0,-0.7743250769,-0.1222602121,-0.7192702514
H,0,-0.83288045,0.1500172594,2.0156450328
H,0,1.813519273,0.1756037451,2.7474259042
H,0,4.1518517458,-0.4265687605,1.1661991544
H,0,3.8107654354,-0.6294083986,-0.5861959361

Table H.1 Substituted Methylfuran Optimized Species (Continued E)

Y(OC[CH_2OH]CCC) (σ = 1)

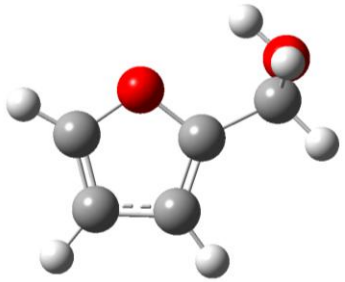

C,0,0.003595318,-0.0032800078,-0.0020678096
C,0,0.0019245048,-0.0008504626,1.3579066436
C,0,1.3795028405,0.001142467,1.7571675127
C,0,2.119711107,0.0065220688,0.6125933551
O,0,1.2832751984,0.0054730836,-0.477037316
C,0,3.5798435795,-0.0171576826,0.3105064011
O,0,4.0266048218,-1.2520199509,-0.2474027086
H,0,-0.7757882716,-0.007986219,-0.7479974513
H,0,-0.8675034591,-0.0017644162,1.9992302417
H,0,1.7689210388,-0.0043641475,2.7651019356
H,0,3.8338677847,0.8247848324,-0.3525575032
H,0,4.1335334572,0.1181668497,1.2429100234
H,0,3.5097910599,-1.4008785595,-1.0507099893

Y(OC[CH_2OJ]CCC) (σ = 1)

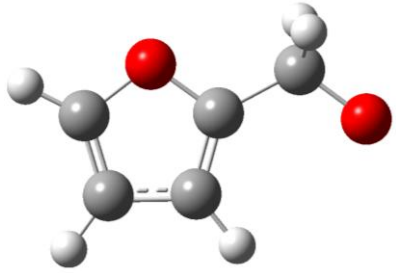

C,0,0.0000914815,-0.0105373995,0.0000868486
C,0,0.0000114704,0.0060549498,1.3604625882
C,0,1.3768368187,0.0101077438,1.7630758302
C,0,2.1085458275,-0.0043569601,0.6145361561
O,0,1.2813915768,-0.0171391152,-0.4757071724
C,0,3.5797096653,-0.0086846908,0.3349811988
O,0,4.3870522449,0.0041536355,1.4290684256
H,0,-0.7780295101,-0.0191631606,-0.7468851556
H,0,-0.8696345074,0.0144159605,2.0015145539
H,0,1.7760918468,0.0220910818,2.7659491103
H,0,3.8593227503,-0.8804834286,-0.2965426847
H,0,3.8604023254,0.8471050789,-0.3176093886

Table H.2 Moments of Inertia[a]

Species	I_a	I_b	I_c
Y(OC[CH_3]CCC[OOH])	383.32705	1282.77699	1549.89644
Y(OC[CH_3]CCC[OOJ])	282.92028	1338.53604	1610.21169
Y(OC[CH_3]CCC[OH])	284.57573	826.71606	1100.04186
Y(OC[CH_3]CCC[OJ])	277.18858	799.37891	1065.38261
Y(OC[CH_3]CC[OOH]C)	262.33416	1468.14815	1713.58575
Y(OC[CH_3]CC[OOJ]C)	334.28175	1305.88209	1628.91786
Y(OC[CH_3]CC[OH]C)	247.59827	908.90208	1145.26546
Y(OC[CH_3]CC[OJ]C)	247.56273	867.24550	1103.57956
Y(OC[CH_3]C[OOH]CC)	562.59519	965.17749	1430.57021
Y(OC[CH_3]C[OOJ]CC)	528.41401	936.58677	1453.73311
Y(OC[CH_3]C[OH]CC)	495.26068	534.93185	1018.92688
Y(OC[CH_3]C[OJ]CC)	472.61877	525.50283	986.87471
Y(OC[CH_2OOH]CCC)	375.58986	1312.47847	1476.28891
Y(OC[CH_2OOJ]CCC)	354.07327	1320.19242	1476.59550
Y(OC[CH_2OH]CCC)	258.40390	931.10811	1093.87028
Y(OC[CH_2OJ]CCC)	234.80539	915.84027	1139.90260

[a] AMU $Bohr^2$

Table H.3 Vibrational Frequencies

Species	Frequencies (cm^{-1})									
Y(OC[CH_3]CCC[OOH])	90.92	126.71	147.47	190.42	245.74	299.33	415.00	479.04	606.67	624.73
	641.85	711.94	767.82	810.51	869.67	965.48	989.15	1036.33	1047.52	1068.03
	1212.26	1238.53	1279.08	1316.54	1407.39	1429.84	1485.54	1503.83	1583.97	1656.04
	3042.73	3097.11	3143.10	3263.19	3285.15	3758.40				
Y(OC[CH_3]CCC[OOJ])	96.64	134.09	212.99	214.80	307.42	337.25	502.46	614.93	640.69	666.24
	711.97	801.25	861.56	974.73	981.25	1020.22	1045.83	1065.96	1138.31	1227.46
	1245.96	1288.97	1411.31	1432.08	1483.77	1497.03	1533.92	1638.94	3043.76	3098.54
	3146.39	3266.93	3309.22							
Y(OC[CH_3]CCC[OH])	148.88	175.78	199.14	279.05	312.16	458.09	611.04	623.89	660.35	711.18
	766.00	836.74	958.93	982.66	1022.97	1051.51	1070.54	1171.50	1235.82	1271.75
	1308.57	1431.15	1439.59	1485.05	1509.21	1655.64	1708.79	3031.29	3080.14	3135.56
	3257.60	3290.33	3819.17							
Y(OC[CH_3]CCC[OJ])	128.05	177.08	293.36	296.25	515.79	589.15	607.71	677.40	722.80	766.34
	810.47	876.54	945.15	1009.28	1043.61	1065.94	1105.26	1286.50	1347.78	1426.37
	1457.54	1478.31	1485.06	1537.48	1787.91	3039.89	3093.45	3147.73	3256.00	3283.03
Y(OC[CH_3]CC[OOH]C)	73.03	107.50	198.29	200.36	213.53	330.73	359.58	461.19	609.54	647.17
	662.18	693.89	738.45	792.97	937.40	947.16	1003.73	1028.02	1067.24	1152.94
	1172.79	1240.58	1317.94	1384.44	1423.90	1428.94	1486.16	1503.79	1601.77	1685.08
	3043.06	3097.25	3142.93	3278.19	3335.53	3744.76				
Y(OC[CH_3]CC[OOJ]C)	102.12	118.56	191.92	202.02	351.26	353.84	501.28	606.18	621.14	642.76
	730.56	744.23	825.41	930.89	994.54	1017.92	1068.32	1139.33	1161.08	1184.86
	1238.87	1291.02	1428.24	1443.26	1484.88	1501.40	1571.96	1655.19	3046.84	3102.85
	3148.89	3305.12	3312.45							
Y(OC[CH_3]CC[OH]C)	101.02	194.32	283.74	294.26	363.59	437.82	594.11	608.03	644.14	671.06
	733.43	801.44	941.97	999.55	1027.55	1067.40	1153.71	1160.90	1201.01	1274.87
	1339.06	1427.24	1485.36	1489.40	1507.30	1603.76	1685.16	3041.63	3095.02	3141.99
	3274.60	3292.13	3828.95							
Y(OC[CH_3]CC[OJ]C)	129.00	180.74	298.06	328.03	470.71	583.06	594.10	595.99	708.98	713.73
	826.91	887.21	943.30	1016.27	1067.34	1128.23	1183.72	1202.89	1315.92	1395.57
	1428.15	1482.55	1494.82	1601.29	1694.14	3047.50	3104.11	3153.52	3279.66	3283.16
Y(OC[CH_3]C[OOH]CC)	57.64	141.82	174.41	178.47	229.21	257.36	408.13	474.79	616.37	629.02
	687.00	734.65	759.04	808.23	845.26	904.33	965.96	1065.85	1070.29	1147.88
	1166.03	1268.48	1292.35	1349.26	1418.24	1458.39	1488.44	1498.32	1569.91	1661.45
	3043.00	3098.04	3150.82	3274.42	3298.91	3764.85				

Table H.3 Vibrational Frequencies (Continued)

Species	Frequencies (cm^{-1})									
Y(OC[CH_3]C[OOJ]CC)	99.12	118.77	196.45	220.27	313.83	321.11	532.52	608.29	619.82	649.63
	749.54	757.31	858.57	908.57	966.44	1051.63	1064.03	1138.43	1169.55	1183.35
	1262.83	1291.36	1425.61	1450.52	1486.50	1498.37	1564.33	1652.95	3044.71	3100.14
	3150.36	3292.02	3314.24							
Y(OC[CH_3]C[OH]CC)	41.90	130.85	215.33	247.87	326.01	441.07	609.63	638.82	660.50	718.96
	732.30	804.41	904.26	963.01	1068.58	1082.79	1098.49	1193.27	1250.01	1301.27
	1321.17	1424.05	1480.11	1489.33	1506.28	1558.71	1721.64	3033.51	3083.34	3140.52
	3251.28	3292.10	3852.15							
Y(OC[CH_3]C[OJ]CC)	118.55	191.78	253.79	295.02	480.28	532.69	638.21	688.93	742.62	783.46
	837.63	883.39	953.87	1024.46	1027.67	1097.83	1159.87	1282.53	1372.30	1390.97
	1441.74	1483.00	1499.23	1595.67	1622.55	3033.40	3085.72	3151.42	3273.53	3295.67
Y(OC[CH_2OOH]CCC)	49.86	102.00	172.14	254.12	296.93	381.55	499.27	614.44	645.98	750.37
	767.06	828.77	875.24	879.11	901.63	940.49	980.49	1018.59	1045.67	1118.62
	1187.75	1233.54	1258.37	1313.38	1377.45	1381.84	1436.14	1465.30	1540.38	1643.58
	3061.85	3119.79	3261.55	3272.67	3295.96	3730.82				
Y(OC[CH_2OOJ]CCC)	53.40	72.80	152.55	297.04	357.06	521.35	613.07	647.19	741.89	761.25
	812.09	838.93	883.94	901.35	939.56	997.01	1046.55	1118.61	1164.22	1192.89
	1238.44	1263.31	1302.44	1364.67	1438.07	1469.57	1536.59	1647.78	3097.25	3165.76
	3264.80	3276.43	3297.39							
Y(OC[CH_2OH]CCC)	63.04	147.50	281.88	364.41	418.07	612.96	638.92	737.43	753.87	822.10
	874.50	900.28	926.67	979.66	1039.24	1044.78	1112.04	1179.42	1197.46	1248.69
	1278.32	1377.36	1420.96	1429.77	1503.97	1550.42	1653.28	2996.38	3117.51	3260.29
	3271.43	3295.89	3812.53							
Y(OC[CH_2OJ]CCC)	66.70	193.98	206.64	455.77	481.82	611.51	650.31	702.84	741.40	825.07
	879.76	897.94	960.12	1029.01	1097.90	1109.57	1129.30	1168.82	1223.61	1252.40
	1316.15	1381.09	1437.33	1541.30	1645.20	2882.75	2884.73	3264.02	3283.50	3297.92

APPENDIX I

CHEMICAL ACTIVATION REACTIONS OF 2-METHYLFURAN RADICAL WITH $^3O_2$

This appendix contains the optimized geometries with symmetry values in parenthesis, moments of inertia, and vibrational frequencies for all calculated species from B3LYP/6-31G(d,p) unless otherwise noted. Calculated enthalpies of formation and elementary rate parameters for species in the 2MF5j + O_2 system are also included.

Table I.1 Pathway I Optimized Species

TS 2MF5OOj (σ = 3)
M06-2X/6-31G(d,p)

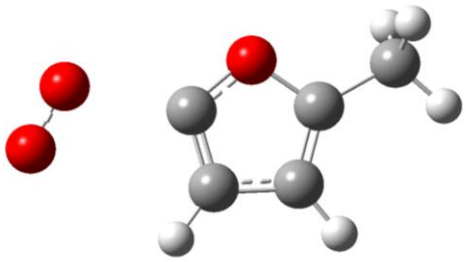

O,0,0.0890695804,0.0000664009,-0.1637277291
C,0,0.0590633208,-0.0000744063,1.1657069684
C,0,1.2781249026,-0.0001886548,1.7416846044
C,0,2.1793446752,-0.0001113319,0.614148341
C,0,1.4219323593,0.0000428081,-0.5131495435
C,0,1.7237344647,0.0001939353,-1.9677934775
H,0,3.2590885527,-0.0001630382,0.647272156
H,0,1.5097805336,-0.0003075456,2.7947833214
O,0,-1.6553837688,-0.0001037682,2.5167682034
O,0,-1.2437341102,-0.0001479913,3.6493173893
H,0,2.8051152035,0.0000859202,-2.112813592
H,0,1.3071299302,-0.8845487892,-2.4575440033
H,0,1.307338356,0.8851594611,-2.4573196386

TS I 1 (σ = 3)

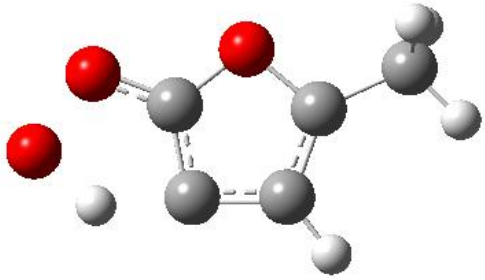

O,0,0.0590623795,0.0248946179,0.0261210475
C,0,0.0943489536,0.0112792737,1.375980499
C,0,1.3542665292,-0.019753519,1.9882753141
C,0,2.1902527306,-0.0258610541,0.8516203595
C,0,1.4120011254,0.0008717731,-0.3064653365
C,0,1.7204201178,0.008557603,-1.753745778
O,0,-1.0028314853,0.02611358,2.07904145
O,0,-0.5961068478,0.0042326859,3.4676568093
H,0,0.6026935004,-0.0170951947,3.210369235
H,0,3.2733463656,-0.0474373463,0.8298332984
H,0,1.2773933736,-0.8606517344,-2.2542484018
H,0,1.3130092931,0.90438877,-2.2372798954
H,0,2.8011842753,-0.0117952066,-1.9047209196

Table I.1 Pathway I Optimized Species (Continued)

MF4j5Q (σ = 3, OI)

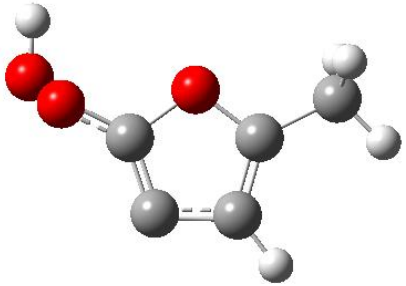

O,0,0.2413651166,-0.6563725827,-0.2700403183
C,0,-0.7229082376,0.3461381758,-0.2574966201
C,0,-0.0968968996,1.50712347,0.0575881162
C,0,1.2862670543,1.2748442051,0.2283936865
C,0,1.4364752723,-0.0736036084,0.0272936201
C,0,2.6235440154,-0.9665559978,0.0668841251
H,0,2.0653133811,1.9799548978,0.4674174026
O,0,-1.953116667,0.0232571955,-0.5780478687
O,0,-2.6472816241,-0.5736083326,0.6536756538
H,0,3.5170860279,-0.3917227376,0.3127859004
H,0,2.4977244613,-1.7513650564,0.819013536
H,0,2.7799452082,-1.4548765702,-0.8997912629
H,0,-2.8172291089,-1.4577930586,0.2968950294

TS I 2 (σ = 3,OI) MP2/6-31G(d,p)

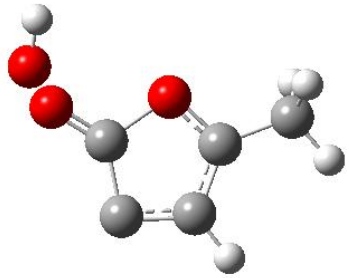

O,0,0.0596987115,-0.0054180263,0.2228156134
C,0,0.2958723323,0.0199109459,1.6760364047
C,0,1.7143852911,0.0036604495,2.025347281
C,0,2.272165175,0.0194298548,0.7427059288
C,0,1.2913825118,-0.011788513,-0.2633877621
C,0,1.4188212875,-0.0469609602,-1.737927568
H,0,3.325453578,0.0259087599,0.5027366332
O,0,-0.7453774325,0.0633452026,2.3579241371
O,0,-1.5176144534,-1.341614216,2.2515673503
H,0,0.9261355912,-0.9378879327,-2.1267422038
H,0,0.921381576,0.8212943555,-2.1696720715
H,0,2.4651187113,-0.0510147036,-2.0284144437
H,0,-2.2903081067,-0.9976854118,1.7754347867

CC(=O)CH=C=C=O (σ = 3)

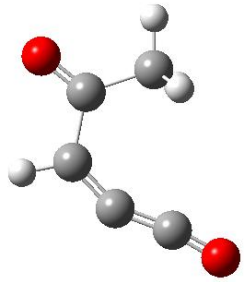

O,0,2.6189511681,-0.3483077608,-0.0002330725
C,0,-1.9863526335,-0.1332469073,0.0003169497
C,0,-0.9241632823,-0.8741770234,0.0002847896
C,0,0.3915905095,-1.068241778,0.0004538642
C,0,1.4517237116,0.0044474804,0.0000850861
C,0,1.0355339632,1.4577186247,-0.0001153892
H,0,0.8158361625,-2.0736307686,-0.0005792284
O,0,-3.0448983233,0.3838414955,0.0002851958
H,0,0.4252268621,1.6860283843,-0.879920682
H,0,0.4256494577,1.686390716,0.8798846941
H,0,1.9296744045,2.0810925372,-0.0004642077

Table I.2 Pathway II Optimized Species

TS II 1 (σ = 3,OI) MP2/6-31G(d,p)

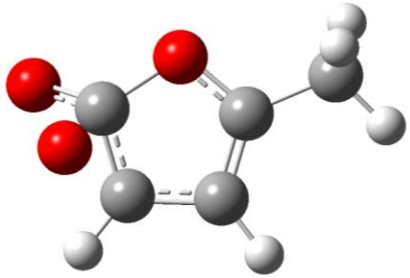

O,0,0.4216575759,-0.945149855,0.0905689068
C,0,-0.8039942327,-0.45079266,-0.4285881259
C,0,-0.6719163736,0.9341586815,-0.535409028
C,0,0.6935314265,1.2466969635,-0.2887727121
C,0,1.2601090873,0.0690560686,0.0545068888
C,0,2.6825349364,-0.2589760996,0.3289170294
H,0,1.1887204405,2.1963183358,-0.3684483234
H,0,-1.4008918697,1.5699464803,-1.0057528321
O,0,-1.9451555955,-0.8175871206,0.1358683682
O,0,-1.8788530917,0.4164134155,0.8542885976
H,0,3.2748910061,0.6487379653,0.3810588796
H,0,2.7577381549,-0.8059944679,1.2657783278
H,0,3.0617195356,-0.8956847072,-0.4682809766

MF45Y(CjCOOj) (σ = 3,OI)

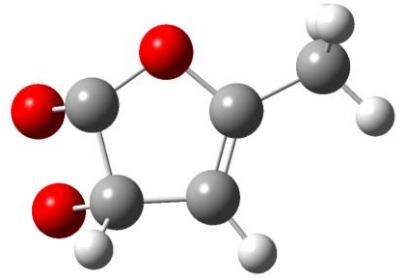

O,0,-0.5380521333,-1.0677560402,0.2952694317
C,0,0.765550508,-0.6800883034,0.5778494006
C,0,0.8957456558,0.8171918409,0.4956811585
C,0,-0.4784424608,1.2135183046,0.074821656
C,0,-1.2356187849,0.1035257417,0.0027553057
C,0,-2.6776547875,-0.0970675932,-0.29415137
H,0,-0.8332035159,2.2237530483,-0.070267419
H,0,1.351010174,1.4121507517,1.2910406062
O,0,1.7184369783,-0.9155234847,-0.3805888001
O,0,1.9248688395,0.5822937866,-0.5603168697
H,0,-3.1675195623,0.8586389198,-0.4889497768
H,0,-2.7991293105,-0.7441376665,-1.1693664122
H,0,-3.1748466003,-0.5899773059,0.5480140894

TS II 2 (σ = 3,OI)

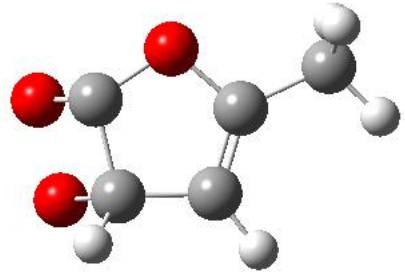

O,0,-0.5305954413,-1.0649306768,0.2593503606
C,0,0.7671772827,-0.6744808468,0.563545318
C,0,0.8924471505,0.8197542536,0.4823422187
C,0,-0.4847475179,1.2185881075,0.0801644449
C,0,-1.2378603145,0.1065287945,-0.0057101813
C,0,-2.6817078457,-0.0965094187,-0.2922309272
H,0,-0.8448443048,2.2298079182,-0.0430113225
H,0,1.3575664444,1.4122190263,1.2736446617
O,0,1.7524860523,-0.950527329,-0.3118430552
O,0,1.917983067,0.5903745512,-0.5894683795
H,0,-3.1766497697,0.8599740604,-0.4697266177
H,0,-2.809219272,-0.7319954086,-1.175026791
H,0,-3.1697615308,-0.6021760319,0.5477282704

Table I.2 Pathway II Optimized Species (Continued)

MF4Oj5O (σ = 3,OI)

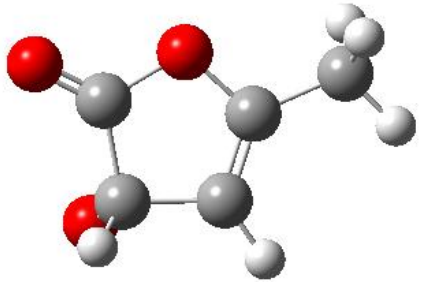

O,0,0.1363313374,-0.1785160469,-0.002468195
C,0,-0.0627231608,0.0345372999,1.3640798525
C,0,1.2503756335,-0.3299731902,2.104802438
C,0,2.1798389874,-0.5876745281,0.9359251041
C,0,1.4632213022,-0.5224719648,-0.1982561027
C,0,1.8546250378,-0.7064900344,-1.6189718598
H,0,3.2185223403,-0.86311041,1.0337218497
H,0,1.5657487718,0.4729496877,2.7886635182
O,0,-1.1096388221,0.4057700912,1.8008006096
H,0,2.9145697659,-0.953837561,-1.696978205
H,0,1.2656824861,-1.5131949803,-2.0689815557
H,0,1.6531548812,0.2040464407,-2.192989504
O,0,1.1610040086,-1.5654992499,2.7002011751

TS II 3 (σ = 3,OI)

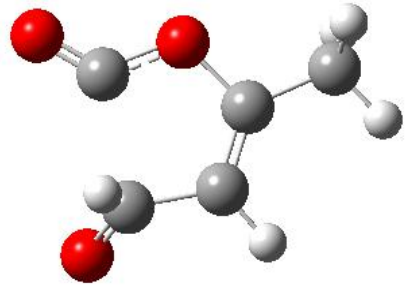

O,0,0.206851611,0.141198699,0.0327714823
C,0,0.0982867782,-0.1299317194,1.3395065078
C,0,2.1290623298,-0.0646925526,1.9131275398
C,0,2.5108191326,0.0280173517,0.4626274409
C,0,1.5429613071,0.1514161503,-0.4425791411
C,0,1.5925720857,0.2747178706,-1.9236217412
H,0,3.5526300332,-0.0396649048,0.1716823256
H,0,1.8601746009,0.9091755072,2.3825194178
O,0,-0.8801899845,-0.2153279305,1.997489351
H,0,2.6288547168,0.2612614168,-2.2656210332
H,0,1.0499162961,-0.5491651111,-2.3996125897
H,0,1.1254684936,1.2096715627,-2.2522250633
O,0,2.4554454124,-1.0221981387,2.6347247879

O=CjOC(C)=CHCH(=O) (σ = 3)

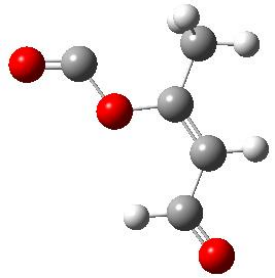

O,0,-0.770926289,-0.4605278834,-0.0027529382
C,0,-2.1244094146,-0.397139069,-0.0038979675
C,0,2.0381647378,-0.6874847915,-0.0006066258
C,0,1.3114901492,0.5896212876,0.0024328831
C,0,-0.0270373409,0.7184956619,0.001472874
C,0,-0.7756545521,2.012118087,0.0045399722
H,0,1.9175919255,1.4891447278,0.0056924769
H,0,1.4167752654,-1.6038653418,-0.003929849
O,0,-2.8541247727,-1.3321699105,-0.0073871995
H,0,-0.0712837256,2.8452398524,0.0076931316
H,0,-1.4203127925,2.0961726863,-0.8772511373
H,0,-1.4220627725,2.0909809923,0.8855293392
O,0,3.255501582,-0.7486832992,0.0004330401

Table I.2 Pathway II Optimized Species (Continued)

TS II 4 (σ = 3)

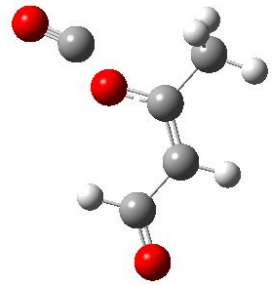

O,0,0.4743376056,-0.2491702897,0.2346488797
C,0,-0.8859891813,0.3624205462,1.1059408473
C,0,3.2731764011,0.0318925604,0.569144086
C,0,2.4836721608,0.6734982783,-0.4817123925
C,0,1.1150090174,0.5830921411,-0.5721003839
C,0,0.293999498,1.3237009007,-1.5816370278
H,0,3.0341532374,1.2270571793,-1.2362430148
H,0,2.7009714567,-0.5251683581,1.3345481446
O,0,-1.548747976,-0.4043910886,1.6577579374
H,0,0.905617749,1.9501752492,-2.2325651429
H,0,-0.2890507967,0.6231629336,-2.1879953796
H,0,-0.4254308817,1.9569190038,-1.0442654491
O,0,4.4908309594,0.1224421839,0.6226567827

n-CC(=O)CjHCH(=O) (σ = 3)

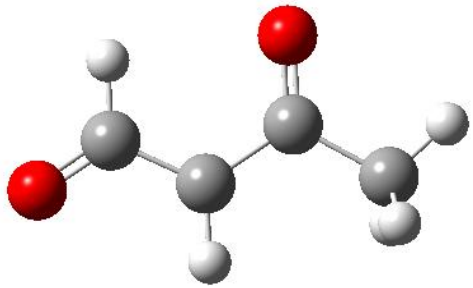

O,0,0.030819725,-0.488724308,0.1629105378
C,0,-0.0063169225,0.0582176474,2.965772641
C,0,1.1608502004,0.1416484342,2.1131368622
C,0,1.0986267428,-0.1552499058,0.6816001207
C,0,2.3778282379,-0.0379963816,-0.1224123151
H,0,2.0976951668,0.4365140021,2.5797299084
H,0,-0.9478120776,-0.2422132001,2.4761345169
H,0,3.1452362531,-0.7117647923,0.2755720774
H,0,2.177680085,-0.2875890489,-1.1647426147
H,0,2.7797448203,0.979719188,-0.0592752053
O,0,0.0487519662,0.3086239412,4.1703248522

Table I.2 Pathway II Optimized Species (Continued)

TS II 5 (σ = 3)

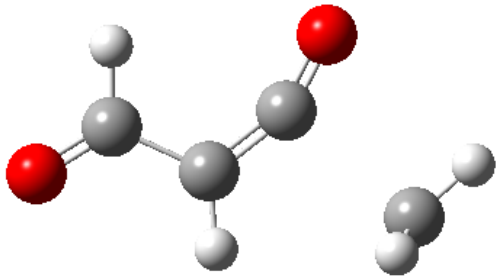

O,0,0.2162178192,-0.0599684041,-0.4028652146
C,0,0.1118477071,0.0120728268,2.8019506438
C,0,1.2286306995,0.0124344724,1.8525412727
C,0,0.9224581493,-0.0238668876,0.5422139896
C,0,2.9943499495,-0.0024937437,-0.4229276349
H,0,2.2421914427,0.0412134608,2.2202906164
H,0,-0.8968610121,-0.0187738054,2.337911771
H,0,3.3684619328,-0.9161915123,0.0239177258
H,0,2.6856595804,-0.0322252551,-1.4602943505
H,0,3.3303271958,0.9449124183,-0.0179198863
O,0,0.2592258988,0.0428712462,4.009580422

O=CHCH=C=O (σ = 1)

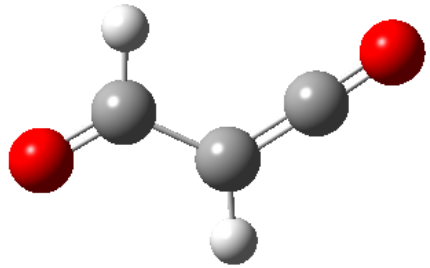

O,0,2.3307255741,-0.2751188397,0.0002484126
C,0,-1.1419102852,-0.3737930924,0.0003603427
C,0,-0.0141007636,0.5671032198,-0.0002850985
C,0,1.2425008649,0.1369932389,-0.0000072337
H,0,-0.1994343611,1.635348586,-0.0010580558
H,0,-0.8614582146,-1.4471163651,0.0011071653
O,0,-2.3040041311,-0.0188803527,0.0001066399

Table I.3 Pathway III Optimized Species

TS III 1 (σ = 3)

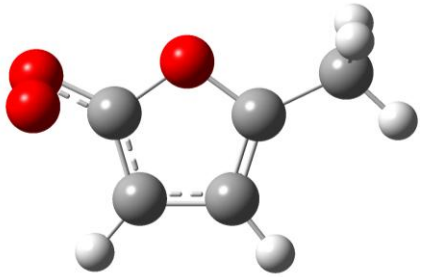

O,0,-0.2249574299,-0.7927970475,-0.2326296664
C,0,0.8336221724,0.0706986264,-0.2612437824
C,0,0.380142251,1.3833862517,-0.0846321294
C,0,-1.0140494996,1.2928536074,0.0899367925
C,0,-1.3478407962,-0.042990915,-0.0024596145
C,0,-2.6314057148,-0.7793198029,0.0933897511
H,0,-1.7091762943,2.1010542294,0.2661868925
H,0,1.0148564058,2.2556636772,-0.0769314379
O,0,2.2611734093,-0.2959270217,0.9099413385
O,0,2.0322735818,-0.4112467658,-0.5510596182
H,0,-2.6086122164,-1.5003884254,0.9184214637
H,0,-3.4530477685,-0.0807199031,0.2625037722
H,0,-2.8318371008,-1.3414155106,-0.8258357618

MF5Yj(COO) (σ = 3)

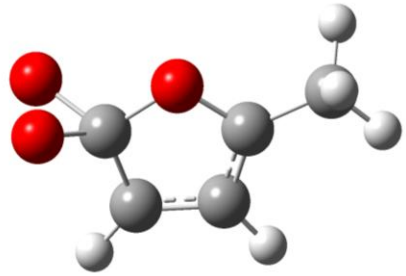

O,0,-0.2286377289,-0.8181757161,-0.0000026916
C,0,0.9018708355,0.0164543084,-0.0000026736
C,0,0.4063815162,1.4029427335,0.0000039312
C,0,-0.9778882424,1.332011596,0.0000070151
C,0,-1.343265806,-0.0116307447,0.0000031853
C,0,-2.6547416476,-0.6991840662,0.0000042038
H,0,-1.6763432356,2.1576946156,0.0000117931
H,0,1.0548462507,2.2653675702,0.0000055466
O,0,1.9788532453,-0.4259363665,0.7597633672
O,0,1.9788490668,-0.425930585,-0.7597781757
H,0,-2.7611156441,-1.3427948705,0.8819031497
H,0,-3.4663862772,0.0312438611,0.0000077801
H,0,-2.7611193327,-1.3427903361,-0.8818976007

TS III 2 (σ = 3) MP2/3-21G

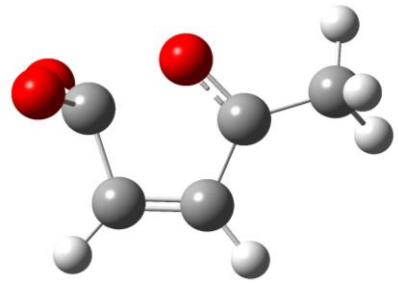

O,0,0.0173311388,0.8433958612,0.0861081512
C,0,0.0175055378,0.1906737400,1.6449711484
C,0,1.4131114841,-0.0988306388,1.8287584571
C,0,2.1701279596,0.2490721645,0.7225155940
C,0,1.3146048611,0.7825706131,-0.2404640841
C,0,1.5415356400,1.3202854048,-1.6074671146
H,0,3.2390982384,0.1372384745,0.6007862671
H,0,1.7194858037,-0.5377955576,2.7656844832
O,0,-0.8637081890,0.7796785426,2.5452752845
O,0,-1.0751002001,-0.6083015811,1.9641290671
H,0,2.2264140567,2.1762948984,-1.5923073711
H,0,1.9812593797,0.5633305394,-2.2675475021
H,0,0.5935766430,1.6453952448,-2.0398853534

Table I.3 Pathway III Optimized Species (Continued)

CC(=O)CH=CHCO2j (σ = 3)

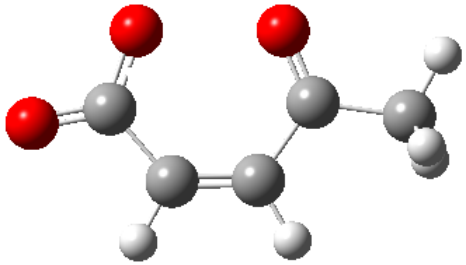

O,0,0.9986749638,-1.2343848311,0.0303266627
C,0,-1.6953535684,-0.017307041,-0.0207146853
C,0,-0.7328097733,1.1255986613,-0.0202108004
C,0,0.6093403395,1.1153501692,-0.0014786772
C,0,1.4615617487,-0.101127337,0.0240428077
C,0,2.9584408575,0.1211961868,0.0421356352
H,0,1.1380062268,2.0655237598,-0.0048452039
H,0,-1.2572441495,2.0783468835,-0.038206681
O,0,-1.2798188885,-1.2442558423,-0.0010904177
O,0,-2.9075713834,0.2059799612,-0.0400580313
H,0,3.2621510845,0.6930635532,-0.842223891
H,0,3.2378835855,0.7128443354,0.9214695801
H,0,3.4783799569,-0.8361654593,0.0600287018

TS III 3 (σ = 3)

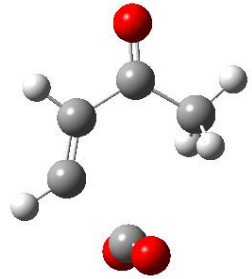

O,0,2.9225663065,0.4058933079,-0.4156686458
C,0,-1.7193010495,-0.134602258,-0.0671505208
C,0,-0.5101662355,1.3733892503,0.0353556284
C,0,0.798894527,1.3331241947,-0.090166722
C,0,1.7300622892,0.1755595998,-0.3390392382
C,0,1.1648018782,-1.2189472211,-0.4843870401
H,0,1.3338260034,2.2832029568,-0.0048359025
H,0,-1.2002330667,2.1889540804,0.2138133487
O,0,-1.7979880005,-0.503179556,1.0715798623
O,0,-2.0087416622,-0.1777271799,-1.2303832252
H,0,0.6203940983,-1.5072097626,0.42062468
H,0,0.4609403578,-1.2609523185,-1.3218459955
H,0,1.9863483737,-1.913997944,-0.6578004891

CC(=O)CH=CjH (σ = 3)

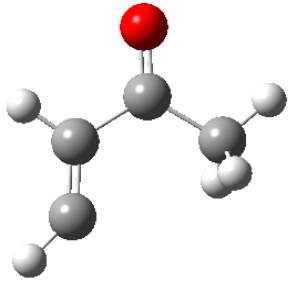

O,0,0.9188417275,-0.1019516611,-0.2391422092
C,0,0.7089821448,0.4058390769,3.285347438
C,0,0.7764208712,-0.1829784603,2.1116715448
C,0,0.8599749141,0.5362509732,0.7971152217
C,0,0.8675067394,2.051749313,0.8181486398
H,0,0.7758394599,-1.2737925217,2.0162456215
H,0,0.6443727303,0.1262629873,4.3285288977
H,0,-0.04150215,2.4291196275,1.2982235519
H,0,1.7164599795,2.4189068179,1.4043671563
H,0,0.9313769936,2.4272246528,-0.2035300683

Table I.3 Pathway III Optimized Species (Continued)

TS III 4 (σ = 3)

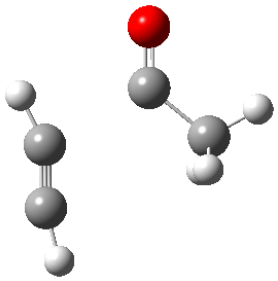

O,0,0.2009409043,0.2650602585,-0.1059872362
C,0,0.2769946356,0.1240737229,3.9493532261
C,0,0.7577410384,-0.2136983315,2.8728397937
C,0,-0.2536972643,0.5837189423,0.9464179942
C,0,-1.4376606697,1.4641457436,1.2448507625
H,0,1.4562448081,-0.7237471192,2.2416389068
H,0,-0.2993813392,0.5392543592,4.744842158
H,0,-2.1542718539,0.8897396031,1.8392436275
H,0,-1.1003042235,2.2971424081,1.868614088
H,0,-1.9071394985,1.8348423526,0.3283203461

CCj(=O) (σ = 3)

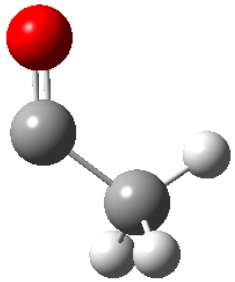

O,0,0.0118826321,-0.0000301528,-0.0009597343
C,0,-0.0138228417,0.000028126,1.1881719684
C,0,1.1624604697,0.0000079497,2.1440768882
H,0,1.090359163,0.880034748,2.7900711442
H,0,1.0902166016,-0.8798955356,2.7902221235
H,0,2.1166564624,-0.0001131847,1.6058631314

TS III 5 (σ = 3)

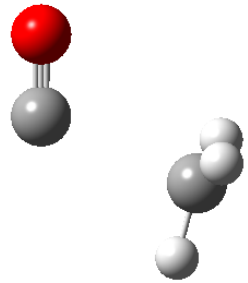

O,0,-0.0981779381,0.3819102261,0.0860037603
C,0,-0.072876288,-0.3898471764,0.9349245028
C,0,1.6380660729,-0.0181064733,2.4878093056
H,0,1.321501744,0.9715538172,2.7955941683
H,0,1.4465778293,-0.8492978457,3.1536772136
H,0,2.464787535,-0.0961983939,1.7915297019

Table I.4 Pathway IV Optimized Species

TS IV 1 (σ = 3)

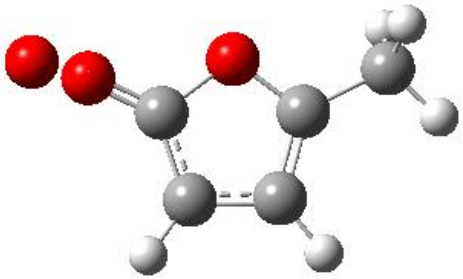

O,0,0.0349560246,0.1863762375,0.1177510304
C,0,0.0817371907,0.3140620103,1.5069002892
C,0,1.4193068374,0.2119540935,1.9125547054
C,0,2.1893437143,0.0514469969,0.7498401573
C,0,1.306180475,0.0361201181,-0.3169798597
C,0,1.5104310075,-0.0962781442,-1.781587806
H,0,3.2632333098,-0.0429838569,0.6756708072
H,0,1.7506569563,0.2650196254,2.9389390699
O,0,-0.996621518,0.502820386,2.1410188662
O,0,-1.7337132627,-1.0379074133,2.5335104482
H,0,2.5715735185,-0.21968197,-2.0062422489
H,0,0.9641228202,-0.9610236317,-2.174281762
H,0,1.1404051107,0.7899660638,-2.3093793141

2MF5Oj (σ = 3)

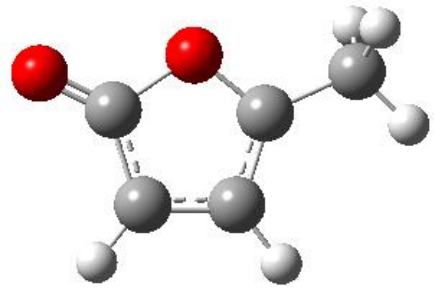

O,0,-0.0223755896,-0.0000216885,-0.0487744299
C,0,-0.0958990503,-0.0000238951,1.3833981439
C,0,1.2727942275,0.0000085961,1.8485792381
C,0,2.1029182768,0.000027018,0.7357496608
C,0,1.2850438213,0.0000084678,-0.3946659678
C,0,1.6060598999,-0.0000014573,-1.8427652404
H,0,3.1840415869,0.0000536419,0.7154140499
H,0,1.5394877193,0.000017227,2.894886519
O,0,-1.1705852207,-0.000046926,1.9404630582
H,0,2.6870057706,0.0001006339,-1.996679984
H,0,1.1788073497,-0.8815027632,-2.335196328
H,0,1.1786280958,0.8813830478,-2.3352471169

TS IV 2 (σ = 3) MP2/3-21G

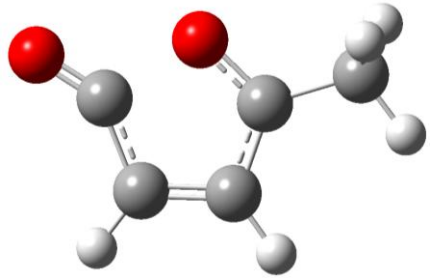

O,0,0.8225101243,0.2086682664,0.5403194744
C,0,0.1889442915,-1.3320176048,0.3490121263
C,0,-1.0832124142,-0.9984581887,-0.2510683574
C,0,-1.2538532007,0.3575525497,-0.4142581206
C,0,-0.1114874378,1.0231878298,0.0638585156
C,0,0.1303721588,2.5021722491,0.0821095519
H,0,-2.113479995,0.8545118599,-0.8368526699
H,0,-1.775249207,-1.7815191035,-0.516872401
O,0,0.8573219366,-2.2411118051,0.7103030464
H,0,1.0307546147,2.7374585837,-0.4958833711
H,0,-0.7257328562,3.0314850974,-0.3424874266
H,0,0.2952509851,2.837869266,1.1118196321

Table I.4 Pathway IV Optimized Species (Continued)

CC(=O)CHCjHC=O (σ = 3)
MP2/6-31G(d)

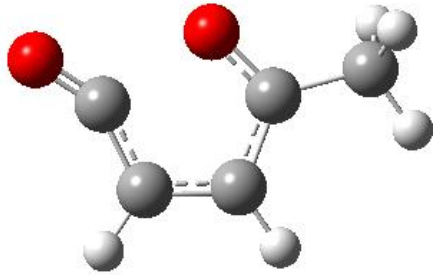

O,0,0.2167406732,-0.1437812332,0.134675393
C,0,-0.0203522537,-0.0983770599,2.060673234
C,0,1.3494521469,0.0488588414,2.372381081
C,0,2.2203806211,0.0960434706,1.2737911881
C,0,1.5228353374,-0.0180927714,0.0213219896
C,0,2.159087343,-0.0037625678,-1.3437739442
H,0,3.2984251282,0.2060659831,1.3556285838
H,0,1.6423608564,0.1153013401,3.4154465531
O,0,-1.1651235407,-0.1994458204,2.4140587311
H,0,3.2477899135,0.1073097666,-1.2621863994
H,0,1.9341746784,-0.9373547379,-1.8776931366
H,0,1.758880878,0.8272349888,-1.9408719986

TS IV 3 (σ = 3)

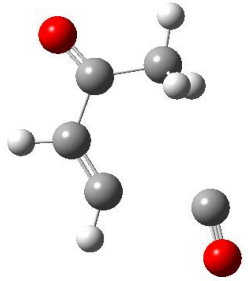

O,0,-2.7619574244,-0.1229968458,-0.1577366147
C,0,2.2287987054,0.5378491341,-0.2036251694
C,0,0.6566842181,-1.1758599989,0.0970588758
C,0,-0.6592035975,-1.1360006638,0.0309686396
C,0,-1.5638418427,0.0610651081,-0.0231618297
C,0,-0.9740255946,1.4475697906,0.1050344623
H,0,-1.2180858759,-2.0776611804,0.0085609177
H,0,1.3724232312,-1.9882756174,0.1381859594
O,0,3.2958909427,0.1537090316,-0.0441106793
H,0,-0.4606376435,1.5545085121,1.0662994757
H,0,-0.2244645863,1.6260194183,-0.670135565
H,0,-1.7780165325,2.1803593115,0.0311945276

Table I.5 Pathway V Optimized Species

TS V 1 (σ = 1) PM3

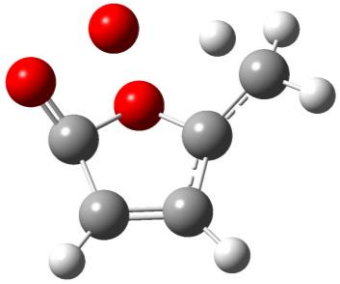

O,0,0.0081738377,-0.1399584987,1.0479247337
C,0,-1.0319137128,0.586563618,0.3739984626
C,0,-0.3760267704,1.6523533177,-0.3693353942
C,0,0.9612813859,1.3126680975,-0.4233409524
C,0,1.0997773091,0.05662881,0.267225104
C,0,1.7346523578,-1.1621024366,-0.1543186852
H,0,1.7542500892,1.8240911343,-0.9652559005
H,0,-0.8779941769,2.4998143719,-0.8306247652
O,0,-1.9607065325,-0.2079362333,0.2105632203
H,0,2.567246789,-1.0485820267,-0.8496942016
H,0,1.9683390591,-1.8959644093,0.623967989
O,0,-0.9560163554,-1.4241679886,-0.7193732692
H,0,0.7640177202,-1.6200717562,-0.7018813413

MF2CjH25Q (σ = 1,OI)
MP2/6-31G(d,p)

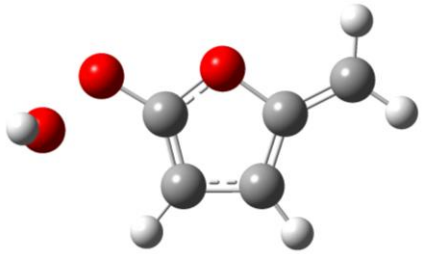

O,0,-0.4971352626,-0.8841927197,-0.0180815892
C,0,0.584470398,-0.1027473421,-0.0217949189
C,0,0.3118539146,1.2139003105,-0.0067628521
C,0,-1.1148785972,1.2761965436,0.0063434384
C,0,-1.6011631875,-0.0159834598,0.0001819345
C,0,-2.8564725003,-0.5803538805,0.0086690425
H,0,-1.7226817908,2.1641267786,0.0170551252
O,0,1.7171033594,-0.8495177274,-0.0343744496
O,0,2.8335989036,0.0897475635,-0.0865560469
H,0,-2.9812771264,-1.6492093252,-0.0020319271
H,0,-3.7237083687,0.0569868151,0.0221900616
H,0,3.1926243834,-0.0635446439,0.8034924853
H,0,1.0225108745,2.0168490873,-0.0202903037

TS V 2 (σ = 1) MP2/6-31G(d,p)

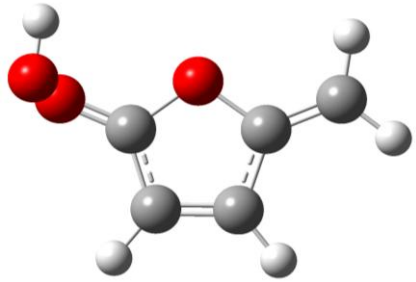

O,0,-0.032880135,-0.1169509004,-0.1210730243
C,0,-0.0899315114,-0.1189704845,1.249535096
C,0,1.2143981993,0.0141246051,1.7765637619
C,0,2.0723037394,0.0460505671,0.7334175544
C,0,1.2973509227,-0.0238019072,-0.4769168378
C,0,1.6752667788,-0.0240237078,-1.7582276527
H,0,3.1468684294,0.1156925829,0.7562682767
O,0,-1.2146475659,-0.170932686,1.8300696492
O,0,-1.8708878124,1.2616683121,1.8447715939
H,0,0.9509505319,-0.0868101634,-2.5529357537
H,0,2.7215320824,0.0421943591,-2.0050335565
H,0,-2.527475831,1.0983092469,1.1508253084
H,0,1.4287323019,0.0530735195,2.8304558868

Table I.5 Pathway V Optimized Species (Continued)

MF2CH25O (σ = 1)

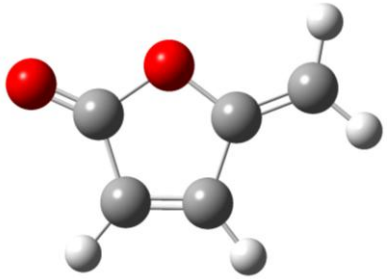

O,0,-0.0647449601,0.0043977696,-0.0322446829
C,0,-0.1034449205,0.0171546196,1.3662239623
C,0,1.3000261015,0.0152640058,1.8322542753
C,0,2.0987995814,0.0019821183,0.7518286035
C,0,1.2546140652,-0.0051872919,-0.43748706
C,0,1.6012555463,-0.018234872,-1.7290337615
H,0,3.1806395846,-0.0031079246,0.7161048615
H,0,1.5639306201,0.0238820487,2.8799168207
O,0,-1.139789924,0.0269278438,1.9751251642
H,0,2.6476100179,-0.0252553234,-2.0080891893
H,0,0.8531180788,-0.0218038882,-2.5118158723

TS V 3 (σ = 1)

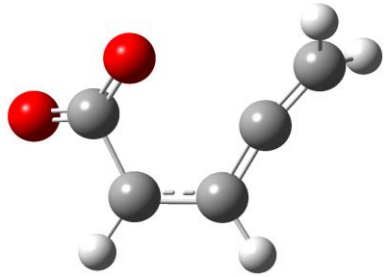

O,0,-0.2551726227,0.5040071984,0.0591113796
C,0,-0.1108183598,-0.0127095077,1.185269947
C,0,1.2301118263,0.1000608358,1.8480009953
C,0,2.3327000435,0.0734422988,1.0083375517
C,0,2.1456003616,0.0806950938,-0.3429830148
C,0,2.2293768045,-0.0301268751,-1.6306174975
H,0,3.3409715013,0.2103657053,1.3942812894
H,0,1.325929699,0.0903476368,2.928497753
O,0,-0.7686048256,-0.8248933128,1.8844050906
H,0,2.7352460172,-0.8797695045,-2.0857106444
H,0,1.7346416344,0.6876553819,-2.279312802

C=C=CHCHCO2 (σ = 1)

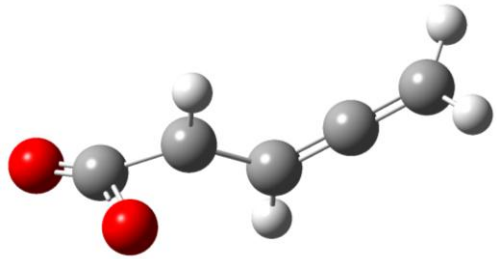

O,0,-2.6687136846,-0.8250908514,0.0179009007
C,0,-1.7187524334,-0.1103967543,-0.1022648829
C,0,-0.3126185961,0.1457343614,-0.4104434889
C,0,0.778460713,-0.1045427714,0.5448455209
C,0,2.0391357788,-0.1193722031,0.1744134752
C,0,3.2866714499,-0.1501937363,-0.2018753954
H,0,0.5078507594,-0.3104041056,1.5789553275
H,0,-0.0269687881,0.3260625474,-1.4438154856
O,0,-1.4054414266,1.1703987981,0.0618361739
H,0,3.748817353,-1.0670405475,-0.5605112302
H,0,3.9093208748,0.7407522627,-0.1669089151

Table I.6 Pathway VI Optimized Species

TS VI 1 (σ = 3,OI) PM3

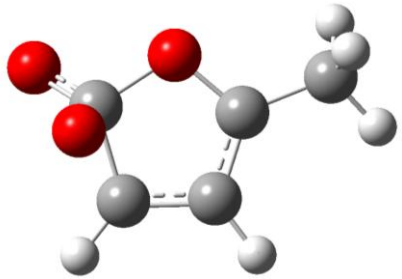

O,0,-0.2003011685,-0.9494837676,0.0512550653
C,0,1.0528339037,-0.223685638,-0.0641468198
C,0,0.6808532846,1.2339133328,-0.3463254222
C,0,-0.7276276254,1.2771982283,-0.246167993
C,0,-1.207498183,-0.0169621677,-0.0345676279
C,0,-2.5951518964,-0.4902969075,0.0976437954
H,0,-1.3392804235,2.1730224257,-0.342590654
H,0,1.3778738557,2.034623268,-0.5871051521
O,0,1.4827952399,0.2313732465,1.1313262441
O,0,1.8870839497,-0.9342688829,-0.8052242972
H,0,-2.805122432,-0.7852121176,1.1357025298
H,0,-3.303834623,0.2994032049,-0.1815218334
H,0,-2.7851158818,-1.364833225,-0.539739835

MF45Y(CCO)5Oj (σ = 3,OI) MP2/3-21G

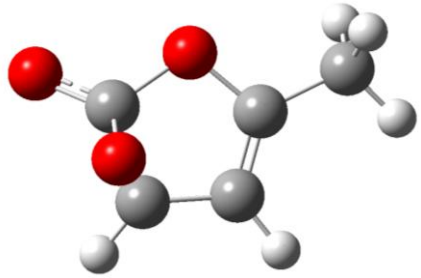

O,0,-0.251838193,-0.9967571333,0.1572392145
C,0,1.0490899084,-0.3631743179,-0.0226461076
C,0,0.7821715328,1.1107037534,-0.3597443958
C,0,-0.696590582,1.203538941,-0.3984845142
C,0,-1.2138451183,0.0190099825,-0.0583108574
C,0,-2.633127615,-0.4263809062,0.103021527
H,0,-1.2605694395,2.0958698197,-0.6176312816
H,0,1.4592976519,1.7046064521,-0.9565097051
O,0,1.3457271692,0.6783649504,1.0125724202
O,0,2.0307481344,-1.1337997578,-0.4795039057
H,0,-2.8110427167,-0.7320382081,1.1390871038
H,0,-3.3098977604,0.3921329479,-0.1548094612
H,0,-2.8278659719,-1.2847525239,-0.5476500366

TS VI 2 (σ = 3) MP2/3-21G

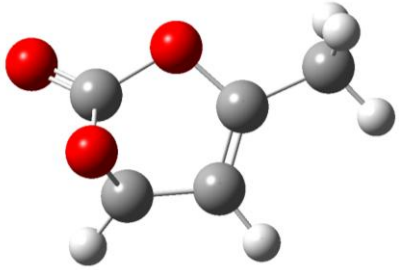

O,0,-0.2590163315,-0.9872891017,0.1904920061
C,0,1.0872920489,-0.4243541642,0.0096163402
C,0,0.7879566646,1.1629161831,-0.3134645903
C,0,-0.6805468132,1.2071370877,-0.3943542118
C,0,-1.1923785732,0.026319144,-0.0523269574
C,0,-2.6193666216,-0.4089919658,0.0657848803
H,0,-1.252233163,2.0811158082,-0.6631424285
H,0,1.4696259459,1.7501092833,-0.9136718865
O,0,1.3388622263,0.6901529,1.0036689879
O,0,2.0065718365,-1.1413054294,-0.4586116197
H,0,-2.8287663484,-0.7068703742,1.0982553191
H,0,-3.2834211088,0.4105698165,-0.2183821717
H,0,-2.7945557624,-1.2724241874,-0.5834206677

Table I.6 Pathway VI Optimized Species (Continued)

Y(OC(C)=CCjOC(=O)) (σ = 3)

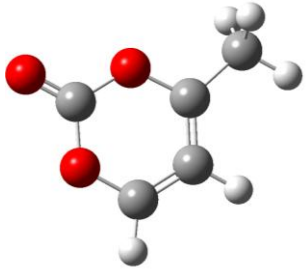

O,0,0.2006046109,-0.9691555945,-0.2404722442
C,0,-1.1267097038,-0.6611444639,-0.2040098755
C,0,-0.5064737698,1.6065011249,0.2700366922
C,0,0.830142265,1.2804526225,0.230642363
C,0,1.2044958091,-0.0204845558,-0.0266674498
C,0,2.5648752272,-0.6080127619,-0.1187116123
H,0,1.5810842275,2.0418995784,0.4008528226
H,0,-0.9451468152,2.5741579749,0.4578680766
O,0,-1.9600784959,-1.4968849588,-0.3907389847
O,0,-1.4690693607,0.6316884588,0.0524381575
H,0,2.7379322996,-1.0544356839,-1.1060672967
H,0,3.3215410573,0.1608563201,0.0523421882
H,0,2.7036826589,-1.4052110708,0.622455163

TS VI 3 (σ = 3)

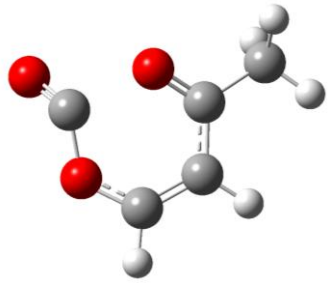

O,0,0.3439843366,-0.9361914784,-0.6622818722
C,0,-1.4162944726,-0.4992334292,-0.1837108468
C,0,-0.370873366,1.6703592209,0.0240964047
C,0,0.9276685346,1.2553986953,-0.0682017999
C,0,1.2343201238,-0.1209373924,-0.2395328135
C,0,2.5907976368,-0.6815478222,0.0947379513
H,0,1.7164607272,1.9890840924,0.045430208
H,0,-0.672212678,2.7100822785,0.0805151493
O,0,-2.0230521373,-1.3301421547,0.4077306775
O,0,-1.4309642881,0.8502779066,0.1249761593
H,0,2.885343127,-1.4308461753,-0.6448564896
H,0,3.3497902128,0.1025534167,0.1478425432
H,0,2.5459060575,-1.1820331585,1.0697707287

CC(=O)CH=CHOCj=O (σ = 3)

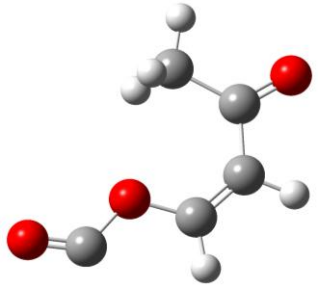

O,0,-3.066961385,-0.0944669012,0.0000610567
C,0,2.5102477649,-0.2314555144,0.0000873689
C,0,0.3653569373,-1.1564373828,0.0000733833
C,0,-0.9651222148,-1.0865941361,0.0001229231
C,0,-1.8672511106,0.0998787989,0.0001220814
C,0,-1.2918853901,1.4999807171,0.0001384488
H,0,-1.4963264094,-2.0313196227,0.0001467886
H,0,0.9115373847,-2.0919316202,0.0000656063
O,0,3.3351110931,0.606132268,0.0000605662
O,0,1.1708899019,-0.0301980066,0.000008868
H,0,-2.1158930797,2.2118062135,0.0001932893
H,0,-0.6589985559,1.6605306561,0.8767919028
H,0,-0.6590919364,1.6605735304,-0.8765762835

Table I.6 Pathway VI Optimized Species (Continued)

TS VI 4 (σ = 3)

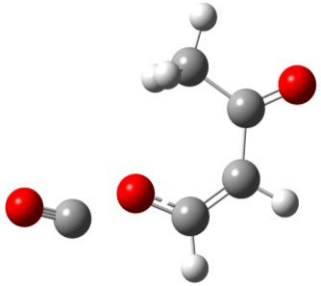

O,0,3.0665109935,0.0507268449,-0.1871410181
C,0,-2.5705377776,-0.0700359489,-0.4737120811
C,0,-0.292721394,-1.2564532609,0.1229988372
C,0,1.05188813,-1.0965675835,-0.0402670185
C,0,1.8538415335,0.1526615899,-0.045084608
C,0,1.1886639227,1.5047671669,0.1004252871
H,0,1.6498230979,-1.9973103272,-0.1459877952
H,0,-0.7283776674,-2.2564594605,0.069084833
O,0,-3.3733104242,0.6389789272,-0.0462764804
O,0,-1.1074833895,-0.2661320575,0.4392303571
H,0,1.9534015785,2.2773008991,0.0119414449
H,0,0.4200523036,1.6471498216,-0.6653477327
H,0,0.682134093,1.586455389,1.0668419747

CC(=O)CjHCH(=O) (σ = 3)

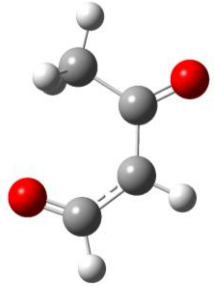

O,0,-3.0735994447,0.062062456,-0.2403073286
C,0,0.3449293798,-1.2304335087,0.1574383238
C,0,-1.0804375717,-1.0882562834,-0.0328544567
C,0,-1.857431398,0.1605577678,-0.0649339745
C,0,-1.184641668,1.5015559069,0.1104837411
H,0,-1.671418646,-1.9905426307,-0.1704156826
H,0,0.7212300516,-2.2719463198,0.1467273968
O,0,1.1247278453,-0.2897656017,0.3234197461
H,0,-1.9441674615,2.2820589907,0.0519246923
H,0,-0.6609856532,1.5497214017,1.0696454541
H,0,-0.4199564337,1.6546828212,-0.6565349118

Table I.7 Pathway VII Optimized Species

TS VII 1 (σ = 3)

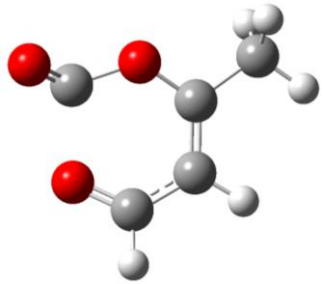

O,0,0.1122002132,-0.9736099625,0.297160677
C,0,-1.178947546,-0.5971346456,0.6260525551
C,0,-0.3400115267,1.7568963319,-0.2674275178
C,0,0.9354123421,1.1643610071,-0.367098468
C,0,1.1378147998,-0.1440186823,0.0014745693
C,0,2.4570025428,-0.8414969838,0.0610635864
H,0,1.7595031437,1.7253648668,-0.7910491527
H,0,-0.5592328422,2.670387533,-0.8350630942
O,0,-2.1495530378,-1.2131910773,0.3339428193
O,0,-1.280214911,1.2770383383,0.4456365722
H,0,3.2582895804,-0.1784512844,-0.2692735623
H,0,2.6681675894,-1.1592803655,1.089035906
H,0,2.4559396523,-1.7414440756,-0.5629948901

Table I.8 Pathway VIII Optimized Species

TS VIII 1 (σ = 3) PM3

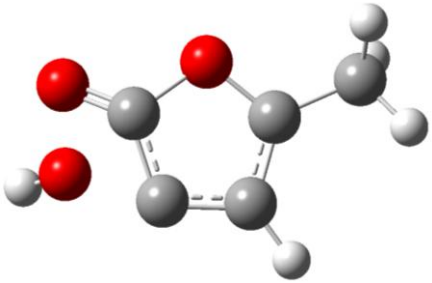

O,0,0.4167429176,-0.9655429123,-0.0645851625
C,0,-0.7863168766,-0.3670107353,-0.5540452355
C,0,-0.5418915514,1.0379237346,-0.5689651844
C,0,0.7945640953,1.2966512905,-0.2444349057
C,0,1.341171028,0.0408657583,0.0321694135
C,0,2.7301385853,-0.324225382,0.3609093563
H,0,1.2995991798,2.2590004347,-0.2127849784
O,0,-1.8630698472,-0.9507822718,-0.2845910674
O,0,-2.1634330632,0.4668820625,0.7646985638
H,0,3.4117736607,0.5091028247,0.1483317394
H,0,2.8201011995,-0.5709859328,1.4286450767
H,0,3.0680338225,-1.1998462536,-0.2105085158
H,0,-2.9178401503,0.5970583825,1.3103848998

MF4OH5Oj (σ = 3)

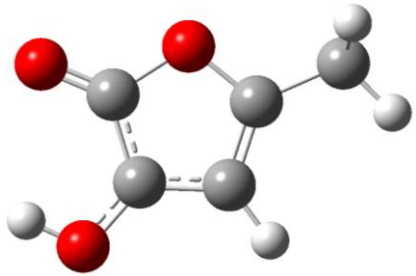

O,0,0.6260096673,1.0180748921,0.0002507223
C,0,-0.7523248125,0.7585632654,0.0002361538
C,0,-0.8922299494,-0.6779403357,0.0001501047
C,0,0.3840500136,-1.2492433158,0.0001242837
C,0,1.275363956,-0.1904091999,0.0001867574
C,0,2.7573632967,-0.1437400453,0.0001937307
H,0,0.641547217,-2.2980784654,0.0000653575
O,0,-1.6096757897,1.6267645467,0.0002747733
O,0,-2.0900798635,-1.2803804286,0.0001078353
H,0,3.1699841152,-1.1546497677,0.0001393697
H,0,3.1318342232,0.3891872834,-0.8818321504
H,0,3.1318287173,0.3890904131,0.8822804396
H,0,-2.7565467911,-0.5706848425,0.0001466223

Table I.9 Pathway IX Optimized Species

TS IX 1 (σ = 3)

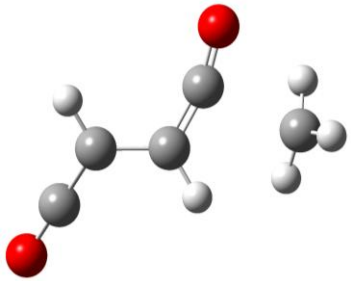

O,0,-2.1234193812,-1.356036166,-0.1530526867
C,0,2.3085827033,0.0194029396,-0.0795652046
C,0,1.1510891477,-0.6213008304,-0.0304917842
C,0,-0.1061199469,-0.0073561615,0.4102591709
C,0,-1.2827808187,-0.5603646562,0.0792017482
C,0,-2.5628271089,1.533951918,-0.145058639
H,0,-0.1029793503,0.9374524395,0.932017301
H,0,1.1751346362,-1.655717091,-0.3593841125
O,0,3.3473017141,0.5651076354,-0.0856884757
H,0,-3.0047095135,1.4466277519,0.8413819
H,0,-1.8783056577,2.3525003143,-0.3306765093
H,0,-3.1095754242,1.1238109065,-0.984586708

O=C=CHCH=C=O (σ = 1)

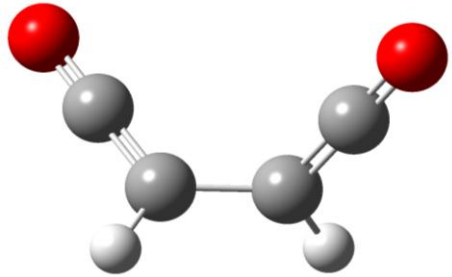

O,0,-2.3931484727,-0.8331211046,0.1535891614
C,0,1.5740890409,-0.0367803282,0.0976933666
C,0,0.6376792659,0.8543138006,0.3822247386
C,0,-0.6377416041,0.8543615277,-0.3820792514
C,0,-1.574130295,-0.0368013346,-0.0976938296
H,0,-0.8510609261,1.5751752864,-1.1670316057
H,0,0.8509817964,1.5750045542,1.1672945782
O,0,2.3931241948,-0.8330424014,-0.153717158

Table I.10 Moments of Inertia[a]

Species	I_a	I_b	I_c	
TS 2MF5OOj	273.74281	1740.04033	2002.51152	M06-2X/6-31G(d,p)
TS I 1	270.71172	1297.43132	1556.92517	
MF4j5Q	357.05674	1297.59786	1535.27298	
TS I 2	403.67758	1206.86748	1497.64711	MP2/6-31G(d,p)
CC(=O)CH=C=C=O	245.33394	1292.21566	1526.40376	
TS II 1	328.35370	1057.79341	1236.67228	MP2/6-31G(d,p)
MF45Y(CjCOOj)	347.73797	1019.09956	1222.29593	
TS II 2	348.86502	1021.92845	1232.92444	
MF4Oj5O	517.13473	929.79159	1333.08688	
TS II 3	626.70240	949.31746	1516.32309	
O=CjOC(C)=CHCH(=O)	464.72762	1616.47478	2070.01875	
TS II 4	523.78562	1643.98754	2110.29589	
n-CC(=O)CjHCH(=O)	184.73040	914.53668	1088.08559	
TS II 5	233.24891	1011.30914	1232.08052	
O=CHCH=C=O	42.01901	738.39159	780.41060	
TS III 1	356.26448	1170.40801	1372.81023	
MF5Yj(COO)	359.77427	1095.50501	1312.19493	
TS III 2	421.90958	1108.82526	1251.28426	MP2/3-21G
CC(=O)CH=CHCO2j	328.45739	1394.86152	1712.12025	
TS III 3	460.25795	1458.68249	1596.44144	
CC(=O)CH=CjH	196.63365	407.65683	593.12707	
TS III 4	213.55826	583.32449	785.75283	
CCj(=O)	21.77583	181.92551	192.55394	
TS III 5	31.77313	273.64103	292.97836	
TS IV 1	385.15947	1315.63921	1547.10544	
2MF5Oj	277.18858	799.37891	1065.38261	
TS IV 2	276.33479	852.12960	1117.17872	MP2/3-21G
CC(=O)CHCjHC=O	279.27095	924.55296	1192.49244	MP2/6-31G(d)
TS IV 3	293.69700	1485.81698	1760.02302	
TS V 1	572.76403	723.17153	1037.82749	PM3
MF2CjH25Q	277.97202	1307.97612	1580.53309	MP2/6-31G(d,p)
TS V 2	369.06606	1224.71247	1468.39741	MP2/6-31G(d,p)
MF2CH25O	268.39560	748.56703	1016.96262	
TS V 3	325.89056	860.42424	1089.11845	
C=C=CHCHCO2	168.70994	1462.82968	1548.99377	
TS VI 1	418.63603	1004.19342	1173.33209	PM3
MF45Y(CCO)5Oj	415.38896	1001.22783	1224.64330	MP2/3-21G

[a] AMU Bohr^2.

Table I.10 Moments of Inertia[a] (Continued)

Species	I_a	I_b	I_c	
TS VI 2	419.45960	987.81797	1222.70060	MP2/3-21G
Y(OC(C)=CCjOC(=O))	483.85239	903.18907	1375.84129	
TS VI 3	503.74101	989.38189	1412.62347	
CC(=O)CH=CHOCj=O	302.45273	1829.66263	2121.02109	
TS VI 4	344.61636	1856.44645	2141.59175	
CC(=O)CjHCH(=O)	244.16776	692.13270	925.32776	
TS VII 1	557.28264	908.01024	1417.12177	
TS VIII 1	359.88311	1164.68457	1350.30289	PM3
MF4OH5Oj	449.12593	1019.20734	1457.13283	
TS IX 1	316.62735	1641.28695	1917.06538	
O=C=CHCH=C=O	185.00294	932.51876	1065.84883	

[a] AMU Bohr^2.

Table I.11 Vibrational Frequencies

Species	Frequencies (cm^{-1})									
TS 2MF5OOj	-218.99	51.38	69.32	89.53	114.07	239.39	290.58	350.53	560.99	634.89
	661.12	805.66	858.97	876.16	957.30	994.92	1035.79	1068.26	1149.22	1243.05
	1249.25	1384.47	1428.38	1483.08	1504.10	1557.78	1680.40	1695.04	3068.31	3137.86
	3171.65	3274.43	3309.09							
TS I 1	-1349.46	117.34	123.26	233.32	278.35	299.39	500.47	544.05	576.16	590.68
	713.08	748.32	842.82	875.38	912.94	988.79	1011.06	1028.22	1049.99	1174.43
	1222.01	1361.11	1415.84	1424.60	1457.88	1475.00	1493.37	1531.46	1944.97	3039.87
	3093.96	3153.40	3232.44							
MF4j5Q	94.75	120.00	144.53	192.71	243.96	297.50	397.36	486.89	570.88	615.45
	634.57	705.70	763.38	794.11	960.55	981.09	1034.72	1061.24	1101.33	1207.38
	1265.24	1304.70	1370.45	1425.82	1484.31	1497.68	1572.15	1616.17	3043.89	3100.07
	3144.68	3276.92	3758.41							
TS I 2	-1379.10	85.12	104.58	119.37	188.25	232.97	301.75	430.48	533.19	545.91
MP2/6-31G(d,p)	605.88	665.49	726.02	767.12	949.83	1010.52	1055.80	1064.07	1184.19	1246.40
	1348.79	1405.37	1430.24	1446.63	1517.79	1542.33	1556.02	1638.78	3135.95	3224.58
	3263.56	3297.81	3846.42							
CC(=O)CH=C=C=O	56.94	59.33	117.22	256.47	278.62	451.79	483.57	498.95	529.84	656.06
	775.54	867.71	986.33	1004.19	1046.56	1245.11	1328.64	1400.86	1474.72	1484.49
	1769.90	1785.16	2259.47	3057.94	3121.28	3139.99	3173.86			
TS II 1	-786.93	104.86	138.86	264.62	319.12	466.70	482.42	567.44	675.42	713.56
MP2/6-31G(d,p)	759.38	814.77	885.51	1026.59	1047.83	1081.84	1121.67	1136.79	1201.37	1253.07
	1342.39	1440.24	1452.75	1529.42	1536.38	1646.06	1846.72	2001.64	3154.49	3251.26
	3277.56	3371.18	3382.34							
MF45Y(CjCOOj)	125.50	146.25	174.78	308.10	412.60	479.71	584.03	607.17	668.57	689.41
	757.56	852.27	910.51	917.54	923.19	1001.34	1025.88	1069.60	1087.25	1142.57
	1198.05	1256.99	1312.99	1334.35	1428.09	1481.05	1493.88	1701.27	3053.00	3111.22
	3113.12	3154.16	3264.33							
TS II 2	-498.41	145.58	161.87	186.16	306.07	413.49	495.55	589.06	657.44	675.35
	754.11	839.94	898.68	908.25	925.48	1000.35	1026.14	1069.60	1091.88	1165.97
	1204.82	1250.50	1314.99	1338.76	1428.38	1481.33	1494.25	1699.36	3052.89	3112.93
	3113.06	3153.91	3264.75							
MF4Oj5O	94.33	156.40	174.68	256.84	292.88	352.37	510.40	586.48	596.75	678.70
	718.40	767.21	851.82	944.95	978.09	1028.89	1058.58	1077.29	1096.65	1181.59
	1238.39	1307.24	1326.59	1428.31	1480.18	1489.44	1687.75	1923.61	3010.75	3052.80
	3113.09	3157.66	3285.13							
TS II 3	-242.45	98.88	153.86	188.72	240.88	290.21	397.81	422.90	492.24	565.08
	572.64	632.12	785.11	926.24	941.72	989.67	1044.93	1074.40	1081.10	1171.38
	1281.40	1367.72	1431.77	1481.46	1497.02	1537.95	1753.14	1944.98	2856.30	3050.29
	3108.93	3156.02	3229.43							

Table I.11 Vibrational Frequencies (Continued A)

Species	Frequencies (cm^{-1})									
O=CjOC(C)=CHCH(=O)	66.89	125.97	137.78	179.23	206.09	243.02	248.68	402.65	442.55	554.00
	560.19	630.15	866.91	903.52	1025.97	1029.02	1066.28	1113.85	1124.97	1204.22
	1325.38	1428.49	1432.38	1481.61	1486.44	1719.06	1781.95	1900.59	2964.62	3049.56
	3106.78	3157.20	3218.91							
TS II 4	-624.54	58.82	117.83	151.12	172.71	202.01	211.49	221.01	361.13	400.21
	497.53	578.01	602.99	836.78	944.92	1019.04	1024.29	1058.63	1125.78	1208.98
	1309.19	1400.41	1416.17	1477.29	1490.26	1577.81	1747.01	2048.60	2976.25	3032.88
	3101.95	3158.40	3209.98							
n-CC(=O)CjHCH(=O)	88.77	108.29	154.57	193.21	378.50	471.79	509.34	604.55	741.62	930.03
	959.82	965.60	1039.11	1137.67	1184.18	1342.59	1401.90	1434.18	1478.36	1486.51
	1623.38	1670.29	3021.87	3046.45	3108.11	3169.31	3195.76			
TS II 5	-278.06	59.34	80.12	141.80	182.65	232.71	430.40	484.22	500.50	564.74
	585.03	696.13	905.61	1000.70	1104.42	1132.25	1312.15	1428.29	1437.13	1443.77
	1774.68	2057.15	2916.02	3122.26	3281.02	3296.99	3304.30			
O=CHCH=C=O	156.24	167.53	495.10	552.98	610.09	639.39	1003.11	1095.71	1124.87	1341.58
	1462.33	1784.43	2229.82	2929.51	3226.76					
TS III 1	-317.86	120.46	140.57	175.00	277.39	294.85	471.92	571.52	615.34	620.69
	712.90	780.87	826.93	871.97	955.05	969.88	1021.20	1053.19	1055.28	1200.10
	1252.19	1326.00	1419.26	1427.50	1480.06	1487.19	1507.81	1584.52	3044.50	3099.86
	3150.69	3267.87	3295.20							
MF5Yj(COO)	127.37	137.80	229.10	275.79	334.19	464.42	524.98	545.52	566.44	659.55
	665.20	847.28	857.62	877.45	894.82	938.26	1011.91	1040.32	1053.54	1138.19
	1268.17	1305.87	1407.81	1428.80	1468.40	1476.51	1478.99	1539.95	3033.21	3083.19
	3145.99	3256.06	3287.77							
TS III 2	-319.50	154.01	182.61	233.40	369.90	394.77	492.89	503.86	562.31	574.55
MP2/3-21G	695.37	748.55	848.46	959.97	987.05	1049.72	1103.23	1147.87	1154.59	1283.41
	1312.69	1330.85	1429.69	1467.04	1519.65	1553.38	1575.96	2501.58	2847.08	2912.89
	2968.76	3231.06	3371.16							
CC(=O)CH=CHCO2j	50.16	95.72	123.51	199.13	272.48	279.52	350.39	480.55	540.00	541.34
	684.09	713.27	800.56	836.56	924.93	995.31	1016.14	1044.24	1198.63	1205.65
	1369.78	1397.41	1421.01	1473.35	1484.22	1602.80	1672.31	1759.83	3047.34	3110.28
	3174.93	3178.76	3194.28							
TS III 3	-370.39	48.33	61.48	139.07	159.51	201.26	221.73	282.63	490.79	502.30
	533.67	570.00	684.51	699.21	767.54	833.03	960.06	1051.96	1064.93	1218.92
	1243.52	1273.37	1401.12	1488.38	1489.19	1658.55	1789.14	2053.93	3057.39	3102.95
	3127.05	3174.16	3245.45							
CC(=O)CH=CjH	47.97	146.74	253.95	473.61	486.90	534.50	700.72	730.56	846.65	855.04
	1014.79	1045.92	1219.83	1249.55	1396.01	1475.19	1485.29	1653.46	1788.91	3053.91
	3081.63	3118.36	3169.98	3264.40						

Table I.11 Vibrational Frequencies (Continued B)

Species	Frequencies (cm^{-1})									
TS III 4	-332.85	34.99	79.12	106.05	143.97	281.82	424.20	511.27	612.56	780.73
	785.12	895.64	952.15	1064.56	1365.87	1464.89	1466.84	1918.77	1928.64	3044.97
	3135.54	3140.24	3381.82	3482.17						
CCj(=O)	110.46	463.10	853.91	951.61	1049.19	1365.38	1469.48	1470.90	1936.57	3037.84
	3132.60	3134.30								
TS III 5	-236.73	12.10	224.21	437.01	476.74	782.15	1425.43	1430.98	2107.16	3123.38
	3291.71	3305.07								
TS IV 1	-576.53	87.95	114.11	133.48	232.18	298.96	376.89	496.81	620.62	624.17
	685.35	742.90	802.38	883.00	924.67	984.96	1022.64	1056.48	1060.17	1177.84
	1267.75	1352.32	1424.40	1439.43	1481.34	1493.02	1517.48	1583.38	3046.70	3103.17
	3150.82	3265.11	3284.27							
2MF5Oj	128.05	177.08	293.36	296.25	515.79	589.15	607.71	677.40	722.80	766.34
	810.47	876.54	945.15	1009.28	1043.61	1065.94	1105.26	1286.50	1347.78	1426.37
	1457.54	1478.31	1485.06	1537.48	1787.91	3039.89	3093.45	3147.73	3256.00	3283.03
TS IV 2	-528.55	99.07	178.41	318.24	325.09	496.91	617.78	662.33	705.57	731.45
MP2/3-21G	784.57	885.99	897.31	1027.12	1077.53	1135.19	1142.87	1324.50	1357.95	1492.60
	1504.73	1523.51	1570.60	1591.83	2256.43	3094.21	3158.62	3190.87	3294.50	3319.06
CC(=O)CHCjHC=O	62.15	143.08	274.56	275.37	416.81	541.03	570.97	580.59	631.88	663.04
MP2/6-31G(d)	738.38	747.73	938.77	1059.57	1099.59	1103.94	1226.22	1298.03	1423.09	1483.82
	1529.96	1544.48	1561.45	2048.48	2837.03	3067.96	3146.38	3162.32	3248.85	3272.64
TS IV 3	-204.96	24.55	42.72	99.39	141.71	163.39	220.46	292.45	472.77	506.13
	561.08	702.77	755.34	876.38	909.20	1036.70	1048.77	1234.40	1257.54	1401.90
	1470.52	1485.14	1651.29	1780.31	2125.08	3062.14	3080.34	3132.12	3173.29	3238.75
TS V 1	-761.72	134.17	241.98	261.82	343.64	408.73	460.96	502.18	570.71	599.37
PM3	752.00	788.42	836.84	894.16	929.24	960.59	978.70	1053.20	1069.17	1122.96
	1174.00	1268.99	1337.04	1364.29	1379.34	1588.71	1624.74	1795.61	1994.81	3104.35
	3129.59	3142.35	3155.33							
MF2CjH25Q	82.51	197.02	222.01	227.69	334.48	345.37	501.98	521.52	613.53	630.87
MP2/6-31G(d,p)	699.11	739.38	741.78	749.32	809.01	925.75	970.37	1001.32	1052.56	1092.79
	1244.40	1315.28	1340.71	1397.88	1432.20	1468.20	1538.38	1748.50	3287.89	3352.98
	3397.38	3406.90	3807.84							
TS V 2	-1505.14	105.22	129.90	219.71	250.43	332.39	382.82	508.87	633.53	656.69
MP2/6-31G(d,p)	696.93	728.34	780.50	850.13	851.48	935.80	963.24	967.01	1032.36	1094.88
	1213.74	1247.84	1300.69	1394.15	1444.00	1501.20	1605.13	1662.21	3285.22	3344.50
	3367.26	3399.58	3854.47							
MF2CH25O	168.55	279.68	322.72	516.83	601.68	645.74	718.07	734.06	746.16	835.85
	884.27	885.00	921.35	962.82	993.53	1089.30	1126.46	1316.94	1362.63	1445.05
	1631.13	1730.06	1882.65	3192.11	3247.14	3279.81	3289.61			
TS V 3	-377.41	101.35	203.47	252.46	368.09	421.92	512.94	554.32	635.87	764.21
	807.04	825.17	901.99	922.67	963.91	1002.16	1134.89	1307.45	1357.38	1397.62
	1444.02	1680.75	1927.30	3146.43	3174.03	3231.44	3236.06			

Table I.11 Vibrational Frequencies (Continued C)

Species	Frequencies (cm^{-1})									
C=C=CHCHCO2	67.93	138.85	211.75	336.55	365.14	463.83	515.20	585.91	659.00	712.50
	885.68	895.49	975.39	1011.82	1064.08	1115.43	1169.43	1194.05	1280.89	1410.65
	1493.04	2009.14	2064.34	3142.19	3163.53	3179.78	3219.09			
TS VI 1	-425.78	48.79	137.27	251.31	278.01	345.29	395.15	445.42	538.98	645.87
PM3	708.66	742.87	859.92	907.42	951.47	961.59	980.42	1041.89	1093.91	1204.00
	1231.03	1346.42	1378.08	1380.84	1396.93	1477.25	1496.87	1638.55	3064.67	3081.65
	3135.95	3150.19	3162.48							
MF45Y(CCO)5Oj	147.69	174.65	261.09	304.14	450.80	459.51	493.90	610.45	648.71	668.16
MP2/3-21G	733.86	817.02	853.15	878.59	951.35	996.00	1055.86	1097.07	1128.86	1158.65
	1176.46	1235.83	1349.94	1388.67	1498.87	1572.38	1589.47	2304.18	3100.61	3168.77
	3189.33	3274.68	3311.22							
TS VI 2	-725.12	147.93	180.86	268.83	310.32	465.95	487.82	520.08	653.76	677.67
MP2/3-21G	703.65	782.14	815.81	825.86	942.66	953.74	1033.06	1077.87	1098.75	1167.53
	1189.52	1235.26	1364.13	1394.02	1498.52	1571.40	1585.81	2030.09	3102.61	3171.62
	3194.60	3265.68	3307.62							
Y(OC(C)=CCjOC(=O))	118.00	129.94	163.50	288.44	295.73	484.21	512.01	528.65	573.77	576.12
	741.59	747.00	856.84	863.85	988.32	1008.55	1042.39	1044.84	1120.06	1236.32
	1269.12	1345.82	1433.43	1475.00	1485.76	1495.94	1554.54	1912.02	3028.24	3076.24
	3141.82	3235.74	3284.21							
TS VI 3	-692.90	81.60	87.90	138.59	226.56	328.30	393.48	424.85	495.92	589.35
	628.81	746.26	759.62	772.96	892.55	951.85	1015.60	1045.46	1094.04	1239.56
	1296.67	1400.25	1408.73	1465.43	1482.36	1501.26	1602.69	1880.27	3046.49	3115.76
	3149.24	3218.54	3234.67							
CC(=O)CH=CHOCj=O	51.58	112.69	113.66	180.75	196.41	275.15	346.93	350.65	499.02	601.35
	608.66	711.89	797.08	819.31	982.08	987.96	1049.97	1079.51	1111.22	1259.75
	1274.37	1401.67	1416.74	1471.71	1489.87	1712.18	1771.72	1909.49	3056.99	3122.05
	3169.38	3203.09	3221.31							
TS VI 4	-636.95	44.33	53.80	113.96	157.27	175.94	234.39	315.56	338.82	415.76
	515.13	590.18	710.60	797.99	847.58	981.88	1005.92	1046.77	1108.93	1243.03
	1271.45	1404.58	1437.60	1467.02	1486.32	1552.72	1742.40	2054.10	3060.09	3126.16
	3126.88	3168.58	3203.92							
CC(=O)CjHCH(=O)	63.23	132.64	217.89	223.75	358.29	501.46	521.35	701.95	715.98	817.81
	971.66	1014.01	1041.54	1052.81	1258.89	1368.12	1410.43	1435.09	1459.66	1482.39
	1626.43	1660.94	2960.15	3064.65	3130.58	3170.66	3196.50			
TS VII 1	-704.31	86.07	121.45	167.26	230.46	324.94	331.67	391.62	493.78	547.90
	587.17	759.63	782.50	798.41	926.67	973.89	1039.76	1057.68	1104.20	1238.40
	1321.39	1376.00	1425.79	1475.48	1480.27	1495.38	1611.82	1883.28	3045.42	3066.79
	3103.29	3154.38	3226.58							

Table I.11 Vibrational Frequencies (Continued D)

Species	Frequencies (cm^{-1})									
TS VIII 1	-633.02	36.33	109.92	228.46	272.66	297.32	395.66	442.19	579.51	605.33
PM3	646.09	662.07	772.34	860.04	947.62	958.30	994.53	1052.44	1087.19	1131.83
	1309.89	1352.85	1370.73	1379.29	1386.82	1557.86	1687.21	1720.10	3064.58	3081.39
	3160.60	3162.86	3970.29							
MF4OH5Oj	120.34	168.10	231.67	263.64	291.82	377.14	528.13	559.97	582.88	586.99
	660.82	685.90	814.34	834.16	930.26	1010.20	1045.55	1047.45	1170.36	1213.12
	1324.10	1418.70	1428.18	1477.92	1488.87	1558.39	1590.81	1774.61	3038.57	3091.30
	3147.00	3273.33	3719.50							
TS IX 1	-385.18	52.33	54.86	71.22	149.11	198.00	237.31	378.05	381.01	447.72
	451.81	561.51	575.33	615.53	638.82	782.73	1041.24	1135.12	1168.33	1286.50
	1426.13	1433.16	1461.23	2108.92	2210.85	3120.31	3198.36	3262.95	3288.62	3301.60
O=C=CHCH=C=O	56.91	161.29	217.99	504.14	541.84	545.91	577.76	618.16	732.14	981.54
	1124.81	1171.52	1368.31	1409.55	2217.86	2228.51	3175.78	3176.63		

Table I.12 Isodesmic Work Reactions and Calculated $\Delta H^{\circ}_{f\,298}$ for TS 2MF5OOj

Isodesmic Work Reactions							$\Delta H^{\circ}_{f\,298}$ M06-2X/6-31G(d,p)
TS 2MF5OOj System							
TS 2MF5OOj	+	CH_4	→	2MF	+	CjH_3	47.53
TS 2MF5OOj	+	CH_3CH_3	→	2MF	+	CH_3CjH_2	47.38
TS 2MF5OOj	+	$CH_3CH_2CH_3$	→	2MF	+	$CH_3CH_2CjH_2$	47.99
TS 2MF5OOj	+	CH_3OOH	→	2MF5OOH	+	CH_3OOj	47.78
TS 2MF5OOj	+	CH_3CH_2OOH	→	2MF5OOH	+	CH_3CH_2OOj	47.76
TS 2MF5OOj	+	$CH_3CH_2CH_2OOH$	→	2MF5OOH	+	$CH_3CH_2CH_2OOj$	47.49
						Average	**47.7 ± 0.2**

Table I.13 Isodesmic Work Reactions and Calculated $\Delta H^{\circ}_{f\,298}$ for 2MF5j + O_2 Reaction Species

Isodesmic Work Reactions							$\Delta H^{\circ}_{f\,298}$ CBS-QB3
TS I 1 System							
TS I 1	+	CH_3CH_3	→	2MF5OOH	+	CH_3CjH_2	36.07
TS I 1	+	$CH_3CH_2CH_3$	→	2MF5OOH	+	$CH_3CH_2CjH_2$	35.69
TS I 1	+	$CH_3CH_2CH_2CH_3$	→	2MF5OOH	+	$CH_3CH_2CH_2CjH_2$	35.84
						Average	**35.9 ± 0.2**
						Atomization	**36.6**
MF4j5Q System							
MF4j5Q	+	CH_3CH_3	→	2MF5OOH	+	CH_3CjH_2	27.97
MF4j5Q	+	$CH_3CH_2CH_3$	→	2MF5OOH	+	$CH_3CH_2CjH_2$	27.59
MF4j5Q	+	$CH_3CH_2CH_2CH_3$	→	2MF5OOH	+	$CH_3CH_2CH_2CjH_2$	27.74
						Average	**27.8 ± 0.2**
						Atomization	**28.5**
TS I 2 System							
TS I 2	+	CH_3CH_3	→	2MF5OOH	+	CH_3CjH_2	47.43
TS I 2	+	$CH_3CH_2CH_3$	→	2MF5OOH	+	$CH_3CH_2CjH_2$	47.05
TS I 2	+	$CH_3CH_2CH_2CH_3$	→	2MF5OOH	+	$CH_3CH_2CH_2CjH_2$	47.20
						Average	**47.2 ± 0.2**
						Atomization	**48.0**
CC(=O)CH=C=C=O System							
CC(=O)CH=C=C=O	+	$CH_2=CH_2$	→	$H_2C=C=C=O$	+	CC(=O)C=C	-8.80
CC(=O)CH=C=C=O	+	CH_3CH_3	→	$H_2C=C=C=O$	+	CC(=O)CC	-8.02
CC(=O)CH=C=C=O	+	$CH_3CH_2CH_3$	→	$H_2C=C=C=O$	+	n-CC(=O)CCC	-7.79
						Average	**-8.2 ± 0.5**
						Atomization	**-6.8**
TS II 1 System							
TS II 1	+	CH_3CH_3	→	2MF5OOH	+	CH_3CjH_2	36.60
TS II 1	+	$CH_3CH_2CH_3$	→	2MF5OOH	+	$CH_3CH_2CjH_2$	36.22
TS II 1	+	$CH_3CH_2CH_2CH_3$	→	2MF5OOH	+	$CH_3CH_2CH_2CjH_2$	36.37
						Average	**36.4 ± 0.2**
						Atomization	**37.1**
MF45Y(CjCOOj) System							
MF45Y(CjCOOj)	+	CH_3CH_3	→	2MF5OOH	+	CH_3CjH_2	23.51
MF45Y(CjCOOj)	+	$CH_3CH_2CH_3$	→	2MF5OOH	+	$CH_3CH_2CjH_2$	23.13
MF45Y(CjCOOj)	+	$CH_3CH_2CH_2CH_3$	→	2MF5OOH	+	$CH_3CH_2CH_2CjH_2$	23.28
						Average	**23.3 ± 0.2**
						Atomization	**24.1**
TS II 2 System							
TS II 2	+	CH_3CH_3	→	2MF5OOH	+	CH_3CjH_2	22.85
TS II 2	+	$CH_3CH_2CH_3$	→	2MF5OOH	+	$CH_3CH_2CjH_2$	22.47
TS II 2	+	$CH_3CH_2CH_2CH_3$	→	2MF5OOH	+	$CH_3CH_2CH_2CjH_2$	22.62
						Average	**22.6 ± 0.2**
						Atomization	**23.4**
MF4Oj5O System							
MF4Oj5O	+	CH_3CH_3	→	2MF5OOH	+	CH_3CjH_2	-51.88
MF4Oj5O	+	$CH_3CH_2CH_3$	→	2MF5OOH	+	$CH_3CH_2CjH_2$	-52.26
MF4Oj5O	+	$CH_3CH_2CH_2CH_3$	→	2MF5OOH	+	$CH_3CH_2CH_2CjH_2$	-52.11
						Average	**-52.1 ± 0.2**
						Atomization	**-51.3**

Table I.13 Isodesmic Work Reactions and Calculated $\Delta H^{\circ}_{f\,298}$ for 2MF5j + O_2 Reaction Species (Continued A)

Isodesmic Work Reactions							$\Delta H^{\circ}_{f\,298}$ CBS-QB3
TS II 3 System							
TS II 3	+	CH_3CH_3	→	2MF5OOH	+	CH_3CjH_2	-45.65
TS II 3	+	$CH_3CH_2CH_3$	→	2MF5OOH	+	$CH_3CH_2CjH_2$	-46.03
TS II 3	+	$CH_3CH_2CH_2CH_3$	→	2MF5OOH	+	$CH_3CH_2CH_2CjH_2$	-45.88
						Average	**-45.9 ± 0.2**
						Atomization	**-45.1**
O=CjOC(C)=CHCH(=O) System							
O=CjOC(C)=CHCH(=O)	+	CH_4	→	CC(=O)CCj	+	HOCH=C=O	-52.88
O=CjOC(C)=CHCH(=O)	+	$CH_3CH_2CH_3$	→	n-CC(=O)CCCj	+	$HOCH_2CH=C=O$	-52.67
O=CjOC(C)=CHCH(=O)	+	CH_3CH_3	→	CC(=O)CCj	+	$HOCH_2CH=C=O$	-52.93
O=CjOC(C)=CHCH(=O)	+	CH_3CH_3	→	n-CC(=O)CCCj	+	HOCH=C=O	-52.71
						Average	**-52.8 ± 0.1**
						Atomization	**-52.5**
TS II 4 System							
TS II 4	+	CH_4	→	CC(=O)CCj	+	HOCH=C=O	-41.64
TS II 4	+	$CH_3CH_2CH_3$	→	n-CC(=O)CCCj	+	$HOCH_2CH=C=O$	-41.42
TS II 4	+	CH_3CH_3	→	CC(=O)CCj	+	$HOCH_2CH=C=O$	-41.68
TS II 4	+	CH_3CH_3	→	n-CC(=O)CCCj	+	HOCH=C=O	-41.46
						Average	**-41.6 ± 0.1**
						Atomization	**-41.2**
***n*-CC(=O)CjHCH(=O) System**							
n-CC(=O)CjHCH(=O)	+	CH_4	→	CC(=O)Cj	+	CC(=O)	-38.09
n-CC(=O)CjHCH(=O)	+	CH_3CH_3	→	CC(=O)CCj	+	CC(=O)	-38.37
n-CC(=O)CjHCH(=O)	+	$CH_3CH_2CH_3$	→	CC(=O)CCj	+	CC(=O)C	-38.48
n-CC(=O)CjHCH(=O)	+	$CH_3CH_2CH_2CH_3$	→	CC(=O)CCj	+	CC(=O)CC	-38.49
						Average	**-38.4 ± 0.2**
						Atomization	**-37.4**
TS II 5 System							
TS II 5	+	CH_4	→	CC(=O)Cj	+	CC(=O)	0.71
TS II 5	+	CH_3CH_3	→	CC(=O)CCj	+	CC(=O)	0.43
TS II 5	+	$CH_3CH_2CH_3$	→	CC(=O)CCj	+	CC(=O)C	0.33
TS II 5	+	$CH_3CH_2CH_2CH_3$	→	CC(=O)CCj	+	CC(=O)CC	0.31
						Average	**0.4 ± 0.2**
						Atomization	**1.4**
O=CHCH=C=O System							
O=CHCH=C=O	+	CH_4	→	$H_2C=C=O$	+	CC(=O)	-40.14
O=CHCH=C=O	+	CH_3CH_3	→	$CH_3CH=C=O$	+	CC(=O)	-40.30
O=CHCH=C=O	+	$CH_3CH_2CH_3$	→	$CH_3CH=C=O$	+	CC(=O)C	-40.40
O=CHCH=C=O	+	$CH_3CH_2CH_3$	→	$CH_3CH_2CH=C=O$	+	CC(=O)	-40.50
						Average	**-40.3 ± 0.2**
						Atomization	**-40.5**
TS III 1 System							
TS III 1	+	CH_3CH_3	→	2MF5OOH	+	CH_3CjH_2	8.77
TS III 1	+	$CH_3CH_2CH_3$	→	2MF5OOH	+	$CH_3CH_2CjH_2$	8.39
TS III 1	+	$CH_3CH_2CH_2CH_3$	→	2MF5OOH	+	$CH_3CH_2CH_2CjH_2$	8.54
						Average	**8.6 ± 0.2**
						Atomization	**9.3**

Table I.13 Isodesmic Work Reactions and Calculated $\Delta H^{\circ}_{f\,298}$ for 2MF5j + O_2 Reaction Species (Continued B)

Isodesmic Work Reactions							$\Delta H^{\circ}_{f\,298}$ CBS-QB3
MF5Yj(COO) System							
MF5Yj(COO)	+	CH_3CH_3	→	2MF5OOH	+	CH_3CjH_2	-6.97
MF5Yj(COO)	+	$CH_3CH_2CH_3$	→	2MF5OOH	+	$CH_3CH_2CjH_2$	-7.35
MF5Yj(COO)	+	$CH_3CH_2CH_2CH_3$	→	2MF5OOH	+	$CH_3CH_2CH_2CjH_2$	-7.20
						Average	**-7.2 ± 0.2**
						Atomization	**-6.4**
TS III 2 System							
TS III 2	+	CH_3CH_3	→	2MF5OOH	+	CH_3CjH_2	-6.19
TS III 2	+	$CH_3CH_2CH_3$	→	2MF5OOH	+	$CH_3CH_2CjH_2$	-6.57
TS III 2	+	$CH_3CH_2CH_2CH_3$	→	2MF5OOH	+	$CH_3CH_2CH_2CjH_2$	-6.42
						Average	**-6.4 ± 0.2**
						Atomization	**-5.6**
CC(=O)CH=CHCO2j System							
CC(=O)CH=CHCO2j	+	CH_4	→	CC(=O)CCj	+	HOCH=C=O	-50.68
CC(=O)CH=CHCO2j	+	$CH_3CH_2CH_3$	→	n-CC(=O)CCCj	+	$HOCH_2CH=C=O$	-50.46
CC(=O)CH=CHCO2j	+	CH_3CH_3	→	CC(=O)CCj	+	$HOCH_2CH=C=O$	-50.73
CC(=O)CH=CHCO2j	+	CH_3CH_3	→	n-CC(=O)CCCj	+	HOCH=C=O	-50.50
						Average	**-50.6 ± 0.1**
						Atomization	**-50.3**
TS III 3 System							
TS III 3	+	CH_4	→	CC(=O)CCj	+	HOCH=C=O	-49.79
TS III 3	+	$CH_3CH_2CH_3$	→	n-CC(=O)CCCj	+	$HOCH_2CH=C=O$	-49.58
TS III 3	+	CH_3CH_3	→	CC(=O)CCj	+	$HOCH_2CH=C=O$	-49.84
TS III 3	+	CH_3CH_3	→	n-CC(=O)CCCj	+	HOCH=C=O	-49.62
						Average	**-49.7 ± 0.1**
						Atomization	**-49.4**
CC(=O)CH=CjH System							
CC(=O)CH=CjH	+	CH_3CH_3	→	CC(=O)C=C	+	CH_3CjH_2	29.98
CC(=O)CH=CjH	+	$CH_3CH_2CH_3$	→	CC(=O)C=C	+	$CH_3CH_2CjH_2$	29.60
CC(=O)CH=CjH	+	$CH_3CH_2CH_2CH_3$	→	CC(=O)C=C	+	$CH_3CH_2CH_2CjH_2$	29.75
CC(=O)CH=CjH	+	$CH_3CH_2CH_2CH_2CH_3$	→	CC(=O)C=C	+	$CH_3CH_2CH_2CH_2CjH_2$	29.87
						Average	**29.8 ± 0.2**
						Atomization	**32.5**
TS III 4 System							
TS III 4	+	CH_3CH_3	→	CC(=O)C=C	+	CH_3CjH_2	56.83
TS III 4	+	$CH_3CH_2CH_3$	→	CC(=O)C=C	+	$CH_3CH_2CjH_2$	56.45
TS III 4	+	$CH_3CH_2CH_2CH_3$	→	CC(=O)C=C	+	$CH_3CH_2CH_2CjH_2$	56.60
TS III 4	+	$CH_3CH_2CH_2CH_2CH_3$	→	CC(=O)C=C	+	$CH_3CH_2CH_2CH_2CjH_2$	56.73
						Average	**56.7 ± 0.2**
						Atomization	**59.4**
CCj(=O) System							
CCj(=O)	+	CC(=O)C	→	CC(=O)Cj	+	CC(=O)	-2.56
CCj(=O)	+	CC(=O)CC	→	CC(=O)CCj	+	CC(=O)	-2.83
CCj(=O)	+	n-CC(=O)CCC	→	n-CC(=O)CCCj	+	CC(=O)	-2.79
CCj(=O)	+	CCC(=O)CC	→	CjCC(=O)CC	+	CC(=O)	-2.89
						Average	**-2.8 ± 0.1**
						Atomization	**-2.2**

Table I.13 Isodesmic Work Reactions and Calculated $\Delta H^{\circ}_{f\,298}$ for 2MF5j + O_2 Reaction Species (Continued C)

Isodesmic Work Reactions							$\Delta H^{\circ}_{f\,298}$ CBS-QB3
TS III 5 System							
TS III 5	+	CC(=O)C	→	CC(=O)Cj	+	CC(=O)	14.36
TS III 5	+	CC(=O)CC	→	CC(=O)CCj	+	CC(=O)	14.10
TS III 5	+	n-CC(=O)CCC	→	n-CC(=O)CCCj	+	CC(=O)	14.13
TS III 5	+	CCC(=O)CC	→	CjCC(=O)CC	+	CC(=O)	14.04
						Average	**14.2 ± 0.1**
						Atomization	**14.7**
TS IV 1 System							
TS IV 1	+	CH_3CH_3	→	2MF5OOH	+	CH_3CjH_2	18.49
TS IV 1	+	$CH_3CH_2CH_3$	→	2MF5OOH	+	$CH_3CH_2CjH_2$	18.11
TS IV 1	+	$CH_3CH_2CH_2CH_3$	→	2MF5OOH	+	$CH_3CH_2CH_2CjH_2$	18.26
						Average	**18.3 ± 0.2**
						Atomization	**19.0**
TS IV 2 System							
TS IV 2	+	CH_3CH_2OH	→	2MF5OOH	+	CH_3CjH_2	-41.56
TS IV 2	+	$CH_3CH_2CH_2OH$	→	2MF5OOH	+	$CH_3CH_2CjH_2$	-42.13
TS IV 2	+	$CH_3CH_2CH_2CH_2OH$	→	2MF5OOH	+	$CH_3CH_2CH_2CjH_2$	-42.21
						Average	**-42.0 ± 0.4**
						Atomization	**-40.6**
CC(=O)CHCjHC=O System							
CC(=O)CHCjHC=O	+	CH_3OH	→	CC(=O)CCj	+	HOCH=C=O	-31.78
CC(=O)CHCjHC=O	+	$CH_3CH_2CH_2OH$	→	n-CC(=O)CCCj	+	$HOCH_2CH=C=O$	-31.60
CC(=O)CHCjHC=O	+	CH_3CH_2OH	→	CC(=O)CCj	+	$HOCH_2CH=C=O$	-31.68
CC(=O)CHCjHC=O	+	CH_3CH_2OH	→	n-CC(=O)CCCj	+	HOCH=C=O	-31.46
						Average	**-31.6 ± 0.1**
						Atomization	**-30.8**
TS IV 3 System							
TS IV 3	+	CH_3OH	→	CC(=O)CCj	+	HOCH=C=O	9.58
TS IV 3	+	$CH_3CH_2CH_2OH$	→	n-CC(=O)CCCj	+	$HOCH_2CH=C=O$	9.76
TS IV 3	+	CH_3CH_2OH	→	CC(=O)CCj	+	$HOCH_2CH=C=O$	9.68
TS IV 3	+	CH_3CH_2OH	→	n-CC(=O)CCCj	+	HOCH=C=O	9.90
						Average	**9.7 ± 0.1**
						Atomization	**10.5**
TS V 1 System							
TS V 1	+	CH_3CH_3	→	2MF5OOH	+	CH_3CjH_2	58.42
TS V 1	+	$CH_3CH_2CH_3$	→	2MF5OOH	+	$CH_3CH_2CjH_2$	58.04
TS V 1	+	$CH_3CH_2CH_2CH_3$	→	2MF5OOH	+	$CH_3CH_2CH_2CjH_2$	58.19
						Average	**58.2 ± 0.2**
						Atomization	**59.0**
MF2CjH25Q System							
MF2CjH25Q	+	CH_3CH_3	→	2MF5OOH	+	CH_3CjH_2	-3.62
MF2CjH25Q	+	$CH_3CH_2CH_3$	→	2MF5OOH	+	$CH_3CH_2CjH_2$	-4.01
MF2CjH25Q	+	$CH_3CH_2CH_2CH_3$	→	2MF5OOH	+	$CH_3CH_2CH_2CjH_2$	-3.85
						Average	**-3.8 ± 0.2**
						Atomization	**-3.1**

Table I.13 Isodesmic Work Reactions and Calculated $\Delta H^{\circ}_{f\,298}$ for 2MF5j + O_2 Reaction Species (Continued D)

Isodesmic Work Reactions							$\Delta H^{\circ}_{f\,298}$ CBS-QB3
TS V 2 System							
TS V 2	+	CH_3CH_3	→	2MF5OOH	+	CH_3CjH_2	-9.86
TS V 2	+	$CH_3CH_2CH_3$	→	2MF5OOH	+	$CH_3CH_2CjH_2$	-10.25
TS V 2	+	$CH_3CH_2CH_2CH_3$	→	2MF5OOH	+	$CH_3CH_2CH_2CjH_2$	-10.10
						Average	**-10.1 ± 0.2**
						Atomization	**-9.3**
MF2CH25O System							
MF2CH25O	+	CH_3CH_3	→	2MF5Oj	+	CH_3CjH_2	-47.06
MF2CH25O	+	$CH_3CH_2CH_3$	→	2MF5Oj	+	$CH_3CH_2CjH_2$	-47.44
MF2CH25O	+	$CH_3CH_2CH_2CH_3$	→	2MF5Oj	+	$CH_3CH_2CH_2CjH_2$	-47.29
MF2CH25O	+	$CH_3CH_2CH_2CH_2CH_3$	→	2MF5Oj	+	$CH_3CH_2CH_2CH_2CjH_2$	-47.16
						Average	**-47.2 ± 0.2**
						Atomization	**-45.9**
TS V 3 System							
TS V 3	+	CH_3CH_3	→	2MF5Oj	+	CH_3CjH_2	32.71
TS V 3	+	$CH_3CH_2CH_3$	→	2MF5Oj	+	$CH_3CH_2CjH_2$	32.33
TS V 3	+	$CH_3CH_2CH_2CH_3$	→	2MF5Oj	+	$CH_3CH_2CH_2CjH_2$	32.48
TS V 3	+	$CH_3CH_2CH_2CH_2CH_3$	→	2MF5Oj	+	$CH_3CH_2CH_2CH_2CjH_2$	32.60
						Average	**32.5 ± 0.2**
						Atomization	**33.8**
C=C=CHCHCO2 System							
C=C=CHCHCO2	+	$CH_2=CH_2$	→	$H_2C=C=C=O$	+	CC(=O)C=C	5.31
C=C=CHCHCO2	+	CH_3CH_3	→	$H_2C=C=C=O$	+	CC(=O)CC	6.09
C=C=CHCHCO2	+	$CH_3CH_2CH_3$	→	$H_2C=C=C=O$	+	n-CC(=O)CCC	6.32
						Average	**5.9 ± 0.5**
						Atomization	**7.3**
TS VI 1 System							
TS VI 1	+	CH_3CH_3	→	2MF5OOH	+	CH_3CjH_2	-12.35
TS VI 1	+	$CH_3CH_2CH_3$	→	2MF5OOH	+	$CH_3CH_2CjH_2$	-12.73
TS VI 1	+	$CH_3CH_2CH_2CH_3$	→	2MF5OOH	+	$CH_3CH_2CH_2CjH_2$	-12.58
						Average	**-12.6 ± 0.2**
						Atomization	**-11.8**
MF45Y(CCO)5Oj System							
MF45Y(CCO)5Oj	+	CH_3CH_3	→	2MF5OOH	+	CH_3CjH_2	-27.91
MF45Y(CCO)5Oj	+	$CH_3CH_2CH_3$	→	2MF5OOH	+	$CH_3CH_2CjH_2$	-28.29
MF45Y(CCO)5Oj	+	$CH_3CH_2CH_2CH_3$	→	2MF5OOH	+	$CH_3CH_2CH_2CjH_2$	-28.14
						Average	**-28.1 ± 0.2**
						Atomization	**-27.4**
TS VI 2 System							
TS VI 2	+	CH_3CH_3	→	2MF5OOH	+	CH_3CjH_2	-36.69
TS VI 2	+	$CH_3CH_2CH_3$	→	2MF5OOH	+	$CH_3CH_2CjH_2$	-37.07
TS VI 2	+	$CH_3CH_2CH_2CH_3$	→	2MF5OOH	+	$CH_3CH_2CH_2CjH_2$	-36.92
						Average	**-36.9 ± 0.2**
						Atomization	**-36.1**

Table I.13 Isodesmic Work Reactions and Calculated $\Delta H^{\circ}_{f\,298}$ for 2MF5j + O_2 Reaction Species (Continued E)

Isodesmic Work Reactions							$\Delta H^{\circ}_{f\,298}$ CBS-QB3
Y(OC(C)=CCjOC(=O)) System							
Y(OC(C)=CCjOC(=O))	+	CH_4	→	$Y(C_4H_4O_2)$	+	CH_3CH_2Oj	-79.08
Y(OC(C)=CCjOC(=O))	+	CH_3CH_3	→	$Y(C_4H_4O_2)$	+	$CH_3CH_2CH_2Oj$	-79.83
Y(OC(C)=CCjOC(=O))	+	$CH_3CH_2CH_3$	→	$Y(C_4H_4O_2)$	+	$CH_3CH_2CH_2CH_2Oj$	-79.50
						Average	**-79.5 ± 0.4**
						Atomization	**-79.7**
TS VI 3 System							
TS VI 3	+	CH_4	→	$Y(C_4H_4O_2)$	+	CH_3CH_2Oj	-37.09
TS VI 3	+	CH_3CH_3	→	$Y(C_4H_4O_2)$	+	$CH_3CH_2CH_2Oj$	-37.84
TS VI 3	+	$CH_3CH_2CH_3$	→	$Y(C_4H_4O_2)$	+	$CH_3CH_2CH_2CH_2Oj$	-37.51
						Average	**-37.5 ± 0.4**
						Atomization	**-37.7**
CC(=O)CH=CHOCj=O System							
CC(=O)CH=CHOCj=O	+	CH_4	→	CC(=O)CCj	+	HOCH=C=O	-53.48
CC(=O)CH=CHOCj=O	+	$CH_3CH_2CH_3$	→	n-CC(=O)CCCj	+	$HOCH_2CH=C=O$	-53.27
CC(=O)CH=CHOCj=O	+	CH_3CH_3	→	CC(=O)CCj	+	$HOCH_2CH=C=O$	-53.53
CC(=O)CH=CHOCj=O	+	CH_3CH_3	→	n-CC(=O)CCCj	+	HOCH=C=O	-53.31
						Average	**-53.4 ± 0.1**
						Atomization	**-53.1**
TS VI 4 System							
TS VI 4	+	CH_4	→	CC(=O)CCj	+	HOCH=C=O	-39.42
TS VI 4	+	$CH_3CH_2CH_3$	→	n-CC(=O)CCCj	+	$HOCH_2CH=C=O$	-39.21
TS VI 4	+	CH_3CH_3	→	CC(=O)CCj	+	$HOCH_2CH=C=O$	-39.47
TS VI 4	+	CH_3CH_3	→	n-CC(=O)CCCj	+	HOCH=C=O	-39.25
						Average	**-39.3 ± 0.1**
						Atomization	**-39.0**
CC(=O)CjHCH(=O) System							
CC(=O)CjHCH(=O)	+	CH_4	→	CC(=O)Cj	+	CC(=O)	-37.39
CC(=O)CjHCH(=O)	+	CH_3CH_3	→	CC(=O)CCj	+	CC(=O)	-37.67
CC(=O)CjHCH(=O)	+	$CH_3CH_2CH_3$	→	CC(=O)CCj	+	CC(=O)C	-37.77
CC(=O)CjHCH(=O)	+	$CH_3CH_2CH_2CH_3$	→	CC(=O)CCj	+	CC(=O)CC	-37.79
						Average	**-37.7 ± 0.2**
						Atomization	**-36.7**
TS VII 1 System							
TS VII 1	+	CH_4	→	$Y(C_4H_4O_2)$	+	CH_3CH_2Oj	-36.73
TS VII 1	+	CH_3CH_3	→	$Y(C_4H_4O_2)$	+	$CH_3CH_2CH_2Oj$	-37.48
TS VII 1	+	$CH_3CH_2CH_3$	→	$Y(C_4H_4O_2)$	+	$CH_3CH_2CH_2CH_2Oj$	-37.15
						Average	**-37.1 ± 0.4**
						Atomization	**-37.4**
TS VIII 1 System							
TS VIII 1	+	CH_3CH_3	→	2MF5OOH	+	CH_3CjH_2	54.35
TS VIII 1	+	$CH_3CH_2CH_3$	→	2MF5OOH	+	$CH_3CH_2CjH_2$	53.97
TS VIII 1	+	$CH_3CH_2CH_2CH_3$	→	2MF5OOH	+	$CH_3CH_2CH_2CjH_2$	54.12
						Average	**54.1 ± 0.2**
						Atomization	**54.9**

Table I.13 Isodesmic Work Reactions and Calculated $\Delta H^{\circ}_{f\,298}$ for 2MF5j + O_2 Reaction Species (Continued F)

Isodesmic Work Reactions							$\Delta H^{\circ}_{f\,298}$ CBS-QB3
MF4OH5Oj System							
MF4OH5Oj	+	CH_3CH_3	→	2MF5OOH	+	CH_3CjH_2	-93.04
MF4OH5Oj	+	$CH_3CH_2CH_3$	→	2MF5OOH	+	$CH_3CH_2CjH_2$	-93.43
MF4OH5Oj	+	$CH_3CH_2CH_2CH_3$	→	2MF5OOH	+	$CH_3CH_2CH_2CjH_2$	-93.28
						Average	**-93.2 ± 0.2**
						Atomization	**-92.5**
TS IX 1 System							
TS IX 1	+	CH_3OH	→	CC(=O)CCj	+	HOCH=C=O	31.23
TS IX 1	+	$CH_3CH_2CH_2OH$	→	n-CC(=O)CCCj	+	$HOCH_2CH=C=O$	31.40
TS IX 1	+	CH_3CH_2OH	→	CC(=O)CCj	+	$HOCH_2CH=C=O$	31.32
TS IX 1	+	CH_3CH_2OH	→	n-CC(=O)CCCj	+	HOCH=C=O	31.54
						Average	**31.4 ± 0.1**
						Atomization	**32.2**
O=C=CHCH=C=O System							
O=C=CHCH=C=O	+	CH#CH	→	$H_2C=C=C=O$	+	$H_2C=C=C=O$	-10.30
O=C=CHCH=C=O	+	CH_3CH_3	→	$H_2C=C=C=O$	+	CC(=O)C	-10.91
O=C=CHCH=C=O	+	CH_3CH_3	→	$H_2C=CHCH=O$	+	$H_2C=CHCH=O$	-10.44
O=C=CHCH=C=O	+	$CH_2=CH_2$	→	$H_2C=C=C=O$	+	$H_2C=CHCH=O$	-10.49
						Average	**-10.5 ± 0.3**
						Atomization	**-10.0**

Table I.14 Calculated $\Delta H^{\circ}_{f\,298}$ for Work Reaction Species

Isodesmic Work Reactions							$\Delta H^{\circ}_{f\,298}$ (kcal mol^{-1}) CBS-QB3
$H_2C{=}C{=}C{=}O$ System							
$H_2C{=}C{=}C{=}O$	+	$CH_2{=}CH_2$	→	$H_2C{=}C{=}O$	+	$CH{\#}CCH_3$	30.93
$H_2C{=}C{=}C{=}O$	+	$CH_2{=}CH_2$	→	$CH_3CH{=}C{=}O$	+	$CH{\#}CH$	30.58
$H_2C{=}C{=}C{=}O$	+	$CH_2{=}CHCH_2CH_3$	→	$CH_3CH{=}C{=}O$	+	$CH{\#}CCH_2CH_3$	30.84
$H_2C{=}C{=}C{=}O$	+	$CH_3CH_2CH_2CH_3$	→	$CH_3CH{=}C{=}O$	+	$CH_2{=}CHCH_2CH_3$	30.52
						Average	**30.7 ± 0.2**
						Atomization	**31.6**
$H_2C{=}CHCH{=}O$ System							
$H_2C{=}CHCH{=}O$	+	$CH_2{=}CH_2$	→	$H_2C{=}C{=}C{=}O$	+	CH_3CH_3	-15.73
$H_2C{=}CHCH{=}O$	+	$CH{\#}CH$	→	$H_2C{=}C{=}C{=}O$	+	$CH_2{=}CH_2$	-15.49
$H_2C{=}CHCH{=}O$	+	$CH_2{=}CHCH_3$	→	$H_2C{=}C{=}C{=}O$	+	$CH_3CH_2CH_3$	-15.72
$H_2C{=}CHCH{=}O$	+	$CH{\#}CCH_3$	→	$H_2C{=}C{=}C{=}O$	+	$CH_2{=}CHCH_3$	-15.77
						Average	**-15.7 ± 0.1**
						Atomization	**-15.3**
$CH_3CH_2CH_2CH_2CjH_2$ System							
$CH_3CH_2CH_2CH_2CjH_2$	+	CH_4	→	$CH_3CH_2CH_2CH_2CH_3$	+	CjH_3	14.64
$CH_3CH_2CH_2CH_2CjH_2$	+	CH_3CH_3	→	$CH_3CH_2CH_2CH_2CH_3$	+	CH_3CjH_2	14.45
$CH_3CH_2CH_2CH_2CjH_2$	+	$CH_3CH_2CH_3$	→	$CH_3CH_2CH_2CH_2CH_3$	+	$CH_3CH_2CjH_2$	14.07
$CH_3CH_2CH_2CH_2CjH_2$	+	$CH_3CH_2CH_2CH_3$	→	$CH_3CH_2CH_2CH_2CH_3$	+	$CH_3CH_2CH_2CjH_2$	14.22
						Average	**14.3 ± 0.3**
						Atomization	**16.7**

Table I.14 Calculated $\Delta H^{\circ}_{f\,298}$ for Work Reaction Species (Continued)

Isodesmic Work Reactions						$\Delta H^{\circ}_{f\,298}$ (kcal mol^{-1}) CBS-QB3
$CH_3CH_2CH_2Oj$ System						
$CH_3CH_2CH_2Oj$	+	CH_4	→	$CH_3CH_2CH_2OH$	+	CjH_3	-8.42
$CH_3CH_2CH_2Oj$	+	CH_3CH_3	→	$CH_3CH_2CH_2OH$	+	CH_3CjH_2	-8.61
$CH_3CH_2CH_2Oj$	+	$CH_3CH_2CH_3$	→	$CH_3CH_2CH_2OH$	+	$CH_3CH_2CjH_2$	-8.99
$CH_3CH_2CH_2Oj$	+	$CH_3CH_2CH_2CH_3$	→	$CH_3CH_2CH_2OH$	+	$CH_3CH_2CH_2CjH_2$	-8.84
						Average	**-8.7 ± 0.3**
						Atomization	**-7.8**
$CH_3CH_2CH_2CH_2Oj$ System						
$CH_3CH_2CH_2CH_2Oj$	+	CH_4	→	$CH_3CH_2CH_2CH_2OH$	+	CjH_3	-13.16
$CH_3CH_2CH_2CH_2Oj$	+	CH_3CH_3	→	$CH_3CH_2CH_2CH_2OH$	+	CH_3CjH_2	-13.35
$CH_3CH_2CH_2CH_2Oj$	+	$CH_3CH_2CH_3$	→	$CH_3CH_2CH_2CH_2OH$	+	$CH_3CH_2CjH_2$	-13.73
$CH_3CH_2CH_2CH_2Oj$	+	$CH_3CH_2CH_2CH_3$	→	$CH_3CH_2CH_2CH_2OH$	+	$CH_3CH_2CH_2CjH_2$	-13.58
						Average	**-13.5 ± 0.3**
						Atomization	**-12.4**
$Y(C_4H_4O_2)$ System						
$Y(C_4H_4O_2)$	+	2 CH_3CH_3	→	$Y(C_4H_8O_2)$	+	2 $CH_2{=}CH_2$	-19.79
$Y(C_4H_4O_2)$	+	2 $CH_3CH_2CH_3$	→	$Y(C_4H_8O_2)$	+	2 $CH_2{=}CHCH_3$	-19.81
$Y(C_4H_4O_2)$	+	2 $CH_3CH_2CH_2CH_3$	→	$Y(C_4H_8O_2)$	+	2 $CH_2{=}CHCH_2CH_3$	-20.40
						Average	**-20.0 ± 0.3**
						Atomization	**-20.4**

Table I.15 Elementary Rate Parameters for Reactions in the 2MF5j + O_2 System

Reactions	Forward			Reverse		
	A	***n***	**E_a**	**A**	***n***	**E_a**
2MF5j + O_2 → TS 2MF5OOj	$2.11x10^{3}$	2.53	0.0			
2MF5OOj → TS 2MF5OOj	$3.93x10^{13}$	0.11	49.9			
2MF5OOj → TS I 1	$5.21x10^{10}$	0.57	37.7	$8.33x10^{9}$	1.43	0.0
TS I 1 → MF4j5Q	$2.53x10^{10}$	1.42	0.0	$1.72x10^{10}$	0.58	8.1
MF4j5Q → TS I 2	$5.89x10^{12}$	0.17	19.8	$7.37x10^{7}$	1.83	0.0
TS I 2 → CC(=O)CH=C=C=O + OH	$1.11x10^{22}$	2.20	0.0	$1.94x10^{3}$	1.80	46.1
MF4j5Q → TS VIII 1	$1.92x10^{10}$	0.71	26.3	$2.26x10^{10}$	1.29	0.0
TS VIII 1 → MF4OH5Oj	$2.34x10^{10}$	0.92	0.0	$1.85x10^{10}$	1.08	147.2
2MF5OOj → TS II 1	$5.69x10^{14}$	-0.93	39.0	$7.63x10^{5}$	2.93	0.0
TS II 1 → MF45Y(CjCOOj)	$5.42x10^{5}$	2.71	0.0	$8.02x10^{14}$	-0.71	14.0
MF45Y(CjCOOj) → TS II 2	$6.53x10^{11}$	0.43	0.0	$6.65x10^{8}$	1.57	0.4
TS II 2 → MF4Oj5O	$2.89x10^{9}$	1.51	0.0	$1.50x10^{11}$	0.49	74.9
MF4Oj5O → TS II 3	$1.32x10^{12}$	0.46	6.6	$3.30x10^{8}$	1.54	0.0
TS II 3 → O=CjOC(C)=CHCH(=O)	$1.77x10^{10}$	1.61	0.0	$2.45x10^{10}$	0.39	7.1
O=CjOC(C)=CHCH(=O) → TS II 4	$3.03x10^{9}$	1.09	11.1	$1.43x10^{11}$	0.91	0.0
TS II 4 → *n*-CC(=O)CjHCH(=O) + CO	$3.80x10^{24}$	0.96	0.0	$5.69x10^{0}$	3.04	22.4
n-CC(=O)CjHCH(=O) → TS II 5	$1.23x10^{10}$	1.38	38.7	$3.54x10^{10}$	0.62	0.0
TS II 5 → O=CHCH=C=O + CjH_3	$3.87x10^{22}$	1.23	0.0	$5.58x10^{2}$	2.77	4.9
2MF5OOj → TS III 1	$6.85x10^{12}$	-0.12	10.9	$6.33x10^{7}$	2.12	0.0
TS III 1 → MF5Yj(COO)	$1.84x10^{7}$	2.03	0.0	$2.36x10^{13}$	-0.03	16.5
MF5Yj(COO) → TS III 2	$1.49x10^{14}$	-0.49	1.7	$2.91x10^{6}$	2.49	0.0
CC(=O)CH=CHCO2j → TS III 1	$1.88x10^{10}$	0.18	59.5	$2.31x10^{10}$	1.82	0.0
TS III 2 → CC(=O)CH=CHCO2j	$3.64x10^{9}$	2.28	0.0	$1.19x10^{11}$	-0.28	44.7
CC(=O)CH=CHCO2j → TS III 3	$9.83x10^{11}$	0.68	1.3	$4.42x10^{8}$	1.32	0.0
TS III 3 → CC(=O)CH=CjH + CO_2	$1.94x10^{21}$	1.41	0.0	$1.12x10^{4}$	2.59	14.3
CC(=O)CH=CjH → TS III 4	$9.50x10^{13}$	0.54	27.5	$4.57x10^{6}$	1.46	0.0
TS III 4 → CCj(=O) + CH≡CH	$3.54x10^{19}$	1.76	0.0	$6.11x10^{5}$	2.24	4.8
CCj(=O) → TS III 5	$6.94x10^{11}$	0.85	17.4	$6.25x10^{8}$	1.15	0.0
TS III 5 → CjH_3 + CO	$1.07x10^{18}$	2.34	0.0	$2.02x10^{7}$	1.66	5.6
MF5Yj(COO) → TS VI 1	$6.98x10^{11}$	0.60	0.0	$6.22x10^{8}$	1.40	5.1
TS VI 1 → MF45Y(CCO)5Oj	$1.61x10^{10}$	0.86	0.0	$2.70x10^{10}$	1.14	15.5
MF45Y(CCO)5Oj → TS VI 2	$2.44x10^{11}$	0.48	0.0	$1.78x10^{9}$	1.52	8.5
MF45Y(CCO)5Oj → TS III 1	$9.11x10^{11}$	0.51	37.1	$4.76x10^{8}$	1.49	0.0
TS VI 2 → Y(OC(C)=CCjOC(=O))	$5.41x10^{8}$	1.82	0.0	$8.02x10^{11}$	0.18	43.0
Y(OC(C)=CCjOC(=O)) → TS VI 3	$3.59x10^{12}$	0.43	42.4	$1.21x10^{8}$	1.57	0.0
TS VI 3 → CC(=O)CH=CHOCj=O	$1.03x10^{9}$	1.71	0.0	$4.20x10^{11}$	0.29	16.2
CC(=O)CH=CHOCj=O → TS VI 4	$1.22x10^{11}$	0.96	14.1	$3.55x10^{9}$	1.04	0.0
TS VI 4 → CC(=O)CjHCH(=O) + CO	$3.25x10^{23}$	1.06	0.0	$6.66x10^{1}$	2.94	24.1
Y(OC(C)=CCjOC(=O)) → TS VII 1	$2.20x10^{12}$	0.45	42.8	$1.97x10^{8}$	1.55	0.0
TS VII 1 → O=CjOC(C)=CHCH(=O)	$1.43x10^{10}$	1.66	0.0	$3.03x10^{10}$	0.34	15.9
2MF5OOj → TS IV 1	$1.21x10^{12}$	0.29	20.3	$3.58x10^{8}$	1.71	0.0

Units: A (mol cm^{-3} s^{-1}), Ea (kcal mol^{-1})

Table I.15 Elementary Rate Parameters for Reactions in the 2MF5j + O_2 System (Continued)

Reactions	Forward			Reverse		
	A	***n***	**E_a**	**A**	***n***	**E_a**
TS IV 1→ 2MF5Oj + O	$1.53x10^{19}$	2.33	0.0	$1.41x10^{6}$	1.67	7.0
2MF5Oj → TS IV 2	$2.15x10^{13}$	-0.09	6.9	$2.02x10^{7}$	2.09	0.0
TS IV 2 → CC(=O)CHCjHC=O	$1.73x10^{9}$	1.58	10.2	$2.51x10^{11}$	0.42	0.0
CC(=O)CHCjHC=O → TS IV 3	$5.22x10^{11}$	1.56	41.2	$8.31x10^{8}$	0.44	0.0
TS IV 3 → CC(=O)CH=CjH + CO	$1.52x10^{21}$	1.44	0.0	$1.43x10^{4}$	2.56	5.9
CC(=O)CHCjHC=O → TS IX 1	$1.98x10^{11}$	1.90	63.0	$2.20x10^{9}$	0.10	0.0
TS IX 1 → O=C=CHCH=C=O + CjH3	$3.30x10^{21}$	1.49	0.0	$6.54x10^{3}$	2.51	6.4
2MF5OOj → TS V 1	$7.73x10^{8}$	1.02	59.7	$5.62x10^{11}$	0.98	0.0
TS V 1 → MF2CjH25Q	$2.22x10^{11}$	1.23	0.0	$1.96x10^{9}$	0.77	61.9
MF2CjH25Q → TS V 2	$5.17x10^{11}$	0.14	0.0	$8.40x10^{8}$	1.86	5.8
TS V 2 → MF2CH25O + OH	$7.88x10^{20}$	2.09	0.0	$2.74x10^{4}$	1.91	28.1
MF2CH25O → TS V 3	$3.92x10^{10}$	1.23	79.7	$1.11x10^{10}$	0.77	0.0
TS V 3 → C=C=CHCHCO2	$6.25x10^{10}$	1.18	0.0	$6.95x10^{9}$	0.82	26.6

Units: A (mol cm^{-3} s^{-1}), Ea (kcal mol^{-1})

REFERENCES

1. Binder, J. B.; Raines, R. T. *J. Am. Chem. Soc.* **2009**, *131*, 1979-1985.

2. Greene, D. L.; Hopson, J. L.; Li, J. *Energy Policy* **2006**, *34*, 515-531.

3. Gomez, L. D.; Steele-King, C. G.; McQueen-Mason, S. J. *New Phytol.* **2008**, *178*, 473-485.

4. Hill, J.; Nelson, E.; Tilman, D.; Polasky, S.; Tiffany, D. *Proc. Natl. Acad. Sci. U.S.A.* **2006**, *103*, 11206-11210.

5. Westbrook, C. K.; Pitz, W. J.; Herbinet, O.; Curran, H. J.; Silke, E. J. *Combust. Flame* **2009**, *156*, 181-199.

6. Simmie, J. M. *Prog. Energy Combust. Sci.* **2003**, *29*, 599-634.

7. Curran, H. J.; Gaffuri, P.; Pitz, W. J.; Westbrook, C. K. *Combust. Flame* **1998**, *114*, 149-177.

8. Curran, H. J.; Gaffuri, P.; Pitz, W. J.; Westbrook, C. K. *Combust. Flame* **2002**, *129*, 253-280.

9. Curran, H. J.; Pitz, W. J.; Westbrook, C. K.; Callahan, C. V.; Dryer, F. L. *Symp. Int. Combust. Proc.* **1998**, *27*, 379-387.

10. Yuan, T.; Zhang, L.; Zhou, Z.; Xie, M.; Ye, L.; Qi, F. *J. Phys. Chem. A* **2011**, *115*, 1593-1601.

11. Pant, K. K.; Kunzru, D. *J. Anal. Appl. Pyrolysis* **1996**, *36*, 103-120.

12. Held, T. J.; Marchese, A. J.; Dryer, F. L. *Combust. Sci. Technol.* **1997**, *123*, 107-146.

13. Chakraborty, J. P.; Kunzru, D. *J. Anal. Appl. Pyrolysis* **2009**, *86*, 44-52.

14. Chaos, M.; Kazakov, A.; Zhao, Z.; Dryer, F. L. *Int. J. Chem. Kinet.* **2007**, *39*, 399-414.

15. Schulz, C.; Sick, V. *Prog. Energy Combust. Sci.* **2005**, *31*, 75-121.

16. Hanson, R. K.; Seitzman, J. M.; Paul, P. H. *Appl. Phys. B: Laser Opt.* **1990**, *50*, 441-454.

17. Einecke, S.; Schulz, C.; Sick, V. *Appl. Phys. B: Laser Opt.* **2000**, *71*, 717-723.

18. Pepiot-Desjardins, P.; Pitsch, H.; Malhotra, R.; Kirby, S. R.; Boehman, A. L. *Combust. Flame* **2008**, *154*, 191-205.

19. Hong, Z.; Davidson, D. F.; Vasu, S. S.; Hanson, R. K. *Fuel* **2009**, *88*, 1901-1906.

20. Gierczak, T.; Burkholder, J. B.; Bauerle, S.; Ravishankara, A. R. *Chem. Phys.* **1998**, *231*, 229-244.

21. Blitz, M. A.; Heard, D. E.; Pilling, M. J. *J. Phys. Chem. A* **2006**, *110*, 6742-6756.

22. Horowitz, A. *J. Phys. Chem.* **1991**, *95*, 10816-10823.

23. Chenoweth, K.; Van Duin, A. C. T.; Dasgupta, S.; Goddard III, W. A. *J. Phys. Chem. A* **2009**, *113*, 1740-1746.

24. Proceedings of the 37th AIAA/ASME/SAE/ASEE Joint Propulsion Conference and Exhibit.

25. He, K.; Androulakis, I. P.; Ierapetritou, M. G. *Energy Fuels* **2010**, *24*, 309-317.

26. Herbinet, O.; Sirjean, B.; Bounaceur, R.; Fournet, R.; Battin-Leclerc, F.; Scacchi, G.; Marquaire, P. M. *J. Phys. Chem. A* **2006**, *110*, 11298-11314.

27. Nakra, S.; Green, R. J.; Anderson, S. L. *Combust. Flame* **2006**, *144*, 662-674.

28. Xing, Y.; Li, D.; Xie, W.; Fang, W.; Guo, Y.; Lin, R. *Fuel* **2010**, *89*, 1422-1428.

29. Xing, Y.; Fang, W.; Xie, W.; Guo, Y.; Lin, R. *Ind. Eng. Chem. Res.* **2008**, *47*, 10034-10040.

30. Li, S. C.; Varatharajan, B.; Williams, F. A. *AIAA J.* **2001**, *39*, 2351-2356.

31. Striebich, R. C.; Lawrence, J. *J. Anal. Appl. Pyrolysis* **2003**, *70*, 339-352.

32. Nageswara Rao, P.; Kunzru, D. *J. Anal. Appl. Pyrolysis* **2006**, *76*, 154-160.

33. Park, S. H.; Kwon, C. H.; Kim, J.; Chun, B. H.; Kang, J. W.; Han, J. S.; Jeong, B. H.; Kim, S. H. *Ind. Eng. Chem. Res.* **2010**, *49*, 8319-8324.

34. Huber, G. W.; Iborra, S.; Corma, A. *Chem. Rev.* **2006**, *106*, 4044-4098.

35. Ragauskas, A. J.; Williams, C. K.; Davison, B. H.; Britovsek, G.; Cairney, J.; Eckert, C. A.; Frederick Jr, W. J.; Hallett, J. P.; Leak, D. J.; Liotta, C. L.; Mielenz, J. R.; Murphy, R.; Templer, R.; Tschaplinski, T. *Science* **2006**, *311*, 484-489.

36. Zidanšek, A.; Blinc, R.; Jeglič, A.; Kabashi, S.; Bekteshi, S.; Šlaus, I. *Int. J. Hydrogen Energy* **2009**, *34*, 6980-6983.

37. Schmidt, L. D.; Dauenhauer, P. J. *Nature* **2007**, *447*, 914-915.

38. Chheda, J. N.; Huber, G. W.; Dumesic, J. A. *Angew. Chem., Int. Ed.* **2007**, *46*, 7164-7183.

39. Lewkowski, J. *ARKIVOC* **2001**, *2001*, 17-54.

40. Lichtenthaler, F. W. *Acc. Chem. Res.* **2002**, *35*, 728-737.

41. Román-Leshkov, Y.; Chheda, J. N.; Dumesic, J. A. *Science* **2006**, *312*, 1933-1937.

42. Román-Leshkov, Y.; Barrett, C. J.; Liu, Z. Y.; Dumesic, J. A. *Nature* **2007**, *447*, 982-986.

43. Hu, S.; Zhang, Z.; Zhou, Y.; Han, B.; Fan, H.; Li, W.; Song, J.; Xie, Y. *Green Chem.* **2008**, *10*, 1280-1283.

44. Mascal, M.; Nikitin, E. B. *Angew. Chem., Int. Ed.* **2008**, *47*, 7924-7926.

45. Simmie, J. M.; Curran, H. J. *J. Phys. Chem. A* **2009**, *113*, 5128- 5137.

46. Becke, A. D. *J. Chem. Phys.* **1993**, *98*, 5648-5652.

47. Lee, C.; Yang, W.; Parr, R. G. *Phys. Rev. B.* **1988**, *37*, 785-789.

48. Bauschlicher Jr, C. W. *Chem. Phys. Lett.* **1995**, *246*, 40-44.

49. Curtiss, L. A.; Raghavachari, K.; Redfern, P. C.; Pople, J. A. *J. Chem. Phys.* **1997**, *106*, 1063-1079.

50. Zhao, Y.; Lynch, B. J.; Truhlar, D. G. *J. Phys. Chem. A* **2004**, *108*, 2715-2719.

51. Zhao, Y.; Truhlar, D. G. *J. Phys. Chem. A* **2004**, *108*, 6908-6918.

52. Boese, A. D.; Martin, J. M. L. *J. Chem. Phys.* **2004**, *121*, 3405-3416.

53. Chai, J. D.; Head-Gordon, M. *J. Chem. Phys.* **2008**, *128*, 084106.

54. Chai, J. D.; Head-Gordon, M. *Phys. Chem. Chem. Phys.* **2008**, *10*, 6615-6620.

55. Zhao, Y.; Truhlar, D. G. *Theor. Chem. Account* **2008**, *120*, 215-241.

56. Zhao, Y.; Truhlar, D. G. *Acc. Chem. Res.* **2008**, *41*, 157-167.

57. Baboul, A. G.; Curtiss, L. A.; Redfern, P. C.; Raghavachari, K. *J. Chem. Phys.* **1999**, *110*, 7650-7657.

58. Curtiss, L. A.; Raghavachari, K.; Redfern, P. C.; Rassolov, V.; Pople, J. A. *J. Chem. Phys.* **1998**, *109*, 7764-7776.

59. Curtiss, L. A.; Redfern, P. C.; Raghavachari, K.; Rassolov, V.; Pople, J. A. *J. Chem. Phys.* **1999**, *110*, 4703-4709.

60. Montgomery Jr, J. A.; Frisch, M. J.; Ochterski, J. W.; Petersson, G. A. *J. Chem. Phys.* **1999**, *110*, 2822-2827.

61. Montgomery Jr, J. A.; Frisch, M. J.; Ochterski, J. W.; Petersson, G. A. *J. Chem. Phys.* **2000**, *112*, 6532-6542.

62. Frisch, M. J.; Trucks, G. W.; Schlegel, H. B.; Scuseria, G. E.; Robb, M. A.; Cheeseman, J. R.; Montgomery, J. A., Jr, ; Vreven, T.; Kudin, K. N.; Burant, J. C.; Millam, J. M.; Iyengar, S. S.; Tomasi, J.; Barone, V.; Mennucci, B.; Cossi, M.; Scalmani, G.; Rega, N.; Petersson, G. A.; Nakatsuji, H.; Hada, M.; Ehara, M.; Toyota, K.; Fukuda, R.; Hasegawa, J.; Ishida, M.; Nakajima, T.; Honda, Y.; Kitao, O.; Nakai, H.; Klene, M.; Li, X.; Knox, J. E.; Hratchian, H. P.; Cross, J. B.; Adamo, C.; Jaramillo, J.; Gomperts, R.; Stratmann, R. E.; Yazyev, O.; Austin, A. J.; Cammi, R.; Pomelli, C.; Ochterski, J. W.; Ayala, P. Y.; Morokuma, K.; Voth, G. A.; Salvador, P.; Dannenberg, J. J.; Zakrzewski, V. G.; Dapprich, S.; Daniels, A. D.; Strain, M. C.; Farkas, O.; Malick, D. K.; Rabuck, A. D.; Raghavachari, K.; Foresman, J. B.; Ortiz, J. V.; Cui, Q.; Baboul, A. G.; Clifford, S.; Cioslowski, J.; Stefanov, B. B.; Liu, G.; Liashenko, A.; Piskorz, P.; Komaromi, I.; Martin, R. L. *Gaussian 03, Revision D.01;* Gaussian, Inc.: Wallingford, CT, 2003.

63. Frisch, M. J.; Trucks, G. W.; Schlegel, H. B.; Scuseria, G. E.; Robb, M. A.; Cheeseman, J. R.; Scalmani, G.; Barone, V.; Mennucci, B.; Petersson, G. A.; Nakatsuji, H.; Caricato, M.; Li, X.; Hratchian, H. P.; Izmaylov, A. F.; Bloino, J.; Zheng, G.; Sonnenberg, J. L.; Hada, M.; Ehara, M.; Toyota, K.; Fukuda, R.; Hasegawa, J.; Ishida, M.; Nakajima, T.; Honda, Y.; Kitao, O.; Nakai, H.; Vreven, T.; Montgomery, J., J. A., ; Peralta, J. E.; Ogliaro, F.; Bearpark, M.; Heyd, J. J.; Brothers, E.; Kudin, K. N.; Staroverov, V. N.; Kobayashi, R.; Normand, J.; Raghavachari, K.; Rendell, A.; Burant, J. C.; Iyengar, S. S.; Tomasi, J.; Cossi, M.; Rega, N.; Millam, J. M.; Klene, M.; Knox, J. E.; Cross, J. B.; Bakken, V.; Adamo, C.; Jaramillo, J.; Gomperts, R.; Stratmann, R. E.; Yazyev, O.; Austin, A. J.; Cammi, R.; Pomelli, C.; Ochterski, J. W.; Martin, R. L.; Morokuma, K.; Zakrzewski, V. G.; Voth, G. A.; Salvador, P.; Dannenberg, J. J.; Dapprich, S.; Daniels, A. D.; Farkas, Ö.; Foresman, J. B.; Ortiz, J. V.; Cioslowski, J.; Fox, D. J. *Gaussian 09, Revision C.01;* Gaussian, Inc.: Wallingford, CT, 2009.

64. Stewart, J. J. P. *J. Comp. Chem.* **1989**, *10*, 209-220.

65. Stewart, J. J. P. *J. Comp. Chem.* **1989**, *10*, 221-264.

66. Frisch, M. J.; Head-Gordon, M.; Pople, J. A. *Chem. Phys. Lett.* **1990**, *166*, 275-280.

67. Frisch, M. J.; Head-Gordon, M.; Pople, J. A. *Chem. Phys. Lett.* **1990**, *166*, 281-289.

68. Head-Gordon, M.; Head-Gordon, T. *Chem. Phys. Lett.* **1994**, *220*, 122-128.

69. Saebo, S.; Almlof, J. *Chem. Phys. Lett.* **1989**, *154*, 83-89.

70. Head-Gordon, M.; Pople, J. A.; Frisch, M. J. *Chem. Phys. Lett.* **1988**, *153*, 503-506.

71. Check, C. E.; Gilbert, T. M. *J. Org. Chem.* **2005**, *70*, 9828-9834.

72. Izgorodina, E. I.; Brittain, D. R. B.; Hodgson, J. L.; Krenske, E. H.; Lin, C. Y.; Namazian, M.; Coote, M. L. *J. Phys. Chem. A* **2007**, *111*, 10754-10768.

73. Redfern, P. C.; Zapol, P.; Curtiss, L. A.; Raghavachari, K. *J. Phys. Chem. A* **2000**, *104*, 5850-5854.

74. Tu, C. Y.; Guo, W. H.; Hu, C. H. *J. Phys. Chem. A* **2008**, *112*, 117-124.

75. Curtiss, L. A.; Raghavachari, K.; Redfern, P. C.; Stefanov, B. B. *J. Chem. Phys.* **1998**, *108*, 692-697.

76. Bartlett, R. J.; Purvis III, G. D. *Int. J. Quant. Chem.* **1978**, *14*, 561-581.

77. Pople, J. A.; Krishnan, R.; Schlegel, H. B.; Binkley, J. S. *Int. J. Quant. Chem.* **1978**, *14*, 545-560.

78. Cizek, J. In *Advances in Chemical Physics*; LeFebvre, R., Moser, C., Eds.; Wiley Interscience: New York, NY, 1969; Vol. 14, p 35-89.

79. Purvis III, G. D.; Bartlett, R. J. *J. Chem. Phys.* **1982**, *76*, 1910-1918.

80. Scuseria, G. E.; Janssen, C. L.; Schaefer III, H. F. *J. Chem. Phys.* **1988**, *89*, 7382-7387.

81. Scuseria, G. E.; Schaefer III, H. F. *J. Chem. Phys.* **1989**, *90*, 3700-3703.

82. Pople, J. A.; Head-Gordon, M.; Raghavachari, K. *J. Chem. Phys.* **1987**, *87*, 5968-5975.

83. Chase, M. W., Jr. *J. Phys. Chem. Ref. Data, Monogr.* **1998**, *9*, 1-1951.

84. Ruscic, B.; Feller, D.; Dixon, D. A.; Peterson, K. A.; Harding, L. B.; Asher, R. L.; Wagner, A. F. *J. Phys. Chem. A* **2001**, *105*, 2-4.

85. Pitzer, K. S. *J. Chem. Phys.* **1937**, *5*, 469-472.

86. Pitzer, K. S. *J. Chem. Phys.* **1946**, *14*, 239-243.

87. Pitzer, K. S.; Gwinn, W. D. *J. Chem. Phys.* **1942**, *10*, 428-440.

88. Kilpatrick, J. E.; Pitzer, K. S. *J. Chem. Phys.* **1949**, *17*, 1064-1075.

89. Pfaendtner, J.; Yu, X.; Broadbelt, L. J. *Theor. Chem. Account* **2007**, *118*, 881-898.

90. Van Speybroeck, V.; Vansteenkiste, P.; Van Neck, D.; Waroquier, M. *Chem. Phys. Lett.* **2005**, *402*, 479-484.

91. Van Speybroeck, V.; Van Neck, D.; Waroquier, M.; Wauters, S.; Saeys, M.; Marin, G. B. *J. Phys. Chem. A* **2000**, *104*, 10939-10950.

92. Ayala, P. Y.; Schlegel, H. B. *J. Chem. Phys.* **1998**, *108*, 2314-2325.

93. Vansteenkiste, P.; Van Neck, D.; Van Speybroeck, V.; Waroquier, M. *J. Chem. Phys.* **2006**, *124*, 044314.

94. Lin, C. Y.; Izgorodina, E. I.; Coote, M. L. *J. Phys. Chem. A* **2008**, *112*, 1956-1964.

95. Sharma, S.; Ramans, S.; Green, W. H. *J. Phys. Chem. A* **2010**, *114*, 5689-5701.

96. Vansteenkiste, P.; Van Speybroeck, V.; Pauwels, E.; Waroquier, M. *Chem. Phys.* **2005**, *314*, 109-117.

97. Vansteenkiste, P.; Van Speybroeck, V.; Marin, G. B.; Waroquier, M. *J. Phys. Chem. A* **2003**, *107*, 3139-3145.

98. Sheng, C. Ph.D. Dissertation. Department of Chemical Engineering, New Jersey Institute of Technology, Newark, NJ, 2002.

99. Scott, A. P.; Radom, L. *J. Phys. Chem.* **1996**, *100*, 16502-16513.

100. Lay, T. H.; Bozzelli, J. W.; Dean, A. M.; Ritter, E. R. *J. Phys. Chem.* **1995**, *99*, 14514-14527.

101. Lay, T. H.; Krasnoperov, L. N.; Venanzi, C. A.; Bozzelli, J. W.; Shokhirev, N. V. *J. Phys. Chem.* **1996**, *100*, 8240-8249.

102. Benson, S. W. *Thermochemical Kinetics*; 2nd ed.; Wiley-Interscience: New York, NY, 1976.

103. Benson, S. W.; Buss, J. H. *J. Chem. Phys.* **1958**, *29*, 546-572.

104. Cohen, N.; Benson, S. W. *Chem. Rev.* **1993**, *93*, 2419-2438.

105. Ritter, E. R. *J. Chem. Inf. Comput. Sci.* **1991**, *31*, 400-408.

106. Ritter, E. R.; Bozzelli, J. W. *Int. J. Chem. Kinet.* **1991**, *23*, 767-778.

107. Sheng, C. Y.; Bozzelli, J. W.; Dean, A. M.; Chang, A. Y. *J. Phys. Chem. A* **2002**, *106*, 7276-7293.

108. Bozzelli, J. W.; Chang, A. Y.; Dean, A. M. *Int. J. Chem. Kinet.* **1997**, *29*, 161-170.

109. Chen, X. H.; Zhang, M.; Huang, G. H.; Hu, G. Y.; Wang, X.; Xu, G. J. *Sci. China Ser. D* **2009**, *52*, 26-33.

110. Zhang, M.; Huang, G. H.; Hu, G. Y.; Zhao, H. J. *Sci. China Ser. D* **2010**, *52*, 1-9.

111. Pitz, W. J.; Mueller, C. J. *Prog. Energy Combust. Sci.* **2011**, *37*, 330-350.

112. Westbrook, C. K.; Pitz, W. J.; Curran, H. J. *J. Phys. Chem. A* **2006**, *110*, 6912-6922.

113. Silke, E. J.; Pitz, W. J.; Westbrook, C. K.; Ribaucour, M. *J. Phys. Chem. A* **2007**, *111*, 3761-3775.

114. Westbrook, C. K.; Pitz, W. J.; Curran, H. C.; Boercker, J.; Kunrath, E. *Int. J. Chem. Kinet.* **2001**, *33*, 868-877.

115. Pitzer, K. S. *J. Am. Chem. Soc.* **1940**, *62*, 1224-1227.

116. Huffman, H. M.; Gross, M. E.; Scott, D. W.; McCullough, J. P. *J. Phys. Chem.* **1961**, *65*, 495-503.

117. Zheng, J.; Yu, T.; Truhlar, D. G. *Phys. Chem. Chem. Phys.* **2011**, *13*, 19318-19324.

118. Karton, A.; Gruzman, D.; Martin, J. M. L. *J. Phys. Chem. A* **2009**, *113*, 8434-8447.

119. Gruzman, D.; Karton, A.; Martin, J. M. L. *J. Phys. Chem. A* **2009**, *113*, 11974-11983.

120. Pedley, J. B. *Thermochemical Data and Structures of Organic Compounds*; Thermodynamics Research Center: College Station, TX, 1994.

121. Blanksby, S. J.; Ellison, G. B. *Acc. Chem. Res.* **2003**, *36*, 255-263.

122. Snitsiriwat, S.; Bozzelli, J. W. *J. Phys. Chem. A* **2013**, *117*, 421-429.

123. Prosen, E. J.; Rossini, F. D. *J. Res. Natl. Bur. Stand.* **1945**, *34*, 263-269.

124. Furka, Á. *Struct. Chem.* **2009**, *20*, 587-604.

125. Scott, D. W. *Chemical Thermodynamic Properties of Hydrocarbons and Related Substances. Properties of the Alkane Hydrocarbons, C1 through C10 in the Ideal Gas State from 0 to 1500 K.*; U.S. Bureau of Mines, Bulletin 666, 1974.

126. Luo, Y.-R. *Comprehensive Handbook of Chemical Bond Energies*; CRC Press: Boca Raton, FL, 2007.

127. Bauschlicher, C. W. *Chem. Phys. Lett.* **1995**, *239*, 252-257.

128. Feng, Y.; Liu, L.; Wang, J. T.; Zhao, S. W.; Guo, Q. X. *J. Org. Chem.* **2004**, *69*, 3129-3138.

129. Stull, D. R.; Westrum E.F, Jr.; Sinke, G. C. *The Chemical Thermodynamics of Organic Compounds*; Wiley: New York, NY, 1969.

130. Yu, T.; Zheng, J.; Truhlar, D. G. *Phys. Chem. Chem. Phys.* **2012**, *14*, 482-494.

131. Lewis, A. C.; Hopkins, J. R.; Carpenter, L. J.; Stanton, J.; Read, K. A.; Pilling, M. J. *Atmos. Chem. Phys.* **2005**, *5*, 1963-1974.

132. Singh, H. B.; Salas, L. J.; Chatfield, R. B.; Czech, E.; Fried, A.; Walega, J.; Evans, M. J.; Field, B. D.; Jacob, D. J.; Blake, D.; Heikes, B.; Talbot, R.; Sachse, G.; Crawford, J. H.; Avery, M. A.; Sandholm, S.; Fuelberg, H. *J. Geophys. Res.* **2004**, *109*, D15S07.

133. Arnold, F.; Knop, G.; Ziereis, H. *Nature* **1986**, *321*, 505-507.

134. Jaeglé, L.; Jacob, D. J.; Brune, W. H.; Wennberg, P. O. *Atmos. Environ.* **2001**, *35*, 469-489.

135. Singh, H. B.; Kanakidou, M.; Crutzen, P. J.; Jacob, D. J. *Nature* **1995**, *378*, 50-54.

136. Warneke, C.; Karl, T.; Judmaier, H.; Hansel, A.; Jordan, A.; Lindinger, W.; Crutzen, P. J. *Global Biogeochem. Cycles* **1999**, *13*, 9-17.

137. Jacob, D. J.; Field, B. D.; Jin, E. M.; Bey, I.; Li, Q.; Logan, J. A.; Yantosca, R. M.; Singh, H. B. *J. Geophys. Res.* **2002**, *107*, 5-1—5-17.

138. Singh, H. B.; Herlth, D.; O`Hara, D.; Sachse, W.; Blake, D. R.; Bradshaw, J. D.; Kanakidou, M.; Crutzen, P. J. *J. Geophys. Res.* **1994**, *99*, 1805-1819.

139. Andreae, M. O.; Merlet, P. *Global Biogeochem. Cycles* **2001**, *15*, 955-966.

140. Talukdar, R. K.; Gierczak, T.; McCabe, D. C.; Ravishankara, A. R. *J. Phys. Chem. A* **2003**, *107*, 5021-5032.

141. Wennberg, P. O.; Hanisco, T. F.; Jaeglé, L.; Jacob, D. J.; Hintsa, E. J.; Lanzendorf, E. J.; Anderson, J. G.; Gao, R. S.; Keim, E. R.; Donnelly, S. G.; Del Negro, L. A.; Fahey, D. W.; McKeen, S. A.; Salawitch, R. J.; Webster, C. R.; May, R. D.; Herman, R. L.; Proffitt, M. H.; Margitan, J. J.; Atlas, E. L.; Schauffler, S. M.; Flocke, F.; McElroy, C. T.; Bui, T. P. *Science* **1998**, *279*, 49-53.

142. Yujing, M.; Mellouki, A. *J. Photochem. Photobiol.* **2000**, *134*, 31-36.

143. Singh, H.; Chen, Y.; Staudt, A.; Jacob, D.; Blake, D.; Heikes, B.; Snow, J. *Nature* **2001**, *410*, 1078-1081.

144. Hassouna, M.; Delbos, E.; Devolder, P.; Viskolcz, B.; Fittschen, C. *J. Phys. Chem. A* **2006**, *110*, 6667-6672.

145. Pichon, S.; Black, G.; Chaumeix, N.; Yahyaoui, M.; Simmie, J. M.; Curran, H. J.; Donohue, R. *Combust. Flame* **2009**, *156*, 494-504.

146. El-Nahas, A. M.; Simmie, J. M.; Navarro, M. V.; Bozzelli, J. W.; Black, G.; Curran, H. J. *Phys. Chem. Chem. Phys.* **2008**, *10*, 7139-7149.

147. Farkas, E.; Kovács, G.; Szilágyi, I.; Dóbé, S.; Bérces, T.; Márta, F. *Int. J. Chem. Kinet.* **2006**, *38*, 32-37.

148. Delbos, E.; Devolder, P.; ElMaimouni, L.; Fittschen, C.; Brudnik, K.; Jodkowski, J. T.; Ratajczak, E. *Phys. Chem. Chem. Phys.* **2002**, *4*, 2941-2949.

149. Imrik, K.; Farkas, E.; Vasvári, G.; Szilágyi, I.; Sarzyński, D.; Dóbé, S.; Bérces, T.; Márta, F. *Phys. Chem. Chem. Phys.* **2004**, *6*, 3958-3968.

150. Serinyel, Z.; Chaumeix, N.; Black, G.; Simmie, J. M.; Curran, H. J. *J. Phys. Chem. A* **2010**, *114*, 12176-12186.

151. Serinyel, Z.; Black, G.; Curran, H. J.; Simmie, J. M. *Combust. Sci. Technol.* **2010**, *182*, 574 - 587.

152. Sebbar, N.; Bozzelli, J. W.; Bockhorn, H. *Z. Phys. Chem.* **2011**, *225*, 993-1018.

153. Swalen, J. D.; Costain, C. C. *J. Chem. Phys.* **1959**, *31*, 1562-1574.

154. Nguyen, H. V. L.; Stahl, W. *ChemPhysChem* **2011**, *12*, 1900-1905.

155. Evangelisti, L.; Favero, L. B.; Maris, A.; Melandri, S.; Vega-Toribio, A.; Lesarri, A.; Caminati, W. *J. Mol. Spectrosc.* **2010**, *259*, 65-69.

156. Pozdeev, N. M.; Mamleev, A. K.; Gunderova, L. N.; Galeev, R. V. *J. Struct. Chem.* **1988**, *29*, 52-58.

157. El-Nahas, A. M.; Bozzelli, J. W.; Simmie, J. M.; Navarro, M. V.; Black, G.; Curran, H. J. *J. Phys. Chem. A* **2006**, *110*, 13618-13623.

158. Bordwell, F. G.; Harrelson J.A, Jr. *Can. J. Chem.* **1990**, *68*, 1714-1718.

159. Bouchoux, G.; Chamot-Rooke, J.; Leblanc, D.; Mourgues, P.; Sablier, M. *ChemPhysChem* **2001**, *2*, 235-241.

160. Cumming, J. B.; Kebarle, P. *J. Am. Chem. Soc.* **1977**, *99*, 5818-5820.

161. Holmes, J. L.; Lossing, F. P.; Terlouw, J. K. *J. Am. Chem. Soc.* **1986**, *108*, 1086-1087.

162. King, K. D.; Golden, D. M.; Benson, S. W. *J. Am. Chem. Soc.* **1970**, *92*, 5541-5546.

163. Leroy, G.; Sana, M.; Wilante, C. *J. Mol. Struct. (THEOCHEM)* **1991**, *228*, 37-45.

164. Reed, D. R.; Hare, M. C.; Fattahi, A.; Chung, G.; Gordon, M. S.; Kass, S. R. *J. Am. Chem. Soc.* **2003**, *125*, 4643-4651.

165. Tsang, W. In *Energetics of Stable Molecules and Reactive Intermediates*; Minas da Piedade, M. E., Ed.; Kluwer Academic Publishers: Dordrecht, Netherlands,1999; Vol. 535, p 323-352.

166. Alnajjar, M. S.; Zhang, X. M.; Gleicher, G. J.; Truksa, S. V.; Franz, J. A. *J. Org. Chem.* **2002**, *67*, 9016-9022.

167. Ruscic, B.; Boggs, J. E.; Burcat, A.; Császár, A. G.; Demaison, J.; Janoschek, R.; Martin, J. M. L.; Morton, M. L.; Rossi, M. J.; Stanton, J. F.; Szalay, P. G.; Westmoreland, P. R.; Zabel, F.; Bérces, T. *J. Phys. Chem. Ref. Data* **2005**, *34*, 573-656.

168. da Silva, G.; Bozzelli, J. W. *J. Phys. Chem. A* **2006**, *110*, 13058-13067.

169. Chao, J.; Zwolinski, B. J. *J. Phys. Chem. Ref. Data* **1976**, *5*, 319-328.

170. Buckley, E.; Herington, E. F. G. *Trans. Faraday Soc.* **1965**, *61*, 1618-1625.

171. Cox, J. D.; Pilcher, G. *Thermochemistry of Organic and Organometallic Compounds*; Academic Press: New York, NY, 1970.

172. Harrop, D.; Head, A. J.; Lewis, G. B. *J. Chem. Thermodyn.* **1970**, *2*, 203-210.

173. Tsang, W. In *Energetics of Organic Free Radicals*; Martinho Simões, J. A., Greenberg, A., Liebman, J. F., Eds.; Blackie Academic and Professional: London, England, 1996.

174. Curtiss, L. A.; Raghavachari, K.; Redfern, P. C.; Pople, J. A. *J. Chem. Phys.* **2000**, *112*, 7374-7383.

175. Sinke, G. C.; Oetting, F. L. *J. Phys. Chem.* **1964**, *68*, 1354-1358.

176. Solly, R. K.; Golden, D. M.; Benson, S. W. *Int. J. Chem. Kinet.* **1970**, *2*, 381-391.

177. Tumanov, V. E.; Kromkin, E. A.; Denisov, E. T. *Russ. Chem. Bull.* **2002**, *51*, 1641-1650.

178. Janoschek, R.; Rossi, M. J. *Int. J. Chem. Kinet.* **2004**, *36*, 661-686.

179. Sellers, P. *J. Chem. Thermodyn.* **1970**, *2*, 211-219.

180. Nickerson, J. K.; Kobe, K. A.; McKetta, J. J. *J. Phys. Chem.* **1961**, *65*, 1037-1043.

181. Goodman, L.; Gu, H.; Pophristic, V. *J. Chem. Phys.* **1999**, *110*, 4268-4275.

182. Lowe, J. P. *Science* **1973**, *179*, 527- 532.

183. Kemp, J. D.; Pitzer, K. S. *J. Chem. Phys.* **1936**, *4*, 749- 750.

184. Mo, Y.; Gao, J. *Acc. Chem. Res.* **2007**, *40*, 113-119.

185. Stull, D. R.; Westrum E.F, Jr.; Sinke, G. C. *The Chemical Thermodynamics of Organic Compounds*; Krieger Publishing Co: Malibar, FL, 1987.

186. Xing, Y.; Fang, W.; Li, D.; Guo, Y.; Lin, R. *J. Chem. Eng. Data* **2009**, *54*, 1865-1870.

187. Xing, E.; Mi, Z.; Xin, C.; Wang, L.; Zhang, X. *J. Mol. Catal. A: Chem.* **2005**, *231*, 161-167.

188. Xing, E.; Zhang, X.; Wang, L.; Mi, Z. *Green Chem.* **2007**, *9*, 589-593.

189. Boyd, R. H.; Sanwal, S. N.; Shary-Tehrany, S.; McNally, D. *J. Phys. Chem.* **1971**, *75*, 1264-1271.

190. Smith, N. K.; Good, W. D. *AIAA J.* **1979**, *17*, 905-907.

191. Zehe, M. J.; Jaffe, R. L. *J. Org. Chem.* **2010**, *75*, 4387-4391.

192. Chickos, J. S.; Hillesheim, D.; Nichols, G. *J. Chem. Thermodyn.* **2002**, *34*, 1647-1658.

193. McMillen, D. F.; Golden, D. M. *Annu. Rev. Phys. Chem.* **1982**, *33*, 493-532.

194. Sumathi, R.; Green Jr, W. H. *J. Phys. Chem. A* **2002**, *106*, 11141-11149.

195. Ashcraft, R. W.; Green, W. H. *J. Phys. Chem. A* **2008**, *112*, 9144-9152.

196. Asatryan, R.; Bozzelli, J. W.; Simmie, J. M. *Int. J. Chem. Kinet.* **2007**, *39*, 378-398.

197. Asatryan, R.; Bozzelli, J. W.; Simmie, J. M. *J. Phys. Chem. A* **2008**, *112*, 3172-3185.

198. Osmont, A.; Catoire, L.; Gökalp, I. *Energy Fuels* **2008**, *22*, 2241-2257.

199. Osmont, A.; Catoire, L.; Escot Bocanegra, P.; Gökalp, I.; Thollas, B.; Kozinski, J. A. *Combust. Flame* **2010**, *157*, 1230-1234.

200. Osmont, A.; Yahyaoui, M.; Catoire, L.; Gökalp, I.; Swihart, M. T. *Combust. Flame* **2008**, *155*, 334-342.

201. Osmont, A.; Catoire, L.; Gökalp, I.; Swihart, M. T. *Energy Fuels* **2007**, *21*, 2027-2032.

202. Osmont, A.; Catoire, L.; Gökalp, I. *Int. J. Chem. Kinet.* **2007**, *39*, 481-491.

203. Nunes, P. M.; Estcio, S. G.; Lopes, G. T.; Costa Cabral, B. J.; Dos Santos, R. M. B.; Simes, J. A. M. *Org. Lett.* **2008**, *10*, 1613-1616.

204. Stanger, A. *Eur. J. Org. Chem.* **2007**, 5717-5725.

205. Tian, Z.; Fattahi, A.; Lis, L.; Kass, S. R. *J. Am. Chem. Soc.* **2006**, *128*, 17087-17092.

206. Bach, R. D.; Dmitrenko, O. *J. Am. Chem. Soc.* **2004**, *126*, 4444-4452.

207. Pedersen, S.; Herek, J. L.; Zewail, A. H. *Science* **1994**, *266*, 1359-1364.

208. Sirjean, B.; Glaude, P. A.; Ruiz-Lopez, M. F.; Fournet, R. *J. Phys. Chem. A* **2006**, *110*, 12693-12704.

209. Tsang, W. *Int. J. Chem. Kinet.* **1978**, *10*, 599-617.

210. Tsang, W. *Int. J. Chem. Kinet.* **1978**, *10*, 1119-1138.

211. O'Neal, H. E.; Benson, S. W. *J. Phys. Chem.* **1968**, *72*, 1866-1887.

212. Billaud, F.; Chaverot, P.; Freund, E. *J. Anal. Appl. Pyrolysis* **1987**, *11*, 39-53.

213. Ondruschka, B.; Zimmermann, G.; Ziegler, U. *J. Anal. Appl. Pyrolysis* **1990**, *18*, 33-39.

214. Hrovat, D. A.; Borden, W. T. *J. Am. Chem. Soc.* **2001**, *123*, 4069-4072.

215. Brown, T. C.; King, K. D.; Nguyen, T. T. *J. Phys. Chem.* **1986**, *90*, 419-424.

216. Kiefer, J. H.; Gupte, K. S.; Harding, L. B.; Klippenstein, S. J. *J. Phys. Chem. A* **2009**, *113*, 13570-13583.

217. Nguyen, M. T.; Matus, M. H.; Lester Jr, W. A.; Dixon, D. A. *J. P. Chem. A* **2008**, *112*, 2082-2087.

218. Matus, M. H.; Nguyen, M. T.; Dixon, D. A. *J. Phys. Chem. A* **2006**, *110*, 8864-8871.

219. Dixon, D. A.; Arduengo III, A. J. *J. Phys. Chem. A* **2006**, *110*, 1968-1974.

220. Nguyen, T. L.; Kim, G. S.; Mebel, A. M.; Nguyen, M. T. *Chem. Phys. Lett.* **2001**, *349*, 571-577.

221. Song, M.-G.; Sheridan, R. S. *J. Phys. Org. Chem.* **2011**, *24*, 889-893.

222. Woodcock, H. L.; Moran, D.; Brooks, B. R.; Schleyer, P. V. R.; Schaefer III, H. F. *J. Am. Chem. Soc.* **2007**, *129*, 3763-3770.

223. Kassaee, M. Z.; Shakib, F. A.; Momeni, M. R.; Ghambarian, M.; Musavi, S. M. *J. Org. Chem.* **2010**, *75*, 2539-2545.

224. Geise, C. M.; Hadad, C. M. *J. Org. Chem.* **2000**, *65*, 8348-8356.

225. Hudzik, J. M.; Asatryan, R.; Bozzelli, J. W. *J. Phys. Chem. A* **2010**, *114*, 9545-9553.

226. Yamaguchi, K.; Jensen, F.; Dorigo, A.; Houk, K. N. *Chem. Phys. Lett.* **1988**, *149*, 537-542.

227. Ess, D. H.; Cook, T. C. *J. Phys. Chem. A* **2012**, *116*, 4922-4929.

228. Sirjean, B.; Fournet, R.; Glaude, P. A.; Ruiz-López, M. F. *Chem. Phys. Lett.* **2007**, *435*, 152-156.

229. Alecu, I. M.; Zheng, J.; Zhao, Y.; Truhlar, D. G. *J. Chem. Theor. Comput.* **2010**, *6*, 2872-2887.

230. Ruscic, B.; Litorja, M.; Asher, R. L. *J. Phys. Chem. A* **1999**, *103*, 8625-8633.

231. Muller, C.; Michel, V.; Scacchi, G.; Côme, G. M. *J. Chem. Phys.* **1995**, *92*, 1154-1178.

232. Murcko, M. A.; Castejon, H.; Wiberg, K. B. *J. Phys. Chem.* **1996**, *100*, 16162-16168.

233. Allinger, N. L.; Fermann, J. T.; Allen, W. D.; Schaefer III, H. F. *J. Chem. Phys.* **1996**, *106*, 5143-5150.

234. Mo, Y. *J. Org. Chem.* **2010**, *75*, 2733-2736.

235. da Silva, G.; Bozzelli, J. W. *J. Phys. Chem. A* **2007**, *111*, 12026-12036.

236. Chen, C. C.; Bozzelli, J. W. *J. Phys. Chem. A* **2003**, *107*, 4531-4546.

237. Cox, J. D.; Wagman, D. D.; Medvedev, V. A. *CODATA Key Values for Thermodynamics*; Hemisphere Publishing, Corp.: New York, NY, 1989.

238. Ruscic, B.; Pinzon, R. E.; Morton, M. L.; Srinivasan, N. K.; Su, M. C.; Sutherland, J. W.; Michael, J. V. *J. Phys. Chem. A* **2006**, *110*, 6592-6601.

239. Seetula, J. A.; Slagle, I. R. *J. Chem. Soc., Faraday Trans.* **1997**, *93*, 1709-1719.

240. Ervin, K. M.; DeTuri, V. F. *J. Phys. Chem. A* **2002**, *106*, 9947-9956.

241. Simmie, J. M.; Black, G.; Curran, H. J.; Hinde, J. P. *J. Phys. Chem. A* **2008**, *112*, 5010-5016.

242. Sukumaran, R. K.; Singhania, R. R.; Mathew, G. M.; Pandey, A. *Renew. Energy* **2009**, *34*, 421-424.

243. Catoire, L.; Yahyaoui, M.; Osmont, A.; Gökalp, I.; Brothier, M.; Lorcet, H.; Guénadou, D. *Energy Fuels* **2008**, *22*, 4265-4273.

244. Kotchoni, S. O.; Gachomo, E. W. *J. Biol. Sci.* **2008**, *8*, 693-701.

245. Demirba, A. *Energy Convers. Manage.* **1998**, *39*, 685-690.

246. Demirba, A. *Energy Convers. Manage.* **2001**, *42*, 1357-1378.

247. McKendry, P. *Bioresour. Technol.* **2002**, *83*, 47-54.

248. Zhao, H.; Holladay, J. E.; Brown, H.; Zhang, Z. C. *Science* **2007**, *316*, 1597-1600.

249. Bicker, M.; Hirth, J.; Vogel, H. *Green Chem.* **2003**, *5*, 280-284.

250. Palmqvist, E.; Hahn-Hägerdal, B. *Bioresour. Technol.* **2000**, *74*, 25-33.

251. Campen, M. G. V.; Johnson, J. R. *J. Am. Chem. Soc.* **1933**, *55*, 430-431.

252. D'Alelio, G. F.; Williams Jr, C. J.; Wilson, C. L. *J. Org. Chem.* **1960**, *25*, 1028-1030.

253. Petfield, R. J. *J. Org. Chem.* **1954**, *19*, 1944-1946.

254. Barluenga, J.; De Prado, A.; Santamaría, J.; Tomás, M. *Chem. Eur. J.* **2007**, *13*, 1326-1331.

255. Murai, A.; Takahashi, K.; Taketsuru, H.; Masamune, T. *J. Chem. Soc., Chem. Commun.* **1981**, 221-222.

256. Goh, Y. W.; Pool, B. R.; White, J. M. *J. Org. Chem.* **2008**, *73*, 151-156.

257. Fisher, B. E.; Hodge, J. E. *J. Org. Chem.* **1964**, *29*, 776-781.

258. Liu, H.; Xu, J.; Du, D.-M. *Org. Lett.* **2007**, *9*, 4725-4728.

259. Zhou, A.; Segi, M.; Nakajima, T. *Tetrahedron Lett.* **2003**, *44*, 1179-1182.

260. Khoumeri, B.; Balbi, N.; Balbi, J. H.; Bighelli, A.; Tomi, F.; Casanova, J. *Thermochim. Acta* **1995**, *259*, 121-131.

261. Beukes, J. A.; Marstokk, K. M.; Mollendal, H. *J. Mol. Struct.* **2001**, *567-568*, 19-27.

262. Glendening, E. D.; Reed, A. E.; Carpenter, J. E.; Weinhold, F. NBO Version 3.1.

263. Pittam, D. A.; Pilcher, G. *J. Chem. Soc., Faraday Trans. 1* **1972**, *68*, 2224-2229.

264. Furuyama, S.; Golden, D. M.; Benson, S. W. *J. Chem. Thermodyn.* **1969**, *1*, 363-375.

265. Pilcher, G.; Pell, A. S.; Coleman, D. J. *Trans. Faraday Soc.* **1964**, *60*, 499-505.

266. Fenwick, J. O.; Harrop, D.; Head, A. J. *J. Chem. Thermodyn.* **1975**, *7*, 943-954.

267. Sebbar, N.; Bockhorn, H.; Bozzelli, J. W. *Phys. Chem. Chem. Phys.* **2002**, *4*, 3691-3703.

268. Guthrie Jr, G. B.; Scott, D. W.; Hubbard, W. N.; Katz, C.; McCullough, J. P.; Gross, M. E.; Williamson, K. D.; Waddington, G. *J. Am. Chem. Soc.* **1952**, *74*, 4662-4669.

269. Pilgrim, J. S.; Taatjes, C. A. *J. Phys. Chem. A* **1997**, *101*, 4172-4177.

270. Barckholtz, C.; Barckholtz, T. A.; Hadad, C. M. *J. Am. Chem. Soc.* **1999**, *121*, 491-500.

271. da Silva, G.; Moore, E. E.; Bozzelli, J. W. *J. Phys. Chem. A* **2006**, *110*, 13979-13988.

272. Mackie, J. C.; Colket, M. B., III; Nelson, P. F.; Esler, M. *Int. J. Chem. Kinet.* **1991**, *23*, 733-760.

273. Davico, G. E.; Bierbaum, V. M.; DePuy, C. H.; Ellison, G. B.; Squires, R. R. *J. Am. Chem. Soc.* **1995**, *117*, 2590-2599.

274. Agapito, F.; Cabral, B. J. C.; Martinho Simões, J. A. *J. Mol. Struct. (THEOCHEM)* **2005**, *719*, 109-114.

275. da Silva, G.; Kim, C. H.; Bozzelli, J. W. *J. Phys. Chem. A* **2006**, *110*, 7925-7934.

276. Curtiss, L. A.; Pople, J. A. *J. Chem. Phys.* **1988**, *88*, 7405-7409.

277. Sebbar, N.; Bockhorn, H.; Bozzelli, J. W. *J. Phys. Chem. A* **2005**, *109*, 2233-2253.

278. Kilpin, K. J.; Jarman, B. P.; Henderson, W.; Nicholson, B. K. *Appl. Organometal. Chem.* **2011**, *25*, 810-814.

279. Corma, A.; De La Torre, O.; Renz, M.; Villandier, N. *Angew. Chem., Int. Ed.* **2011**, *50*, 2375-2378.

280. Zheng, H. Y.; Zhu, Y. L.; Huang, L.; Zeng, Z. Y.; Wan, H. J.; Li, Y. W. *Catal. Commun.* **2008**, *9*, 342-348.

281. Lessard, J.; Morin, J. F.; Wehrung, J. F.; Magnin, D.; Chornet, E. *Top. Catal.* **2010**, *53*, 1231-1234.

282. Aliaga, C.; Tsung, C. K.; Alayoglu, S.; Komvopoulos, K.; Yang, P.; Somorjai, G. A. *J. Phys. Chem. C* **2011**, *115*, 8104-8109.

283. Zheng, H. Y.; Zhu, Y. L.; Teng, B. T.; Bai, Z. Q.; Zhang, C. H.; Xiang, H. W.; Li, Y. W. *J. Mol. Catal. A: Chem.* **2006**, *246*, 18-23.

284. Wu, X.; Huang, Z.; Yuan, T.; Zhang, K.; Wei, L. *Combust. Flame* **2009**, *156*, 1365-1376.

285. Aschmann, S. M.; Nishino, N.; Arey, J.; Atkinson, R. *Environ. Sci. Technol.* **2011**, *45*, 1859-1865.

286. Gómez Alvarez, E.; Borrás, E.; Viidanoja, J.; Hjorth, J. *Atmos. Environ.* **2009**, *43*, 1603-1612.

287. Zhang, W.; Du, B.; Mu, L.; Feng, C. *J. Mol. Struct. (THEOCHEM)* **2008**, *851*, 353-357.

288. Bierbach, A.; Barnes, I.; Becker, K. H. *Atmos. Environ.* **1995**, *29*, 2651-2660.

289. Cabañas, B.; Villanueva, F.; Martín, P.; Baeza, M. T.; Salgado, S.; Jiménez, E. *Atmos. Environ.* **2005**, *39*, 1935-1944.

290. Villanueva, F.; Cabañas, B.; Monedero, E.; Salgado, S.; Bejan, I.; Martin, P. *Atmos. Environ.* **2009**, *43*, 2804-2813.

291. Simmie, J. M.; Metcalfe, W. K. *J. Phys. Chem. A* **2011**, *115*, 8877-8888.

292. Hudzik, J. M.; Bozzelli, J. W. *J. Phys. Chem. A* **2010**, *114*, 7984-7995.

293. Blanksby, S. J.; Ramond, T. M.; Davico, G. E.; Nimlos, M. R.; Kato, S.; Bierbaum, V. M.; Lineberger, W. C.; Ellison, G. B.; Okumura, M. *J. Am. Chem. Soc.* **2001**, *123*, 9585-9596.

294. Wijaya, C. D.; Sumathi, R.; Green Jr, W. H. *J. Phys. Chem. A* **2003**, *107*, 4908-4920.

295. Tumanov, V. E.; Denisov, E. T. *Kinet. Catal.* **2004**, *45*, 621-627.

296. da Silva, G.; Chen, C. C.; Bozzelli, J. W. *Chem. Phys. Lett.* **2006**, *424*, 42-45.

297. Su, Y.; Brown, H. M.; Huang, X.; Zhou, X. d.; Amonette, J. E.; Zhang, Z. C. *Appl. Catal., A* **2009**, *361*, 117-122.

298. Zhang, Z.; Zhao, Z. K. *Bioresour. Technol.* **2010**, *101*, 1111-1114.

299. Dutta, S.; De, S.; Alam, M. I.; Abu-Omar, M. M.; Saha, B. *J. Catal.* **2012**, *288*, 8-15.

300. Paine III, J. B.; Pithawalla, Y. B.; Naworal, J. D. *J. Anal. Appl. Pyrolysis* **2008**, *83*, 37-63.

301. Wei, L.; Tang, C.; Man, X.; Jiang, X.; Huang, Z. *Energy Fuels* **2012**, *26*, 2075-2081.

302. Vasiliou, A.; Nimlos, M. R.; Daily, J. W.; Ellison, G. B. *J. Phys. Chem. A* **2009**, *113*, 8540-8547.

303. Tian, Z.; Yuan, T.; Fournet, R.; Glaude, P. A.; Sirjean, B.; Battin-Leclerc, F.; Zhang, K.; Qi, F. *Combust. Flame* **2011**, *158*, 756-773.

304. Mousavipour, S. H.; Ramazani, S.; Shahkolahi, Z. *J. Phys. Chem. A* **2009**, *113*, 2838-2846.

305. Burnett, L. W.; Johns, I. B.; Holdren, R. F.; Hixon, R. M. *Ind. Eng. Chem.* **1948**, *40*, 502-505.

306. Lifshitz, A.; Tamburu, C.; Shashua, R. *J. Phys. Chem. A* **1997**, *101*, 1018-1029.

307. Lifshitz, A.; Tamburu, C.; Shashua, R. *J. Phys. Chem. A* **1998**, *102*, 10655-10670.

308. Sirjean, B.; Fournet, R. *J. Phys. Chem. A* **2012**, *116*, 6675-6684.

309. Li, S.; Zhang, J.; Gao, H.; Zhou, W.; Zhou, Z. *J. Mol. Struct. (THEOCHEM)* **2010**, *948*, 108-110.

310. Assary, R. S.; Redfern, P. C.; Hammond, J. R.; Greeley, J.; Curtiss, L. A. *Chem. Phys. Lett.* **2010**, *497*, 123-128.

311. Simmie, J. M. *J. Phys. Chem. A* **2012**, *116*, 4528-4538.

312. Hudzik, J. M. Ph.D. Dissertation. Department of Chemistry and Environmental Science, New Jersey Institute of Technology, Newark, NJ, 2013.

313. Chang, A. Y.; Bozzelli, J. W.; Dean, A. M. *Z. Phys. Chem.* **2000**, *214*, 1533-1568.

314. Prosen, E. J.; Maron, F. W.; Rossini, F. D. *J. Res. Natl. Bur. Stand.* **1951**, *46*, 106-112.

315. Hudzik, J. M.; Bozzelli, J. W. *J. Phys. Chem. A* **2012**, *116*, 5707-5722.

316. Guthrie, J. P. *Can. J. Chem.* **1978**, *56*, 962-973.

317. Sumathi, R.; Green Jr, W. H. *J. Phys. Chem. A* **2002**, *106*, 7937-7949.

318. Merle, J. K.; Hadad, C. M. *J. Phys. Chem. A* **2004**, *108*, 8419-8433.

319. Fadden, M. J.; Hadad, C. M. *J. Phys. Chem. A* **2000**, *104*, 8121-8130.

320. da Silva, G.; Chen, C. C.; Bozzelli, J. W. *J. Phys. Chem. A* **2007**, *111*, 8663-8676.